ABSTRACT

WILCOX, ESTHER MAGDALENE. Direct Synthesis of Acetic Acid from Carbon Dioxide and Methane. (Under the direction of Dr. George W. Roberts and Dr. James J. Spivey)

The catalytic activation of carbon dioxide in reactions with methane has been investigated. Of specific concern was the direct synthesis of acetic acid from methane and carbon dioxide using a heterogeneous catalyst:

$$CO_2 + CH_4 \rightarrow CH_3COOH$$

$\Delta G_r^0 = +71$ kJ/mol $\qquad\qquad$ $\Delta H_r^0 = +36$ kJ/mol

Equilibrium thermodynamic calculations were performed on this reaction to understand its potential behavior in the laboratory. This reaction was found to be severely limited by thermodynamics at all conditions of practical interest. Equilibrium calculations were performed on other reaction systems to investigate potential methods for overcoming the thermodynamic limitations of the direct synthesis reaction. Promising approaches include the synthesis of acetic anhydride from ketene, the synthesis of vinyl acetate from ethylene and oxygen, and the synthesis of vinyl acetate from acetylene.

Diffuse reflectance infrared Fourier transform spectroscopy (DRIFTS) experiments definitively showed the formation of adsorbed acetates, monomeric and dimeric acetic acid from carbon dioxide and methane over solid Pt and Pd catalysts. Further reaction experiments, conducted using a micro-reactor system with an online mass spectrometer, confirmed the formation of gas phase acetic acid from carbon dioxide and methane using

either a 5% Pd/alumina or 5% Pt/alumina catalyst. In addition to acetic acid, carbon monoxide, hydrogen and water were observed under some conditions.

The effective catalysts for the direct synthesis reaction adsorbed both methane and carbon dioxide. Methane appeared to adsorb on the metal, and carbon dioxide on the alumina support. The effective catalysts also had small metal clusters dispersed on the support, which increases the number of adjacent carbon dioxide adsorbing and methane adsorbing sites.

Preliminary experiments showed that vinyl acetate could be synthesized from carbon dioxide, methane and acetylene. The most effective catalyst appeared to be an admixture of Pt or Pd/Al_2O_3 and Zn-acetate/carbon. These experiments suggest that the direct synthesis of acetic acid can be driven by coupling it with a thermodynamically favorable reaction that consumes acetic acid.

DIRECT SYNTHESIS OF ACETIC ACID FROM CARBON DIOXIDE AND METHANE

By

ESTHER MAGDALENE WILCOX

A dissertation submitted to the Graduate Faculty of
North Carolina State University
in partial fulfillment of the
requirements for the Degree of
Doctor of Philosophy

CHEMICAL ENGINEERING

Raleigh

June 21st, 2004

APPROVED BY:

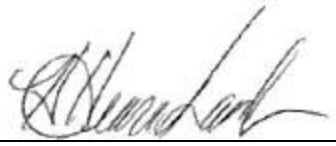

Dr. H. Henry Lamb

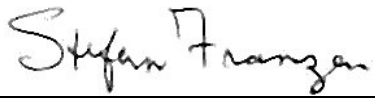

Dr. Stefan Franzen

Dr. George W. Roberts
Chair of Advisory Committee

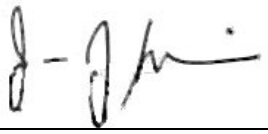

Dr. J. Jerry Spivey
Co-Chair of Advisory Committee

Für Oma und Opa,

Lina und Theo Sauer

BIOGRAPHY

Esther Magdalene Wilcox, the only child of Harold and Gerda Wilcox, was born on July 29th, 1977 in Nuremberg, Germany. The family lived in several places including Tennessee, Kentucky and Kuwait. In 1980 they decided to settle down in Fort Collins, Colorado.

It was during Junior High and High School that Esther truly began to love science and math. She also took advantage of Colorado State University, and took over 60 hours worth of German and general university courses while she was still in high school. After graduating from Fort Collins High School in 1995, she attended the University of Tulsa. While in college, she worked as an engineering intern at a local oil refinery, was a resident assistant, tutored math and chemistry and also conducted undergraduate research. In 1998, she graduated cum laude with a Bachelors of Arts in German and a Bachelors of Science in Chemical Engineering. The joy of research led her to North Carolina State University where she entered the Doctoral program in chemical engineering. She graduated with her Ph.D. in 2004 and has accepted a Post Doctoral position at the University of Colorado, in Boulder.

ACKNOWLEDGEMENTS

First and foremost, I would like to express my deepest appreciation to my parents for their constant support and encouragement. To my father, Dr. Harold Wilcox: I couldn't imagine a better dad. Not only did you teach me the value of education at a young age, but you have also taught me about enjoying life and never letting my inner kid die. I am also thankful for all the building projects you let me help with, I'm sure that had a significant influence on my choice of paths. To my mother, Gerda Wilcox: You have shown me how to balance all the things in my life. I am so grateful for all the adventures you have taken me on. You two have always believed in me and what I could achieve. Not only are you wonderful parents, but also great friends.

I would like to thank all my relatives in Germany including, but not limited to: Lina, Theo, Herbert, Christa, Sonja, and Claudia, for the fun summers, great company and outstanding food.

I am grateful to my junior high and high school science and math teachers; especially Mr. Viney and Mr. Lundt, who passed on to me their excitement and love of science. I hope that you will continue to enlighten the minds of your students.

Many thanks to my advisors, Dr. Roberts and Dr. Spivey. You have taught me about research and so much more. I am also very thankful for the funding you provided over the years. Thank you for your patience, support and motivation. I am also grateful to Dr. Lamb, Dr. Franzen and Dr. Haney for their help with data analysis.

To my fellow graduate students: thanks for the stimulating conversations and for all the help over the years. In particular: Susan, Nick and Brian for lending me tools or a hand

when I needed it. To Paul: You have made everyday in the office interesting. Thanks for the entertainment and coffee.

To all my friends: thank you for your confidence in me and for always keeping my life exciting. To Sara & Emily: Thanks for remaining my friends after all these years and miles in between. To Brent, Kelly, Jenn Greb, Courtney, Cicily, Stacy, Nicole, Robbie and Whitlock (in no particular order): Thanks for showing me that life doesn't always have to be serious. I've enjoyed the randomness of each experience. You will always remain the benchmark for true adventures.

To Jason, Jake, Hung, and Jonathan: You were always there for me through thick and thin. You have made the hard times in these past years bearable, and the good times memorable.

Last but certainly not least, Sean; Thanks for the random late night chats about everything and nothing. I don't think I could have made it through these past years without you.

I am eternally grateful to all of you.

Esther

TABLE OF CONTENTS

TABLE OF CONTENTS CONTINUED

TABLE OF CONTENTS CONTINUED

LIST OF TABLES

LIST OF TABLES CONTINUED

LIST OF FIGURES

LIST OF FIGURES CONTINUED

LIST OF FIGURES CONTINUED

LIST OF FIGURES CONTINUED

LIST OF FIGURES CONTINUED

LIST OF FIGURES CONTINUED

CHAPTER 1

INTRODUCTION

1.1 MOTIVATION

1.1.1 CARBON DIOXIDE EMISSIONS REDUCTION

Carbon dioxide is one of the main contributors to the greenhouse effect. Due to the structure of carbon dioxide, it absorbs the radiation reflected from the earth [1, 2]. This process causes an increase in the global temperature [1, 2]. There is great concern about the long term effects of global warming. The total amount of carbon dioxide produced worldwide, both naturally and synthetically, exceeds the amount that can be removed by natural sinks such as plants and oceans. Thus the amount of carbon dioxide in the atmosphere increases every year. The largest contributor of carbon dioxide emissions is the burning of fossil-fuels. Due to the concern about the increasing carbon dioxide emissions, the Kyoto treaty calls for a worldwide reduction in greenhouse gas emissions [3].

There are two main routes to reducing carbon dioxide emissions: reduce the amount of carbon dioxide produced, and/or sequester the carbon dioxide produced. Technology is continually being developed to reduce emissions from fossil-fuel combustion. There has also been a great deal of research and development in the area of alternative fuels [4-8].

Methods to sequester the carbon dioxide include the use of supercritical carbon dioxide as solvent, bioconversion of carbon dioxide to useful products, and the use of carbon dioxide as a chemical feedstock [1, 6, 9-13]. There has been a great deal of research in all of these areas. However, this research will focus only on the use of carbon dioxide as a chemical feedstock.

The use of carbon dioxide as a chemical feedstock has several advantages, other than the mitigation of a greenhouse gas. Carbon dioxide is an abundant and inexpensive carbon source. However, the main challenge is the activation of carbon dioxide, as it is a stable molecule [6, 13-15]. This leads to thermodynamic and kinetic problems. There is currently a great deal of research that has been and is being conducted on efficient methods to activate carbon dioxide, including bioconversion, photochemical reduction, electrochemical reduction, and various thermal catalytic methods [1, 6, 9-17].

Technology exists for the conversion of CO_2 and CH_4 to synthesis gas (H_2 and CO) [15, 18-22], which can then be used to produce simple organic compounds, including methanol . However, it would be more efficient to use the CO_2 directly in synthesis of the desired product. Direct synthesis of acetic acid from carbon dioxide and methane is one reaction that, if successful, can have lasting environmental benefits and result in the mitigation of greenhouse gas emissions, providing an environmentally benign route to this important chemical intermediate.

Though the absolute amount of CO_2 emission reduction may appear small, it could significantly help the United States achieve the goals of the Kyoto treaty, as the following calculation shows. The Kyoto treaty calls for a reduction of greenhouse gas emissions of 7% from 1990 levels, corresponding to a reduction of 280×10^6 ton/yr. Acetic acid is produced at a rate of more than 6×10^6 ton/yr worldwide, and the demand is increasing at 2% to 3% per year [23]. At this rate, 4.4×10^6 ton/yr of CO_2 would be consumed if all acetic acid were manufactured by the methane/CO_2 process. This corresponds to 0.1% of the $4{,}400 \times 10^6$

ton/yr emissions of CO_2 in the United States, representing 1.6% of the emission reduction required by the Kyoto treaty.

This calculation does not account for the fact that this type of chemistry could be used for a wide range of related carboxylation reactions. If the reaction of CO_2 with CH_4 to form acetic acid can be demonstrated experimentally, it should be possible to extend the underlying chemistry to related carboxylation reactions, e.g.:

$$CO_2 + C_2H_6 \longrightarrow \text{propionic acid}$$

Such an extension would expand the potential reduction in CO_2 emissions substantially. Collectively, if such reactions accounted for as much as, say, 44×10^6 ton/yr (or 1%) of the total CO_2 emissions, this would significantly help the United States achieve the targets of the Kyoto treaty. Under the assumption above, at least (44/280), or 16% of the CO_2 emission reduction, and perhaps more, could be achieved by the use of this technology.

Although this technology may not be implemented to the extent assumed in these calculations, there is a clear potential and an incentive to carry out this research as one way, among others, to prevent CO_2 emissions. The process addressed in this proposal is a simple, heterogeneous catalytic process, which utilizes CO_2 and CH_4 directly.

1.1.2 METHANE USE

While not commonly thought of, methane is actually the third most abundant greenhouse gas in the atmosphere, after water and carbon dioxide [24-26]. Approximately a third of the methane released into the atmosphere comes from natural sources including

wetlands, oceans and hydrates. Anthropological sources of methane emissions include: waste decomposition, rice cultivation, biomass burning and extraction of fossil fuels. It is of interest to reduce the amount of methane emissions from anthropological sources, or mitigate the released methane.

Methane is a naturally occurring and abundant carbon source. The world wide natural gas reserves are estimated to be around 5000 trillion cubic feet [27, 28]. Most of these sources are methane hydrates in the ocean or natural gas in fossil fuel reservoirs. Methane is also a by product of waste decomposition, as biogas.

Currently, most methane used is used primarily as an energy source. It is increasingly being burned by power plants for energy, rather than other fossil fuels. Liquid natural gas (LNG) is becoming a popular form of storing and transporting methane. There are currently few industrial applications involving methane, due to its unreactive nature.

In addition to mitigation of a greenhouse gas, the use of methane is of interest simply because it is abundant and inexpensive. Unfortunately, methane is the least reactive alkane [27, 28]. There is currently a great deal of research that has been and is being conducted on efficient methods to activate methane [27-45]. There are two main focuses for the use of methane as a chemical feedstock. The first is in the dry reforming reaction with carbon dioxide to give synthesis gas. Synthesis gas can then be used to produce organic chemicals. This step is often the most costly part of the overall process. The direct synthesis of chemicals from methane eliminates the need for the intermediate synthesis gas production step, but these types of direct processes have not been widely reported. There is a need for

further research in methane activation, especially with single reactants such as CO_2. This proposed research would contribute to the field of methane activation.

1.1.3 Acetic Acid Uses and Current Production

Acetic acid is an important industrial chemical produced at an annual rate of more than 6.8 million metric tons worldwide[23]. Acetic acid finds use in a variety of industrial applications including the production of acetic anhydride, acrylates, and terephthalic acid and as a solvent in pharmaceutical syntheses [23, 46]. Using over 44% of the acetic acid produced in 2001, vinyl acetate production is the largest consumer of acetic acid [23, 47]. Vinyl acetate and its derivatives, such as polyvinyl acetate, polyvinyl alcohol and ethylene-vinyl acetate copolymer, are widely used in the production of adhesives and coating materials [46, 47].

Currently, the industrial production of acetic acid is accomplished primarily by the homogeneous catalyzed carbonylation of methanol using the Monsanto/BP process [23]:

$$CH_3OH + CO \xrightarrow{[Rh(CO)_2I_2]^-} CH_3COOH$$

This process relies on a multiphase reaction of methanol and carbon monoxide with a rhodium or iridium catalyst dissolved in the liquid phase. Due to the expense of the catalyst, the economics of the process depends on successful recovery and recycling of the catalyst. This separation and the purification of the acetic acid from the water and by-products are costly and energy consuming. In addition, the methyl iodine (CH_3I) promoter used is toxic and corrosive. The potential occupational and environmental hazards of the promoter and the

carbon monoxide provide a clear incentive to develop benign manufacturing processes for acetic acid. The direct synthesis of acetic acid from methane and carbon dioxide using a solid catalyst may provide an economic and environmentally sound process. Furthermore, the key patents on the Monsanto/BP technology expired in 2000, leading to a recent flurry of research and development on a heterogeneous route to acetic acid synthesis. This suggests that the opportunity exists for a new technology, such as this one, to be commercially practiced.

Current technology already exists for the synthesis of acetic acid from carbon dioxide and methane. However, this is an indirect method, involving the formation of carbon monoxide and hydrogen from methane and carbon dioxide. The carbon monoxide can then be used in the standard synthesis of acetic acid from carbon monoxide and methanol. The synthesis gas (carbon monoxide and hydrogen) can also be used to produce acetic acid.

Dry reforming is the process of converting carbon dioxide and methane to synthesis gas, carbon monoxide and hydrogen. This reaction is thermodynamically limited; therefore it is carried out at high temperature, 600°C and above [12]. Coke formation on the catalyst is an intermediate step [48-63]. A nickel catalyst is typically used for this reaction, does not deactivate with coke formation [48-63]. Due to the high temperatures required, this process is energy intensive.

The carbon monoxide from the formed synthesis gas can be used in the acetic acid synthesis from methanol and carbon monoxide. Acetic acid is currently produced industrially by the carbonylation of methanol using an aqueous rhodium or iridium catalyst. This Monsanto/BP process is well understood [46, 64-66].

Acetic acid can also be formed directly from synthesis gas [67-76]. This reaction is typically run using a rhodium catalyst. While selectivities up to 70% for acetic acid can be achieved, the conversions are less than 2% based on either carbon monoxide or hydrogen.

Overall this indirect route of acetic acid synthesis from carbon dioxide and methane is inefficient. The dry reforming step is energy intensive, and the synthesis gas route to acetic acid gives very low conversions.

Due to the interest of using methane as a feedstock, and the value of producing acetic acid, several groups have studied the formation of acetic acid from methane, carbon monoxide and an oxidant. Three main types of oxidants have been used, oxygen, hydrogen peroxide (H_2O_2) and potassium peroxodisulfate ($K_2S_2O_8$), or combinations thereof.

The first investigators to examine the synthesis of acetic acid from methane and carbon monoxide was Lin and Sen [77]. Using a rhodium chloride catalyst in an aqueous medium, and oxygen as the oxidant, they were able to form acetic acid. They examined the effect of various promoters including HI, KI and a 5% Pd/carbon catalyst. In the absence of any promoter, they report the yield of acetic acid to be 0.014, determined by NMR, after 72 hours at 140°C. The highest yield of acetic acid was 0.276 after 420 hours at 95°C using an HI promoter. The yield of acetic acid was approximately the same for experiments run using an HI promoter as with those using a KI promoter. The advantage of the HI promoter is the lower yields of methanol and formic acid compared to the KI promoter. Additionally, the yield of acetic acid increased with increasing reaction time.

As a continuation of the work, Lin et al. also examined the reaction using a $CuCl_2$ catalysts and trifluoroacetic acid (CF_3COOH) [78]. From a system containing 0.1 mmol

$CuCl_2$, 1 mg 5% Pd/carbon catalyst, 1 mL water, 3 mL CF_3COOH, 900 psi CH_4, 200 psi CO_2 and 100 psi O_2, they reported high yields of acetic acid after 90 hours at 90°C. They also observed small amounts of methanol, formic acid and $CF_3COO_2CH_3$.

Chepkaikin et al. studied the reaction of methane with carbon monoxide using oxygen as an oxidant [79-83]. Their work is based on the use of various homogeneous rhodium catalysts. In all cases CF_3COOH was used in the reaction systems. Using a $RhCl_3$ catalyst and a CuI promoter in CF_3COOH and water, they report their highest yields of acetic acid up to 0.07 from inlet pressures of CH_4, CO_2 and O_2 of 6 MPa, 1.84 MPa and 0.56 MPa, respectively. From this same system, a yield of 0.02 of formic acid and 0.11 of CF_3COOCH_3 was reported. Carbon dioxide was also formed from the reaction of carbon monoxide and oxygen.

Using a dielectric barrier discharge reactor, Larkin et al. also examined the reaction of methane with carbon monoxide and oxygen [84]. Using an inlet flow rate of 10 mL/min of CO, 145 mL/min of CH_4 and 45 mL/min of O_2, they report their highest selectivity of acetic acid to be 16%. At these conditions the conversion of methane was only 17%. The highest conversion of methane was found to be 20% using an inlet flow rater of 40 ml/min of CO, 120 mL/min of CH_4 and 20 mL/min of O_2. At these conditions, the selectivity of acetic acid was only 12%. In addition to acetic acid, methyl formate, carbon dioxide and formaldehyde were observed in the products.

These studies show that methane can be reacted with carbon monoxide and oxygen to give acetic acid. However, in all cases, the yield of acetic acid was small. In addition, these systems produced many side products.

The Fugiwara group extensively studied the reaction of carbon monoxide with methane using various homogeneous catalysts in CF_3COOH and $K_2S_2O_8$ [85-93]. Using 20 atm of CO, 40 atm of CH_4 and a $Cu(OAc)_2$ catalysts, they report an 8% yield of acetic acid based on methane after 20 hours at 80°C [85]. Using 20 atm of CH_4, 15 atm of CO and a mixture of $Cu(OAc)_2$ and $Pd(OAc)_2$ catalysts, they report a 410% yield of acetic acid based on palladium after 40 hours at 80°C [86, 87]. They found that using $CuSO_4$ as the catalyst, that a yield of 3900% of acetic acid based on copper was achieved [88]. For this reaction, they used 40 atm of CH_4 and 20 atm of CO, reacting for 40 hours at 80°C.

Again using the $Cu(OAc)_2$ catalyst, they report a 9% yield of acetic acid based on methane with 40 atm of CH_4 and 20 atm of CO at 80° for 20 hours [89]. They also found that the copper catalyst alone performed better than the palladium catalyst alone or a mixture of the palladium an copper catalysts. Their studies show that the yield of acetic acid increases with increasing inlet CH_4 pressure. The yield increases with reaction time up to about 25 hours, after which it remains fairly constant. Additionally, the yield increases with less catalyst.

In studies with other catalysts, they reported a 26% yield of acetic acid with a $CaCl_2$ catalyst in the presence of 40 atm CO and 5 atm of CH_4 at 85° for 15 hours [93]. They obtained a 93% yield of acetic acid based on methane using a $VO(acac)_2$ catalyst, 5 atm of CH_4 and 20 atm of CO at 80°C for 20 hours. In this study, they report that the yield of acetic acid increases with increasing methane pressure up to 20 atm, at which point it remains constant [90, 92]. They also examined several lanthanide catalysts [91]. In the presence of 40 atm of CH_4 and 20 atm of CO at 80° for 20 hours, they report that all of the catalysts tried

gave above a 20% yield of acetic acid based on methane. Most of them gave yields above 30%. The best catalyst, Yb_2O_3, gave a 100% yield of acetic acid based on methane.

In all of their publications, they do not report the formation of any side products, such as methanol, methyl formate or carbon dioxide. It is likely that these products are formed in their reaction systems. Additionally, the use of CF_3COOH solvent is called into question by us [94]. Methane is likely to react with the solvent to form acetic acid and CHF_3. Other research in the literature supports this, and is discussed in detail later. The high yields of acetic acid reported may be due to this reaction, rather than that of methane with carbon monoxide and the oxidant.

In addition to their work with $K_2S_2O_8$ as the oxidant, Asudullah et al. (part of the Fugiwara group), examined the effects of using H_2O_2 in the reaction of methane and carbon monoxide [95]. Using 20 atm of CH_4, 10 atm CO, 1 mL H_2O_2, 9 mL NaClO and 183 μmol of $Yb(OAc)_3$ catalyst, they report a 5% yield of acetic acid based on methane after 20 hours at 80°C. They found that the best temperature for the reaction was around 50°C. To optimize the yield, 5 atm of CO and over 20 atm CH_4 is best. Additionally, the longer the reaction time, the higher the yield of acetic acid. The formation of other products was not reported.

Nizova et al. also examined the reaction of methane and carbon monoxide with H_2O_2 [96]. Using a $NaVO_3$ catalyst, 50 bar CH_4 and 30 bar CO in H_2O_2, they report a 2.2% yield of acetic acid based on methane after 50 hours at 40°C. They also found large amounts of methanol in the product.

These studies show that hydrogen peroxide can be used as an oxidant, rather than oxygen or $K_2S_2O_8$. However, the yields are lower than those reported from the use of $K_2S_2O_8$.

A few groups have studied the formation of acetic acid from methane without carbon monoxide or carbon dioxide, rather with an oxidant only. Seki et al. examined the reaction of methane with hydrogen peroxide using various vanadium catalysts dissolved in $(CF_3CO)_2O$ at 80° for 24 hours [97, 98]. The highest conversion of methane reported was when a VOF_3 catalyst was used. However, this catalyst gave one of the worst selectivities of acetic acid. A V_2O_5 catalyst gave the highest selectivity of acetic acid, 87%, but only a 1% conversion of methane. In addition to acetic acid, other by products were formed including methanol, and carbon dioxide.

Suss-Fink et al. studied the reaction of methane with oxygen and hydrogen peroxide [99]. The examined the formation of methanol from metavanadate and pyrazine-2-carboxylic acid. While the objective was to form methanol, they report the formation of acetic acid caused by the termination step in a radical mechanism. The selectivity or yield of acetic acid was reported, nor were the conversions of methane.

Rather than using hydrogen peroxide or oxygen, Periana et al. examined the reaction of methane with sulfuric acid catalyzed with palladium [100]. Using labeled methane and NMR analysis, they showed the formation of acetic acid with two labeled carbons. This indicates that the methane was the only carbon source. They report a 59% selectivity of acetic acid after 3 hours. Other products reported include carbon dioxide, and methanol.

These results show that acetic acid can be produced from methane and an oxidant. In these cases, methane is the only carbon source. Various intermediate species are produced, including methanol and carbon dioxide, which then react either with each other or methane to give acetic acid or other compounds. While these studies show the formation of acetic acid from methane, they all include several intermediate steps and generally have low conversions of methane and/or low selectivities of acetic acid.

As continuations of the studies of acetic acid synthesis from carbon monoxide, methane and an oxidant, several groups examined the possibility of replacing the carbon monoxide with carbon dioxide.

As a continuation of their work with carbon monoxide and methane [85-93], the Fugiwara group examined the possibility of reacting carbon dioxide with methane to produce acetic acid [87, 101]. Taniguchi et al. used a system consisting of a homogeneous catalyst and potassium peroxodisulfate ($K_2S_2O_8$) dissolved in trifluoroacetic acid (CF_3COOH) [101]. This mixture was placed in a 25 mL autoclave, which was then pressurized with carbon dioxide and methane. The mixture was heated to 80°C for 20 hours. After the reaction, the products were analyzed by GLC. Various catalysts and initial pressures of carbon dioxide and methane were tested. They reported that a VO(acetylacetonate)$_2$ catalyst performed the best, giving 97% yield of acetic acid using 5 atm methane, and 20 atm CO_2. More interestingly, they reported that the inlet pressure of carbon dioxide had no effect on the reaction. In fact, they report that the reaction occurred in the absence of carbon dioxide.

Kurioka et al. examined the reaction of methane with carbon dioxide using oxygen as an oxidant [87]. Again, a mixture of a $Pd(OAc)_2$ and a $Cu(OAc)_2$ catalysts were dissolved in

CF_3COOH. Using 40 atm of CH_4, and 20 atm of CO_2 they report an acetic acid yield of 1650% based on the palladium.

The direct synthesis of acetic acid from carbon dioxide and methane is thermodynamically limited, as discussed in detail in chapter 3. The high yields that they report are contrary to what thermodynamics predict. However, the thermodynamics for methane reacting with CF_3COOH to give acetic acid and CHF_3 is very favorable [94]. At their reaction conditions, thermodynamics predict a 98% conversion of methane to CF_3COOH.

Further work was conducted on this theory by two groups. Zerella et al. carried out the same reaction using the same system as described above [102]. By using $^{13}CO_2$ and NMR analysis, they confirmed that the majority of acetic acid produced by this system is from the reaction of methane with CF_3COOH. Only small amounts of acetic acid with a C^{13} carbon was found. Further analysis also revealed that the initial amount of CF_3COOH had greatly decreased and that large amounts of CHF_3 was formed.

Golombok et al. also looked at this system to determine the actual cause of the formation of acetic acid [103]. Using $^{13}CH_4$, or $^{13}CO_2$ and NMR analysis, they found that the carbon dioxide does not react in this system. They report that the acetic acid is formed from the methane and oxidants only.

Park et al. also examined the reaction of methane with CF_3COOH [104]. Using various vanadium catalysts dissolved in CF_3COOH, they report the formation of large amounts of CF_3COOCH_3. The addition of H_2O_2 as an oxidant was reported to regenerate the catalyst, and increase the yields of CF_3COOCH_3. While they did not test for acetic acid, this

work shows that methane is likely to react with CF_3COOH. Kitmamura et al. also reported similar results [105]. Using various vanadium catalyst, CF_3COOH and $K_2S_2O_8$ they reported high conversions, 95%, of methane to CF_3COOCH_3 and/or CH_3COOCH_3. Of several different oxidants tried, $K_2S_2O_8$ performed the best for the partial oxidation of methane.

Whether the methane reacts with the CF_3COOH or the oxidant, it is clear that it does not react to a great extent with carbon dioxide. In all cases where CF_3COOH and $K_2S_2O_8$ are used, the results of acetic acid formation from methane are questionable.

Rather than using $K_2S_2O_8$, other groups have examined the possibility of forming acetic acid from carbon dioxide and methane in the presence of other oxidants, including H_2O_2, oxygen, and starches.

As a continuation of their work with carbon monoxide, Nizova et al. examined the synthesis of acetic acid from methane, carbon dioxide and H_2O_2 as an oxidant [96]. By heating a mixture of sodium vanadate, H_2O_2, methane and carbon dioxide to 40°C for 30 hours, they reported a 2000% yield of acetic acid based on the vanadium. No acetic acid was detected in the absence of either methane or carbon dioxide. Additionally, large amounts of methanol were observed.

In addition to their work with carbon monoxide, Larkin et al. studied the reaction of methane, carbon dioxide and oxygen using a barrier discharge reactor [84]. Using an inlet flow rate of 40 mL/min of CO_2, 120 mL/min of CH_4, and 40 mL/min of O_2 they report the highest conversions with a 22% conversion of CH_4, 4% conversion of CO_2 and 77% conversion of O_2. With this same inlet flow rates, they also report a 22% selectivity of acetic acid. Several other oxygenates were formed, including methyl formate and formaldehyde.

However, from the conversions reported, it appears as though the carbon dioxide is not an important reactant. In fact, they report a 21% conversion of methane and 16% selectivity of acetic acid when no carbon dioxide was present in the system.

Zou et al. also used a dielectric barrier discharge reactor, however, they used a starch as the oxidant [106]. Using a total inlet flow rate of 90 Nml/min consisting of 35 % CH_4 and 65% CO_2, they report their highest selectivity of acetic acid to be only 7.2%. At these same conditions, the conversion of methane was reported to be about 25% and 18% for carbon dioxide. The other products observed included hydrogen, carbon monoxide, alcohols, formaldehyde and other acids.

Only three other groups have investigated the direct synthesis of acetic acid from carbon dioxide and methane without the use of an oxidant. One group used a plasma reactor, and the other two solid catalysts.

The use of plasma reactors has recently been investigated by Li et al. in hopes of overcoming the thermodynamic limitations of the direct synthesis of acetic acid from carbon dioxide and methane [107]. They used dielectric barrier discharge reactors consisting of a quartz dielectric tube, an aluminum foil high voltage electrode attached to the inner surface of the quartz tube and a stainless steel tube around the reactor to serve as the grounded electrode. Different reactors were used to examine the effect of the discharge gap, and afterglow zones. The inlet ratio of carbon dioxide and methane was also examined. For all their reactions, carbon monoxide, hydrogen and gaseous hydrocarbons were the main products. The highest conversion of methane was reported to be around 57% using an inlet methane volume fraction of 0.34. The highest selectivity of acids was less than 10% using an

inlet methane volume fraction of 0.67 and a discharge gap of 1.1 mm. By adjusting the inlet ratio of methane and carbon dioxide, they were able to vary the composition of the products. In all cases, their main products were either carbon monoxide or gaseous hydrocarbons.

A South African patent by Freund and Wambach claims a process for the direct synthesis of acetic acid from CO_2 and CH_4 using a solid catalyst [108]. The catalyst is not clearly identified. It is described as containing "one or more metals of groups VIA, VIIA, VIIIA" on one of many supports including aluminum oxide, aluminum hydroxide, and silicon dioxide. Reaction conditions between 100 – 600 °C and 0.1 – 20 MPa are claimed to give selectivities between 70 – 95% and an unspecified "sufficient conversion for commercial scale". No actual data or experimental examples are given in the patent to support the claims, nor is there an equivalent patent filed in the United States. Given the poor thermodynamics of the reaction, discussed in detail in chapter 4, it is unlikely that such high conversions can be achieved under the conditions described in the patent.

More recently, Huang et al. reported the formation of acetic acid, alcohols, formic acid and other organic compounds from carbon dioxide and methane using a solid catalyst [109]. They used copper and cobalt catalysts of varying Cu/Co ratios. The support used was not mentioned. On the idea that CH_x adsorbed species are the intermediate species in the reaction, they used a cyclic method. The catalyst was first exposed to a flow of methane, then to an inert gas to purge the system, and finally to a flow of carbon dioxide. This cycle was repeated 20 times. Liquid products were collected by an ice trap and analyzed by gas chromatography. The highest percent of acetic acid found in the products was about 28%, when no cleaning gas was used between the reaction gases. They report that 250°C was the

optimum temperature for this system, and that a Cu/Co ratio of 5 is most favorable for acetic acid production. They did not report the total amount of liquid product obtained nor any conversions.

Due to the flurry of research in acetic acid synthesis from carbon dioxide and methane, the reaction route is becoming a great interest. Two groups have examined the possible reaction route, one over a solid catalyst, and the other for a plasma reaction.

Huang et al. proposed that the reaction occurs with an intermediate CH_x adsorbed species [109]. They report that the CH_x adsorbed species can be formed either from methane or from carbon dioxide and hydrogen. They propose that the adsorbed CH_x species then reacts with carbon dioxide to give oxygenate species. Using temperature programmed surface reaction (TPSR) studies, they found a peak at 200°C when exposing a methane pretreated catalyst to either a carbon dioxide in argon mixture or a carbon dioxide, hydrogen and argon mixture. They interpret these results as indicating that the same reaction occurs between adsorbed CHx species with carbon dioxide only and with carbon dioxide and hydrogen. When hydrogen was added to the mixture, the peak intensity at 200°C was higher, interpreted as meaning that the hydrogen is beneficial to the reaction. Using infrared spectroscopy, they report seeing peaks associated with CH_x adsorbed species. They also propose that the thermodynamic limitations of the direct synthesis of acetic acid can be overcome by reacting carbon dioxide with the CH_x adsorbed species only.

Theoretical studies of the reaction route in a gas discharge reactor were recently reported by Wang et al. [110]. Using density functional theory (DFT), they examined several different reaction routes for the synthesis of acetic acid from carbon dioxide and methane.

Three main routes were examined, first one in which the carbon dioxide is reacted with an electron to give CO_2^-, the others in which carbon dioxide reacts with an electron to give either O˙ and CO or O, CO and an electron. In all routes examined, the methane was dissociated to give CH_3 and H. For the non CO route, the CO_2^- species reacts with H to give COOH-, which then in turn reacts with CH_3 to give acetic acid and an electron. The synthesis route from the CO_2^- species was found to be more thermodynamically favorable than those routes involving CO.

In addition to the studies on producing acetic acid from methane, the reaction of other hydrocarbons, both alkanes and aromatics, with carbon monoxide or carbon dioxide and an oxidant to form oxygenates has been examined by several groups [111-129]. In all cases, the systems used were similar to those discussed in the previous sections. Most notably, the Fugiwara group has reported high yields of butyric acid from propane and carbon monoxide [111, 114, 115, 118]. Using a $Co(OAc)_2$ catalyst, they report a 20% yield of butyric acid based on propane after 15 hours at 80°C [114]. This value was reported when 6 bar of propane and 40 bar of propane were introduced to the catalytic system containing $K_2S_2O_8$ and CF_3COOH. When the same catalyst, solvent and oxidant was used, but with 1 atm of propane and 30 atm of carbon monoxide, a 58% yield of butyric acid based on propane was reported after 15 hours at 70°C [111].

Using the same solvent and oxidant and a $CaCl_2$ catalyst, they report a 95% yield of butyric acid based on propane when 1 bar of propane was reacted with 30 bar of carbon monoxide for 20 hours at 80°C [115, 118]. Moreover, they also report the formation of cyclic acids from the reaction of cyclical hydrocarbons with carbon monoxide in $K_2S_2O_8$ and

CF_3COOH [113]. Using a Mg catalyst, 5 mmol of cyclohexane, and 50 atm of carbon monoxide, they report an 80% conversion of cyclohexane and a 91% yield of cyclohexanecarboxylic acid based on cyclohexane.

These studies show that systems which catalyze the formation of acetic acid from methane, should also catalyze the formation of higher carboxylic acids from higher hydrocarbons.

1.2 RESEARCH OBJECTIVES

The direct synthesis of acetic acid from carbon dioxide and methane using a heterogeneous catalyst may provide both environmental and economic benefits. The main objective of the proposed research is to gain a better understanding of the formation of the carbon-carbon bond in the direct carboxylation of methane with carbon dioxide over a solid catalyst to form acetic acid:

$$CO_2 + CH_4 \rightarrow CH_3COOH \qquad \text{(R 1-1)}$$

$\Delta G_r^0 = +71$ kJ/mol * $\qquad\qquad$ $\Delta H_r^0 = +36$ kJ/mol *

* ΔG_r^0 and ΔH_r^0 values calculated from ΔG_f^0 and ΔH_f^0 values obtained from CRC [130]

This research attempts to answer the following questions:

1) What behavior do thermodynamics predict for the direct synthesis reaction, side reactions or other similar reactions?

2) What methods may be used to overcome the poor thermodynamics of the direct synthesis reaction? What behavior does thermodynamics predict for these methods?

3) Can the acetic acid be formed from carbon dioxide and methane over solid catalysts? What catalysts are effective for the direct synthesis reaction?

4) How does temperature and inlet mole fraction of methane affect the direct synthesis reaction?

5) What characteristics make an effective catalyst for the direct synthesis reaction?

6) Can the formation of vinyl acetate from acetylene, carbon dioxide and methane drive the equilibrium of the direct synthesis reaction? How does this reaction system behave? What are possible effective catalysts?

1.3 DISSERTATION OVERVIEW

This dissertation focuses on showing the formation of an adsorbed acetate and gas phase acetic acid formed from carbon dioxide and methane over a solid catalyst. Different catalysts were tried and found to have varying effectiveness for the reaction. To better understand the differences in the catalysts and why some are more effective than others, catalyst characterizations were performed. Also, some preliminary experiments to overcome the thermodynamic limitations of the direct synthesis reaction were performed.

Chapter 2 discusses thermodynamic calculations performed on the direct synthesis reaction, the side reaction of forming methyl formate from carbon dioxide and methane, The synthesis of acetic acid from methane, carbon monoxide and oxygen, and the synthesis of propionic acid from carbon dioxide and ethane. Methods to overcome the poor thermodynamics of the direct synthesis of acetic acid from carbon dioxide and methane are also discussed in chapter 2. In chapter 3 the formation of adsorbed acetate on the surface of catalysts is demonstrated, as well as the formation of gas phase acetic acid and the dependence on the concentration of methane and carbon dioxide on the formation of acetic

acid. Catalysts characterizations to help understand the differences between the catalysts and their effectiveness on the reaction are also discussed in chapter 3. In chapter 4, preliminary experiments on methods to overcome the thermodynamic limitations of the direct synthesis reaction are shown. Suggestions for future research are given in chapter 8. The appendices include detailed tables of the thermodynamic calculations and other data not found in the previous chapters.

1.4 REFERENCES

1. Halmann, M.M.S., M., *Greenhouse Gas Carbon Dioxide Mitigation: Science and Technology*. 1999, New York: Lewis Publishers.

2. Paul, J. and C. Pradier, *Carbon Dioxide Chemisrty: Environmental Issues*. 1994, Cambridge: Royal Society of Chemistry.

3. United.Nations. *Kyoto Protocol*. in *Framework Convention on Climate Change*. 1997. Kyoto, Japan.

4. Eliasson, B.R., P.W.; Wokaun, A., *Greenhouse Gas Control Technologies*. 1999, New York: Elsevier Science Ltd.

5. Larminie, J.D., A., *Fuel Cell Systems Explained*. 2000, New York: John Wiley & Sons Ltd.

6. Riemer, P.W.F.S., A.Y.; Thambimuthu, K.V., *Greenhouse Gas Mitigation: Technologies for Activities Implemented Jointly*. 1998, New York: Elsevier.

7. Heck, R.M.F., R.J., *Catalytic Air Pollution Control: Commercial Technology*. 2002, New York: John Wiley & Sons, Inc.

8. Turner, M.O.C., B., *The Whole World's Watching: Decarbonization the Economy and Saving the World*. 2001, New York: John Wiley & Sons, Ltd.

9. Anastas, P.T.W., T.C., *Green Chemistry: Frontiers in Benign Chemical Syntheses and Processes*. 1998, New York: Oxford University Press.

10. Anastas, P.T.W., J.C., *Green Chemistry: Theory and Practice*. 1998, New York: Oxford University Press.

11. Hake, J.F.B., N.; Kleemann, M., *Strategies and Technologies for Greenhouse Gas Mitigations*. 1999, Brookfield: Ashgate Publishing Ltd.

12. Liu, C.M., R.G.; Aresta, M., *Utilization of Greenhouse Gases*. 2003, Washington, DC: American Chemical Society.

13. Halmann, M.M., *Chemical Fixation of Carbon Dioxide: Methods for Recycling CO2 into Useful Products.* 1993, Ann Arbor: CRC Press.

14. Yin, X.M., J.R., *Recent Developments in the Activation of Carbon Dioxide by Metal Complexes.* Coordination Chemistry Reviews, 1999. **181**: p. 27.

15. Xu, X.D. and J.A. Moulijn, *Mitigation of CO2 by chemical conversion: Plausible chemical reactions and promising products.* Energy & Fuels, 1996. **10**(2): p. 305-325.

16. Abraham, M.A.H., R.P., *Reaction Engineering for Pollution Prevention*. 2000, New York: Elsevier.

17. Nakicenovie, Y.K.N., W.D.; Toth, F.L., *Costs, Impacts and Benefits of CO2 Mitigation*. 1993, Laxenburg: IIASA.

18. Pena, M.A., J.P. Gomez, and J.L.G. Fierro, *New catalytic routes for syngas and hydrogen production.* Applied Catalysis a-General, 1996. **144**(1-2): p. 7-57.

19. Tsang, S.C., J.B. Claridge, and M.L.H. Green, *Recent Advances in the Conversion of Methane to Synthesis Gas.* Catalysis Today, 1995. **23**(1): p. 3-15.

20. Yan, Z., H.S. Shang, C.X. Xiao, and Y. Kou, *Catalysis in the simultaneous utilization of greenhouse gases*, in *Utilization of Greenhouse Gases*. 2003. p. 42-56.

21. Hu, Y.H. and E. Ruckenstein, *Binary MgO-based solid solution catalysts for methane conversion to syngas.* Catalysis Reviews-Science and Engineering, 2002. **44**(3): p. 423-453.

22. Kirk, R.E.O., D.F, *Encyclopedia of Chemical Technology*. 4th ed. 1997, New York: John Wiley & Sons.

23. [Anon], *Product focus - Acetic Acid.* Chemical Week, 2002. **164**(21): p. 33-33.

24. Bell, P.R., *Methane Hydrates*. 1982, Oak Ridge: Insitute for Energy Analysis.

25. Etiope, G.K., R.W., *Geologic Emissions of Methane to the Atmosphere.* Chemosphere, 2002. **49**: p. 777.

26. Wuebbles, D.J.H., K., *Atmospheric Methane and Global Change.* Earth-Science Reviews, 2002. **57**: p. 177.

27. Crabtree, R.H., *Aspects of Methane Chemistry.* Chemical Reviews, 1995. **95**(4): p. 21.

28. Crabtree, R.H., *The Organometallic Chemistry of Alkanes.* Chemical Reviews, 1985. **85**(4): p. 25.

29. Grigoryan, E.A., *Catalytic activation and functionalization of methane.* Kinetics and Catalysis, 1999. **40**(3): p. 350-363.

30. Crabtree, R.H., *Current Ideas and Future-Prospects in Metal-Catalyzed Methane Conversion.* Natural Gas Conversion Ii, 1994. **81**: p. 8.

31. Kozlov, Y.N., G.V. Nizova, and G.B. Shul'pin, *The mechanism of hydrogen peroxide-induced aerobic oxidation of alkanes in catalysis by a vanadium complex and pyrazine-2-carboxylic acid.* Russian Journal of Physical Chemistry, 2001. **75**(5): p. 770-774.

32. Fujiwara, Y. and C.G. Jia, *New developments in transition metal-catalyzed synthetic reactions via C-H bond activation.* Pure and Applied Chemistry, 2001. **73**(2): p. 319-324.

33. Ueda, W., N.F. Chen, and K. Oshihara, *Selective oxidation of C-1-C-3 alkanes over molybdenum- and vanadium-based oxide catalysts.* Kinetics and Catalysis, 1999. **40**(3): p. 401-404.

34. Bergman, R.G., *Activation of Alkanes With Organotransition Metal-Complexes.* Science, 1984. **223**(4639): p. 7.

35. Taylor, C.E., R.R. Anderson, and R.P. Noceti, *Activation of methane with organopalladium complexes.* Catalysis Today, 1997. **35**(4): p. 7.

36. Wittborn, A.M.C., M. Costas, M.R.A. Blomberg, and P.E.M. Siegbahn, *The C-H activation reaction of methane for all transition metal atoms from the three transition rows.* Journal of Chemical Physics, 1997. **107**(11): p. 11.

37. Westerberg, J. and M.R.A. Blomberg, *Methane activation by naked Rh+ atoms. A theoretical study.* Journal of Physical Chemistry a, 1998. **102**(37): p. 5.

38. Vikulov, K., G. Martra, S. Coluccia, D. Miceli, F. Arena, A. Parmaliana, and E. Paukshtis, *FTIR spectroscopic investigation of the active sites on different types of silica catalysts for methane partial oxidation to formaldehyde.* Catalysis Letters, 1996. **37**(3-4): p. 5.

39. Shen, G.C. and M. Ichikawa, *Methane hydrogenation and confirmation of CHx intermediate species on NaY encapsulated cobalt clusters and Co/SiO2 catalysts: EXAFS, FTIR, UV characterization and catalytic performances.* Journal of the Chemical Society-Faraday Transactions, 1997. **93**(6): p. 9.

40. Burch, R., D.J. Crittle, and M.J. Hayes, *C-H bond activation in hydrocarbon oxidation on heterogeneous catalysts.* Catalysis Today, 1999. **47**(1-4): p. 6.

41. Burch, R. and M.J. Hayes, *C-H bond activation in hydrocarbon oxidation on solid catalysts.* Journal of Molecular Catalysis a-Chemical, 1995. **100**(1-3): p. 13-33.

42. Sen, A., *Organometallic Approaches to Methane Activation.* Abstracts of Papers of the American Chemical Society, 1992. **203**: p. 0.

43. Sen, A., M.R. Lin, L.C. Kao, and A.C. Hutson, *C-H Activation in Aqueous-Medium - the Diverse Roles of Platinum(Ii) and Metallic Platinum in the Catalytic and Stoichiometric Oxidative Functionalization of Organic Substrates Including Alkanes.* Journal of the American Chemical Society, 1992. **114**(16): p. 8.

44. Sen, A., *Catalytic functionalization of carbon-hydrogen and carbon- carbon bonds in protic media.* Accounts of Chemical Research, 1998. **31**(9): p. 550-557.

45. Gretz, E., T.F. Oliver, and A. Sen, *Carbon-Hydrogen Bond Activation By Electrophilic Transition- Metal Compounds - Palladium(Ii)-Mediated Oxidation of Arenes and Alkanes Including Methane.* Journal of the American Chemical Society, 1987. **109**(26): p. 3.

46. Agreda, V. and J. Zoeller, *Acetic Acid and its Derivatives*. 1993, New York: Marcel Dekker.

47. [Anon], *Product Focus - Vinyl Acetate Monomer.* Chemical Week, 2003. **165**(23): p. 31-31.

48. Tomishige, K., M. Nurunnabi, K. Maruyama, and K. Kunimori, *Effect of oxygen addition to steam and dry reforming of methane on bed temperature profile over Pt and Ni catalysts.* Fuel Processing Technology, 2004. **85**(8-10): p. 1103-1120.

49. Quincoces, C.E., E.I. Basaldella, S.P. De Vargas, and M.G. Gonzalez, *Ni/gamma-Al2O3 catalyst from kaolinite for the dry reforming of methane.* Materials Letters, 2004. **58**(3-4): p. 272-275.

50. Tsyganok, A.I., T. Tsunoda, S. Hamakawa, K. Suzuki, K. Takehira, and T. Hayakawa, *Dry reforming of methane over catalysts derived from nickel-containing Mg-Al layered double hydroxides.* Journal of Catalysis, 2003. **213**(2): p. 191-203.

51. Becerra, A., M.E. Iriarte, M. Dimitrjewits, and A. Castro-Luna, *Promoting effects of rhodium on supported nickel catalysts in the dry reforming of methane.* Boletin De La Sociedad Chilena De Quimica, 2002. **47**(4): p. 385-392.

52. Courson, C., L. Udron, D. Swierczynski, C. Petit, and A. Kiennemann, *Hydrogen production from biomass gasification on nickel catalysts - Tests for dry reforming of methane.* Catalysis Today, 2002. **76**(1): p. 75-86.

53. Frusteri, F., L. Spadaro, F. Arena, and A. Chuvilin, *TEM evidence for factors affecting the genesis of carbon species on bare and K-promoted Ni/MgO catalysts during the dry reforming of methane.* Carbon, 2002. **40**(7): p. 1063-1070.

54. Yan, Z.F., R.G. Ding, X.M. Liu, and L.H. Song, *Promotion effects of nickel catalysts of dry reforming with methane.* Chinese Journal of Chemistry, 2001. **19**(8): p. 738-744.

55. Shamsi, A. and C.D. Johnson, *Carbon deposition on methane dry reforming catalysts at higher pressures.* Abstracts of Papers of the American Chemical Society, 2001. **221**: p. U501-U501.

56. Becerra, A., M. Dimitrijewits, C. Arciprete, and A.C. Luna, *Stable Ni/Al2O3 catalysts for methane dry reforming - Effects of pretreatment.* Granular Matter, 2001. **3**(1-2): p. 79-81.

57. Dimitrijewits, M.I., M.M. Guraya, C.P. Arciprete, A.C. Luna, and A. Becerra, *Catalytic behaviour Ni/(y)-Al2O3 microporous catalysts in the methane dry-reforming reaction.* Granular Matter, 2001. **3**(1-2): p. 101-104.

58. Shamsi, A. and D.K. Lyons, *Methane dry reforming over carbide, nickel-based, and noble metal catalysts.* Abstracts of Papers of the American Chemical Society, 2000. **219**: p. U250-U250.

59. Ross, J.R.H., A.N.J. van Keulen, A.M. O'Connor, and M.E.S. Hegarty, *Effect of the method preparation and pretreatment on the dispersion and catalytic behavior of finely divided Pt or Ni particles supported on zirconia for the dry reforming of*

methane. Abstracts of Papers of the American Chemical Society, 2000. **219**: p. U253-U253.

60. Provendier, H., C. Petit, C. Estournes, and A. Kiennemann, *Dry reforming of methane. Interest of La-Ni-Fe solid solutions compared to LaNiO3 and LaFeO3*, in *Natural Gas Conversion V*. 1998. p. 741-746.

61. York, A.P.E., T. Suhartanto, and M.L.H. Green, *Influence of molybdenum and tungsten dopants on nickel catalysts for the dry reforming of methane with carbon dioxide to synthesis gas*, in *Natural Gas Conversion V*. 1998. p. 777-782.

62. Nam, J.W., H. Chae, S.H. Lee, H. Jung, and K.Y. Lee, *Methane dry reforming over well-dispersed Ni catalyst prepared from perovskite-type mixed oxides*, in *Natural Gas Conversion V*. 1998. p. 843-848.

63. Gronchi, P., D. Fumagalli, R. DelRosso, and P. Centola, *Carbon deposition in methane reforming with carbon dioxide - Dry reforming.* Journal of Thermal Analysis, 1996. **47**(1): p. 227-234.

64. Maitlis, P.M., A. Haynes, G.J. Sunley, and M.J. Howard, *Methanol carbonylation revisited: Thirty years on.* Journal of the Chemical Society-Dalton Transactions, 1996(11): p. 2187-2196.

65. Yoneda, N., S. Kusano, M. Yasui, P. Pujado, and S. Wilcher, *Recent advances in processes and catalysts for the production of acetic acid.* Applied Catalysis a-General, 2001. **221**(1-2): p. 253-265.

66. Wang, Y.H., D.H. He, and B.Q. Xu, *Studies of producing acetic acid by carbonylation of methanol.* Progress in Chemistry, 2003. **15**(3): p. 215-221.

67. Dettmeier, U., E.I. Leupold, H. Poll, H.J. Schmidt, and J. Schutz, *Direct Synthesis of Acetic-Acid from Synthesis Gas.* Erdol & Kohle Erdgas Petrochemie, 1985. **38**(2): p. 59-62.

68. Maruya, K., K. Okumura, and T. Komiya, *Selective formation of acetic acid from syngas in the presence of H2O over zirconium hydroxide.* Chemistry Letters, 2001(1): p. 10-11.

69. Xu, B.Q., K.Q. Sun, Q.M. Zhu, and W.M.H. Sachtler, *Unusual selectivity of oxygenate synthesis - Formation of acetic acid from syngas over unpromoted Rh in NaY zeolite.* Catalysis Today, 2000. **63**(2-4): p. 453-460.

70. Xu, B.Q. and W.M.H. Sachtler, *Selective one step synthesis of acetic acid from syngas over Rh NaY catalyst.* Chemical Journal of Chinese Universities-Chinese, 1999. **20**(5): p. 794-796.

71. Xu, B.Q. and W.M.H. Sachtler, *Rh/NaY: A selective catalyst for direct synthesis of acetic acid from syngas.* Journal of Catalysis, 1998. **180**(2): p. 194-206.

72. Knifton, J.F., *The Selective Generation of Acetic-Acid Directly from Synthesis Gas.* Acs Symposium Series, 1987. **328**: p. 98-107.

73. Nakajo, T., K. Sano, S. Matsuhira, and H. Arakawa, *Direct Synthesis of Acetic-Acid from Synthesis Gas over Rh-Mn-Zr-Li-Sio2 Catalyst.* Chemistry Letters, 1986(9): p. 1557-1560.

74. *Acetic-Acid Made Directly from Syngas.* Chemical & Engineering News, 1986. **64**(18): p. 43-43.

75. Knifton, J.F., *The Selective Generation of Acetic-Acid Directly from Synthesis Gas.* Abstracts of Papers of the American Chemical Society, 1986. **191**: p. 92-PETR.

76. Knifton, J.F., *Syngas Reactions .9. Acetic-Acid from Synthesis Gas.* Journal of Catalysis, 1985. **96**(2): p. 439-453.

77. Lin, M. and A. Sen, *Direct Catalytic Conversion of Methane to Acetic-Acid in an Aqueous-Medium.* Nature, 1994. **368**(6472): p. 613-615.

78. Lin, M.R., T. Hogan, and A. Sen, *A highly catalytic bimetallic system for the low-temperature selective oxidation of methane and lower alkanes with dioxygen as the oxidant.* Journal of the American Chemical Society, 1997. **119**(26): p. 6048-6053.

79. Chepaikin, E.G., A.P. Bezruchenko, A.A. Leshcheva, G.N. Boyko, I.V. Kuzmenkov, E.H. Grigoryan, and A.E. Shilov, *Functionalisation of methane under dioxygen and carbon monoxide catalyzed by rhodium complexes - Oxidation and oxidative carbonylation.* Journal of Molecular Catalysis a-Chemical, 2001. **169**(1-2): p. 89-98.

80. Chepaikin, E.G., A.P. Bezruchenko, and A.A. Leshcheva, *Homogeneous rhodium-copper-halide catalytic systems for the oxidation and oxidative carbonylation of methane.* Kinetics and Catalysis, 2002. **43**(4): p. 507-513.

81. Chepaikin, E.G., G.N. Boyko, A.P. Bezruchenko, A.A. Leshcheva, and E.H. Grigoryan, *Oxidative carbonylation of methane in the presence of Rh complexes in aqueous acetic acid.* Journal of Molecular Catalysis a-Chemical, 1998. **129**(1): p. 15-18.

82. Chepaikin, E.G., A.P. Bezruchenko, A.A. Leshcheva, and E.A. Grigoryan, *New catalytic system for functionalization of methane.* Doklady Physical Chemistry, 2000. **373**(1-3): p. 105-107.

83. Chepaikin, E.G., G.N. Boiko, A.P. Bezruchenko, A.A. Leshcheva, and E.A. Grigoryan, *Oxidative carbonylation of methane in the presence of rhodium complexes.* Doklady Akademii Nauk, 1997. **353**(2): p. 217-219.

84. Larkin, D.W.C., T.A.; Lobban, L.L.; Mallinson, R.G., *Oxygen Pathways and Carbon Dioxide Utilization in Methane Partial Oxidation in Ambient Temperature Electric Discharges.* Energy & Fuels, 1998(12).

85. Nakata, K., T. Miyata, Y. Yamaoka, Y. Taniguchi, K. Takaki, and Y. Fujiwara, *Organic-Synthesis Via C-H Bond Activation of Small Alkanes Such As Methane, Ethane, and Propane,* in *Natural Gas Conversion Ii*. 1994. p. 6.

86. Fujiwara, Y., Y. Taniguchi, K. Takaki, M. Kurioka, T. Jintoku, and T. Kitamura, *Palladium-catalyzed acetic acid synthesis from methane and carbon dioxide*, in *Natural Gas Conversion Iv*, BJ22F, Editor. 1997. p. 275-278.

87. Kurioka, M., K. Nakata, T. Jintoku, Y. Taniguchi, K. Takaki, and Y. Fujiwara, *Palladium-Catalyzed Acetic-Acid Synthesis from Methane and Carbon-Monoxide or Dioxide.* Chemistry Letters, 1995(3): p. 244-244.

88. Nishiguchi, T., K. Nakata, K. Takaki, and Y. Fujiwara, *Transition-Metal Catalyzed Acetic-Acid Synthesis from Methane and Co.* Chemistry Letters, 1992(7): p. 1141-1142.

89. Nakata, K., Y. Yamaoka, T. Miyata, Y. Taniguchi, K. Takaki, and Y. Fujiwara, *Palladium(Ii) and/or Copper(Ii)-Catalyzed Carboxylation of Small Alkanes Such As Methane and Ethane With Carbon-Monoxide.* Journal of Organometallic Chemistry, 1994. **473**(1-2): p. 6.

90. Fujiwara, Y., T. Kitamura, Y. Taniguchi, T. Hayashida, and T. Jintoku, *Transition metal catalyzed acetic acid synthesis from methane and carbon monoxide,* in *Natural Gas Conversion V*. 1998. p. 349-353.

91. Asadullah, M., Y. Taniguchi, T. Kitamura, and Y. Fujiwara, *Ln(2)O(3)/K2S2O8 promoted synthesis of acetic acid from methane and carbon monoxide under mild conditions.* Sekiyu Gakkaishi-Journal of the Japan Petroleum Institute, 1998. **41**(3): p. 236-239.

92. Taniguchi, Y., T. Hayashida, H. Shibasaki, D.G. Piao, T. Kitamura, T. Yamaji, and Y. Fujiwara, *Highly efficient vanadium-catalyzed transformation of CH4 and CO to acetic acid.* Organic Letters, 1999. **1**(4): p. 557-559.

93. Asadullah, M., T. Kitamura, and Y. Fujiwara, *Calcium-catalyzed selective and quantitative transformation of CH4 and CO into acetic acid.* Angewandte Chemie-International Edition, 2000. **39**(14): p. 2475-+.

94. Wilcox, E.M.R., G.W.; SPivey, J.J., *Thermodynamics of light alkane carboxylation.* Applied Catalysis a-General, 2002. **226**.

95. Asadullah, M., Y. Taniguchi, T. Kitamura, and Y. Fujiwara, *Direct carboxylation reaction of methane with CO by a Yb(OAc)(3)/Mn(OAc)(2)/NaClO/H2O catalytic system under very mild conditions.* Applied Organometallic Chemistry, 1998. **12**(4): p. 277-284.

96. Nizova, G.V., G. Suss-Fink, S. Stanislas, and G.B. Shul'pin, *Carboxylation of methane with CO or CO2 in aqueous solution catalysed by vanadium complexes.* Chemical Communications, 1998(17): p. 1885-1886.

97. Seki, Y., J.S. Min, M. Misono, and N. Mizuno, *Reaction mechanism of oxidation of methane with hydrogen peroxide catalyzed by 11-molybdo-1-vanadophosphoric acid catalyst precursor.* Journal of Physical Chemistry B, 2000. **104**(25): p. 5940-5944.

98. Seki, Y., N. Mizuno, and M. Misono, *High-yield liquid-phase oxygenation of methane with hydrogen peroxide catalyzed by 12-molybdovanadophosphoric acid catalyst precursor.* Applied Catalysis a-General, 1997. **158**(1-2): p. L47-L51.

99. Suss-Fink, G., S. Stanislas, G.B. Shul'pin, and G.V. Nizova, *Catalytic functionalization of methane.* Applied Organometallic Chemistry, 2000. **14**(10): p. 623-628.

100. Periana, R.A., O. Mironov, D. Taube, G. Bhalla, and C.J. Jones, *Catalytic, oxidative condensation of CH4 to CH3COOH in one step via CH activation.* Science, 2003. **301**(5634): p. 814-818.

101. Taniguchi, Y., T. Hayashida, T. Kitamura, and Y. Fujiwara, *Vanadium-catalyzed acetic acid synthesis from methane and carbon dioxide,* in *Advances in Chemical Conversions for Mitigating Carbon Dioxide*. 1998. p. 439-442.

102. Zerella, M., S. Mukhopadhyay, and A.T. Bell, *Synthesis of mixed acid anhydrides from methane and carbon dioxide in acid solvents.* Organic Letters, 2003. **5**(18): p. 3193-3196.

103. Golombok, M. and W. Teunissen, *A chemical alternative to natural gas flaring.* Industrial & Engineering Chemistry Research, 2003. **42**(20): p. 5003-5006.

104. Park, E.D., Y.S. Hwang, C.W. Lee, and J.S. Lee, *Copper- and vanadium-catalyzed methane oxidation into oxygenates with in situ generated H2O2 over Pd/C.* Applied Catalysis a-General, 2003. **247**(2): p. 269-281.

105. Kitamura, T., D.G. Piao, Y. Taniguchi, and Y. Fujiwara, *Heteropolyacid-catalyzed partial oxidation of methane in trifluoroacetic acid.* Natural Gas Conversion V, 1998. **119**: p. 5.

106. Zou, J.J., Y.P. Zhang, C.J. Liu, Y. Li, and B. Eliasson, *Starch-enhanced synthesis of oxygenates from methane and carbon dioxide using dielectric-barrier discharges.* Plasma Chemistry and Plasma Processing, 2003. **23**(1): p. 69-82.

107. Li, Y., C.J. Liu, B. Eliasson, and Y. Wang, *Synthesis of oxygenates and higher hydrocarbons directly from methane and carbon dioxide using dielectric-barrier discharges: Product distribution.* Energy & Fuels, 2002. **16**(4): p. 864-870.

108. Freund, H.J. and J. Wambach, *Process for the Preparation of Acetic Acid*. 1995: Republic of South Africa.

109. Huang, W., K.C. Xie, J.P. Wang, Z.H. Gao, L.H. Yin, and Q.M. Zhu, *Possibility of direct conversion of CH4 and CO2 to high-value products.* Journal of Catalysis, 2001. **201**(1): p. 100-104.

110. Wang, J.G., C.J. Liu, Y.P. Zhang, and B. Eliasson, *A DFT study of synthesis of acetic acid from methane and carbon dioxide.* Chemical Physics Letters, 2003. **368**(3-4): p. 313-318.

111. Asadullah, M., Y. Taniguchi, T. Kitamura, and Y. Fujiwara, *Cobalt catalyzed carboxylation reaction of saturated hydrocarbons with CO in the presence of K2S2O8 and TFA under mild conditions.* Tetrahedron Letters, 1999. **40**(50): p. 8867-8871.

112. Nakata, K., T. Miyata, Y. Taniguchi, K. Takaki, and Y. Fujiwara, *Carboxylation of Gaseous Alkanes with Co Catalyzed by Pd-Cu- Based Catalysts - a Spectroscopic Study.* Journal of Organometallic Chemistry, 1995. **489**(1-2): p. 71-75.

113. Asadullah, M., T. Kitamura, and Y. Fujiwara, *Mg/K2S2O8-promoted direct carboxylation of saturated hydrocarbons with CO.* Applied Organometallic Chemistry, 1999. **13**(7): p. 539-547.

114. Asadullah, M., Y. Taniguchi, T. Kitamura, and Y. Fujiwara, *One-step carboxylation reaction of saturated hydrocarbons with CO by Co(OAc)(2) catalyst under mild conditions.* Applied Catalysis a-General, 2000. **194**: p. 443-452.

115. Asadullah, M., T. Kitamura, and Y. Fujiwara, *CaCl2-catalyzed functionalization of saturated hydrocarbons with CO to carboxylic acids and esters.* Journal of Catalysis, 2000. **195**(1): p. 180-186.

116. Shen, C.Y., E.A. Garcia-Zayas, and A. Sen, *A bimetallic system for the catalytic hydroxylation of remote primary C-H bonds in functionalized organics using dioxygen.* Journal of the American Chemical Society, 2000. **122**(17): p. 4029-4031.

117. Nakata, K., T. Miyata, T. Jintoku, A. Kitani, Y. Taniguchi, K. Takaki, and Y. Fujiwara, *Palladium and Copper-Catalyzed Carboxylation of Alkanes with Carbon-Monoxide - Remarkable Effect of the Mixed-Metal Salts.* Bulletin of the Chemical Society of Japan, 1993. **66**(12): p. 3755-3759.

118. Asadullah, M., T. Kitamura, and Y. Fujiwara, *Transformation of propane and CO to carboxylic acid and ester by highly active CaCl2 catalyst.* Catalysis Letters, 2000. **69**(1-2): p. 37-41.

119. Fujiwara, Y., T. Jintoku, and K. Takaki, *Look What Pd Catalyzes.* Chemtech, 1990. **20**(10): p. 5.

120. Fujiwara, Y., I. Kawata, H. Sugimoto, and H. Taniguchi, *Palladium-Catalyzed One-Step Synthesis of Aromatic-Acids From Aromatic-Compounds With Carbon-Monoxide.* Journal of Organometallic Chemistry, 1983. **256**(2): p. 2.

121. Fujiwara, Y., K. Takaki, and Y. Taniguchi, *Exploitation of synthetic reactions via C-H bond activation by transition metal catalysts. Carboxylation and aminomethylation of alkanes or arenes.* Synlett, 1996(7): p. 591-&.

122. Suss-Fink, G., L. Gonzalez, and G.B. Shul'pin, *Alkane oxidation with hydrogen peroxide catalyzed homogeneously by vanadium-containing polyphosphomolybdates.* Applied Catalysis a-General, 2001. **217**(1-2): p. 111-117.

123. Suss-Fink, G., S. Stanislas, G.B. Shul'pin, G.V. Nizova, H. Stoeckli-Evans, A. Neels, C. Bobillier, and S. Claude, *Oxidative functionalisation of alkanes: synthesis, molecular structure and catalytic implications of anionic vanadium(v) oxo and peroxo complexes containing bidentate N,O ligands.* Journal of the Chemical Society-Dalton Transactions, 1999(18): p. 3169-3175.

124. Jintoku, T., Y. Fujiwara, I. Kawata, T. Kawauchi, and H. Taniguchi, *Palladium-Catalyzed Synthesis of Aromatic-Acids From Carbon- Monoxide and Aromatic-*

Compounds Via the Aromatic C-H Bond Activation. Journal of Organometallic Chemistry, 1990. **385**(2): p. 10.

125. Taniguchi, Y., Y. Yamaoka, K. Nakata, K. Takaki, and Y. Fujiwara, *Palladium(Ii) Catalyzed Carboxylation of Aromatic-Compounds With Co Under Very Mild Conditions.* Chemistry Letters, 1995(5): p. 2.

126. Lu, W.J., Y. Yamaoka, Y. Taniguchi, T. Kitamura, K. Takaki, and Y. Fujiwara, *Palladium(II)-catalyzed carboxylation of benzene and other aromatic compounds with carbon monoxide under very mild conditions.* Journal of Organometallic Chemistry, 1999. **580**(2): p. 5.

127. Sugimoto, H., I. Kawata, H. Taniguchi, and Y. Fujiwara, *Palladium-Catalyzed Carboxylation of Aromatic-Compounds With Carbon-Dioxide.* Journal of Organometallic Chemistry, 1984. **266**(3): p. 3.

128. Tang, H., C.Y. Shen, M.R. Lin, and Y. Sen, *Cobalt porphyrin-catalyzed alkane oxidations using dioxygen as oxidant.* Inorganica Chimica Acta, 2000. **300**: p. 1109-1111.

129. Lin, M.R., T.E. Hogan, and A. Sen, *Catalytic carbon-carbon and carbon-hydrogen bond cleavage in lower alkanes. Low-temperature hydroxylations and hydroxycarbonylations with dioxygen as the oxidant.* Journal of the American Chemical Society, 1996. **118**(19): p. 4574-4580.

130. Chemical.Rubber.Company, *CRC Handbook of Chemistry and Physics*. 83 ed. 2002, Cleveland: Chemical Rubber Company Press.

CHAPTER 2:

THERMODYNAMIC ANALYSIS OF REACTIONS

2.1 INTRODUCTION

Equilibrium thermodynamic calculations were performed on the direct synthesis of acetic acid from methane and carbon dioxide to understand the potential behavior of the reaction between carbon dioxide and methane and to determine the feasibility of the reaction in the laboratory. Equilibrium thermodynamic calculations were also performed on the synthesis of methyl formate from carbon dioxide and methane to determine if this side reaction could cause any significant interference with the direct synthesis reaction. Thermodynamic calculations were performed on the synthesis of acetic acid from carbon monoxide, oxygen and methane to compare this reaction with that of carbon dioxide and methane, and to compare theoretical values with those claimed in the literature. Calculations were performed on the synthesis of propionic acid from carbon dioxide and ethane to determine the feasibility of this reaction and to compare it to the synthesis of acetic acid.

For the direct synthesis reaction to be industrially useful, methods to overcome the thermodynamic limitation must be devised. In order to drive the equilibrium, the acetic acid must be removed from the system. This can be accomplished by removing it physically or chemically. Chemical removal involves coupling the direct synthesis reaction with a second reaction in which acetic acid is consumed. The second reaction should be thermodynamically and it should produce a useful chemical.

Possible methods to drive the equilibrium were examined. Chemical methods include the formation of methyl acetate from methanol, the formation of acetic anhydride from

ketene, the formation of vinyl acetate from ethylene and oxygen and the formation of vinyl acetate from acetylene. A cyclic adsorption/desorption of acetic acid from the chemical surface, a physically method, was also examined.

The Gibbs free energy change on reaction at 298.15 K (ΔG_r^0) for each reaction was calculated by:

$$\Delta G_r^0 = \sum_i n_i \Delta G_{fi}^0 \qquad \text{(E 2-1)}$$

where ΔG_{fi}^0 is the molar Gibbs free energy of formation of species i, and ν_i the stoichiometric coefficient of species i [1]. By convention, the stoichiometric coefficients of products are taken to be positive, and the stoichiometric coefficients of reactants are negative. The enthalpy change on reaction at 298.15 K (ΔH_r^0) for each reaction was calculated by:

$$\Delta H_r^0 = \sum_i n_i \Delta H_{fi}^0 \qquad \text{(E 2-2)}$$

where ΔH_{fi}^0 is the molar heat of formation of species i [1]. The Gibbs free energy and heat of formation at 298.15 K for each chemical was obtained from the CRC handbook of chemistry and physics [2]. The ΔG_r^0 and ΔH_r^0 values are for the gas phase reaction only.

When the Gibbs free energy change on reaction (ΔG_r) is negative, the reaction is spontaneous. However, then ΔG_r is positive, the reaction is thermodynamically limited. The equilibrium constant can be used to determine the extent to which the reaction occurs. This is defined by:

$$\Delta G_r(T) = -RT \ln[K_a(T)] \qquad \text{(E 2-3)}$$

where R is the gas constant, and $K_p(T)$ is the equilibrium constant at temperature T.

The enthalpy change on reaction (ΔH_r^0) indicates whether the reaction is exothermic or endothermic. For exothermic reactions ΔH_r^0 is negative, and for endothermic it is positive. Endothermic reactions become more thermodynamically favorable at higher temperatures, and exothermic reaction at lower. This can be seen by:

$$\ln \frac{K_a(T_2)}{K_a(T_1)} = -\frac{\Delta H_r^0}{R}\left(\frac{1}{T_2} - \frac{1}{T_1}\right) \qquad \text{(E 2-4)}$$

To obtain specific equilibrium conversion values, the equilibrium thermodynamic calculations were performed using AspenPlus™ simulation software. The RGIBBS reactor in AspenPlus™ was used to perform a Gibbs free energy minimization which determined the equilibrium phase and chemical compositions. Molecular interactions were taken into account in the equation of state. The calculations were performed for a wide range of temperatures, 300 – 2000 K, and pressures, 1 – 200 atm (up to 1000 atm for the direct synthesis reaction). An inlet total mole flow of 1 mole/hr was used for all calculations. Unless otherwise noted, no restrictions were placed on the chemical systems.

The thermodynamic calculations were performed using the Peng-Robinson equation of state:

$$p = \frac{RT}{V_m - b} - \frac{a}{V_m(V_m + b) + b(V_m - b)} \quad \text{(E 2-5)}$$

where p is the pressure, R the ideal gas constant, T the temperature, Vm the molar volume and:

$$a = \sum_i \sum_j x_i x_j \left(a_i a_j\right)^{0.5} \left(1 - k_{aij}\right) \quad \text{(E 2-6)}$$

$$a_i = 0.45724 \frac{\left(RT_c\right)^2}{P_c} \left[1 + \left(0.37464 + 1.54226w - 0.26992w^2\right)\left(1 - \sqrt{T/T_c}\right)\right]^2 \quad \text{(E 2-7)}$$

$$b = \sum_i x_i b_i \quad \text{(E 2-8)}$$

$$b_i = 0.07780 \frac{RT_c}{P_c} \quad \text{(E 2-9)}$$

$$k_{ij} = k_{ji} \quad \text{(E 2-10)}$$

where T_{ci} is the critical temperature, p_{ci} the critical pressure and k_{ij} the interaction parameter[3, 4].

The interaction parameters were obtained from the AspenPlus ™ database. When no interaction parameter was available the default of 0.0 was used. The following interaction parameters were used: 0.0919 for CO_2 and CH_4, 0.3000 for CO and CH_4, 0.1322 for CO_2 and C_2H_6, 0.2300 for CO2 and CH_3OH, -0.0493 for CO_2 and CH_3COOCH_3, 0.1200 for CO_2 and H_2O, -0.0778 for H_2O and CH_3OH, 0.552 for CO_2 and C_2H_2, and 0.0215 for CH_4 and C_2H_4.

The equilibrium fractional conversion of reactant A (XA) was calculated using:

$$XA = \#\ \text{Moles of A reacted} / \#\ \text{Inlet moles of A} \qquad \text{(E 2 -11)}$$

When the outlet moles of A given by AspenPlus™ did not have enough significant figures, the number of outlet moles of the desired product times the stoichiometric ratio of the product and A was used as the number of moles of A that reacted.

The equilibrium yield of product B (Y B) was calculated using:

$$Y\,B = \text{Outlet moles of B} / \text{total outlet moles of products} \qquad \text{(E 2 -12)}$$

2.2 ACETIC ACID FROM CO_2 AND CH_4

Thermodynamic calculations were performed on the direct synthesis of acetic acid from carbon dioxide and methane:

$$CO_2 + CH_4 \leftrightarrow CH_3COOH \qquad \text{(R 2-1)}$$

$\Delta G_r^0 = +\ 71$ kJ/mol $\qquad\qquad$ $\Delta H_r^0 = +\ 36$ kJ/mol

An inlet mole fraction of 0.95 of carbon dioxide and 0.05 of methane was chosen to help maximize the equilibrium fractional conversion of methane.

As expected, the fractional conversion of methane increases with increasing temperature and with increasing pressure, figures 2-1 and 2-2. At pressures above 25 atm and temperatures below 700 K, the system was found to be a "liquid" phase, whereas at all other temperatures and pressures it was a gas. AspenPlus™ cannot distinguish between a liquid phase and a supercritical phase. The critical point of carbon dioxide is 304 K and

72.8 atm [2]. Given that carbon dioxide is the major component it is likely that the system is a supercritical fluid, rather than a liquid.

The highest fractional conversion of methane was only 1.292 x 10^{-4} at 2000 K and 1000 atm. This reaction is thermodynamically limited at all conditions of practical interest.

Detailed tables of the data obtained can be found in Appendix A.2.3.

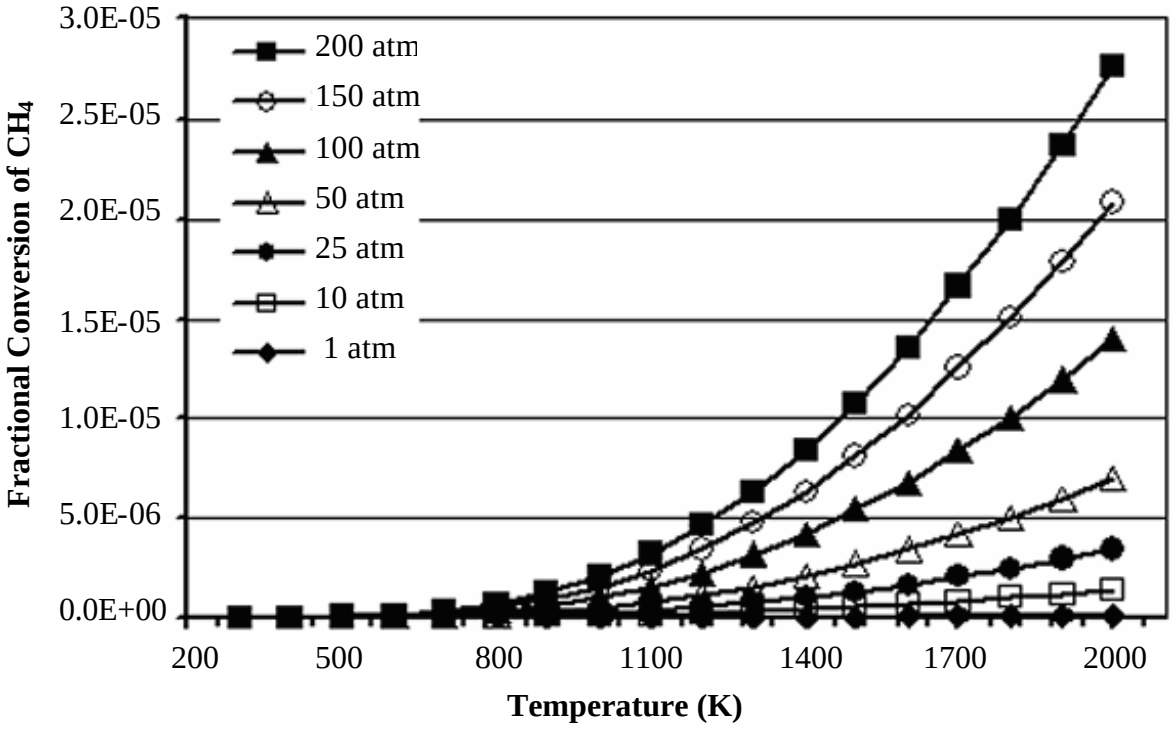

Figure 2-1: Equilibrium fractional conversion of methane for reaction R 2-1 at 1 - 200 atm and 300 – 1000 K obtained from AspenPlus ™ using the Peng-Robinson equation of state and 0.95 inlet mole fraction of carbon dioxide.

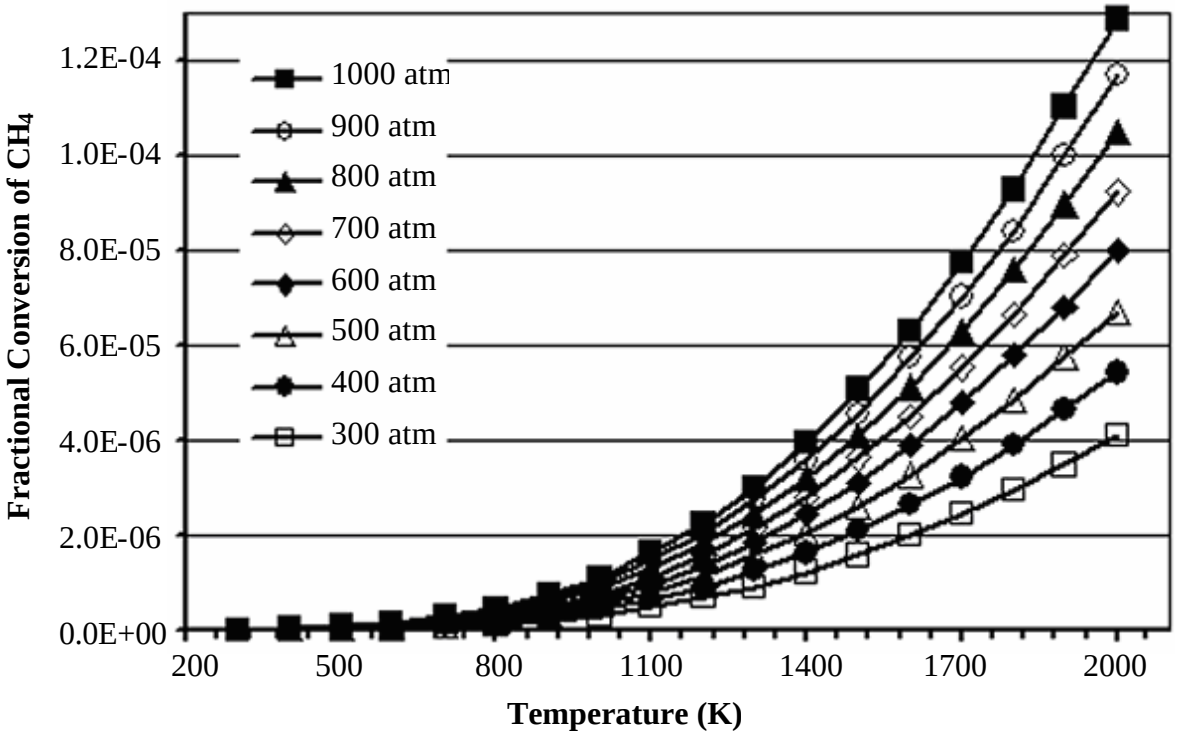

Figure 2-2: Equilibrium fractional conversion of methane for reaction R 2-1 at 300 - 1000 atm and 300 – 1000 K obtained from AspenPlus ™ using the Peng-Robinson equation of state and 0.95 inlet mole fraction of carbon dioxide.

2.3 METHYL FORMATE

A possible side reaction is the formation of methyl formate rather than acetic acid from carbon dioxide and methane:

$$CO_2 + CH_4 \leftrightarrow HCOOCH_3 \qquad \text{(R 2-2)}$$

$\Delta G_r^0 = +145$ kJ/mol $\qquad\qquad$ $\Delta H_r^0 = +111$ kJ/mol

In order to compare the results from these calculations to those from the direct synthesis of acetic acid reaction, an inlet composition of 0.95 mole CO_2 and 0.05 mole CH_4 was used.

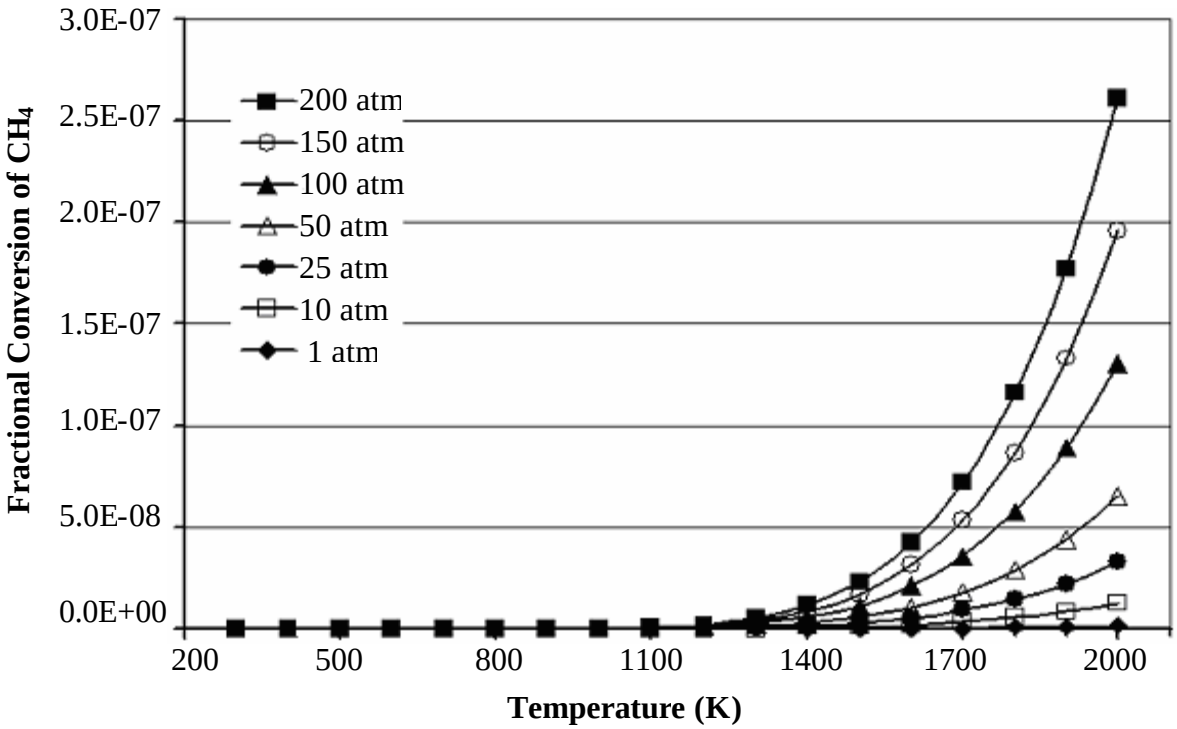

Figure 2-3: Equilibrium fractional conversion of methane for reaction R 2-2 at varying temperatures and pressures obtained from Aspen using the Peng-Robinson equation of state.

The fractional conversion of methane increases with increasing temperature and increasing pressure, figure 2-3. The fractional conversions of methane in this reaction are on the order of 100 times lower than those of the direct synthesis of acetic acid. It is unlikely that this side reaction will cause problems with the direct synthesis reaction. It is possible for this side reaction to occur. Therefore the products of the reaction of carbon dioxide and methane were analyzed for methyl formate. Detailed tables of the data obtained can be found in Appendix A.3.

2.4 ACETIC ACID FROM CO, O_2 AND CH_4

Some of the current research on the synthesis of acetic acid from methane is based on reaction (R 2-3) [5-9]. In order to better understand the results reported in the literature, the equilibrium thermodynamics were examined for this reaction:

$$CO + \tfrac{1}{2} O_2 + CH_4 \leftrightarrow CH_3COOH \qquad \text{(R 2-3)}$$

$\Delta G_r^0 = -187$ kJ/mol $\qquad\qquad$ $\Delta H_r^0 = -247$ kJ/mol

A stoichiometric inlet composition of the reactants was used; 0.4 mole CO, 0.2 mole O_2 and 0.4 mole CH_4.

Only carbon monoxide, oxygen, methane and acetic acid were allowed in the system, thus these calculations neglect the complete combustion of methane:

$$2\ O_2 + CH_4 \leftrightarrow CO_2 + 2\ H_2O \qquad \text{(R 2-4)}$$

$\Delta G_r^0 = -802$ kJ/mol $\qquad\qquad$ $\Delta H_r^0 = -803$ kJ/mol

the partial combustion of methane to hydrogen:

$$\tfrac{1}{2}\ O_2 + CH_4 \leftrightarrow CO + 2\ H_2 \qquad \text{(R 2-5)}$$

$\Delta G_r^0 = -87$ kJ/mol $\qquad\qquad$ $\Delta H_r^0 = -36$ kJ/mol

the partial combustion of methane to water:

$$3/2\ O_2 + CH_4 \leftrightarrow CO + 2\ H_2O \qquad \text{(R 2-6)}$$

$\Delta G_r^0 = -544$ kJ/mol $\qquad\qquad$ $\Delta H_r^0 = -520$ kJ/mol

and the oxidation of carbon monoxide to form carbon dioxide:

$$CO + \tfrac{1}{2}\ O_2 \leftrightarrow CO_2 \qquad \text{(R 2-7)}$$

$\Delta G_r^0 = -257$ kJ/mol $\qquad\qquad$ $\Delta H_r^0 = -283$ kJ/mol

The reaction can go to completion at 500 K and below for all pressures examined, figure 2-4. The fractional conversion of methane increases with increasing pressure, but decreases with increasing temperature. Given the thermodynamic calculations, the high yields of acetic acid reported in the literature are obtainable [5-9]. However, it is likely that side reactions would occur, thus in order for this reaction system to work efficiently, a highly selective catalyst must be used. Detailed tables of the data obtained can be found in Appendix A.4.

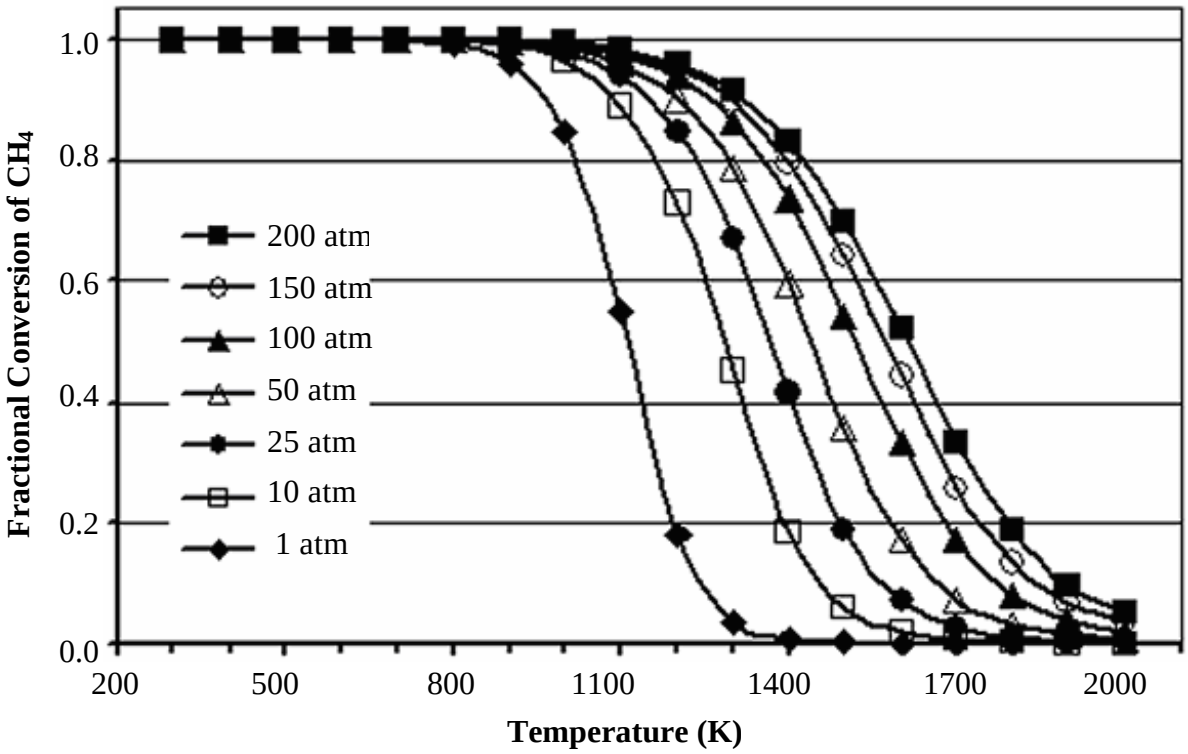

Figure 2-4: Equilibrium fractional conversion of methane for reaction R 2-3 at 1 - 200 atm and 300 – 1000 K obtained from AspenPlus ™ using the Peng-Robinson equation of state and a stoichiometric inlet composition.

2.5 PROPIONIC ACID

If the formation of acetic acid is achieved from methane and carbon dioxide, the same system might be used to synthesize higher acids from higher alkanes. The equilibrium thermodynamics were examined for the formation of propionic acid from carbon dioxide and ethane:

$$CO_2 + C_2H_6 \leftrightarrow C_2H_5COOH \qquad \text{(R 2-8)}$$

$\Delta G_r^0 = +42$ kJ/mol $\qquad\qquad$ $\Delta H_r^0 = -33$ kJ/mol

In order to compare the results from these calculations to those performed on the direct synthesis of acetic acid, an inlet composition of 0.95 mole CO_2 and 0.05 mole C_2H_4 was used.

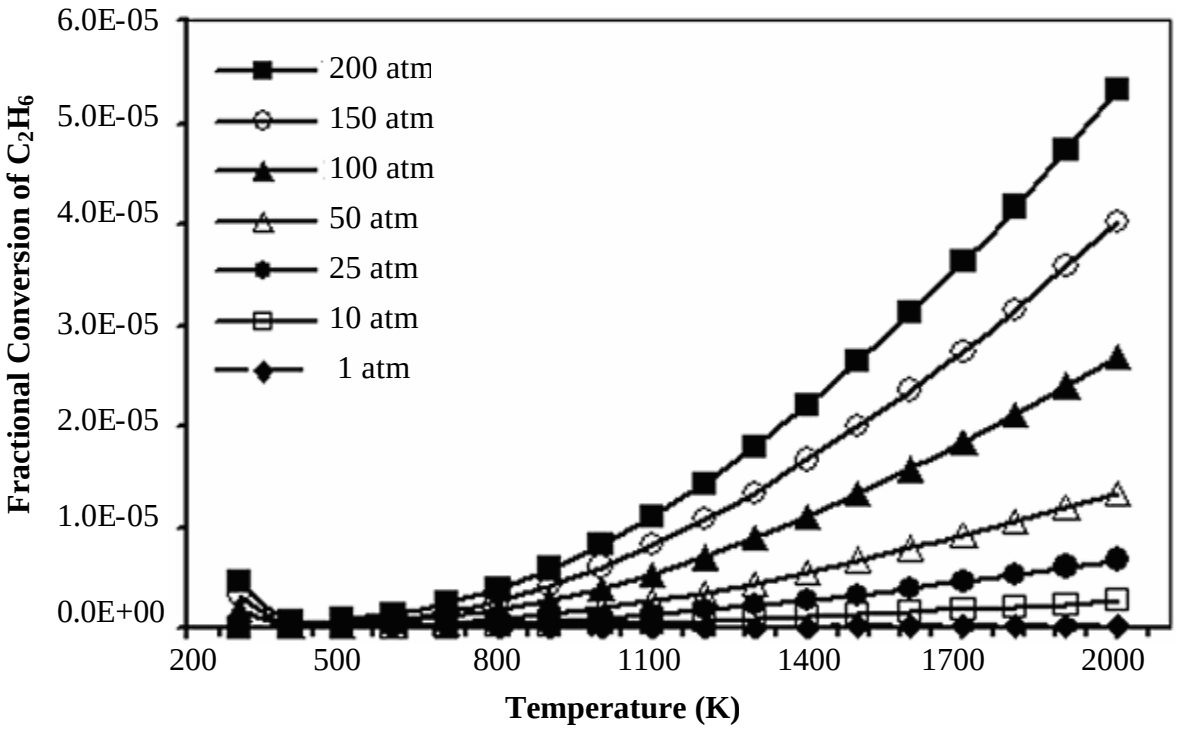

Figure 2-5: Equilibrium fractional conversion of ethane for reaction R 2-8 at varying temperatures and pressures obtained from Aspen using the Peng-Robinson equation of state.

The fractional conversion of ethane increases with increasing temperature and pressure, figure 2-5. While the maximum fractional conversion of ethane was only 5.328×10^{-5} at 2000 K and 200 atm, the fractional conversions of ethane are approximately twice that of the conversions of methane in the acetic acid reaction. The thermodynamics for the synthesis of propionic acid from carbon dioxide and ethane, while still limited, are better than that of the acetic acid synthesis from carbon dioxide and methane.

2.6 METHYL ACETATE

Due to its fast evaporation rate, methyl acetate is commonly used in fast drying paints, coatings and adhesives [10, 11]. It is also used in inks, electronic cleaners, battery electrolytes and as a process solvent for pharmaceuticals, agricultural chemicals and other organic syntheses[10]. Methyl acetate is produced industrially by the acid-catalyzed esterification of acetic acid with methanol [10].

To drive the equilibrium of the direct synthesis reaction (R 4 -1), the formation of methyl acetate (CH_3COOCH_3) from methanol was examined. First, acetic acid is formed from the direct synthesis reaction, (R 2-1). The acetic acid is then reacted with methanol (CH_3OH) to form methyl acetate and water:

$$CH_3OH + CH_3COOH \rightarrow CH_3COOCH_3 + H_2O \qquad \text{(R 2 -9)}$$

$\Delta G_r^0 = -18$ kJ/mol $\qquad\qquad$ $\Delta H_r^0 = -21$ kJ/mol

This gives the overall reaction:

$$CO_2 + CH_4 + CH_3OH \rightarrow CH_3COOCH_3 + H_2O \qquad \text{(R 2 -10)}$$

$\Delta G_r^0 = +53$ kJ/mol $\qquad\qquad$ $\Delta H_r^0 = +15$ kJ/mol

Equilibrium thermodynamic calculations were performed on this system.

The side reaction of methanol decomposition:

$$4\ CH_3OH \rightarrow CO_2 + 3\ CH_4 + 2\ H_2O \qquad \text{(R 2 -11)}$$

$\Delta G_r^0 = -354$ kJ/mol $\qquad\qquad$ $\Delta H_r^0 = -397$ kJ/mol

was restricted by setting the extent of that reaction to zero. A stoichiometric inlet composition of 0.333 mole fraction CO_2, 0.333 mole fraction CH_4 and 0.333 mole fraction

CH_3OH was used. While no acetic acid occurs in the overall reaction (R 2 -10), acetic acid was allowed in the system, thus permitting reactions (R 2 -1) and (R 2 -9).

The equilibrium fractional conversion of methane increases with increasing pressure. The equilibrium fractional conversion of methane decreases with increasing temperature until it reaches a minimum around 400 or 500 K, after which it increases with increasing temperature, figure 2-6. The higher conversions at the lower temperatures are due to the presence of a liquid phase. At 300 K and all pressures, and 400 K at 50 atm and above, both a liquid and vapor phase were present. The equilibrium fractional conversion of methanol is qualitatively the same as the methane. The equilibrium fractional yield of methyl acetate is greater than 0.990 at all conditions, figure 2 -7. As the temperature and pressure increases, the acetic acid reaction becomes increasingly favorable, thus the equilibrium fractional yield of methyl acetate decreases with increasing temperature and decreases with increasing pressure, figure 2 -8.

While this system is more thermodynamically favorable than the direct synthesis reaction, the thermodynamics are still limited. At the best conditions, 200 atm and 300 K, the equilibrium fractional conversions of methane and methanol were only 1.8106×10^{-3}, and the equilibrium fractional yield of methyl acetate was greater than 0.9999. Detailed tables of the data can be found in Appendix B.1.

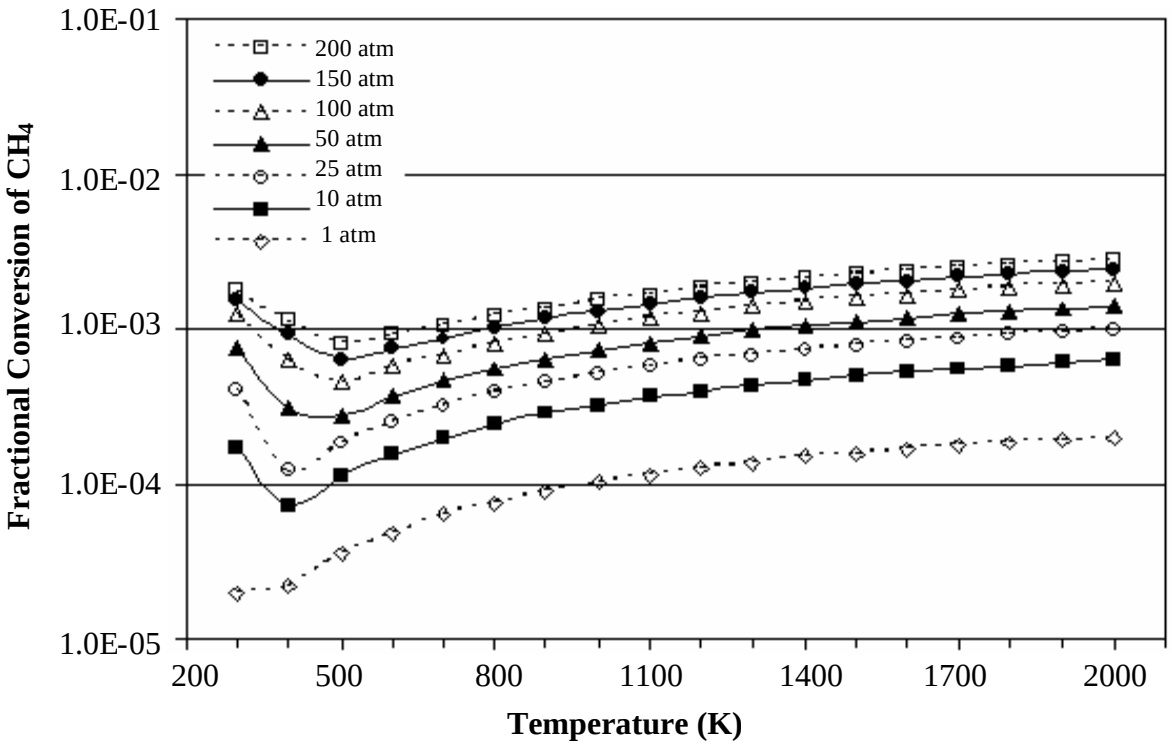

Figure 2 -6: Equilibrium fractional conversion of methane for reaction (R 2 -10) from 300 - 2000K and 1 -200 atm obtain from AspenPlus™ using a stoichiometric inlet and Peng -Robinson equation of state.

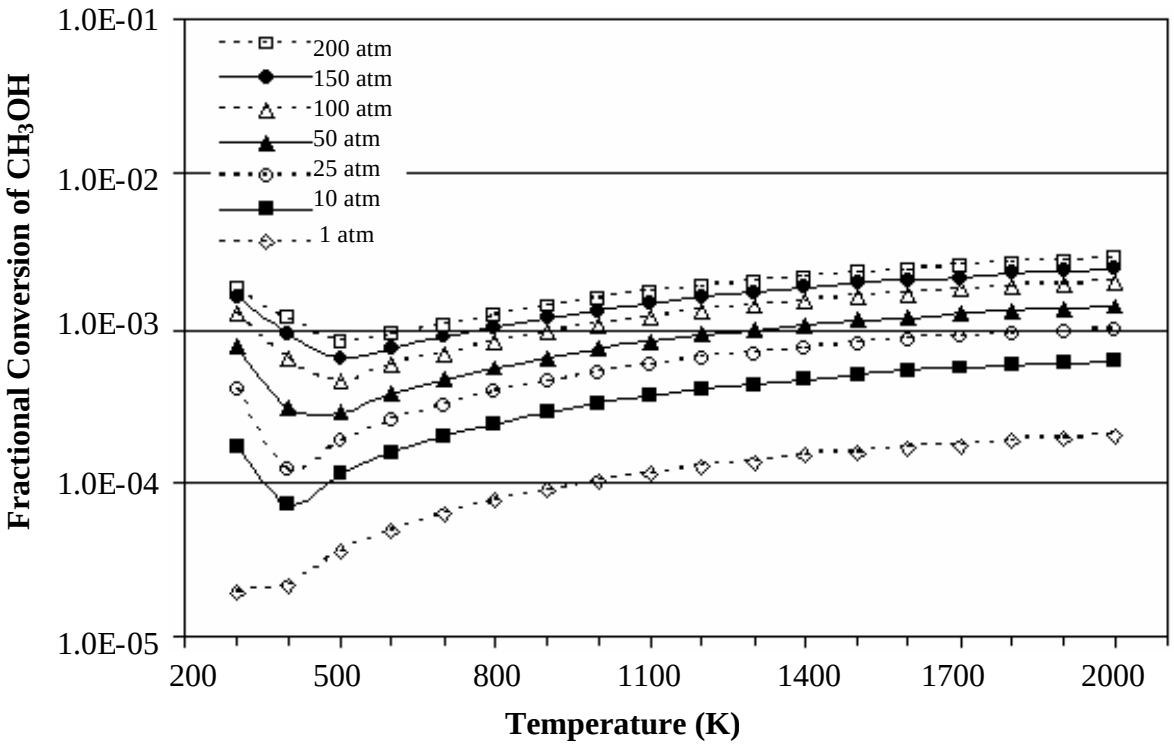

Figure 2-7: Equilibrium fractional conversion of methanol for reaction (R 2 -10) from 300 - 2000K and 1 -200 atm obtain from AspenPlus™ using a stoichiometric inlet and Peng -Robinson equation of state.

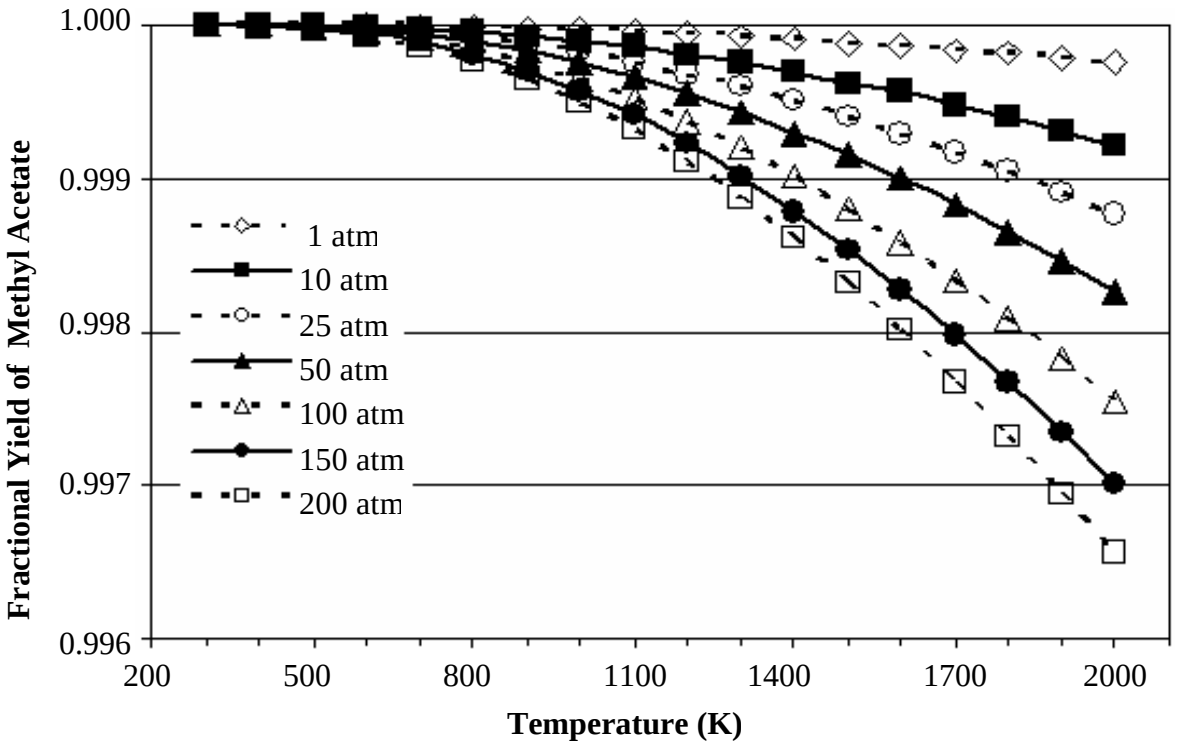

Figure 2 -8: Equilibrium fractional yield of methyl acetate for reaction (R 2 -10) from 300 - 2000K and 1 -200 atm obtain from AspenPlus™ using a stoichiometric inlet and Peng -Robinson equation of state.

2.7 ACETIC ANHYDRIDE

Acetic anhydride is used in the synthesis of cellulose acetate and acetylsalicylic acid [10, 11]. Acetic anhydride can be made from the dehydration of acetic acid, the carbonylation of methyl acetate or the reaction of ketene with acetic acid [10-13]. Approximately 1.3 million metric tons of acetic anhydride was produced in 2001 using 19% of the acetic acid produced [14].

The formation of acetic anhydride ($(CH_3CO)_2O$) was examined as a means to drive the equilibrium of the direct synthesis reaction (R 2 -1). First, acetic acid is formed from the direct synthesis reaction, (R 2-1). The acetic acid is then reacted with ketene (CH_2CO) to form acetic anhydride:

$$CH_3COOH + CH_2CO \rightarrow (CH_3CO)_2O \qquad \text{(R 2 -12)}$$

$\Delta G_r^0 = -51$ kJ/mol $\qquad\qquad$ $\Delta H_r^0 = -93$ kJ/mol

This gives the overall reaction:

$$CO_2 + CH_4 + CH_2CO \rightarrow (CH_3CO)_2O \qquad \text{(R 2 -13)}$$

$\Delta G_r^0 = +20$ kJ/mol $\qquad\qquad$ $\Delta H_r^0 = -57$ kJ/mol

Equilibrium thermodynamic calculations were performed on this system. The dehydration of acetic acid to acetic anhydride:

$$2\ CH_3COOH \rightarrow (CH_3CO)_2O + H_2O \qquad \text{(R 2 -14)}$$

$\Delta G_r^0 = +47$ kJ/mol $\qquad\qquad$ $\Delta H_r^0 = +50$ kJ/mol

was restricted, because no water was allowed in the system.

A stoichiometric inlet composition of 0.333 mole fraction of CO_2, 0.333 mole fraction of CH_4 and 0.333 mole fraction of CH_2CO was used. While no acetic acid occurs in the overall reaction (R 2 -13), acetic acid was allowed in the system, thus permitting reactions (R 2 -1) and (R 2 -12).

The equilibrium fractional conversion of methane increases with increasing pressure. The equilibrium fractional conversion of methane decreases with increasing temperature until it reaches a minimum around 600 or 700 K, and then it increases with increasing

temperature, figure 2 -9. This is due to a decreasing amount of methane being converted to acetic anhydride and an increasing amount being converted to acetic acid. The equilibrium fractional conversion of ketene increases with increasing pressure and decreases with increasing temperature, figure 2 -10. The equilibrium fractional yield of acetic anhydride is nearly unity below 600 K at all pressures, figure 2 -11. It decreases with increasing temperature and increases with increasing pressure. At lower temperatures, the formation of acetic anhydride is more favorable than the formation of acetic acid, however as the temperature increases, the acetic acid reaction becomes increasingly favorable.

At 300 K and 25 atm and above the system was a liquid, whereas it was a vapor at all other temperatures and pressures. The equilibrium fractional conversion of ketene was much greater when the system was a liquid, than when it was a vapor. At reasonable temperatures and pressures, 300 K and 25 atm, the equilibrium fractional conversion of methane and ketene is 0.947 and the equilibrium fractional yield of acetic anhydride is 1.0.

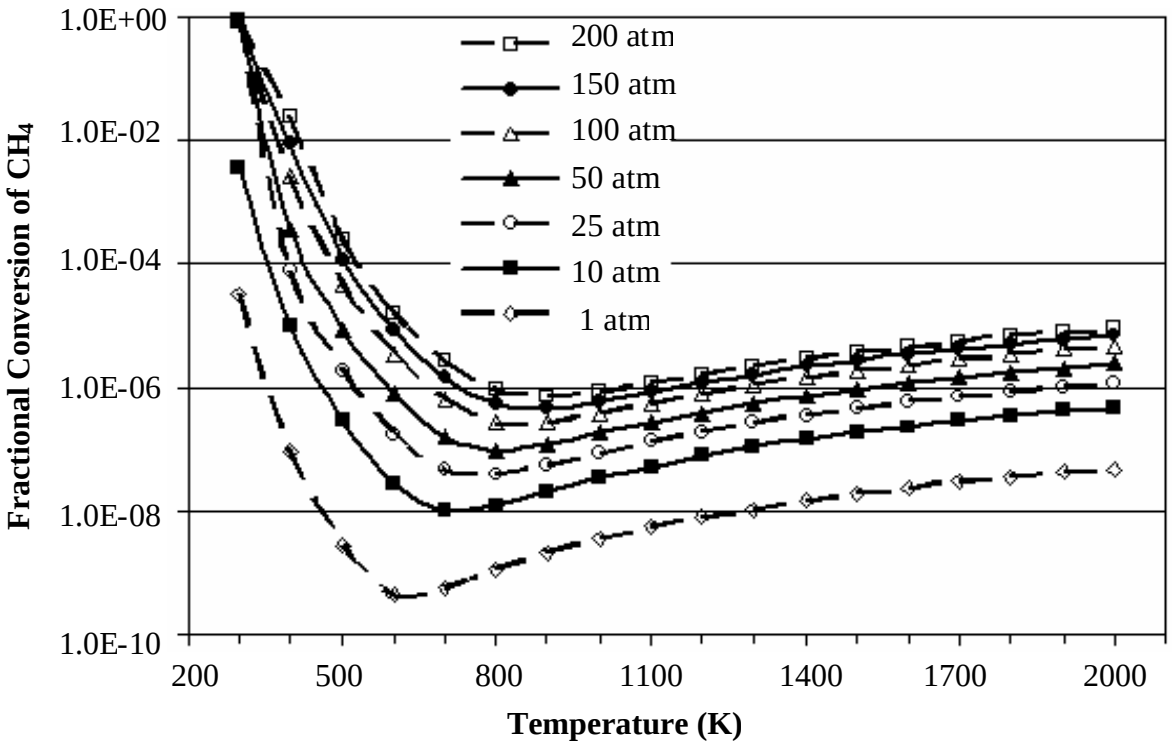

Figure 2 -9: Equilibrium fractional conversion of methane for reaction (R 2 -12) from 300 - 2000K and 1 -200 atm obtain from AspenPlus™ using a stoichiometric inlet and Peng -Robinson equation of state.

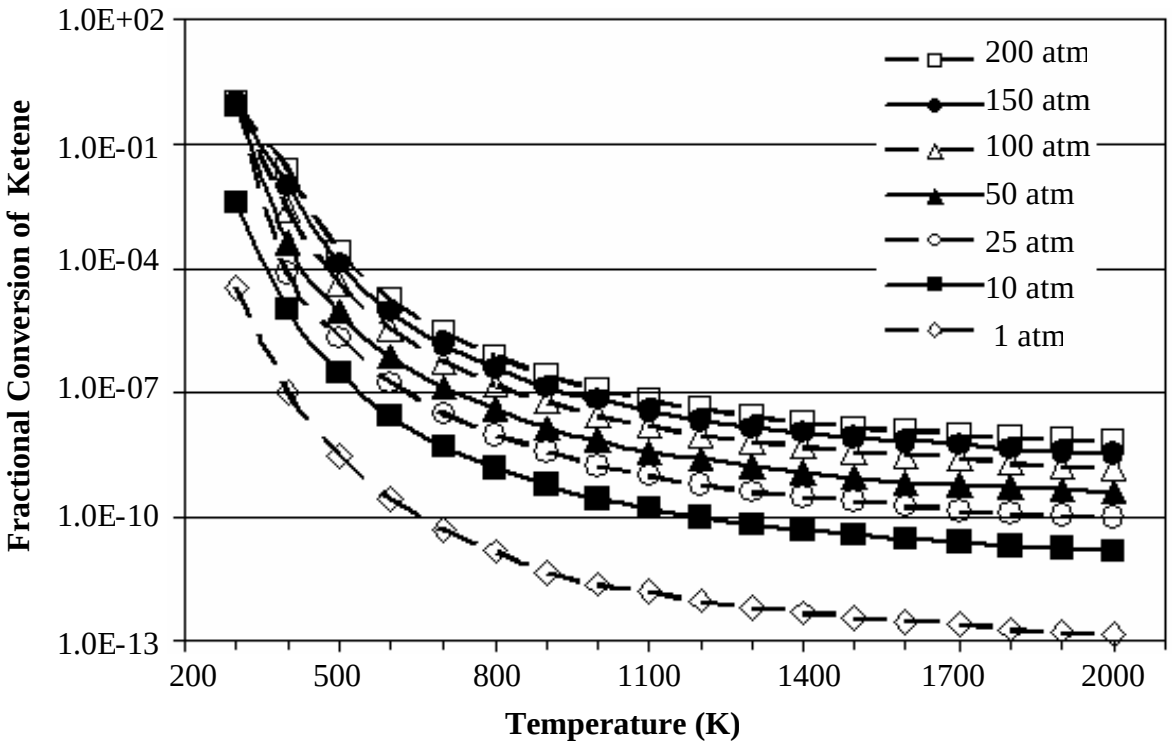

Figure 2 -10: Equilibrium fractional conversion of ketene for reaction (R 2 -12) from 300 - 2000K and 1 -200 atm obtain from AspenPlus™ using a stoichiometric inlet and Peng -Robinson equation of state.

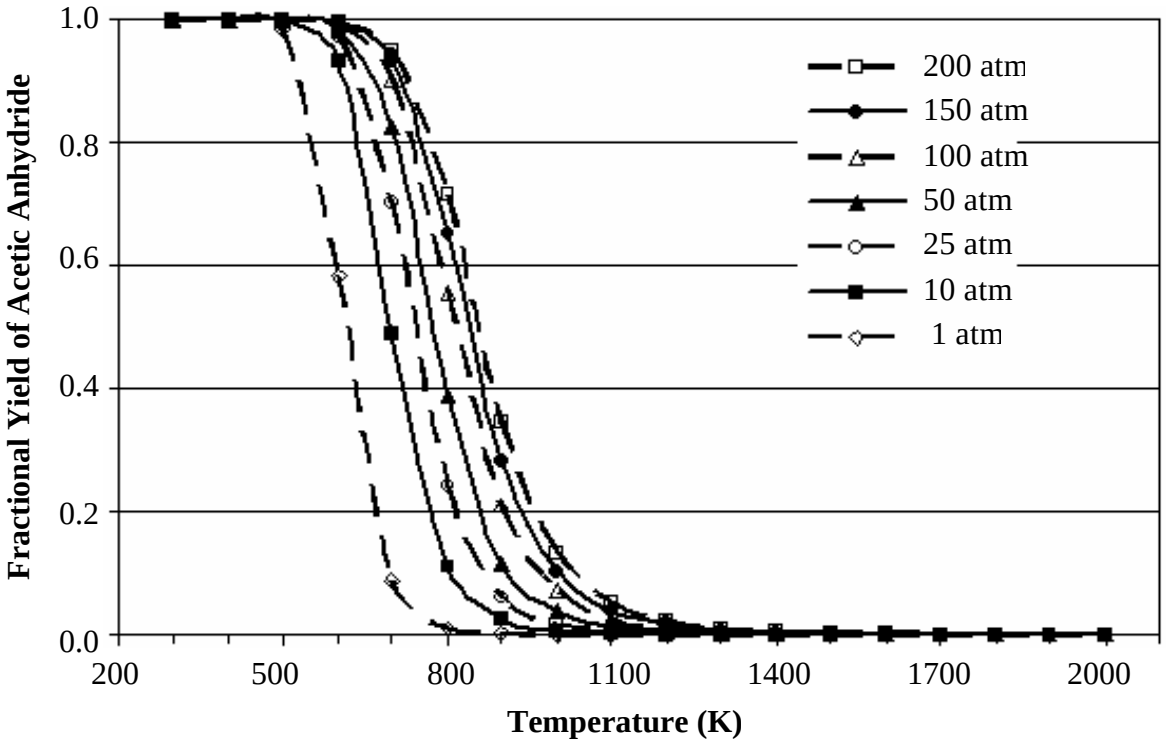

Figure 2 -11: Equilibrium fractional yield of acetic anhydride for reaction (R 2 -12) from 300 - 2000K and 1 -200 atm obtain from AspenPlus™ using a stoichiometric inlet and Peng -Robinson equation of state.

The equilibrium fractional conversions of methane for this system are higher than those of the direct synthesis reaction alone, (R 2 -1). The thermodynamics for this reaction system are favorable at reasonable conditions. Additionally, the acetic anhydride produced can be reacted with water to give acetic acid:

$$(CH_3CO)_2O + H_2O \rightarrow 2\,CH_3COOH \qquad \text{(R 2 -15)}$$

$\Delta G_r^0 = -47$ kJ/mol $\qquad\qquad$ $\Delta H_r^0 = -50$ kJ/mol

While this system is theoretically a valid method to overcome the thermodynamic limitations of the direct synthesis reaction (R 4 -1), it is not likely to be an industrially useful

solution. The current method of producing ketene is by the decomposition of acetic acid to ketene and water [11]:

$$CH_3COOH \rightarrow CH_2CO + H_2O \qquad \text{(R 2 -16)}$$

$\Delta G_r^0 = +97$ kJ/mol $\qquad\qquad$ $\Delta H_r^0 = +143$ kJ/mol

Half of the acetic acid produced from the reaction system described above can be used to form ketene to be used as a reactant in the system. However, this process is not likely to be economically viable. Detailed tables of the data can be found in Appendix B.2.

2.8 VINYL ACETATE FROM ETHYLENE AND OXYGEN

Vinyl acetate is an important industrial chemical widely used in coatings and adhesives [10, 15]. The current production method is to react acetic acid with ethylene and oxygen [15]. Over 4.3 million metric tons of vinyl acetate was produced in 2003 [15] using approximately 45% of the acetic acid produced [14].

To drive the equilibrium of the direct synthesis reaction (R 4 -1), the formation of vinyl acetate ($CH_3CO_2CH=CH_2$) using ethylene (C_2H_4) and oxygen was examined. This process consists of two reactions. First, acetic acid is formed from the direct synthesis reaction, (R 2-1). The acetic acid is then reacted with ethylene and oxygen to form vinyl acetate:

$$CH_3COOH + C_2H_4 + ½\ O_2 \rightarrow CH_3CO_2CH{=}CH_2 + H_2O \qquad \text{(R 2 -17)}$$

$\Delta G_r^0 = -151$ kJ/mol $\qquad\qquad \Delta H_r^0 = -176$ kJ/mol

This gives the overall reaction:

$$CO_2 + CH_4 + C_2H_4 + ½\ O_2 \rightarrow CH_3CO_2CH{=}CH_2 + H_2O \qquad \text{(R 2 -18)}$$

$\Delta G_r^0 = -80$ kJ/mol $\qquad\qquad \Delta H_r^0 = -141$ kJ/mol

Equilibrium thermodynamic calculations were performed on this system. The side reactions of methane combustion:

$$CH_4 + 2\ O_2 \rightarrow CO_2 + H_2O \qquad \text{(R 2 -19)}$$

$\Delta G_r^0 = -802$ kJ/mol $\qquad\qquad \Delta H_r^0 = -803$ kJ/mol

ethylene combustion:

$$C_2H_4 + 3\ O_2 \rightarrow 2\ CO_2 + 2\ H_2O \qquad \text{(R 2 -20)}$$

$\Delta G_r^0 = -1316$ kJ/mol $\qquad\qquad \Delta H_r^0 = -1323$ kJ/mol

and partial oxidation of ethylene:

$$C_2H_4 + O_2 \rightarrow CO_2 + CH_4 \qquad \text{(R 2 -21)}$$

$\Delta G_r^0 = -514$ kJ/mol $\qquad\qquad \Delta H_r^0 = -521$ kJ/mol

were restricted by setting the extents of those reactions to zero. A stoichiometric inlet composition of 0.286 mole fraction of CO_2, 0.286 mole fraction of CH_4, and 0.286 mole fraction of C_2H_4 and 0.142 mole fraction of O_2 was used. While no acetic acid occurs in the overall reaction (R 2 -18), acetic acid was allowed in the system, thus permitting reactions (R 2 -1) and (R 2 -17).

The equilibrium fractional conversion of methane in the reaction system increased with increasing pressure and decreased with increasing temperature, figure 2 -12. Likewise, the equilibrium fractional conversion of ethylene increased with increasing pressure and decreased with increasing temperature, figure 2 -13. The equilibrium yield of vinyl acetate increased with increasing pressure and decreased with increasing temperature, however, it was above 0.999 for all temperatures and pressures, figure 2 -14.

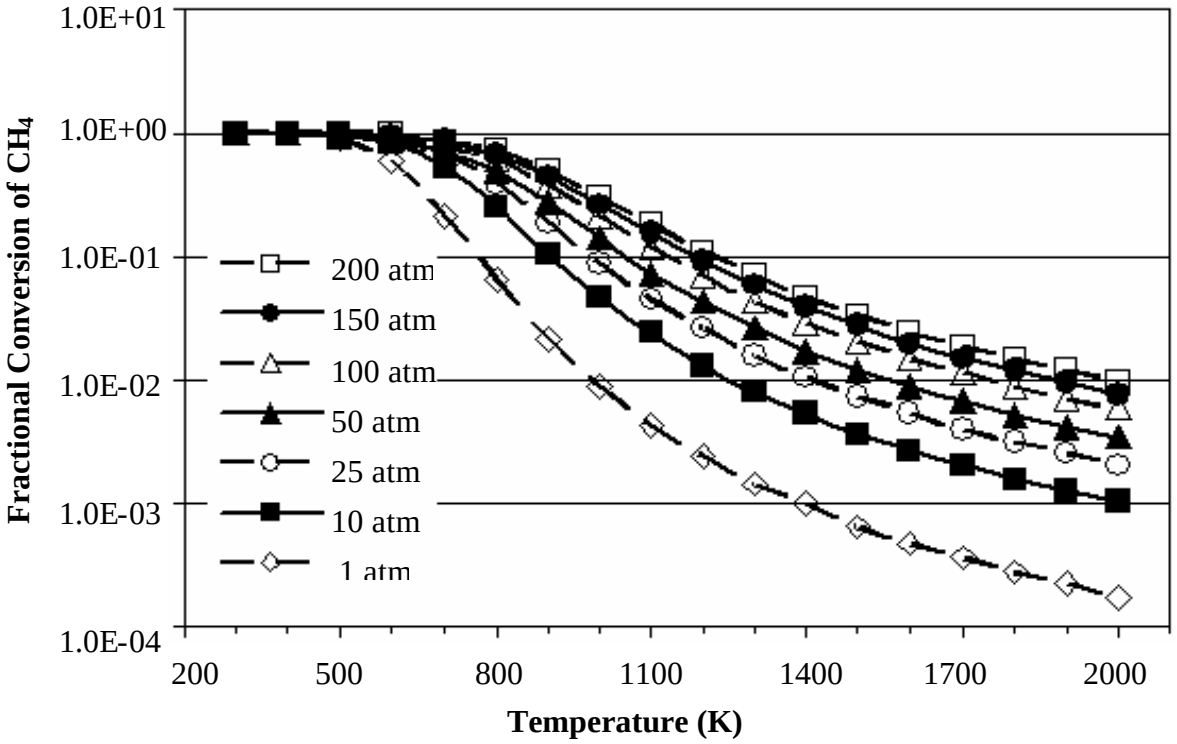

Figure 2 -12: Equilibrium fractional conversion of methane for reaction (R 2 -18) from 300 - 2000K and 1 -200 atm obtain from AspenPlus™ using a stoichiometric inlet and Peng -Robinson equation of state.

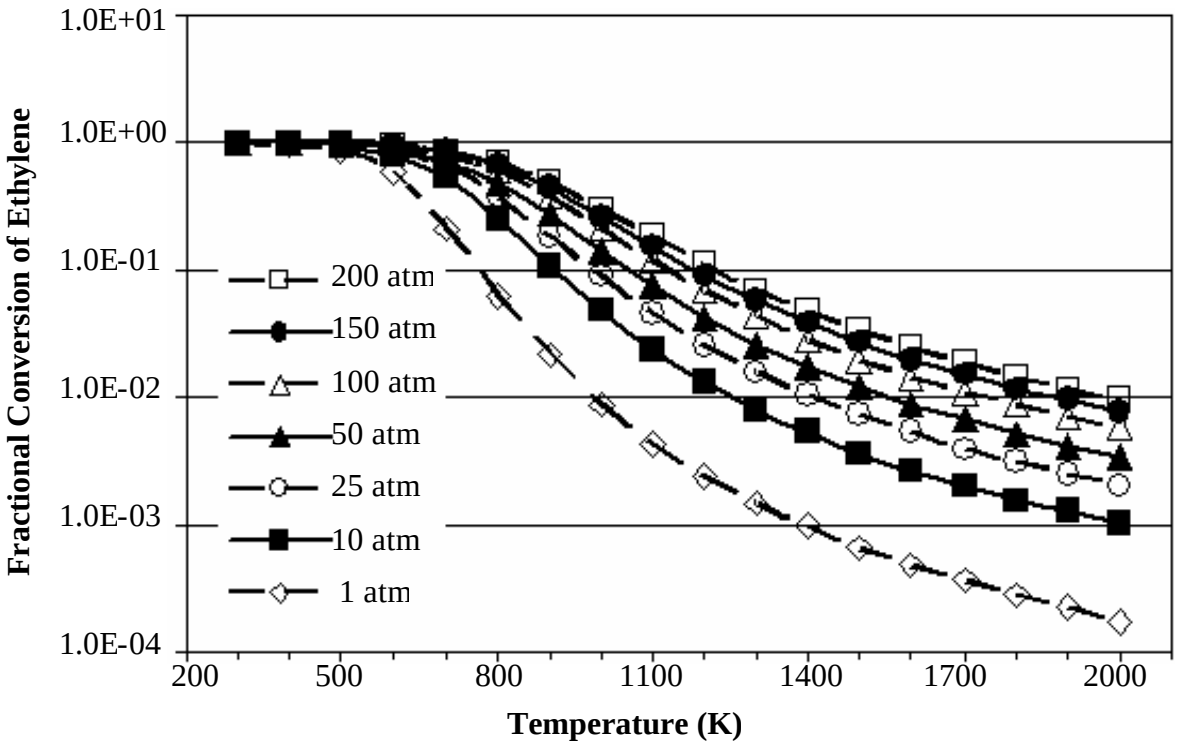

Figure 2 -13: Equilibrium fractional conversion of ethylene for reaction (R 2 -18) from 300 - 2000K and 1 -200 atm obtain from AspenPlus™ using a stoichiometric inlet and Peng -Robinson equation of state.

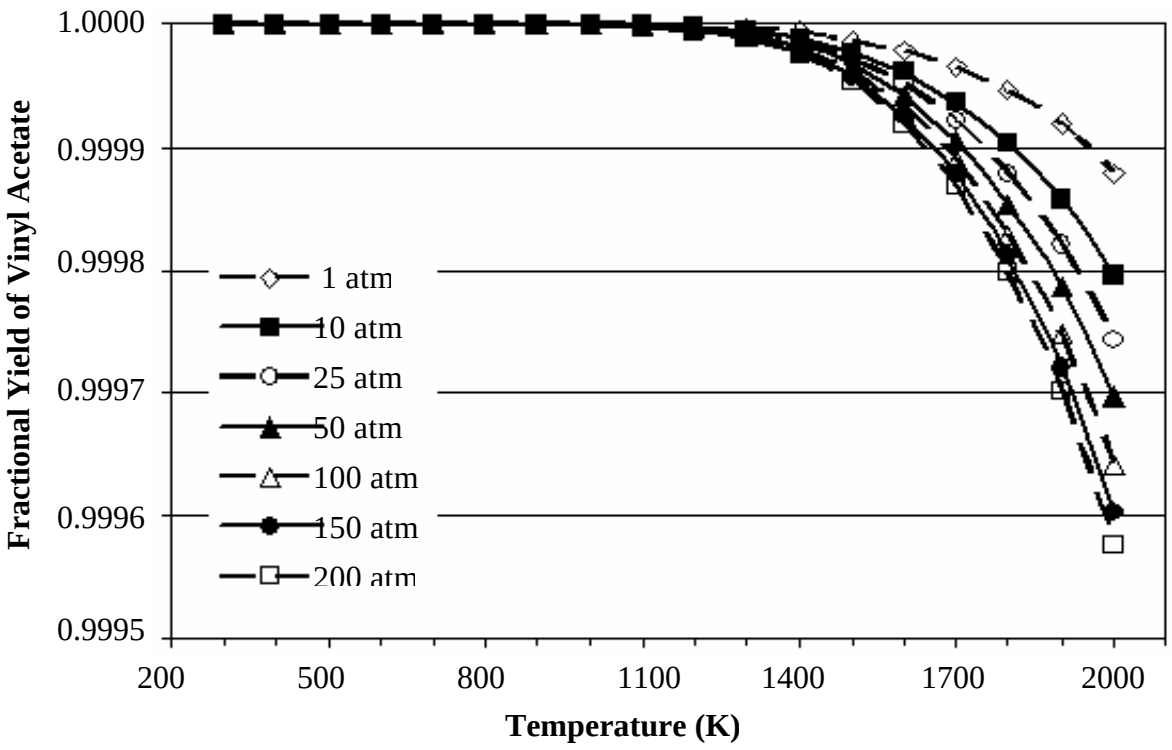

Figure 2 -14: Equilibrium fractional yield of vinyl acetate for reaction (R 2 -18) from 300 - 2000K and 1 -200 atm obtain from AspenPlus™ using a stoichiometric inlet and Peng -Robinson equation of state.

At 300 K and all pressures, 400 K and 25 atm and above, and 500 K and 200 atm, the system was a liquid, whereas it was a vapor at all other temperatures and pressures. The fractional conversion of ethylene was not affected by the phase of the system. At reasonable temperatures and pressures, 300 K and 1 atm, the equilibrium fractional conversion of methane and ethylene is 0.9999997 and the equilibrium fractional yield of vinyl acetate is 1.000.

This system is a significant improvement over the direct synthesis reaction, however, the calculations did restrict the combustion of methane and ethylene and the partial oxidation

of ethylene. These reactions are very likely to occur, thus giving much lower yields of vinyl acetate. This method may be feasible given a highly selective catalyst. Detailed tables of the data can be found in Appendix B.3.

2.9 VINYL ACETATE FROM ACETYLENE

Vinyl acetate is an important industrial chemical widely used in coatings and adhesives [10, 15]. Vinyl acetate can be produced by reacting vinyl acetate with acetylene [12]. Over 4.3 million metric tons of vinyl acetate was produced in 2003 [15] using approximately 45% of the acetic acid produced [14].

To drive the equilibrium of the direct synthesis reaction (R 2 -1), the formation of vinyl acetate ($CH_3CO_2CH=CH_2$) using acetylene (C_2H_2) was examined. This process consists of two reactions. First, acetic acid is formed from the direct synthesis reaction. The acetic acid is then reacted with ethylene and oxygen to form vinyl acetate:

$$CH_3COOH + C_2H_2 \rightarrow CH_3CO_2CH=CH_2 \qquad \text{(R 2 -22)}$$

$\Delta G_r^0 = -65$ kJ/mol $\qquad\qquad$ $\Delta H_r^0 = -110$ kJ/mol

This gives the overall reaction:

$$CO_2 + CH_4 + C_2H_2 \rightarrow CH_3CO_2CH=CH_2 \qquad \text{(R 2 -23)}$$

$\Delta G_r^0 = +7$ kJ/mol $\qquad\qquad$ $\Delta H_r^0 = -75$ kJ/mol

Equilibrium thermodynamic calculations were performed on this system. A stoichiometric inlet composition of 0.333 mole fraction of CO_2, 0.333 mole fraction of CH_4

and 0.333 mole fraction of C_2H_2 was used. While no acetic acid occurs in the overall reaction (R 2 -23), acetic acid was allowed in the system.

The equilibrium fractional conversion of methane increases with increasing pressure. The equilibrium fractional conversion of methane decreases with increasing temperature until it reaches a minimum around 600 or 700 K, and then it increases with increasing temperature, figure 2 -15. This is due to a decreasing amount of methane being converted to acetic anhydride and an increasing amount being converted to acetic acid. The equilibrium fractional conversion of acetylene increases with increasing pressure and decreases with increasing temperature, figure 2 -16. The equilibrium fractional yield of vinyl acetate is nearly one below 600 K at all pressures, figure 2 -17. It decreases with increasing temperature and increases with increasing pressure. At lower temperatures, the formation of vinyl acetate is more favorable than the formation of acetic acid, however as the temperature increases, the acetic acid reaction is more favorable.

At 300 K and 10 atm and above, and 400 K and 200 atm, the system was a liquid, whereas it was a vapor at all other temperatures and pressures. The fractional conversion of acetylene was much greater when the system was a liquid, than when it was a vapor. At reasonable temperatures and pressures, 300 K and 10 atm, the equilibrium fractional conversion of methane and acetylene is 0.981 and the equilibrium fractional yield of vinyl acetate is 1.000.

This system is a significant improvement over the direct synthesis reaction, and it does not have the side reactions that the ethylene system does. Detailed tables of the data can be found in Appendix B.4.

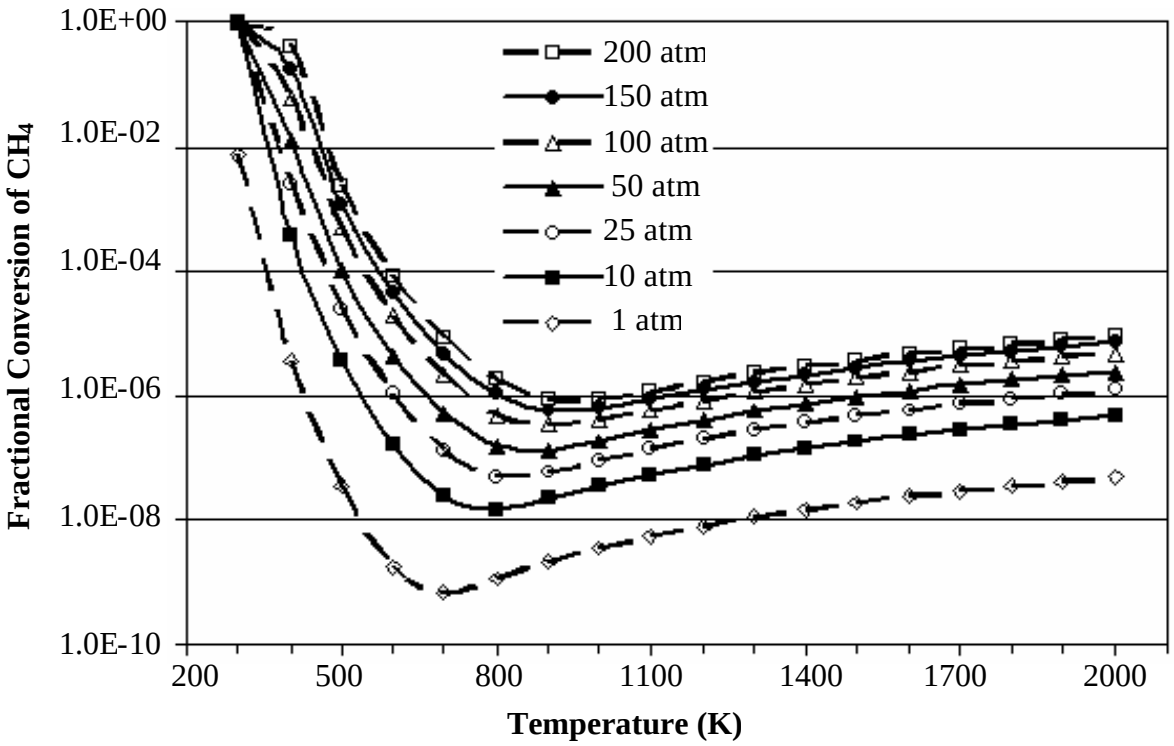

Figure 2 -15: Equilibrium fractional conversion of methane for reaction (R 2 -23) from 300 - 2000K and 1 -200 atm obtain from AspenPlus™ using a stoichiometric inlet and Peng -Robinson equation of state.

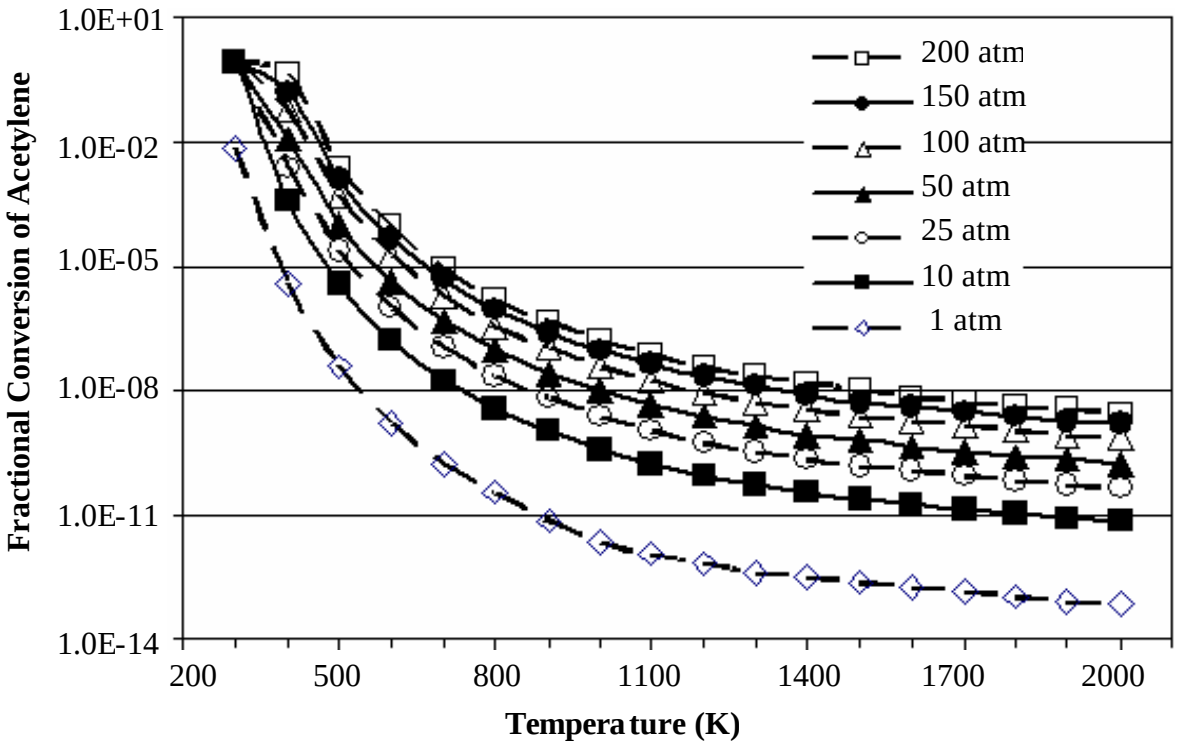

Figure 2 -16: Equilibrium fractional conversion of acetylene for reaction (R 2 -23) from 300 - 2000K and 1 -200 atm obtain from AspenPlus™ using a stoichiometric inlet and Peng -Robinson equation of state.

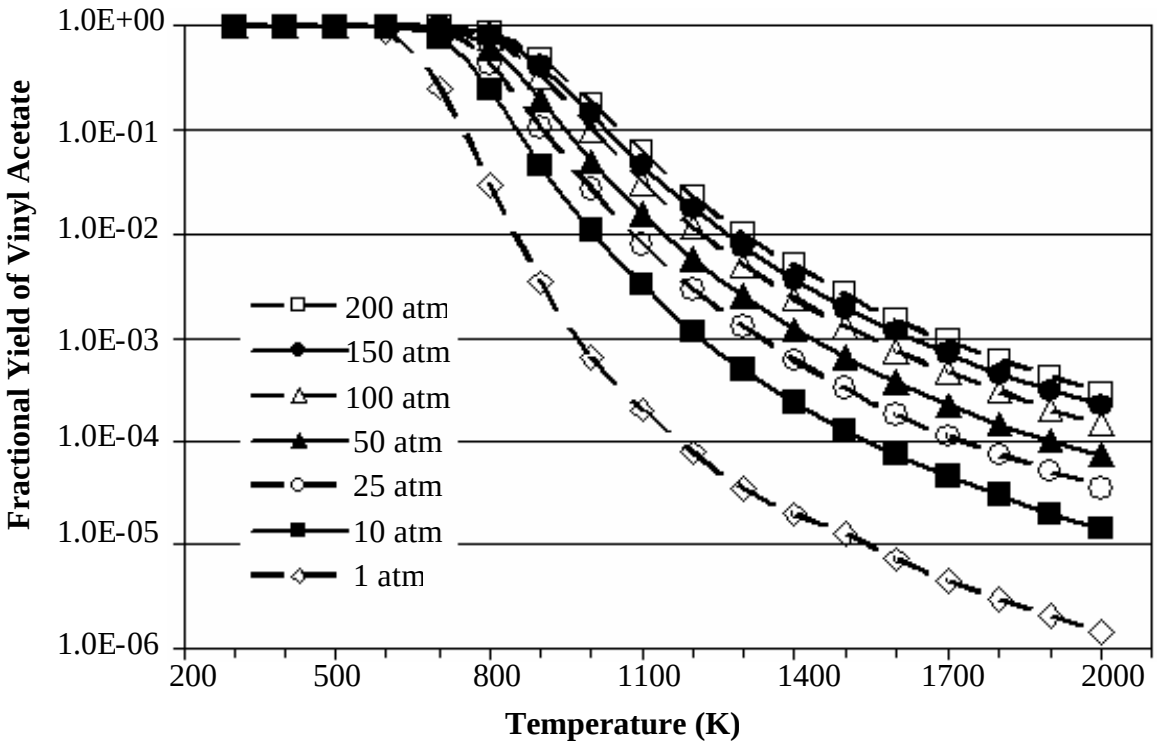

Figure 2 -17: Equilibrium fractional yield of vinyl acetate for reaction (R 2 -23) from 300 - 2000K and 1 -200 atm obtain from AspenPlus™ using a stoichiometric inlet and Peng -Robinson equation of state.

2.10 CYCLIC ADSORPTION/DESORPTION

The equilibrium thermodynamics are unfavorable for the direct synthesis reaction, (R 2 -1). A catalyst will not affect the overall thermodynamics of the reaction. However, individual portions of the reaction with the catalyst may be thermodynamically favorable. If these individual reaction steps can be separated and optimized, perhaps the thermodynamics can be overcome by using the reaction with the catalyst. A cyclic adsorption -desorption of

adsorbed species on the catalyst may be a feasible method to drive the equilibrium of the direct synthesis reaction.

For this method, the carbon dioxide and methane would react with a catalyst site to form adsorbed acetic acid:

$$CO_2 + CH_4 + * \leftrightarrow CH_3COOH\text{-}* \quad \text{(R 2 -24)}$$

where * is a catalyst site, and CH_3COOH -* is adsorbed acetic acid. Under a different set of conditions, the adsorbed species would then be removed, the product recovered and the catalyst site regenerated:

$$CH_3COOH\text{-}* \leftrightarrow CH_3COOH + * \quad \text{(R 2 -25)}$$

However, acetic acid does not normally adsorb molecularly to catalyst sites. It is more common for it to adsorb dissociatively as an acetate species. Acetic acid commonly adsorbs strongly as a monodentate acetate species on metal oxides [16, 17]:

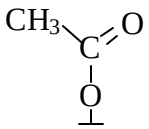

Figure 2 -18: Monodentate adsorbed acetate species

Using a mondentate adsorbed acetate species, a possible method for overcoming the thermodynamics of the direct synthesis reaction would be to react CO_2 and CH_4 with a hydroxyl catalyst site to form an adsorbed acetate and water:

$$CO_2 + CH_4 + * \text{-}OH \leftrightarrow CH_3COO\text{-}* + H_2O \quad \text{(R 2 -26)}$$

The water can be removed from the system by the unreacted gases or a sweep gas.

To remove the acetate as acetic acid, the catalyst would first be removed from the reaction conditions, then exposed to conditions which are favorable for the desorption. Gas phase acetic acid may likely be formed from steaming the adsorbed acetate species off the catalyst:

$$CH_3COO\text{-}* + H_2O \leftrightarrow *\text{-}OH + CH_3COOH \qquad \text{(R 2 -27)}$$

This would also regenerate the catalyst sites, so that the catalyst can be exposed to the reaction conditions again and form adsorbed acetate species. Figure 2 -19 illustrates this catalytic cyclic adsorption/desorption.

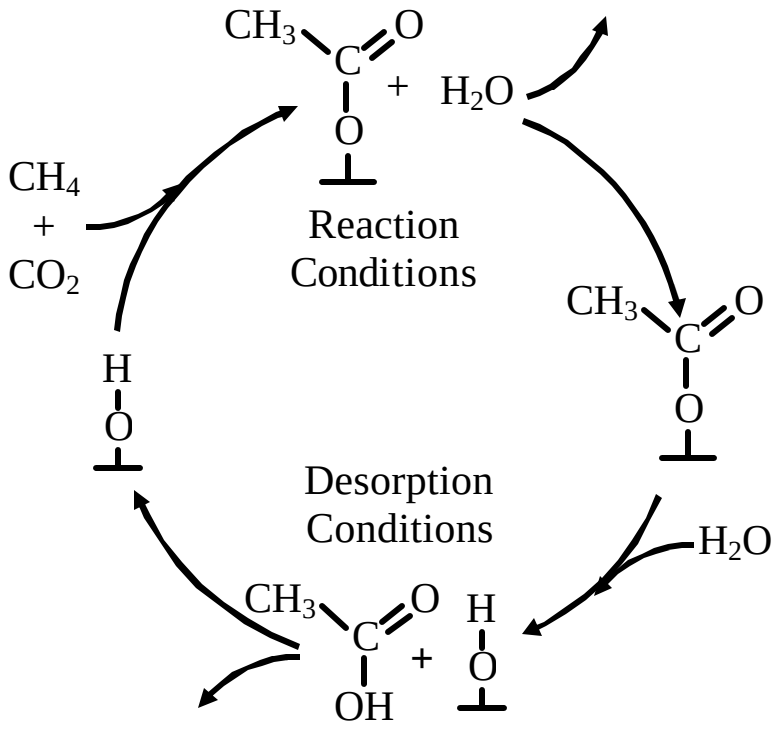

Figure 2 -19: Catalytic Cyclic Adsorption/Desorption

This cyclic adsorption/desorption may be a feasible method to overcome the thermodynamic limitations of the direct synthesis reaction. Due to the lack of thermodynamic data for solids in the AspenPlus™ database, no simulations could be run for this system.

2.11 CONCLUSIONS

The equilibrium thermodynamic calculations on the direct synthesis of acetic acid showed that the fractional conversion of methane increased with increasing temperature, pressure and inlet mole fraction of carbon dioxide. Unfortunately, the highest fractional conversion of methane was found to be only 1.292×10^{-4} at 2000 K, and 1000 atm calculated from the Peng-Robinson equation of state with an inlet mole fraction of 0.95 carbon dioxide. In order for this reaction to be industrially viable, methods must be found to overcome the thermodynamic limitations.

A possible side reaction for the direct synthesis reaction is the formation of methyl formate from carbon dioxide and methane. Equilibrium thermodynamic calculations performed on this side reaction showed that the conversions of methane in this reaction are on the order of 100 times less than those in the direct synthesis reaction. While this side reaction is possible, it should not cause significant interference.

Most of the literature on the synthesis of acetic acid from methane uses carbon monoxide and oxygen in the reaction rather than carbon dioxide. Equilibrium thermodynamic calculations performed on the system showed that complete conversion of

methane to acetic acid was possible at low temperatures and pressures. However, these calculations neglected side reactions such as the combustion of methane and the oxidation of carbon monoxide. If the catalyst was highly selective, then it is theoretically possible to achieve the high yields of acetic acid reported in the literature.

Since methane is the least active alkane, if a reaction system can be found to produce acetic acid from methane and carbon dioxide, the same reaction system might be used to produce higher acids from higher alkanes. The equilibrium thermodynamics of the synthesis of propionic acid from carbon dioxide and ethane showed that the fractional conversion of ethane increases with increasing temperature and pressure. The maximum fractional conversion of ethane was only 5.328×10^{-5} at 2000 K and 200 atm calculated using the Peng-Robinson equation of state and an inlet mole fraction of 0.95 carbon dioxide. The fractional conversions of ethane were approximately twice that of the conversions of methane in the acetic acid reaction.

The direct synthesis of acetic acid from carbon dioxide and methane is thermodynamically limited at all conditions of interest. To overcome the thermodynamic limitations the acetic acid must be either chemically or physically removed from the system. Thermodynamic calculations were performed on four chemical systems: synthesis of methyl acetate from methanol, synthesis of acetic anhydride from ketene, synthesis of vinyl acetate from ethylene and oxygen, and the synthesis of vinyl acetate form acetylene.

The methyl acetate system was more favorable than the direct synthesis of acetic acid, however, it was still limited with a maximum equilibrium fractional conversion of methane of 1.8106×10^{-3} at 300 K and 2000 atm. Additionally, the decomposition of methanol was

restricted. It is likely that this reaction would occur, resulting in a lower actual methane conversion.

The synthesis of acetic anhydride was significantly more favorable with an equilibrium fractional conversion of methane of 0.947 at only 300 K and 25 atm. The acetic anhydride could be reacted with water to give acetic acid. However, ketene is industrially produced from acetic acid. While part of the acetic acid produced in this system could be used to make the ketene required, it is unlikely that this process would be economical.

The synthesis of vinyl acetate from ethylene and oxygen was significantly more favorable than the direct synthesis reaction with an equilibrium fractional conversion of methane of 0.9999997 at only 300 K and 1 atm. However, the oxidation of methane and ethylene was not allowed. Given a highly selective catalyst, this system may be an effective method to overcome the thermodynamic limitations of the direct synthesis reaction.

The synthesis of vinyl acetate from acetylene was also significantly more favorable with an equilibrium fractional conversion of methane of 0.981 at only 300 K and 10 atm. While this system is less favorable than the ethylene system, it does not have the oxidative side reactions. This system may be an effective method to overcome the thermodynamic limitations of the direct synthesis of acetic acid and still results in a valuable industrial chemical.

A cyclic adsorption/desorption method using the catalyst was proposed. No thermodynamic simulations were performed, however, this method may be effective in overcoming the thermodynamic limitations.

While the direct synthesis of acetic acid from methane and carbon dioxide is thermodynamically limited, it may be possible to overcome the thermodynamics by chemically or physically removing the acetic acid from the system.

2.12 REFERENCES

1. Sandler, S.I., *Chemical and Engineering Thermodynamics*. 1999, New York: John Wiley & Sons, Inc.

2. Chemical.Rubber.Company, *CRC Handbook of Chemistry and Physics*. 83 ed. 2002, Cleveland: Chemical Rubber Company Press.

3. Aspen.Technology, *Aspen Physical Property System: Physical Property Methods and Models*. 2001, Cambridge, MA: Aspen Technology.

4. Prausnitz, J.M.L., R.N.; Azevedo, E.G., *Molecular Thermodynamics of Fluid-Phase Equilibria*. 1999, New Jersey: Prentice Hall PTR.

5. Lin, M. and A. Sen, *Direct Catalytic Conversion of Methane to Acetic-Acid in an Aqueous-Medium.* Nature, 1994. **368**(6472): p. 613-615.

6. Larkin, D.W.C., T.A.; Lobban, L.L.; Mallinson, R.G., *Oxygen Pathways and Carbon Dioxide Utilization in Methane Partial Oxidation in Ambient Temperature Electric Discharges.* Energy & Fuels, 1998(12).

7. Chepaikin, E.G., A.P. Bezruchenko, A.A. Leshcheva, G.N. Boyko, I.V. Kuzmenkov, E.H. Grigoryan, and A.E. Shilov, *Functionalisation of methane under dioxygen and carbon monoxide catalyzed by rhodium complexes - Oxidation and oxidative carbonylation.* Journal of Molecular Catalysis a-Chemical, 2001. **169**(1-2): p. 89-98.

8. Chepaikin, E.G., G.N. Boiko, A.P. Bezruchenko, A.A. Leshcheva, and E.A. Grigoryan, *Oxidative carbonylation of methane in the presence of rhodium complexes.* Doklady Akademii Nauk, 1997. **353**(2): p. 217-219.

9. Chepaikin, E.G., G.N. Boyko, A.P. Bezruchenko, A.A. Leshcheva, and E.H. Grigoryan, *Oxidative carbonylation of methane in the presence of Rh complexes in aqueous acetic acid.* Journal of Molecular Catalysis a-Chemical, 1998. **129**(1): p. 15-18.

10. Kirk, R.E.O., D.F, *Encyclopedia of Chemical Technology*. 4th ed. 1997, New York: John Wiley & Sons.

11. Agreda, V. and J. Zoeller, *Acetic Acid and its Derivatives*. 1993, New York: Marcel Dekker.

12. Kirk, R.E.O., D.F, *Encyclopedia of Chemical Technology*. 4th ed. 1955, New York: John Wiley & Sons.

13. Considine, D.M., *Chemical and Process Technology Encyclopedia*. 1974, New York: McGraw-Hill Book Company.

14. [Anon], *Product focus - Acetic Acid.* Chemical Week, 2002. **164**(21): p. 33-33.

15. [Anon], *Product Focus - Vinyl Acetate Monomer.* Chemical Week, 2003. **165**(23): p. 31-31.

16. Pei, Z.F. and V. Ponec, *On the intermediates of the acetic acid reactions on oxides: An IR study.* Applied Surface Science, 1996. **103**(2): p. 12.

17. Chateau, L., J.P. Hindermann, A. Kiennemann, and E. Tempesti, *On the mechanism of carbonylation in acetic acid and higher acid synthesis from methanol and syngas mixtures on supported rhodium catalysts.* Journal of Molecular Catalysis a-Chemical, 1996. **107**(1-3): p. 12.

CHAPTER 3:

ACETIC ACID SYNTHESIS

3.1 INTRODUCTION

From the thermodynamic calculations discussed in chapter 2, the direct synthesis of acetic acid from carbon dioxide and methane is limited at all practical conditions. However, all of the methods proposed to overcome the thermodynamics assume the formation of acetic acid from carbon dioxide and methane as an intermediate step. Reaction studies were performed to show the formation of acetic acid from carbon dioxide and methane.

The direct synthesis of acetic acid from carbon dioxide and methane reaction was tested using four different commercial catalysts: reduced 5% Pd/carbon, unreduced 5% Pd/carbon, 5% Pd/alumina and 5% Pt/alumina. The carbon and alumina supports were also tested. Catalyst characterizations were performed to better understand the fundamental differences between the catalysts. These characterizations were also used to try to identify qualities required for a catalyst to be effective in the direct synthesis reaction. The characterizations include metal loading, surface area, pore volume, metal dispersion, CO_2 adsorption and desorption, CH_4 adsorption and desorption and TEM.

Diffuse reflectance infrared Fourier transform spectroscopy (DRIFTS) was chosen to examine the various catalysts for the formation of adsorbed acetates, dimer and monomer acetic acid from carbon dioxide and methane. While not a very common technique, DRIFTS has been shown to be an effect method to determine adsorbed species on powdered catalysts [1-15]. This is an ideal technique, as it can be used under reaction conditions such as high

temperature and pressure and can be used with a powder sample [9, 16-18]. Additionally, DRIFTS can show IR peaks associated with both adsorbed and gas phase species [9, 16-18].

Further experiments were conducted to confirm the formation of gas phase acetic acid from carbon dioxide and methane using a flow through reactor system with an online mass spectrometer. Detailed experiments were then conducted to explore the effects of inlet gas concentrations on the direct synthesis of acetic acid from carbon dioxide and methane.

3.2 CATALYSTS

The use of catalysts cannot change the overall thermodynamics of the reaction. Catalysts are used to reduce the activation energy barrier for the reaction. The catalyst enhances the rate of conversion of the reactants to desired products without itself being consumed. There are considerable interactions with the reactants and the catalyst as well as the products with the catalyst. The net effect, however, is that the catalyst remains unchanged while providing an easier alternative path for the conversion of reactants to products.

Four catalysts were tested for the formation of adsorbed acetate and gas phase acetic acid from carbon dioxide and methane: reduced 5% Pd/carbon, un-reduced 5% Pd/carbon, 5% Pd/alumina and 5% Pt/alumina. A carbon support and alumina support were also used.

The palladium on carbon catalysts were chosen because they were used in preliminary experiments [19] and because palladium has been shown to activate methane [20-39]. These catalysts and the carbon support were provided by Calgon Carbon and

prepared by impregnation. The two carbon supported catalysts were reported to be made in the same batch. Half of the catalyst made was then reduced by Calgon Carbon, denoted as the reduced 5% Pd/carbon, whereas the other half was not, denoted as un-reduced 5% Pd/carbon.

A 5% palladium on alumina, 5% platinum on alumina and the gamma alumina support were also tested. Alumina is known to adsorb carbon dioxide [40-58] and thus was chosen as the support for the catalysts. The 5% palladium on alumina support was used as a comparison between supports to the 5% palladium on carbon catalysts. Platinum has been shown to activate methane [29, 59-81] and thus was chosen. The platinum on alumina catalysts was also used as a comparison between metals to the 5% palladium on alumina catalyst. The alumina and alumina supported catalysts were provided by Johnson Matthey and prepared by incipient wetness. Table 5-1 lists the information for the catalysts tested.

Table 3-1: Catalyst information and relative reaction performance

Abbreviation?	Carbon	5% Pd/C Red.	5% Pd/C Not Red.	Alumina	5% Pd/Al	5% Pt/Al
Support	Carbon	Carbon	Carbon	γ-Alumina	γ-Alumina	γ-Alumina
Metal/ Reported Loading	N/A	Palladium/ 5%	Palladium/ 5%	N/A	Palladium/ 5%	Platinum/ 5%
Preparation Technique	N/A	Impregnation Reduced	Impregnation	N/A	Incipient Wetness	Incipient Wetness
Provided by	Calgon Carbon			Johnson Matthey		

3.3 EXPERIMENTAL

3.3.1 METAL LOADING

The metal loading of each of the catalysts was determined by either Inductively Coupled Plasma Spectroscopy (ICP) or Nuclear Activation Analysis (NAA). The ICP analyses were carried out by the Soil Science Department at North Carolina State University. The metal was removed from the support by refluxing a catalyst sample in Aqua Regia on a hot plate. The final solution then underwent the ICP testing. It was apparent when all the metal was removed from the alumina support, as the color of the solid changed from black to white. However, it was not apparent when all the metal was removed from the carbon supported catalysts, as the solid remained black. Thus the carbon supported catalysts underwent additional NAA analysis. The alumina samples could not be analyzed by NAA, as the aluminum causes interference. The NAA analyses were carried out by the Nuclear Engineering Department at North Carolina State University.

3.3.2 SURFACE AREA AND PORE VOLUME

The surface area measurements were based on the Brunauer-Emmet-Teller (BET) surface area theory. Assuming a clean surface and a monolayer adsorption of the adsorbing gas, the surface area can be calculated by:

$$S = V \times A \times N \times [1-P/P_0/M] \qquad \text{(E 7-1)}$$

where S is the surface area, V is the volume of gas adsorbed, A is Avogadro's number, N is the area of each adsorbed gas molecule, P is the pressure at which the gas was adsorbed, P_0 is

the saturation pressure of liquefied gas at the adsorbing temperature, and M is the molar volume of the gas [82]. For nitrogen, P_0 at 77 K is 1.013 x 10^5 Pa, and N is 0.16 nm^2 [83]. The conditions of the experiments were such that the assumptions for this method are valid.

The total pore volume of a catalyst can be determined by liquid absorption. Assuming a clean surface, negligible volume of gas adsorbed on the surface and straight, non-connecting pores, the total pore volume is equivalent to the volume of liquid condensed in the pores from a condensable gas near its saturation vapor pressure [83]

The surface area and pore volume experiments were conducted using a Micromeritics FlowSorb II 2300 system. Approximately 0.1 grams of catalyst were used for each experiment. The initial catalyst weight and total weight (glass tube, quartz wool and catalyst) were recorded. The catalysts were then degassed at 240°C for 2 hours. The tests were then run according to the instruction manual [82]. The final total weight was recorded, as well as the display value. Nitrogen was used as the absorbing gas for both the surface area and pore volume experiments.

The dry catalyst weight was determined by subtracting the difference in weight due to the degas from the initial catalyst weight:

$$\text{Dry Catalyst Weight} = \text{Initial Catalyst Weight} - \Delta \text{ Total Weight} \qquad \text{(E 7-2)}$$

The display on the FlowSorb II 2300 system gives the total surface area in square meters. This value was used to determine the surface area per gram of catalyst by:

$$\text{Surface Area } (m^2/g) = \text{Display Values } (m^2) \,/\, \text{Dry Catalyst Weight } (g) \qquad \text{(E 7-3)}$$

According to the Micromeritics Instruction manual [82], the error associated with the surface area is 2 percent of the value. From this, the surface area error was calculated by:

$$\text{Surface Area Error } (m^2/g) = 2\% \times \text{Surface Area } (m^2/g) \quad \text{(E 7-4)}$$

From the pore volume experiments (different than the surface area), the display value on the FlowSorb II 2300 system gives 100 times the pore volume in cubic centimeters. This value was used to determine the pore volume per gram of catalyst by:

$$\text{Pore Volume } (cm^3/g) = (\text{Display Values } (cm^3)/100)/ \text{ Dry Catalyst Weight } (g) \quad \text{(E 7-5)}$$

According to the Micromeritics Instruction manual [82], the error associated with the pore volume is 3 percent of the value. From this the surface area error was calculated by:

$$\text{Pore Volume Error } (cm^3/g) = 3\% \times \text{Pore Volume } (cm^3/g) \quad \text{(E 7-6)}$$

3.3.3 PULSE CHEMISORPTION

Pulse chemisorption can be used to determine the amount of a gas that adsorbs onto a catalyst sample. A known volume of the gas is pulsed through the sample. As the gas flows over the sample, some of it is adsorbed. With each progressive pulse, the sample adsorbs less gas. Eventually the sample will become completely saturated with the gas, and the amount of gas pulsed into the catalyst will equal the amount detected leaving the catalyst. The total amount of gas adsorbed can then be calculated by subtracting the amount exiting the catalyst from the amount that was pulsed into the catalyst [84]. Figure 7-1 shows an example of the data profile for a pulse chemisorption experiment.

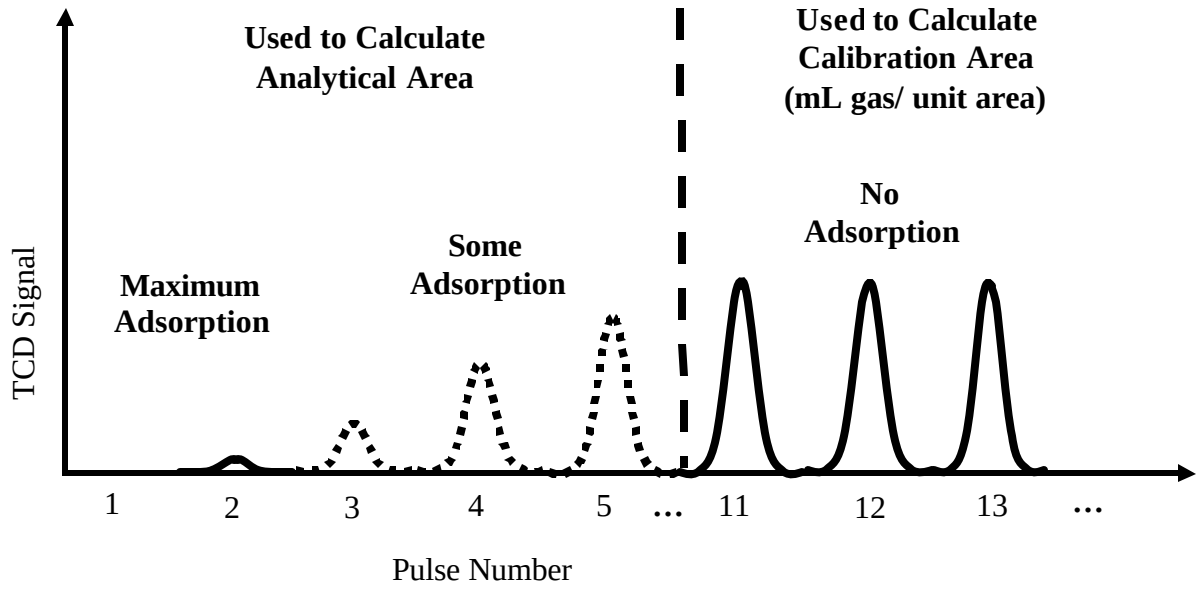

Figure 3-1: Pulse chemisorption example data

In addition to determining the amount of gas adsorbed by the catalyst, pulse chemisorption can be used to calculate the metal dispersion of the catalyst. The metal dispersion is the ratio of the number of exposed metal atoms t to the total number of metal atoms. Carbon monoxide is commonly used in determining the metal dispersion, as carbon monoxide does not adsorb on supports and adsorbs in a consistent manner on metals [83, 84]. The number of exposed metal atoms can be determined from the total amount of carbon monoxide adsorbed on the sample and the stoichiometry of adsorption (number of carbon monoxide atoms adsorbed per metal atom) [83, 84].

The following experiments were performed using the Altamira system and the thermal conductivity detector (TCD). Approximately 0.1 grams of catalyst were used for each experiment and the catalyst weight was recorded. The sample was purged in a 25 sccm flow of helium at room temperature for 30 minutes. In a 25 sccm flow of helium, the

temperature was ramped up to 400°C at 10°C/min, held at 400°C for 30 minutes then cooled back down to 25°C at 30°C/min and held at 25°C for 30 min. Then, using a 50 sccm flow of helium as the carrier gas, the reaction gas (CO, CO_2 or CH_4) was pulsed through the reactor forty times. The sample loop was filled for two minutes with a flow of 25 sccm of the reaction gas. The helium was allowed to flow through the 121 μL sample loop for two minutes for each pulse. The carbon dioxide and methane gases were pure research grade. The carbon monoxide was a mixture of 10% carbon monoxide in helium. New catalyst samples were used for each experiment.

Each pulse of reaction gas results in a peak from the baseline of the TCD output. The area under each peak is proportional to the amount of gas. The peak areas were determined using the Altamira software.

A calibration value is needed to determine the amount of gas per unit area. The calibration value is calculated by:

$$CV\ (\mu L\ gas/\ unit\ area) = PLV \times \%\ gas/\ ACPA \qquad (E\ 7\text{-}7)$$

where CV is the calibration value, PLV the pulse loop volume (121 μL), % gas is the percent of reaction gas, and ACPA is the average calibration peak area. The average calibration peak area was determined by averaging the peak area for the last 30 pulses in each experiment.

The analytical area is needed to determine the amount of gas adsorbed. The first ten pulse peaks were used in the calculation of the analytical area by:

$$Total\ Analytical\ Area = \#\ of\ pulses \times ACPA - sum\ of\ analytical\ peak\ areas \qquad (E\ 7\text{-}8)$$

The micro liters of gas adsorbed can then be found by:

μL gas adsorbed = total analytical area x calibration value (E 7-9)

The standard deviation of the calibration peak areas (SDCPA) is used to find the error of gas adsorbed:

Error μL gas adsorbed = SDCPA x calibration value (E 7-10)

The micro moles of gas adsorbed per gram of catalyst is then found by:

μmol of gas adsorbed per gram = μL of gas adsorbed / (RT/P) / CW (E 7-11)

where R is the ideal gas constant, T the temperature of adsorption, P the pressure of adsorption, and CW is the weight of the catalyst.

Likewise, the error of micro moles of gas adsorbed is calculated by:

Error μmol of gas adsorbed per gram = Error μL gas adsorbed / (RT/P) / CW (E 7-12)

From the carbon monoxide pulse chemisorption experiments, the metal dispersion of the catalysts can be determined. The percent metal dispersion can then be calculated by:

% Dispersion = (mol CO adsorbed/g cat) x MW / stoich / metal load x 100% (E 7-13)

The % metal loading values obtained from ICP and NAA analyses carried out at NCSU, were used in this calculation. The stoichiometry (atoms of CO adsorbed per metal atom) values were taken from the literature. The stoichiometry for CO on palladium is 0.5, and on platinum is 1 [85-87].

3.3.4 TEMPERATURE PROGRAMMED DESORPTION

Temperature programmed desorption (TPD) is used to determine the temperature of maximum desorption and the activation energy of desorption for a particular adsorbate. The activation energy of desorption is usually determined by using varying coverage. However, this method is not feasible given the Altamira design. Instead, the activation energy of desorption was determined by using varying ramp rates during the desorption process. This method assumes that the surface for adsorption is homogeneous, that readsorption of desorbed gas does not occur, that the concentration of the adsorbate in the gas phase is uniform through the bed, that the desorption rate is first order in coverage and that the temperature increase is linear with time. Using high flow rates helps assure that readsorption of the desorbed gas does not occur. The experimental procedure used a constant ramp rate, which ensures that the temperature increase with time was constant.

The activation energy of desorption can be determined by starting with a mass balance on the desorbing species:

$$-V_m \, d\theta/dt = k_{do} \exp[-E_d/RT] \, \theta \qquad \text{(E 7-13)}$$

where V_m is the volume of a monolayer, θ is the fractional surface the coverage, k_d is the pre-exponential factor for the rate constant, E_d is the activation energy of desorption, R is the ideal gas constant, and T is the temperature. $d\theta/dt$ can be expressed in terms of the ramp rate, β:

$$d\theta/dt = (dT/dt) \, d\theta/dT = (\beta) \, d\theta/dT \qquad \text{(E 7-14)}$$

This can then be substituted into the mass balance (E 7-13), which can be rearranged to give:

$$d\theta/dT = -k_{do}\ \theta \exp[-Ed/RT]/(\beta\ V_m) \qquad \text{(E 7-15)}$$

At the maximum in desorption rate, $d^2\theta/dT^2 = 0$, which gives:

$$[d^2\theta/dT^2] \mid_{Tm} = -\{k_{do}/\beta Vm\}\{d\theta/dT + E_d\theta/RT^2\}\exp[-E_d/RT] \mid_{Tm} = 0 \qquad \text{(E 7-16)}$$

Rearranging (E 7-16) gives:

$$(d\theta/dT) \mid_{Tm} = -\ E_d\theta/(\ RT_m^{\ 2}) \qquad \text{(E 7-17)}$$

Which can be equated to (E 7-15):

$$(d\theta/dT) \mid_{Tm} = -k_{do}\ \theta \exp[-Ed/RT_m]/(\beta\ V_m) = -\ E_d\theta/(\ RT_m^{\ 2}) \qquad \text{(E 7-18)}$$

This can be rearranged to:

$$-E_d/R = \ln(\beta/T_m^{\ 2}) + \ln[E_d\ V_m\ /\ R\ k_{do}] \qquad \text{(E 7-19)}$$

Which can then be put into a linear form:

$$2\ln T_m - \ln\beta = E_d/RT_m + \ln[E_d\ V_m\ /\ R\ k_{do}] \qquad \text{(E 7-20)}$$

The data can then be plotted as $2\ln T_m - \ln\beta$ versus $1/T_m$. From equation (E 7-20), a line fitted to the data will have a slope of E_d/R and an intercept of $\ln[E_d\ V_m\ /\ R\ k_{do}]$.

These experiments were performed using the Altamira system and the online mass spectrometer (MS). Only the alumina support and the two alumina supported catalysts were evaluated. The experiments were run using approximately 0.5 grams of catalyst. This amount of catalyst was required in order to obtain decent desorption peaks. When the typical amount (0.1 grams) was used, the amount of gas adsorbed was too low to see distinct desorption peaks. Due to the large amount of catalyst required for each TPD experiment and the limited amount available, new samples were not used for each experiment. The same sample of each catalyst was used in each set of experiments.

First the catalyst was pretreated in flowing helium at 25 sccm and 25°C for 30 minutes. The temperature was then increased to 400°C at a rate of 10°C per minute. The catalyst was held at 400°C for 30 minutes. The temperature was then decreased back to 25°C at a rate up to 20°C per minute. The catalyst was held at 25°C for 30 minutes. This pretreatment process was used to ensure that the catalyst surface was clean, i.e. no water or previous experimental gas was left on the surface.

Next, the catalyst was exposed to the experimental gas, pure carbon dioxide, pure methane or helium bubbled through glacial acetic acid, at 25 sccm and 25°C for 30 minutes. As determined by the pulse chemisorption experiments, this procedure ensures that 100% coverage is achieved, i.e. that the maximum amount of experimental gas is adsorbed on the surface. Then the catalyst is exposed to helium at 50 sccm and 25°C for 30 minutes in order to remove any physisorbed experimental gas.

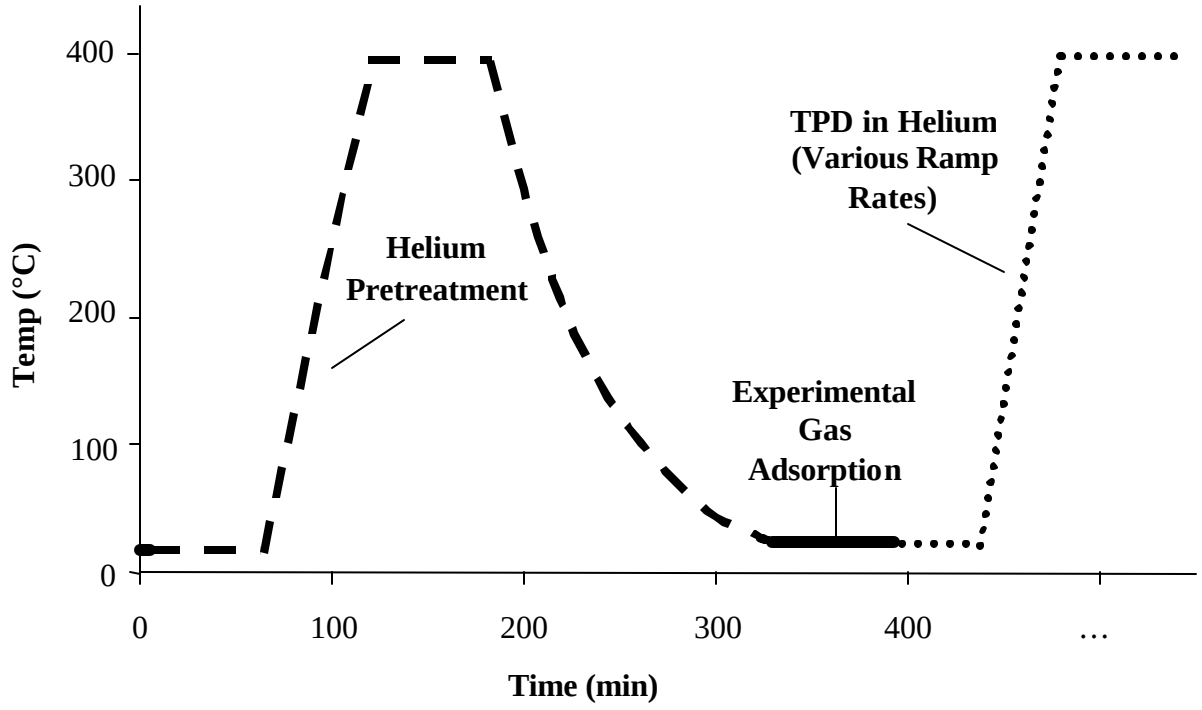

Figure 3-2: TPD Experimental Profile

Finally, the temperature was increased to 400°C at one of four ramp rates (19°C/min, 15°C/min, 10°C/min or 5°C/min). The catalyst was held at 400°C for 30 minutes. Mass spec data for helium (4 m/z), carbon dioxide (44 m/z and 28 m/z), methane (16 m/z and 15 m/z) and acetic acid (43 m/z and 60 m/z) was collected throughout each experiment. A profile of the experimental procedure can be seen in figure 7-3.

For each experiment, the mass spectrum data at each value was plotted versus time and versus temperature. From the plot versus temperature, distinct peaks were visible. The temperature of maximum desorption was determined by finding the local maximum of the peak. A plot was then made of $2\ln T_m - \ln\beta$ versus $1/T_m$. Using JMP statistics software, a

straight line was fitted to the data points. The software gave the slope, intercept, error associated with the slope and intercept and the R^2 value. From equation (E 7-20), the slope is E_d/R and the intercept $\ln[E_d V_m / R k_{do}]$. The activation energy of desorption was calculated by multiplying the slope by the ideal gas constant. The error in the activation energy was calculated by multiplying the error in the slope by the ideal gas constant.

The plot of mass spectrum data versus time from each experiment was used to determine the amount of gas desorbed per gram of catalyst. A standard value of mol gas/unit area was determined from 20 pulse chemisorption peaks through an empty reactor (for carbon dioxide and methane only). The areas under the curves were calculated using the trapezoidal method. These values were compared to the values obtained from the pulse chemisorption experiments.

Finally, the full mass spectrum data was examined to determine if any other desorption species were present.

3.3.5 TRANSMISSION ELECTRON MICROSCOPY

Transmission electron microscopy (TEM) was used to view the surface of the catalysts. From the TEM images, the metal cluster sizes and distribution on the catalyst support can be seen. TEM uses an electron source to bombard the thin sample with electrons. The electrons are then either transmitted through atoms or backscattered. The electrons are scattered by atoms as a result of the Coulomb interaction with the positively charged nucleus and with the negatively charged electron cloud. The amount of backscatter

is proportional to the atomic number[88]. A detector below the sample is used to detect transmitted electrons. This results in an image in which the areas of transmitted electrons are light in color and areas of backscatter are dark. A diagram of the TEM process can be seen in figure 3-3.

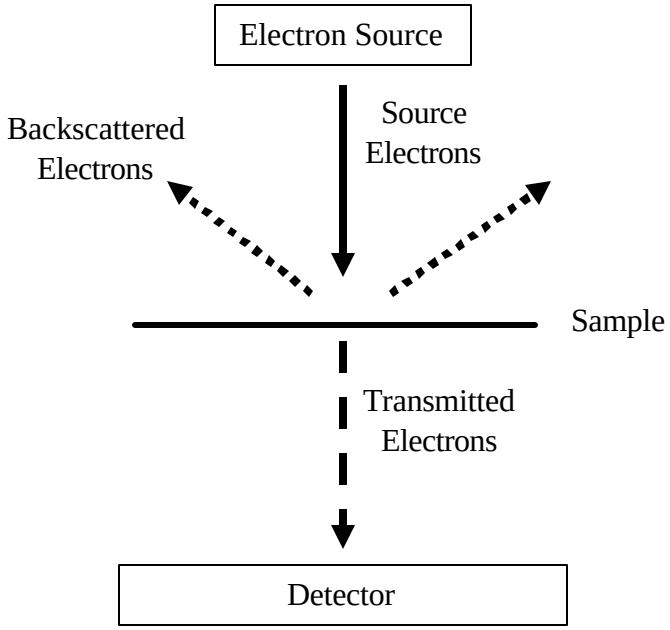

Figure 3-3: TEM Process

3.3.6 Diffuse Reflectance Infrared Fourier Transform Spectroscopy

A Nicolet Magna 560 IR Optical Bench equipped with a high-temperature, high-pressure DRIFTS chamber was used. The chamber was heated using a Spectratech Omega CN8500 temperature control system with a thermocouple placed in the bottom of the sample cup. This temperature control system was not equipped with any digital or analog inputs or

outputs, thus the temperature of the chamber had to be recorded by hand and be adjusted manually with no control over ramp rate. Cooling water continuously flowed through cooling lines on the outside of the chamber to prevent overheating and allow for faster cooling rates. A Tylan 120-28 mass flow controller was used to control the inlet gas flow rate. This controller also did not have any digital or analog input or output, thus requiring manual control and recording. An inline saturator placed after the mass flow controller and before the chamber was used in studies with liquids. For liquid studies, the valves were switched to allow gas flow through the saturator. The IR spectra were recorded using Omnic software.

This system was equipped with both a deuterated triglycerine sulfate (DTGS) and a mercury-cadmium-telluride (MCT) detector. The DTGS detector responds to changes in the temperature of the detector material [89]. The advantages are that it can be used at room temperature, has a high signal/noise ratio, and responds to a wide range of wavelengths ($4000 - 400\ cm^{-1}$) [89]. However, it has a limited sensitivity, and a slow response to intensity changes [89]. The MCT detector uses the energy in the infrared signal to excite electrons in the detector, boosting them into higher energy levels [89]. This detector must be cooled with liquid nitrogen, because at room temperature there is enough energy present to cause random noise [89]. The advantage of this detector is its high sensitivity [89]. However, the range of wavelengths detectable is limited to $4000 - 750\ cm^{-1}$ [89]. Due to the higher sensitivity and faster response rate, the MCT detector was used in all experiments. A flow diagram of the system is shown in figure 3-4.

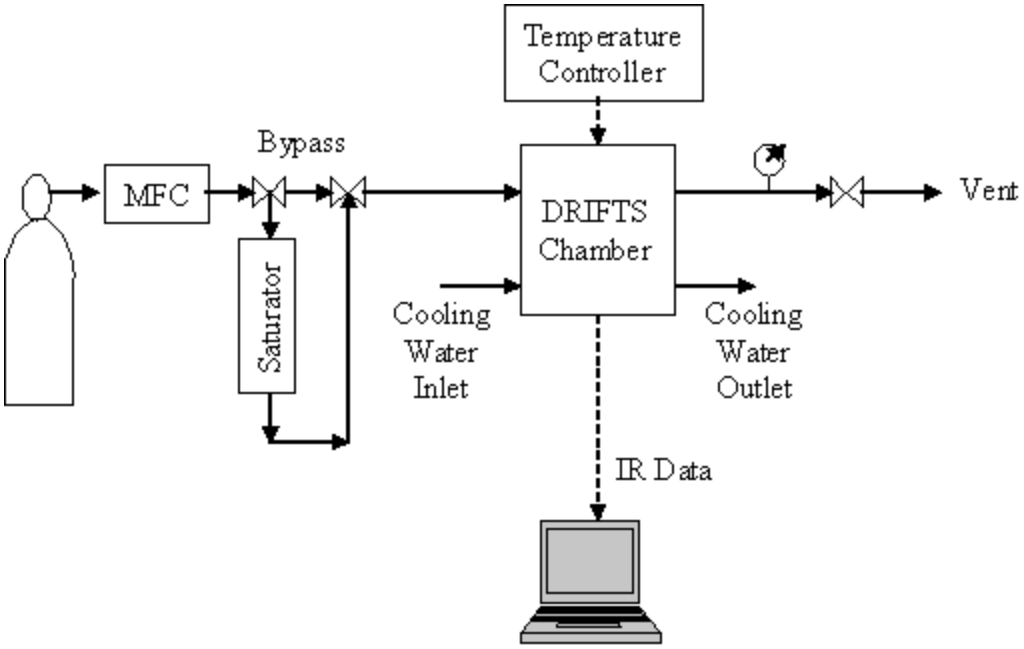

Figure 3-4: Flow diagram of DRIFTS system

Infrared (IR) spectroscopy relies on the IR absorption in molecules. For a molecule to absorb IR, the vibrations or rotations within a molecule must cause a net change in the dipole moment of the molecule [16, 90]. Molecules without dipole moments, such as helium, oxygen and nitrogen, cannot be detected with IR spectroscopy [16, 90]. When the frequency of the IR radiation matches a vibrational frequency, stretches or bendings, in the molecule, the radiation will be absorbed [16, 90]. It is these peaks of IR absorption which are used to determine the molecules present, based on the types of bonds which adsorb IR at the given frequency.

Diffuse reflectance occurs when light impinges on the surface of a material and is partially reflected and transmitted. Light that passes into the material may be absorbed or

reflected out again. The radiation that reflects from an absorbing material is composed of surface-reflected and bulk re-emitted components, which summed are the diffuse reflectance of the sample [9, 16, 91]. The incident beam enters the cell through a KBr window and is diffusely reflected off the sample in all directions. The reflected light is collected over a large angle and directed to the detector. This phenomenon is illustrated in figure 3-5.

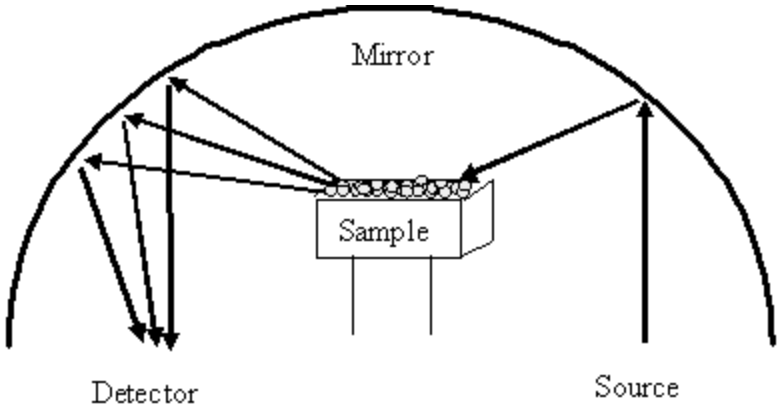

Figure 3-5: DRIFTS Cell

Each catalyst and support was diluted with KBr to 10% in order to reduce the effect of specular reflection, i.e. restrahlen bands [89, 90]. The mixtures were then ground using a mortar and pestle to provide a more even distribution of particle sizes, which yields more accurate spectra [89, 90]. The KBr/catalyst mixture was then placed in the 0.01 gram volume sample cup in the DRIFTS chamber and smoothed using a flat spatula. The DRIFTS chamber top was then tightly fastened to the base and the cooling water lines connected.

For each experiment, the sample was heated to 400°C in a flow of 25 sccm of research grade helium. Once the sample temperature reached 400°C, it was held there for 1 hour to clean the catalyst surface and remove any air and water on the catalyst or in the chamber. Still in flowing helium, the sample was then cooled back down to room temperature and held for 30 minutes. For some experiments, the sample underwent an additional pretreatment. For these pretreatments, the sample was exposed to a 25 sccm flow of either research grade oxygen, research grade hydrogen, research grade methane or research grade carbon dioxide at 25 °C for 2 hours. If an additional pretreatment was used, the sample was then exposed to a 25 sccm flow of research grade helium for 30 minutes to flush out any remaining pretreatment gas. Unless otherwise noted no additional pretreatment was used.

After the pretreatment, a background spectrum was taken at 25°C in a 25 sccm flow of research grade helium. This spectrum, as well as all others taken, was automatically converted by the software into an absorbance spectrum. The software then automatically "subtracted" the absorbance background spectrum from any further absorbance spectra taken. This procedure is done to eliminate the water peaks which occur due to the water vapor in the air in the IR path through areas other than the DRIFTS chamber.

The sample was then exposed to a 25 sccm flow of the experimental gas. For the reaction experiments a premixed 50% carbon dioxide and 50% methane gas mixture was used. The pure acetic acid experiments used a flow of research grade helium through a saturator filled with glacial acetic acid.

Under the 25 sccm flow of the experimental gas, the sample was kept at 25°C temperature for 30 minutes. Still in the flowing experimental gas, the temperature was increased to 50°C, 100°C, 150°C, 200°C, 250°C, 300°C, 350°C and 400°C incrementally. The sample was held at each temperature for 30 minutes before increasing the temperature again. Absorbance spectra were taken every 5 minutes during this entire experimental portion. After each experiment, the sample was cooled back down to room temperature and the sample removed from the DRIFTS chamber. The experimental profile is shown in figure 3-6.

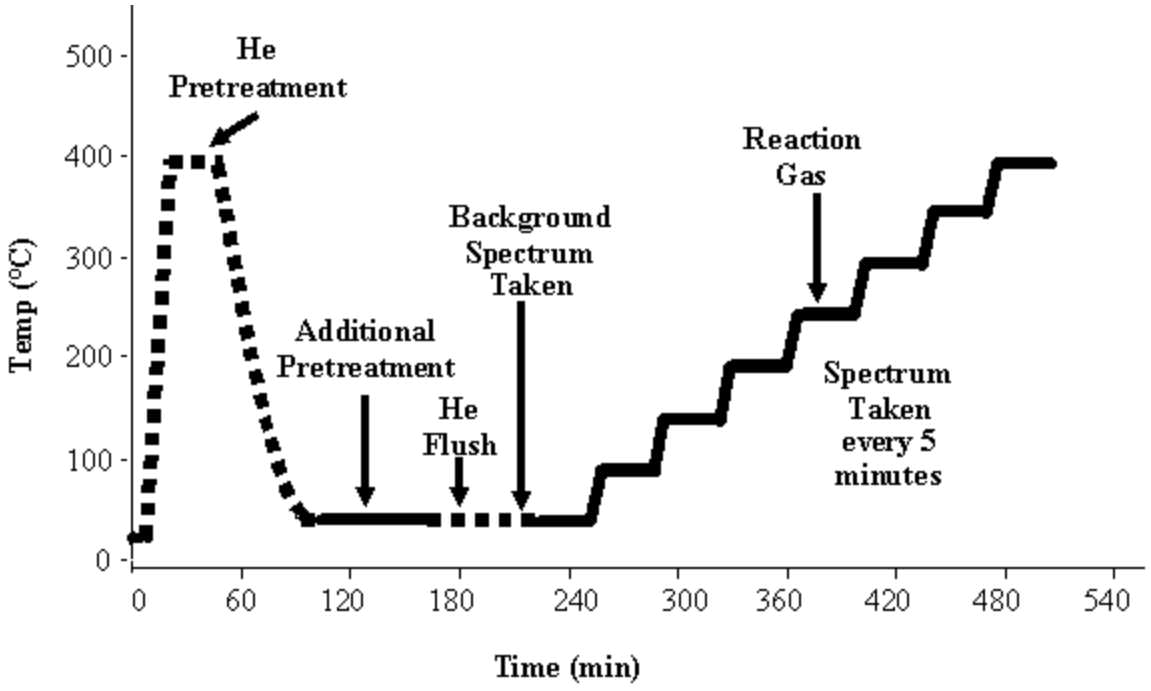

Figure 3-6: DRIFTS experimental profile

While the system was designed for high pressure experiments, none were conducted. When high pressure or sealed cell experiments were attempted, a crack was discovered in the DRIFTS chamber, and the experiments could not be run properly. Calibrations of the peak intensities to be able to qualitatively determine the amount of a given compound present was not possible given the setup. This calibration would have required running the experimental gases at different concentrations, which was not possible with only one mass flow controller.

3.3.7 Flow Through Reactor Experiments

An Altamira AMI 1 reaction system equipped with a thermal conductivity detector and online mass spectrometer was used. Switching valves were used to select from one of three treatment gases, whose flow was then adjusted by a Tylan™ mass flow controller. The selected treatment gas could either flow through a sample loop, to be used for pulse experiments, or through the catalyst bed. After the reactor, the treatment gas went directly to a vent line. An Omega™ three gas mixing rotameter placed before the inlet was used to mix pure gases. For experiments using liquids, saturators immediately prior to the reactor tube were used. Each gas individually flowed through separate AllTech ™ purifiers to remove any water, oxygen and C_2+ hydrocarbons.

The flow for a single carrier gas for the thermal conductivity detector (TCD) was adjusted using a MKS™ mass flow controller. After the mass flow controller, the carrier gas flowed through the reference side of the TCD. The carrier gas could then either flow directly to the reactor and to the sample side of the TCD, or through the sample loop, into the reactor

and through the sample side of the TCD. A flow diagram of the Altamira system is shown in figure 3-7.

The powder catalyst sample was placed between two quartz wool plugs, used to keep the sample in place and prevent it from contaminating the system, in a 1/8" quartz reactor tube. A furnace was raised up around the reactor tube. To provide good thermal conductivity, the furnace was filled with ceramic beads. To measure the sample temperature, a thermocouple was placed in the reactor tube touching the sample. The temperature was controlled by a second thermocouple placed in the furnace. This system was not equipped to be pressurized, therefore all pressures were atmospheric.

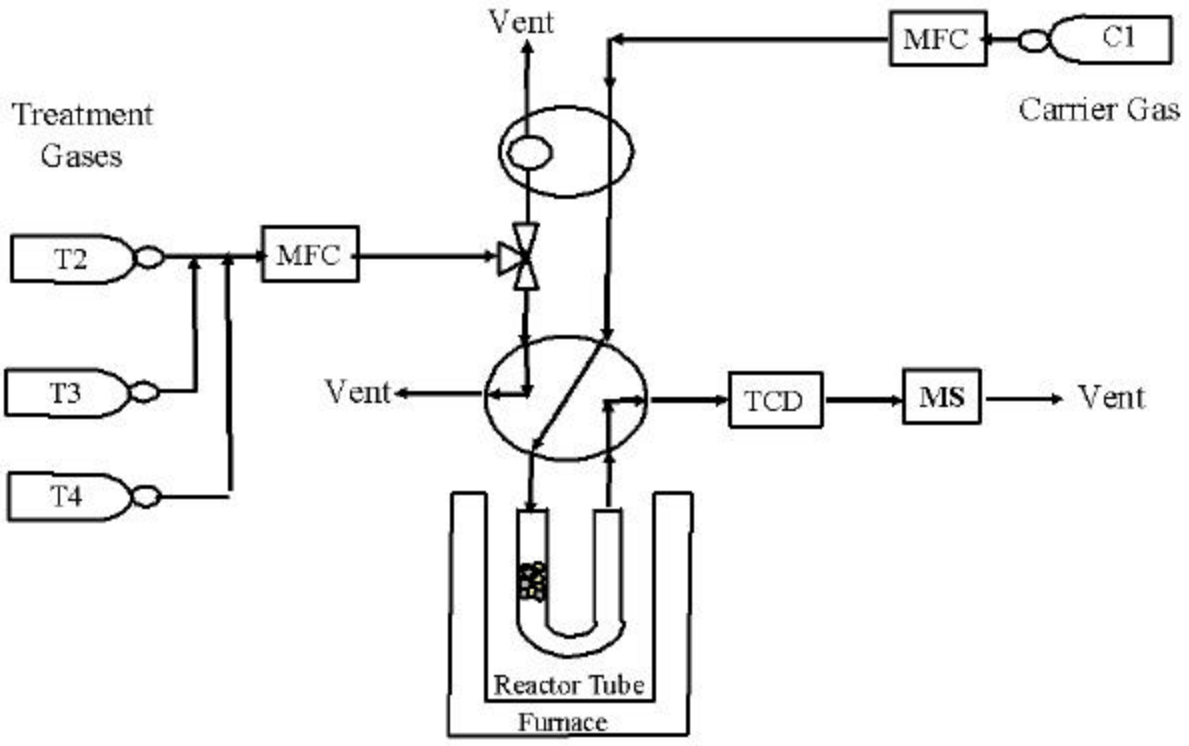

Figure 3-7: Flow diagram of Altamira reaction system

An Ametek™ quadrupole mass spectrometer with up to 100 mass-to-charge ratio (m/z) capability was used to determine the composition of the outlet gas. A capillary tube placed in the outlet side of the quartz reactor tube was used to constantly feed a sample of the outlet gas to the mass spectrometer.

Altamira software was used to control the selection of the treatment gases, flow rates of the treatment and carrier gases and the temperature of the furnace. The experimental profiles were programmed into the software. This software was also used to record the flow rates, temperature and TCD output. Dycor™ software was used to control the mass spectrometer and record the mass spectrometer data.

As indicated by the name, a thermal conductivity detector uses the difference in thermal conductivities between a carrier gas stream and that of the sample gas stream to give quantitative analysis of the sample [92]. The gases flow over electrically heated tungsten wires. The thermal conductivity is detected by changes in the resistance of the wire due to temperature changes of the wire, which results from the thermal conductivity change of the gas. Thermal conductivity detectors require known sample gas volume standards for calibration. A major draw back to thermal conductivity detectors is that they can only be used for quantitative analysis, and not qualitative analysis.

A mass spectrometer consists of three main elements: an ion source, a mass analyzer and a detector, all contained in a vacuum chamber. A heated tungsten filament gives off electrons which then collide with a molecule [92-94]. This collision knocks off an electron in the molecule to give a positive ion. These collisions can produce either a molecular ion or it can produce a fragment ion. The electrons are then collected by an electron trap, which is a

positively charged metal plate, and the positive ion fragments are deflected to the detector by an ion repeller, which is another slightly positively charged metal plate.

A quadrupole mass filter was used as the mass analyzer. A quadrupole mass filter consists of two pairs of metal rod electrodes arranged in a cross configuration [92-94]. Opposite rods are connected electrically, with one pair attached to the positive side of a variable dc source and the other pair to the negative terminal. A variable radio-frequency (RF) ac potential is applied to each pair of electrodes. At a given RF potential and dc current, an ion will either be attracted to the rods, thus neutralizing the fragment which is then carried away, or it will be defected by the rods and sent to the detector. Specific molecular weight molecules can then be selectively filtered and sent to the detector by adjusting the RF potential and dc current.

A Faraday cup detector is aligned with the filter, so that ions exiting the filter will strike the collector electrode [92-94]. This electrode is surrounded by a cage that prevents reflected ions and ejected secondary electrons from escaping. The electrode and cage are connected to a ground potential through a large resistor. When the ion strikes the negatively charged electrode, it is neutralized by the flow of electrons from the ground through the resistor. It is the magnitude of the resulting potential drop across the resistor which is measured and converted into partial pressure.

Each molecular compound gives a unique mass spectrum based upon how it fragments and the amount of fragmentation. The chemical composition of a sample can be determined by analyzing the partial pressures of the m/z peaks in the mass spectrum.

The same catalysts that were tested in the DRIFTS experiments were used in these reaction experiments. These include a reduced 5% Pd/carbon, un-reduced 5% Pd/carbon, 5% Pd/alumina and 5% Pt/alumina. Information about the catalysts can be found in section 5-4.

For each experiment, approximately 0.5 grams of fresh sample was packed between fresh quartz wool plugs in the quartz reactor tube. The sample was then pretreated in a flow of 50 sccm research grade helium for 30 minutes. The temperature was raised to 400°C at 20°C/min and held for 1 hour in the flow of helium. The sample was then cooled back down to 50°C and held for 30 minutes. This pretreatment was used to clean the catalyst surface and remove any air or water vapor from the reactor tube. The same pretreatment was used in the DRIFTS experiments discussed in chapter 5. For some experiments, an additional pretreatment at 50°C for 30 minutes in a 50 sccm flow of research grade carbon dioxide was used.

After the pretreatment, the sample was exposed to a 50 sccm flow of the experimental gas. The experimental gas consisted of either pure research grade methane, or varying ratios of research grade carbon dioxide and research grade methane. Mixtures of approximately 25% carbon dioxide and 75% methane, 50% carbon dioxide and 50% methane, and 75% carbon dioxide and 25% methane were prepared using the mixing rotameter, research grade carbon dioxide, and research grade methane. The sample was exposed to the experimental gas at 50°C for 30 minutes. With the experimental gas still flowing, the temperature was increased to 400°C at a rate of 20°C/minute. The temperature was held at 400°C for 1 hour. The sample was then cooled down to 50°C in the flow of experimental gas. The experimental profile can be seen in figure 6-2. The helium, methane and carbon dioxide

were all run through separate AllTech™ gas purifiers placed immediately after the cylinders to remove any water, oxygen or C2+ impurities.

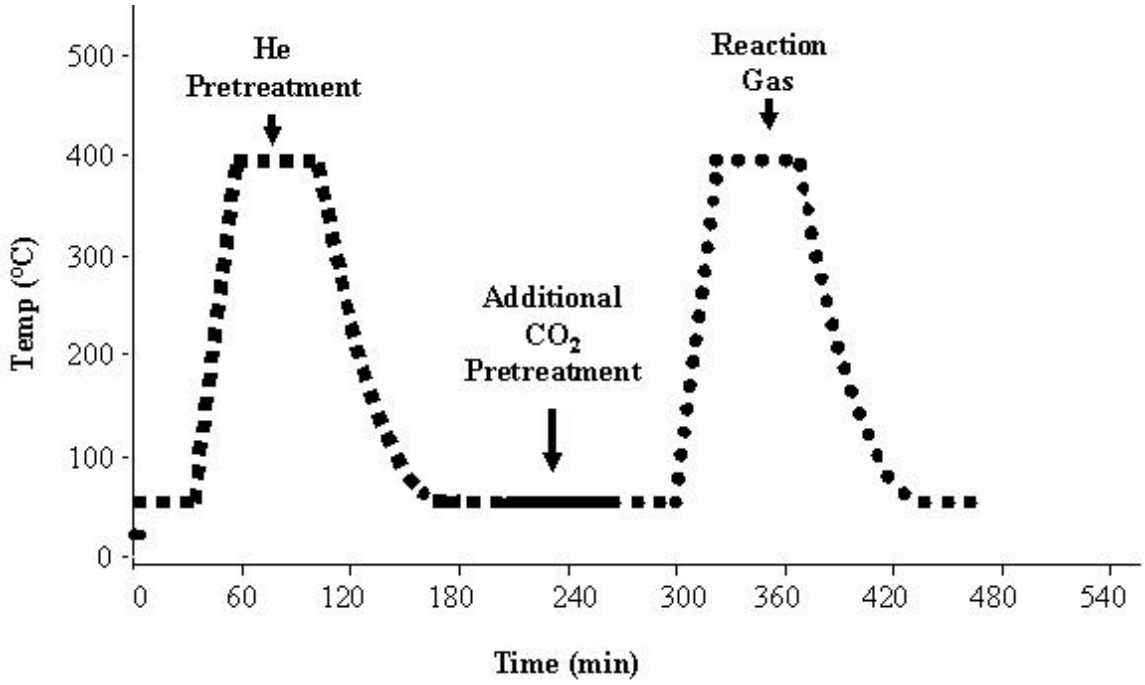

Figure 3-8: Reaction experimental profile

The exiting experimental gas was continuously analyzed using the online quadrupole mass spectrometer. An analog mass spectrum from 1 – 100 m/z was recorded using the Dycor™ software continuously throughout the entire experiment. The flow rates and temperatures were recorded throughout the experiment using the Altamira software.

For each experiment, the Altamira™ data files were converted into excel spreadsheets. The flow rates were examined to ensure that no major fluctuations occurred. The temperature of the sample and corresponding time was then saved in a new spreadsheet.

The mass spectrum data was first analyzed using the Dycor™ software. The mass spectrum was examined for any m/z peaks associated with compounds other than helium, carbon dioxide, methane and acetic acid. In order to obtain the value of individual m/z peaks for each sampling time, a Perl data filter program was used to sort through the comma delimited converted Dycor™ data files. The following m/z values were chosen: 2 m/z for hydrogen, 4 m/z for helium, 16 m/z for methane, 18 m/z for water, 28 m/z for carbon monoxide, 44 m/z for carbon dioxide and 60 m/z for acetic acid. These m/z values are those corresponding to the largest fraction displayed by each molecule [95, 96], except acetic acid. A 43 m/z value is the largest fraction for acetic acid and 45 m/z the next largest[95, 96], however, due to the large amount of carbon dioxide in the system, it was found that the 44 m/z peak of carbon dioxide interfered with the 43 m/z of acetic acid and carbon dioxide also displays a fraction at 45 m/z. Thus the third largest m/z fraction for acetic acid, 60 m/z [95, 96], was chosen. Mass spectra of these pure components are given in Appendix D.1.

The recorded partial pressure value for each m/z and each sampling time were then inserted into the temperature spreadsheet. Due to the inaccuracy of the mixing rotameter, the mass spectrometer could not be calibrated. Instead literature values were used for the sensitivity factors. These sensitivity factors are a ratio of the sensitivity of the mass spectrometer to a given compound with respect to nitrogen. The sensitivity factors used were: 0.23 for helium, 0.9 for carbon dioxide, 1.08 for methane, 1.09 for carbon dioxide, 0.7 for hydrogen and 1.17 for water [97]. A selectivity factor for acetic acid could not be found, so a value of 1.00 was used.

The partial pressure data for each m/z was then divided by the corresponding selectivity factor to give a more accurate value. The total pressure for each sampling time was calculated by summing the partial pressures for each m/z. The mole fraction for each component was calculated by dividing the partial pressure of the component by the total pressure. Plots were made of the mole fractions versus time and also the temperature versus time.

Using the ideal gas law and the inlet volumetric flow rate, the total inlet molar flow rate was calculated. The outlet molar flow rates were calculated using mass balances assuming the dry reforming reaction. The total fractional conversion of methane was calculated by subtracting the outlet molar flow of methane from the inlet molar flow of methane and dividing by the inlet molar flow of methane. The fractional conversion of methane to acetic acid was calculated by dividing the amount of methane reacted to acetic acid from the inlet molar flow of methane. The outlet molar flow rate of acetic acid was used as the amount of methane reacted to acetic acid. The outlet mole fraction of acetic acid for this calculation was adjusted by subtracting the baseline mole fraction of acetic acid. The outlet molar flow was then calculated by multiplying the adjusted mole fraction by the total outlet flow rate. The total fractional conversion of methane and the fractional conversion of methane to acetic acid have some error associated with assuming that the direct synthesis reaction and reverse water gas shift reaction occur to an insignificant amount compared to the dry reforming reaction.

3.4 RESULTS & DISCUSSION

The metal loadings of the alumina supported catalysts were reported to be 5 wt% by the manufacturer, Johnson Matthey. The ICP analyses conducted at NCSU verified that the metal loading was indeed approximately 5 wt% for both the Pd/alumina and Pt/alumina catalysts. Calgon Carbon reported a 5 wt% metal loading for both the reduced and un-reduced catalysts. The ICP analyses conducted at NCSU found that the un-reduced Pd/carbon catalyst only had a 3.35 wt% metal loading, and the reduced Pd/carbon catalysts a 3.26 wt% metal loading. The NAA analyses conducted at NCSU agreed with the ICP. The NAA analyses gave a 3.52 wt% metal loading for the un-reduced catalyst and a 3.41 % metal loading for the reduced catalyst. The results obtained from the ICP and NAA analyses can be found in table 3-2.

Table 3-2: Metal loading of catalysts determined at NCSU by ICP and/or NAA

Catalyst	Carbon Support	5% Pd/C Red.	5% Pd/C Not Red.	Alumina	5% Pd/Al	5% Pt/Al
ICP % Metal Loading	**N/A**	**3.26 %**	**3.35 %**	**N/A**	**4.98 %**	**4.95 %**
ICP Error	N/A	0.16 %	0.10 %	N/A	0.12 %	0.16 %
NAA % Metal Loading	**N/A**	**3.41 %**	**3.52 %**	**N/A**	**N/A**	**N/A**
NAA Error	N/A	0.33 %	0.34 %	N/A	N/A	N/A

Background surface area and pore volume experiments were run to ensure that the degassing procedure was adequate, that the glass tube and quartz wool did not contribute to the weight change of the sample during the degassing procedure, that the glass tube and quartz wool did not contribute to the surface area or pore volume values, and that the system was working properly.

To ensure that the degassing procedure was adequate, the total weight of a sample was measured every 15 minutes during degassing. After one hour, no further weight change was observed. Therefore, it was concluded that the 2 hour degas was sufficient.

To ensure that the glass tube and the quartz wool do not contribute a significant amount during the degassing process, the glass tube alone and a glass tube with approximately the same amount of quartz wool used in the experiments underwent the degas process. The glass tube alone showed no weight change after degas process. The weight change observed from the quartz wool was only 0.0002 grams. It was concluded that no significant weight change occurs during the degas process due to the glass tube or the quartz wool.

The surface area and pore volume experiments then were conducted on an empty tube and a tube with approximately the same amount of quartz wool as used in the experiments. For both the empty tube and the tube with quartz wool, the surface area measured was 0.00 and the pore volume was 0.00. Therefore neither the glass tube nor the quartz wool contribute to the surface area or pore volume values.

Surface area and pore volume experiments were also run on standard samples provided by Micromeritics. The results obtained were within the given limits, indicating that the FlowSorb II 2300 system was working properly.

There was a significant difference between the measured surface areas of the alumina supported catalysts and the carbon supported catalysts. The carbon supported catalysts had surface areas almost twice that of the alumina supported catalysts. The alumina support, 5% Pd/alumina and 5% Pt/alumina all had similar surface areas. The alumina support had a

slightly higher surface area than that of the alumina supported catalysts. The carbon support and the carbon supported catalysts showed a greater difference. The un-reduced 5% Pd/carbon catalyst had the largest surface area. The carbon support had the next highest, and the reduced 5% Pd/carbon catalyst had the lowest of the carbon based materials. The reduced 5% Pd/carbon catalyst surface area was more than 150 m^2/g lower than that of the un-reduced 5% Pd/carbon catalyst, and more than 100 m^2/g lower than that of the carbon support alone. This indicates that either the reduced catalyst was not made in the same batch as that of the un-reduced catalyst (as reported by Calgon-Carbon) or that the reduction process significantly reduced the surface area of the catalyst. The surface area data can be found in table 3-3.

Table 3-3: Surface area values for catalysts

Catalyst	Carbon Support	5% Pd/C Red.	5% Pd/C Not Red.	Alumina	5% Pd/Al	5% Pt/Al
Surface Area (m^2/g)	**602.7**	**503.6**	**660.9**	**283.3**	**278.8**	**274.3**
2% Error (m^2/g)	12.1	10.1	13.2	5.7	5.6	5.5

The pore volume of the carbon supported catalysts was slightly higher than that of the alumina supported catalysts. The alumina support and alumina supported catalysts had similar pore volumes. The carbon support and carbon supported catalysts also had similar pore volumes. Pore volume data can be found in table 3-4.

Table 3-4: Pore volume values for catalysts

Catalyst	Carbon Support	5% Pd/C Red.	5% Pd/C Not Red.	Alumina	5% Pd/Al	5% Pt/Al
Pore Volume (cm^3/g)	**0.54**	**0.48**	**0.50**	**0.46**	**0.42**	**0.45**
3% Error (cm^3/g)	0.02	0.01	0.02	0.01	0.01	0.01

As determined by pulse chemisorption, the alumina supported catalysts adsorbed a much greater amount of carbon monoxide than the carbon supported catalysts. Neither the carbon support nor the alumina support alone adsorbed any carbon monoxide. The 5% Pd/alumina catalyst adsorbed the most carbon monoxide, 84.18 μmol CO/g. The 5% Pt/alumina adsorbed the second most, 70.46 μmol CO/g, followed by the un-reduced 5% Pd/carbon, 13.83 μmol CO/g, and the reduced catalyst, 7.90 μmol CO/g. The 5% Pd/alumina and 5% Pt/alumina had a much greater metal dispersion (31.2% and 27.5% respectively) than the un-reduced and reduced 5% Pd/carbon catalysts (6.88% and 3.10% respectively). The significant difference in the metal dispersion between the alumina supported and carbon supported catalysts may contribute to the difference in the effectiveness of the catalysts for the direct synthesis of acetic acid reaction. The values of the carbon monoxide adsorption and the metal dispersion for the catalysts can be found in table 3-5.

Table 3-5: CO adsorption and metal dispersion

Catalyst	Carbon Support	5% Pd/C Red.	5% Pd/C Not Red.	Alumina Support	5% Pd/Al	5% Pt/Al
mmol CO/g	**0.11**	**7.90**	**13.8**	**0.13**	**84.2**	**70.5**
Error μmol CO/g	0.33	0.06	0.34	0.21	0.66	0.13
Metal Dispersion	**N/A**	**3.10%**	**6.88%**	**N/A**	**31.2%**	**27.5%**
Error (Metal Dispersion)	N/A	0.03%	0.17%	N/A	0.26%	0.05%

The carbon support and the reduced 5% Pd/carbon catalyst did not adsorb any carbon dioxide. The un-reduced 5% Pd/carbon catalyst adsorbed only 4.20 μmol CO_2/g. The alumina support alone had the greatest amount of carbon dioxide adsorption, 77.3 μmol CO_2/g. The 5% Pd/alumina and 5% Pt/alumina catalysts adsorbed 21.0 and 31.0 μmol CO_2/g respectively.

Since the alumina supported catalysts adsorbed less carbon dioxide than the alumina support alone, it appears that the carbon dioxide adsorbs to the alumina support rather than the metal. The values of carbon dioxide adsorption for each of the supports and catalysts can be found in table 3-6.

Table 3-6: CO_2 adsorption values

Catalyst	Carbon Support	5% Pd/C Red.	5% Pd/C Not Red.	Alumina Support	5% Pd/Al	5% Pt/Al
mmol CO_2/g	**0.30**	**0.43**	**4.20**	**77.3**	**21.0**	**31.0**
Error μmol CO_2/g	0.43	0.11	0.29	0.51	0.50	0.49

The carbon dioxide TPD experiments further confirmed that the carbon dioxide adsorbs on the alumina rather than the metals. The temperatures of maximum desorption, T_m, for the samples at each ramp rate, β, are no more than 2°C different. The activation energies of desorption, E_d, for carbon dioxide on all three samples are within the error limits of each other. The similar T_ms and E_ds suggest that the adsorbed species is the same on all three samples. Since the alumina adsorbs carbon dioxide and the adsorbed species is the same on the alumina and alumina supported catalysts, the carbon dioxide must be adsorbing on the alumina support, rather than the metals, on the two catalysts. The T_ms can be found in table 3-7, the activation energies in table 3-8.

Table 3-7: T_ms from CO_2 TPDs on alumina support and alumina supported catalysts

β (°C/min)	Alumina T_m (°C)	5% Pd/Alumina T_m (°C)	5% Pt/Alumina T_m (°C)
19.07	90.3	90.3	89.9
15.25	85.5	87.7	85.5
10.17	80.6	81.7	80.6
5.08	73.3	73.2	72.6

Table 3-8: E_ds from CO_2 TPDs on alumina support and alumina supported catalysts

	Alumina	5% Pd/Alumina	5% Pt/Alumina
E_d (kJ/mol)	**76.75**	**74.15**	**75.41**
Error (kJ/mol)	7.45	4.92	5.02

From the integration of the mass spectrometer signal over time, it was determined that the amount of carbon dioxide adsorbed per gram is a bit less than that calculated from the pulse chemisorption experiments. This suggests that some of the adsorbed carbon dioxide in the pulse chemisorption experiments was physisorbed rather than chemisorbed. Also, the

carbon dioxide desorbed for each ramp rate was also very similar. This indicates that the pretreatment was adequate to regenerate the catalyst surface. The amount of carbon dioxide desorbed per gram for each of the catalysts at each ramp rate can be found in table 3-9.

Table 3-9: μmol CO_2 /g adsorbed from TPD experiments

β (°C/min)	Alumina μmol CO_2/g	5% Pd/Alumina μmol CO_2/g	5% Pt/Alumina μmol CO_2/g
19.07	71.18	20.25	29.58
15.25	67.58	19.99	29.67
10.17	69.95	19.22	29.31
5.08	68.75	19.09	30.05

The full mass spectrum taken during the experiments showed only helium and carbon dioxide. Therefore, the carbon dioxide that adsorbs onto the surface is removed as carbon dioxide rather than carbon monoxide or another species.

The alumina and carbon supports alone and the reduced 5% Pd/carbon catalysts did not adsorb any methane, determined by pulse chemisorption. The un-reduced 5% Pd/carbon catalyst adsorbed only 1.07 μmol CH_4/g. The 5% Pd/alumina and 5% Pt/alumina catalysts adsorbed 12.6 and 32.7 μmol CH_4/g respectively. The lack of methane adsorption on the alumina support and the large amount of methane adsorption on the alumina supported catalysts indicates that the methane adsorbs on the metal rather than the support. The values of methane adsorption for each of the supports and catalysts can be found in table 3-10.

Table 3-10: CH_4 adsorption values

Catalyst	Carbon Support	5% Pd/C Red.	5% Pd/C Not Red.	Alumina Support	5% Pd/Al	5% Pt/Al
mmol CH_4/g	**0.26**	**0.56**	**1.07**	**0.48**	**12.6**	**32.7**
Error μmol CH_4/g	0.63	0.59	0.12	0.61	0.86	1.92

As expected from the pulse chemisorption experiments, no methane desorption peaks were observed for the alumina support during TPD. This further confirms that the methane adsorbs to the metal rather than the alumina. Both the 5% Pd/alumina and 5% Pt/alumina catalysts had two distinct methane desorption peaks. This suggests that methane was adsorbed to two different sites, or in two different configurations on the same type of site.

While both the 5% Pd/alumina and 5% Pt/alumina catalysts had two desorption peaks for methane, the T_ms and activation energies were different for each catalyst. This indicates that the methane bonds differently to the different metals.

The activation energy of desorption for both the methane species on the 5% Pd/alumina catalyst were higher than those of the 5% Pt/alumina. Perhaps this difference in methane adsorption influences the effectiveness of the catalyst in the direct synthesis reaction. The T_ms can be found in table 3-11, the activation energies in table 3-12.

Table 3-11: T_ms from CH_4 TPDs on alumina supported catalysts

β (°C/min)	Peak 1 5% Pd/Alumina T_m (°C)	Peak 2 5% Pd/Alumina T_m (°C)	Peak 1 5% Pt/Alumina T_m (°C)	Peak 2 5% Pt/Alumina T_m (°C)
19.07	94.77	226.89	92.23	213.62
15.25	89.98	219.73	86.75	205.08
10.17	85.44	213.48	76.25	197.75
5.08	78.65	206.95	64.89	187.77

Table 3-12: E_ds from CH_4 TPDs on alumina supported catalysts

	Peak 1 5% Pd/Alumina	Peak 2 5% Pd/Alumina	Peak 1 5% Pt/Alumina	Peak 2 5% Pt/Alumina
E_d (kJ/mol)	**84.1**	**123.5**	**43.3**	**89.1**
Error (kJ/mol)	9.0	13.3	3.4	12.7

From the integration of the mass spectrometer signal over time, it was determined that the amount of methane desorbed per gram is nearly the same as that calculated from the pulse chemisorption experiments. The methane desorbed for each ramp rate was also very similar. This indicates that the pretreatment was adequate to regenerate the catalyst surface. The amount of methane desorbed per gram for each of the catalysts at each ramp rate can be found in table 3-13.

Table 3-13: μmol CH_4 /g adsorbed from TPD experiments

β (°C/min)	Alumina μmol CH_4/g	5% Pd/Alumina μmol CH_4/g	5% Pt/Alumina μmol CH_4/g
19.07	Undetectable	12.13	28.93
15.25	Undetectable	11.76	29.56
10.17	Undetectable	11.87	28.34
5.08	Undetectable	12.35	29.21

The full mass spectrum taken during the experiments showed only helium and methane. Therefore, the methane that adsorbs onto the surface is removed as methane rather than hydrogen or other species. This also indicates that methane does not decompose to carbon and hydrogen at these temperatures.

The acetic acid TPD experiments resulted in two distinct desorption peaks for both the alumina support and the alumina supported catalysts. At the lower temperature, the adsorbed acetic acid desorbs as acetic acid. At the higher temperature, the adsorbed acetic acid is decomposed into carbon dioxide and methane.

The alumina supported catalysts had similar T_ms and E_ds for the lower temperature desorption peak. The alumina support had slightly lower T_ms and E_d for the low temperature peak. It is likely that the supported catalysts have a similar adsorbed acetate species, while the alumina has a slightly different adsorbed species.

Since the adsorbed acetate decomposes at higher temperatures, the T_ms and E_ds for the high temperature desorption peak were determined from the carbon dioxide and methane values, which were similar. The T_ms for the high temperature peaks on the alumina support and alumina supported catalysts were similar, as were the activation energies of desorption. For this high temperature peak, the adsorbate is similar, or the method of decomposition is the same. The T_ms can be found in table 3-14, the activation energies in table 3-15.

Table 3-14: T_ms of acetic acid TPDs on alumina supported catalysts

β (°C/min)	Peak 1 Alumina T_m (°C)	Peak 1 5% Pd/Al T_m (°C)	Peak 1 5% Pt/Al T_m (°C)	Peak 2 Alumina T_m (°C)	Peak 2 5% Pd/Al T_m (°C)	Peak 2 5% Pt/Al T_m (°C)
19.07	164.35	194.75	194.86	371.58	370.43	368.65
15.25	159.87	187.99	189.99	369.87	367.10	365.77
10.17	154.25	181.66	183.73	357.98	354.58	354.98
5.08	149.48	174.45	178.54	347.58	346.46	348.57

Table 3-15: E_ds of acetic acid TPDs on alumina supported catalysts

	Peak 1 Alumina	Peak 1 5% Pd/Al	Peak 1 5% Pt/Al	Peak 2 Alumina	Peak 12 5% Pd/Al	Peak 2 5% Pt/Al
E_d (kJ/mol)	**106**	**127**	**132**	**160**	**159**	**170**
Error (kJ/mol)	17	22	23	19	25	21

The amount of desorbed acetic acid could not be determined from these experiments. While the amount of carbon dioxide or methane desorbed could be used to calculate the amount of acetic acid adsorbed, the desorption was not complete, even after 30 minutes at 400°C.

The full mass spectrum taken around 400°C showed the presence of ketene and water. This suggests that in addition to the decomposition of acetic acid to carbon dioxide and methane, that the adsorbed acetate decomposed to ketene and water. This occurred on the alumina support as well as the two alumina supported catalysts. The full mass spectrum also showed stronger carbon dioxide and methane peaks than ketene and water. While the decomposition to ketene and water occurs, the decomposition to carbon dioxide and methane is preferred.

The TEM images show distinct differences between the carbon supported catalysts and the alumina supported catalysts. The carbon supported catalysts had large metal clusters, which were far apart from each other on the carbon support. The alumina catalysts had very small metal clusters close together on the alumina support.

The TEM image for the reduced 5% Pd/carbon catalyst, figure 3-9, shows that the palladium clusters range from about 5 nm to 50 nm. More than half of the clusters seen in the image are larger than 25 nm in size. The palladium clusters are far apart from each other on the support with distances up to 100 nm apart. In a 200 nm x 200 nm region, there were fewer than 20 clusters observed.

The un-reduced 5% Pd/carbon catalyst, figure 3-10, has palladium clusters that range from about 10 nm up to 100 nm. Most of the clusters are larger than 25 nm. The clusters are not well dispersed over the support. There are some areas with many large clusters, and areas with many small clusters. The large clusters tend to be near other large clusters. In a 200nm by 200 nm region with smaller clusters, there are less than 40 clusters.

The 5% Pd/Alumina catalyst, figure 3-11, has very fine palladium clusters, ranging from about 1 nm to 5 nm. The clusters are also very close to each other and widely dispersed on the catalyst surface. The support is well covered by the palladium with few areas with a low cluster density. However, the palladium does not completely cover the alumina, which would allow interaction between adsorbed species on the alumina and adsorbed species on the palladium.

The 5% Pt/Alumina catalyst, figure 3-12, has very fine platinum clusters. The cluster sizes range from about 1 nm to 5 nm. The clusters are also very close to each other and

widely dispersed on the catalyst surface. The support is well covered by the platinum with few areas with a low cluster density. The platinum does not completely cover the alumina, which would allow interaction between adsorbed species on the alumina and adsorbed species on the platinum.

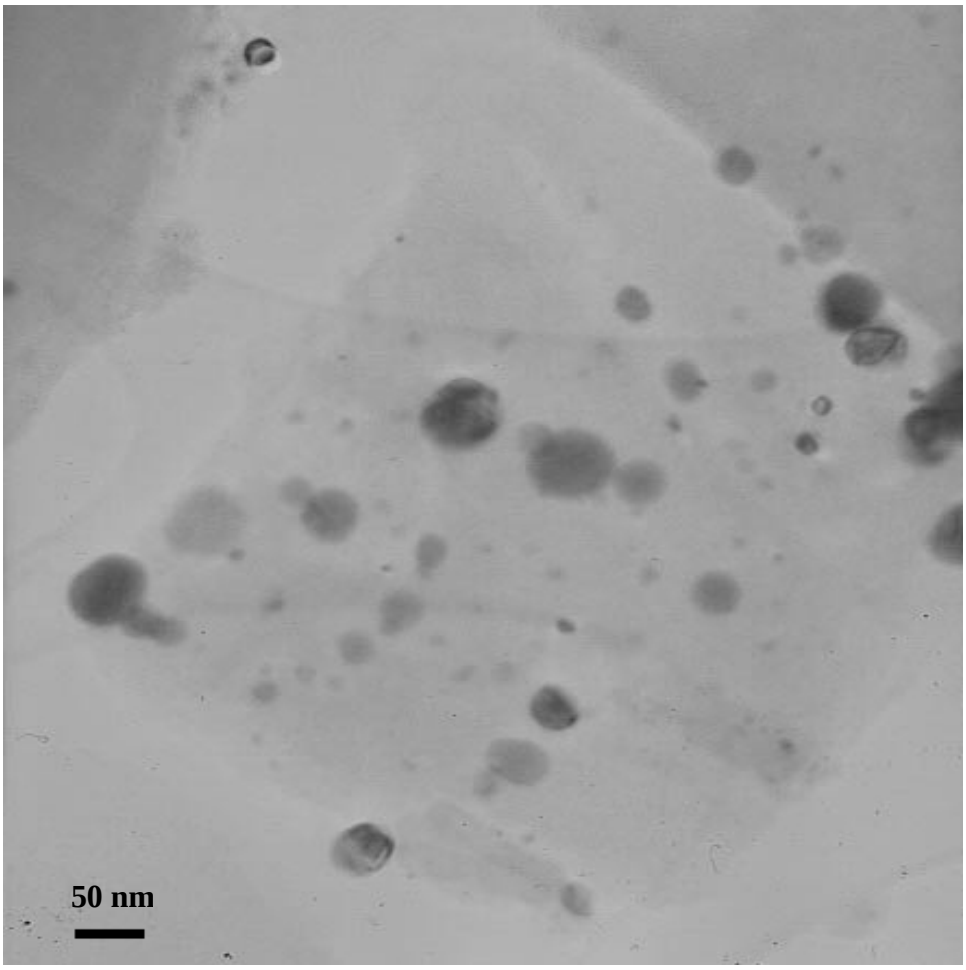

Figure 3-9: TEM of reduced 5% Pd/Carbon catalyst

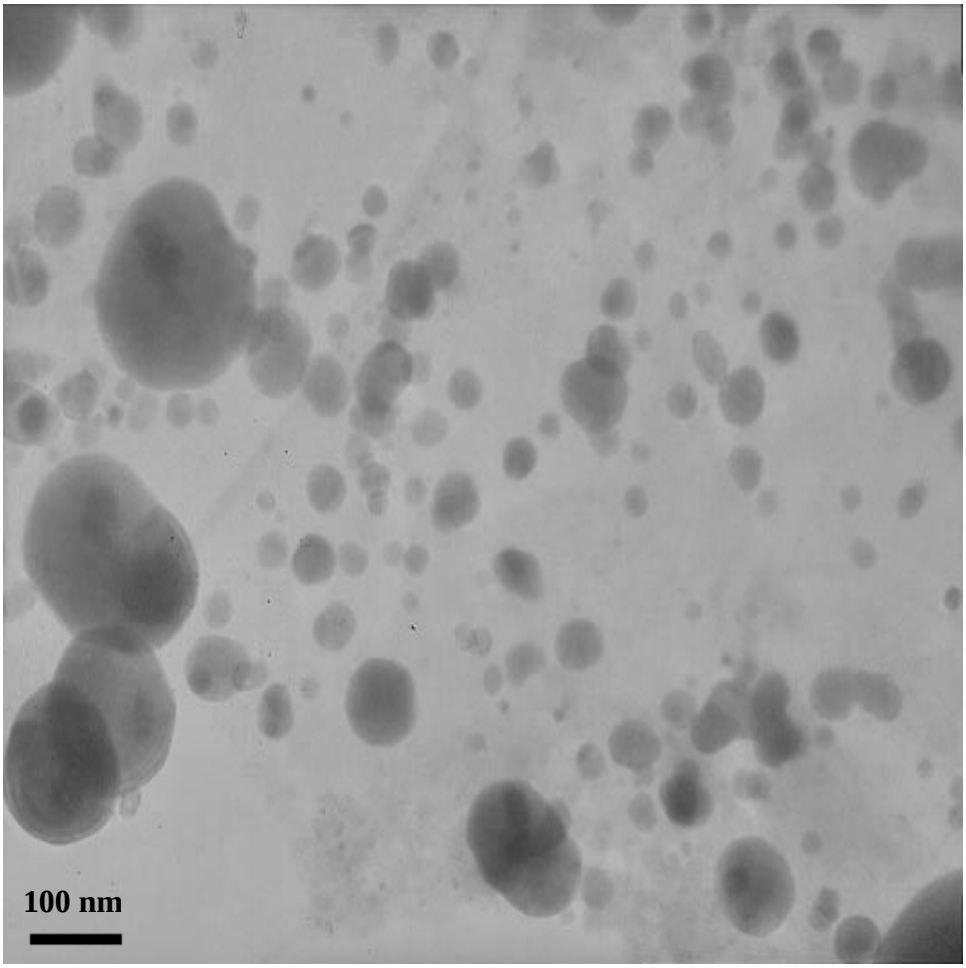

Figure 3-10: TEM of un-reduced 5% Pd/Carbon catalyst

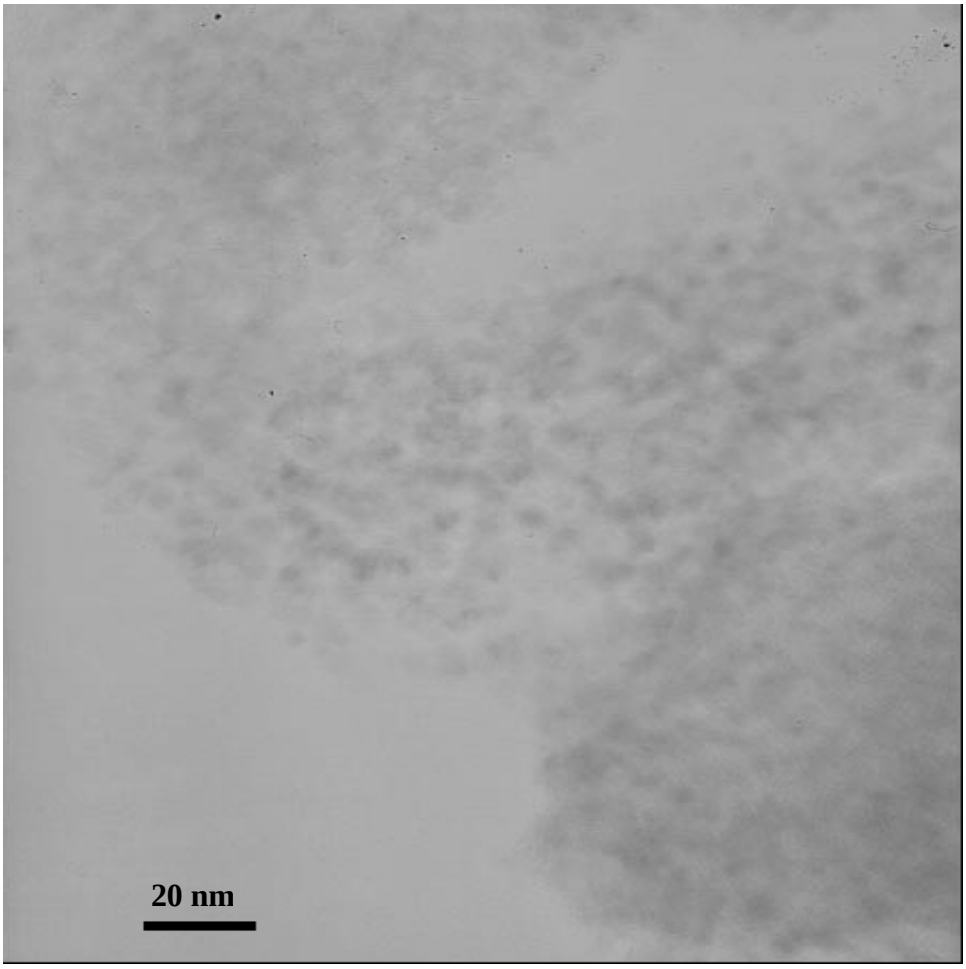

Figure 3-11: TEM of 5% Pd/Alumina catalyst

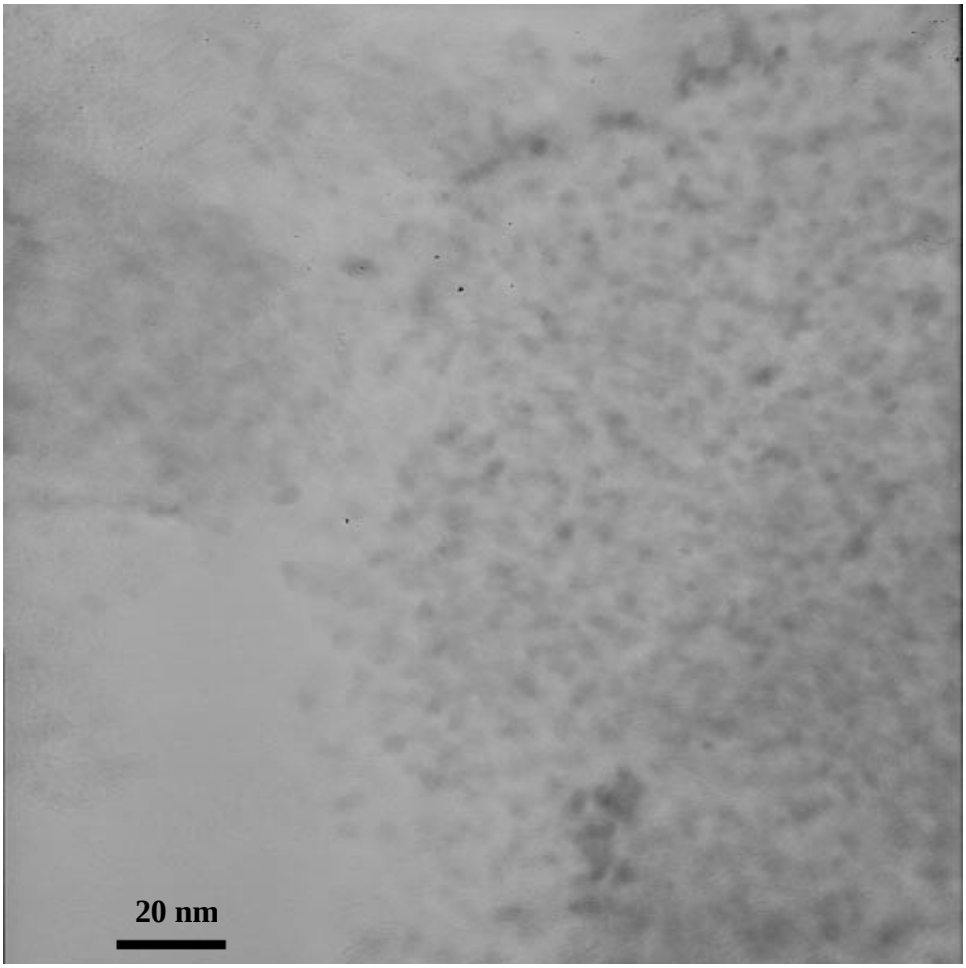

Figure 3-12: TEM of 5% Pt/Alumina catalyst

For the DRIFTS experiments, each experiment was first run using a sample of pure KBr. These experiments were run to ensure that the KBr did not adsorb any experimental gases, and that the carbon dioxide and methane did react in the absence of a catalyst. During the reaction experiment, no acetate or acetic acid was seen for any of the various pretreatments. The acetic acid experiment spectra showed only peaks associated with the

monomer and dimer forms of acetic acid, figure 3-13. No peaks associated with adsorbed acetate species were seen.

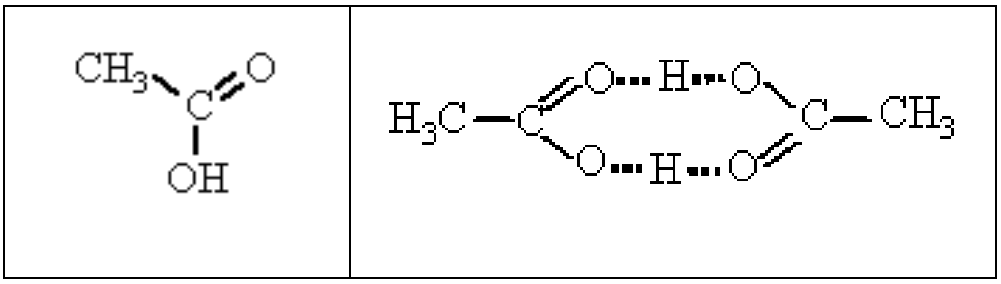

Figure 3-13: Monomer acetic acid and dimer acetic acid

The pure acetic acid DRIFTS experiments over the carbon support, alumina support and the catalysts, show peaks corresponding to the monomer, dimer and adsorbed acetate. These spectra of the carbon support and carbon supported catalysts were virtually identical, as were the alumina support and alumina supported catalyst spectra.

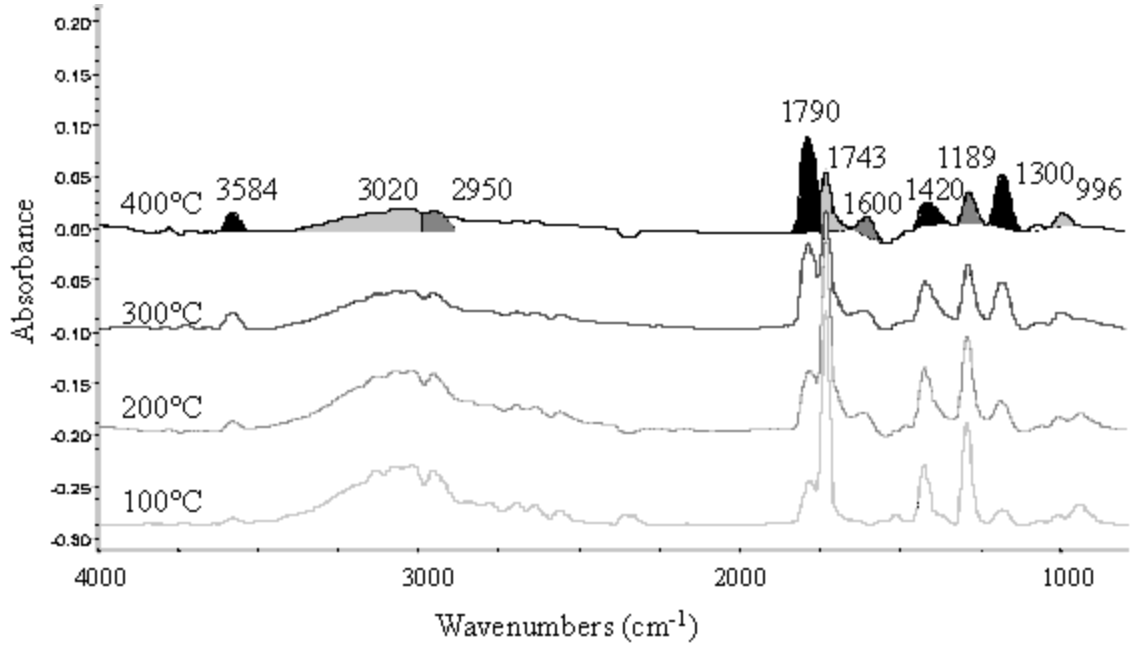

Figure 3-14: Spectra of acetic acid at various temperatures over un-reduced 5% Pd/carbon catalyst

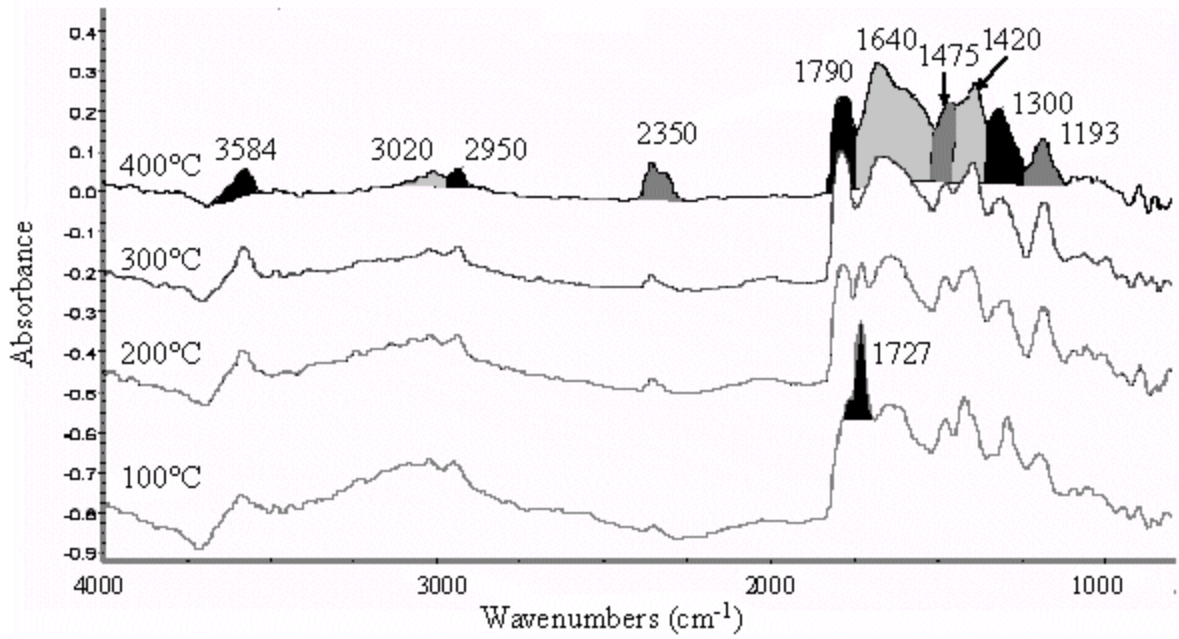

Figure 3-15: Spectra of acetic acid at various temperatures over 5% Pt/alumina catalyst

The O-H stretch of the monomer form of acetic acid gives a peak at 3584 cm^{-1} [98-101]. The O-H stretch of the dimer form of acetic acid gives a broad peak around 3020 cm^{-1} [98-101]. The dimer also has peaks associated with O-H deformation at 1420 cm^{-1} and 996 cm^{-1} [98-101]. The C-H_3 stretching vibration at 2950 cm^{-1} overlaps the O-H stretch at 3020 cm^{-1}. However, the overlap does split enough to be able to clearly see the C-H_3 stretch at 2950 cm^{-1}. An additional C-H_3 stretching vibration gives a peak at 1300 cm^{-1} [98-101]. The peak at 1189 cm^{-1} represents a C-O stretch [98-101]. The most characteristic peaks associated with acetic acid are at 1,790 cm^{-1}, 1,743 cm^{-1} and 1600 cm^{-1}. The 1,790 cm^{-1} peak corresponds to the C=O stretch of the monomer of acetic acid [98-101]. The 1,743 cm^{-1} peak corresponds to the C=O stretch of the acetic acid dimer on the carbon supported catalysts and the same vibration shows up as 1727 on the alumina supported catalysts [98-101]. The peaks at 1600 cm^{-1} represents the O-C=O of an adsorbed species on the carbon supported catalysts [1, 102-104]. This peak indicates that the acetic acid adsorbs in a monodentate form on the surface of the catalyst [103, 104]. The monodentate adsorbed acetate on the alumina supported catalysts gives a peak at 1640 cm^{-1}. This peak is shifted from the 1600 cm^{-1} peak associated with the same vibration on the carbon catalysts. This shift occurs because of differing bond strengths between the acetate and the two catalyst surfaces. The peak at 1475 cm^{-1} seen on with the alumina supported catalysts is associated with the O-C-O stretch of a bidentate adsorbed acetate[104].

As the temperature increases, the intensity of the dimer peaks, 3020 cm^{-1}, 1,743 cm^{-1}, 1420 cm^{-1}, and 996 cm^{-1}, decrease while the intensity of the monomer peaks, 3584 cm^{-1} and 1790 cm^{-1}, increase.

The adsorbed acetate peaks at 1600 cm $^{-1}$, 1640 cm $^{-1}$, and 1420 cm $^{-1}$ increases with the increasing temperature. This indicates that more acetic acid is being adsorbed onto the catalyst surface. As the temperature increases, it would be expected that the adsorbed acetic acid would be removed from the catalysts surface rather than adsorbed. The increase in adsorbed species may be due to the longer exposure to the acetic acid, rather than the temperature.

For the alumina supported catalysts, around 200°C a peak at 2350 cm^{-1} begins to appear and increases with the increasing temperature. This peak corresponds to the O=C=O stretch in carbon dioxide [98, 99, 101, 105]. This indicates that the acetic acid decomposes to carbon dioxide and methane. The methane peaks overlap with the acetic acid peaks at 2950 cm $^{-1}$ and 1300 cm $^{-1}$.

No reaction was seen using the reduced 5% Pd/carbon catalyst for any of the pretreatment types or temperatures. This catalyst is completely ineffective for the direct synthesis of acetic acid from carbon dioxide and methane. The reaction between carbon dioxide and methane does not take place in the presence of this catalyst. The spectra from the reaction experiments, figure 3-16, showed only peaks associated with methane and carbon dioxide. The peaks at 3010 cm^{-1} and 1300cm^{-1} correspond to the C-H stretch in methane [98, 99, 101, 105]. The peaks at 3660 cm^{-1} and 2350 cm^{-1} correspond to the O=C=O stretch in carbon dioxide [98, 99, 101, 105]. The multiple peaks for methane and carbon dioxide are due to Fermi resonance overtones [90, 91].

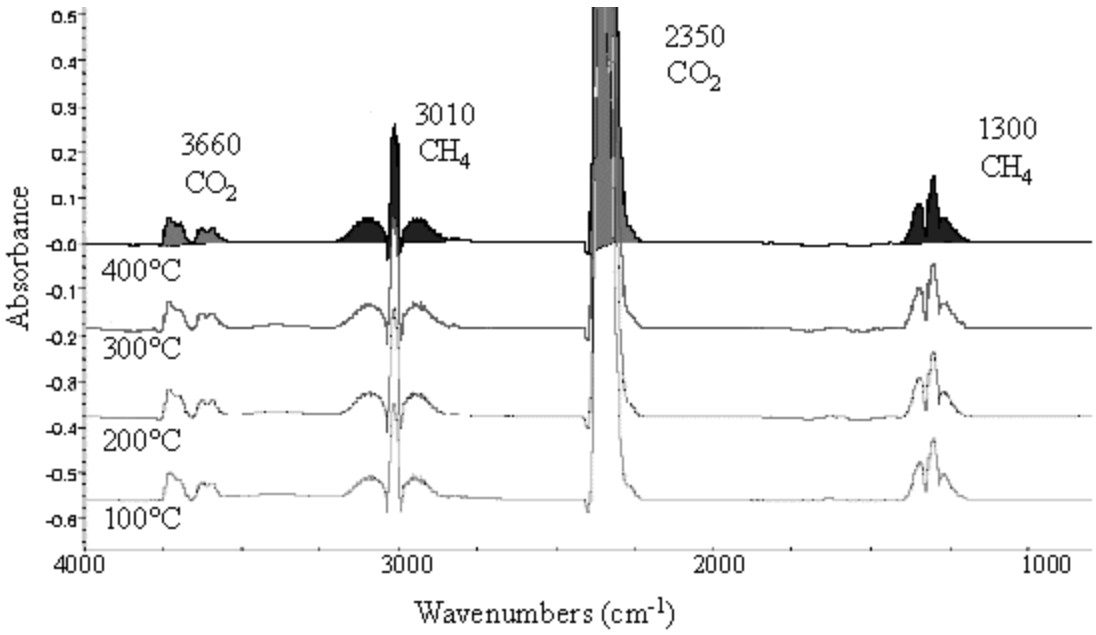

Figure 3-16: Spectra of CO_2/CH_4 at various temperatures over reduced 5% Pd/carbon catalyst

The reaction experiments using a hydrogen, oxygen, methane or helium only pretreatment over the un-reduced 5% Pd/carbon catalyst showed only peaks associated with methane and carbon dioxide at all temperatures. However, when an additional carbon dioxide pretreatment was used, peaks associated with acetic acid were seen when the temperature reached 400°C, figure 3-17.

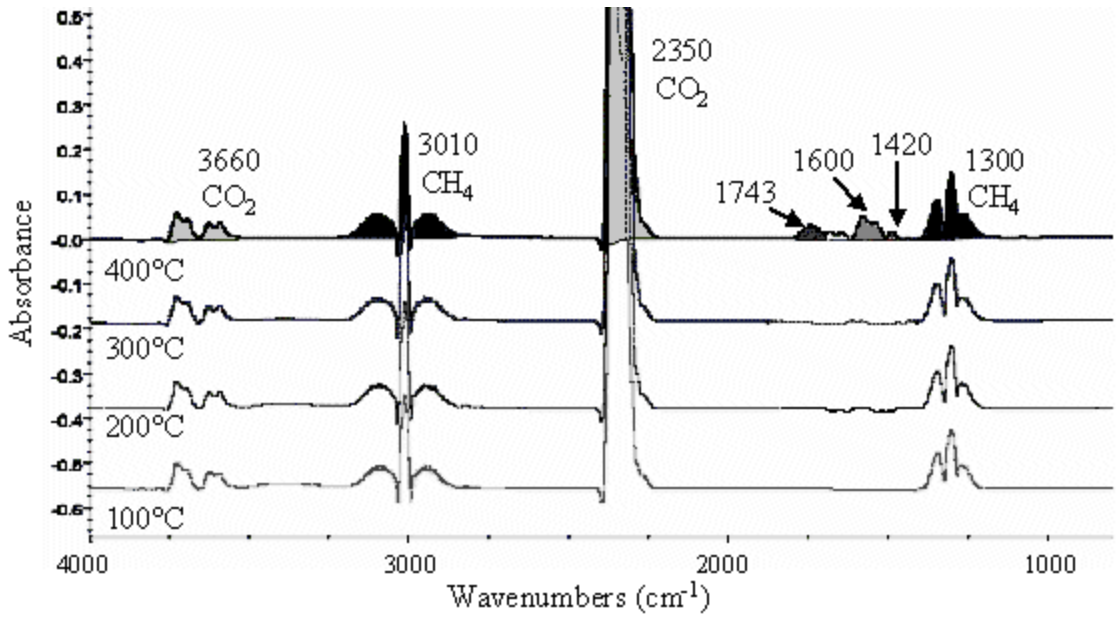

Figure 3-17 Spectra of CO_2/CH_4 at various temperatures over un-reduced 5% Pd/carbon catalyst pretreated with carbon dioxide.

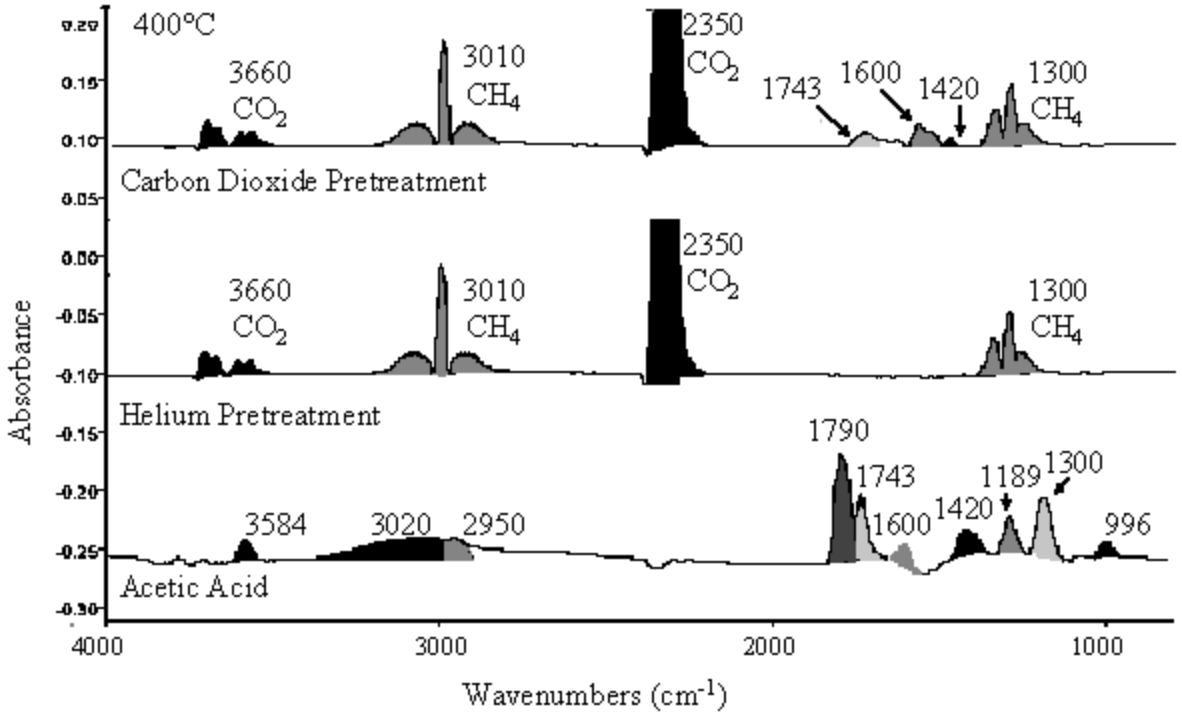

Figure 3-18: Spectra of acetic acid and CO_2/CH_4 over un-reduced 5% Pd/carbon catalyst at 400°C

Using the alumina supported catalysts, the reaction experiments for all the various pretreatments gave the same results. A very strong peak at 1640 cm^{-1} was seen in all the spectra as well. While this is the same wavenumber that the monodentate adsorbed acetate was seen in the acetic acid experiment, it can also be associated with the O-C=O stretch of monodentate adsorbed carbon dioxide [2, 3, 48, 106]. Since no other peaks associated with the acetic acid or acetate at 100°C and since alumina adsorbs a significant amount of carbon dioxide, it is more likely that this peak corresponds to the adsorbed carbon dioxide rather than the acetate.

Around 200°C the spectra begin to show small peaks at 1790 cm^{-1}, 1475 $cm^{-1}$and 1189 cm^{-1}. The 1790 cm^{-1} and 1475 cm^{-1} peaks correspond to the C=O stretch of the monomer form of acetic acid and O-C=O stretch of an adsorbed bidentate acetate, respectively. The 1189 cm^{-1} peak represents the C-O stretch of both the dimer and monomer form of acetic acid. The other acetic acid peaks seen in the acetic acid experiment are overlapped with those of the carbon dioxide, methane and adsorbed carbonate.

As the temperature increases, the strength of the 1790 cm^{-1}, 1475 $cm^{-1}$and 1189 cm^{-1} peaks increase. Additionally, the carbon dioxide peak at 3660 cm^{-1} clearly decreases with increasing temperature indicating that the carbon dioxide is being consumed. While not clearly seen in the spectra, the 2350 cm^{-1} carbon dioxide peak and 3010 cm^{-1} methane peak also decrease with increasing temperature. The peak at 1640 cm^{-1} corresponding to the O-C=O stretch of monodentate adsorbed carbon dioxide or monodentate adsorbed acetate increases with temperature. This may be due either to an increasing amount of adsorbed carbon dioxide or adsorbed acetate.

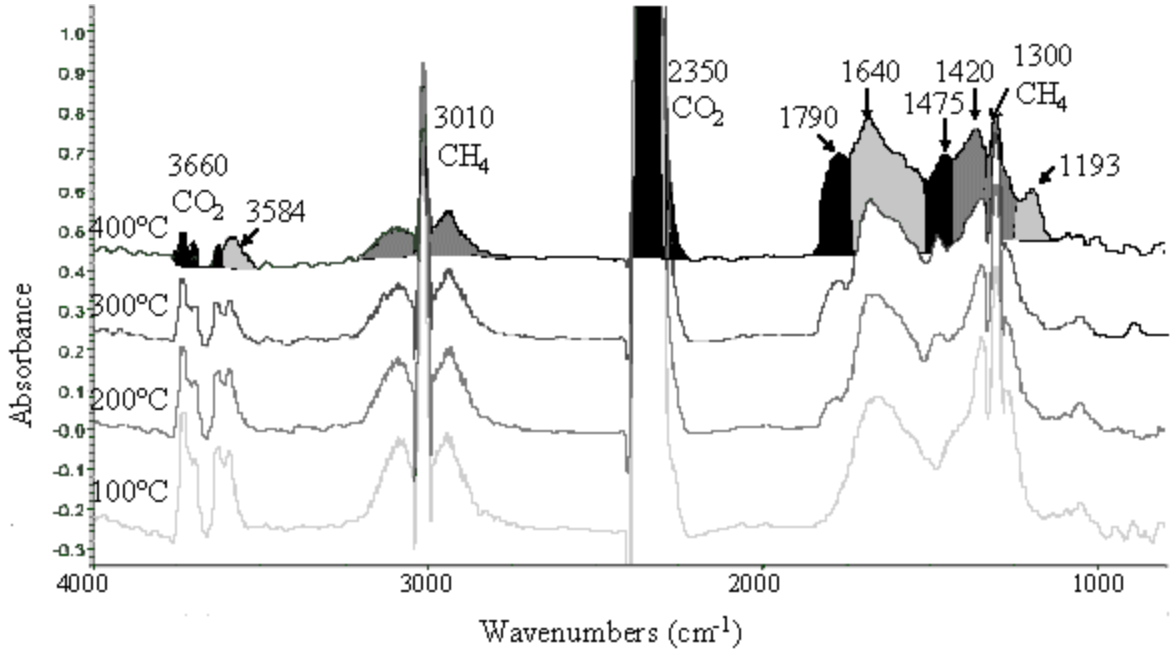

Figure 3-19: Spectra of CO_2/CH_4 at various temperatures over 5% Pd/alumina catalyst

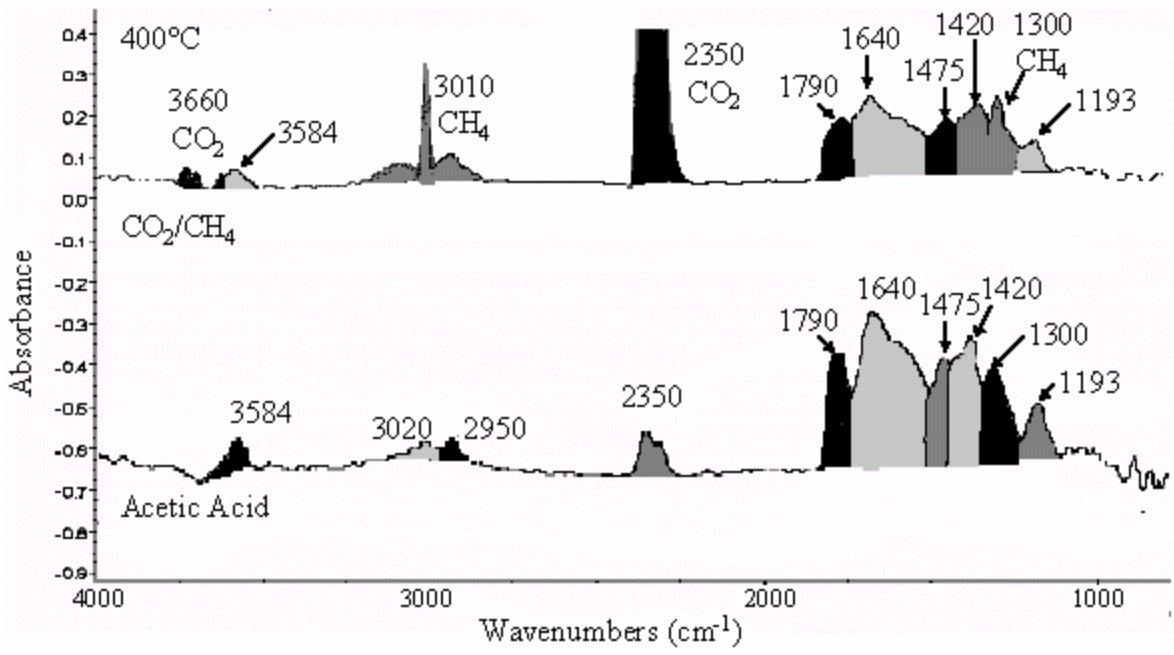

Figure 3-20: Spectra of acetic acid and CO_2/CH_4 over 5% Pd/alumina catalyst at 400°C

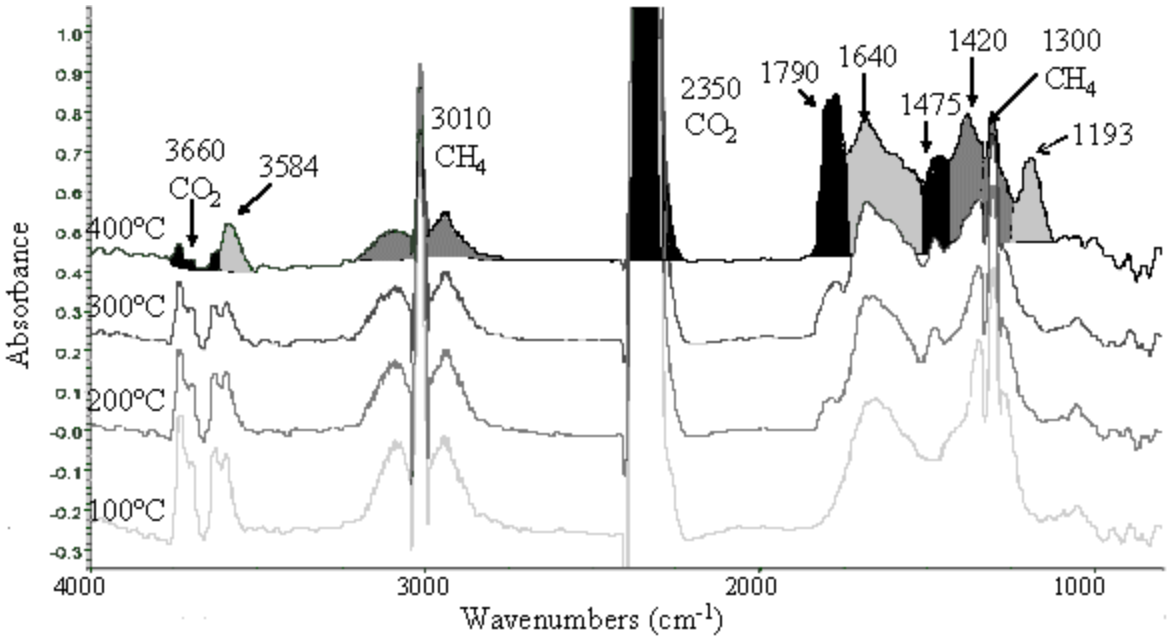

Figure 3-21: Spectra of CO_2/CH_4 at various temperatures over 5% Pt/alumina catalyst

Table 3-16: Peak assignments for spectra

Peak	Vibration	Reference(s)
3584 cm^{-1}	O-H stretch (acetic acid monomer)	[98-101]
3660 cm^{-1}	O=C=O stretch of CO_2	[98, 99, 101, 105]
3020 cm^{-1}	O-H stretch (acetic acid dimer)	[98-101]
3010 cm^{-1}	CH_3 stretch of CH_4	[98, 99, 101, 105]
2950 cm^{-1}	C-H_3 stretch (all forms of acetic acid)	[98-101]
2350 cm^{-1}	O=C=O stretch of CO_2	[98, 99, 101, 105]
1790 cm^{-1}	C=O stretch (acetic acid monomer)	[98-101]
1743 cm^{-1}	C=O stretch (acetic acid dimer)	[98-101]
1727 cm^{-1}	C=O stretch (acetic acid dimer)	[98-101]
1640 cm^{-1}	O-C=O (adsorbed monodentate CO_2 & acetate)	[1, 102-104]
1600 cm^{-1}	O-C=O (monodentate adsorbed acetate)	[1, 102-104]
1475 cm^{-1}	O-C-O stretch (adsorbed bidentate acetate)	[104]
1420 cm^{-1}	O-H deformation (acetic acid dimer)	[98-101]
1300 cm^{-1}	C-H_3 stretch (all forms of acetic acid & CH_4)	[98-101]
1189 cm^{-1}	C-O stretch (all forms of acetic acid)	[98-101]
996 cm^{-1}	O-H deformation (acetic acid dimer)	[98-101]

During all the DRIFTS reaction experiments, no peaks were observed associated with carbon monoxide. Gas phase carbon monoxide has a strong peak at 2143 cm^{-1} [98, 99, 101] and bonded carbon monoxide usually yields a peak between 1800 cm^{-1} and 2100 cm^{-1} depending on the orientation [17, 91, 102]. None of these peaks would overlap the peaks observed in the reaction experiment; therefore the dry reforming reaction was not seen to occur over this catalyst under the reaction conditions examined.

Methyl acetate exhibits very strong peaks at 1754 cm^{-1}, 1207 cm^{-1} and 1166 cm^{-1} associated with the C=O stretch, C-O stretch and CH_3 rock respectively [99-101, 105]. These peaks are close to those observed in the acetic acid spectra and the reaction experiment. However, if a large amount of methyl acetate was formed, these peaks would be discernable. It is unlikely that a significant amount of methyl formate is being produced under the reaction conditions.

Flow through reactor background experiments were run to ensure that no acetic acid was formed from carbon dioxide and methane in the absence of a catalyst. The carbon dioxide pretreated pure methane experiment and the carbon dioxide pretreatment 50% carbon dioxide and 50% methane experiment were run using an empty reactor tube, quartz wool plugs only, the carbon support and alumina support. From these experiments, only m/z peaks associated with helium, carbon dioxide and methane were observed. No peaks corresponding to carbon monoxide, hydrogen, water, acetic acid or any other organic compound were observed. Therefore any product seen during the reaction experiments using the catalysts is formed by the catalyst, not the reactor tube, quartz wool or support.

From the carbon dioxide pretreatment pure methane experiment, no gas phase acetic acid was observed using the reduced 5% Pd/carbon catalyst, the un-reduced 5% Pd/carbon catalyst, the carbon support nor the alumina support. The carbon dioxide pretreated 50% carbon dioxide 50% methane experiment for the same samples showed similar results. The only gases observed during the experiments were methane and carbon dioxide. This indicates that either no carbon dioxide was adsorbed onto the sample surface, or that the adsorbed carbon dioxide did not react with the methane to any measurable extent. Due to the lack of reaction in these experiments, no further experiments were conducted on this catalyst. This catalyst is completely ineffective for the direct synthesis of acetic acid from carbon dioxide and methane.

More promising results were obtained when the alumina supported catalysts were used. From the carbon dioxide pretreatment pure methane experiment, gas phase acetic acid was first seen when the temperature reached 350°C for the 5% Pt/alumina catalyst, and at 400°C for the 5% Pd/alumina catalyst, figures 3-22 and 3-23. The mole fraction of acetic acid increased with the increasing temperature, and reached a maximum of about 2.0×10^{-6} for the 5% Pt/alumina catalyst, and 1.7×10^{-6} for the 5% Pd/alumina catalyst. The acetic acid then sharply decreased. The only carbon dioxide in the system during the pure methane reaction was that which was adsorbed on the catalyst during the pretreatment. The decline in the acetic acid peak probably occurred because the available carbon dioxide was consumed. This experiment suggests that the reaction occurs with an adsorbed carbon dioxide species. No carbon monoxide, hydrogen or water formation was seen, suggesting that the only reaction that occurred was the direct synthesis of acetic acid.

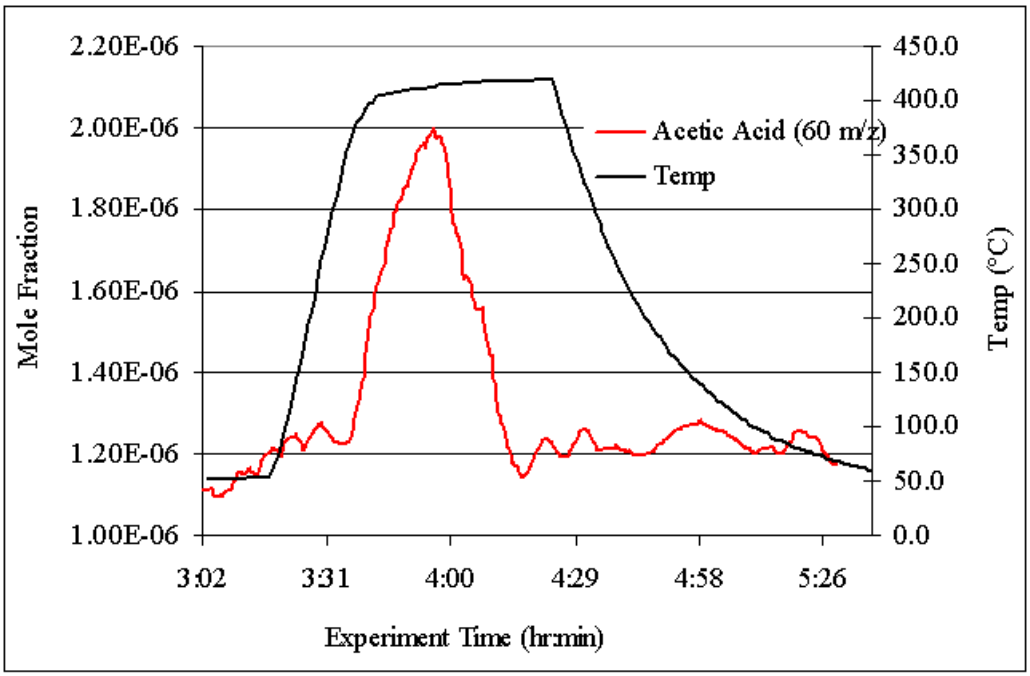

Figure 3-22: Acetic acid mole fraction and temperature for carbon dioxide pretreated 5% Pt/alumina exposed to pure methane

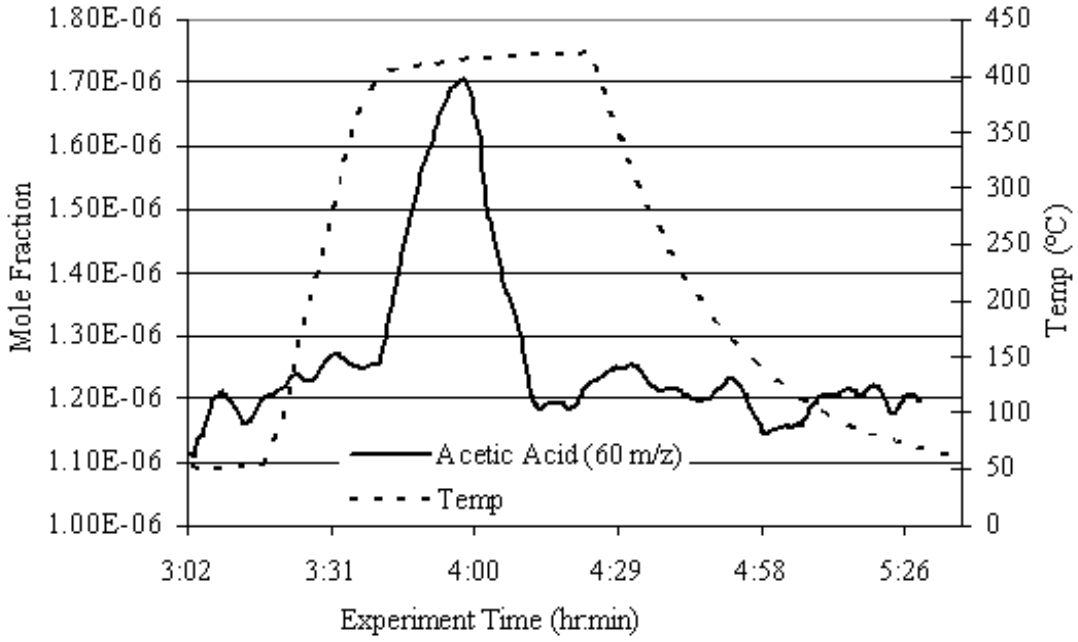

Figure 3-23: Acetic acid mole fraction and temperature for carbon dioxide pretreated 5% Pd/alumina exposed to pure methane

When the 5% Pt/alumina catalyst was pretreated with methane and then exposed to pure carbon dioxide, similar results were observed. Acetic acid formation was again seen, however, not until the temperature reached about 375°C. The maximum peak of the acetic acid was only 1.3×10^{-6}.

When the catalysts were pretreated in carbon dioxide then exposed to a mixture of ~50% carbon dioxide and 50% methane, gas phase acetic acid was also observed. The formation of acetic acid is first observed at around 250°C for the 5% Pt/alumina and at 390°C for the 5% Pd/alumina. The mole fraction of acetic acid increases to about 1.65×10^{-5} for the 5% Pt/alumina and 1.7×10^{-5} for the 5% Pd/alumina and remains steady until the temperature begins to decrease. This indicates that the consumed adsorbed carbon dioxide was continuously replaced by the carbon dioxide in the gas stream.

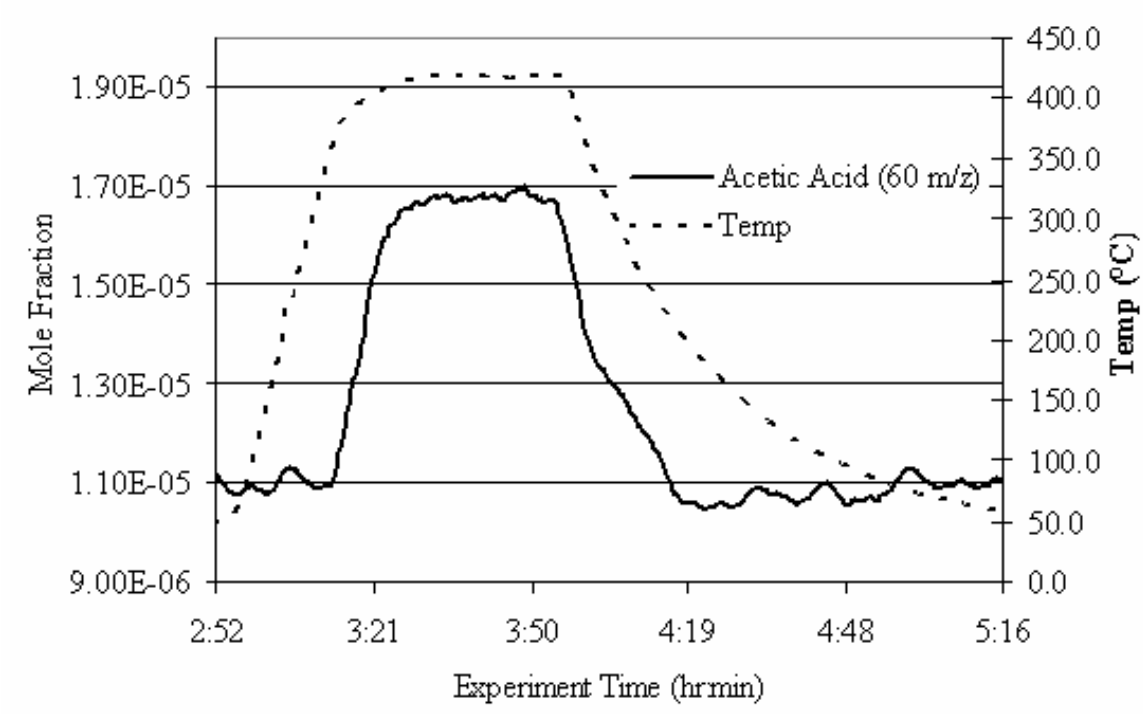

Figure 3-24: Acetic acid mole fraction and temperature for carbon dioxide pretreated 5% Pd/alumina exposed to 53% carbon dioxide 47% methane

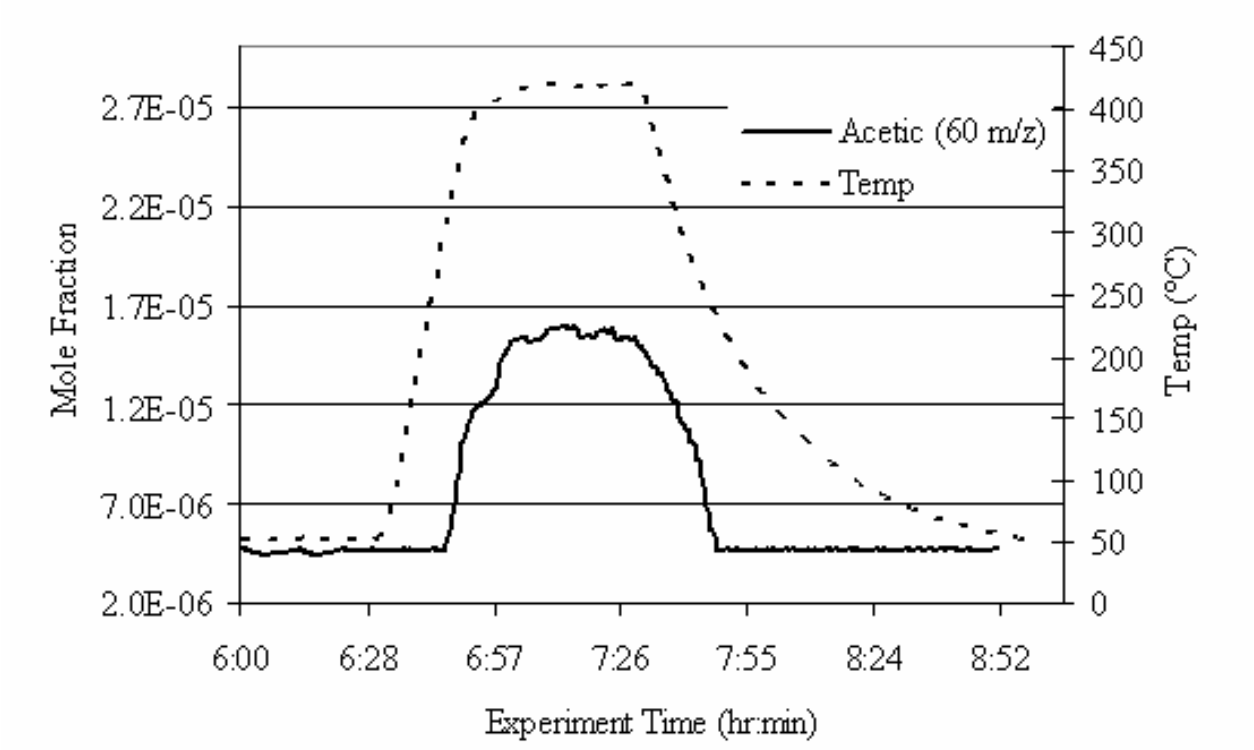

Figure 3-25: Acetic acid mole fraction and temperature for carbon dioxide pretreated 5% Pt/alumina exposed to 53% carbon dioxide 47% methane

After subtracting out the baseline, the mole fraction of acetic acid was approximately 9.6×10^{-6} for the 5% Pt/alumina and 6.1×10^{-6} for the 5% Pd/alumina. The fractional conversion of methane to acetic acid was calculated to be about 2.92×10^{-5} and 1.78×10^{-5} for the Pt and Pd catalysts respectively.

In addition to the acetic acid, carbon monoxide, hydrogen and water were formed, figures 3-26 and 3-27. The formation of both carbon monoxide and hydrogen begins to occur around 325°C for the 5% Pd/alumina and around 225°C for the 5% Pt/alumina. The mole fractions of carbon monoxide and hydrogen increase as the temperature increases, and remain steady at 400°C until the temperature begins to drop.

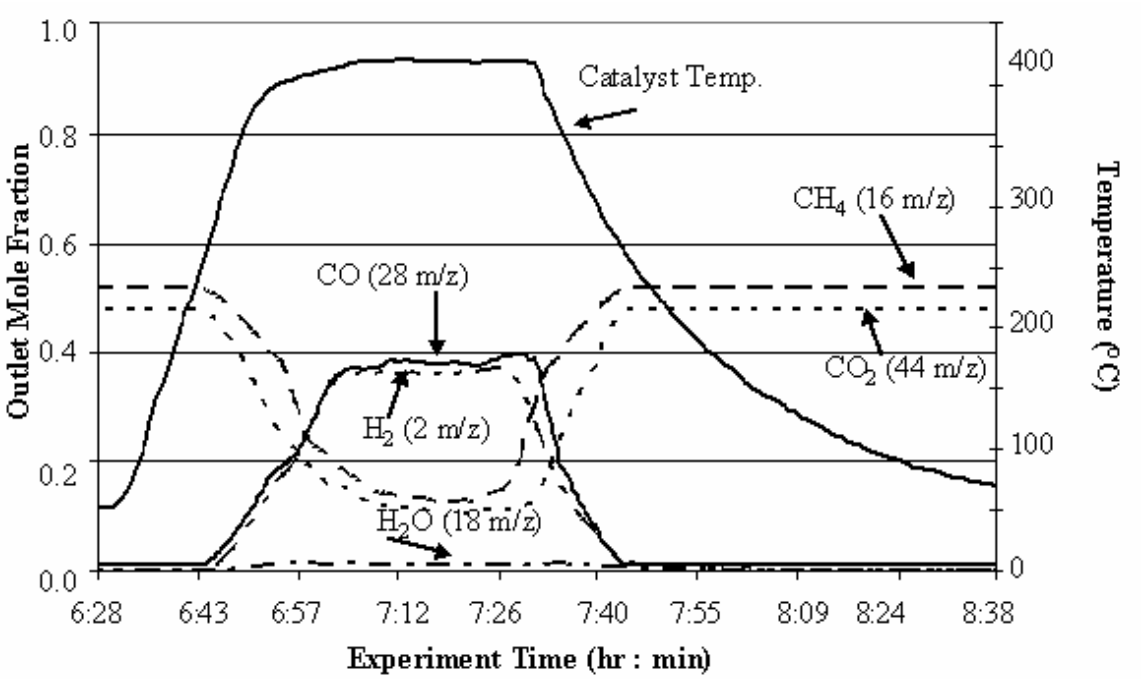

Figure 3-26: CO_2, CH_4, CO, H_2 and H_2O mole fractions and temperature for carbon dioxide pretreated 5% Pt/alumina exposed to 53% carbon dioxide 47% methane

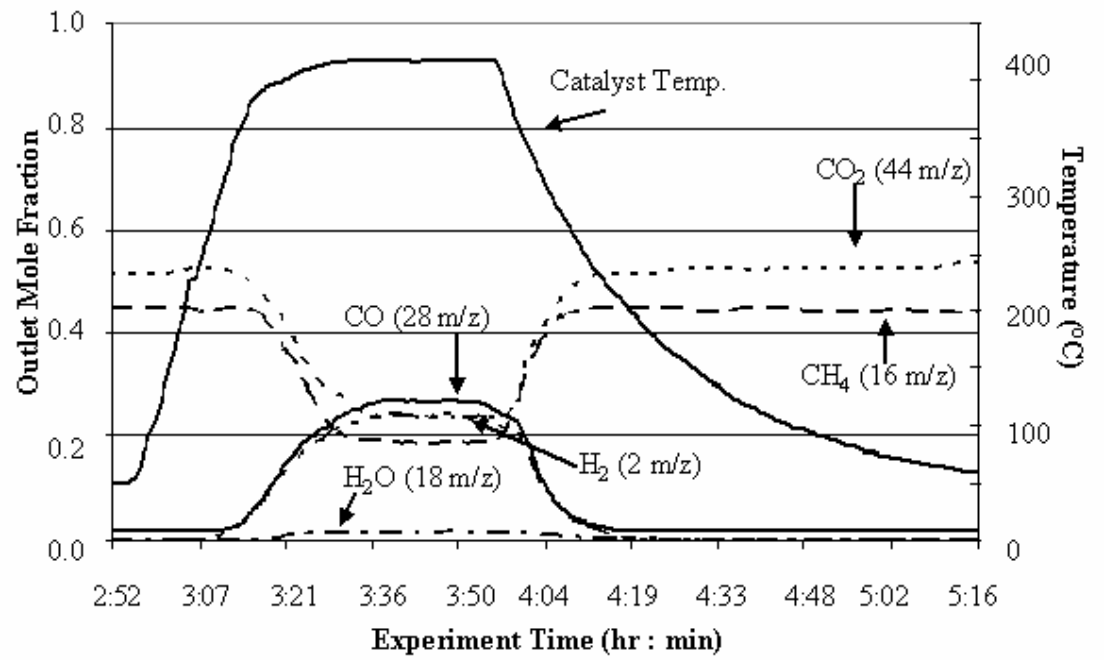

Figure 3-27: CO_2, CH_4, CO, H_2 and H_2O mole fractions and temperature for carbon dioxide pretreated 5% Pd/alumina exposed to 53% carbon dioxide 47% methane

Calculations from mass balances using the inlet molar flow rate of methane, and the inlet and outlet mole fraction of methane, were performed assuming the dry reforming reaction. The outlet mole fractions of carbon monoxide, hydrogen and carbon dioxide determined by this calculation were nearly the same as those observed in the experiment.

This suggests that the dry reforming reaction is occurring:

$$CO_2 + CH_4 \rightarrow 2\ CO + 2\ H_2 \qquad \text{(R 6-1)}$$

$\Delta G_r^0 = +\ 171$ kJ/mol * $\qquad\qquad$ $\Delta H_r^0 = +\ 247$ kJ/mol *

* ΔG_r^0 and ΔH_r^0 values calculated from ΔG_f^0 and ΔH_f^0 values obtained from CRC [107]

The thermodynamics for the dry reforming reaction are highly unfavorable and worse than that of the direct synthesis of acetic acid from carbon dioxide and methane reaction. Typically the dry reforming reaction is run at high temperatures, 600°C and above, in order to overcome the thermodynamic limitations [108]. Thermodynamically, this reaction should not occur to a great extent at 400°C. The formation of carbon monoxide and hydrogen may occur by a different reaction. However, the stoichiometry from the experiments supports the dry reforming reaction.

The DRIFTS experiments did not show any carbon monoxide formation. It is not clear what caused this reaction to occur in this system. This experiment was run three times with fresh samples, and gave the same results.

Given the high amounts of hydrogen in the system, water formation is likely due to the reverse water gas shift reaction:

$$H_2 + CO_2 \rightarrow CO + H_2O \qquad \text{(R 6-2)}$$

ΔG_r^0 = + 29 kJ/mol * $\qquad\qquad$ ΔH_r^0 = + 41 kJ/mol *

* ΔG_r^0 and ΔH_r^0 values calculated from ΔG_f^0 and ΔH_f^0 values obtained from CRC [107]

Taking into account the reverse water gas shift reaction and the baseline of carbon monoxide due to overlapping m/z fractions of the carbon dioxide, the difference between the carbon monoxide and hydrogen can be accounted for.

At 400°C, as the inlet mole fraction of carbon dioxide increased the outlet mole fraction of water increased, and the mole fractions of carbon monoxide, hydrogen and acetic acid decreased, table 3-17 and 3-18. This trend occurred for both the helium pretreatment only and the additional carbon dioxide pretreatment for both of the catalysts. Graphs of the mole fractions of CO_2, CH_4, CO, H_2 and H_2O mole fractions and temperature for the carbon dioxide pretreatment experiments using various inlet mole fraction ratios can be found in Appendix D.3.

Table 3-17: Outlet mole fractions of CO_2, CH_4, CO, H_2, H_2O and CH_3COOH at 400°C for carbon dioxide pretreated 5% Pt/alumina catalyst exposed to varying inlet mole fractions of carbon dioxide and methane

Mole Fractions	Inlet	Outlet	Inlet	Outlet	Inlet	Outlet
CO_2	0.35	0.05	0.48	0.11	0.83	0.50
CH_4	0.65	0.24	0.52	0.13	0.17	0.03
CO	0.00	0.36	0.00	0.39	0.00	0.23
H_2	0.00	0.34	0.00	0.37	0.00	0.21
H_2O	0.00	6.33E-03	0.00	1.30E-02	0.00	2.60E-02
CH_3COOH	0.00	1.35E-05	0.00	1.07E-05	0.00	6.02E-06

Table 3-18: Outlet mole fractions of CO_2, CH_4, CO, H_2, H_2O and CH_3COOH at 400°C for carbon dioxide pretreated 5% Pd/alumina catalyst exposed to varying inlet mole fractions of carbon dioxide and methane

Mole Fractions	Inlet	Outlet	Inlet	Outlet	Inlet	Outlet
CO_2	0.35	0.09	0.53	0.25	0.77	0.44
CH_4	0.65	0.30	0.47	0.19	0.23	0.03
CO	0.00	0.31	0.00	0.28	0.00	0.27
H_2	0.00	0.29	0.00	0.26	0.00	0.25
H_2O	0.00	7.20E-03	0.00	1.20E-02	0.00	2.07E-02
CH_3COOH	0.00	1.60E-05	0.00	6.10E-06	0.00	2.40E-06

As the inlet mole fraction of methane decreases, the total fractional conversion of methane increased, while the fractional conversion of methane to acetic acid decreased, table 6-2 and ?-?. The behavior of the fractional conversion of methane to acetic acid with respect to the inlet mole fraction of methane is opposite of that predicted by the thermodynamic calculations. The increasing consumption of methane in the formation of carbon monoxide and hydrogen may contribute to the decrease in the conversion of methane to acetic acid with decreasing inlet mole fraction of methane. The fractional conversion of methane to acetic acid values are merely a very rough estimate, given the number of assumptions used in the calculations. While the numbers may be off by as much as an order of magnitude, the trend should still hold.

Table 3-19: Total fractional conversion of methane and fractional conversion of methane to acetic acid for carbon dioxide pretreated 5% Pd/alumina catalyst exposed to varying inlet mole fractions of carbon dioxide and methane at 400°C

Inlet Mole Fraction of CH_4	Total Fractional Conversion of CH_4	Fractional Conversion of CH_4 to CH_3COOH
0.65	0.34	4 E-05
0.47	0.40	2 E-05
0.23	0.76	2 E-05

Table 3-20: Total fractional conversion of methane and fractional conversion of methane to acetic acid for carbon dioxide pretreated 5% Pt/alumina catalyst exposed to varying inlet mole fractions of carbon dioxide and methane at 400°C

Inlet Mole Fraction of CH_4	Total Fractional Conversion of CH_4	Fractional Conversion of CH_4 to CH_3COOH
0.65	0.42	5 E-05
0.52	0.58	4 E-05
0.17	0.97	3 E-05

The experiments conducted with a helium pretreatment only gave similar results to that of the carbon dioxide pretreated experiments. Again, the formation of carbon monoxide, hydrogen and water was observed. At 400°C, as the inlet mole fraction of carbon dioxide increased the outlet mole fraction of water increased, while the mole fractions of carbon monoxide, hydrogen and acetic acid decreased, tables 3-21 - 3-22. Graphs of the mole fractions of CO_2, CH_4, CO, H_2 and H_2O mole fractions and temperature for the helium only pretreatment experiments using various inlet mole fraction ratios can be found in Appendix D.2.

Table 3-21: Outlet mole fractions of CO_2, CH_4, CO, H_2, H_2O and CH_3COOH at 400°C for helium pretreated 5% Pd/alumina catalyst exposed to varying inlet mole fractions of carbon dioxide and methane

Mole Fractions	Inlet	Outlet	Inlet	Outlet	Inlet	Outlet
CO_2	0.35	0.11	0.47	0.20	0.80	0.52
CH_4	0.65	0.33	0.53	0.24	0.20	0.05
CO	0.00	0.29	0.00	0.27	0.00	0.22
H_2	0.00	0.27	0.00	0.25	0.00	0.20
H_2O	0.00	4.15E-03	0.00	1.63E-02	0.00	2.25E-02
CH_3COOH	0.00	9.40E-06	0.00	3.00E-06	0.00	1.50E-06

Table 3-22: Total fractional conversion of methane and fractional conversion of methane to acetic acid for helium pretreated 5% Pd/alumina catalyst exposed to varying inlet mole fractions of carbon dioxide and methane at 400°C

Inlet Mole Fraction of CH_4	Total Fractional Conversion of CH_4	Fractional Conversion of CH_4 to CH_3COOH
0.65	0.30	2.02E-05
0.53	0.36	7.84E-06
0.20	0.69	9.56E-06

Table 3-23: Outlet mole fractions of CO_2, CH_4, CO, H_2, H_2O and CH_3COOH at 400°C for helium pretreated 5% Pt/alumina catalyst exposed to varying inlet mole fractions of carbon dioxide and methane

Mole Fractions	Inlet	Outlet	Inlet	Outlet	Inlet	Outlet
CO_2	0.36	0.11	0.48	0.12	0.80	0.45
CH_4	0.64	0.31	0.52	0.17	0.20	0.02
CO	0.00	0.3	0.00	0.36	0.00	0.23
H_2	0.00	0.27	0.00	0.34	0.00	0.20
H_2O	0.00	4.60E-03	0.00	1.13E-02	0.00	9.51E-02
CH_3COOH	0.00	1.27E-05	0.00	9.60E-06	0.00	5.60E-06

Table 3-24: Total fractional conversion of methane and fractional conversion of methane to acetic acid for helium pretreated 5% Pt/alumina catalyst exposed to varying inlet mole fractions of carbon dioxide and methane at 400°C

Inlet Mole Fraction of CH_4	Total Fractional Conversion of CH_4	Fractional Conversion of CH_4 to CH_3COOH
0.64	0.32	3.83E-05
0.52	0.56	2.92E-05
0.20	0.92	2.80E-05

The results of the DRIFTS experiments showed significant differences between the effectiveness of the catalysts used for the direct synthesis of acetic acid from carbon dioxide and methane. From the flow through reactor experiments, the formation of carbon monoxide, hydrogen and water was observed. This is not in agreement with the DRIFTS results. Also, acetic acid formation was observed using an un-reduced 5% Pd/carbon catalysts from DRIFTS, while the acetic acid was not seen during the flow through experiments.

The four catalysts performed differently from each other. The catalyst characterization results discussed earlier may give some insight into the differences between the catalyst effectiveness for this reaction. The carbon supported catalysts performed poorly, while the alumina supported catalysts performed better, and the 5% Pt/alumina performed the best. The pore volume and surface areas of the catalysts do not provide any useful information regarding an active catalyst for this reaction, as the carbon supported catalysts had both higher surface areas and pore volumes than the alumina supported catalysts.

The lack of formation of acetic acid in the absence of a catalyst or in the presence of the support only indicates that the reaction requires an active metal. The alumina supported

catalysts have a higher metal loading and dispersion than of the carbon supported catalysts. The significant differences in the metal loading and dispersion may contribute to the difference in the effectiveness of the catalysts for the direct synthesis of acetic acid reaction.

The experiments also suggest that the reaction takes place between an adsorbed carbon dioxide and an adsorbed methane species. The large difference of carbon dioxide adsorption between the alumina supported catalysts and the carbon supported catalysts may contribute to the difference in the effectiveness of the catalysts.

The results of the pulse chemisorption experiments help to explain the significant differences between the effectiveness of the catalysts in the direct synthesis of acetic acid from carbon dioxide and methane as inferred from the DRIFTS experiments. The catalysts that showed the formation of acetate from carbon dioxide and methane: un-reduced 5% Pd/carbon, 5% Pd/alumina and 5% Pt/alumina, all adsorbed both carbon dioxide and methane. The catalysts that did not show any formation of acetate on the surface: carbon support, alumina support and reduced 5% Pd/carbon catalyst, did not adsorb any methane. Only the alumina support adsorbed carbon dioxide. The alumina support adsorbs more carbon dioxide than the alumina supported catalysts, thus the support itself may play an important role in the direct synthesis reaction. Figure 7-2 graphically shows the results from the adsorption experiments.

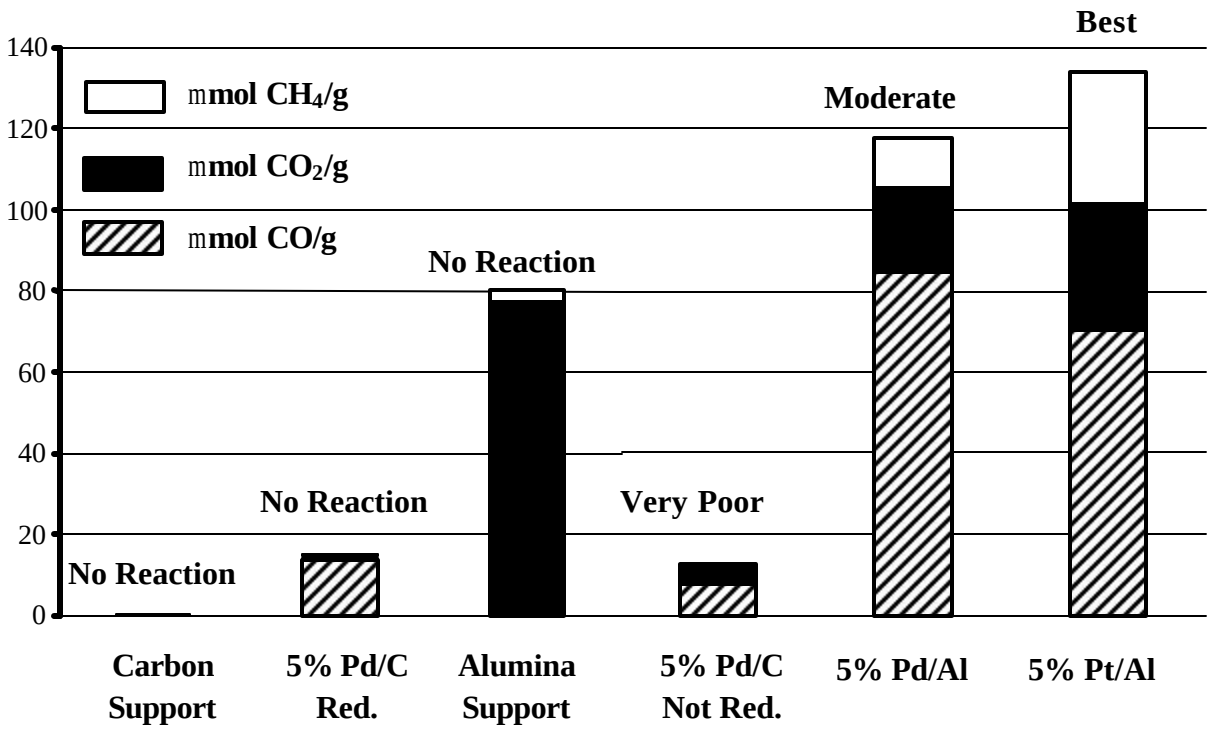

Figure 3-28: Pulse chemisorption results

The adsorption and desorption experiments showed that the carbon dioxide adsorbs onto the alumina support, rather than the metal, and that the methane adsorbs onto the metal, rather than the supports .Since the carbon dioxide adsorbs on the alumina support rather than the metal, the support itself may play an important role in the reaction. It appears that the reaction on the alumina catalysts takes place between an adsorbed carbon dioxide on the alumina and an adsorbed methane on the metal. The more active catalysts had smaller evenly dispersed metal clusters. This indicates that there would be more adjacent alumina and metal sites for the reaction to occur.

3.5 CONCLUSIONS

The catalyst characterizations revealed differences between the catalysts that may help to explain the difference in their effectiveness. The carbon supported catalysts had a lower metal loading and a lower dispersion than the alumina supported catalysts. Since methane adsorbed only on the metal, and not on the support, it is likely that the reaction required metal sites. Therefore, the lower exposed metal area of the carbon supported catalysts should make them less effective for the direct synthesis reaction.

The carbon support and carbon supported catalysts had a slightly higher pore volume than the alumina and alumina supported catalysts. The carbon support and carbon supported catalysts had a much higher surface area than the alumina support and alumina supported catalysts. It is unlikely that surface area alone influences the effectiveness of the catalysts.

The metal dispersion for the carbon supported catalysts was much less than that of the alumina supported catalysts. The higher metal dispersion and metal loading indicates that the alumina supported catalysts had more active sites for the reaction. The pulse chemisorption experiments showed that the carbon supported catalysts adsorbed less carbon dioxide and methane than the alumina supported catalysts. It is likely that the reaction occurs between adsorbed molecules. Thus effective catalysts for the reaction should adsorb both reactants. The alumina support itself adsorbed more carbon dioxide than the alumina supported catalysts, whereas the alumina support did not adsorb any methane.

Temperature programmed desorption experiments supported the pulse chemisorption results. The carbon dioxide only had one adsorbed species, which was the same for the alumina support and the alumina supported catalysts. The alumina supported catalysts both

had two different adsorbed methane species. The methane species were different for both catalysts. The acetic acid desorbed as acetic acid at low temperatures, but was decomposed and desorbed as carbon dioxide and methane at higher temperatures.

TEM images showed that the carbon supported catalysts had large metal clusters, which were far apart on the support. The alumina supported catalysts had small metal clusters, which were close together and well dispersed over the support.

The characterizations show that the effective catalysts for the direct synthesis reaction adsorb both methane and carbon dioxide. The support plays an important role in the reaction, as the carbon dioxide does not adsorb to the metal. Therefore, an effective catalyst should have small metal clusters widely dispersed on the support to maximize the metal/support interface with adjacent carbon dioxide adsorbing and methane adsorbing sites.

The diffuse reflectance infrared Fourier transform spectroscopy experiments definitively showed the formation of acetate species from carbon dioxide and methane over the unreduced 5% Pd/carbon, 5% Pd/alumina and 5% Pt/alumina catalysts. In addition to adsorbed acetates, liquid phase acetic acid was formed over a carbon dioxide pretreated unreduced 5% Pd/carbon catalyst at 400°C, and gas phase acetic acid was formed over the 5% Pd/alumina and 5% Pt/alumina catalysts at 200°C.

The reduced 5% Pd/carbon catalyst did not show any peaks corresponding to acetic acid or an adsorbed acetate from carbon dioxide and methane. Several pretreatment methods were tested with no success. The unreduced 5% Pd/carbon catalyst did show peaks corresponding to both an adsorbed acetate and gas phase acetic acid when exposed to carbon dioxide and methane. These peaks did not appear until the catalyst temperature reached

400°C. The adsorbed acetate and gas phase acetic acid peaks were only seen when the catalyst was pretreated with carbon dioxide. In all other pretreatments, helium only, hydrogen, oxygen and methane, only carbon dioxide and methane peaks were observed during the experiment.

The alumina supported catalysts performed much better than the carbon supported catalysts. With the helium pretreatment only, both the 5% Pd/alumina and 5% Pt/alumina catalysts had strong distinct adsorbed acetate and gas phase acetic acid peaks from the reaction of carbon dioxide and methane. The reaction spectra from the other pretreatments did not differ from the helium only spectra. For both the alumina supported catalyst, adsorbed acetate peaks were seen at 200°C, and gas phase acetic acid peaks appear at 300°C.

None of the catalysts showed peaks corresponding to methyl formate or carbon monoxide. Therefore these catalysts are selective to the direct synthesis of acetic acid from carbon dioxide and methane. They do not allow the dry reforming reaction, or the formation of methyl acetate.

Neither the pure KBr, carbon support nor the alumina support showed the formation of an adsorbed acetate or gas phase acetic acid from carbon dioxide and methane. Therefore the direct synthesis reaction does not occur in the gas phase and requires an active metal. The reaction mechanism likely includes intermediate adsorbed carbon dioxide and/or methane species.

Reaction experiments using a mixture of methane and carbon dioxide over the carbon and alumina supports showed no formation of acetic acid. The supports alone do not catalyze the direct synthesis reaction nor any other reaction between carbon dioxide and

methane. The reduced 5% Pd/carbon catalyst also showed no formation of gas phase acetic acid from carbon dioxide and methane. This catalyst likewise did not catalyze any reaction, which agrees with the previous DRIFTS results.

The un-reduced 5% Pd/carbon catalyst also did not show the formation of gas phase acetic acid from carbon dioxide and methane, nor any other reaction. The previous DRIFTS results showed a small amount of dimer acetic acid formed. If acetic acid was formed during the reaction experiments, it either did not enter the gas phase, or was too minute to be detected by the mass spectrometer.

The 5% Pd/alumina and 5% Pt/alumina catalysts did show the formation of gas phase acetic acid from carbon dioxide and methane. When the catalysts were pretreated with carbon dioxide and then exposed to a flow of pure methane, a sharp peak in the mole fraction of acetic acid was observed. When the catalysts were pretreated with carbon dioxide and then exposed to a mixture of carbon dioxide and methane, the acetic acid peak was not sharp, and the decline corresponded to a reduction in the temperature. This suggests that the carbon dioxide in the gas phase can replace pre-adsorbed carbon dioxide on the catalyst surface.

In addition to the direct synthesis reaction, the dry reforming and reverse water gas shift reactions appeared to occur. It is unclear why these additional reactions occurred, as the DRIFTS data did not show formation of carbon monoxide. The formation of carbon monoxide and hydrogen occurred at a lower temperature than the direct synthesis of acetic acid reaction, and these were the dominant products.

The total fractional conversion of methane for both catalysts increased as the inlet mole fraction of carbon dioxide increased. The fractional conversion of methane to acetic

acid and the mole fraction of acetic acid decreased as the inlet mole fraction of carbon dioxide increased. This behavior is opposite of that predicted by the thermodynamic calculations. This behavior may be explained by the dry reforming reaction. As the inlet mole fraction of methane decreases, more of the methane is converted in the dry reforming reaction, leaving less methane available for the direct synthesis reaction.

Pretreating the catalysts in carbon dioxide increases the total fractional conversions of methane, and the fractional conversions of methane to acetic acid. The 5% Pt/alumina catalyst gave higher conversions of methane and higher mole fractions of acetic acid than the 5% Pd/alumina catalyst.

The formation of gas phase acetic acid from carbon dioxide and methane has been definitively shown. However, in order for this reaction to become industrially useful, the yield and selectivity of acetic acid must be significantly increased.

While this research was focused on finding a catalyst for the direct synthesis of acetic acid from carbon dioxide and methane, good catalysts for what may be the dry reforming reaction were found. The 5% Pd/alumina and 5% Pt/alumina both gave high conversions of methane to synthesis gas at temperatures lower than the dry reforming reaction is typically run. Further studies need to be conducted to determine exactly what is causing the formation of carbon monoxide and hydrogen in this system.

3.6 REFERENCES

1. Augustine, S.M. and J.P. Blitz, *The Use of Drifts-Ms and Kinetic-Studies to Determine the Role of Acetic-Acid in the Palladium-Catalyzed Vapor-Phase Synthesis of Vinyl-Acetate*. Journal of Catalysis, 1993. **142**(1): p. 13.

2. Benitez, J.J., R. Alvero, M.J. Capitan, I. Carrizosa, and J.A. Odriozola, *Drifts Study of Adsorbed Formate Species in the Carbon-Dioxide and Hydrogen Reaction Over Rhodium Catalysts.* Applied Catalysis, 1991. **71**(2): p. 13.

3. Benitez, J.J., R. Alvero, I. Carrizosa, and J.A. Odriozola, *Insitu Drifts Study of Adsorbed Species in the Hydrogenation of Carbon Oxides.* Catalysis Today, 1991. **9**(1-2): p. 8.

4. Benitez, J.J., I. Carrizosa, and J.A. Odriozola, *Diffuse-Reflectance Ft-Ir Characterization of Active-Sites Under Reaction Conditions - the Production of Oxygenates in the Co H-2 Reaction.* Applied Spectroscopy, 1994. **48**(10): p. 5.

5. Benitez, J.J., I. Carrizosa, and J.A. Odriozola, *In-Situ Diffuse-Reflectance Infrared (Drifts) Identification of Active-Sites in the Co+H2 Reaction Over Lanthanide-Modified Rh Al2o3 Catalysts.* Applied Surface Science, 1995. **84**(4): p. 9.

6. Bhumkar, S.C. and L.L. Lobban, *Diffuse Reflectance Infrared and Transient Studies of Oxidative Coupling of Methane Over Li Mgo Catalyst.* Industrial & Engineering Chemistry Research, 1992. **31**(8): p. 9.

7. Blatter, F., F. Moreau, and H. Frei, *Diffuse-Reflectance Spectroscopy of Visible Alkene-O-2 Charge- Transfer Absorptions in Zeolite-Y and Determination of Photooxygenation Quantum Efficiencies.* Journal of Physical Chemistry, 1994. **98**(50): p. 5.

8. Blitz, J.P. and S.M. Augustine, *Characterization of Heterogeneous Catalysts By Ft-Ir Diffuse- Reflectance Spectroscopy.* Spectroscopy, 1994. **9**(8): p. 7.

9. Frei, R.W. and J.D. MacNeil, *Diffuse Reflectance Spectroscopy in Environmental Problem-Solving*. 1973, Cleveland: CRC Press.

10. Hrebicik, M. and K. Volka, *Diffuse-reflectance infrared spectroscopy - Theory and application.* Chemicke Listy, 1996. **90**(2): p. 13.

11. Iwaoka, T., S.H. Wang, and P.R. Griffiths, *Diffuse Reflectance Infrared Spectrometry of Inorganic Materials.* Spectrochimica Acta Part a-Molecular and Biomolecular Spectroscopy, 1985. **41**(1-2): p. 5.

12. Llewellyn, P.L. and C.R. Theocharis, *A Diffuse Reflectance Fourier-Transform Infrared Study of Carbon-Dioxide Adsorption On Silicalite-I.* Journal of Chemical Technology and Biotechnology, 1991. **52**(4): p. 8.

13. Maulhardt, H. and D. Kunath, *Diffuse-Reflectance Spectroscopy in the Infrared.* Talanta, 1982. **29**(3): p. 5.

14. Moradi, K., C. Depecker, J. Barbillat, and J. Corset, *Diffuse reflectance infrared spectroscopy: an experimental measure and interpretation of the sample volume size involved in the light scattering process.* Spectrochimica Acta Part a-Molecular and Biomolecular Spectroscopy, 1999. **55**(1): p. 22.

15. O'Connor, A.M., F.C. Meunier, and J.R.H. Ross, *An in-situ DRIFTS study of the mechanism of the CO2 reforming of CH4 over a Pt/ZrO2 catalyst.* Natural Gas Conversion V, 1998. **119**: p. 6.

16. Stuart, B., *Modern Infrared Spectroscopy*. 1996, New York: John Wiley.

17. Delannay, F., *Characterization of Heterogeneous Catalysts.* 1984, New York: Marcel Dekker.

18. Skoog, D.A. and J.J. Leary, *Principles of Instrumental Analysis*. 1992, New York: Saunders.

19. Spivey, J. and R. Makarand, *Method of Preparing Acetic Acid by Carboxylation of Methane*. 1999.

20. Gretz, E., T.F. Oliver, and A. Sen, *Carbon-Hydrogen Bond Activation by Electrophilic Transition-Metal Compounds - Palladium(Ii)-Mediated Oxidation of Arenes and Alkanes Including Methane.* Journal of the American Chemical Society, 1987. **109**(26): p. 8109-8111.

21. Schild, C., A. Wokaun, and A. Baiker, *On the Mechanism of Co and Co2 Hydrogenation Reactions on Zirconia-Supported Catalysts - a Diffuse Reflectance Ftir Study .1. Identification of Surface Species and Methanation Reactions on Palladium Zirconia Catalysts.* Journal of Molecular Catalysis, 1990. **63**(2): p. 223-242.

22. Beattie, J.K., A.F. Masters, and M.L. Sparkes, *Alkane Activation by Homogeneous Palladium Complexes.* Applied Organometallic Chemistry, 1991. **5**(6): p. 521-523.

23. Wang, Y.N., R.G. Herman, and K. Klier, *Dissociative Adsorption of Methane on Pd(679) Surface.* Surface Science, 1992. **279**(1-2): p. 33-48.

24. Hoyos, L.J., H. Praliaud, and M. Primet, *Catalytic Combustion of Methane over Palladium Supported on Alumina and Silica in Presence of Hydrogen-Sulfide.* Applied Catalysis a-General, 1993. **98**(2): p. 125-138.

25. Erdohelyi, A., J. Cserenyi, E. Papp, and F. Solymosi, *Catalytic Reaction of Methane with Carbon-Dioxide over Supported Palladium.* Applied Catalysis a-General, 1994. **108**(2): p. 205-219.

26. Burch, R. and M.J. Hayes, *C-H bond activation in hydrocarbon oxidation on solid catalysts.* Journal of Molecular Catalysis a-Chemical, 1995. **100**(1-3): p. 13-33.

27. Muto, K., N. Katada, and M. Niwa, *Complete oxidation of methane on supported palladium catalyst: Support effect.* Applied Catalysis a-General, 1996. **134**(2): p. 203-215.

28. Solymosi, F., I. Kovacs, and K. Revesz, *Selective oxygen addition to adsorbed CH2 and CH3 on Pd(100).* Surface Science, 1996. **356**(1-3): p. 121-129.

29. Aryafar, M. and F. Zaera, *Kinetic study of the catalytic oxidation of alkanes over nickel, palladium, and platinum foils.* Catalysis Letters, 1997. **48**(3-4): p. 173-183.

30. da Rocha, M.G.C. and R. Frety, *Catalytic œombustion of methane: Activation and characterization of Pd/Al2O3*, in *3rd World Congress on Oxidation Catalysis*. 1997. p. 767-776.

31. Klier, K., J.S. Hess, and R.G. Herman, *Structure sensitivity of methane dissociation on palladium single crystal surfaces.* Journal of Chemical Physics, 1997. **107**(10): p. 4033-4043.

32. Taylor, C.E., R.R. Anderson, and R.P. Noceti, *Activation of methane with organopalladium complexes.* Catalysis Today, 1997. **35**(4): p. 407-413.

33. Hei, M.J., H.B. Chen, J. Yi, Y.J. Lin, Y.Z. Lin, G. Wei, and D.W. Liao, *CO2-reforming of methane on transition metal surfaces.* Surface Science, 1998. **417**(1): p. 82-96.

34. Yu, T.C. and H. Shaw, *The effect of sulfur poisoning on methane oxidation over palladium supported on gamma-alumina catalysts.* Applied Catalysis B-Environmental, 1998. **18**(1-2): p. 105-114.

35. Park, E.D., S.H. Choi, and J.S. Lee, *Characterization of Pd/C and Cu catalysts for the oxidation of methane to a methanol derivative.* Journal of Catalysis, 2000. **194**(1): p. 33-44.

36. Guczi, L., L. Borko, Z. Schay, D. Bazin, and F. Mizukami, *CO hydrogenation and methane activation over Pd-Co/SiO2 catalysts prepared by sol/gel method.* Catalysis Today, 2001. **65**(1): p. 51-57.

37. Hayes, R.E., S.T. Kolaczkowski, P.K.C. Li, and S. Awdry, *The palladium catalysed oxidation of methane: reaction kinetics and the effect of diffusion barriers.* Chemical Engineering Science, 2001. **56**(16): p. 4815-4835.

38. Ciuparu, D., M.R. Lyubovsky, E. Altman, L.D. Pfefferle, and A. Datye, *Catalytic combustion of methane over palladium-based catalysts.* Catalysis Reviews-Science and Engineering, 2002. **44**(4): p. 593-649.

39. Michalkiewicz, B., K. Kalucki, and J.G. Sosnicki, *Catalytic system containing metallic palladium in the process of methane partial oxidation.* Journal of Catalysis, 2003. **215**(1): p. 14-19.

40. Zhang, X.L., B. Dai, A.M. Zhu, W.M. Gong, and C.H. Liu, *The simultaneous activation of methane and carbon dioxide to C-2 hydrocarbons under pulse corona plasma over La2O3/gamma-Al2O3 catalyst.* Catalysis Today, 2002. **72**(3-4): p. 223-227.

41. Zhang, X.L., W.M. Gong, B. Dai, and C.H. Liu, *Effect of La2O3/gamma-Al2O3 catalyst on the activation of CH4 and CO2 to C-2 hydrocarbons under non-equilibrium plasma.* Chinese Chemical Letters, 2002. **13**(2): p. 175-176.

42. Harlick, P.J.E. and F.H. Tezel, *Adsorption of carbon dioxide, methane, and nitrogen: Pure and binary mixture adsorption by ZSM-5 with SiO2/Al2O3 ratio of 30.* Separation Science and Technology, 2002. **37**(1): p. 33-60.

43. Sloczynski, J., R. Grabowski, A. Kozlowska, M. Lachowska, and J. Skrzypek, *Methanol synthesis from CO2 and H2 on Cu/ZnO/Al2O3-ZrO2 catalysts. Catalytic activity and adsorption of reactants.* Polish Journal of Chemistry, 2001. **75**(5): p. 733-742.

44. Yong, Z., V. Mata, and A.E. Rodrigues, *Adsorption of carbon dioxide on basic alumina at high temperatures.* Journal of Chemical and Engineering Data, 2000. **45**(6): p. 1093-1095.

45. Horiuchi, T., H. Hidaka, T. Fukui, Y. Kubo, M. Horio, K. Suzuki, and T. Mori, *Effect of added basic metal oxides on CO2 adsorption on alumina at elevated temperatures.* Applied Catalysis a-General, 1998. **167**(2): p. 195-202.

46. Tamura, H., N. Katayama, and R. Furuichi, *The Co2+ adsorption properties of Al2O3, Fe2O3, Fe2O3, TiO2, and MnO2 evaluated by modeling with the Frumkin isotherm.* Journal of Colloid and Interface Science, 1997. **195**(1): p. 192-202.

47. Aksoylu, A.E., A.N. Akin, S.G. Sunol, and Z.I. Onsan, *The effect of metal loading on the adsorption parameters of carbon dioxide on coprecipitated nickel-alumina catalysts.* Turkish Journal of Chemistry, 1996. **20**(1): p. 88-94.

48. Manchado, M.C., J.M. Guil, A.P. Masia, A.R. Paniego, and J.M.T. Menayo, *Adsorption of H-2, O2, Co, and Co2 on a Gamma-Alumina - Volumetric and Calorimetric Studies.* Langmuir, 1994. **10**(3): p. 685-691.

49. Lercher, J.A., C. Colombier, and H. Noller, *Acid-Base Properties of Alumina Magnesia Mixed Oxides .4. Infrared Study of Adsorption of Carbon-Dioxide.* Journal of the Chemical Society-Faraday Transactions I, 1984. **80**: p. 949-959.

50. Tanaka, Y., T. Iizuka, and K. Tanabe, *Infrared Spectroscopic Study of Co and Co2 Adsorption on Rh-Zro2, Rh-Al2o3 and Rh-Mgo.* Journal of the Chemical Society-Faraday Transactions I, 1982. **78**: p. 2215-2225.

51. Morterra, C., A. Zecchina, S. Coluccia, and A. Chiorino, *Ir Spectroscopic Study of Co2 Adsorption onto Eta-Al2o3.* Journal of the Chemical Society-Faraday Transactions I, 1977. **73**: p. 1544-1560.

52. Takeuchi, K. and Y. Uraguchi, *Chromatographic Studies of Co and Co2 Adsorption on Activated Alumina by Weighted Fourier-Analysis.* Journal of Chemical Engineering of Japan, 1977. **10**(4): p. 297-302.

53. Morterra, C., S. Coluccia, G. Ghiotti, and A. Zecchina, *Ir Spectroscopic Characterization of Alpha Alumina Surface Properties - Carbon-Dioxide Adsorption.* Zeitschrift Fur Physikalische Chemie-Frankfurt, 1977. **104**(4-6): p. 275-290.

54. Malinowski, M., S. Malinowski, and S. Krzyzanowski, *Investigation of Surface Phenomena on Solid Catalysts by Simultaneous Thermogravimetry and Dta .5. Adsorption of Carbon-Dioxide on Surface of Zeolites and Silica-Alumina Gels Treated with Sodium-Hydroxide.* Journal of Thermal Analysis, 1976. **10**(3): p. 331-337.

55. Rosynek, M.P., *Isotherms and Energetics of Carbon-Dioxide Adsorption on Gamma-Alumina at 100-300 Degrees.* Journal of Physical Chemistry, 1975. **79**(13): p. 1280-1284.

56. Gregg, S.J. and J.D.F. Ramsay, *A Study of Adsorption of Carbon Dioxide by Alumina Using Infrared and Isotherm Measurements.* Journal of Physical Chemistry, 1969. **73**(5): p. 1243-&.

57. Parkyns, N.D., *Surface Properties of Metal Oxides .2. An Infrared Study of Adsorption of Carbon Dioxide on Gamma-Alumina.* Journal of the Chemical Society a -Inorganic Physical Theoretical, 1969(3): p. 410-&.

58. Jones, W.M. and R.E. Evans, *Adsorption of Carbon Dioxide at High Pressures (1-100 Atm) by Alumina Determined from Measurement of Dielectric Constant.* Transactions of the Faraday Society, 1966. **62**(522P): p. 1596-&.

59. Achatz, U., C. Berg, S. Joos, B.S. Fox, M.K. Beyer, G. Niedner-Schatteburg, and V.E. Bondybey, *Methane activation by platinum cluster ions in the gas phase: effects of cluster charge on the Pt-4 tetramer.* Chemical Physics Letters, 2000. **320**(1-2): p. 53-58.

60. Aghalayam, P., Y.K. Park, N. Fernandes, V. Papavassiliou, A.B. Mhadeshwar, and D.G. Vlachos, *A C1 mechanism for methane oxidation on platinum.* Journal of Catalysis, 2003. **213**(1): p. 23-38.

61. Anderson, A.B. and J.J. Maloney, *Activation of Methane on Iron, Nickel, and Platinum Surfaces - a Molecular-Orbital Study.* Journal of Physical Chemistry, 1988. **92**(3): p. 809-812.

62. Biswas, B., M. Sugimoto, and S. Sakaki, *C-H bond activation of benzene and methane by M(eta(2)-O2CH)(2) (M = Pd or Pt). A theoretical study.* Organometallics, 2000. **19**(19): p. 3895-3908.

63. Bradford, M.C.J., *Isothermal, non-oxidative, two-step CH4 conversion over unsupported and supported Ru and Pt catalysts.* Catalysis Letters, 2000. **66**(3): p. 113-120.

64. Burch, R., P.K. Loader, and F.J. Urbano, *Some aspects of hydrocarbon activation on platinum group metal combustion catalysts.* Catalysis Today, 1996. **27**(1-2): p. 243-248.

65. Choudhary, T.V., E. Aksoylu, and D.W. Goodman, *Nonoxidative activation of methane.* Catalysis Reviews-Science and Engineering, 2003. **45**(1): p. 151-203.

66. Crabtree, R.H., *Aspects of Methane Chemistry.* Chemical Reviews, 1995. **95**(4): p. 987-1007.

67. FerreiraAparicio, P., I. RodriguezRamos, and A. GuerreroRuiz, *Methane interaction with silica and alumina supported metal catalysts.* Applied Catalysis a-General, 1997. **148**(2): p. 343-356.

68. Grigoryan, E.A., *Catalytic activation and functionalization of methane.* Kinetics and Catalysis, 1999. **40**(3): p. 350-363.

69. Heiberg, H., O. Swang, O.B. Ryan, and O. Gropen, *C-H activation at a cationic platinum (II) center: A quantum chemical investigation.* Journal of Physical Chemistry A, 1999. **103**(48): p. 10004-10008.

70. Heinemann, C., R. Wesendrup, and H. Schwarz, *Pt+-Mediated Activation of Methane - Theory and Experiment.* Chemical Physics Letters, 1995. **239**(1-3): p. 75-83.

71. Hwang, D.Y. and A.M. Mebel, *Theoretical study of the reaction mechanism of platinum oxide with methane.* Chemical Physics Letters, 2002. **365**(1-2): p. 140-147.

72. Labinger, J.A., J.E. Bercaw, G.A. Luinstra, D.K. Lyon, and A.M. Herring, *Organometallic Methane Activation - Functionalization by Aqueous Platinum Complexes*, in *Natural Gas Conversion Ii*. 1994. p. 515-520.

73. Luinstra, G.A., L. Wang, S.S. Stahl, J.A. Labinger, and J.E. Bercaw, *C-H Activation by Aqueous Platinum Complexes - a Mechanistic Study.* Journal of Organometallic Chemistry, 1995. **504**(1-2): p. 75-91.

74. Mallens, E.P.J., J. Hoebink, and G.B. Marin, *An Investigation on the Reaction-Mechanism for the Partial Oxidation of Methane to Synthesis Gas over Platinum.* Catalysis Letters, 1995. **33**(3-4): p. 291-304.

75. Nelson, K.T. and K. Foger, *Activation of Methane under Mild Conditions*, in *Natural Gas Conversion Ii*. 1994. p. 545-550.

76. Periana, R.A., D.J. Taube, S. Gamble, H. Taube, T. Satoh, and H. Fujii, *Platinum catalysts for the high-yield oxidation of methane to a methanol derivative.* Science, 1998. **280**(5363): p. 560-564.

77. Souza, M., D.A.G. Aranda, and M. Schmal, *Reforming of methane with carbon dioxide over Pt/ZrO2/Al2O3 catalysts.* Journal of Catalysis, 2001. **204**(2): p. 498-511.

78. Trevor, D.J., D.M. Cox, and A. Kaldor, *Methane Activation on Unsupported Platinum Clusters.* Journal of the American Chemical Society, 1990. **112**(10): p. 3742-3749.

79. Valden, M., N. Xiang, J. Pere, and M. Pessa, *Dissociative chemisorption of methane on clean and oxygen precovered Pt(111).* Applied Surface Science, 1996. **99**(2): p. 83-89.

80. Wittborn, A.M.C., M. Costas, M.R.A. Blomberg, and P.E.M. Siegbahn, *The C-H activation reaction of methane for all transition metal atoms from the three transition rows.* Journal of Chemical Physics, 1997. **107**(11): p. 4318-4328.

81. Wolf, D., *High yields of methanol from methane by C-H bond activation at low temperatures.* Angewandte Chemie-International Edition, 1998. **37**(24): p. 3351-3353.

82. Micromeritics.Instument.Corporation, *Flowsorb II 2300 Instruction Manual.* 1986, Norcross: Micromeritics Instument Corporation.

83. White, M., *Heterogeneous Catalysis*. 1990, Englewood Cliffs: Prentice-Hall.

84. Zeton.Altamira, *Zeton Altamira Notes*. Temperature-Programmed Desorption of Adsorbed Species from Catalyst Surfaces. Vol. 1.3. 1989, Pittsburgh, PA: Zeton Altamira.

85. Bourane, A., O. Dulaurent, and D. Bianchi, *Comparison of the coverage of the linear CO species on Pt/Al2O3 measured under adsorption equilibrium conditions by using FTIR and mass spectroscopy.* Journal of Catalysis, 2000. **195**(2): p. 406-411.

86. Chafik, T., O. Dulaurent, J.L. Gass, and D. Bianchi, *Heat of adsorption of carbon monoxide on a Pt/Rh/CeO2/Al2O2 three-way catalyst using in-situ infrared spectroscopy at high temperatures.* Journal of Catalysis, 1998. **179**(2): p. 503-514.

87. Dulaurent, O. and D. Bianchi, *Adsorption isobars for CO on a Pt/Al2O3 catalyst at high temperatures using FTIR spectroscopy: isosteric heat of adsorption and adsorption model.* Applied Catalysis a-General, 2000. **196**(2): p. 271-280.

88. Amelinckx, S.D.v.D., *Handbook of Microscopy*. 1997, New York: VCH.

89. Nicolet, *Magna-IR 560 Instruction Manual*. 1995, Madison: Nicolet.

90. McHale, J.L., *Molecular Spectroscopy*. 1999, New Jersey: Prentice Hall.

91. Niemantsverdriet, J.W., *Spectroscopy in Catalysis*. 2000, New York: Wiley-VCH.

92. Skoog, D.A.L., J.J., *Principles of Instumental Analysis*. 4th ed. 1992, New York: Harcourt Brace College Publishers.

93. Busch, K.L.G., G.L.; McLuckey, S.A., *Mass Spectrometry*. 1988, New York: VCH Publishers.

94. March, R.E.H., R.J., *Quardupole Storgae Mass Spectrometry*. 1989, New York: John Wiley & Sons.

95. Cornu, A.M., R., *Compilation of Mass Spectral Data.* 1975, New York: Heyden & Sons Ltd.

96. NIST, *Standard Reference Database*. 2001.

97. Millard, B.J., *Quantitative Mass Spectrometry*. 1988, Philadelphia: Heyden & Son Ltd.

98. Smith, B.C., *Infrared Spectral Interpretation: A Systematic Approach*. 1999, New York: CRC Press.

99. Dolphin, D.W., A., *Tabulation of Infrared Spectral Data.* 1977, New York: John Wiley & Sons.

100. Roeges, N.P., *A Guide to the Complete Interpretation of Infrared Spectra of Organic Structrures*. 1994, New York: John Wiley & Sons.

101. Aldrich.Chemical.Company, *The Aldrich Library of FT-IR Spectra*. 1997, Milwaukee: Aldrich.

102. Urban, M.W., *Vibrational Spectroscopy of Molecules and Macromolecules on Surfaces*. 1993, New York: John Wiley & Sons.

103. Chateau, L., J.P. Hindermann, A. Kiennemann, and E. Tempesti, *On the mechanism of carbonylation in acetic acid and higher acid synthesis from methanol and syngas mixtures on supported rhodium catalysts.* Journal of Molecular Catalysis a-Chemical, 1996. **107**(1-3): p. 12.

104. Pei, Z.F. and V. Ponec, *On the intermediates of the acetic acid reactions on oxides: An IR study.* Applied Surface Science, 1996. **103**(2): p. 12.

105. Szymanski, H.A., *Infrared Band Handbook*. 1970, New York: Plenum.

106. Kiselev, A.V.L., V.I., *Infrared Spectra of Surface Componds*. 1975, New York: John Wiley & Sons.

107. Chemical.Rubber.Company, *CRC Handbook of Chemistry and Physics*. 83 ed. 2002, Cleveland: Chemical Rubber Company Press.

108. Liu, C.M., R.G.; Aresta, M., *Utilization of Greenhouse Gases*. 2003, Washington, DC: American Chemical Society.

CHAPTER 4

PRELIMINARY EXPERIMENTS FOR VINYL ACETATE SYNTHESIS

4.1 INTRODUCTION

As discussed in chapter 3, gas phase acetic acid can be formed from carbon dioxide and methane using either a 5% Pd/alumina or 5% Pt/alumina catalyst. However, very little acetic acid was produced from this reaction, due to the thermodynamic limitations discussed in chapter 2. In order for the direct synthesis of acetic acid from carbon dioxide and methane to be industrially useful, the thermodynamic limitations must be overcome and the conversion of methane and the yield of acetic acid must be increased. One method to overcome the thermodynamics, as discussed in chapter 2, is the synthesis of vinyl acetate from carbon dioxide, methane and acetylene. Over 44% of the acetic acid produced in 2003 was used in the production of vinyl acetate [1]. While this reaction would not yield acetic acid as the end product, vinyl acetate is industrially useful chemical, with over 5 million metric tons produced worldwide in 2003 [2].

Currently vinyl acetate is produced industrially by a catalytic vapor phase reaction of acetic acid with ethylene and oxygen [2, 3]. In the past, vinyl acetate was produced by the reaction of acetic acid with acetylene [4-6]:

$$CH_3COOH + C_2H_2 \rightarrow CH_3CO_2CH{=}CH_2 \qquad \text{(R 4-1)}$$

ΔG_r^0 = - 65 kJ/mol * $\qquad\qquad$ ΔH_r^0 = - 110 kJ/mol *

* ΔG_r^0 and ΔH_r^0 values calculated from ΔG_f^0 and ΔH_f^0 values obtained from CRC [7]

This thermodynamically favorable reaction might be coupled with the direct synthesis reaction:

$$CO_2 + CH_4 \rightarrow CH_3COOH \qquad \text{(R 4-2)}$$

ΔG_r^0 = + 71 kJ/mol * $\qquad\qquad$ ΔH_r^0 = + 36 kJ/mol *

* ΔG_r^0 and ΔH_r^0 values calculated from ΔG_f^0 and ΔH_f^0 values obtained from CRC [7]

to drive the equilibrium of the latter reaction. Coupling of reactions (R 4-1) and (R 4-2) gives an overall reaction for the formation of vinyl acetate from carbon dioxide, methane and acetylene:

$$CO_2 + CH_4 + C_2H_2 \rightarrow CH_3CO_2CH{=}CH_2 \qquad \text{(R 4-3)}$$

ΔG_r^0 = + 7 kJ/mol * $\qquad\qquad$ ΔH_r^0 = - 75 kJ/mol *

* ΔG_r^0 and ΔH_r^0 values calculated from ΔG_f^0 and ΔH_f^0 values obtained from CRC [7]

Equilibrium calculations on this reaction, Chapter 2, predicted an equilibrium fractional conversion of methane as high as 0.941 at 300 K and 10 atm.

Preliminary experiments were conducted to determine the feasibility of producing vinyl acetate from carbon dioxide, methane and acetylene.

4.2 CATALYSTS

The formation of vinyl acetate from carbon dioxide, methane and acetylene, as described above, requires the formation of acetic acid from carbon dioxide and methane, (R 4-2). Catalysts for reaction (R 4-3) must catalyze the direct synthesis of acetic acid from carbon dioxide and methane. Due to their success in the direct synthesis of acetic acid from carbon dioxide and methane experiments, chapters 5 and 6, the 5% Pd/alumina and 5% Pt/alumina catalysts were examined for vinyl acetate synthesis. A detailed description of these catalysts can be found in section 3-2.

While these catalysts have been shown to form acetic acid from carbon dioxide and methane, they may not catalyze the vinyl acetate reaction, (R 4-1). A zinc-acetate on carbon catalyst was used industrially for the synthesis of vinyl acetate from acetylene and acetic acid [4-6]. For the vinyl acetate synthesis from carbon dioxide, methane, and acetylene, admixtures of a zinc-acetate on carbon catalyst and the 5% Pd/alumina catalyst, and the same zinc-acetate on carbon catalyst and the 5% Pt/alumina catalyst evaluated, along with the individual catalysts. The admixtures were used in the hope that the alumina supported catalysts would form acetic acid from carbon dioxide and methane, and then the zinc-acetate on carbon catalyst would form vinyl acetate from the acetic acid and acetylene.

Since vinyl acetate is not currently produced via the acetylene reaction, R 4-1, the industrial catalyst was not available. The zinc-acetate on carbon catalyst was synthesized in-house via the incipient wetness technique. The same carbon support that was used for the carbon supported palladium catalysts was provided by Calgon Carbon. The pore volume of the support was roughly determined and used to calculate the volume of solution required.

Enough zinc acetate to give a 5 weight percent of zinc on the support was diluted to the required volume. This solution was then gradually added to the support. After the water had been evaporated, the catalyst was calcined at 500°C for 3 hours.

The catalyst admixtures were prepared by adding approximately equal weight amounts of the zinc-acetate on carbon catalyst to the 5% Pd/alumina and 5% Pt/alumina catalysts. The mixtures were shaken vigorously in a sample vial prior to use.

4.3 EXPERIMENTAL PROCEDURES

These experiments were run using the Altamira™ reaction system described in section 3.3. For each experiment, approximately 0.5 grams of sample was packed between quartz wool plugs in the quartz reactor tube. The sample was pretreated in a flow of 50 sccm research grade helium for 30 minutes. The temperature was raised to 400°C at 20°C/min and held for 1 hour in the flow of helium. The sample was then cooled to 50°C and held for 30 minutes. This pretreatment was used to clean the catalyst surface and remove any air or water vapor from the reactor tube.

After the pretreatment, the sample was exposed to a 50 sccm flow of the experimental gas for 30 minutes at 50°C. The temperature was then increased to 400°C at a rate of 20°C/min. The sample was held at 400°C for 1 hour, then, still in the flow of experimental gas, was cooled down to 50°C. The experimental gas consisted of either acetylene bubbled through acetic acid or an approximately equal volume mixture of carbon dioxide, methane and acetylene mixed using a mixing rotameter. Figure 4-1 shows the experimental profile.

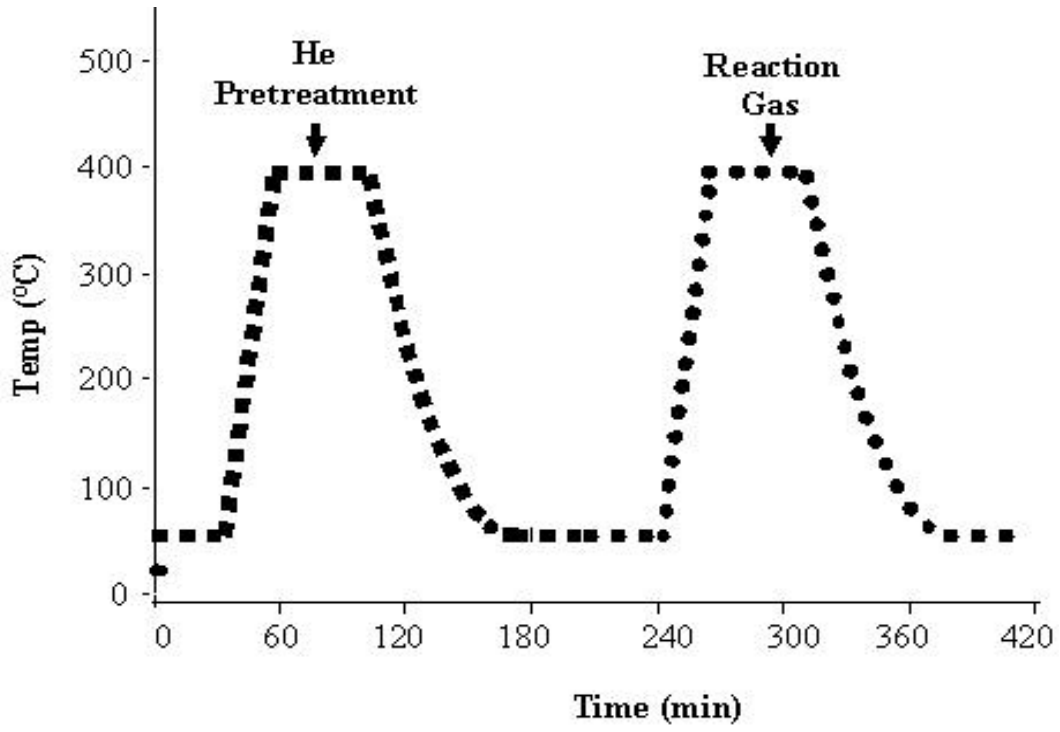

Figure 4-1: Vinyl Acetate Reaction Experimental Profile

The helium, carbon dioxide and methane gases were purified individually using Alltech™ gas purifiers to remove water, oxygen and C_2 + hydrocarbons. The acetylene was purified using three Alltech™ purifiers to remove water, oxygen and sulfur.

The exiting experimental gas was continuously analyzed using the online Ametek™ quadrupole mass spectrometer. An analog mass spectrum from 1 – 100 m/z was recorded using the Dycor™ software continuously throughout the entire experiment. The flow rates and temperatures were recorded throughout the entire experiment using the Altamira™ software.

4.4 BACKGROUND EXPERIMENTS

Background experiments were run to ensure that no vinyl acetate was formed in the absence of a catalyst. An experiment with a carbon dioxide, methane and acetylene mixture using the alumina support showed only mass spectra peaks associated with helium, carbon dioxide, methane and acetylene. No peaks corresponding to carbon monoxide, hydrogen, acetic acid, vinyl acetate or any other organic compound were observed. Therefore any product seen during the experiments with a catalyst is formed by the catalyst, not the reactor tube, quartz wool or alumina support.

4.5 DATA ANALYSIS

For each experiment, the Altamira™ data files were converted into excel spreadsheets. The flow rates were examined to ensure that no major fluctuations occurred. The temperature of the sample at each recorded time was then saved in a new spreadsheet.

The mass spectrum data was first analyzed using the Dycor™ software. The mass spectra were examined for any peaks associated with compounds other than helium, carbon dioxide, methane, acetylene, acetic acid or vinyl acetate. In order to obtain the value of individual m/z mass spectrometer signals for each sampling time, a Perl data filter program was used to sort through the comma delimited converted Dycor™ data files. To eliminate noise, the m/z data was smoothed using an 11 point adjacent averaging in Origin™. The smoothed m/z mass spectrometer signals values for each sampling time were then inserted

into the temperature spreadsheet. Plots were made of temperature and the selected m/z peak mass spectrometer signal versus time.

The following m/z values were chosen: 2 m/z for hydrogen, 4 m/z for helium, 16 m/z for methane, 14 m/z for water, 26 m/z for acetylene, 24 m/z for carbon monoxide, 44 m/z for carbon dioxide, 60 m/z for acetic acid and 46 m/z for vinyl acetate. These m/z values are those corresponding to the largest fraction displayed by each molecule [8, 9], except acetic acid and vinyl acetate. A 43 m/z value is the largest fraction for acetic acid and 45 m/z the next largest[8, 9]. However, due to the large amount of carbon dioxide in the system the 44 m/z peak of carbon dioxide interfered with the 43 m/z of acetic acid. Moreover, carbon dioxide also has a peak at 45 m/z. Thus, the third largest m/z fraction for acetic acid, 60 m/z [8, 9], was chosen. A 43 m/z value is also the largest fraction for vinyl acetate [8, 9]. Since the carbon dioxide interferes with the 43 m/z peak, and 43 m/x is the largest fraction for acetic acid, the next largest peak, 46 m/z, was chosen for vinyl acetate. Mass spectra of the hydrogen, helium, carbon dioxide, carbon monoxide, methane and acetic acid pure components are given in Appendix D.1. Mass spectra for acetylene and vinyl acetate are given in Appendix E.1.

Due to the inaccuracy of the mixing rotameter, the m/z peaks of given compounds could not be calibrated. Selectivity factors for acetylene, acetic acid and vinyl acetate were not available in the literature. Therefore, the mole fractions of the components and conversions were not calculated.

4.6 RESULTS & DISCUSSION

When the Zn-acetate/carbon catalyst was exposed to acetylene bubbled through acetic acid, vinyl acetate was observed, figure 4-2. The vinyl acetate was first seen when the temperature reached about 225°C. The mass spectrometer signal sharply increased until it reached a maximum of 7.52×10^{-12}, at which point it began to decrease as the temperature increased. At 400°C, it remained steady at about 1.61×10^{-13}. As the temperature began to decrease, the mass spectrometer signal of vinyl acetate once again increased. A maximum mass spectrometer signal of 1.15×10^{-11} was reached around 275°C. The mass spectrometer signal then decreased as the temperature continued to decrease.

Thermodynamics indicate that this reaction is more favorable at lower temperatures. The lack of formation of vinyl acetate below 200°C may be due to poor kinetics. The thermodynamics at 400°C are limited, thus the mass spectrometer signal of vinyl acetate was lower at this temperature. Once the temperature had decreased back down, the thermodynamics once again became favorable and an increase in vinyl acetate was seen. As the temperature continued to decrease, the vinyl acetate likewise decreased, likely due to poor kinetics again. It appears that 225°C - 275°C is the ideal temperature range at which the reaction is not completely limited by either thermodynamics or kinetics.

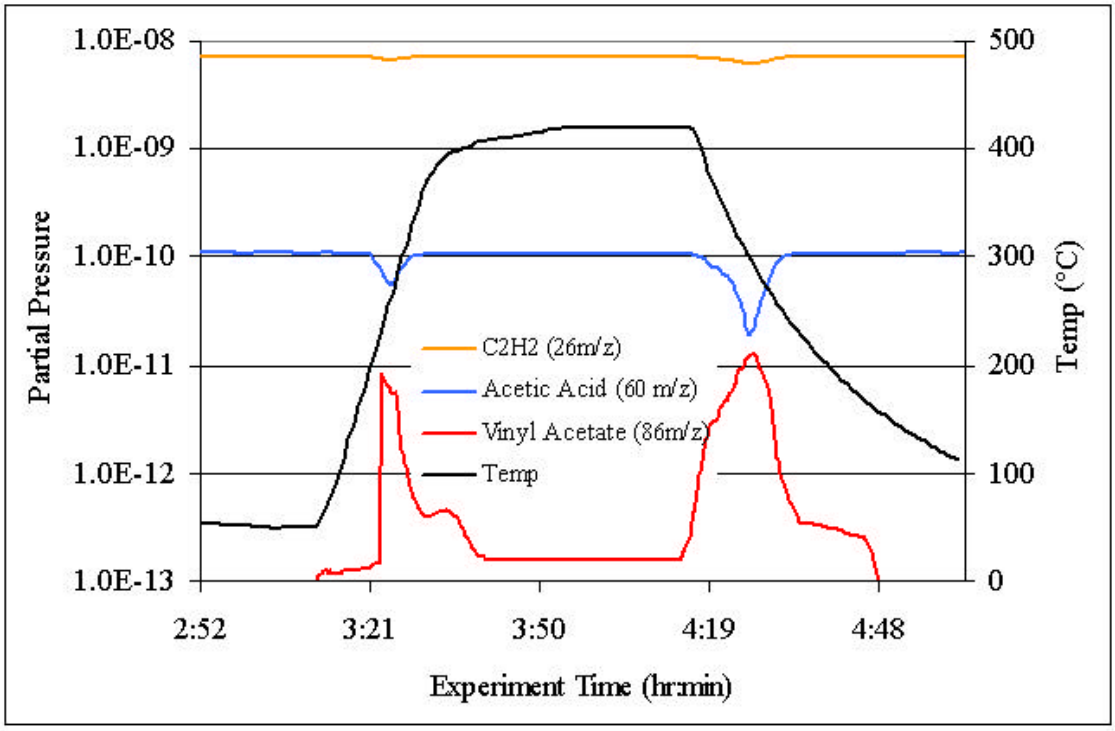

Figure 4-2: C_2H_2, acetic acid and vinyl acetate mass spectrometer signals, determined by quadrupole mass spectrometer, and sample temperature versus experiment time for Zn -acetate/carbon catalyst exposed to acetylene bubbled through acetic acid

This experiment shows that the Zn-acetate/carbon catalyst can facilitate the reaction between acetylene and acetic acid. It also shows that the ideal temperature range for the reaction between acetylene and acetic acid using the Zn-acetate/carbon catalyst is 225°C -275°C.

The carbon dioxide, methane, and acetylene mixture experiment was run using the Zn-acetate/carbon catalyst alone. This experiment showed no formation of acetic acid or vinyl acetate. The formation of carbon monoxide and hydrogen also was not observed. Minimal amounts of organic compounds other than acetic acid and vinyl acetate were

observed. However, these were barely above the baseline and within the noise value of the mass spectrometer.

The Zn-acetate/carbon catalyst alone does not catalyze the formation of vinyl acetate from carbon dioxide, methane and acetylene. Since no acetic acid was observed, the limitation of this catalyst is probably its inability to catalyze the direct synthesis of acetic acid from carbon dioxide and methane. This experiment also shows that the Zn-acetate does not react with the acetylene to form vinyl acetate to any measurable extent.

The 5% Pd/alumina and 5% Pt/alumina catalysts showed the formation of vinyl acetate in addition to acetic acid when exposed to a mixture of carbon dioxide, methane and acetylene, figure 4-3 and figure 4-4 respectively. The formation of vinyl acetate was first observed around 150°C, and acetic acid was first observed around 225°C for both catalysts. The mass spectrometer signals of both species reached a maximum at 400°C and remained steady until the temperature began to decrease.

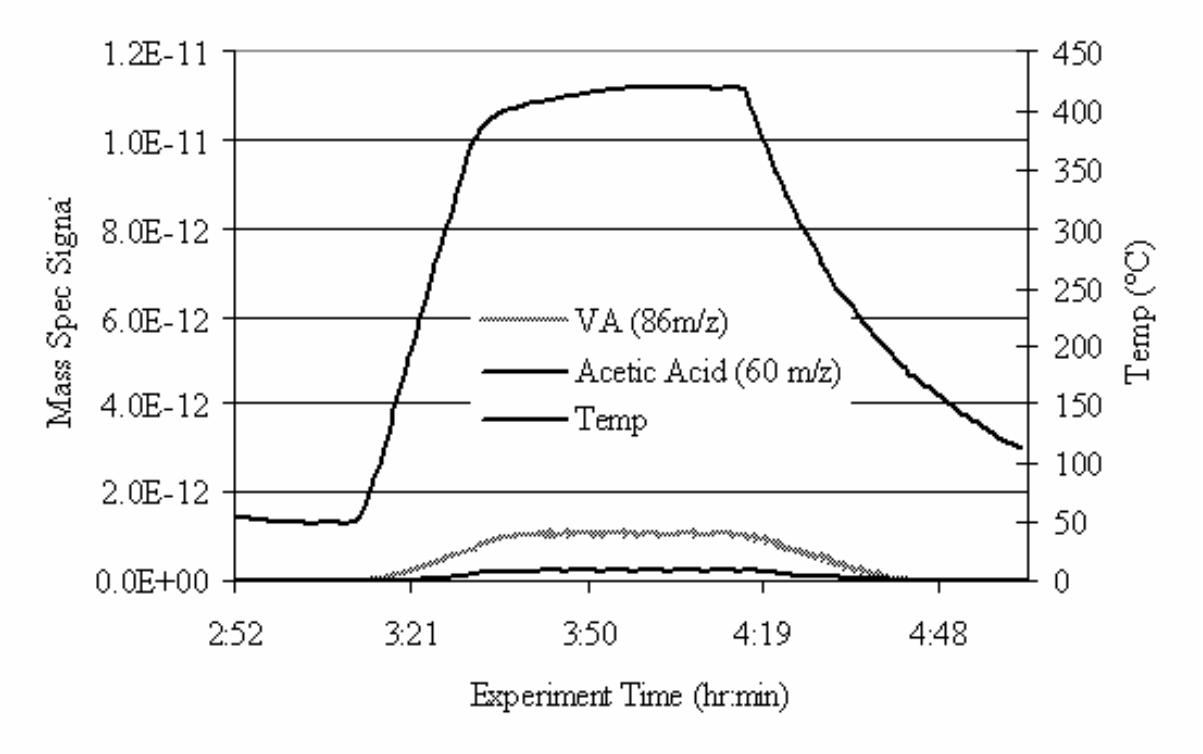

Figure 4-3: Acetic acid and vinyl acetate mass spectrometer signals, determined by quadrupole mass spectrometer, and sample temperature versus experiment time for 5% Pd/alumina exposed to a mixture of carbon dioxide, methane and acetylene

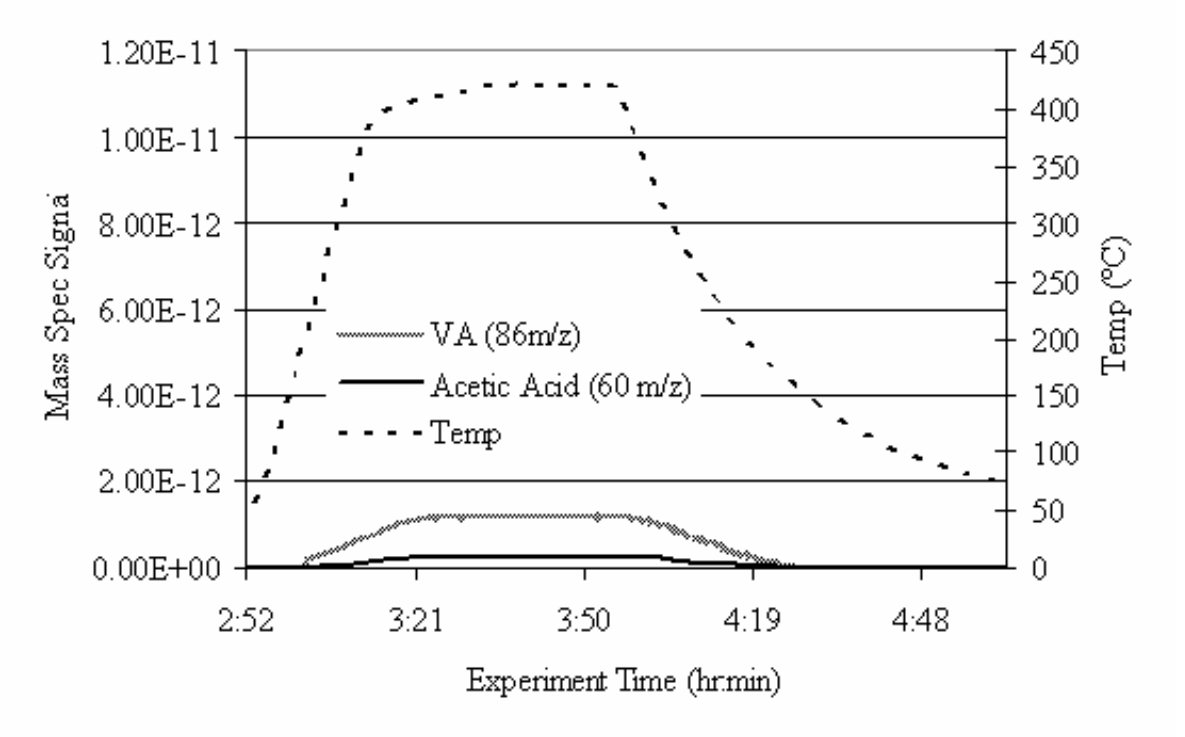

Figure 4-4: Acetic acid and vinyl acetate mass spectrometer signals, determined by quadrupole mass spectrometer, and sample temperature versus experiment time for 5% Pt/alumina exposed to a mixture of carbon dioxide, methane and acetylene

The maximum mass spectrometer signal of acetic acid was slightly lower than the lowest mass spectrometer signal of acetic acid observed during the carbon dioxide and methane experiment using these catalysts, discussed in section 3.4. The maximum mass spectrometer signal of acetic acid was about 2.17×10^{-13} for the 5% Pd/Alumina catalyst and 2.34×10^{-13} for the 5% Pt/Alumina catalyst. The maximum mass spectrometer signal of vinyl acetate was 1.04×10^{-12} for the 5% Pd/Alumina catalyst and 1.14×10^{-12} for the 5% Pt/Alumina catalyst. The higher mass spectrometer signal of the 46 m/z peak of vinyl acetate, relative to the 60 m/z peak of acetic acid, indicates that the mole fraction of vinyl acetate was

higher than the mole fraction of acetic acid. This is in qualitatively agreement with the thermodynamic calculations, section 2.9.

The equilibrium thermodynamic calculations predict that the formation of vinyl acetate would be more favorable at lower temperatures. However, this is not observed from experimentally. The lack of vinyl acetate formation at lower temperatures may be due to poor kinetics, rather than thermodynamics.

In addition to the acetic acid and vinyl acetate, carbon monoxide and hydrogen were observed over both catalysts, figure 4-5 and figure 4-6. This is consistent with the results from the carbon dioxide and methane experiments discussed in section 3.8. The relatively small decrease in acetylene can be associated with the formation of vinyl acetate. This indicates that the carbon monoxide and hydrogen were formed from carbon dioxide and methane, not from acetylene.

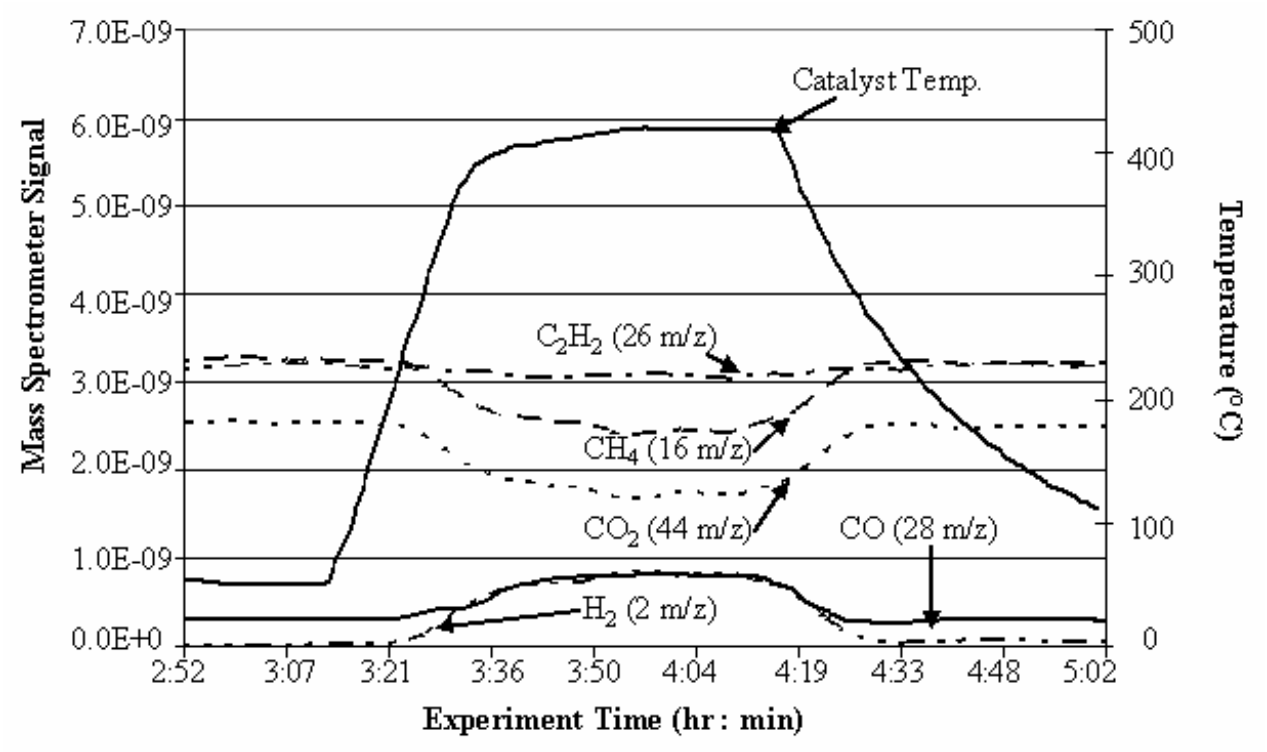

Figure 4-5: CO_2, CH_4, C_2H_2, CO and H_2 mass spectrometer signals, determined by quadrupole mass spectrometer, and sample temperature versus experiment time for 5% Pd/alumina exposed to a mixture of carbon dioxide, methane and acetylene

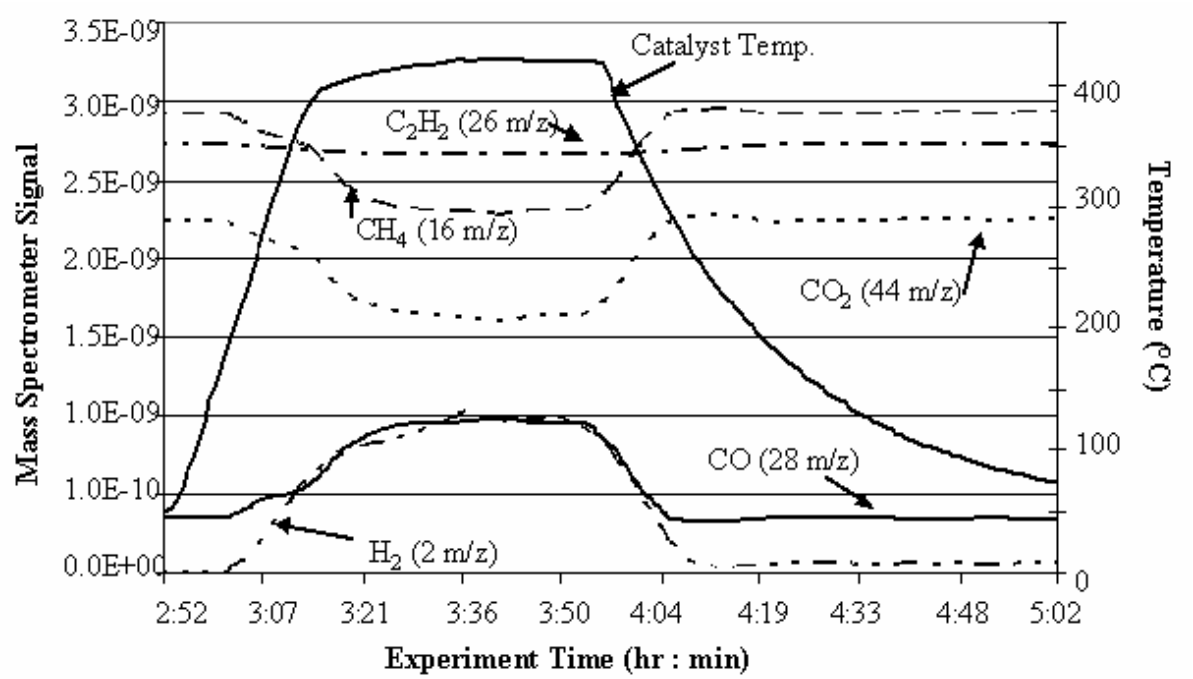

Figure 4-6: CO_2, CH_4, C_2H_2, CO and H_2 mass spectrometer signals, determined by quadrupole mass spectrometer, and sample temperature versus experiment time for 5% Pt/alumina exposed to a mixture of carbon dioxide, methane and acetylene

The mass spectrometer signal of acetylene decreases as the mass spectrometer signal of vinyl acetate increases. This indicates that the acetylene is reacted to form the vinyl acetate. It is not obvious whether the vinyl acetate was formed from acetic acid and acetylene alone, or if the carbon monoxide and hydrogen played a role in vinyl acetate formation.

When an admixtures of 5% Pd/alumina and Zn-acetate/carbon, and 5% Pt/alumina and Zn-acetate/carbon catalysts were used, interesting results were observed. The formation of both acetic acid and vinyl acetate was seen, figure 4-7 and figure 4-8. However, the mass spectrometer signals of acetic acid and vinyl acetate reached a maximum at 300°C, as

opposed to 400°C with the 5% Pt/alumina and 5% Pd/alumina catalysts. The mass spectrometer signals sharply increased up to 300°C, and then gradually declined as the temperature remained at 400°C. After about 30 minutes at 400°C, the mass spectrometer signals leveled off until the temperature began to decrease and the mass spectrometer signals dropped back to the baseline levels.

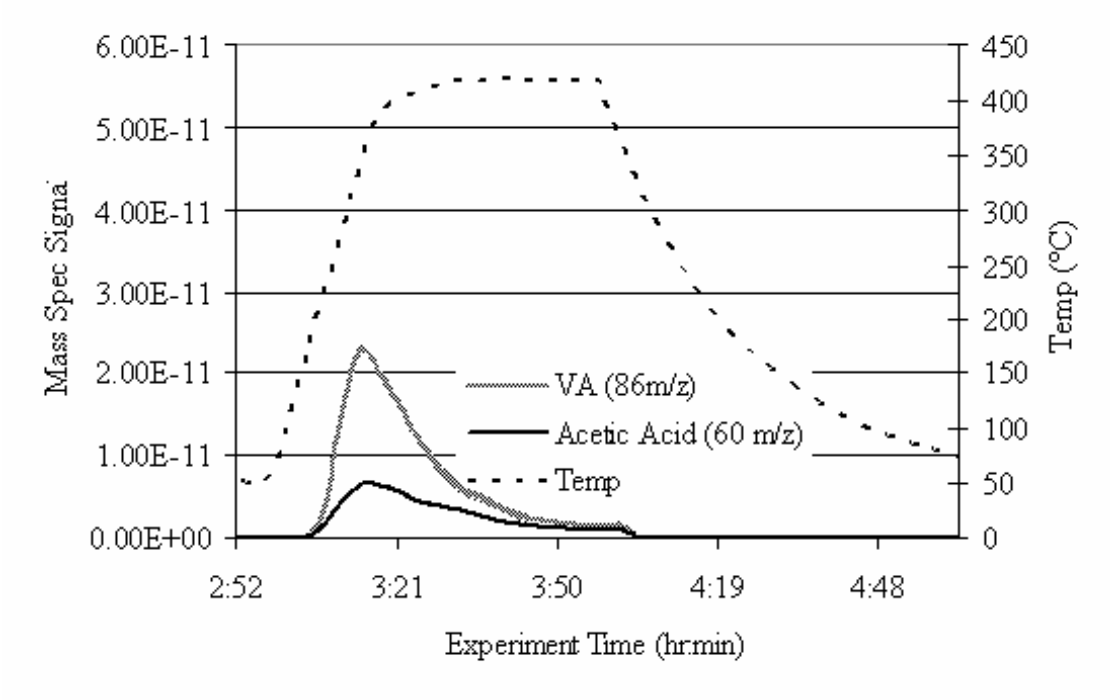

Figure 4-7: Acetic acid and vinyl acetate mass spectrometer signals, determined by quadrupole mass spectrometer, and sample temperature versus experiment time for 5% Pd/alumina & Zn-acetate/carbon admixture exposed to a mixture of carbon dioxide, methane and acetylene

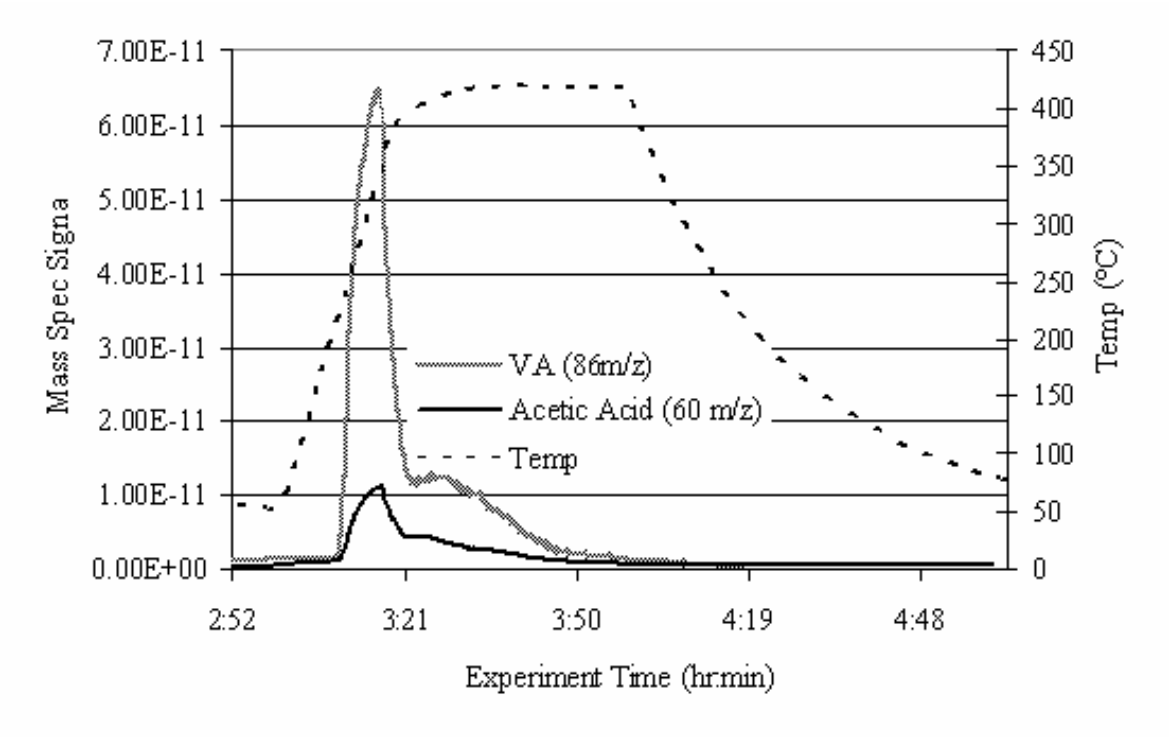

Figure 4-8: Acetic acid and vinyl acetate mass spectrometer signals, determined by quadrupole mass spectrometer, and sample temperature versus experiment time for 5% Pt/alumina & Zn-acetate/carbon admixture exposed to a mixture of carbon dioxide, methane and acetylene

The maximum mass spectrometer signals of acetic acid and vinyl acetate were significantly higher than observed when using the 5% Pd/alumina or 5% Pt/alumina catalysts alone. The maximum mass spectrometer signal of acetic acid was about 6.65×10^{-12} for the 5% Pd/Alumina and Zn-acetate/Carbon admixture and 1.07×10^{-11} for the 5% Pt/Alumina and Zn-acetate/Carbon admixture. The maximum mass spectrometer signal of vinyl acetate was 2.27×10^{-11} for the 5% Pd/Alumina and Zn-acetate/Carbon admixture and 4.6×10^{-11} for the 5% Pt/Alumina and Zn-acetate/Carbon admixture.

The equilibrium thermodynamic calculations predict that the formation of vinyl acetate would be more favorable at lower temperatures. The lack of formation of acetic acid

and vinyl acetate at low temperatures, 50°C, may be due to kinetic limitations, rather than thermodynamic limitations. As the temperature increases, the kinetic limitations are overcome, thus the reaction is then thermodynamically limited. The sharp peak at 300°C may be the ideal temperature at which the reaction is not completely limited by either thermodynamics or kinetics.

The large vinyl acetate and acetic acid peaks are observed only as the temperature increases, and not again at 300°C, when the temperature decreases. If 300°C is the ideal temperature for this reaction, a second peak as the temperature decreases would be expected. The lack of this peak may be due to deactivation of the Zn-acetate catalyst or possibly polymerization of the vinyl acetate on the metal of the alumina catalysts

In addition to the acetic acid and vinyl acetate, carbon monoxide and hydrogen were observed, figure 4-9 and figure 4-10. The mass spectrometer signals of both carbon monoxide and hydrogen are considerably less than those observed with the 5% Pd/alumina or the 5% Pt/alumina catalysts alone. Perhaps Zn-acetate/carbon hinders the formation of carbon monoxide and hydrogen from carbon dioxide and methane or the Pd or Pt metal is deactivated by the vinyl acetate, leading to a decrease in CO and H_2 formation.

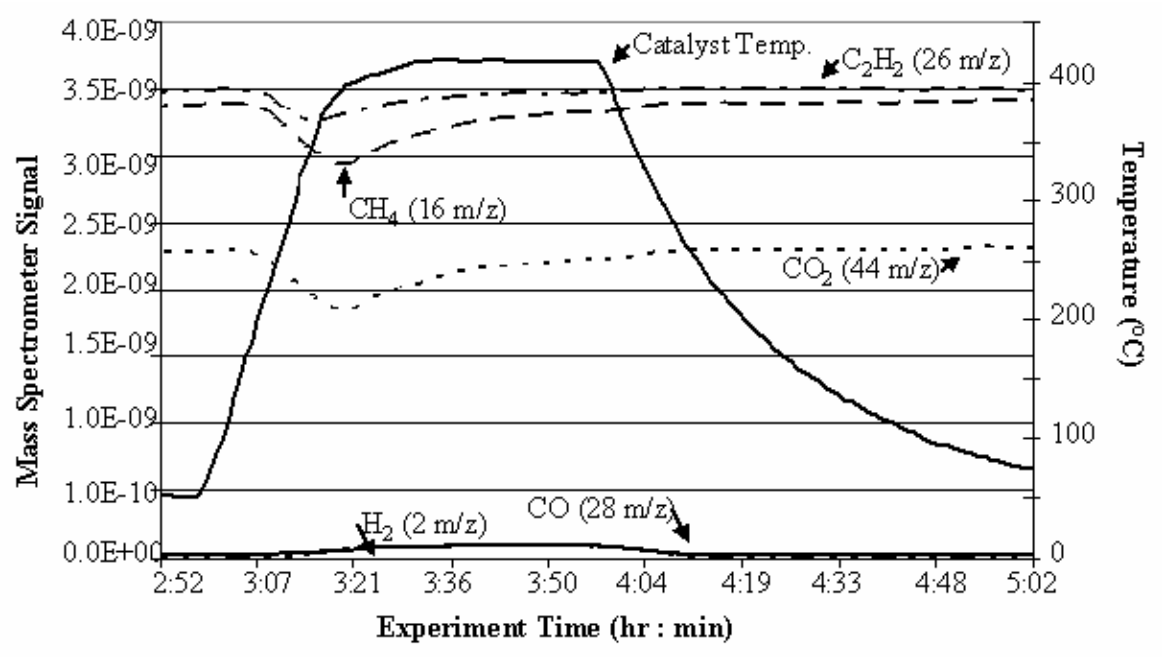

Figure 4-9: CO_2, CH_4, C_2H_2, CO and H_2 mass spectrometer signals, determined by quadrupole mass spectrometer, and sample temperature versus experiment time for 5% Pd/alumina & Zn-acetate/carbon admixture exposed to a mixture of carbon dioxide, methane and acetylene

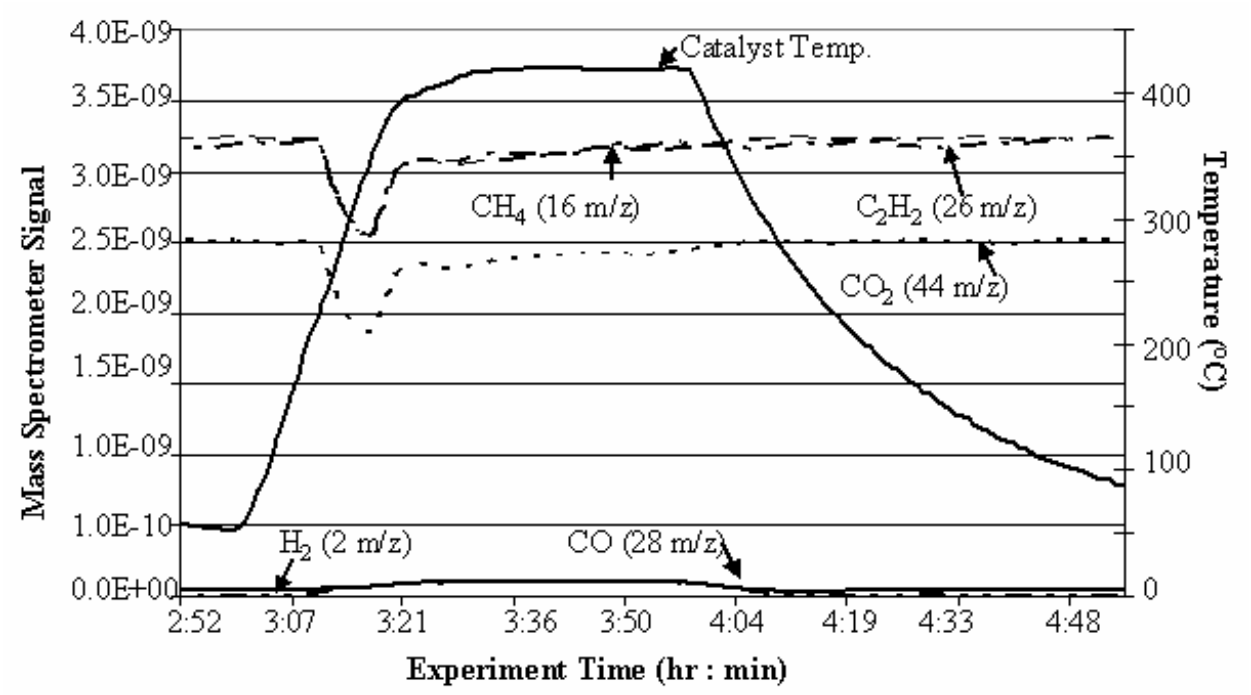

Figure 4-10: CO_2, CH_4, C_2H_2, CO and H_2 mass spectrometer signals, determined by quadrupole mass spectrometer, and sample temperature versus experiment time for 5% Pt/alumina & Zn-acetate/carbon admixture exposed to a mixture of carbon dioxide, methane and acetylene

The decrease in mass spectrometer signals of acetylene, carbon dioxide and methane at 300°C qualitatively correspond to the increase in the mass spectrometer signals of acetic acid and vinyl acetate at the same temperature. The formation of carbon monoxide and hydrogen does not begin to occur until around 400°C.

4.7 CONCLUSIONS

The Zn-acetate/carbon catalyst alone did not show the formation of acetic acid or vinyl acetate when exposed to a mixture of carbon dioxide, methane and acetylene. Vinyl

acetate was observed when the catalyst was exposed to acetylene and acetic acid. The Zn-acetate/carbon catalyst can facilitate the formation of vinyl acetate from acetylene and methane, but cannot catalyze the direct synthesis reaction. Therefore another catalyst is required to form the acetic acid from carbon dioxide and methane.

Both the 5% Pd/alumina and 5% Pt/alumina catalysts alone showed the formation of vinyl acetate when exposed to a mixture of carbon dioxide and methane, while the alumina support and Zn-acetate/carbon catalyst alone did not. The mass spectrometer signals of acetic acid and vinyl acetate observed from the alumina supported catalysts reached a maximum at 400°C. The thermodynamics predict that the overall reaction is more favorable at lower temperatures. The observed increase in mass spectrometer signals with temperature may be due to kinetic limitations, rather than thermodynamics.

Admixtures of the alumina supported catalysts and the Zn-acetate/carbon catalysts gave much higher maximum mass spectrometer signals of acetic acid and vinyl acetate than the alumina supported catalysts alone. Unlike the alumina supported catalysts alone, the maximum mass spectrometer signals of acetic acid and vinyl acetate were observed at 300°C. As the temperature increased to 400°C, the mass spectrometer signals decreased. After approximately 30 minutes at 400°C, the mass spectrometer signals remained steady and then decreased to the baseline values as the temperature decreased. The lack of acetic acid and vinyl acetate at low temperatures may be due to kinetic limitations, whereas the minimal amounts at higher temperatures may be due to thermodynamic limitations. It appears that 300°C is the optimal temperature for this reaction using the admixtures, where neither the kinetics nor the thermodynamics completely hinder the reaction.

Vinyl acetate formation using the admixtures was only seen at 300°C as the temperature was increased, not at 300°C when the temperature decreased. However, vinyl acetate from acetic acid and acetylene over the Zn-acetate/carbon catalyst was seen both as the temperature increased and decreased. It is not certain what causes the lack of vinyl acetate over the admixtures as the temperature decreases. This may be due to poisoning or deactivation of the catalysts.

These experiments have shown that the thermodynamic limitations of the direct synthesis of acetic acid can be overcome by reacting the formed acetic acid in another more thermodynamically favorable reaction. The formation of vinyl acetate from carbon dioxide, methane and acetylene was definitively shown. To maximize the formation of vinyl acetate, admixtures of a catalyst which facilitates the formation of acetic acid from carbon dioxide and methane and a catalyst which facilitates the formation of vinyl acetate from acetic acid and acetylene is required. More research is required to understand this reaction system.

4.8 REFERENCES

1. [Anon], *Product focus - Acetic Acid.* Chemical Week, 2002. **164**(21): p. 33-33.
2. [Anon], *Product Focus - Vinyl Acetate Monomer.* Chemical Week, 2003. **165**(23): p. 31-31.
3. Kirk, R.E.O., D.F, *Encyclopedia of Chemical Technology*. 4th ed. 1997, New York: John Wiley & Sons.
4. Kirk, R.E.O., D.F, *Encyclopedia of Chemical Technology*. 4th ed. 1955, New York: John Wiley & Sons.

5. Agreda, V. and J. Zoeller, *Acetic Acid and its Derivatives*. 1993, New York: Marcel Dekker.

6. Considine, D.M., *Chemical and Process Technology Encyclopedia*. 1974, New York: McGraw-Hill Book Company.

7. Chemical.Rubber.Company, *CRC Handbook of Chemistry and Physics*. 83 ed. 2002, Cleveland: Chemical Rubber Company Press.

8. Cornu, A.M., R., *Compilation of Mass Spectral Data.* 1975, New York: Heyden & Sons Ltd.

9. NIST, *Standard Reference Database*. 2001.

CHAPTER 5

SUGGESTIONS FOR FUTURE WORK

5.1 INTRODUCTION

This research has demonstrated the formation of acetic acid from carbon dioxide and methane over solid catalysts. However, there is still a considerable amount of research which may be done to better understand this reaction and to optimize it. Additionally, research should be done on systems to overcome the thermodynamic limitations of the direct synthesis of acetic acid from carbon dioxide and methane. Some of these possible research ideas are described in the following sections.

5.2 DETERMINATION OF REACTION MECHANISM

The results from DRIFTS experiments, flow through reactor experiments, and catalyst characterizations indicate that the reaction mechanism of the direct synthesis reaction requires both adsorbed carbon dioxide and methane. However, the exact reaction mechanism was not determined. Additionally, it was uncertain whether the acetic acid formed in the flow through reactor experiments was formed directly from the carbon dioxide and methane, or from the carbon monoxide and hydrogen that were observed. Future work on the reaction mechanism may provide valuable information on the direct synthesis reaction.

5.3 EFFECT CATALYSTS ON DIRECT ACETIC ACID SYNTHESIS

Only four catalysts were used in this research: reduced 5% Pd/carbon, un-reduced 5% Pd/carbon, 5% Pd/alumina and 5% Pd/alumina. The carbon supported catalysts were ineffective for the direct synthesis of acetic acid from carbon dioxide and methane, while the alumina supported catalysts were effective. Other catalysts may be even more effective. Further research should be conducted using different metals and/or supports. Additionally, the metal loading may effect the formation of acetic acid and should be studied.

5.4 CARBON MONOXIDE FORMATION

Using the flow through reactor system with an online mass spectrometer, the formation of large amounts of carbon monoxide and hydrogen was observed over 5% Pd/alumina and 5% Pt/alumina catalysts exposed to carbon dioxide and methane. The thermodynamics for the dry reforming reaction are worse than those of the direct synthesis reaction:

$$CO_2 + CH_4 \rightarrow 2\ CO + 2\ H_2 \qquad \text{(R 5-1)}$$

$\Delta G_r^0 = +\ 171$ kJ/mol * $\qquad\qquad$ $\Delta H_r^0 = +\ 247$ kJ/mol *

* ΔG_r^0 and ΔH_r^0 values calculated from ΔG_f^0 and ΔH_f^0 values obtained from CRC [1]

The cause of the formation of carbon monoxide and hydrogen was not determined in this research. Further studies are needed to understand this side reaction. It would be of great industrial use if the formation of synthesis gas from carbon dioxide and methane can be

achieved to a sufficient degree at these mild conditions. Using labeled carbon on either the carbon dioxide or methane might be useful in determining where the carbon in the carbon monoxide is coming from: the carbon dioxide, methane, or both.

5.5 VINYL ACETATE SYNTHESIS FROM ACETYLENE

Preliminary experiments were conducted that showed significant formation of vinyl acetate from carbon dioxide, methane and acetylene over admixtures of 5% Pd/alumina or 5% Pt/alumina and Zn-acetate/carbon catalysts. These preliminary results indicate that this may be an effective method to overcome the thermodynamic limitations of the direct synthesis reaction and produce an industrially useful chemical.

Further research is needed to understand and optimize the formation of vinyl acetate from carbon dioxide, methane and acetylene. Rather than using an admixture of catalysts, a single catalyst may be found that will facilitate both the direct synthesis reaction and the formation of vinyl acetate from the formed acetic acid and acetylene. This catalyst may consist of Pt and Zn on an alumina support. Additionally, the effects of temperature, pressure and inlet concentrations on this reaction system should be studied to determine the optimal conditions.

5.6 OTHER METHODS TO OVERCOME THERMODYNAMICS

Thermodynamic calculations performed on the synthesis of acetic anhydride from carbon dioxide, methane and ketene indicated that high conversions of methane could be achieved at relatively mild conditions. Similarly, vinyl acetate synthesis from carbon dioxide, methane, ethylene and oxygen also resulted in promising thermodynamics. These reaction systems may be successful methods to overcome the thermodynamic limitations of the direct synthesis reaction and produce useful industrial chemicals. Research is required to determine if these reaction systems are indeed possible, and the optimum catalysts and conditions.

5.7 REFERENCES

1. Chemical.Rubber.Company, *CRC Handbook of Chemistry and Physics*. 83 ed. 2002, Cleveland: Chemical Rubber Company Press.

APPENDIX A:

THERMODYNAMIC ANALYSIS OF REACTIONS

A.1. CALCULATIONS FOR EQUILIBRIUM THERMODYNAMICS OF DIRECT SYNTHESIS

Equilibrium thermodynamic calculations were performed on the direct synthesis of acetic acid from carbon dioxide and methane:

$$CO_2 + CH_4 \leftrightarrow CH_3COOH \qquad \text{(R A-1)}$$

A detailed description of the calculations performed to determine the equilibrium fractional conversion of methane at varying temperatures, pressures and inlet mole fractions of carbon dioxide is given in sections A.1.1 and A.1.2. The data obtained from those calculations can be found in section A.1.3. A list of the symbols used in sections A.1.1 and A.1.2 is given in table A-1.

Table A-1: Definition of symbols used in sections A.1.1 and A.1.2:

Symbol:	**Definition:**
Cp	Heat Capacity of Reaction
G(Tr)	Gibbs Free Energy of Reaction at Tr
H(Tr)	Heat of Reaction at Tr
Kp(T)	Equilibrium Constant in Terms of Pressures at T
Kp(Tr)	Equilibrium Constant in Terms of Pressures at Tr
na	Number of Moles of Acetic Acid
nch	Number of Moles of Methane
nco	Number of Moles of Carbon Dioxide
noch	Initial Number of Moles of Methane
noco	Initial Number of Moles of Carbon Dioxide
nt	Total Number of Moles
nto	Initial Total Number of Moles
P	Total Pressure
pa	Partial Pressure of Acetic Acid
pch	Partial Pressure of Methane
pco	Partial Pressure of Carbon Dioxide
R	Ideal Gas Constant
T	Temperature
Tr	289.15 Kelvin
X CH_4	Equilibrium Fractional Conversion of Methane
ya	Mole Fraction of Acetic Acid
ych	Mole Fraction of Methane
yco	Mole Fraction of Carbon Dioxide
yoa	Initial mole fraction of Acetic Acid, assumed to be zero
yoch	Initial mole fraction of Methane
yoco	Initial mole fraction of Carbon Dioxide

A.1.1. FINDING THE EQUILIBRIUM CONSTANT (K_P) AT ANY TEMPERATURE:

The equilibrium constant of the reaction at a given temperature can be found by starting with the definition of the Gibbs free energy of the reaction in terms of equilibrium constant, the standard temperature and the ideal gas constant:

$$\mathrm{G}(Tr) = -R\,Tr\,\ln(\mathrm{Kp}(Tr)) \qquad \text{(E A-1)}$$

Solving for Kp(Tr) from equation (E A-1) gives:

$$\mathrm{Kp}(Tr) = \mathbf{e}^{\left(-\frac{\mathrm{G}(Tr)}{R\,Tr}\right)} \qquad \text{(E A-2)}$$

which can be used to find the equilibrium constant of the reaction at a standard temperature, if the Gibbs free energy at that temperature is known.

The equilibrium constant of the reaction at any temperature can be found by starting with the relationship between the equilibrium constant and the heat of the reaction, the heat capacity of the reaction and the temperature:

$$\frac{\partial}{\partial T}\ln(Kp) = \frac{\mathrm{H}(Tr) + Cp\,(T - Tr)}{R\,T^2} \qquad \text{(E A-3)}$$

Integrating equation (E A-3) from Tr to T gives:

$$\ln\left(\frac{\mathrm{Kp}(T)}{\mathrm{Kp}(Tr)}\right) = \frac{(\mathrm{H}(Tr) - Tr\,Cp)\left(\frac{1}{Tr} - \frac{1}{T}\right)}{R} + \frac{Cp\,\ln\left(\frac{T}{Tr}\right)}{R} \qquad \text{(E A-4)}$$

Solving equation (E A-4) for Kp gives:

$$\mathrm{Kp}(T) = \mathbf{e}^{\left(\frac{Tr^2\, Cp + \mathrm{H}(Tr)\, T - \mathrm{H}(Tr)\, Tr - Tr\, Cp\, T + Cp\, \ln\left(\frac{T}{Tr}\right) Tr\, T}{R\, Tr\, T}\right)} \mathrm{Kp}(Tr) \qquad \text{(E A-5)}$$

which can be used to find the equilibrium constant of the reaction at any temperature, if the heat capacity, heat of reaction and the equilibrium constant at a given temperature is known.

A.1.2. FINDING THE EQUILIBRIUM FRACTIONAL CONVERSION OF METHANE:

The equilibrium fractional conversion of methane can be found by starting with the definition of the equilibrium constant in terms of the partial pressures of the components of the reaction:

$$Kp = \frac{pa}{pco\ pch} \qquad \text{(E A-6)}$$

The partial pressures of each component can be expressed in terms of its mole fraction and the total pressure:

$$pa = ya\ P \qquad \text{(E A-7)}$$

$$pco = yco\ P \qquad \text{(E A-8)}$$

$$pch = ych\ P \qquad \text{(E A-9)}$$

The equilibrium constant can then be written in terms of the mole fractions of the components and the total pressure by substituting equations (E A-7), (E A-8) and (E A-9) into equation (E A-6):

$$Kp = \frac{ya}{P\ yco\ ych} \qquad \text{(E A-10)}$$

The number of moles of methane can be expressed in terms of the number of initial moles of methane and the equilibrium fractional conversion of methane:

$$nch = noch\ (1 - X) \qquad \text{(E A-11)}$$

Likewise, the number of moles of carbon dioxide can be expressed in terms of the number of initial moles of carbon dioxide and the equilibrium fractional conversion of methane:

$$nco = noco - noch\ X \qquad \text{(E A-12)}$$

The number of moles of acetic acid can also be expressed in terms of the number of initial moles of acetic acid in terms of equilibrium fractional conversion of methane, assuming no initial moles of acetic acid:

$$na = noch\ X \qquad \text{(E A-13)}$$

The total number of moles can be written as the sum of the number of moles of each of the components:

$$nt = nch + nco + na \qquad \text{(E A-14)}$$

The total number of moles can be re-written in terms of the initial moles of methane and carbon dioxide, and equilibrium fractional conversion of methane by substituting equations (E A-11), (E A-12) and (E A-13) into equation (E A-14):

$$nt = noch\ (1 - X) + noco \qquad \text{(E A-15)}$$

The mole fractions of each component can be expressed in terms of number of moles of the component and the total number of moles:

$$ya = \frac{na}{nt} \qquad \text{(E A-16)}$$

$$ych = \frac{nch}{nt} \qquad \text{(E A-17)}$$

$$yco = \frac{nco}{nt} \qquad \text{(E A-18)}$$

The mole fractions of each component can then be re-written in terms of the initial number of moles of carbon dioxide and methane and equilibrium fractional conversion of methane by substituting equations (E A-12), (E A-13), (E A-14), and (E A-15) into the above equations (E A-16), (E A-17), and (E A-18):

$$ya = \frac{noch\ X}{noch\ (1 - X) + noco} \qquad \text{(E A-19)}$$

$$ych = \frac{noch\ (1 - X)}{noch\ (1 - X) + noco} \qquad \text{(E A-20)}$$

$$yco = \frac{noco - noch\ X}{noch\ (1 - X) + noco} \qquad \text{(E A-21)}$$

The initial number of moles of methane and carbon dioxide can be written in terms of the inlet mole fractions of each, respectively, and the initial total number of moles, still assuming no initial number of moles of acetic acid:

$$noch = yoch\ nto \tag{E A-22}$$

$$noco = yoco\ nto \tag{E A-23}$$

Since the initial mole fractions of the components add up to one, the initial mole fraction of methane can be expressed in terms of initial mole fraction of carbon dioxide:

$$noch = 1 - noco \tag{E A-24}$$

Now the mole fractions of each of the component can be re-written in terms of the initial total number of moles, the initial mole fraction of carbon dioxide and equilibrium fractional conversion of methane by substituting previous equations (E A-22), (E A-23), (E A-24) into equations (E A-19), (E A-20), and (E A-21):

$$ya = \frac{(1 - yoco)\ X\ nto}{(1 - yoco)\ (1 - X)\ nto + yoco\ nto} \tag{E A-25}$$

$$ych = \frac{(1 - yoco)\ (1 - X)\ nto}{(1 - yoco)\ (1 - X)\ nto + yoco\ nto} \tag{E A-26}$$

$$yco = \frac{yoco\ nto - (1 - yoco)\ X\ nto}{(1 - yoco)\ (1 - X)\ nto + yoco\ nto} \tag{E A-27}$$

Finally, the equilibrium constant can now be expressed in terms of the initial mole fraction of carbon dioxide, the equilibrium fractional conversion of methane and the total pressure by substituting equations (E A-25), (E A-26) and (E A-27) into equation (E A-10) and simplifying:

$$Kp = -\frac{X\,(1 - X + yoco\,X)}{P\,(yoco - X + yoco\,X)\,(-1 + X)} \qquad \text{(E A-28)}$$

By using equations (E A-5) and (E A-28) the equilibrium fractional conversion of methane can be found at any given temperature, pressure and inlet mole fraction of carbon dioxide.

A.1.3. Equilibrium Fractional Conversion of Methane Data

To calculate the equilibrium constant for the reaction at any temperature, first the equilibrium constant at a given temperature must be found. To do so, the heat of formation ($?Hf°$), Gibbs free energy of formation ($?Gf°$), heat capacity ($Cp°$) and entropy ($?S°$) for the reaction at a given temperature must be known. The data for the reaction were calculated by subtracting the data for the sum of the products from the sum of the reactants. The data for each of the components at 298.15 K was taken from the CRC Handbook of Chemistry and Physics [1]. This data, as well as the calculated data for the reactant can be found in table A-2.

Table A-2: Thermodynamic values used in equilibrium calculations

	Kcal/mol ?Hf°	Kcal/mol ?Gf°	Kcal/K mol Cp	Kcal/K mol ?S°
Acetic Acid	-103.31	-89.40	0.0159	0.0675
Carbon Dioxide	-94.051	-94.254	0.00887	0.05106
Methane	-17.88	-12.13	0.008439	0.044492
Reaction	**8.621**	**16.98**	**-0.00141**	**-0.0281**

From these values the equilibrium constant for the reaction at 298.15 K was calculated to be 3.543×10^{-13} atm^{-1} from equation (E A-2). The equilibrium fractional conversion of methane was calculated using equation (E A-28) for varying temperatures, pressures, and inlet mole fractions of carbon dioxide. The values of these calculations can be found in tables A-3 and A-4.

Table A-3: Equilibrium fractional conversion of methane calculated for reaction (R A-1) at 150 atm and varying temperatures and inlet mole fractions of carbon dioxide.

Inlet Mole Fraction of CO_2	400 K	500 K	600 K	700 K	800 K	900 K	1000 K
0.10	2.34 E-11	1.94 E-10	7.77 E-10	2.06 E-09	4.22 E-09	7.30 E-09	1.12 E-08
0.15	3.71 E-11	3.08 E-10	1.23 E-09	3.27 E-09	6.70 E-09	1.16 E-08	1.78 E-08
0.20	5.25 E-11	4.36 E-10	1.75 E-09	4.63 E-09	9.49 E-09	1.64 E-08	2.53 E-08
0.25	7.01 E-11	5.82 E-10	2.33 E-09	6.17 E-09	1.27 E-08	2.19 E-08	3.37 E-08
0.30	9.01 E-11	7.48 E-10	3.00 E-09	7.93 E-09	1.63 E-08	2.81 E-08	4.33 E-08
0.35	1.13 E-10	9.40 E-10	3.76 E-09	9.97 E-09	2.04 E-08	3.54 E-08	5.44 E-08
0.40	1.40 E-10	1.16 E-09	4.66 E-09	1.23 E-08	2.53 E-08	4.38 E-08	6.74 E-08
0.45	1.72 E-10	1.43 E-09	5.72 E-09	1.51 E-08	3.11 E-08	5.37 E-08	8.27 E-08
0.50	2.10 E-10	1.75 E-09	6.99 E-09	1.85 E-08	3.80 E-08	6.57 E-08	1.01 E-07
0.55	2.57 E-10	2.13 E-09	8.54 E-09	2.26 E-08	4.64 E-08	8.03 E-08	1.24 E-07
0.60	3.15 E-10	2.62 E-09	1.05 E-08	2.78 E-08	5.69 E-08	9.85 E-08	1.52 E-07
0.65	3.90 E-10	3.24 E-09	1.30 E-08	3.44 E-08	7.05 E-08	1.22 E-07	1.88 E-07
0.70	4.90 E-10	4.07 E-09	1.63 E-08	4.32 E-08	8.86 E-08	1.53 E-07	2.36 E-07
0.75	6.31 E-10	5.24 E-09	2.10 E-08	5.55 E-08	1.14 E-07	1.97 E-07	3.03 E-07
0.80	8.41 E-10	6.98 E-09	2.80 E-08	7.41 E-08	1.52 E-07	2.63 E-07	4.04 E-07
0.85	1.19 E-09	9.89 E-09	3.96 E-08	1.05 E-07	2.15 E-07	3.72 E-07	5.73 E-07
0.90	1.89 E-09	1.57 E-08	6.29 E-08	1.67 E-07	3.42 E-07	5.91 E-07	9.09 E-07
0.95	3.99 E-09	3.32 E-08	1.33 E-07	3.52 E-07	7.21 E-07	1.25 E-06	1.92 E-06

Table A-4: Equilibrium fractional conversion of methane calculated for reaction (R A-1) with an inlet mole fraction of carbon dioxide of 0.95 and varying temperatures and pressures.

	1 atm	10 atm	25 atm	50 atm	75 atm	100 atm	125 atm	150 atm
350 K	5.76 E-12	5.76 E-11	1.44 E-10	2.88 E-10	4.32 E-10	5.76 E-10	7.20 E-10	8.64 E-10
400 K	2.66 E-11	2.66 E-10	6.66 E-10	1.33 E-09	2.00 E-09	2.66 E-09	3.33 E-09	3.99 E-09
450 K	8.67 E-11	8.67 E-10	2.17 E-09	4.33 E-09	6.50 E-09	8.67 E-09	1.08 E-08	1.30 E-08
500 K	2.21 E-10	2.21 E-09	5.53 E-09	1.11 E-08	1.66 E-08	2.21 E-08	2.76 E-08	3.32 E-08
550 K	4.73 E-10	4.73 E-09	1.18 E-08	2.36 E-08	3.54 E-08	4.73 E-08	5.91 E-08	7.09 E-08
600 K	8.85 E-10	8.85 E-09	2.21 E-08	4.43 E-08	6.64 E-08	8.85 E-08	1.11 E-07	1.33 E-07
650 K	1.50 E-09	1.50 E-08	3.75 E-08	7.50 E-08	1.12 E-07	1.50 E-07	1.87 E-07	2.25 E-07
700 K	2.34 E-09	2.34 E-08	5.86 E-08	1.17 E-07	1.76 E-07	2.34 E-07	2.93 E-07	3.52 E-07
750 K	3.44 E-09	3.44 E-08	8.61 E-08	1.72 E-07	2.58 E-07	3.44 E-07	4.31 E-07	5.17 E-07
800 K	4.81 E-09	4.81 E-08	1.20 E-07	2.40 E-07	3.61 E-07	4.81 E-07	6.01 E-07	7.21 E-07
850 K	6.43 E-09	6.43 E-08	1.61 E-07	3.22 E-07	4.83 E-07	6.43 E-07	8.04 E-07	9.65 E-07
900 K	8.32 E-09	8.32 E-08	2.08 E-07	4.16 E-07	6.24 E-07	8.32 E-07	1.04 E-06	1.25 E-06
950 K	1.04 E-08	1.04 E-07	2.61 E-07	5.22 E-07	7.84 E-07	1.04 E-06	1.31 E-06	1.57 E-06
1000 K	1.28 E-08	1.28 E-07	3.20 E-07	6.40 E-07	9.60 E-07	1.28 E-06	1.60 E-06	1.92 E-06

A.2. ASPEN DATA FOR DIRECT SYNTHESIS

The equilibrium thermodynamic calculations for reaction (R A-1) were performed using the AspenPlus™ engineering simulation software. The RGIBBS reactor model was used to perform a Gibbs free energy minimization on the system to give the chemical and phase equilibrium composition at various temperatures and pressures. These calculations do not take into account any surface interactions. Molecular interactions between molecules are taken into account in the equation of state. The inlet composition, inlet temperature, inlet pressure, reactor temperature and reactor pressure were specified for each reaction. The inlet conditions were set equal to the reactor conditions.

For the Aspen calculations, an inlet mole fraction of 0.95 CO_2 and 0.05 CH_4, and an inlet total number of moles of 1 was used. The Aspen calculations were performed for a wide range of pressures and temperatures, 1 - 1000 atm and 300 – 2000 K. Additionally, the calculations were performed for each of three equations of state; ideal gas, Redlich-Kwong and Peng-Robinson.

The equilibrium fractional conversion of methane (X_{CH4}) was calculated using equation (E A-29):

$$X_{CH4} = \#\text{ Moles of } CH_4 \text{ reacted} / \#\text{ Inlet moles of } CH_4 \qquad \text{(E A-29)}$$

Since the outlet moles of methane given by Aspen did not have enough significant figures, the number of outlet moles of acetic acid was used as the number of moles of methane that reacted.

A.2.1. IDEAL GAS EQUATION OF STATE

Data of the outlet moles for carbon dioxide (CO_2), methane (CH_4) and acetic acid (CH_3COOH) and the equilibrium fractional conversion of methane (X_{CH4}) obtained by using the ideal gas equation of state in Aspen at varying temperatures and pressures can be found in tables A-5 - A-19. The equilibrium fractional conversions of methane only can be found in tables A-20 – A-22. An inlet mole flow of 0.95 CO_2 and 0.05 CH_4 was used for all calculations. The inlet temperature and pressure was set equal to that of the reactor. This equation of state assumes no molecular interactions; therefore there no interaction parameters were used.

Table A-5: Outlet moles and the equilibrium fractional conversion of methane for reaction (R A-1) obtained by using the ideal gas equation of state in Aspen at varying temperatures and 1 atm.

1 atm	300 K	400 K	500 K	600 K	700 K
Phase	Vapor	Vapor	Vapor	Vapor	Vapor
CO_2	0.9500000	0.9500000	0.9500000	0.9500000	0.9500000
CH_4	0.0500000	0.0500000	0.0500000	0.0500000	0.0500000
CH_3COOH	0.0000E+00	8.4084E-13	6.7313E-12	2.7158E-11	7.4857E-11
X CH_4	**0.000E+00**	**1.682E-11**	**1.346E-10**	**5.432E-10**	**1.497E-09**

1 atm	800 K	900 K	1000 K	1100 K	1200 K
Phase	Vapor	Vapor	Vapor	Vapor	Vapor
CO_2	0.9500000	0.9500000	0.9500000	0.9500000	0.9500000
CH_4	0.0500000	0.0500000	0.0499999	0.0500000	0.0500000
CH_3COOH	1.6331E-10	3.0511E-10	5.1125E-10	7.9056E-10	1.1496E-09
X CH_4	**3.266E-09**	**6.102E-09**	**1.023E-08**	**1.581E-08**	**2.299E-08**

1 atm	1300 K	1400 K	1500 K	1600 K	1700 K
Phase	Vapor	Vapor	Vapor	Vapor	Vapor
CO_2	0.9500000	0.9500000	0.9500000	0.9500000	0.9500000
CH_4	0.0500000	0.0500000	0.0500000	0.0500000	0.0500000
CH_3COOH	1.5927E-09	2.1220E-09	2.7378E-09	3.4388E-09	4.2227E-09
X CH_4	**3.185E-08**	**4.244E-08**	**5.476E-08**	**6.878E-08**	**8.445E-08**

1 atm	1800 K	1900 K	2000 K
Phase	Vapor	Vapor	Vapor
CO_2	0.9500000	0.9500000	0.9500000
CH_4	0.0499999	0.0499999	0.0499999
CH_3COOH	5.0857E-09	6.0235E-09	7.0314E-09
X CH_4	**1.017E-07**	**1.205E-07**	**1.406E-07**

Table A-6: Outlet moles and the equilibrium fractional conversion of methane for reaction (R A-1) obtained by using the ideal gas equation of state in Aspen at varying temperatures and 10 atm.

10 atm	300 K	400 K	500 K	600 K	700 K
Phase	Vapor	Vapor	Vapor	Vapor	Vapor
CO_2	0.9500000	0.9500000	0.9500000	0.9500000	0.9500000
CH_4	0.0500000	0.0500000	0.0500000	0.0500000	0.0500000
CH_3COOH	2.5441E-13	8.4083E-12	6.7313E-11	2.7158E-10	7.4857E-10
X CH_4	**5.088E-12**	**1.682E-10**	**1.346E-09**	**5.432E-09**	**1.497E-08**

10 atm	800 K	900 K	1000 K	1100 K	1200 K
Phase	Vapor	Vapor	Vapor	Vapor	Vapor
CO_2	0.9500000	0.9500000	0.9500000	0.9500000	0.9500000
CH_4	0.0500000	0.0500000	0.0499999	0.0499999	0.0499999
CH_3COOH	1.6331E-09	3.0512E-09	5.1127E-09	7.9057E-09	1.1496E-08
X CH_4	**3.266E-08**	**6.102E-08**	**1.023E-07**	**1.581E-07**	**2.299E-07**

10 atm	1300 K	1400 K	1500 K	1600 K	1700 K
Phase	Vapor	Vapor	Vapor	Vapor	Vapor
CO_2	0.9500000	0.9500000	0.9500000	0.9500000	0.9500000
CH_4	0.0499999	0.0499999	0.0499999	0.0499999	0.0499999
CH_3COOH	1.5927E-08	2.1220E-08	2.7378E-08	3.4389E-08	4.2227E-08
X CH_4	**3.185E-07**	**4.244E-07**	**5.476E-07**	**6.878E-07**	**8.445E-07**

10 atm	1800 K	1900 K	2000 K
Phase	Vapor	Vapor	Vapor
CO_2	0.9499999	0.9499999	0.9499999
CH_4	0.0499999	0.0499999	0.0499999
CH_3COOH	5.0857E-08	6.0235E-08	7.0314E-08
X CH_4	**1.017E-06**	**1.205E-06**	**1.406E-06**

Table A-7: Outlet moles and the equilibrium fractional conversion of methane for reaction (R A-1) obtained by using the ideal gas equation of state in Aspen at varying temperatures and 25 atm.

25 atm	300 K	400 K	500 K	600 K	700 K
Phase	Vapor	Vapor	Vapor	Vapor	Vapor
CO_2	0.9500000	0.9500000	0.9500000	0.9500000	0.9500000
CH_4	0.0500000	0.0500000	0.0500000	0.0500000	0.0500000
CH_3COOH	6.3600E-13	2.1021E-11	1.6828E-10	6.7895E-10	1.8715E-09
X CH_4	**1.272E-11**	**4.204E-10**	**3.366E-09**	**1.358E-08**	**3.743E-08**

25 atm	800 K	900 K	1000 K	1100 K	1200 K
Phase	Vapor	Vapor	Vapor	Vapor	Vapor
CO_2	0.9500000	0.9500000	0.9500000	0.9500000	0.9500000
CH_4	0.0500000	0.0499999	0.0499999	0.0499999	0.0499999
CH_3COOH	4.0826E-09	7.6281E-09	1.2782E-08	1.9764E-08	2.8740E-08
X CH_4	**8.165E-08**	**1.526E-07**	**2.556E-07**	**3.953E-07**	**5.748E-07**

25 atm	1300 K	1400 K	1500 K	1600 K	1700 K
Phase	Vapor	Vapor	Vapor	Vapor	Vapor
CO_2	0.9500000	0.9499999	0.9499999	0.9499999	0.9499999
CH_4	0.0499999	0.0499999	0.0499999	0.0499999	0.0499998
CH_3COOH	3.9817E-08	5.3049E-08	6.8445E-08	8.5972E-08	1.0557E-07
X CH_4	**7.963E-07**	**1.061E-06**	**1.369E-06**	**1.719E-06**	**2.111E-06**

25 atm	1800 K	1900 K	2000 K
Phase	Vapor	Vapor	Vapor
CO_2	0.9499999	0.9499998	0.9499998
CH_4	0.0499998	0.0499998	0.0499998
CH_3COOH	1.2714E-07	1.5059E-07	1.7578E-07
X CH_4	**2.543E-06**	**3.012E-06**	**3.516E-06**

Table A-8: Outlet moles and the equilibrium fractional conversion of methane for reaction (R A-1) obtained by using the ideal gas equation of state in Aspen at varying temperatures and 50 atm.

50 atm	300 K	400 K	500 K	600 K	700 K
Phase	Vapor	Vapor	Vapor	Vapor	Vapor
CO_2	0.9500000	0.9500000	0.9500000	0.9500000	0.9500000
CH_4	0.0500000	0.0500000	0.0500000	0.0500000	0.0500000
CH_3COOH	1.2700E-12	4.2042E-11	3.3656E-10	1.3580E-09	3.7429E-09
X CH_4	**2.540E-11**	**8.408E-10**	**6.731E-09**	**2.716E-08**	**7.486E-08**

50 atm	800 K	900 K	1000 K	1100 K	1200 K
Phase	Vapor	Vapor	Vapor	Vapor	Vapor
CO_2	0.9500000	0.9500000	0.9500000	0.9500000	0.9499999
CH_4	0.0499999	0.0499999	0.0499999	0.0499999	0.0499999
CH_3COOH	8.1653E-09	1.5256E-08	2.5563E-08	3.9529E-08	5.7481E-08
X CH_4	**1.633E-07**	**3.051E-07**	**5.113E-07**	**7.906E-07**	**1.150E-06**

50 atm	1300 K	1400 K	1500 K	1600 K	1700 K
Phase	Vapor	Vapor	Vapor	Vapor	Vapor
CO_2	0.9499999	0.9499999	0.9499999	0.9499998	0.9499998
CH_4	0.0499999	0.0499998	0.0499998	0.0499998	0.0499997
CH_3COOH	7.9634E-08	1.0610E-07	1.3689E-07	1.7194E-07	2.1113E-07
X CH_4	**1.593E-06**	**2.122E-06**	**2.738E-06**	**3.439E-06**	**4.223E-06**

50 atm	1800 K	1900 K	2000 K
Phase	Vapor	Vapor	Vapor
CO_2	0.9499997	0.9499997	0.9499996
CH_4	0.0499997	0.0499997	0.0499996
CH_3COOH	2.5428E-07	3.0112E-07	3.5157E-07
X CH_4	**5.086E-06**	**6.022E-06**	**7.031E-06**

Table A-9: Outlet moles and the equilibrium fractional conversion of methane for reaction (R A-1) obtained by using the ideal gas equation of state in Aspen at varying temperatures and 100 atm.

100 atm	300 K	400 K	500 K	600 K	700 K
Phase	Liquid	Vapor	Vapor	Vapor	Vapor
CO_2	0.9500000	0.9500000	0.9500000	0.9500000	0.9500000
CH_4	0.0499999	0.0500000	0.0500000	0.0500000	0.0499999
CH_3COOH	2.7526E-08	8.4083E-11	6.7313E-10	2.7159E-09	7.4860E-09
X CH_4	**5.505E-07**	**1.682E-09**	**1.346E-08**	**5.432E-08**	**1.497E-07**

100 atm	800 K	900 K	1000 K	1100 K	1200 K
Phase	Vapor	Vapor	Vapor	Vapor	Vapor
CO_2	0.9500000	0.9500000	0.9499999	0.9499999	0.9499999
CH_4	0.0499999	0.0499999	0.0499999	0.0499999	0.0499998
CH_3COOH	1.6331E-08	3.0512E-08	5.1126E-08	7.9057E-08	1.1496E-07
X CH_4	**3.266E-07**	**6.102E-07**	**1.023E-06**	**1.581E-06**	**2.299E-06**

100 atm	1300 K	1400 K	1500 K	1600 K	1700 K
Phase	Vapor	Vapor	Vapor	Vapor	Vapor
CO_2	0.9499998	0.9499998	0.9499997	0.9499997	0.9499996
CH_4	0.0499998	0.0499997	0.0499997	0.0499996	0.0499995
CH_3COOH	1.5927E-07	2.1220E-07	2.7378E-07	3.4389E-07	4.2227E-07
X CH_4	**3.185E-06**	**4.244E-06**	**5.476E-06**	**6.878E-06**	**8.445E-06**

100 atm	1800 K	1900 K	2000 K
Phase	Vapor	Vapor	Vapor
CO_2	0.9499995	0.9499994	0.9499993
CH_4	0.0499994	0.0499994	0.0499993
CH_3COOH	5.0856E-07	6.0234E-07	7.0313E-07
X CH_4	**1.017E-05**	**1.205E-05**	**1.406E-05**

Table A-10: Outlet moles and the equilibrium fractional conversion of methane for reaction (R A-1) obtained by using the ideal gas equation of state in Aspen at varying temperatures and 150 atm.

150 atm	300 K	400 K	500 K	600 K	700 K
Phase	Liquid	Vapor	Vapor	Vapor	Vapor
CO_2	0.9500000	0.9500000	0.9500000	0.9500000	0.9500000
CH_4	0.0499999	0.0500000	0.0500000	0.0500000	0.0499999
CH_3COOH	2.7526E-08	1.2613E-10	1.0097E-09	4.0739E-09	1.1229E-08
X CH_4	**5.505E-07**	**2.523E-09**	**2.019E-08**	**8.148E-08**	**2.246E-07**

150 atm	800 K	900 K	1000 K	1100 K	1200 K
Phase	Vapor	Vapor	Vapor	Vapor	Vapor
CO_2	0.9500000	0.9500000	0.9499999	0.9499999	0.9499998
CH_4	0.0499999	0.0499999	0.0499999	0.0499998	0.0499998
CH_3COOH	2.4496E-08	4.5769E-08	7.6690E-08	1.1859E-07	1.7244E-07
X CH_4	**4.899E-07**	**9.154E-07**	**1.534E-06**	**2.372E-06**	**3.449E-06**

150 atm	1300 K	1400 K	1500 K	1600 K	1700 K
Phase	Vapor	Vapor	Vapor	Vapor	Vapor
CO_2	0.9499998	0.9499997	0.9499996	0.9499995	0.9499994
CH_4	0.0499997	0.0499996	0.0499995	0.0499994	0.0499993
CH_3COOH	2.3890E-07	3.1829E-07	4.1067E-07	5.1583E-07	6.3340E-07
X CH_4	**4.778E-06**	**6.366E-06**	**8.213E-06**	**1.032E-05**	**1.267E-05**

150 atm	1800 K	1900 K	2000 K
Phase	Vapor	Vapor	Vapor
CO_2	0.9499992	0.9499991	0.9499989
CH_4	0.0499992	0.0499991	0.0499989
CH_3COOH	7.6284E-07	9.0351E-07	1.0547E-06
X CH_4	**1.526E-05**	**1.807E-05**	**2.109E-05**

Table A-11: Outlet moles and the equilibrium fractional conversion of methane for reaction (R A-1) obtained by using the ideal gas equation of state in Aspen at varying temperatures and 200 atm.

200 atm	300 K	400 K	500 K	600 K	700 K
Phase	Liquid	Vapor	Vapor	Vapor	Vapor
CO_2	0.9500000	0.9500000	0.9500000	0.9500000	0.9500000
CH_4	0.0499999	0.0500000	0.0500000	0.0499999	0.0499999
CH_3COOH	2.7526E-08	1.6672E-10	1.3463E-09	5.4318E-09	1.4972E-08
X CH_4	**5.505E-07**	**3.334E-09**	**2.693E-08**	**1.086E-07**	**2.994E-07**

200 atm	800 K	900 K	1000 K	1100 K	1200 K
Phase	Vapor	Vapor	Vapor	Vapor	Vapor
CO_2	0.9500000	0.9499999	0.9499999	0.9499998	0.9499998
CH_4	0.0499999	0.0499999	0.0499999	0.0499998	0.0499997
CH_3COOH	3.2661E-08	6.1025E-08	1.0225E-07	1.5811E-07	2.2992E-07
X CH_4	**6.532E-07**	**1.220E-06**	**2.045E-06**	**3.162E-06**	**4.598E-06**

200 atm	1300 K	1400 K	1500 K	1600 K	1700 K
Phase	Vapor	Vapor	Vapor	Vapor	Vapor
CO_2	0.9499997	0.9499996	0.9499995	0.9499993	0.9499992
CH_4	0.0499996	0.0499995	0.0499994	0.0499993	0.0499991
CH_3COOH	3.1854E-07	4.2439E-07	5.4755E-07	6.8777E-07	8.4452E-07
X CH_4	**6.371E-06**	**8.488E-06**	**1.095E-05**	**1.376E-05**	**1.689E-05**

200 atm	1800 K	1900 K	2000 K
Phase	Vapor	Vapor	Vapor
CO_2	0.9499989	0.9499988	0.9499986
CH_4	0.0499989	0.0499988	0.0499985
CH_3COOH	1.0171E-06	1.2047E-06	1.4062E-06
X CH_4	**2.034E-05**	**2.409E-05**	**2.812E-05**

Table A-12: Outlet moles and the equilibrium fractional conversion of methane for reaction (R A-1) obtained by using the ideal gas equation of state in Aspen at varying temperatures and 300 atm.

300 atm	300 K	400 K	500 K	600 K	700 K
Phase	Liquid	Vapor	Vapor	Vapor	Vapor
CO_2	0.9500000	0.9500000	0.9500000	0.9500000	0.9500000
CH_4	0.0499999	0.0500000	0.0500000	0.0499999	0.0499999
CH_3COOH	2.7526E-08	2.5225E-10	2.0236E-09	8.1478E-09	2.2458E-08
X CH_4	**5.505E-07**	**5.045E-09**	**4.047E-08**	**1.630E-07**	**4.492E-07**

300 atm	800 K	900 K	1000 K	1100 K	1200 K
Phase	Vapor	Vapor	Vapor	Vapor	Vapor
CO_2	0.9500000	0.9499999	0.9499998	0.9499998	0.9499997
CH_4	0.0499999	0.0499999	0.0499998	0.0499997	0.0499996
CH_3COOH	4.8992E-08	9.1537E-08	1.5338E-07	2.3717E-07	3.4488E-07
X CH_4	**9.798E-07**	**1.831E-06**	**3.068E-06**	**4.743E-06**	**6.898E-06**

300 atm	1300 K	1400 K	1500 K	1600 K	1700 K
Phase	Vapor	Vapor	Vapor	Vapor	Vapor
CO_2	0.9499995	0.9499994	0.9499992	0.9499990	0.9499987
CH_4	0.0499995	0.0499993	0.0499991	0.0499989	0.0499987
CH_3COOH	4.7780E-07	6.3658E-07	8.2133E-07	1.0317E-06	1.2668E-06
X CH_4	**9.556E-06**	**1.273E-05**	**1.643E-05**	**2.063E-05**	**2.534E-05**

300 atm	1800 K	1900 K	2000 K
Phase	Vapor	Vapor	Vapor
CO_2	0.9499985	0.9499982	0.9499979
CH_4	0.0499984	0.0499981	0.0499978
CH_3COOH	1.5257E-06	1.8070E-06	2.1093E-06
X CH_4	**3.051E-05**	**3.614E-05**	**4.219E-05**

Table A-13: Outlet moles and the equilibrium fractional conversion of methane for reaction (R A-1) obtained by using the ideal gas equation of state in Aspen at varying temperatures and 400 atm.

400 atm	300 K	400 K	500 K	600 K	700 K
Phase	Liquid	Liquid	Vapor	Vapor	Vapor
CO_2	0.9500000	0.9499998	0.9500000	0.9500000	0.9500000
CH_4	0.0499999	0.0499997	0.0500000	0.0499999	0.0499999
CH_3COOH	2.7564E-08	2.1933E-07	2.6692E-09	1.0864E-08	2.9944E-08
X CH_4	**5.513E-07**	**4.387E-06**	**5.338E-08**	**2.173E-07**	**5.989E-07**

400 atm	800 K	900 K	1000 K	1100 K	1200 K
Phase	Vapor	Vapor	Vapor	Vapor	Vapor
CO_2	0.9499999	0.9499999	0.9499998	0.9499997	0.9499995
CH_4	0.0499999	0.0499998	0.0499998	0.0499996	0.0499995
CH_3COOH	6.5322E-08	1.2205E-07	2.0451E-07	3.1623E-07	4.5984E-07
X CH_4	**1.306E-06**	**2.441E-06**	**4.090E-06**	**6.325E-06**	**9.197E-06**

400 atm	1300 K	1400 K	1500 K	1600 K	1700 K
Phase	Vapor	Vapor	Vapor	Vapor	Vapor
CO_2	0.9499994	0.9499992	0.9499989	0.9499986	0.9499983
CH_4	0.0499993	0.0499991	0.0499989	0.0499986	0.0499983
CH_3COOH	6.3707E-07	8.4878E-07	1.0951E-06	1.3755E-06	1.6890E-06
X CH_4	**1.274E-05**	**1.698E-05**	**2.190E-05**	**2.751E-05**	**3.378E-05**

400 atm	1800 K	1900 K	2000 K
Phase	Vapor	Vapor	Vapor
CO_2	0.9499980	0.9499976	0.9499972
CH_4	0.0499979	0.0499975	0.0499971
CH_3COOH	2.0342E-06	2.4093E-06	2.8124E-06
X CH_4	**4.068E-05**	**4.819E-05**	**5.625E-05**

Table A-14: Outlet moles and the equilibrium fractional conversion of methane for reaction (R A-1) obtained by using the ideal gas equation of state in Aspen at varying temperatures and 500 atm.

500 atm	300 K	400 K	500 K	600 K	700 K
Phase	Liquid	Liquid	Vapor	Vapor	Vapor
CO_2	0.9500000	0.9499998	0.9500000	0.9500000	0.9500000
CH_4	0.0499999	0.0499997	0.0500000	0.0499999	0.0499999
CH_3COOH	2.7526E-08	2.1933E-07	3.3657E-09	1.3580E-08	3.7430E-08
X CH_4	**5.505E-07**	**4.387E-06**	**6.731E-08**	**2.716E-07**	**7.486E-07**

500 atm	800 K	900 K	1000 K	1100 K	1200 K
Phase	Vapor	Vapor	Vapor	Vapor	Vapor
CO_2	0.9499999	0.9499998	0.9499997	0.9499996	0.9499994
CH_4	0.0499999	0.0499998	0.0499997	0.0499996	0.0499994
CH_3COOH	8.1653E-08	1.5256E-07	2.5563E-07	3.9528E-07	5.7480E-07
X CH_4	**1.633E-06**	**3.051E-06**	**5.113E-06**	**7.906E-06**	**1.150E-05**

500 atm	1300 K	1400 K	1500 K	1600 K	1700 K
Phase	Vapor	Vapor	Vapor	Vapor	Vapor
CO_2	0.9499992	0.9499989	0.9499986	0.9499983	0.9499979
CH_4	0.0499992	0.0499989	0.0499986	0.0499982	0.0499978
CH_3COOH	7.9633E-07	1.0610E-06	1.3689E-06	1.7194E-06	2.1113E-06
X CH_4	**1.593E-05**	**2.122E-05**	**2.738E-05**	**3.439E-05**	**4.223E-05**

500 atm	1800 K	1900 K	2000 K
Phase	Vapor	Vapor	Vapor
CO_2	0.9499975	0.9499970	0.9499965
CH_4	0.0499974	0.0499969	0.0499964
CH_3COOH	2.5427E-06	3.0116E-06	3.5155E-06
X CH_4	**5.085E-05**	**6.023E-05**	**7.031E-05**

Table A-15: Outlet moles and the equilibrium fractional conversion of methane for reaction (R A-1) obtained by using the ideal gas equation of state in Aspen at varying temperatures and 600 atm.

600 atm	300 K	400 K	500 K	600 K	700 K
Phase	Liquid	Liquid	Vapor	Vapor	Vapor
CO_2	0.9500000	0.9499998	0.9500000	0.9500000	0.9500000
CH_4	0.0499999	0.0499997	0.0500000	0.0499999	0.0499999
CH_3COOH	2.7526E-08	2.1933E-07	4.0389E-09	1.6296E-08	4.4916E-08
X CH_4	**5.505E-07**	**4.387E-06**	**8.078E-08**	**3.259E-07**	**8.983E-07**

600 atm	800 K	900 K	1000 K	1100 K	1200 K
Phase	Vapor	Vapor	Vapor	Vapor	Vapor
CO_2	0.9499999	0.9499998	0.9499997	0.9499995	0.9499993
CH_4	0.0499999	0.0499998	0.0499996	0.0499995	0.0499993
CH_3COOH	9.7983E-08	1.8307E-07	3.0676E-07	4.7434E-07	6.8976E-07
X CH_4	**1.960E-06**	**3.661E-06**	**6.135E-06**	**9.487E-06**	**1.380E-05**

600 atm	1300 K	1400 K	1500 K	1600 K	1700 K
Phase	Vapor	Vapor	Vapor	Vapor	Vapor
CO_2	0.9499990	0.9499987	0.9499984	0.9499979	0.9499975
CH_4	0.0499990	0.0499987	0.0499983	0.0499979	0.0499974
CH_3COOH	9.5559E-07	1.2732E-06	1.6426E-06	2.0633E-06	2.5335E-06
X CH_4	**1.911E-05**	**2.546E-05**	**3.285E-05**	**4.127E-05**	**5.067E-05**

600 atm	1800 K	1900 K	2000 K
Phase	Vapor	Vapor	Vapor
CO_2	0.9499969	0.9499964	0.9499958
CH_4	0.0499969	0.0499963	0.0499957
CH_3COOH	3.0512E-06	3.6138E-06	4.2185E-06
X CH_4	**6.102E-05**	**7.228E-05**	**8.437E-05**

Table A-16: Outlet moles and the equilibrium fractional conversion of methane for reaction (R A-1) obtained by using the ideal gas equation of state in Aspen at varying temperatures and 700 atm.

700 atm	300 K	400 K	500 K	600 K	700 K
Phase	Liquid	Liquid	Vapor	Vapor	Vapor
CO_2	0.9500000	0.9499998	0.9500000	0.9500000	0.9499999
CH_4	0.0499999	0.0499997	0.0500000	0.0499999	0.0499999
CH_3COOH	2.7526E-08	2.1933E-07	4.7121E-09	1.9044E-08	5.2402E-08
X CH_4	**5.505E-07**	**4.387E-06**	**9.424E-08**	**3.809E-07**	**1.048E-06**

700 atm	800 K	900 K	1000 K	1100 K	1200 K
Phase	Vapor	Vapor	Vapor	Vapor	Vapor
CO_2	0.9499999	0.9499998	0.9499996	0.9499994	0.9499992
CH_4	0.0499998	0.0499997	0.0499996	0.0499994	0.0499992
CH_3COOH	1.1431E-07	2.1359E-07	3.5788E-07	5.5340E-07	8.0472E-07
X CH_4	**2.286E-06**	**4.272E-06**	**7.158E-06**	**1.107E-05**	**1.609E-05**

700 atm	1300 K	1400 K	1500 K	1600 K	1700 K
Phase	Vapor	Vapor	Vapor	Vapor	Vapor
CO_2	0.9499989	0.9499985	0.9499981	0.9499976	0.9499970
CH_4	0.0499988	0.0499985	0.0499980	0.0499975	0.0499970
CH_3COOH	1.1149E-06	1.4853E-06	1.9164E-06	2.4071E-06	2.9557E-06
X CH_4	**2.230E-05**	**2.971E-05**	**3.833E-05**	**4.814E-05**	**5.911E-05**

700 atm	1800 K	1900 K	2000 K
Phase	Vapor	Vapor	Vapor
CO_2	0.9499964	0.9499958	0.9499951
CH_4	0.0499964	0.0499957	0.0499950
CH_3COOH	3.5597E-06	4.2161E-06	4.9215E-06
X CH_4	**7.119E-05**	**8.432E-05**	**9.843E-05**

Table A-17: Outlet moles and the equilibrium fractional conversion of methane for reaction (R A-1) obtained by using the ideal gas equation of state in Aspen at varying temperatures and 800 atm.

800 atm	300 K	400 K	500 K	600 K	700 K
Phase	Liquid	Liquid	Vapor	Vapor	Vapor
CO_2	0.9500000	0.9499998	0.9500000	0.9500000	0.9499999
CH_4	0.0499999	0.0499997	0.0499999	0.0499999	0.0499999
CH_3COOH	2.7526E-08	2.1933E-07	5.3852E-09	2.1727E-08	5.9888E-08
X CH_4	**5.505E-07**	**4.387E-06**	**1.077E-07**	**4.345E-07**	**1.198E-06**

800 atm	800 K	900 K	1000 K	1100 K	1200 K
Phase	Vapor	Vapor	Vapor	Vapor	Vapor
CO_2	0.9499999	0.9499998	0.9499996	0.9499994	0.9499991
CH_4	0.0499998	0.0499997	0.0499995	0.0499993	0.0499990
CH_3COOH	1.3064E-07	2.4410E-07	4.0901E-07	6.3245E-07	9.1967E-07
X CH_4	**2.613E-06**	**4.882E-06**	**8.180E-06**	**1.265E-05**	**1.839E-05**

800 atm	1300 K	1400 K	1500 K	1600 K	1700 K
Phase	Vapor	Vapor	Vapor	Vapor	Vapor
CO_2	0.9499987	0.9499983	0.9499978	0.9499972	0.9499966
CH_4	0.0499987	0.0499983	0.0499978	0.0499972	0.0499966
CH_3COOH	1.2741E-06	1.6975E-06	2.1901E-06	2.7510E-06	3.3779E-06
X CH_4	**2.548E-05**	**3.395E-05**	**4.380E-05**	**5.502E-05**	**6.756E-05**

800 atm	1800 K	1900 K	2000 K
Phase	Vapor	Vapor	Vapor
CO_2	0.9499959	0.9499952	0.9499944
CH_4	0.0499959	0.0499951	0.0499943
CH_3COOH	4.0682E-06	4.8183E-06	5.6245E-06
X CH_4	**8.136E-05**	**9.637E-05**	**1.125E-04**

Table A-18: Outlet moles and the equilibrium fractional conversion of methane for reaction (R A-1) obtained by using the ideal gas equation of state in Aspen at varying temperatures and 900 atm.

900 atm	300 K	400 K	500 K	600 K	700 K
Phase	Liquid	Liquid	Vapor	Vapor	Vapor
CO_2	0.9500000	0.9499998	0.9500000	0.9500000	0.9499999
CH_4	0.4999990	0.0499997	0.0499999	0.0499999	0.0499999
CH_3COOH	2.7526E-08	2.1933E-07	6.0584E-09	2.4443E-08	6.7374E-08
X CH_4	**5.505E-07**	**4.387E-06**	**1.212E-07**	**4.889E-07**	**1.347E-06**

900 atm	800 K	900 K	1000 K	1100 K	1200 K
Phase	Vapor	Vapor	Vapor	Vapor	Vapor
CO_2	0.9499999	0.9499997	0.9499995	0.9499993	0.9499990
CH_4	0.0499998	0.0499997	0.0499995	0.0499992	0.0499989
CH_3COOH	1.4698E-07	2.7461E-07	4.6013E-07	7.1151E-07	1.0346E-06
X CH_4	**2.940E-06**	**5.492E-06**	**9.203E-06**	**1.423E-05**	**2.069E-05**

900 atm	1300 K	1400 K	1500 K	1600 K	1700 K
Phase	Vapor	Vapor	Vapor	Vapor	Vapor
CO_2	0.9499986	0.9499981	0.9499975	0.9499969	0.9499962
CH_4	0.0499985	0.0499980	0.0499975	0.0499969	0.0499962
CH_3COOH	1.4334E-06	1.9097E-06	2.4639E-06	3.0948E-06	3.8001E-06
X CH_4	**2.867E-05**	**3.819E-05**	**4.928E-05**	**6.190E-05**	**7.600E-05**

900 atm	1800 K	1900 K	2000 K
Phase	Vapor	Vapor	Vapor
CO_2	0.9499954	0.9499946	0.9499937
CH_4	0.0499954	0.0499946	0.0499936
CH_3COOH	4.5667E-06	5.4206E-06	6.3275E-06
X CH_4	**9.133E-05**	**1.084E-04**	**1.265E-04**

Table A-19: Outlet moles and the equilibrium fractional conversion of methane for reaction (R A-1) obtained by using the ideal gas equation of state in Aspen at varying temperatures and 1000 atm.

1000 atm	300 K	400 K	500 K	600 K	700 K
Phase	Liquid	Liquid	Vapor	Vapor	Vapor
CO_2	0.9500000	0.9499998	0.9500000	0.9500000	0.9499999
CH_4	0.0499999	0.0499997	0.0499999	0.0499999	0.0499999
CH_3COOH	2.7526E-08	2.1933E-07	6.7315E-09	2.7159E-08	7.4860E-08
X CH_4	**5.505E-07**	**4.387E-06**	**1.346E-07**	**5.432E-07**	**1.497E-06**

1000 atm	800 K	900 K	1000 K	1100 K	1200 K
Phase	Vapor	Vapor	Vapor	Vapor	Vapor
CO_2	0.9499998	0.9499997	0.9499995	0.9499992	0.9499988
CH_4	0.0499998	0.0499996	0.0499994	0.0499992	0.0499988
CH_3COOH	1.6331E-07	3.0512E-07	5.1126E-07	7.9056E-07	1.1496E-06
X CH_4	**3.266E-06**	**6.102E-06**	**1.023E-05**	**1.581E-05**	**2.299E-05**

1000 atm	1300 K	1400 K	1500 K	1600 K	1700 K
Phase	Vapor	Vapor	Vapor	Vapor	Vapor
CO_2	0.9499984	0.9499979	0.9499973	0.9499966	0.9499958
CH_4	0.0499984	0.0499978	0.0499972	0.0499965	0.0499957
CH_3COOH	1.5926E-06	2.1219E-06	2.7377E-06	3.4387E-06	4.2223E-06
X CH_4	**3.185E-05**	**4.244E-05**	**5.475E-05**	**6.877E-05**	**8.445E-05**

1000 atm	1800 K	1900 K	2000 K
Phase	Vapor	Vapor	Vapor
CO_2	0.9499949	0.9499940	0.9499930
CH_4	0.0499949	0.0499939	0.0499929
CH_3COOH	5.0851E-06	6.0228E-06	7.0304E-06
X CH_4	**1.017E-04**	**1.205E-04**	**1.406E-04**

Table A-20: Equilibrium fractional conversion of methane for reaction (R A-1) obtained by using the ideal gas equation of state in Aspen at varying temperatures and 1 - 100 atm.

T (K)	1 atm	10 atm	25 atm	50 atm	100 atm
300 K	0.000E+00	5.088E-12	1.272E-11	2.540E-11	**5.505E-07**
400 K	1.682E-11	1.682E-10	4.204E-10	8.408E-10	1.682E-09
500 K	1.346E-10	1.346E-09	3.366E-09	6.731E-09	1.346E-08
600 K	5.432E-10	5.432E-09	1.358E-08	2.716E-08	5.432E-08
700 K	1.497E-09	1.497E-08	3.743E-08	7.486E-08	1.497E-07
800 K	3.266E-09	3.266E-08	8.165E-08	1.633E-07	3.266E-07
900 K	6.102E-09	6.102E-08	1.526E-07	3.051E-07	6.102E-07
1000 K	1.023E-08	1.023E-07	2.556E-07	5.113E-07	1.023E-06
1100 K	1.581E-08	1.581E-07	3.953E-07	7.906E-07	1.581E-06
1200 K	2.299E-08	2.299E-07	5.748E-07	1.150E-06	2.299E-06
1300 K	3.185E-08	3.185E-07	7.963E-07	1.593E-06	3.185E-06
1400 K	4.244E-08	4.244E-07	1.061E-06	2.122E-06	4.244E-06
1500 K	5.476E-08	5.476E-07	1.369E-06	2.738E-06	5.476E-06
1600 K	6.878E-08	6.878E-07	1.719E-06	3.439E-06	6.878E-06
1700 K	8.445E-08	8.445E-07	2.111E-06	4.223E-06	8.445E-06
1800 K	1.017E-07	1.017E-06	2.543E-06	5.086E-06	1.017E-05
1900 K	1.205E-07	1.205E-06	3.012E-06	6.022E-06	1.205E-05
2000 K	1.406E-07	1.406E-06	3.516E-06	7.031E-06	1.406E-05

NOTE: Values in bold indicate liquid phase.

Table A-21: Equilibrium fractional conversion of methane for reaction (R A-1) obtained by using the ideal gas equation of state in Aspen at varying temperatures and 150 - 500 atm.

T (K)	150 atm	200 atm	300 atm	400 atm	500 atm
300 K	**5.505E-07**	**5.505E-07**	**5.505E-07**	**5.513E-07**	**5.505E-07**
400 K	2.523E-09	3.334E-09	5.045E-09	**4.387E-06**	**4.387E-06**
500 K	2.019E-08	2.693E-08	4.047E-08	5.338E-08	6.731E-08
600 K	8.148E-08	1.086E-07	1.630E-07	2.173E-07	2.716E-07
700 K	2.246E-07	2.994E-07	4.492E-07	5.989E-07	7.486E-07
800 K	4.899E-07	6.532E-07	9.798E-07	1.306E-06	1.633E-06
900 K	9.154E-07	1.220E-06	1.831E-06	2.441E-06	3.051E-06
1000 K	1.534E-06	2.045E-06	3.068E-06	4.090E-06	5.113E-06
1100 K	2.372E-06	3.162E-06	4.743E-06	6.325E-06	7.906E-06
1200 K	3.449E-06	4.598E-06	6.898E-06	9.197E-06	1.150E-05
1300 K	4.778E-06	6.371E-06	9.556E-06	1.274E-05	1.593E-05
1400 K	6.366E-06	8.488E-06	1.273E-05	1.698E-05	2.122E-05
1500 K	8.213E-06	1.095E-05	1.643E-05	2.190E-05	2.738E-05
1600 K	1.032E-05	1.376E-05	2.063E-05	2.751E-05	3.439E-05
1700 K	1.267E-05	1.689E-05	2.534E-05	3.378E-05	4.223E-05
1800 K	1.526E-05	2.034E-05	3.051E-05	4.068E-05	5.085E-05
1900 K	1.807E-05	2.409E-05	3.614E-05	4.819E-05	6.023E-05
2000 K	2.109E-05	2.812E-05	4.219E-05	5.625E-05	7.031E-05

NOTE: Values in bold indicate liquid phase.

Table A-22: Equilibrium fractional conversion of methane for reaction (R A-1) obtained by using the ideal gas equation of state in Aspen at varying temperatures and 600 - 1000 atm.

T (K)	600 atm	700 atm	800 atm	900 atm	1000 atm
300 K	**5.505E-07**	**5.505E-07**	**5.505E-07**	**5.505E-07**	**5.505E-07**
400 K	**4.387E-06**	**4.387E-06**	**4.387E-06**	**4.387E-06**	**4.387E-06**
500 K	8.078E-08	9.424E-08	1.077E-07	1.212E-07	1.346E-07
600 K	3.259E-07	3.809E-07	4.345E-07	4.889E-07	5.432E-07
700 K	8.983E-07	1.048E-06	1.198E-06	1.347E-06	1.497E-06
800 K	1.960E-06	2.286E-06	2.613E-06	2.940E-06	3.266E-06
900 K	3.661E-06	4.272E-06	4.882E-06	5.492E-06	6.102E-06
1000 K	6.135E-06	7.158E-06	8.180E-06	9.203E-06	1.023E-05
1100 K	9.487E-06	1.107E-05	1.265E-05	1.423E-05	1.581E-05
1200 K	1.380E-05	1.609E-05	1.839E-05	2.069E-05	2.299E-05
1300 K	1.911E-05	2.230E-05	2.548E-05	2.867E-05	3.185E-05
1400 K	2.546E-05	2.971E-05	3.395E-05	3.819E-05	4.244E-05
1500 K	3.285E-05	3.833E-05	4.380E-05	4.928E-05	5.475E-05
1600 K	4.127E-05	4.814E-05	5.502E-05	6.190E-05	6.877E-05
1700 K	5.067E-05	5.911E-05	6.756E-05	7.600E-05	8.445E-05
1800 K	6.102E-05	7.119E-05	8.136E-05	9.133E-05	1.017E-04
1900 K	7.228E-05	8.432E-05	9.637E-05	1.084E-04	1.205E-04
2000 K	8.437E-05	9.843E-05	1.125E-04	1.265E-04	1.406E-04

NOTE: Values in bold indicate liquid phase.

A.2.2. REDLICH-KWONG-SOAVE EQUATION OF STATE

Data of the outlet moles for carbon dioxide (CO_2), methane (CH_4) and acetic acid (CH_3COOH) and the equilibrium fractional conversion of methane (X_{CH4}) obtained by using the Redlich-Kwong-Soave equation of state in Aspen at varying temperatures and pressures can be found in tables A-23 - A-37. The equilibrium fractional conversions of methane only can be found in tables A-38 – A-40. An inlet mole flow of 0.95 CO_2 and 0.05 CH_4 was used for all calculations. The interaction parameter used for carbon dioxide and methane was 0.0933 obtained from the AspenPlus™ database. No other interaction parameters were available. The inlet temperature and pressure was set equal to that of the reactor.

Table A-23: Outlet moles and the equilibrium fractional conversion of methane for reaction (R A-1) obtained by using the Redlich-Kwong-Soave equation of state in Aspen at varying temperatures and 1 atm.

1 atm	300 K	400 K	500 K	600 K	700 K
Phase	Vapor	Vapor	Vapor	Vapor	Vapor
CO_2	0.9500000	0.9500000	0.9500000	0.9500000	0.9500000
CH_4	0.0500000	0.0500000	0.0500000	0.0500000	0.0500000
CH_3COOH	0.0000E+00	8.4867E-13	6.7625E-12	2.7225E-11	7.4959E-11
X CH_4	**0.000E+00**	**1.697E-11**	**1.353E-10**	**5.445E-10**	**1.499E-09**

1 atm	800 K	900 K	1000 K	1100 K	1200 K
Phase	Vapor	Vapor	Vapor	Vapor	Vapor
CO_2	0.9500000	0.9500000	0.9500000	0.9500000	0.9500000
CH_4	0.0500000	0.0500000	0.0500000	0.0500000	0.0500000
CH_3COOH	1.6342E-10	3.0524E-10	5.1134E-10	7.9059E-10	1.1496E-09
X CH_4	**3.268E-09**	**6.105E-09**	**1.023E-08**	**1.581E-08**	**2.299E-08**

1 atm	1300 K	1400 K	1500 K	1600 K	1700 K
Phase	Vapor	Vapor	Vapor	Vapor	Vapor
CO_2	0.9500000	0.9500000	0.9500000	0.9500000	0.9500000
CH_4	0.0500000	0.0500000	0.0500000	0.0500000	0.0500000
CH_3COOH	1.5926E-09	2.1217E-09	2.7375E-09	3.4385E-09	4.2222E-09
X CH_4	**3.185E-08**	**4.243E-08**	**5.475E-08**	**6.877E-08**	**8.444E-08**

1 atm	1800 K	1900 K	2000 K
Phase	Vapor	Vapor	Vapor
CO_2	0.9500000	0.9500000	0.9500000
CH_4	0.0499999	0.0499999	0.0499999
CH_3COOH	5.0850E-09	6.0228E-09	7.0306E-09
X CH_4	**1.017E-07**	**1.205E-07**	**1.406E-07**

Table A-24: Outlet moles and the equilibrium fractional conversion of methane for reaction (R A-1) obtained by using the Redlich-Kwong-Soave equation of state in Aspen at varying temperatures and 10 atm.

10 atm	300 K	400 K	500 K	600 K	700 K
Phase	Vapor	Vapor	Vapor	Vapor	Vapor
CO_2	0.9500000	0.9500000	0.9500000	0.9500000	0.9500000
CH_4	0.0500000	0.0500000	0.0500000	0.0500000	0.0500000
CH_3COOH	3.1674E-13	9.2333E-12	7.0502E-11	2.7835E-10	7.5876E-10
X CH_4	**6.335E-12**	**1.847E-10**	**1.410E-09**	**5.567E-09**	**1.518E-08**

10 atm	800 K	900 K	1000 K	1100 K	1200 K
Phase	Vapor	Vapor	Vapor	Vapor	Vapor
CO_2	0.9500000	0.9500000	0.9500000	0.9500000	0.9500000
CH_4	0.0500000	0.0500000	0.0499999	0.0499999	0.0499999
CH_3COOH	1.6452E-09	3.0630E-09	5.1215E-09	7.9093E-09	1.1492E-08
X CH_4	**3.290E-08**	**6.126E-08**	**1.024E-07**	**1.582E-07**	**2.298E-07**

10 atm	1300 K	1400 K	1500 K	1600 K	1700 K
Phase	Vapor	Vapor	Vapor	Vapor	Vapor
CO_2	0.9500000	0.9500000	0.9500000	0.9500000	0.9500000
CH_4	0.0499999	0.0499999	0.0499999	0.0499999	0.0499999
CH_3COOH	1.5914E-08	2.1197E-08	2.7351E-08	3.4346E-08	4.2174E-08
X CH_4	**3.183E-07**	**4.239E-07**	**5.470E-07**	**6.869E-07**	**8.435E-07**

10 atm	1800 K	1900 K	2000 K
Phase	Vapor	Vapor	Vapor
CO_2	0.9499999	0.9499999	0.9499999
CH_4	0.0499999	0.0499999	0.0499999
CH_3COOH	5.0795E-08	6.0165E-08	7.0237E-08
X CH_4	**1.016E-06**	**1.203E-06**	**1.405E-06**

Table A-25: Outlet moles and the equilibrium fractional conversion of methane for reaction (R A-1) obtained by using the Redlich-Kwong-Soave equation of state in Aspen at varying temperatures and 25 atm.

25 atm	300 K	400 K	500 K	600 K	700 K
Phase	Liquid	Vapor	Vapor	Vapor	Vapor
CO_2	0.9500000	0.9500000	0.9500000	0.9500000	0.9500000
CH_4	0.0500000	0.0500000	0.0500000	0.0500000	0.0500000
CH_3COOH	5.0792E-11	2.6656E-11	1.8887E-10	7.2680E-10	1.9351E-09
X CH_4	**1.016E-09**	**5.331E-10**	**3.777E-09**	**1.454E-08**	**3.870E-08**

25 atm	800 K	900 K	1000 K	1100 K	1200 K
Phase	Vapor	Vapor	Vapor	Vapor	Vapor
CO_2	0.9500000	0.9500000	0.9500000	0.9500000	0.9500000
CH_4	0.0500000	0.0499999	0.0499999	0.0499999	0.0499999
CH_3COOH	4.1578E-09	7.7007E-09	1.2836E-08	1.9786E-08	2.8716E-08
X CH_4	**8.316E-08**	**1.540E-07**	**2.567E-07**	**3.957E-07**	**5.743E-07**

25 atm	1300 K	1400 K	1500 K	1600 K	1700 K
Phase	Vapor	Vapor	Vapor	Vapor	Vapor
CO_2	0.9500000	0.9499999	0.9499999	0.9499999	0.9499999
CH_4	0.0499999	0.0499999	0.0499999	0.0499999	0.0499998
CH_3COOH	3.9738E-08	5.2908E-08	6.8240E-08	8.5703E-08	1.0524E-07
X CH_4	**7.948E-07**	**1.058E-06**	**1.365E-06**	**1.714E-06**	**2.105E-06**

25 atm	1800 K	1900 K	2000 K
Phase	Vapor	Vapor	Vapor
CO_2	0.9499999	0.9499998	0.9499998
CH_4	0.0499998	0.0499998	0.0499998
CH_3COOH	1.2675E-07	1.5015E-07	1.7531E-07
X CH_4	**2.535E-06**	**3.003E-06**	**3.506E-06**

Table A-26: Outlet moles and the equilibrium fractional conversion of methane for reaction (R A-1) obtained by using the Redlich-Kwong-Soave equation of state in Aspen at varying temperatures and 50 atm.

50 atm	300 K	400 K	500 K	600 K	700 K
Phase	Liquid	Liquid	Vapor	Vapor	Vapor
CO_2	0.9500000	0.9500000	0.9500000	0.9500000	0.9500000
CH_4	0.0500000	0.0500000	0.0500000	0.0500000	0.0500000
CH_3COOH	5.0380E-11	5.5598E-10	4.0281E-10	1.5314E-09	3.9964E-09
X CH_4	**1.008E-09**	**1.112E-08**	**8.056E-09**	**3.063E-08**	**7.993E-08**

50 atm	800 K	900 K	1000 K	1100 K	1200 K
Phase	Vapor	Vapor	Vapor	Vapor	Vapor
CO_2	0.9500000	0.9500000	0.9500000	0.9500000	0.9499999
CH_4	0.0499999	0.0499999	0.0499999	0.0499999	0.0499999
CH_3COOH	8.4619E-09	1.5541E-08	2.5775E-08	3.9608E-08	5.7379E-08
X CH_4	**1.692E-07**	**3.108E-07**	**5.155E-07**	**7.922E-07**	**1.148E-06**

50 atm	1300 K	1400 K	1500 K	1600 K	1700 K
Phase	Vapor	Vapor	Vapor	Vapor	Vapor
CO_2	0.9499999	0.9499999	0.9499999	0.9499998	0.9499998
CH_4	0.0499999	0.0499998	0.0499998	0.0499998	0.0499997
CH_3COOH	7.9314E-08	1.0553E-07	1.3607E-07	1.7087E-07	2.0981E-07
X CH_4	**1.586E-06**	**2.111E-06**	**2.721E-06**	**3.417E-06**	**4.196E-06**

50 atm	1800 K	1900 K	2000 K
Phase	Vapor	Vapor	Vapor
CO_2	0.9499997	0.9499997	0.9499996
CH_4	0.0499997	0.0499997	0.0499996
CH_3COOH	2.5274E-07	2.9943E-07	3.4965E-07
X CH_4	**5.055E-06**	**5.989E-06**	**6.993E-06**

Table A-27: Outlet moles and the equilibrium fractional conversion of methane for reaction (R A-1) obtained by using the Redlich-Kwong-Soave equation of state in Aspen at varying temperatures and 100 atm.

100 atm	300 K	400 K	500 K	600 K	700 K
Phase	Liquid	Liquid	Vapor	Vapor	Vapor
CO_2	0.9500000	0.9500000	0.9500000	0.9500000	0.9500000
CH_4	0.0500000	0.0500000	0.0500000	0.0500000	0.0499999
CH_3COOH	9.2999E-10	8.3601E-10	1.0568E-09	3.4262E-09	8.4901E-09
X CH_4	**1.860E-08**	**1.672E-08**	**2.114E-08**	**6.852E-08**	**1.698E-07**

100 atm	800 K	900 K	1000 K	1100 K	1200 K
Phase	Vapor	Vapor	Vapor	Vapor	Vapor
CO_2	0.9500000	0.9500000	0.9499999	0.9499999	0.9499999
CH_4	0.0499999	0.0499999	0.0499999	0.0499999	0.0499998
CH_3COOH	1.7485E-08	3.1606E-08	5.1924E-08	7.9334E-08	1.1452E-07
X CH_4	**3.497E-07**	**6.321E-07**	**1.038E-06**	**1.587E-06**	**2.290E-06**

100 atm	1300 K	1400 K	1500 K	1600 K	1700 K
Phase	Vapor	Vapor	Vapor	Vapor	Vapor
CO_2	0.9499998	0.9499998	0.9499997	0.9499997	0.9499996
CH_4	0.0499998	0.0499997	0.0499997	0.0499996	0.0499995
CH_3COOH	1.5797E-07	2.0994E-07	2.7051E-07	3.3961E-07	4.1702E-07
X CH_4	**3.159E-06**	**4.199E-06**	**5.410E-06**	**6.792E-06**	**8.340E-06**

100 atm	1800 K	1900 K	2000 K
Phase	Vapor	Vapor	Vapor
CO_2	0.9499995	0.9499994	0.9499993
CH_4	0.0499995	0.0499994	0.0499993
CH_3COOH	5.0241E-07	5.9539E-07	6.9550E-07
X CH_4	**1.005E-05**	**1.191E-05**	**1.391E-05**

Table A-28: Outlet moles and the equilibrium fractional conversion of methane for reaction (R A-1) obtained by using the Redlich-Kwong-Soave equation of state in Aspen at varying temperatures and 150 atm.

150 atm	300 K	400 K	500 K	600 K	700 K
Phase	Liquid	Liquid	Vapor	Vapor	Vapor
CO_2	0.9500000	0.9500000	0.9500000	0.9500000	0.9500000
CH_4	0.0500000	0.0500000	0.0500000	0.0499999	0.0499999
CH_3COOH	2.0028E-09	1.0473E-09	1.9511E-09	5.6993E-09	1.3459E-08
X CH_4	**4.006E-08**	**2.095E-08**	**3.902E-08**	**1.140E-07**	**2.692E-07**

150 atm	800 K	900 K	1000 K	1100 K	1200 K
Phase	Vapor	Vapor	Vapor	Vapor	Vapor
CO_2	0.9500000	0.9500000	0.9499999	0.9499999	0.9499998
CH_4	0.0499999	0.0499999	0.0499999	0.0499998	0.0499998
CH_3COOH	2.7019E-08	4.8129E-08	7.8380E-08	1.1912E-07	1.7394E-07
X CH_4	**5.404E-07**	**9.626E-07**	**1.568E-06**	**2.382E-06**	**3.479E-06**

150 atm	1300 K	1400 K	1500 K	1600 K	1700 K
Phase	Vapor	Vapor	Vapor	Vapor	Vapor
CO_2	0.9499998	0.9499997	0.9499996	0.9499995	0.9499994
CH_4	0.0499997	0.0499996	0.0499996	0.0499994	0.0499993
CH_3COOH	2.3595E-07	3.1321E-07	4.0334E-07	5.0625E-07	6.2165E-07
X CH_4	**4.719E-06**	**6.264E-06**	**8.067E-06**	**1.013E-05**	**1.243E-05**

150 atm	1800 K	1900 K	2000 K
Phase	Vapor	Vapor	Vapor
CO_2	0.9499993	0.9499991	0.9499990
CH_4	0.0499992	0.0499991	0.0499989
CH_3COOH	7.4907E-07	8.8794E-07	1.0376E-06
X CH_4	**1.498E-05**	**1.776E-05**	**2.075E-05**

Table A-29: Outlet moles and the equilibrium fractional conversion of methane for reaction (R A-1) obtained by using the Redlich-Kwong-Soave equation of state in Aspen at varying temperatures and 200 atm.

200 atm	300 K	400 K	500 K	600 K	700 K
Phase	Liquid	Liquid	Vapor	Vapor	Vapor
CO_2	0.9500000	0.9500000	0.9500000	0.9500000	0.9500000
CH_4	0.0500000	0.0500000	0.0499999	0.0499999	0.0499999
CH_3COOH	2.9940E-09	1.3407E-09	6.0062E-09	8.3505E-09	1.8873E-08
X CH_4	**5.988E-08**	**2.681E-08**	**1.201E-07**	**1.670E-07**	**3.775E-07**

200 atm	800 K	900 K	1000 K	1100 K	1200 K
Phase	Vapor	Vapor	Vapor	Vapor	Vapor
CO_2	0.9500000	0.9499999	0.9499999	0.9499998	0.9499998
CH_4	0.0499999	0.0499999	0.0499998	0.0499998	0.0499997
CH_3COOH	3.7011E-08	6.5048E-08	1.0508E-07	1.5891E-07	2.2795E-07
X CH_4	**7.402E-07**	**1.301E-06**	**2.102E-06**	**3.178E-06**	**4.559E-06**

200 atm	1300 K	1400 K	1500 K	1600 K	1700 K
Phase	Vapor	Vapor	Vapor	Vapor	Vapor
CO_2	0.9499997	0.9499996	0.9499995	0.9499993	0.9499992
CH_4	0.0499996	0.0499995	0.0499994	0.0499993	0.0499991
CH_3COOH	3.1323E-07	4.1536E-07	5.3458E-07	6.7083E-07	8.2375E-07
X CH_4	**6.265E-06**	**8.307E-06**	**1.069E-05**	**1.342E-05**	**1.647E-05**

200 atm	1800 K	1900 K	2000 K
Phase	Vapor	Vapor	Vapor
CO_2	0.9499990	0.9499988	0.9499986
CH_4	0.0499990	0.0499988	0.0499986
CH_3COOH	9.9276E-07	1.1771E-06	1.3759E-06
X CH_4	**1.986E-05**	**2.354E-05**	**2.752E-05**

Table A-30: Outlet moles and the equilibrium fractional conversion of methane for reaction (R A-1) obtained by using the Redlich-Kwong-Soave equation of state in Aspen at varying temperatures and 300 atm.

300 atm	300 K	400 K	500 K	600 K	700 K
Phase	Liquid	Liquid	Vapor	Vapor	Vapor
CO_2	0.9500000	0.9500000	0.9500000	0.9500000	0.9499999
CH_4	0.0500000	0.0500000	0.0499999	0.0499999	0.0499999
CH_3COOH	4.8638E-09	3.5118E-09	6.4548E-09	1.4722E-08	5.4963E-08
X CH_4	**9.728E-08**	**7.024E-08**	**1.291E-07**	**2.944E-07**	**1.099E-06**

300 atm	800 K	900 K	1000 K	1100 K	1200 K
Phase	Vapor	Vapor	Vapor	Vapor	Vapor
CO_2	0.9499999	0.9499999	0.9499998	0.9499998	0.9499997
CH_4	0.0499999	0.0499999	0.0499998	0.0499997	0.0499996
CH_3COOH	5.8165E-08	9.9842E-08	1.5900E-07	2.3832E-07	3.4000E-07
X CH_4	**1.163E-06**	**1.997E-06**	**3.180E-06**	**4.766E-06**	**6.800E-06**

300 atm	1300 K	1400 K	1500 K	1600 K	1700 K
Phase	Vapor	Vapor	Vapor	Vapor	Vapor
CO_2	0.9499995	0.9499994	0.9499992	0.9499990	0.9499988
CH_4	0.0499995	0.0499993	0.0499992	0.0499990	0.0499987
CH_3COOH	4.6563E-07	6.1625E-07	7.9235E-07	9.9391E-07	1.2205E-06
X CH_4	**9.313E-06**	**1.233E-05**	**1.585E-05**	**1.988E-05**	**2.441E-05**

300 atm	1800 K	1900 K	2000 K
Phase	Vapor	Vapor	Vapor
CO_2	0.9499985	0.9499983	0.9499980
CH_4	0.0499985	0.0499982	0.0499979
CH_3COOH	1.4714E-06	1.7455E-06	2.0416E-06
X CH_4	**2.943E-05**	**3.491E-05**	**4.083E-05**

Table A-31: Outlet moles and the equilibrium fractional conversion of methane for reaction (R A-1) obtained by using the Redlich-Kwong-Soave equation of state in Aspen at varying temperatures and 400 atm.

400 atm	300 K	400 K	500 K	600 K	700 K
Phase	Liquid	Liquid	Liquid	Vapor	Vapor
CO_2	0.9500000	0.9500000	0.9500000	0.9500000	0.9500000
CH_4	0.0499999	0.0499999	0.0499999	0.0499999	0.0499999
CH_3COOH	6.6036E-09	6.5467E-09	1.0849E-08	2.2321E-08	4.4207E-08
X CH_4	**1.321E-07**	**1.309E-07**	**2.170E-07**	**4.464E-07**	**8.841E-07**

400 atm	800 K	900 K	1000 K	1100 K	1200 K
Phase	Vapor	Vapor	Vapor	Vapor	Vapor
CO_2	0.9499999	0.9499999	0.9499998	0.9499997	0.9499996
CH_4	0.0499999	0.0499998	0.0499997	0.0499996	0.0499995
CH_3COOH	8.0548E-08	1.3556E-07	2.1327E-07	3.1724E-07	4.5043E-07
X CH_4	**1.611E-06**	**2.711E-06**	**4.265E-06**	**6.345E-06**	**9.009E-06**

400 atm	1300 K	1400 K	1500 K	1600 K	1700 K
Phase	Vapor	Vapor	Vapor	Vapor	Vapor
CO_2	0.9499994	0.9499992	0.9499990	0.9499987	0.9499984
CH_4	0.0499993	0.0499991	0.0499989	0.0499986	0.0499983
CH_3COOH	6.1507E-07	8.1264E-07	1.0439E-06	1.3091E-06	1.6076E-06
X CH_4	**1.230E-05**	**1.625E-05**	**2.088E-05**	**2.618E-05**	**3.215E-05**

400 atm	1800 K	1900 K	2000 K
Phase	Vapor	Vapor	Vapor
CO_2	0.9499981	0.9499977	0.9499973
CH_4	0.0499980	0.0499977	0.0499973
CH_3COOH	1.9386E-06	2.3009E-06	2.6928E-06
X CH_4	**3.877E-05**	**4.602E-05**	**5.386E-05**

Table A-32: Outlet moles and the equilibrium fractional conversion of methane for reaction (R A-1) obtained by using the Redlich-Kwong-Soave equation of state in Aspen at varying temperatures and 500 atm.

500 atm	300 K	400 K	500 K	600 K	700 K
Phase	Liquid	Liquid	Liquid	Liquid	Vapor
CO_2	0.9500000	0.9500000	0.9500000	0.9500000	0.9499999
CH_4	0.0499999	0.0499999	0.0499999	0.0499999	0.0499999
CH_3COOH	8.2111E-09	9.8843E-09	1.6011E-08	3.0853E-08	5.8502E-08
X CH_4	**1.642E-07**	**1.977E-07**	**3.202E-07**	**6.171E-07**	**1.170E-06**

500 atm	800 K	900 K	1000 K	1100 K	1200 K
Phase	Vapor	Vapor	Vapor	Vapor	Vapor
CO_2	0.9499999	0.9499998	0.9499997	0.9499996	0.9499994
CH_4	0.0499999	0.0499998	0.0499997	0.0499996	0.0499994
CH_3COOH	1.0380E-07	1.7184E-07	2.6756E-07	3.9540E-07	5.5907E-07
X CH_4	**2.076E-06**	**3.437E-06**	**5.351E-06**	**7.908E-06**	**1.118E-05**

500 atm	1300 K	1400 K	1500 K	1600 K	1700 K
Phase	Vapor	Vapor	Vapor	Vapor	Vapor
CO_2	0.9499992	0.9499990	0.9499987	0.9499984	0.9499980
CH_4	0.0499992	0.0499990	0.0499987	0.0499983	0.0499980
CH_3COOH	7.6146E-07	1.0046E-06	1.2895E-06	1.6165E-06	1.9853E-06
X CH_4	**1.523E-05**	**2.009E-05**	**2.579E-05**	**3.233E-05**	**3.971E-05**

500 atm	1800 K	1900 K	2000 K
Phase	Vapor	Vapor	Vapor
CO_2	0.9499976	0.9499972	0.9499967
CH_4	0.0499976	0.0499971	0.0499966
CH_3COOH	2.3948E-06	2.8436E-06	3.3298E-06
X CH_4	**4.790E-05**	**5.687E-05**	**6.660E-05**

Table A-33: Outlet moles and the equilibrium fractional conversion of methane for reaction (R A-1) obtained by using the Redlich-Kwong-Soave equation of state in Aspen at varying temperatures and 600 atm.

600 atm	300 K	400 K	500 K	600 K	700 K
Phase	Liquid	Liquid	Liquid	Liquid	Liquid
CO_2	0.9500000	0.9500000	0.9500000	0.9500000	0.9499999
CH_4	0.0499999	0.0499999	0.0499999	0.0499999	0.0499999
CH_3COOH	9.6830E-09	1.3291E-08	2.1635E-08	4.0027E-08	7.3519E-08
X CH_4	**1.937E-07**	**2.658E-07**	**4.327E-07**	**8.005E-07**	**1.470E-06**

600 atm	800 K	900 K	1000 K	1100 K	1200 K
Phase	Vapor	Vapor	Vapor	Vapor	Vapor
CO_2	0.9499999	0.9499998	0.9499997	0.9499995	0.9499993
CH_4	0.0499998	0.0499997	0.0499996	0.0499995	0.0499993
CH_3COOH	1.2760E-07	2.0838E-07	3.2160E-07	4.7257E-07	6.6577E-07
X CH_4	**2.552E-06**	**4.168E-06**	**6.432E-06**	**9.451E-06**	**1.332E-05**

600 atm	1300 K	1400 K	1500 K	1600 K	1700 K
Phase	Vapor	Vapor	Vapor	Vapor	Vapor
CO_2	0.9499991	0.9499988	0.9499985	0.9499981	0.9499976
CH_4	0.0499991	0.0499988	0.0499984	0.0499980	0.0499976
CH_3COOH	9.0475E-07	1.1920E-06	1.5291E-06	1.9165E-06	2.3539E-06
X CH_4	**1.809E-05**	**2.384E-05**	**3.058E-05**	**3.833E-05**	**4.708E-05**

600 atm	1800 K	1900 K	2000 K
Phase	Vapor	Vapor	Vapor
CO_2	0.9499972	0.9499966	0.9499960
CH_4	0.0499971	0.0499966	0.0499960
CH_3COOH	2.8403E-06	3.3740E-06	3.9531E-06
X CH_4	**5.681E-05**	**6.748E-05**	**7.906E-05**

Table A-34: Outlet moles and the equilibrium fractional conversion of methane for reaction (R A-1) obtained by using the Redlich-Kwong-Soave equation of state in Aspen at varying temperatures and 700 atm.

700 atm	300 K	400 K	500 K	600 K	700 K
Phase	Liquid	Liquid	Liquid	Liquid	Liquid
CO_2	0.9500000	0.9500000	0.9500000	0.9500000	0.9499999
CH_4	0.0499999	0.0499999	0.0499999	0.0499999	0.0499999
CH_3COOH	1.1019E-08	1.6645E-08	2.7487E-08	4.9592E-08	8.8845E-08
X CH_4	**2.204E-07**	**3.329E-07**	**5.497E-07**	**9.918E-07**	**1.777E-06**

700 atm	800 K	900 K	1000 K	1100 K	1200 K
Phase	Vapor	Vapor	Vapor	Vapor	Vapor
CO_2	0.9499998	0.9499998	0.9499996	0.9499995	0.9499992
CH_4	0.0499998	0.0499997	0.0499996	0.0499994	0.0499992
CH_3COOH	1.5169E-07	2.4491E-07	3.7516E-07	5.4857E-07	7.7041E-07
X CH_4	**3.034E-06**	**4.898E-06**	**7.503E-06**	**1.097E-05**	**1.541E-05**

700 atm	1300 K	1400 K	1500 K	1600 K	1700 K
Phase	Vapor	Vapor	Vapor	Vapor	Vapor
CO_2	0.9499990	0.9499986	0.9499982	0.9499978	0.9499973
CH_4	0.0499989	0.0499986	0.0499982	0.0499970	0.0499972
CH_3COOH	1.0449E-06	1.3751E-06	1.7629E-06	2.2091E-06	2.7135E-06
X CH_4	**2.090E-05**	**2.750E-05**	**3.526E-05**	**4.418E-05**	**5.427E-05**

700 atm	1800 K	1900 K	2000 K
Phase	Vapor	Vapor	Vapor
CO_2	0.9499967	0.9499961	0.9499954
CH_4	0.0499967	0.0499961	0.0499954
CH_3COOH	3.2752E-06	3.8924E-06	4.5628E-06
X CH_4	**6.550E-05**	**7.785E-05**	**9.126E-05**

Table A-35: Outlet moles and the equilibrium fractional conversion of methane for reaction (R A-1) obtained by using the Redlich-Kwong-Soave equation of state in Aspen at varying temperatures and 800 atm.

800 atm	300 K	400 K	500 K	600 K	700 K
Phase	Liquid	Liquid	Liquid	Liquid	Liquid
CO_2	0.9500000	0.9500000	0.9500000	0.9499999	0.9499999
CH_4	0.0499999	0.0499999	0.0499999	0.0499999	0.0499999
CH_3COOH	1.2220E-08	1.9883E-08	3.3397E-08	5.9342E-08	1.0442E-07
X CH_4	**2.444E-07**	**3.977E-07**	**6.679E-07**	**1.187E-06**	**2.088E-06**

800 atm	800 K	900 K	1000 K	1100 K	1200 K
Phase	Vapor	Vapor	Vapor	Vapor	Vapor
CO_2	0.9499998	0.9499997	0.9499996	0.9499994	0.9499991
CH_4	0.0499998	0.0499997	0.0499995	0.0499993	0.0499991
CH_3COOH	1.7584E-07	2.8122E-07	4.2805E-07	6.2326E-07	8.7290E-07
X CH_4	**3.517E-06**	**5.624E-06**	**8.561E-06**	**1.247E-05**	**1.746E-05**

800 atm	1300 K	1400 K	1500 K	1600 K	1700 K
Phase	Vapor	Vapor	Vapor	Vapor	Vapor
CO_2	0.9499988	0.9499984	0.9499980	0.9499975	0.9499969
CH_4	0.0499988	0.0499984	0.0499980	0.0499975	0.0499969
CH_3COOH	1.1819E-06	1.5538E-06	1.9910E-06	2.4945E-06	3.0645E-06
X CH_4	**2.364E-05**	**3.108E-05**	**3.982E-05**	**4.989E-05**	**6.129E-05**

800 atm	1800 K	1900 K	2000 K
Phase	Vapor	Vapor	Vapor
CO_2	0.9499963	0.9499956	0.9499948
CH_4	0.0499963	0.0499956	0.0499948
CH_3COOH	3.7000E-06	4.3990E-06	5.1593E-06
X CH_4	**7.400E-05**	**8.798E-05**	**1.032E-04**

Table A-36: Outlet moles and the equilibrium fractional conversion of methane for reaction (R A-1) obtained by using the Redlich-Kwong-Soave equation of state in Aspen at varying temperatures and 900 atm.

900 atm	300 K	400 K	500 K	600 K	700 K
Phase	Liquid	Liquid	Liquid	Liquid	Liquid
CO_2	0.9500000	0.9500000	0.9500000	0.9499999	0.9499999
CH_4	0.0499999	0.0499999	0.0499999	0.0499999	0.0499998
CH_3COOH	1.3290E-08	2.2964E-08	3.9250E-08	6.9121E-08	1.2000E-07
X CH_4	**2.658E-07**	**4.593E-07**	**7.850E-07**	**1.382E-06**	**2.400E-06**

900 atm	800 K	900 K	1000 K	1100 K	1200 K
Phase	Vapor	Vapor	Vapor	Vapor	Vapor
CO_2	0.9499998	0.9499997	0.9499995	0.9499993	0.9499990
CH_4	0.0499998	0.0499996	0.0499995	0.0499993	0.0499990
CH_3COOH	1.9988E-07	3.1715E-07	4.8011E-07	6.9652E-07	9.7317E-07
X CH_4	**3.998E-06**	**6.343E-06**	**9.602E-06**	**1.393E-05**	**1.946E-05**

900 atm	1300 K	1400 K	1500 K	1600 K	1700 K
Phase	Vapor	Vapor	Vapor	Vapor	Vapor
CO_2	0.9499987	0.9499983	0.9499978	0.9499972	0.9499966
CH_4	0.0499986	0.0499982	0.0499977	0.0499972	0.0499965
CH_3COOH	1.3156E-06	1.7281E-06	2.2134E-06	2.7730E-06	3.4071E-06
X CH_4	**2.631E-05**	**3.456E-05**	**4.427E-05**	**5.546E-05**	**6.814E-05**

900 atm	1800 K	1900 K	2000 K
Phase	Vapor	Vapor	Vapor
CO_2	0.9499959	0.9499951	0.9499943
CH_4	0.0499958	0.0499950	0.0499942
CH_3COOH	4.1148E-06	4.9222E-06	5.7429E-06
X CH_4	**8.230E-05**	**9.844E-05**	**1.149E-04**

Table A-37: Outlet moles and the equilibrium fractional conversion of methane for reaction (R A-1) obtained by using the Redlich-Kwong-Soave equation of state in Aspen at varying temperatures and 1000 atm.

1000 atm	300 K	400 K	500 K	600 K	700 K
Phase	Liquid	Liquid	Liquid	Liquid	Liquid
CO_2	0.9500000	0.9500000	0.9500000	0.9499999	0.9499999
CH_4	0.0499999	0.0499999	0.0499999	0.0499999	0.0499998
CH_3COOH	1.4235E-08	2.5866E-08	4.4965E-08	7.8807E-08	1.3547E-07
X CH_4	**2.847E-07**	**5.173E-07**	**8.993E-07**	**1.576E-06**	**2.709E-06**

1000 atm	800 K	900 K	1000 K	1100 K	1200 K
Phase	Vapor	Vapor	Vapor	Vapor	Vapor
CO_2	0.9499999	0.9499996	0.9499995	0.9499992	0.9499989
CH_4	0.0499997	0.0499996	0.0499994	0.0499992	0.0499989
CH_3COOH	2.2366E-07	3.5255E-07	5.3124E-07	7.6255E-07	1.0712E-06
X CH_4	**4.473E-06**	**7.051E-06**	**1.062E-05**	**1.525E-05**	**2.142E-05**

1000 atm	1300 K	1400 K	1500 K	1600 K	1700 K
Phase	Vapor	Vapor	Vapor	Vapor	Vapor
CO_2	0.9499986	0.9499981	0.9499976	0.9499970	0.9499963
CH_4	0.0499985	0.0499981	0.0499975	0.0499969	0.0499962
CH_3COOH	1.4462E-06	1.8982E-06	2.4305E-06	3.0447E-06	3.7415E-06
X CH_4	**2.892E-05**	**3.796E-05**	**4.861E-05**	**6.089E-05**	**7.483E-05**

1000 atm	1800 K	1900 K	2000 K
Phase	Vapor	Vapor	Vapor
CO_2	0.9499955	0.9499946	0.9499937
CH_4	0.0499954	0.0499946	0.0499936
CH_3COOH	4.5199E-06	5.3782E-06	6.3138E-06
X CH_4	**9.040E-05**	**1.076E-04**	**1.263E-04**

Table A-38: Equilibrium fractional conversion of methane for reaction (R A-1) obtained by using the Redlich-Kwong-Soave equation of state in Aspen at varying temperatures and 1 - 100 atm.

T (K)	1 atm	10 atm	25 atm	50 atm	100 atm
300 K	0.000E+00	6.335E-12	**1.016E-09**	**1.008E-09**	**1.860E-08**
400 K	1.697E-11	1.847E-10	5.331E-10	**1.112E-08**	**1.672E-08**
500 K	1.353E-10	1.410E-09	3.777E-09	8.056E-09	2.114E-08
600 K	5.445E-10	5.567E-09	1.454E-08	3.063E-08	6.852E-08
700 K	1.499E-09	1.518E-08	3.870E-08	7.993E-08	1.698E-07
800 K	3.268E-09	3.290E-08	8.316E-08	1.692E-07	3.497E-07
900 K	6.105E-09	6.126E-08	1.540E-07	3.108E-07	6.321E-07
1000 K	1.023E-08	1.024E-07	2.567E-07	5.155E-07	1.038E-06
1100 K	1.581E-08	1.582E-07	3.957E-07	7.922E-07	1.587E-06
1200 K	2.299E-08	2.298E-07	5.743E-07	1.148E-06	2.290E-06
1300 K	3.185E-08	3.183E-07	7.948E-07	1.586E-06	3.159E-06
1400 K	4.243E-08	4.239E-07	1.058E-06	2.111E-06	4.199E-06
1500 K	5.475E-08	5.470E-07	1.365E-06	2.721E-06	5.410E-06
1600 K	6.877E-08	6.869E-07	1.714E-06	3.417E-06	6.792E-06
1700 K	8.444E-08	8.435E-07	2.105E-06	4.196E-06	8.340E-06
1800 K	1.017E-07	1.016E-06	2.535E-06	5.055E-06	1.005E-05
1900 K	1.205E-07	1.203E-06	3.003E-06	5.989E-06	1.191E-05
2000 K	1.406E-07	1.405E-06	3.506E-06	6.993E-06	1.391E-05

NOTE: Values in bold indicate liquid phase.

Table A-39: Equilibrium fractional conversion of methane for reaction (R A-1) obtained by using the Redlich-Kwong-Soave equation of state in Aspen at varying temperatures and 150 - 500 atm.

T (K)	150 atm	200 atm	300 atm	400 atm	500 atm
300 K	**4.006E-08**	**5.988E-08**	**9.728E-08**	**1.321E-07**	**1.642E-07**
400 K	**2.095E-08**	**2.681E-08**	**7.024E-08**	**1.309E-07**	**1.977E-07**
500 K	3.902E-08	1.201E-07	1.291E-07	**2.170E-07**	**3.202E-07**
600 K	1.140E-07	1.670E-07	2.944E-07	4.464E-07	**6.171E-07**
700 K	2.692E-07	3.775E-07	1.099E-06	8.841E-07	1.170E-06
800 K	5.404E-07	7.402E-07	1.163E-06	1.611E-06	2.076E-06
900 K	9.626E-07	1.301E-06	1.997E-06	2.711E-06	3.437E-06
1000 K	1.568E-06	2.102E-06	3.180E-06	4.265E-06	5.351E-06
1100 K	2.382E-06	3.178E-06	4.766E-06	6.345E-06	7.908E-06
1200 K	3.479E-06	4.559E-06	6.800E-06	9.009E-06	1.118E-05
1300 K	4.719E-06	6.265E-06	9.313E-06	1.230E-05	1.523E-05
1400 K	6.264E-06	8.307E-06	1.233E-05	1.625E-05	2.009E-05
1500 K	8.067E-06	1.069E-05	1.585E-05	2.088E-05	2.579E-05
1600 K	1.013E-05	1.342E-05	1.988E-05	2.618E-05	3.233E-05
1700 K	1.243E-05	1.647E-05	2.441E-05	3.215E-05	3.971E-05
1800 K	1.498E-05	1.986E-05	2.943E-05	3.877E-05	4.790E-05
1900 K	1.776E-05	2.354E-05	3.491E-05	4.602E-05	5.687E-05
2000 K	2.075E-05	2.752E-05	4.083E-05	5.386E-05	6.660E-05

NOTE: Values in bold indicate liquid phase.

Table A-40: Equilibrium fractional conversion of methane for reaction (R A-1) obtained by using the Redlich-Kwong-Soave equation of state in Aspen at varying temperatures and 600 - 1000 atm.

T (K)	600 atm	700 atm	800 atm	900 atm	1000 atm
300 K	**1.937E-07**	**2.204E-07**	**2.444E-07**	**2.658E-07**	**2.847E-07**
400 K	**2.658E-07**	**3.329E-07**	**3.977E-07**	**4.593E-07**	**5.173E-07**
500 K	**4.327E-07**	**5.497E-07**	**6.679E-07**	**7.850E-07**	**8.993E-07**
600 K	**8.005E-07**	**9.918E-07**	**1.187E-06**	**1.382E-06**	**1.576E-06**
700 K	**1.470E-06**	**1.777E-06**	**2.088E-06**	**2.400E-06**	**2.709E-06**
800 K	2.552E-06	3.034E-06	3.517E-06	3.998E-06	4.473E-06
900 K	4.168E-06	4.898E-06	5.624E-06	6.343E-06	7.051E-06
1000 K	6.432E-06	7.503E-06	8.561E-06	9.602E-06	1.062E-05
1100 K	9.451E-06	1.097E-05	1.247E-05	1.393E-05	1.525E-05
1200 K	1.332E-05	1.541E-05	1.746E-05	1.946E-05	2.142E-05
1300 K	1.809E-05	2.090E-05	2.364E-05	2.631E-05	2.892E-05
1400 K	2.384E-05	2.750E-05	3.108E-05	3.456E-05	3.796E-05
1500 K	3.058E-05	3.526E-05	3.982E-05	4.427E-05	4.861E-05
1600 K	3.833E-05	4.418E-05	4.989E-05	5.546E-05	6.089E-05
1700 K	4.708E-05	5.427E-05	6.129E-05	6.814E-05	7.483E-05
1800 K	5.681E-05	6.550E-05	7.400E-05	8.230E-05	9.040E-05
1900 K	6.748E-05	7.785E-05	8.798E-05	9.844E-05	1.076E-04
2000 K	7.906E-05	9.126E-05	1.032E-04	1.149E-04	1.263E-04

NOTE: Values in bold indicate liquid phase.

A.2.3. PENG-ROBINSON EQUATION OF STATE

Data of the outlet moles for carbon dioxide (CO_2), methane (CH_4) and acetic acid (CH_3COOH) and the equilibrium fractional conversion of methane (X_{CH4}) obtained by using the Peng-Robinson equation of state in Aspen at varying temperatures and pressures can be found in tables A-41 - A-55. The equilibrium fractional conversions of methane only can be found in tables A-56 – A-58. The interaction parameter used for carbon dioxide and methane was 0.0919 obtained from the AspenPlus ™ database. No other interaction parameters were available. An inlet mole flow of 0.95 CO_2 and 0.05 CH_4 was used for all calculations. The inlet temperature and pressure was set equal to that of the reactor.

Table A-41: Outlet moles and the equilibrium fractional conversion of methane for reaction (R A-1) obtained by using the Peng-Robinson equation of state in Aspen at varying temperatures and 1 atm.

1 atm	300 K	400 K	500 K	600 K	700 K
Phase	Vapor	Vapor	Vapor	Vapor	Vapor
CO_2	0.9500000	0.9500000	0.9500000	0.9500000	0.9500000
CH_4	0.0500000	0.0500000	0.0500000	0.0500000	0.0500000
CH_3COOH	0.0000E+00	8.4593E-13	6.7645E-12	2.7232E-11	7.4975E-11
X CH_4	**0.000E+00**	**1.692E-11**	**1.353E-10**	**5.446E-10**	**1.500E-09**

1 atm	800 K	900 K	1000 K	1100 K	1200 K
Phase	Vapor	Vapor	Vapor	Vapor	Vapor
CO_2	0.9500000	0.9500000	0.9500000	0.9500000	0.9500000
CH_4	0.0500000	0.0500000	0.0500000	0.0500000	0.0500000
CH_3COOH	1.6345E-10	3.0529E-10	5.1140E-10	7.9067E-10	1.1497E-09
X CH_4	**3.269E-09**	**6.106E-09**	**1.023E-08**	**1.581E-08**	**2.299E-08**

1 atm	1300 K	1400 K	1500 K	1600 K	1700 K
Phase	Vapor	Vapor	Vapor	Vapor	Vapor
CO_2	0.9500000	0.9500000	0.9500000	0.9500000	0.9500000
CH_4	0.0500000	0.0500000	0.0500000	0.0500000	0.0500000
CH_3COOH	1.5927E-09	2.1219E-09	2.7376E-09	3.4386E-09	4.2223E-09
X CH_4	**3.185E-08**	**4.244E-08**	**5.475E-08**	**6.877E-08**	**8.445E-08**

1 atm	1800 K	1900 K	2000 K
Phase	Vapor	Vapor	Vapor
CO_2	0.9500000	0.9500000	0.9500000
CH_4	0.0499999	0.0499999	0.0499999
CH_3COOH	5.0852E-09	6.0230E-09	7.0308E-09
X CH_4	**1.017E-07**	**1.205E-07**	**1.406E-07**

Table A-42: Outlet moles and the equilibrium fractional conversion of methane for reaction (R A-1) obtained by using the Peng-Robinson equation of state in Aspen at varying temperatures and 10 atm.

10 atm	300 K	400 K	500 K	600 K	700 K
Phase	Vapor	Vapor	Vapor	Vapor	Vapor
CO_2	0.9500000	0.9500000	0.9500000	0.9500000	0.9500000
CH_4	0.0500000	0.0500000	0.0500000	0.0500000	0.0500000
CH_3COOH	3.1729E-13	9.2610E-12	7.0704E-11	2.7905E-10	7.6036E-10
X CH_4	**6.346E-12**	**1.852E-10**	**1.414E-09**	**5.581E-09**	**1.521E-08**

10 atm	800 K	900 K	1000 K	1100 K	1200 K
Phase	Vapor	Vapor	Vapor	Vapor	Vapor
CO_2	0.9500000	0.9500000	0.9500000	0.9500000	0.9500000
CH_4	0.0500000	0.0500000	0.0499999	0.0499999	0.0499999
CH_3COOH	1.6481E-09	3.0676E-09	5.1279E-09	7.9177E-09	1.1503E-08
X CH_4	**3.296E-08**	**6.135E-08**	**1.026E-07**	**1.584E-07**	**2.301E-07**

10 atm	1300 K	1400 K	1500 K	1600 K	1700 K
Phase	Vapor	Vapor	Vapor	Vapor	Vapor
CO_2	0.9500000	0.9500000	0.9500000	0.9500000	0.9500000
CH_4	0.0499999	0.0499999	0.0499999	0.0499999	0.0499999
CH_3COOH	1.5926E-08	2.1211E-08	2.7360E-08	3.4362E-08	4.2191E-08
X CH_4	**3.185E-07**	**4.242E-07**	**5.472E-07**	**6.872E-07**	**8.438E-07**

10 atm	1800 K	1900 K	2000 K
Phase	Vapor	Vapor	Vapor
CO_2	0.9499999	0.9499999	0.9499999
CH_4	0.0499999	0.0499999	0.0499999
CH_3COOH	5.0811E-08	6.0181E-08	7.0253E-08
X CH_4	**1.016E-06**	**1.204E-06**	**1.405E-06**

Table A-43: Outlet moles and the equilibrium fractional conversion of methane for reaction (R A-1) obtained by using the Peng-Robinson equation of state in Aspen at varying temperatures and 25 atm.

25 atm	300 K	400 K	500 K	600 K	700 K
Phase	Liquid	Vapor	Vapor	Vapor	Vapor
CO_2	0.9500000	0.9500000	0.9500000	0.9500000	0.9500000
CH_4	0.0500000	0.0500000	0.0500000	0.0500000	0.0500000
CH_3COOH	5.0151E-11	2.6851E-11	1.9090E-10	7.2606E-10	1.9451E-09
X CH_4	**1.003E-09**	**5.370E-10**	**3.818E-09**	**1.452E-08**	**3.890E-08**

25 atm	800 K	900 K	1000 K	1100 K	1200 K
Phase	Vapor	Vapor	Vapor	Vapor	Vapor
CO_2	0.9500000	0.9500000	0.9500000	0.9500000	0.9500000
CH_4	0.0500000	0.0499999	0.0499999	0.0499999	0.0499999
CH_3COOH	4.1759E-09	7.7290E-09	1.2876E-08	1.9838E-08	2.8780E-08
X CH_4	**8.352E-08**	**1.546E-07**	**2.575E-07**	**3.968E-07**	**5.756E-07**

25 atm	1300 K	1400 K	1500 K	1600 K	1700 K
Phase	Vapor	Vapor	Vapor	Vapor	Vapor
CO_2	0.9500000	0.9499999	0.9499999	0.9499999	0.9499999
CH_4	0.0499999	0.0499999	0.0499999	0.0499999	0.0499998
CH_3COOH	3.9813E-08	5.2993E-08	6.8333E-08	8.5802E-08	1.0534E-07
X CH_4	**7.963E-07**	**1.060E-06**	**1.367E-06**	**1.716E-06**	**2.107E-06**

25 atm	1800 K	1900 K	2000 K
Phase	Vapor	Vapor	Vapor
CO_2	0.9499999	0.9499998	0.9499998
CH_4	0.0499998	0.0499998	0.0499998
CH_3COOH	1.2686E-07	1.5025E-07	1.7541E-07
X CH_4	**2.537E-06**	**3.005E-06**	**3.508E-06**

Table A-44: Outlet moles and the equilibrium fractional conversion of methane for reaction (R A-1) obtained by using the Peng-Robinson equation of state in Aspen at varying temperatures and 50 atm.

50 atm	300 K	400 K	500 K	600 K	700 K
Phase	Liquid	Liquid	Vapor	Vapor	Vapor
CO_2	0.9500000	0.9500000	0.9500000	0.9500000	0.9500000
CH_4	0.0500000	0.0500000	0.0500000	0.0500000	0.0500000
CH_3COOH	4.5970E-11	5.6960E-10	4.0795E-10	1.5491E-09	4.0361E-09
X CH_4	**9.194E-10**	**1.139E-08**	**8.159E-09**	**3.098E-08**	**8.072E-08**

50 atm	800 K	900 K	1000 K	1100 K	1200 K
Phase	Vapor	Vapor	Vapor	Vapor	Vapor
CO_2	0.9500000	0.9500000	0.9500000	0.9500000	0.9499999
CH_4	0.0499999	0.0499999	0.0499999	0.0499999	0.0499999
CH_3COOH	8.5332E-09	1.5652E-08	2.5931E-08	3.9813E-08	5.7631E-08
X CH_4	**1.707E-07**	**3.130E-07**	**5.186E-07**	**7.963E-07**	**1.153E-06**

50 atm	1300 K	1400 K	1500 K	1600 K	1700 K
Phase	Vapor	Vapor	Vapor	Vapor	Vapor
CO_2	0.9499999	0.9499999	0.9499999	0.9499998	0.9499998
CH_4	0.0499999	0.0499999	0.0499998	0.0499998	0.0499997
CH_3COOH	7.9610E-08	1.0587E-07	1.3644E-07	1.7126E-07	2.1022E-07
X CH_4	**1.592E-06**	**2.117E-06**	**2.729E-06**	**3.425E-06**	**4.204E-06**

50 atm	1800 K	1900 K	2000 K
Phase	Vapor	Vapor	Vapor
CO_2	0.9499997	0.9499997	0.9499996
CH_4	0.0499997	0.0499997	0.0499996
CH_3COOH	2.5315E-07	2.9984E-07	3.5005E-07
X CH_4	**5.063E-06**	**5.997E-06**	**7.001E-06**

Table A-45: Outlet moles and the equilibrium fractional conversion of methane for reaction (R A-1) obtained by using the Peng-Robinson equation of state in Aspen at varying temperatures and 100 atm.

100 atm	300 K	400 K	500 K	600 K	700 K
Phase	Liquid	Liquid	Vapor	Vapor	Vapor
CO_2	0.9500000	0.9500000	0.9500000	0.9500000	0.9500000
CH_4	0.0500000	0.0500000	0.0500000	0.0500000	0.0499999
CH_3COOH	8.7529E-10	8.4669E-10	1.0812E-09	3.4983E-09	8.6460E-09
X CH_4	**1.751E-08**	**1.693E-08**	**2.162E-08**	**6.997E-08**	**1.729E-07**

100 atm	800 K	900 K	1000 K	1100 K	1200 K
Phase	Vapor	Vapor	Vapor	Vapor	Vapor
CO_2	0.9500000	0.9500000	0.9499999	0.9499999	0.9499999
CH_4	0.0499999	0.0499999	0.0499999	0.0499999	0.0499998
CH_3COOH	1.7761E-08	3.2034E-08	5.2526E-08	8.0121E-08	1.1550E-07
X CH_4	**3.552E-07**	**6.407E-07**	**1.051E-06**	**1.602E-06**	**2.310E-06**

100 atm	1300 K	1400 K	1500 K	1600 K	1700 K
Phase	Vapor	Vapor	Vapor	Vapor	Vapor
CO_2	0.9499998	0.9499998	0.9499997	0.9499997	0.9499996
CH_4	0.0499998	0.0499997	0.0499997	0.0499996	0.0499995
CH_3COOH	1.5912E-07	2.1125E-07	2.7195E-07	3.4115E-07	4.1863E-07
X CH_4	**3.182E-06**	**4.225E-06**	**5.439E-06**	**6.823E-06**	**8.373E-06**

100 atm	1800 K	1900 K	2000 K
Phase	Vapor	Vapor	Vapor
CO_2	0.9499995	0.9499994	0.9499993
CH_4	0.0499995	0.0499994	0.0499993
CH_3COOH	5.0405E-07	5.9703E-07	6.9709E-07
X CH_4	**1.008E-05**	**1.194E-05**	**1.394E-05**

Table A-46: Outlet moles and the equilibrium fractional conversion of methane for reaction (R A-1) obtained by using the Peng-Robinson equation of state in Aspen at varying temperatures and 150 atm.

150 atm	300 K	400 K	500 K	600 K	700 K
Phase	Liquid	Liquid	Vapor	Vapor	Vapor
CO_2	0.9500000	0.9500000	0.9500000	0.9500000	0.9500000
CH_4	0.0500000	0.0500000	0.0500000	0.0499999	0.0499999
CH_3COOH	1.8515E-09	1.0023E-09	2.0081E-09	5.8610E-09	1.3802E-08
X CH_4	**3.703E-08**	**2.005E-08**	**4.016E-08**	**1.172E-07**	**2.760E-07**

150 atm	800 K	900 K	1000 K	1100 K	1200 K
Phase	Vapor	Vapor	Vapor	Vapor	Vapor
CO_2	0.9500000	0.9500000	0.9499999	0.9499999	0.9499998
CH_4	0.0499999	0.0499999	0.0499999	0.0499998	0.0499998
CH_3COOH	2.7620E-08	4.9057E-08	7.9685E-08	1.2083E-07	1.7351E-07
X CH_4	**5.524E-07**	**9.811E-07**	**1.594E-06**	**2.417E-06**	**3.470E-06**

150 atm	1300 K	1400 K	1500 K	1600 K	1700 K
Phase	Vapor	Vapor	Vapor	Vapor	Vapor
CO_2	0.9499998	0.9499997	0.9499996	0.9499995	0.9499994
CH_4	0.0499997	0.0499996	0.0499995	0.0499994	0.0499993
CH_3COOH	2.3846E-07	3.1608E-07	4.0651E-07	5.0966E-07	6.2522E-07
X CH_4	**4.769E-06**	**6.322E-06**	**8.130E-06**	**1.019E-05**	**1.250E-05**

150 atm	1800 K	1900 K	2000 K
Phase	Vapor	Vapor	Vapor
CO_2	0.9499992	0.9499991	0.9499990
CH_4	0.0499992	0.0499991	0.0499989
CH_3COOH	7.5272E-07	8.9159E-07	1.0411E-06
X CH_4	**1.505E-05**	**1.783E-05**	**2.082E-05**

Table A-47: Outlet moles and the equilibrium fractional conversion of methane for reaction (R A-1) obtained by using the Peng-Robinson equation of state in Aspen at varying temperatures and 200 atm.

200 atm	300 K	400 K	500 K	600 K	700 K
Phase	Liquid	Liquid	Liquid	Vapor	Vapor
CO_2	0.9500000	0.9500000	0.9500000	0.9500000	0.9500000
CH_4	0.0500000	0.0500000	0.0499999	0.0499999	0.0499999
CH_3COOH	2.7370E-09	1.2769E-09	6.0568E-09	8.6331E-09	1.9464E-08
X CH_4	**5.474E-08**	**2.554E-08**	**1.211E-07**	**1.727E-07**	**3.893E-07**

200 atm	800 K	900 K	1000 K	1100 K	1200 K
Phase	Vapor	Vapor	Vapor	Vapor	Vapor
CO_2	0.9500000	0.9499999	0.9499999	0.9499998	0.9499998
CH_4	0.0499999	0.0499999	0.0499998	0.0499998	0.0499997
CH_3COOH	3.8043E-08	6.6638E-08	1.0732E-07	1.6185E-07	2.3160E-07
X CH_4	**7.609E-07**	**1.333E-06**	**2.146E-06**	**3.237E-06**	**4.632E-06**

200 atm	1300 K	1400 K	1500 K	1600 K	1700 K
Phase	Vapor	Vapor	Vapor	Vapor	Vapor
CO_2	0.9499997	0.9499996	0.9499995	0.9499993	0.9499992
CH_4	0.0499996	0.0499995	0.0499994	0.0499993	0.0499991
CH_3COOH	3.1757E-07	4.2033E-07	5.4010E-07	6.7678E-07	8.3000E-07
X CH_4	**6.351E-06**	**8.407E-06**	**1.080E-05**	**1.354E-05**	**1.660E-05**

200 atm	1800 K	1900 K	2000 K
Phase	Vapor	Vapor	Vapor
CO_2	0.9499990	0.9499988	0.9499986
CH_4	0.0499990	0.0499988	0.0499986
CH_3COOH	9.9918E-07	1.1836E-06	1.3822E-06
X CH_4	**1.998E-05**	**2.367E-05**	**2.764E-05**

Table A-48: Outlet moles and the equilibrium fractional conversion of methane for reaction (R A-1) obtained by using the Peng-Robinson equation of state in Aspen at varying temperatures and 300 atm.

300 atm	300 K	400 K	500 K	600 K	700 K
Phase	Liquid	Liquid	Liquid	Vapor	Vapor
CO_2	0.9500000	0.9500000	0.9500000	0.9500000	0.9500000
CH_4	0.0500000	0.0500000	0.0499999	0.0499999	0.0499999
CH_3COOH	4.3842E-09	3.4463E-09	7.0597E-09	1.5320E-08	3.2133E-08
X CH_4	**8.768E-08**	**6.893E-08**	**1.412E-07**	**3.064E-07**	**6.427E-07**

300 atm	800 K	900 K	1000 K	1100 K	1200 K
Phase	Vapor	Vapor	Vapor	Vapor	Vapor
CO_2	0.9499999	0.9499999	0.9499998	0.9499998	0.9499997
CH_4	0.0499999	0.0499999	0.0499998	0.0499997	0.0499996
CH_3COOH	6.0329E-08	1.0317E-07	1.6370E-07	2.4452E-07	3.4773E-07
X CH_4	**1.207E-06**	**2.063E-06**	**3.274E-06**	**4.890E-06**	**6.955E-06**

300 atm	1300 K	1400 K	1500 K	1600 K	1700 K
Phase	Vapor	Vapor	Vapor	Vapor	Vapor
CO_2	0.9499995	0.9499994	0.9499992	0.9499990	0.9499988
CH_4	0.0499995	0.0499993	0.0499992	0.0499989	0.0499987
CH_3COOH	4.7488E-07	6.2691E-07	8.0425E-07	1.0068E-06	1.2342E-06
X CH_4	**9.498E-06**	**1.254E-05**	**1.608E-05**	**2.014E-05**	**2.468E-05**

300 atm	1800 K	1900 K	2000 K
Phase	Vapor	Vapor	Vapor
CO_2	0.9499985	0.9499982	0.9499979
CH_4	0.0499985	0.0499982	0.0499979
CH_3COOH	1.4855E-06	1.7598E-06	2.0557E-06
X CH_4	**2.971E-05**	**3.520E-05**	**4.111E-05**

Table A-49: Outlet moles and the equilibrium fractional conversion of methane for reaction (R A-1) obtained by using the Peng-Robinson equation of state in Aspen at varying temperatures and 400 atm.

400 atm	300 K	400 K	500 K	600 K	700 K
Phase	Liquid	Liquid	Liquid	Liquid	Vapor
CO_2	0.9500000	0.9500000	0.9500000	0.9500000	0.9500000
CH_4	0.0499999	0.0499999	0.0499999	0.0499999	0.0499999
CH_3COOH	5.9027E-09	6.3673E-09	1.1136E-08	2.4729E-08	4.6271E-08
X CH_4	**1.181E-07**	**1.273E-07**	**2.227E-07**	**4.946E-07**	**9.254E-07**

400 atm	800 K	900 K	1000 K	1100 K	1200 K
Phase	Vapor	Vapor	Vapor	Vapor	Vapor
CO_2	0.9499999	0.9499999	0.9499998	0.9499997	0.9499995
CH_4	0.0499999	0.0499998	0.0499997	0.0499996	0.0499995
CH_3COOH	8.4136E-08	1.4109E-07	2.2109E-07	3.2760E-07	4.6343E-07
X CH_4	**1.683E-06**	**2.822E-06**	**4.422E-06**	**6.552E-06**	**9.269E-06**

400 atm	1300 K	1400 K	1500 K	1600 K	1700 K
Phase	Vapor	Vapor	Vapor	Vapor	Vapor
CO_2	0.9499994	0.9499992	0.9499989	0.9499987	0.9499984
CH_4	0.0499993	0.0499991	0.0499989	0.0499986	0.0499983
CH_3COOH	6.3069E-07	8.3074E-07	1.0643E-06	1.3313E-06	1.6312E-06
X CH_4	**1.261E-05**	**1.661E-05**	**2.129E-05**	**2.663E-05**	**3.262E-05**

400 atm	1800 K	1900 K	2000 K
Phase	Vapor	Vapor	Vapor
CO_2	0.9499980	0.9499977	0.9499973
CH_4	0.0499980	0.0499976	0.0499972
CH_3COOH	1.9632E-06	2.3258E-06	2.7176E-06
X CH_4	**3.926E-05**	**4.652E-05**	**5.435E-05**

Table A-50: Outlet moles and the equilibrium fractional conversion of methane for reaction (R A-1) obtained by using the Peng-Robinson equation of state in Aspen at varying temperatures and 500 atm.

500 atm	300 K	400 K	500 K	600 K	700 K
Phase	Liquid	Liquid	Liquid	Liquid	Vapor
CO_2	0.9500000	0.9500000	0.9500000	0.9500000	0.9499999
CH_4	0.0499999	0.0499999	0.0499999	0.0499999	0.0499999
CH_3COOH	7.3010E-09	9.5849E-09	1.6385E-08	3.2265E-08	6.1510E-08
X CH_4	**1.460E-07**	**1.917E-07**	**3.277E-07**	**6.453E-07**	**1.230E-06**

500 atm	800 K	900 K	1000 K	1100 K	1200 K
Phase	Vapor	Vapor	Vapor	Vapor	Vapor
CO_2	0.9499999	0.9499998	0.9499997	0.9499996	0.9499994
CH_4	0.0499998	0.0499998	0.0499997	0.0499995	0.0499994
CH_3COOH	1.0904E-07	1.7994E-07	2.7905E-07	4.1066E-07	5.7832E-07
X CH_4	**2.181E-06**	**3.599E-06**	**5.581E-06**	**8.213E-06**	**1.157E-05**

500 atm	1300 K	1400 K	1500 K	1600 K	1700 K
Phase	Vapor	Vapor	Vapor	Vapor	Vapor
CO_2	0.9499992	0.9499990	0.9499987	0.9499983	0.9499980
CH_4	0.0499992	0.0499989	0.0499986	0.0499983	0.0499979
CH_3COOH	7.8471E-07	1.0316E-06	1.3200E-06	1.6500E-06	2.0212E-06
X CH_4	**1.569E-05**	**2.063E-05**	**2.640E-05**	**3.300E-05**	**4.042E-05**

500 atm	1800 K	1900 K	2000 K
Phase	Vapor	Vapor	Vapor
CO_2	0.9499976	0.9499971	0.9499966
CH_4	0.0499975	0.0499971	0.0499966
AcOH	2.4323E-06	2.8820E-06	3.3682E-06
X CH_4	**4.865E-05**	**5.764E-05**	**6.736E-05**

Table A-51: Outlet moles and the equilibrium fractional conversion of methane for reaction (R A-1) obtained by using the Peng-Robinson equation of state in Aspen at varying temperatures and 600 atm.

600 atm	300 K	400 K	500 K	600 K	700 K
Phase	Liquid	Liquid	Liquid	Liquid	Liquid
CO_2	0.9500000	0.9500000	0.9500000	0.9499999	0.9499999
CH_4	0.0499999	0.0499999	0.0499999	0.0499999	0.0499999
CH_3COOH	8.5819E-09	1.2880E-08	2.2104E-08	4.1911E-08	7.7521E-08
X CH_4	**1.716E-07**	**2.576E-07**	**4.421E-07**	**8.382E-07**	**1.550E-06**

600 atm	800 K	900 K	1000 K	1100 K	1200 K
Phase	Vapor	Vapor	Vapor	Vapor	Vapor
CO_2	0.9499999	0.9499998	0.9499997	0.9499995	0.9499993
CH_4	0.0499998	0.0499997	0.0499996	0.0499995	0.0499993
CH_3COOH	1.3469E-07	2.1935E-07	3.3721E-07	4.9338E-07	6.9211E-07
X CH_4	**2.694E-06**	**4.387E-06**	**6.744E-06**	**9.868E-06**	**1.384E-05**

600 atm	1300 K	1400 K	1500 K	1600 K	1700 K
Phase	Vapor	Vapor	Vapor	Vapor	Vapor
CO_2	0.9499991	0.9499988	0.9499984	0.9499980	0.9499976
CH_4	0.0499990	0.0499987	0.0499984	0.0499980	0.0499976
CH_3COOH	9.3671E-07	1.2294E-06	1.5715E-06	1.9632E-06	2.4041E-06
X CH_4	**1.873E-05**	**2.459E-05**	**3.143E-05**	**3.926E-05**	**4.808E-05**

600 atm	1800 K	1900 K	2000 K
Phase	Vapor	Vapor	Vapor
CO_2	0.9499971	0.9499966	0.9499960
CH_4	0.0499971	0.0499966	0.0499959
CH_3COOH	2.8931E-06	3.4283E-06	4.0077E-06
X CH_4	**5.786E-05**	**6.857E-05**	**8.015E-05**

Table A-52: Outlet moles and the equilibrium fractional conversion of methane for reaction (R A-1) obtained by using the Peng-Robinson equation of state in Aspen at varying temperatures and 700 atm.

700 atm	300 K	400 K	500 K	600 K	700 K
Phase	Liquid	Liquid	Liquid	Liquid	Liquid
CO_2	0.9500000	0.9500000	0.9500000	0.9499999	0.9499999
CH_4	0.0499999	0.0499999	0.0499999	0.0499999	0.0499999
CH_3COOH	9.7478E-09	1.6141E-08	2.8070E-08	5.1988E-08	9.4030E-08
X CH_4	**1.950E-07**	**3.228E-07**	**5.614E-07**	**1.040E-06**	**1.881E-06**

700 atm	800 K	900 K	1000 K	1100 K	1200 K
Phase	Vapor	Vapor	Vapor	Vapor	Vapor
CO_2	0.9499998	0.9499997	0.9499996	0.9499994	0.9499992
CH_4	0.0499998	0.0499997	0.0499996	0.0499994	0.0499992
CH_3COOH	1.6077E-07	2.5900E-07	3.9526E-07	5.7546E-07	8.0458E-07
X CH_4	**3.215E-06**	**5.180E-06**	**7.905E-06**	**1.151E-05**	**1.609E-05**

700 atm	1300 K	1400 K	1500 K	1600 K	1700 K
Phase	Vapor	Vapor	Vapor	Vapor	Vapor
CO_2	0.9499989	0.9499986	0.9499982	0.9499977	0.9499972
CH_4	0.0499989	0.0499985	0.0499981	0.0499977	0.0499972
CH_3COOH	1.0865E-06	1.4240E-06	1.8185E-06	2.2707E-06	2.7802E-06
X CH_4	**2.173E-05**	**2.848E-05**	**3.637E-05**	**4.541E-05**	**5.560E-05**

700 atm	1800 K	1900 K	2000 K
Phase	Vapor	Vapor	Vapor
CO_2	0.9499967	0.9499960	0.9499954
CH_4	0.0499966	0.0499960	0.0499953
CH_3COOH	3.3456E-06	3.9651E-06	4.6362E-06
X CH_4	**6.691E-05**	**7.930E-05**	**9.272E-05**

Table A-53: Outlet moles and the equilibrium fractional conversion of methane for reaction (R A-1) obtained by using the Peng-Robinson equation of state in Aspen at varying temperatures and 800 atm.

800 atm	300 K	400 K	500 K	600 K	700 K
Phase	Liquid	Liquid	Liquid	Liquid	Liquid
CO_2	0.9500000	0.9500000	0.9500000	0.9499999	0.9499999
CH_4	0.0499999	0.0499999	0.0499999	0.0499999	0.0499998
CH_3COOH	1.0802E-08	1.9303E-08	3.4122E-08	6.2294E-08	1.1081E-07
X CH_4	**2.160E-07**	**3.861E-07**	**6.824E-07**	**1.246E-06**	**2.216E-06**

800 atm	800 K	900 K	1000 K	1100 K	1200 K
Phase	Vapor	Vapor	Vapor	Vapor	Vapor
CO_2	0.9499998	0.9499997	0.9499995	0.9499993	0.9499991
CH_4	0.0499998	0.0499997	0.0499995	0.0499993	0.0499990
CH_3COOH	1.8706E-07	2.9866E-07	4.5297E-07	6.5669E-07	9.1551E-07
X CH_4	**3.741E-06**	**5.973E-06**	**9.059E-06**	**1.313E-05**	**1.831E-05**

800 atm	1300 K	1400 K	1500 K	1600 K	1700 K
Phase	Vapor	Vapor	Vapor	Vapor	Vapor
CO_2	0.9499988	0.9499984	0.9499979	0.9499974	0.9499969
CH_4	0.0499987	0.0499983	0.0499979	0.0499974	0.0499968
CH_3COOH	1.2339E-06	1.6152E-06	2.0612E-06	2.5727E-06	3.1493E-06
X CH_4	**2.468E-05**	**3.230E-05**	**4.122E-05**	**5.145E-05**	**6.299E-05**

800 atm	1800 K	1900 K	2000 K
Phase	Vapor	Vapor	Vapor
CO_2	0.9499962	0.9499955	0.9499947
CH_4	0.0499962	0.0499955	0.0499947
CH_3COOH	3.7899E-06	4.4923E-06	5.2541E-06
X CH_4	**7.580E-05**	**8.985E-05**	**1.051E-04**

Table A-54: Outlet moles and the equilibrium fractional conversion of methane for reaction (R A-1) obtained by using the Peng-Robinson equation of state in Aspen at varying temperatures and 900 atm.

900 atm	300 K	400 K	500 K	600 K	700 K
Phase	Liquid	Liquid	Liquid	Liquid	Liquid
CO_2	0.9500000	0.9500000	0.9500000	0.9499999	0.9499999
CH_4	0.0499999	0.0499999	0.0499999	0.0499999	0.0499998
CH_3COOH	1.1750E-08	2.2331E-08	4.0148E-08	7.2672E-08	1.2768E-07
X CH_4	**2.350E-07**	**4.466E-07**	**8.030E-07**	**1.453E-06**	**2.554E-06**

900 atm	800 K	900 K	1000 K	1100 K	1200 K
Phase	Vapor	Vapor	Vapor	Vapor	Vapor
CO_2	0.9499998	0.9499997	0.9499995	0.9499993	0.9499990
CH_4	0.0499997	0.0499996	0.0499994	0.0499992	0.0499989
CH_3COOH	2.1335E-07	3.3811E-07	5.1013E-07	7.3688E-07	1.0248E-06
X CH_4	**4.267E-06**	**6.762E-06**	**1.020E-05**	**1.474E-05**	**2.050E-05**

900 atm	1300 K	1400 K	1500 K	1600 K	1700 K
Phase	Vapor	Vapor	Vapor	Vapor	Vapor
CO_2	0.9499986	0.9499982	0.9499977	0.9499971	0.9499965
CH_4	0.0499986	0.0499982	0.0499977	0.0499971	0.0499964
CH_3COOH	1.3789E-06	1.8030E-06	2.2994E-06	2.8690E-06	3.5117E-06
X CH_4	**2.758E-05**	**3.606E-05**	**4.599E-05**	**5.738E-05**	**7.023E-05**

900 atm	1800 K	1900 K	2000 K
Phase	Vapor	Vapor	Vapor
CO_2	0.9499958	0.9499950	0.9499941
CH_4	0.0499957	0.0499949	0.0499941
CH_3COOH	4.2261E-06	5.0103E-06	5.8613E-06
X CH_4	**8.452E-05**	**1.002E-04**	**1.172E-04**

Table A-55: Outlet moles and the equilibrium fractional conversion of methane for reaction (R A-1) obtained by using the Peng-Robinson equation of state in Aspen at varying temperatures and 1000 atm.

1000 atm	300 K	400 K	500 K	600 K	700 K
Phase	Liquid	Liquid	Liquid	Liquid	Liquid
CO_2	0.9500000	0.9500000	0.9500000	0.9499999	0.9499999
CH_4	0.0499999	0.0499999	0.0499999	0.0499999	0.0499998
CH_3COOH	1.2594E-08	2.5203E-08	4.6066E-08	8.3001E-08	1.4449E-07
X CH_4	**2.519E-07**	**5.041E-07**	**9.213E-07**	**1.660E-06**	**2.890E-06**

1000 atm	800 K	900 K	1000 K	1100 K	1200 K
Phase	Vapor	Vapor	Vapor	Vapor	Vapor
CO_2	0.9499998	0.9499996	0.9499994	0.9499992	0.9499989
CH_4	0.0499997	0.0499996	0.0499994	0.0499991	0.0499988
CH_3COOH	2.3948E-07	3.7719E-07	5.6658E-07	8.1589E-07	1.1322E-06
X CH_4	**4.790E-06**	**7.544E-06**	**1.133E-05**	**1.632E-05**	**2.264E-05**

1000 atm	1300 K	1400 K	1500 K	1600 K	1700 K
Phase	Vapor	Vapor	Vapor	Vapor	Vapor
CO_2	0.9499985	0.9499980	0.9499975	0.9499968	0.9499961
CH_4	0.0499984	0.0499980	0.0499974	0.0499968	0.0499961
CH_3COOH	1.5214E-06	1.9874E-06	2.5332E-06	3.1598E-06	3.8674E-06
X CH_4	**3.043E-05**	**3.975E-05**	**5.066E-05**	**6.320E-05**	**7.735E-05**

1000 atm	1800 K	1900 K	2000 K
Phase	Vapor	Vapor	Vapor
CO_2	0.9499953	0.9499945	0.9499935
CH_4	0.0499953	0.0499944	0.0499935
CH_3COOH	4.6545E-06	5.5191E-06	6.4582E-06
X CH_4	**9.309E-05**	**1.104E-04**	**1.292E-04**

Table A-56: Equilibrium fractional conversion of methane for reaction (R A-1) obtained by using the Peng-Robinson equation of state in Aspen at varying temperatures and 1 - 100 atm.

T (K)	1 atm	10 atm	25 atm	50 atm	100 atm
300 K	0.000E+00	6.346E-12	**1.003E-09**	**9.194E-10**	**1.751E-08**
400 K	1.692E-11	1.852E-10	5.370E-10	**1.139E-08**	**1.693E-08**
500 K	1.353E-10	1.414E-09	3.818E-09	8.159E-09	2.162E-08
600 K	5.446E-10	5.581E-09	1.452E-08	3.098E-08	6.997E-08
700 K	1.500E-09	1.521E-08	3.890E-08	8.072E-08	1.729E-07
800 K	3.269E-09	3.296E-08	8.352E-08	1.707E-07	3.552E-07
900 K	6.106E-09	6.135E-08	1.546E-07	3.130E-07	6.407E-07
1000 K	1.023E-08	1.026E-07	2.575E-07	5.186E-07	1.051E-06
1100 K	1.581E-08	1.584E-07	3.968E-07	7.963E-07	1.602E-06
1200 K	2.299E-08	2.301E-07	5.756E-07	1.153E-06	2.310E-06
1300 K	3.185E-08	3.185E-07	7.963E-07	1.592E-06	3.182E-06
1400 K	4.244E-08	4.242E-07	1.060E-06	2.117E-06	4.225E-06
1500 K	5.475E-08	5.472E-07	1.367E-06	2.729E-06	5.439E-06
1600 K	6.877E-08	6.872E-07	1.716E-06	3.425E-06	6.823E-06
1700 K	8.445E-08	8.438E-07	2.107E-06	4.204E-06	8.373E-06
1800 K	1.017E-07	1.016E-06	2.537E-06	5.063E-06	1.008E-05
1900 K	1.205E-07	1.204E-06	3.005E-06	5.997E-06	1.194E-05
2000 K	1.406E-07	1.405E-06	3.508E-06	7.001E-06	1.394E-05

NOTE: Values in bold indicate liquid phase.

Table A-57: Equilibrium fractional conversion of methane for reaction (R A-1) obtained by using the Peng-Robinson equation of state in Aspen at varying temperatures and 150 - 500 atm.

T (K)	150 atm	200 atm	300 atm	400 atm	500 atm
300 K	**3.703E-08**	**5.474E-08**	**8.768E-08**	**1.181E-07**	**1.460E-07**
400 K	**2.005E-08**	**2.554E-08**	**6.893E-08**	**1.273E-07**	**1.917E-07**
500 K	4.016E-08	**1.211E-07**	**1.412E-07**	**2.227E-07**	**3.277E-07**
600 K	1.172E-07	1.727E-07	3.064E-07	**4.946E-07**	**6.453E-07**
700 K	2.760E-07	3.893E-07	6.427E-07	9.254E-07	1.230E-06
800 K	5.524E-07	7.609E-07	1.207E-06	1.683E-06	2.181E-06
900 K	9.811E-07	1.333E-06	2.063E-06	2.822E-06	3.599E-06
1000 K	1.594E-06	2.146E-06	3.274E-06	4.422E-06	5.581E-06
1100 K	2.417E-06	3.237E-06	4.890E-06	6.552E-06	8.213E-06
1200 K	3.470E-06	4.632E-06	6.955E-06	9.269E-06	1.157E-05
1300 K	4.769E-06	6.351E-06	9.498E-06	1.261E-05	1.569E-05
1400 K	6.322E-06	8.407E-06	1.254E-05	1.661E-05	2.063E-05
1500 K	8.130E-06	1.080E-05	1.608E-05	2.129E-05	2.640E-05
1600 K	1.019E-05	1.354E-05	2.014E-05	2.663E-05	3.300E-05
1700 K	1.250E-05	1.660E-05	2.468E-05	3.262E-05	4.042E-05
1800 K	1.505E-05	1.998E-05	2.971E-05	3.926E-05	4.865E-05
1900 K	1.783E-05	2.367E-05	3.520E-05	4.652E-05	5.764E-05
2000 K	2.082E-05	2.764E-05	4.111E-05	5.435E-05	6.736E-05

NOTE: Values in bold indicate liquid phase.

Table A-58: Equilibrium fractional conversion of methane for reaction (R A-1) obtained by using the Peng-Robinson equation of state in Aspen at varying temperatures and 600 - 1000 atm.

T (K)	600 atm	700 atm	800 atm	900 atm	1000 atm
300 K	**1.716E-07**	**1.950E-07**	**2.160E-07**	**2.350E-07**	**2.519E-07**
400 K	**2.576E-07**	**3.228E-07**	**3.861E-07**	**4.466E-07**	**5.041E-07**
500 K	**4.421E-07**	**5.614E-07**	**6.824E-07**	**8.030E-07**	**9.213E-07**
600 K	**8.382E-07**	**1.040E-06**	**1.246E-06**	**1.453E-06**	**1.660E-06**
700 K	**1.550E-06**	**1.881E-06**	**2.216E-06**	**2.554E-06**	**2.890E-06**
800 K	2.694E-06	3.215E-06	3.741E-06	4.267E-06	4.790E-06
900 K	4.387E-06	5.180E-06	5.973E-06	6.762E-06	7.544E-06
1000 K	6.744E-06	7.905E-06	9.059E-06	1.020E-05	1.133E-05
1100 K	9.868E-06	1.151E-05	1.313E-05	1.474E-05	1.632E-05
1200 K	1.384E-05	1.609E-05	1.831E-05	2.050E-05	2.264E-05
1300 K	1.873E-05	2.173E-05	2.468E-05	2.758E-05	3.043E-05
1400 K	2.459E-05	2.848E-05	3.230E-05	3.606E-05	3.975E-05
1500 K	3.143E-05	3.637E-05	4.122E-05	4.599E-05	5.066E-05
1600 K	3.926E-05	4.541E-05	5.145E-05	5.738E-05	6.320E-05
1700 K	4.808E-05	5.560E-05	6.299E-05	7.023E-05	7.735E-05
1800 K	5.786E-05	6.691E-05	7.580E-05	8.452E-05	9.309E-05
1900 K	6.857E-05	7.930E-05	8.985E-05	1.002E-04	1.104E-04
2000 K	8.015E-05	9.272E-05	1.051E-04	1.172E-04	1.292E-04

NOTE: Values in bold indicate liquid phase.

A.2.4. DIFFERENCES BETWEEN EQUATIONS OF STATE

The values for the equilibrium fractional conversion of methane from each equation of state were compared. The percent differences were calculated using equations (E A-30), (E A-31) and (E A-32).

$$\% \text{ Difference (Ideal \& R-K)} = (X_{R\text{-}K} - X_{Ideal})/X_{Ideal} \times 100\% \quad \text{(E A-30)}$$

$$\% \text{ Difference (Ideal \& P-R)} = (X_{P\text{-}R} - X_{Ideal})/X_{Ideal} \times 100\% \quad \text{(E A-31)}$$

$$\% \text{ Difference (R-K \& P-R)} = (X_{P\text{-}R} - X_{R\text{-}K})/X_{R\text{-}K} \times 100\% \quad \text{(E A-32)}$$

where X_{Ideal}, $X_{R\text{-}K}$ and $X_{P\text{-}R}$ are the equilibrium fractional conversions of methane obtained from the ideal gas, Redlich-Kwong and Peng-Robinson equations of state, respectively.

The equilibrium fractional conversions of methane for each equation of state and the percent differences between them at varying temperatures and pressures can be found in tables A-59 – A-73.

Table A-59: Equilibrium fractional conversion of methane (X_{CH4}) for reaction RA1 obtained from Aspen at 1 atm and varying temperatures and equations of state and the % differences between the conversions from the equations of state.

	X CH_4			**Differences**		
1 atm	Ideal	R-K	P-R	Ideal & R-K	Ideal & P-R	P-R & R-K
300 K	0.00E+00	0.00E+00	0.00E+00	0.00%	0.00%	0.00%
400 K	1.682E-11	1.697E-11	1.692E-11	0.93%	0.61%	-0.32%
500 K	1.346E-10	1.353E-10	1.353E-10	0.46%	0.49%	0.03%
600 K	5.432E-10	5.445E-10	5.446E-10	0.25%	0.27%	0.03%
700 K	1.497E-09	1.499E-09	1.500E-09	0.14%	0.16%	0.02%
800 K	3.266E-09	3.268E-09	3.269E-09	0.07%	0.09%	0.02%
900 K	6.102E-09	6.105E-09	6.106E-09	0.04%	0.06%	0.02%
1000 K	1.023E-08	1.023E-08	1.023E-08	0.02%	0.03%	0.01%
1100 K	1.581E-08	1.581E-08	1.581E-08	0.00%	0.01%	0.01%
1200 K	2.299E-08	2.299E-08	2.299E-08	0.00%	0.01%	0.01%
1300 K	3.185E-08	3.185E-08	3.185E-08	-0.01%	0.00%	0.01%
1400 K	4.244E-08	4.243E-08	4.244E-08	-0.01%	0.00%	0.01%
1500 K	5.476E-08	5.475E-08	5.475E-08	-0.01%	-0.01%	0.01%
1600 K	6.878E-08	6.877E-08	6.877E-08	-0.01%	-0.01%	0.00%
1700 K	8.445E-08	8.444E-08	8.445E-08	-0.01%	-0.01%	0.00%
1800 K	1.017E-07	1.017E-07	1.017E-07	-0.01%	-0.01%	0.00%
1900 K	1.205E-07	1.205E-07	1.205E-07	-0.01%	-0.01%	0.00%
2000 K	1.406E-07	1.406E-07	1.406E-07	-0.01%	-0.01%	0.00%

NOTE: Values in bold indicate liquid phase.

Table A-60: Equilibrium fractional conversion of methane for reaction (R A-1) obtained from Aspen at 10 atm and varying temperatures and equations of state and the % differences between the conversions from the equations of state.

	X CH_4			**Differences**		
10 atm	Ideal	R-K	P-R	Ideal & R-K	Ideal & P-R	P-R & R-K
300 K	5.088E-12	6.335E-12	6.346E-12	24.5%	24.7%	0.17%
400 K	1.682E-10	1.847E-10	1.852E-10	9.81%	10.14%	0.30%
500 K	1.346E-09	1.410E-09	1.414E-09	4.74%	5.04%	0.29%
600 K	5.432E-09	5.567E-09	5.581E-09	2.49%	2.75%	0.25%
700 K	1.497E-08	1.518E-08	1.521E-08	1.36%	1.58%	0.21%
800 K	3.266E-08	3.290E-08	3.296E-08	0.74%	0.92%	0.18%
900 K	6.102E-08	6.126E-08	6.135E-08	0.39%	0.54%	0.15%
1000 K	1.023E-07	1.024E-07	1.026E-07	0.17%	0.30%	0.13%
1100 K	1.581E-07	1.582E-07	1.584E-07	0.04%	0.15%	0.11%
1200 K	2.299E-07	2.298E-07	2.301E-07	-0.03%	0.06%	0.09%
1300 K	3.185E-07	3.183E-07	3.185E-07	-0.08%	0.00%	0.08%
1400 K	4.244E-07	4.239E-07	4.242E-07	-0.11%	-0.04%	0.06%
1500 K	5.476E-07	5.470E-07	5.473E-07	-0.10%	-0.07%	0.06%
1600 K	6.878E-07	6.869E-07	6.872E-07	-0.13%	-0.08%	0.05%
1700 K	8.445E-07	8.435E-07	8.438E-07	-0.13%	-0.09%	0.04%
1800 K	1.017E-06	1.016E-06	1.016E-06	-0.12%	-0.09%	0.03%
1900 K	1.205E-06	1.203E-06	1.204E-06	-0.12%	-0.09%	0.03%
2000 K	1.406E-06	1.405E-06	1.405E-06	-0.11%	-0.09%	0.02%

NOTE: Values in bold indicate liquid phase.

Table A-61: Equilibrium fractional conversion of methane for reaction (R A-1) obtained from Aspen at 25 atm and varying temperatures and equations of state and the % differences between the conversions from the equations of state.

	X CH_4			**Differences**		
25 atm	Ideal	R-K	P-R	Ideal & R-K	Ideal & P-R	P-R & R-K
300 K	1.272E-11	**1.016E-09**	**1.003E-09**	7886.2%	7785.4%	-1.3%
400 K	4.204E-10	5.331E-10	5.370E-10	26.81%	27.73%	0.73%
500 K	3.366E-09	3.777E-09	3.818E-09	12.24%	13.44%	1.07%
600 K	1.358E-08	1.443E-08	1.452E-08	7.05%	6.94%	0.61%
700 K	3.743E-08	3.870E-08	3.890E-08	3.40%	3.93%	0.52%
800 K	8.165E-08	8.316E-08	8.352E-08	1.84%	2.28%	0.44%
900 K	1.526E-07	1.540E-07	1.546E-07	0.95%	1.32%	0.37%
1000 K	2.556E-07	2.567E-07	2.575E-07	0.43%	0.74%	0.31%
1100 K	3.953E-07	3.957E-07	3.968E-07	0.11%	0.37%	0.26%
1200 K	5.748E-07	5.743E-07	5.756E-07	-0.08%	0.14%	0.22%
1300 K	7.963E-07	7.948E-07	7.963E-07	-0.20%	-0.01%	0.19%
1400 K	1.061E-06	1.058E-06	1.060E-06	-0.27%	-0.11%	0.16%
1500 K	1.369E-06	1.365E-06	1.367E-06	-0.30%	-0.16%	0.14%
1600 K	1.719E-06	1.714E-06	1.716E-06	-0.31%	-0.20%	0.12%
1700 K	2.111E-06	2.105E-06	2.107E-06	-0.31%	-0.22%	0.10%
1800 K	2.543E-06	2.535E-06	2.537E-06	-0.30%	-0.22%	0.08%
1900 K	3.012E-06	3.003E-06	3.005E-06	-0.29%	-0.22%	0.07%
2000 K	3.516E-06	3.506E-06	3.508E-06	-0.27%	-0.22%	0.06%

NOTE: Values in bold indicate liquid phase.

Table A-62: Equilibrium fractional conversion of methane for reaction (R A-1) obtained from Aspen at 50 atm and varying temperatures and equations of state and the % differences between the conversions from the equations of state.

	X CH_4			**Differences**		
50 atm	Ideal	R-K	P-R	Ideal & R-K	Ideal & P-R	P-R & R-K
300 K	2.540E-11	**1.008E-09**	**9.194E-10**	3866.9%	3519.7%	-4.8%
400 K	8.408E-10	**1.112E-08**	**1.139E-08**	1222.44%	1254.84%	2.45%
500 K	6.731E-09	8.056E-09	8.159E-09	19.68%	21.21%	1.28%
600 K	2.716E-08	3.063E-08	3.098E-08	12.77%	14.08%	1.16%
700 K	7.486E-08	7.993E-08	8.072E-08	6.77%	7.83%	0.99%
800 K	1.633E-07	1.692E-07	1.707E-07	3.63%	4.51%	0.84%
900 K	3.051E-07	3.108E-07	3.130E-07	1.87%	2.59%	0.71%
1000 K	5.113E-07	5.155E-07	5.186E-07	0.83%	1.44%	0.61%
1100 K	7.906E-07	7.922E-07	7.963E-07	0.20%	0.72%	0.52%
1200 K	1.150E-06	1.148E-06	1.153E-06	-0.18%	0.26%	0.44%
1300 K	1.593E-06	1.586E-06	1.592E-06	-0.40%	-0.03%	0.37%
1400 K	2.122E-06	2.111E-06	2.117E-06	-0.53%	-0.22%	0.32%
1500 K	2.738E-06	2.721E-06	2.729E-06	-0.60%	-0.33%	0.27%
1600 K	3.439E-06	3.417E-06	3.425E-06	-0.63%	-0.40%	0.23%
1700 K	4.223E-06	4.196E-06	4.204E-06	-0.63%	-0.43%	0.19%
1800 K	5.086E-06	5.055E-06	5.063E-06	-0.61%	-0.44%	0.16%
1900 K	6.022E-06	5.989E-06	5.997E-06	-0.56%	-0.42%	0.14%
2000 K	7.031E-06	6.993E-06	7.001E-06	-0.54%	-0.43%	0.11%

NOTE: Values in bold indicate liquid phase.

Table A-63: Equilibrium fractional conversion of methane for reaction (R A-1) obtained from Aspen at 100 atm and varying temperatures and equations of state and the % differences between the conversions from the equations of state.

	X CH_4			**Differences**		
100 atm	Ideal	R-K	P-R	Ideal & R-K	Ideal & P-R	P-R & R-K
300 K	**5.505E-07**	**1.860E-08**	**1.751E-08**	-96.6%	-96.8%	-5.9%
400 K	1.682E-09	**1.672E-08**	**1.693E-08**	894.27%	906.97%	1.28%
500 K	1.346E-08	2.114E-08	2.162E-08	56.99%	60.62%	2.31%
600 K	5.432E-08	6.852E-08	6.997E-08	26.15%	28.81%	2.10%
700 K	1.497E-07	1.698E-07	1.729E-07	13.41%	15.50%	1.84%
800 K	3.266E-07	3.497E-07	3.552E-07	7.07%	8.76%	1.58%
900 K	6.102E-07	6.321E-07	6.407E-07	3.58%	4.99%	1.35%
1000 K	1.023E-06	1.038E-06	1.051E-06	1.56%	2.74%	1.16%
1100 K	1.581E-06	1.587E-06	1.602E-06	0.35%	1.35%	0.99%
1200 K	2.299E-06	2.290E-06	2.310E-06	-0.38%	0.47%	0.85%
1300 K	3.185E-06	3.159E-06	3.182E-06	-0.81%	-0.09%	0.73%
1400 K	4.244E-06	4.199E-06	4.225E-06	-1.06%	-0.45%	0.62%
1500 K	5.476E-06	5.410E-06	5.439E-06	-1.19%	-0.67%	0.53%
1600 K	6.878E-06	6.792E-06	6.823E-06	-1.24%	-0.80%	0.45%
1700 K	8.445E-06	8.340E-06	8.373E-06	-1.24%	-0.86%	0.39%
1800 K	1.017E-05	1.005E-05	1.008E-05	-1.21%	-0.89%	0.33%
1900 K	1.205E-05	1.191E-05	1.194E-05	-1.15%	-0.88%	0.27%
2000 K	1.406E-05	1.391E-05	1.394E-05	-1.09%	-0.86%	0.23%

NOTE: Values in bold indicate liquid phase.

Table A-64: Equilibrium fractional conversion of methane for reaction (R A-1) obtained from Aspen at 150 atm and varying temperatures and equations of state and the % differences between the conversions from the equations of state.

	X CH_4			**Differences**		
150 atm	Ideal	R-K	P-R	Ideal & R-K	Ideal & P-R	P-R & R-K
300 K	**5.505E-07**	**4.006E-08**	**3.703E-08**	-92.7%	-93.3%	-7.6%
400 K	2.523E-09	**2.095E-08**	**2.005E-08**	730.37%	694.62%	-4.30%
500 K	2.019E-08	3.902E-08	4.016E-08	93.24%	98.88%	2.92%
600 K	8.148E-08	1.140E-07	1.172E-07	39.90%	43.87%	2.84%
700 K	2.246E-07	2.692E-07	2.760E-07	19.86%	22.91%	2.54%
800 K	4.899E-07	5.404E-07	5.524E-07	10.30%	12.75%	2.22%
900 K	9.154E-07	9.626E-07	9.811E-07	5.16%	7.18%	1.93%
1000 K	1.534E-06	1.568E-06	1.594E-06	2.20%	3.91%	1.66%
1100 K	2.372E-06	2.382E-06	2.417E-06	0.45%	1.89%	1.44%
1200 K	3.449E-06	3.455E-06	3.494E-06	0.17%%	1.32%	1.15%
1300 K	4.778E-06	4.719E-06	4.769E-06	-1.24%	-0.19%	1.06%
1400 K	6.366E-06	6.264E-06	6.322E-06	-1.60%	-0.70%	0.92%
1500 K	8.213E-06	8.067E-06	8.130E-06	-1.78%	-1.01%	0.79%
1600 K	1.032E-05	1.013E-05	1.019E-05	-1.86%	-1.20%	0.67%
1700 K	1.267E-05	1.243E-05	1.250E-05	-1.85%	-1.29%	0.57%
1800 K	1.526E-05	1.498E-05	1.505E-05	-1.80%	-1.33%	0.49%
1900 K	1.807E-05	1.776E-05	1.783E-05	-1.72%	-1.32%	0.41%
2000 K	2.109E-05	2.075E-05	2.082E-05	-1.62%	-1.28%	0.34%

NOTE: Values in bold indicate liquid phase.

Table A-65: Equilibrium fractional conversion of methane for reaction (R A-1) obtained from Aspen at 200 atm and varying temperatures and equations of state and the % differences between the conversions from the equations of state.

	X CH_4			**Differences**		
200 atm	Ideal	R-K	P-R	Ideal & R-K	Ideal & P-R	P-R & R-K
300 K	**5.505E-07**	**5.988E-08**	**5.474E-08**	-89.1%	-90.1%	-8.6%
400 K	3.334E-09	**2.681E-08**	**2.554E-08**	704.14%	665.92%	-4.75%
500 K	2.693E-08	1.201E-07	**1.211E-07**	346.12%	349.88%	0.84%
600 K	1.086E-07	1.670E-07	1.727E-07	53.73%	58.93%	3.38%
700 K	2.994E-07	3.775E-07	3.893E-07	26.06%	30.01%	3.13%
800 K	6.532E-07	7.402E-07	7.609E-07	13.32%	16.48%	2.79%
900 K	1.220E-06	1.301E-06	1.333E-06	6.59%	9.20%	2.44%
1000 K	2.045E-06	2.102E-06	2.146E-06	2.77%	4.96%	2.13%
1100 K	3.162E-06	3.178E-06	3.237E-06	0.50%	2.36%	1.85%
1200 K	4.598E-06	4.559E-06	4.632E-06	-0.86%	0.73%	1.60%
1300 K	6.371E-06	6.265E-06	6.351E-06	-1.67%	-0.30%	1.39%
1400 K	8.488E-06	8.307E-06	8.407E-06	-2.13%	-0.96%	1.20%
1500 K	1.095E-05	1.069E-05	1.080E-05	-2.37%	-1.36%	1.03%
1600 K	1.376E-05	1.342E-05	1.354E-05	-2.46%	-1.60%	0.89%
1700 K	1.689E-05	1.647E-05	1.660E-05	-2.46%	-1.72%	0.76%
1800 K	2.034E-05	1.986E-05	1.998E-05	-2.39%	-1.76%	0.65%
1900 K	2.409E-05	2.354E-05	2.367E-05	-2.29%	-1.75%	0.55%
2000 K	2.812E-05	2.752E-05	2.764E-05	-2.16%	-1.71%	0.46%

NOTE: Values in bold indicate liquid phase.

Table A-66: Equilibrium fractional conversion of methane for reaction (R A-1) obtained from Aspen at 300 atm and varying temperatures and equations of state and the % differences between the conversions from the equations of state.

	X CH_4			**Differences**		
300 atm	Ideal	R-K	P-R	Ideal & R-K	Ideal & P-R	P-R & R-K
300 K	**5.505E-07**	**9.728E-08**	**8.768E-08**	-82.3%	-84.1%	-9.9%
400 K	5.045E-09	**7.024E-08**	**6.893E-08**	1292.17%	1266.21%	-1.86%
500 K	4.047E-08	1.291E-07	**1.412E-07**	218.98%	248.87%	9.37%
600 K	1.630E-07	2.944E-07	3.064E-07	80.69%	88.03%	4.06%
700 K	4.492E-07	7.084E-07	7.379E-07	57.71%	64.28%	4.17%
800 K	9.798E-07	1.163E-06	1.207E-06	18.73%	23.14%	3.72%
900 K	1.831E-06	1.997E-06	2.063E-06	9.07%	12.71%	3.34%
1000 K	3.068E-06	3.180E-06	3.274E-06	3.66%	6.73%	2.95%
1100 K	4.743E-06	4.766E-06	4.890E-06	0.49%	3.10%	2.60%
1200 K	6.898E-06	6.800E-06	6.955E-06	-1.42%	0.83%	2.28%
1300 K	9.556E-06	9.313E-06	9.498E-06	-2.55%	-0.61%	1.99%
1400 K	1.273E-05	1.233E-05	1.254E-05	-3.19%	-1.52%	1.73%
1500 K	1.643E-05	1.585E-05	1.608E-05	-3.53%	-2.08%	1.50%
1600 K	2.063E-05	1.988E-05	2.014E-05	-3.66%	-2.41%	1.30%
1700 K	2.534E-05	2.441E-05	2.468E-05	-3.65%	-2.57%	1.12%
1800 K	3.051E-05	2.943E-05	2.971E-05	-3.56%	-2.63%	0.96%
1900 K	3.614E-05	3.491E-05	3.520E-05	-3.40%	-2.61%	0.82%
2000 K	4.219E-05	4.083E-05	4.111E-05	-3.21%	-2.54%	0.69%

NOTE: Values in bold indicate liquid phase.

Table A-67: Equilibrium fractional conversion of methane for reaction (R A-1) obtained from Aspen at 400 atm and varying temperatures and equations of state and the % differences between the conversions from the equations of state.

	X CH_4			**Differences**		
400 atm	Ideal	R-K	P-R	Ideal & R-K	Ideal & P-R	P-R & R-K
300 K	**5.513E-07**	**1.321E-07**	**1.181E-07**	-76.0%	-78.6%	-10.6%
400 K	**4.387E-06**	**1.309E-07**	**1.273E-07**	-97.02%	-97.10%	-2.74%
500 K	5.338E-08	**2.170E-07**	**2.227E-07**	306.43%	317.22%	2.65%
600 K	2.173E-07	4.464E-07	**4.946E-07**	105.46%	127.63%	10.79%
700 K	5.989E-07	8.841E-07	9.254E-07	47.63%	54.52%	4.67%
800 K	1.306E-06	1.611E-06	1.683E-06	23.31%	28.80%	4.45%
900 K	2.441E-06	2.711E-06	2.822E-06	11.07%	15.60%	4.08%
1000 K	4.090E-06	4.265E-06	4.422E-06	4.29%	8.11%	3.67%
1100 K	6.325E-06	6.345E-06	6.552E-06	0.32%	3.59%	3.26%
1200 K	9.197E-06	9.009E-06	9.269E-06	-2.05%	0.78%	2.89%
1300 K	1.274E-05	1.230E-05	1.261E-05	-3.45%	-1.00%	2.54%
1400 K	1.698E-05	1.625E-05	1.661E-05	-4.26%	-2.12%	2.23%
1500 K	2.190E-05	2.088E-05	2.129E-05	-4.67%	-2.82%	1.95%
1600 K	2.751E-05	2.618E-05	2.663E-05	-4.83%	-3.22%	1.70%
1700 K	3.378E-05	3.215E-05	3.262E-05	-4.82%	-3.42%	1.47%
1800 K	4.068E-05	3.877E-05	3.926E-05	-4.70%	-3.49%	1.27%
1900 K	4.819E-05	4.602E-05	4.652E-05	-4.50%	-3.46%	1.08%
2000 K	5.625E-05	5.386E-05	5.435E-05	-4.25%	-3.37%	0.92%

NOTE: Values in bold indicate liquid phase.

Table A-68: Equilibrium fractional conversion of methane for reaction (R A-1) obtained from Aspen at 500 atm and varying temperatures and equations of state and the % differences between the conversions from the equations of state.

	X CH_4			**Differences**		
500 atm	Ideal	R-K	P-R	Ideal & R-K	Ideal & P-R	P-R & R-K
300 K	**5.505E-07**	**1.642E-07**	**1.460E-07**	-70.2%	-73.5%	-11.1%
400 K	**4.387E-06**	**1.977E-07**	**1.917E-07**	-95.49%	-95.63%	-3.03%
500 K	6.731E-08	**3.202E-07**	**3.277E-07**	375.70%	386.81%	2.34%
600 K	2.716E-07	**6.171E-07**	**6.453E-07**	127.20%	137.60%	4.58%
700 K	7.486E-07	1.170E-06	1.230E-06	56.30%	64.33%	5.14%
800 K	1.633E-06	2.076E-06	2.181E-06	27.12%	33.54%	5.05%
900 K	3.051E-06	3.437E-06	3.599E-06	12.64%	17.95%	4.71%
1000 K	5.113E-06	5.351E-06	5.581E-06	4.67%	9.16%	4.29%
1100 K	7.906E-06	7.908E-06	8.213E-06	0.03%	3.89%	3.86%
1200 K	1.150E-05	1.118E-05	1.157E-05	-2.74%	0.61%	3.44%
1300 K	1.593E-05	1.523E-05	1.569E-05	-4.38%	-1.46%	3.05%
1400 K	2.122E-05	2.009E-05	2.063E-05	-5.32%	-2.77%	2.70%
1500 K	2.738E-05	2.579E-05	2.640E-05	-5.80%	-3.57%	2.37%
1600 K	3.439E-05	3.233E-05	3.300E-05	-5.98%	-4.03%	2.07%
1700 K	4.223E-05	3.971E-05	4.042E-05	-5.97%	-4.27%	1.81%
1800 K	5.085E-05	4.790E-05	4.865E-05	-5.82%	-4.34%	1.57%
1900 K	6.023E-05	5.687E-05	5.764E-05	-5.58%	-4.30%	1.35%
2000 K	7.031E-05	6.660E-05	6.736E-05	-5.28%	-4.19%	1.15%

NOTE: Values in bold indicate liquid phase.

Table A-69: Equilibrium fractional conversion of methane for reaction (R A-1) obtained from Aspen at 600 atm and varying temperatures and equations of state and the % differences between the conversions from the equations of state.

	X CH_4			**Differences**		
600 atm	Ideal	R-K	P-R	Ideal & R-K	Ideal & P-R	P-R & R-K
300 K	**5.505E-07**	**1.937E-07**	**1.716E-07**	-64.8%	-68.8%	-11.4%
400 K	**4.387E-06**	**2.658E-07**	**2.576E-07**	-93.94%	-94.13%	-3.09%
500 K	8.078E-08	**4.327E-07**	**4.421E-07**	435.67%	447.27%	2.17%
600 K	3.259E-07	**8.005E-07**	**8.382E-07**	145.63%	157.19%	4.71%
700 K	8.983E-07	**1.470E-06**	**1.550E-06**	63.68%	72.59%	5.44%
800 K	1.960E-06	2.552E-06	2.694E-06	30.23%	37.46%	5.55%
900 K	3.661E-06	4.168E-06	4.387E-06	13.82%	19.81%	5.27%
1000 K	6.135E-06	6.432E-06	6.744E-06	4.84%	9.93%	4.85%
1100 K	9.487E-06	9.451E-06	9.868E-06	-0.37%	4.01%	4.40%
1200 K	1.380E-05	1.332E-05	1.384E-05	-3.48%	0.34%	3.96%
1300 K	1.911E-05	1.809E-05	1.873E-05	-5.32%	-1.98%	3.53%
1400 K	2.546E-05	2.384E-05	2.459E-05	-6.37%	-3.44%	3.14%
1500 K	3.285E-05	3.058E-05	3.143E-05	-6.91%	-4.33%	2.77%
1600 K	4.127E-05	3.833E-05	3.926E-05	-7.11%	-4.85%	2.44%
1700 K	5.067E-05	4.708E-05	4.808E-05	-7.09%	-5.11%	2.14%
1800 K	6.102E-05	5.681E-05	5.786E-05	-6.91%	-5.18%	1.86%
1900 K	7.228E-05	6.748E-05	6.857E-05	-6.64%	-5.13%	1.61%
2000 K	8.437E-05	7.906E-05	8.015E-05	-6.29%	-5.00%	1.38%

NOTE: Values in bold indicate liquid phase.

Table A-70: Equilibrium fractional conversion of methane for reaction (R A-1) obtained from Aspen at 700 atm and varying temperatures and equations of state and the % differences between the conversions from the equations of state.

	X CH_4			**Differences**		
700 atm	Ideal	R-K	P-R	Ideal & R-K	Ideal & P-R	P-R & R-K
300 K	**5.505E-07**	**2.204E-07**	**1.950E-07**	-60.0%	-64.6%	-11.5%
400 K	**4.387E-06**	**3.329E-07**	**3.228E-07**	-92.41%	-92.64%	-3.03%
500 K	9.424E-08	**5.497E-07**	**5.614E-07**	483.33%	495.70%	2.12%
600 K	3.809E-07	**9.918E-07**	**1.040E-06**	160.40%	172.99%	4.83%
700 K	1.048E-06	**1.777E-06**	**1.881E-06**	69.54%	79.44%	5.84%
800 K	2.286E-06	3.034E-06	3.215E-06	32.69%	40.64%	5.99%
900 K	4.272E-06	4.898E-06	5.180E-06	14.66%	21.26%	5.76%
1000 K	7.158E-06	7.503E-06	7.905E-06	4.83%	10.45%	5.36%
1100 K	1.107E-05	1.097E-05	1.151E-05	-0.87%	3.99%	4.90%
1200 K	1.609E-05	1.541E-05	1.609E-05	-4.26%	-0.02%	4.43%
1300 K	2.230E-05	2.090E-05	2.173E-05	-6.28%	-2.54%	3.98%
1400 K	2.971E-05	2.750E-05	2.848E-05	-7.42%	-4.13%	3.55%
1500 K	3.833E-05	3.526E-05	3.637E-05	-8.01%	-5.11%	3.16%
1600 K	4.814E-05	4.418E-05	4.541E-05	-8.23%	-5.67%	2.79%
1700 K	5.911E-05	5.427E-05	5.560E-05	-8.19%	-5.94%	2.46%
1800 K	7.119E-05	6.550E-05	6.691E-05	-7.99%	-6.02%	2.15%
1900 K	8.432E-05	7.785E-05	7.930E-05	-7.68%	-5.95%	1.87%
2000 K	9.843E-05	9.126E-05	9.272E-05	-7.29%	-5.80%	1.61%

NOTE: Values in bold indicate liquid phase.

Table A-71: Equilibrium fractional conversion of methane for reaction (R A-1) obtained from Aspen at 800 atm and varying temperatures and equations of state and the % differences between the conversions from the equations of state.

	X CH_4			**Differences**		
800 atm	Ideal	R-K	P-R	Ideal & R-K	Ideal & P-R	P-R & R-K
300 K	**5.505E-07**	**2.444E-07**	**2.160E-07**	-55.6%	-60.8%	-11.6%
400 K	**4.387E-06**	**3.977E-07**	**3.861E-07**	-90.94%	-91.20%	-2.91%
500 K	1.077E-07	**6.679E-07**	**6.824E-07**	520.16%	533.63%	2.17%
600 K	4.345E-07	**1.187E-06**	**1.246E-06**	173.12%	186.71%	4.97%
700 K	1.198E-06	**2.088E-06**	**2.216E-06**	74.35%	85.03%	6.12%
800 K	2.613E-06	3.517E-06	3.741E-06	34.60%	43.18%	6.38%
900 K	4.882E-06	5.624E-06	5.973E-06	15.21%	22.35%	6.20%
1000 K	8.180E-06	8.561E-06	9.059E-06	4.65%	10.75%	5.82%
1100 K	1.265E-05	1.247E-05	1.313E-05	-1.45%	3.83%	5.36%
1200 K	1.839E-05	1.746E-05	1.831E-05	-5.09%	-0.45%	4.88%
1300 K	2.548E-05	2.364E-05	2.468E-05	-7.24%	-3.15%	4.41%
1400 K	3.395E-05	3.108E-05	3.230E-05	-8.47%	-4.85%	3.95%
1500 K	4.380E-05	3.982E-05	4.122E-05	-9.09%	-5.89%	3.53%
1600 K	5.502E-05	4.989E-05	5.145E-05	-9.32%	-6.48%	3.13%
1700 K	6.756E-05	6.129E-05	6.299E-05	-9.28%	-6.77%	2.77%
1800 K	8.136E-05	7.400E-05	7.580E-05	-9.05%	-6.84%	2.43%
1900 K	9.637E-05	8.798E-05	8.985E-05	-8.70%	-6.77%	2.12%
2000 K	1.125E-04	1.032E-04	1.051E-04	-8.27%	-6.59%	1.84%

NOTE: Values in bold indicate liquid phase.

Table A-72: Equilibrium fractional conversion of methane for reaction (R A-1) obtained from Aspen at 900 atm and varying temperatures and equations of state and the % differences between the conversions from the equations of state.

	X CH_4			**Differences**		
900 atm	Ideal	R-K	P-R	Ideal & R-K	Ideal & P-R	P-R & R-K
300 K	**5.505E-07**	**2.658E-07**	**2.350E-07**	-51.7%	-57.3%	-11.6%
400 K	**4.387E-06**	**4.593E-07**	**4.466E-07**	-89.53%	-89.82%	-2.75%
500 K	1.212E-07	**7.850E-07**	**8.030E-07**	547.86%	562.68%	2.29%
600 K	4.889E-07	**1.382E-06**	**1.453E-06**	182.78%	197.31%	5.14%
700 K	1.347E-06	**2.400E-06**	**2.554E-06**	78.11%	89.50%	6.39%
800 K	2.940E-06	3.998E-06	4.267E-06	36.00%	45.16%	6.74%
900 K	5.492E-06	6.343E-06	6.762E-06	15.49%	23.12%	6.61%
1000 K	9.203E-06	9.602E-06	1.020E-05	4.34%	10.87%	6.25%
1100 K	1.423E-05	1.393E-05	1.474E-05	-2.11%	3.57%	5.79%
1200 K	2.069E-05	1.946E-05	2.050E-05	-5.94%	-0.95%	5.30%
1300 K	2.867E-05	2.631E-05	2.758E-05	-8.21%	-3.80%	4.81%
1400 K	3.819E-05	3.456E-05	3.606E-05	-9.51%	-5.59%	4.33%
1500 K	4.928E-05	4.427E-05	4.599E-05	-10.17%	-6.68%	3.88%
1600 K	6.190E-05	5.546E-05	5.738E-05	-10.40%	-7.30%	3.46%
1700 K	7.600E-05	6.814E-05	7.023E-05	-10.34%	-7.59%	3.07%
1800 K	9.133E-05	8.230E-05	8.452E-05	-9.90%	-7.46%	2.71%
1900 K	1.084E-04	9.848E-05	1.009E-04	-9.19%	-6.90%	2.48%
2000 K	1.265E-04	1.149E-04	1.172E-04	-9.24%	-7.37%	2.06%

NOTE: Values in bold indicate liquid phase.

Table A-73: Equilibrium fractional conversion of methane for reaction (R A-1) obtained from Aspen at 1000 atm and varying temperatures and equations of state and the % differences between the conversions from the equations of state.

	X CH_4			**Differences**		
1000 atm	Ideal	R-K	P-R	Ideal & R-K	Ideal & P-R	P-R & R-K
300 K	**5.505E-07**	**2.847E-07**	**2.519E-07**	-48.3%	-54.2%	-11.5%
400 K	**4.387E-06**	**5.173E-07**	**5.041E-07**	-88.21%	-88.51%	-2.56%
500 K	1.346E-07	**8.993E-07**	**9.213E-07**	567.98%	584.34%	2.45%
600 K	5.432E-07	**1.576E-06**	**1.660E-06**	190.17%	205.61%	5.32%
700 K	1.497E-06	**2.709E-06**	**2.890E-06**	80.96%	93.01%	6.66%
800 K	3.266E-06	4.473E-06	4.790E-06	36.96%	46.65%	7.07%
900 K	6.102E-06	7.051E-06	7.544E-06	15.54%	23.62%	6.99%
1000 K	1.023E-05	1.062E-05	1.133E-05	3.91%	10.82%	6.65%
1100 K	1.581E-05	1.533E-05	1.630E-05	-3.04%	3.08%	6.31%
1200 K	2.299E-05	2.142E-05	2.264E-05	-6.82%	-1.51%	5.70%
1300 K	3.185E-05	2.892E-05	3.043E-05	-9.19%	-4.48%	5.19%
1400 K	4.244E-05	3.796E-05	3.975E-05	-10.54%	-6.34%	4.70%
1500 K	5.475E-05	4.861E-05	5.066E-05	-11.22%	-7.47%	4.23%
1600 K	6.877E-05	6.089E-05	6.320E-05	-11.46%	-8.11%	3.78%
1700 K	8.445E-05	7.483E-05	7.735E-05	-11.39%	-8.41%	3.36%
1800 K	1.017E-04	9.040E-05	9.309E-05	-11.12%	-8.47%	2.98%
1900 K	1.205E-04	1.076E-04	1.104E-04	-10.70%	-8.36%	2.62%
2000 K	1.406E-04	1.263E-04	1.292E-04	-10.19%	-8.14%	2.29%

NOTE: Values in bold indicate liquid phase.

A.3. ASPEN DATA FOR METHYL FORMATE REACTION

Equilibrium thermodynamic calculations were performed on the synthesis of acetic acid from carbon monoxide, oxygen and methane:

$$CO_2 + CH_4 \leftrightarrow HCOOCH_3 \qquad \text{(R A-2)}$$

The calculations were performed using the AspenPlus™ engineering simulation software. The RGIBBS reactor model was used to perform a Gibbs free energy minimization on the system to give the chemical and phase equilibrium composition at various temperatures and pressures. These calculations do not take into account any surface interactions. Molecular interactions between molecules are taken into account in the equation of state. The inlet composition, inlet temperature, inlet pressure, reactor temperature and reactor pressure were specified for each reaction. The inlet conditions were set equal to the reactor conditions.

For the Aspen calculations, an inlet mole fraction of 0.95 CO_2 and 0.05 CH_4, and an inlet total number of moles of 1 was used. The Aspen calculations were performed for a wide range of pressures and temperatures, 1 - 200 atm and 300 – 2000 K. The calculations were performed using the Peng-Robinson equation of state.

The equilibrium fractional conversion of methane (X_{CH4}) was calculated using equation EA29. Since the outlet moles of methane given by Aspen did not have enough significant figures, the number of outlet moles of acetic acid was used as the number of moles of methane that reacted.

Table A-74: Outlet moles and the equilibrium fractional conversion of methane for reaction (R A-2) obtained by using the Peng-Robinson equation of state in Aspen at varying temperatures and 1 atm.

1 atm	300 K	400 K	500 K	600 K	700 K
Phase	Vapor	Vapor	Vapor	Vapor	Vapor
CO_2	0.9500000	0.9500000	0.9500000	0.9500000	0.9500000
CH_4	0.0500000	0.0500000	0.0500000	0.0500000	0.0500000
$HCOOCH_3$	0.0000000	0.0000000	0.0000000	0.0000000	1.0926E-16
X CH_4	**0.0000000**	**0.0000000**	**0.0000000**	**0.0000000**	**2.185E-15**

1 atm	800 K	900 K	1000 K	1100 K	1200 K
Phase	Vapor	Vapor	Vapor	Vapor	Vapor
CO_2	0.9500000	0.9500000	0.9500000	0.9500000	0.9500000
CH_4	0.0500000	0.0500000	0.0500000	0.0500000	0.0500000
$HCOOCH_3$	1.3419E-15	9.5714E-15	4.6494E-14	1.7069E-13	5.0741E-13
X CH_4	**2.684E-14**	**1.914E-13**	**9.299E-13**	**3.414E-12**	**1.015E-11**

1 atm	1300 K	1400 K	1500 K	1600 K	1700 K
Phase	Vapor	Vapor	Vapor	Vapor	Vapor
CO_2	0.9500000	0.9500000	0.9500000	0.9500000	0.9500000
CH_4	0.0500000	0.0500000	0.0500000	0.0500000	0.0500000
$HCOOCH_3$	1.2811E-12	2.8427E-12	5.6858E-12	1.0447E-11	1.7894E-11
X CH_4	**2.562E-11**	**5.685E-11**	**1.137E-10**	**2.089E-10**	**3.579E-10**

1 atm	1800 K	1900 K	2000 K
Phase	Vapor	Vapor	Vapor
CO_2	0.9500000	0.9500000	0.9500000
CH_4	0.0500000	0.0500000	0.0500000
$HCOOCH_3$	2.8897E-11	4.4399E-11	6.5380E-11
X CH_4	**5.779E-10**	**8.880E-10**	**1.308E-09**

Table A-75: Outlet moles and the equilibrium fractional conversion of methane for reaction (R A-2) obtained by using the Peng-Robinson equation of state in Aspen at varying temperatures and 10 atm.

10 atm	300 K	400 K	500 K	600 K	700 K
Phase	Vapor	Vapor	Vapor	Vapor	Vapor
CO_2	0.9500000	0.9500000	0.9500000	0.9500000	0.9500000
CH_4	0.0500000	0.0500000	0.0500000	0.0500000	0.0500000
$HCOOCH_3$	0.0000000	0.0000000	0.0000000	3.9509E-17	1.0103E-15
X CH_4	**0.0000000**	**0.0000000**	**0.0000000**	**7.902E-16**	**2.021E-14**

10 atm	800 K	900 K	1000 K	1100 K	1200 K
Phase	Vapor	Vapor	Vapor	Vapor	Vapor
CO_2	0.9500000	0.9500000	0.9500000	0.9500000	0.9500000
CH_4	0.0500000	0.0500000	0.0500000	0.0500000	0.0500000
$HCOOCH_3$	1.3518E-14	9.6118E-14	4.6625E-13	1.7102E-12	5.0807E-12
X CH_4	**2.704E-13**	**1.922E-12**	**9.325E-12**	**3.420E-11**	**1.016E-10**

10 atm	1300 K	1400 K	1500 K	1600 K	1700 K
Phase	Vapor	Vapor	Vapor	Vapor	Vapor
CO_2	0.9500000	0.9500000	0.9500000	0.9500000	0.9500000
CH_4	0.0500000	0.0500000	0.0500000	0.0500000	0.0500000
$HCOOCH_3$	1.2822E-11	2.8444E-11	5.6879E-11	1.0449E-10	1.7896E-10
X CH_4	**2.564E-10**	**5.689E-10**	**1.138E-09**	**2.090E-09**	**3.579E-09**

10 atm	1800 K	1900 K	2000 K
Phase	Vapor	Vapor	Vapor
CO_2	0.9500000	0.9500000	0.9500000
CH_4	0.0500000	0.0500000	0.0500000
$HCOOCH_3$	2.8897E-10	4.4398E-10	6.5376E-10
X CH_4	**5.779E-09**	**8.880E-09**	**1.308E-08**

Table A-76: Outlet moles and the equilibrium fractional conversion of methane for reaction (R A-2) obtained by using the Peng-Robinson equation of state in Aspen at varying temperatures and 25 atm.

25 atm	300 K	400 K	500 K	600 K	700 K
Phase	Liquid	Vapor	Vapor	Vapor	Vapor
CO_2	0.9500000	0.9500000	0.9500000	0.9500000	0.9500000
CH_4	0.0500000	0.0500000	0.0500000	0.0500000	0.0500000
$HCOOCH_3$	0.0000000	0.0000000	0.0000000	1.0233E-16	2.8026E-15
X CH_4	**0.0000000**	**0.0000000**	**0.0000000**	**2.047E-15**	**5.605E-14**

25 atm	800 K	900 K	1000 K	1100 K	1200 K
Phase	Vapor	Vapor	Vapor	Vapor	Vapor
CO_2	0.9500000	0.9500000	0.9500000	0.9500000	0.9500000
CH_4	0.0500000	0.0500000	0.0500000	0.0500000	0.0500000
$HCOOCH_3$	3.4145E-14	2.4194E-13	1.1710E-12	4.2890E-12	1.2729E-11
X CH_4	**6.829E-13**	**4.839E-12**	**2.342E-11**	**8.578E-11**	**2.546E-10**

25 atm	1300 K	1400 K	1500 K	1600 K	1700 K
Phase	Vapor	Vapor	Vapor	Vapor	Vapor
CO_2	0.9500000	0.9500000	0.9500000	0.9500000	0.9500000
CH_4	0.0500000	0.0500000	0.0500000	0.0500000	0.0500000
$HCOOCH_3$	3.2101E-11	7.1176E-11	1.4228E-10	2.6133E-10	4.4747E-10
X CH_4	**6.420E-10**	**1.424E-09**	**2.846E-09**	**5.227E-09**	**8.949E-09**

25 atm	1800 K	1900 K	2000 K
Phase	Vapor	Vapor	Vapor
CO_2	0.9500000	0.9500000	0.9500000
CH_4	0.0500000	0.0500000	0.0500000
$HCOOCH_3$	7.2247E-10	1.1099E-09	1.6342E-09
X CH_4	**1.445E-08**	**2.220E-08**	**3.268E-08**

Table A-77: Outlet moles and the equilibrium fractional conversion of methane for reaction (R A-2) obtained by using the Peng-Robinson equation of state in Aspen at varying temperatures and 50 atm.

50 atm	300 K	400 K	500 K	600 K	700 K
Phase	Liquid	Liquid	Vapor	Vapor	Vapor
CO_2	0.9500000	0.9500000	0.9500000	0.9500000	0.9500000
CH_4	0.0500000	0.0500000	0.0500000	0.0500000	0.0500000
$HCOOCH_3$	0.0000E+00	0.0000E+00	0.0000E+00	2.1341E-16	5.7517E-15
X CH_4	**0.000E+00**	**0.000E+00**	**0.000E+00**	**4.268E-15**	**1.150E-13**

50 atm	800 K	900 K	1000 K	1100 K	1200 K
Phase	Vapor	Vapor	Vapor	Vapor	Vapor
CO_2	0.9500000	0.9500000	0.9500000	0.9500000	0.9500000
CH_4	0.0500000	0.0500000	0.0500000	0.0500000	0.0500000
$HCOOCH_3$	6.9433E-14	4.8927E-13	2.3596E-12	8.6170E-12	2.5546E-11
X CH_4	**1.389E-12**	**9.785E-12**	**4.719E-11**	**1.723E-10**	**5.109E-10**

50 atm	1300 K	1400 K	1500 K	1600 K	1700 K
Phase	Vapor	Vapor	Vapor	Vapor	Vapor
CO_2	0.9500000	0.9500000	0.9500000	0.9500000	0.9500000
CH_4	0.0500000	0.0500000	0.0500000	0.0500000	0.0500000
$HCOOCH_3$	6.4352E-11	1.4257E-10	2.8484E-10	5.2296E-10	8.9519E-10
X CH_4	**1.287E-09**	**2.851E-09**	**5.697E-09**	**1.046E-08**	**1.790E-08**

50 atm	1800 K	1900 K	2000 K
Phase	Vapor	Vapor	Vapor
CO_2	0.9500000	0.9500000	0.9500000
CH_4	0.0500000	0.0500000	0.0500000
$HCOOCH_3$	1.4451E-09	2.2197E-09	3.2679E-09
X CH_4	**2.890E-08**	**4.439E-08**	**6.536E-08**

Table A-78: Outlet moles and the equilibrium fractional conversion of methane for reaction (R A-2) obtained by using the Peng-Robinson equation of state in Aspen at varying temperatures and 100 atm.

100 atm	300 K	400 K	500 K	600 K	700 K
Phase	Liquid	Liquid	Vapor	Vapor	Vapor
CO_2	0.9500000	0.9500000	0.9500000	0.9500000	0.9500000
CH_4	0.0500000	0.0500000	0.0500000	0.0500000	0.0500000
$HCOOCH_3$	0.0000000	0.0000000	0.0000000	4.6193E-16	1.2076E-14
X CH_4	**0.0000000**	**0.0000000**	**0.0000000**	**9.239E-15**	**2.415E-13**

100 atm	800 K	900 K	1000 K	1100 K	1200 K
Phase	Vapor	Vapor	Vapor	Vapor	Vapor
CO_2	0.9500000	0.9500000	0.9500000	0.9500000	0.9500000
CH_4	0.0500000	0.0500000	0.0500000	0.0500000	0.0500000
$HCOOCH_3$	1.4330E-13	9.9924E-13	4.7867E-12	1.7412E-11	5.1433E-11
X CH_4	**2.866E-12**	**1.998E-11**	**9.573E-11**	**3.482E-10**	**1.029E-09**

100 atm	1300 K	1400 K	1500 K	1600 K	1700 K
Phase	Vapor	Vapor	Vapor	Vapor	Vapor
CO_2	0.9500000	0.9500000	0.9500000	0.9500000	0.9500000
CH_4	0.0500000	0.0500000	0.0500000	0.0500000	0.0500000
$HCOOCH_3$	1.2929E-10	2.8600E-10	5.7077E-10	1.0471E-09	1.7914E-09
X CH_4	**2.586E-09**	**5.720E-09**	**1.142E-08**	**2.094E-08**	**3.583E-08**

100 atm	1800 K	1900 K	2000 K
Phase	Vapor	Vapor	Vapor
CO_2	0.9500000	0.9500000	0.9500000
CH_4	0.0500000	0.0500000	0.0500000
$HCOOCH_3$	2.8906E-09	4.4388E-09	6.5337E-09
X CH_4	**5.781E-08**	**8.878E-08**	**1.307E-07**

Table A-79: Outlet moles and the equilibrium fractional conversion of methane for reaction (R A-2) obtained by using the Peng-Robinson equation of state in Aspen at varying temperatures and 150 atm.

150 atm	300 K	400 K	500 K	600 K	700 K
Phase	Liquid	Liquid	Vapor	Vapor	Vapor
CO_2	0.9500000	0.9500000	0.9500000	0.9500000	0.9500000
CH_4	0.0500000	0.0500000	0.0500000	0.0500000	0.0500000
$HCOOCH_3$	0.0000000	0.0000000	8.6169E-18	2.2008E-15	7.2430E-14
X CH_4	**0.0000000**	**0.0000000**	**1.723E-16**	**4.402E-14**	**1.449E-12**

150 atm	800 K	900 K	1000 K	1100 K	1200 K
Phase	Vapor	Vapor	Vapor	Vapor	Vapor
CO_2	0.9500000	0.9500000	0.9500000	0.9500000	0.9500000
CH_4	0.0500000	0.0500000	0.0500000	0.0500000	0.0500000
$HCOOCH_3$	2.2128E-13	1.5283E-12	7.2761E-12	2.6358E-11	7.7637E-11
X CH_4	**4.426E-12**	**3.057E-11**	**1.455E-10**	**5.272E-10**	**1.553E-09**

150 atm	1300 K	1400 K	1500 K	1600 K	1700 K
Phase	Vapor	Vapor	Vapor	Vapor	Vapor
CO_2	0.9500000	0.9500000	0.9500000	0.9500000	0.9500000
CH_4	0.0500000	0.0500000	0.0500000	0.0500000	0.0500000
$HCOOCH_3$	1.9476E-10	4.3023E-10	8.5773E-10	1.5724E-09	2.6886E-09
X CH_4	**3.895E-09**	**8.605E-09**	**1.715E-08**	**3.145E-08**	**5.377E-08**

150 atm	1800 K	1900 K	2000 K
Phase	Vapor	Vapor	Vapor
CO_2	0.9500000	0.9500000	0.9500000
CH_4	0.0500000	0.0499999	0.0499999
$HCOOCH_3$	4.3366E-09	6.6574E-09	9.7976E-09
X CH_4	**8.673E-08**	**1.331E-07**	**1.960E-07**

Table A-80: Outlet moles and the equilibrium fractional conversion of methane for reaction (R A-2) obtained by using the Peng-Robinson equation of state in Aspen at varying temperatures and 200 atm.

200 atm	300 K	400 K	500 K	600 K	700 K
Phase	Liquid	Liquid	Liquid	Vapor	Vapor
CO_2	0.9500000	0.9500000	0.9500000	0.9500000	0.9500000
CH_4	0.0500000	0.0500000	0.0500000	0.0500000	0.0500000
$HCOOCH_3$	0.0000000	0.0000000	2.2007E-17	2.3653E-15	2.6314E-14
X CH_4	**0.0000000**	**0.0000000**	**4.401E-16**	**4.731E-14**	**5.263E-13**

200 atm	800 K	900 K	1000 K	1100 K	1200 K
Phase	Vapor	Vapor	Vapor	Vapor	Vapor
CO_2	0.9500000	0.9500000	0.9500000	0.9500000	0.9500000
CH_4	0.0500000	0.0500000	0.0500000	0.0500000	0.0500000
$HCOOCH_3$	3.0306E-13	2.0749E-12	9.8228E-12	3.5447E-11	1.0414E-10
X CH_4	**6.061E-12**	**4.150E-11**	**1.965E-10**	**7.089E-10**	**2.083E-09**

200 atm	1300 K	1400 K	1500 K	1600 K	1700 K
Phase	Vapor	Vapor	Vapor	Vapor	Vapor
CO_2	0.9500000	0.9500000	0.9500000	0.9500000	0.9500000
CH_4	0.0500000	0.0500000	0.0500000	0.0500000	0.0500000
$HCOOCH_3$	2.6075E-10	5.7522E-10	1.1457E-09	2.0987E-09	3.5867E-09
X CH_4	**5.215E-09**	**1.150E-08**	**2.291E-08**	**4.197E-08**	**7.173E-08**

200 atm	1800 K	1900 K	2000 K
Phase	Vapor	Vapor	Vapor
CO_2	0.9500000	0.9500000	0.9500000
CH_4	0.0499999	0.0499999	0.0499999
$HCOOCH_3$	5.7931E-09	8.8756E-09	1.3060E-08
X CH_4	**1.159E-07**	**1.775E-07**	**2.612E-07**

Table A-81: Equilibrium fractional conversion of methane for reaction (R A-2) obtained by using the Peng-Robinson equation of state in Aspen at varying temperatures and 1 - 50 atm.

T (K)	1 atm	10 atm	25 atm	50 atm
300 K	0.000E+00	0.000E+00	**0.000E+00**	**0.000E+00**
400 K	0.000E+00	0.000E+00	0.000E+00	**0.000E+00**
500 K	0.000E+00	0.000E+00	0.000E+00	0.000E+00
600 K	0.000E+00	7.902E-16	2.047E-15	4.268E-15
700 K	2.185E-15	2.021E-14	5.605E-14	1.150E-13
800 K	2.684E-14	2.704E-13	6.829E-13	1.389E-12
900 K	1.914E-13	1.922E-12	4.839E-12	9.785E-12
1000 K	9.299E-13	9.325E-12	2.342E-11	4.719E-11
1100 K	3.414E-12	3.420E-11	8.578E-11	1.723E-10
1200 K	1.015E-11	1.016E-10	2.546E-10	5.109E-10
1300 K	2.562E-11	2.564E-10	6.420E-10	1.287E-09
1400 K	5.685E-11	5.689E-10	1.424E-09	2.851E-09
1500 K	1.137E-10	1.138E-09	2.846E-09	5.697E-09
1600 K	2.089E-10	2.090E-09	5.227E-09	1.046E-08
1700 K	3.579E-10	3.579E-09	8.949E-09	1.790E-08
1800 K	5.779E-10	5.779E-09	1.445E-08	2.890E-08
1900 K	8.880E-10	8.880E-09	2.220E-08	4.439E-08
2000 K	1.308E-09	1.308E-08	3.268E-08	6.536E-08

NOTE: Values in bold indicate liquid phase.

Table A-82: Equilibrium fractional conversion of methane for reaction (R A-2) obtained by using the Peng-Robinson equation of state in Aspen at varying temperatures and 100 - 200 atm.

T (K)	100 atm	150 atm	200 atm
300 K	**0.000E+00**	**0.000E+00**	**0.000E+00**
400 K	**0.000E+00**	**0.000E+00**	**0.000E+00**
500 K	0.000E+00	1.723E-16	**4.401E-16**
600 K	9.239E-15	4.402E-14	4.731E-14
700 K	2.415E-13	1.449E-12	5.263E-13
800 K	2.866E-12	4.426E-12	6.061E-12
900 K	1.998E-11	3.057E-11	4.150E-11
1000 K	9.573E-11	1.455E-10	1.965E-10
1100 K	3.482E-10	5.272E-10	7.089E-10
1200 K	1.029E-09	1.553E-09	2.083E-09
1300 K	2.586E-09	3.895E-09	5.215E-09
1400 K	5.720E-09	8.605E-09	1.150E-08
1500 K	1.142E-08	1.715E-08	2.291E-08
1600 K	2.094E-08	3.145E-08	4.197E-08
1700 K	3.583E-08	5.377E-08	7.173E-08
1800 K	5.781E-08	8.673E-08	1.159E-07
1900 K	8.878E-08	1.331E-07	1.775E-07
2000 K	1.307E-07	1.960E-07	2.612E-07

NOTE: Values in bold indicate liquid phase.

A.4. ASPEN DATA FOR CARBON MONOXIDE REACTION

Equilibrium thermodynamic calculations were performed on the synthesis of acetic acid from carbon monoxide, oxygen and methane:

$$CO + ½\ O_2 + CH_4 \leftrightarrow CH_3COOH \qquad \text{(R A-3)}$$

The calculations were performed using the AspenPlus™ engineering simulation software. The RGIBBS reactor model was used to perform a Gibbs free energy minimization on the system to give the chemical and phase equilibrium composition at various temperatures and pressures. These calculations do not take into account any surface interactions. Molecular interactions between molecules are taken into account in the equation of state. The inlet composition, inlet temperature, inlet pressure, reactor temperature and reactor pressure were specified for each reaction. The inlet conditions were set equal to the reactor conditions.

For the Aspen calculations, an inlet mole fraction of 0.4 CO, 0.2 O_2 and 0.4 CH_4, and an inlet total number of moles of 1 was used. The Aspen calculations were performed for a wide range of pressures and temperatures, 1 - 200 atm and 300 – 2000 K. The calculations were performed using the Peng-Robinson equation of state.

The equilibrium fractional conversion of methane (X_{CH4}) was calculated using equation EA29:

Table A-83: Outlet moles and the equilibrium fractional conversion of methane for reaction (R A-3) obtained by using the Peng-Robinson equation of state in Aspen at varying temperatures and 1 atm.

1 atm	300 K	400 K	500 K	600 K	700 K
Phase	Liquid	Vapor	Vapor	Vapor	Vapor
CO	4.0492E-18	9.5541E-10	3.8541E-07	2.0951E-05	3.6065E-04
O_2	6.7135E-16	4.7770E-10	1.9270E-07	1.0476E-05	1.8033E-04
CH_4	1.5591E-15	9.5540E-10	3.8541E-07	2.0951E-05	3.6065E-04
CH_3COOH	0.400000	0.400000	0.400000	0.399979	0.399639
X CH_4	**1.000000**	**1.000000**	**0.999999**	**0.999948**	**0.999099**

1 atm	800 K	900 K	1000 K	1100 K	1200 K
Phase	Vapor	Vapor	Vapor	Vapor	Vapor
CO	3.0275E-03	0.015889	0.061006	0.178791	0.327486
O_2	1.5138E-06	7.9447E-03	0.030503	0.089395	0.163743
CH_4	3.0275E-03	0.158893	0.061006	0.178791	0.327486
CH_3COOH	0.396973	0.384111	0.338994	0.221209	0.072514
X CH_4	**0.992431**	**0.960277**	**0.847485**	**0.553023**	**0.181285**

1 atm	1300 K	1400 K	1500 K	1600 K	1700 K
Phase	Vapor	Vapor	Vapor	Vapor	Vapor
CO	0.385055	0.396742	0.399150	0.399737	0.399906
O_2	0.192528	0.198371	0.199575	0.199869	0.199953
CH_4	0.385055	0.396742	0.399150	0.399737	0.399906
CH_3COOH	0.014945	3.2583E-03	8.5053E-04	2.6300E-04	9.3845E-05
X CH_4	**0.037362**	**8.146E-03**	**2.126E-03**	**6.575E-04**	**2.346E-04**

1 atm	1800 K	1900 K	2000 K
Phase	Vapor	Vapor	Vapor
CO	0.399962	0.399983	0.399992
O_2	0.199811	0.199992	0.199996
CH_4	0.399623	0.399983	0.399992
AcOH	3.7745E-05	1.6787E-05	8.1303E-06
X CH_4	**9.436E-05**	**4.197E-05**	**2.033E-05**

Table A-84: Outlet moles and the equilibrium fractional conversion of methane for reaction (R A-3) obtained by using the Peng-Robinson equation of state in Aspen at varying temperatures and 10 atm.

10 atm	300 K	400 K	500 K	600 K	700 K
Phase	Liquid	Liquid	Vapor	Vapor	Vapor
CO	0.000000	9.1211E-14	8.4128E-08	4.8785E-06	8.6540E-05
O_2	0.000000	4.5279E-13	4.2064E-08	2.4393E-06	4.3270E-05
CH_4	0.000000	9.0228E-13	8.4128E-08	4.8785E-06	8.6540E-05
CH_3COOH	0.400000	0.400000	0.400000	0.399995	0.399914
X CH_4	**1.000000**	**1.000000**	**1.000000**	**0.999988**	**0.999784**

10 atm	800 K	900 K	1000 K	1100 K	1200 K
Phase	Vapor	Vapor	Vapor	Vapor	Vapor
CO	7.3685E-04	0.003864	0.014546	0.043454	0.108602
O_2	3.6843E-04	1.9321E-03	0.007273	0.021727	0.054301
CH_4	7.3685E-04	0.003864	0.014546	0.043454	0.108602
CH_3COOH	0.399263	0.396136	0.385454	0.356547	0.291399
X CH_4	**0.998158**	**0.990340**	**0.963636**	**0.891366**	**0.728496**

10 atm	1300 K	1400 K	1500 K	1600 K	1700 K
Phase	Vapor	Vapor	Vapor	Vapor	Vapor
CO	0.219561	0.325486	0.375616	0.391944	0.397067
O_2	0.109780	0.162743	0.187808	0.195972	0.198534
CH_4	0.219561	0.325486	0.375616	0.391944	0.397067
CH_3COOH	0.180439	0.074514	0.024385	8.0563E-03	2.9330E-03
X CH_4	**0.451098**	**0.186285**	**0.060961**	**0.020141**	**7.333E-03**

10 atm	1800 K	1900 K	2000 K
Phase	Vapor	Vapor	Vapor
CO	0.398812	0.399470	0.399743
O_2	0.199406	0.199735	0.199872
CH_4	0.398812	0.399470	0.399743
CH_3COOH	1.1877E-03	5.2957E-04	2.5675E-04
X CH_4	**2.969E-03**	**1.324E-03**	**6.419E-04**

Table A-85: Outlet moles and the equilibrium fractional conversion of methane for reaction (R A-3) obtained by using the Peng-Robinson equation of state in Aspen at varying temperatures and 25 atm.

25 atm	300 K	400 K	500 K	600 K	700 K
Phase	Liquid	Liquid	Liquid	Vapor	Vapor
CO	0.000000	8.8942E-13	1.3115E-09	2.4238E-06	4.6081E-05
O_2	0.000000	4.5231E-13	6.5577E-10	1.2119E-06	2.3041E-05
CH_4	0.000000	9.0227E-13	1.3115E-09	2.4238E-06	4.6081E-05
CH_3COOH	0.400000	0.400000	0.400000	0.399998	0.399954
X CH_4	**1.000000**	**1.000000**	**1.000000**	**0.999994**	**0.999885**

25 atm	800 K	900 K	1000 K	1100 K	1200 K
Phase	Vapor	Vapor	Vapor	Vapor	Vapor
CO	4.048600E-04	0.002157	0.008167	0.024334	0.060932
O_2	2.024300E-04	1.078570E-03	0.004084	0.012167	0.030466
CH_4	4.048600E-04	0.002157	0.008167	0.024334	0.060932
CH_3COOH	0.399595	0.397843	0.391833	0.375666	0.339068
X CH_4	**0.998988**	**0.994607**	**0.979582**	**0.939165**	**0.847670**

25 atm	1300 K	1400 K	1500 K	1600 K	1700 K
Phase	Vapor	Vapor	Vapor	Vapor	Vapor
CO	0.131328	0.233805	0.324321	0.370885	0.388798
O_2	0.065664	0.116902	0.162160	0.185442	0.194399
CH_4	0.131328	0.233805	0.324321	0.370885	0.388798
CH_3COOH	0.268672	0.166196	0.075679	0.029115	0.011202
X CH_4	**0.671680**	**0.415489**	**0.189198**	**0.072788**	**0.028006**

25 atm	1800 K	1900 K	2000 K
Phase	Vapor	Vapor	Vapor
CO	0.395373	0.397921	0.398989
O_2	0.197686	0.198961	0.199494
CH_4	0.395373	0.397921	0.398989
CH_3COOH	4.6272E-03	2.0790E-03	1.0112E-03
X CH_4	**0.011568**	**5.198E-03**	**2.528E-03**

Table A-86: Outlet moles and the equilibrium fractional conversion of methane for reaction (R A-3) obtained by using the Peng-Robinson equation of state in Aspen at varying temperatures and 50 atm.

50 atm	300 K	400 K	500 K	600 K	700 K
Phase	Liquid	Liquid	Liquid	Vapor	Vapor
CO	0.000000	8.8428E-13	1.2530E-09	1.0759E-06	2.6214E-05
O_2	0.000000	4.3692E-13	6.2649E-10	5.3793E-07	1.3107E-05
CH_4	0.000000	8.8574E-13	1.2130E-09	1.0759E-06	2.6214E-05
CH_3COOH	0.400000	0.400000	0.400000	0.399999	0.399974
X CH_4	**1.000000**	**1.000000**	**1.000000**	**0.999997**	**0.999935**

50 atm	800 K	900 K	1000 K	1100 K	1200 K
Phase	Vapor	Vapor	Vapor	Vapor	Vapor
CO	2.4599E-04	0.001351	0.005197	0.015575	0.039028
O_2	1.2300E-04	6.7571E-04	0.002598	0.007788	0.019514
CH_4	2.4599E-04	0.001351	0.005196	0.015575	0.039028
CH_3COOH	0.399754	0.398649	0.394804	0.384425	0.360972
X CH_4	**0.999385**	**0.996622**	**0.987009**	**0.961062**	**0.902430**

50 atm	1300 K	1400 K	1500 K	1600 K	1700 K
Phase	Vapor	Vapor	Vapor	Vapor	Vapor
CO	0.085125	0.161802	0.256625	0.331547	0.370691
O_2	0.042563	0.080901	0.128312	0.165773	0.185345
CH_4	0.085125	0.161802	0.256625	0.331547	0.370691
CH_3COOH	0.314875	0.238199	0.143375	0.068453	0.029309
X CH_4	**0.787187**	**0.595496**	**0.358438**	**0.171133**	**0.073273**

50 atm	1800 K	1900 K	2000 K
Phase	Vapor	Vapor	Vapor
CO	0.387349	0.394213	0.397164
O_2	0.193675	0.197107	0.198582
CH_4	0.387349	0.394213	0.397164
CH_3COOH	0.012651	5.7867E-03	2.8362E-03
X CH_4	**0.031627**	**0.014467**	**7.090E-03**

Table A-87: Outlet moles and the equilibrium fractional conversion of methane for reaction (R A-3) obtained by using the Peng-Robinson equation of state in Aspen at varying temperatures and 100 atm.

100 atm	300 K	400 K	500 K	600 K	700 K
Phase	Liquid	Liquid	Liquid	Vapor	Vapor
CO	0.000000	8.6262E-13	1.1599E-09	2.0778E-07	1.2328E-05
O_2	0.000000	4.2476E-13	5.7994E-10	1.0389E-07	6.1641E-06
CH_4	0.000000	8.5170E-13	1.5989E-09	2.0778E-07	1.2328E-05
CH_3COOH	0.400000	0.400000	0.400000	0.400000	0.399988
X CH_4	**1.000000**	**1.000000**	**1.000000**	**1.000000**	**0.999969**

100 atm	800 K	900 K	1000 K	1100 K	1200 K
Phase	Vapor	Vapor	Vapor	Vapor	Vapor
CO	1.3819E-04	0.000811	0.003221	0.009816	0.024774
O_2	6.9094E-05	4.0533E-04	0.001610	0.004908	0.012387
CH_4	1.381870E-04	0.000811	0.003221	0.009816	0.024774
CH_3COOH	0.399862	0.399189	0.396779	0.390184	0.375227
X CH_4	**0.999655**	**0.997973**	**0.991948**	**0.975460**	**0.938066**

100 atm	1300 K	1400 K	1500 K	1600 K	1700 K
Phase	Vapor	Vapor	Vapor	Vapor	Vapor
CO	0.054336	0.105946	0.181980	0.266497	0.331207
O_2	0.027168	0.052973	0.090990	0.133249	0.165604
CH_4	0.054339	0.105946	0.181980	0.266497	0.331207
CH_3COOH	0.345665	0.294055	0.218020	0.133503	0.068793
X CH_4	**0.864161**	**0.735136**	**0.545050**	**0.333757**	**0.171982**

100 atm	1800 K	1900 K	2000 K
Phase	Vapor	Vapor	Vapor
CO	0.367238	0.384320	0.392156
O_2	0.183619	0.192160	0.196078
CH_4	0.367238	0.384320	0.392156
CH_3COOH	0.032762	0.015680	7.8439E-03
X CH_4	**0.081905**	**0.039199**	**0.019610**

Table A-88: Outlet moles and the equilibrium fractional conversion of methane for reaction (R A-3) obtained by using the Peng-Robinson equation of state in Aspen at varying temperatures and 150 atm.

150 atm	300 K	400 K	500 K	600 K	700 K
Phase	Liquid	Liquid	Liquid	Liquid	Liquid
CO	0.000000	8.2862E-13	1.0878E-09	1.6243E-07	7.3315E-06
O_2	0.000000	4.1643E-13	5.4391E-10	8.1215E-08	3.6657E-06
CH_4	0.000000	8.3290E-13	1.0878E-09	1.6243E-07	7.3315E-06
CH_3COOH	0.400000	0.400000	0.400000	0.400000	0.399993
X CH_4	**1.000000**	**1.000000**	**1.000000**	**1.000000**	**0.999982**

150 atm	800 K	900 K	1000 K	1100 K	1200 K
Phase	Vapor	Vapor	Vapor	Vapor	Vapor
CO	9.4252E-05	0.000586	0.002395	0.007415	0.018869
O_2	4.7126E-05	2.9285E-04	0.001198	0.003708	0.009434
CH_4	9.4252E-05	0.000586	0.002395	0.007415	0.018869
CH_3COOH	0.399906	0.399414	0.397605	0.392585	0.381131
X CH_4	**0.999764**	**0.998536**	**0.994013**	**0.981462**	**0.952828**

150 atm	1300 K	1400 K	1500 K	1600 K	1700 K
Phase	Vapor	Vapor	Vapor	Vapor	Vapor
CO	0.041565	0.081639	0.143694	0.222157	0.295684
O_2	0.027826	0.040819	0.071847	0.111078	0.147842
CH_4	0.041565	0.081639	0.143694	0.222157	0.295684
CH_3COOH	0.358435	0.318361	0.256306	0.177843	0.104316
X CH_4	**0.896087**	**0.795904**	**0.640766**	**0.444608**	**0.260789**

150 atm	1800 K	1900 K	2000 K
Phase	Vapor	Vapor	Vapor
CO	0.345604	0.372651	0.385982
O_2	0.172802	0.186325	0.192991
CH_4	0.345604	0.372651	0.285982
CH_3COOH	0.054396	0.027349	0.014048
X CH_4	**0.135991**	**0.068373**	**0.035120**

Table A-89: Outlet moles and the equilibrium fractional conversion of methane for reaction (R A-3) obtained by using the Peng-Robinson equation of state in Aspen at varying temperatures and 200 atm.

200 atm	300 K	400 K	500 K	600 K	700 K
Phase	Liquid	Liquid	Liquid	Liquid	Liquid
CO	0.000000	8.1181E-13	1.0295E-09	1.4040E-07	5.3676E-06
O_2	0.000000	4.0423E-13	5.1475E-10	7.0199E-08	2.6838E-06
CH_4	0.000000	8.0623E-13	1.0295E-09	1.4040E-07	5.3676E-06
CH_3COOH	0.400000	0.400000	0.400000	0.400000	0.399995
X CH_4	**1.000000**	**1.000000**	**1.000000**	**1.000000**	**0.999987**

200 atm	800 K	900 K	1000 K	1100 K	1200 K
Phase	Liquid	Vapor	Vapor	Vapor	Vapor
CO	7.1339E-05	0.000461	0.001928	0.006048	0.015504
O_2	3.5670E-05	2.3048E-04	0.000964	0.003024	0.007752
CH_4	7.1339E-05	0.000461	0.001928	0.006048	0.015504
CH_3COOH	0.399929	0.399539	0.398072	0.393952	0.384496
X CH_4	**0.999822**	**0.998848**	**0.995180**	**0.984880**	**0.961240**

200 atm	1300 K	1400 K	1500 K	1600 K	1700 K
Phase	Vapor	Vapor	Vapor	Vapor	Vapor
CO	0.034290	0.067618	0.120340	0.191311	0.266108
O_2	0.017145	0.033809	0.061701	0.095655	0.133054
CH_4	0.034290	0.067618	0.120340	0.191311	0.266108
CH_3COOH	0.365710	0.332382	0.279660	0.208689	0.133892
X CH_4	**0.914276**	**0.830955**	**0.699149**	**0.521723**	**0.334730**

200 atm	1800 K	1900 K	2000 K
Phase	Vapor	Vapor	Vapor
CO	0.324630	0.360230	0.379079
O_2	0.162316	0.180115	0.189540
CH_4	0.324630	0.360230	0.379079
CH_3COOH	0.075370	0.039770	0.020921
X CH_4	**0.188426**	**0.099424**	**0.052302**

Table A-90: Equilibrium fractional conversion of methane for reaction (R A-3) obtained by using the Peng-Robinson equation of state in Aspen at varying temperatures and 1 - 50 atm.

T (K)	1 atm	10 atm	25 atm	50 atm
300 K	**1.00000**	**1.00000**	**1.00000**	**1.00000**
400 K	1.00000	**1.00000**	**1.00000**	**1.00000**
500 K	1.00000	1.00000	**1.00000**	**1.00000**
600 K	0.99995	0.99999	0.99999	1.00000
700 K	0.99910	0.99978	0.99988	0.99993
800 K	0.99243	0.99816	0.99899	0.99939
900 K	0.96028	0.99034	0.99461	0.99662
1000 K	0.84749	0.96364	0.97958	0.98701
1100 K	0.55302	0.89137	0.93916	0.96106
1200 K	0.18129	0.72850	0.84767	0.90243
1300 K	0.03736	0.45110	0.67168	0.78719
1400 K	8.146E-03	0.18629	0.41549	0.59550
1500 K	2.126E-03	0.06096	0.18920	0.35844
1600 K	6.575E-04	0.02014	0.07279	0.17113
1700 K	2.346E-04	7.333E-03	0.02801	0.07327
1800 K	9.436E-05	2.969E-03	0.01157	0.03163
1900 K	4.197E-05	1.324E-03	5.198E-03	0.01447
2000 K	2.033E-05	6.419E-04	2.528E-03	7.090E-03

NOTE: Values in bold indicate liquid phase.

Table A-91: Equilibrium fractional conversion of methane for reaction (R A-3) obtained by using the Peng-Robinson equation of state in Aspen at varying temperatures and 100 - 200 atm.

T (K)	100 atm	150 atm	200 atm
300 K	**1.00000**	**1.00000**	**1.00000**
400 K	**1.00000**	**1.00000**	**1.00000**
500 K	**1.00000**	**1.00000**	**1.00000**
600 K	**1.00000**	**1.00000**	**1.00000**
700 K	0.99997	**0.99998**	**0.99999**
800 K	0.99965	0.99976	**0.99982**
900 K	0.99797	0.99854	0.99885
1000 K	0.99195	0.99401	0.99518
1100 K	0.97546	0.98146	0.98488
1200 K	0.93807	0.95283	0.96124
1300 K	0.86416	0.89609	0.91428
1400 K	0.73514	0.79590	0.83096
1500 K	0.54505	0.64077	0.69915
1600 K	0.33376	0.44461	0.52172
1700 K	0.17198	0.26079	0.33473
1800 K	0.08190	0.13599	0.18843
1900 K	0.03920	0.06837	0.09942
2000 K	0.01961	0.03512	0.05230

NOTE: Values in bold indicate liquid phase.

A.5. ASPEN DATA FOR PROPIONIC ACID

Equilibrium thermodynamic calculations were performed on the synthesis of acetic acid from carbon monoxide, oxygen and methane:

$$CO_2 + C_2H_6 \leftrightarrow C_2H_5COOH \qquad \text{(R A-4)}$$

The calculations were performed using the AspenPlus™ engineering simulation software. The RGIBBS reactor model was used to perform a Gibbs free energy minimization on the system to give the chemical and phase equilibrium composition at various temperatures and pressures. These calculations do not take into account any surface interactions. Molecular interactions between molecules are taken into account in the equation of state. The inlet composition, inlet temperature, inlet pressure, reactor temperature and reactor pressure were specified for each reaction. The inlet conditions were set equal to the reactor conditions.

For the Aspen calculations, an inlet mole fraction of 0.95 CO_2 and 0.05 CH_4, and an inlet total number of moles of 1 was used. The Aspen calculations were performed for a wide range of pressures and temperatures, 1 - 200 atm and 300 – 2000 K. The calculations were performed using the Peng-Robinson equation of state.

The equilibrium fractional conversion of methane (X_{CH4}) was calculated using equation EA29. Since the outlet moles of methane given by Aspen did not have enough significant figures, the number of outlet moles of acetic acid was used as the number of moles of methane that reacted.

Table A-92: Outlet moles and the equilibrium fractional conversion of methane for reaction (R A-4) obtained by using the Peng-Robinson equation of state in Aspen at varying temperatures and 1 atm.

1 atm	300 K	400 K	500 K	600 K	700 K
Phase	Vapor	Vapor	Vapor	Vapor	Vapor
CO_2	0.9500000	0.9500000	0.9500000	0.9500000	0.9500000
C_2H_6	0.0500000	0.0500000	0.0500000	0.0500000	0.0500000
C_2H_5COOH	1.8724E-12	2.0232E-11	8.6353E-11	2.3347E-10	4.8657E-10
X C_2H_6	**3.745E-11**	**4.046E-10**	**1.727E-09**	**4.669E-09**	**9.731E-09**

1 atm	800 K	900 K	1000 K	1100 K	1200 K
Phase	Vapor	Vapor	Vapor	Vapor	Vapor
CO_2	0.9500000	0.9500000	0.9500000	0.9500000	0.9500000
C_2H_6	0.0500000	0.0500000	0.0500000	0.0500000	0.0500000
C_2H_5COOH	8.6025E-10	1.3605E-09	1.9856E-09	2.7315E-09	3.5909E-09
X C_2H_6	**1.721E-08**	**2.721E-08**	**3.971E-08**	**5.463E-08**	**7.182E-08**

1 atm	1300 K	1400 K	1500 K	1600 K	1700K
Phase	Vapor	Vapor	Vapor	Vapor	Vapor
CO_2	0.9500000	0.9500000	0.9500000	0.9500000	0.9500000
C_2H_6	0.0500000	0.0500000	0.0499999	0.0499999	0.0499999
C_2H_5COOH	4.5554E-09	5.6167E-09	6.7666E-09	7.9974E-09	9.3019E-09
X C_2H_6	**9.111E-08**	**1.123E-07**	**1.353E-07**	**1.599E-07**	**1.860E-07**

1 atm	1800 K	1900 K	2000 K
Phase	Vapor	Vapor	Vapor
CO_2	0.9500000	0.9500000	0.9500000
C_2H_6	0.0499999	0.0499999	0.0499999
C_2H_5COOH	1.0674E-08	1.2107E-08	1.3597E-08
X C_2H_6	**2.135E-07**	**2.421E-07**	**2.719E-07**

Table A-93: Outlet moles and the equilibrium fractional conversion of methane for reaction (R A-4) obtained by using the Peng-Robinson equation of state in Aspen at varying temperatures and 10 atm.

10 atm	300 K	400 K	500 K	600 K	700 K
Phase	Vapor	Vapor	Vapor	Vapor	Vapor
CO_2	0.9500000	0.9500000	0.9500000	0.9500000	0.9500000
C_2H_6	0.0500000	0.0500000	0.0500000	0.0500000	0.0500000
C_2H_5COOH	2.3190E-11	2.2157E-10	9.0319E-10	2.3912E-09	4.9303E-09
X C_2H_6	**4.638E-10**	**4.431E-09**	**1.806E-08**	**4.782E-08**	**9.861E-08**

10 atm	800 K	900 K	1000 K	1100 K	1200 K
Phase	Vapor	Vapor	Vapor	Vapor	Vapor
CO_2	0.9500000	0.9500000	0.9500000	0.9500000	0.9500000
C_2H_6	0.0499999	0.0499999	0.0499999	0.0499999	0.0499999
C_2H_5COOH	8.6653E-09	1.3654E-08	1.9892E-08	2.7331E-08	3.5903E-08
X C_2H_6	**1.733E-07**	**2.731E-07**	**3.978E-07**	**5.466E-07**	**7.181E-07**

10 atm	1300 K	1400 K	1500 K	1600 K	1700 K
Phase	Vapor	Vapor	Vapor	Vapor	Vapor
CO_2	0.9500000	0.9499999	0.9499999	0.9499999	0.9499999
C_2H_6	0.0499999	0.0499999	0.0499999	0.0499999	0.0499999
C_2H_5COOH	4.5526E-08	5.6118E-08	6.7597E-08	7.9888E-08	9.2919E-08
X C_2H_6	**9.105E-07**	**1.122E-06**	**1.352E-06**	**1.598E-06**	**1.858E-06**

10 atm	1800 K	1900 K	2000 K
Phase	Vapor	Vapor	Vapor
CO_2	0.9499999	0.9499999	0.9499999
C_2H_6	0.0499999	0.0499998	0.0499998
C_2H_5COOH	1.0663E-07	1.2095E-07	1.3584E-07
X C_2H_6	**2.133E-06**	**2.419E-06**	**2.717E-06**

Table A-94: Outlet moles and the equilibrium fractional conversion of methane for reaction (R A-4) obtained by using the Peng-Robinson equation of state in Aspen at varying temperatures and 25 atm.

25 atm	300 K	400 K	500 K	600 K	700 K
Phase	Vapor	Vapor	Vapor	Vapor	Vapor
CO_2	0.9500000	0.9500000	0.9500000	0.9500000	0.9500000
C_2H_6	0.0500000	0.0500000	0.0500000	0.0499999	0.0499999
C_2H_5COOH	8.7014E-11	6.4673E-10	2.4321E-09	6.2167E-09	1.2593E-08
X C_2H_6	**1.740E-09**	**1.293E-08**	**4.864E-08**	**1.243E-07**	**2.519E-07**

25 atm	800 K	900 K	1000 K	1100 K	1200 K
Phase	Vapor	Vapor	Vapor	Vapor	Vapor
CO_2	0.9500000	0.9500000	0.9500000	0.9499999	0.9499999
C_2H_6	0.0499999	0.0499999	0.0499999	0.0499999	0.0499999
C_2H_5COOH	2.1920E-08	3.4349E-08	4.9874E-08	6.8389E-08	8.9727E-08
X C_2H_6	**4.384E-07**	**6.870E-07**	**9.975E-07**	**1.368E-06**	**1.795E-06**

25 atm	1300 K	1400 K	1500 K	1600 K	1700 K
Phase	Vapor	Vapor	Vapor	Vapor	Vapor
CO_2	0.9499999	0.9499999	0.9499998	0.9499998	0.9499998
C_2H_6	0.0499998	0.0499998	0.0499998	0.0499998	0.0499997
C_2H_5COOH	1.1369E-07	1.4009E-07	1.6871E-07	1.9936E-07	2.3188E-07
X C_2H_6	**2.274E-06**	**2.802E-06**	**3.374E-06**	**3.987E-06**	**4.638E-06**

25 atm	1800 K	1900 K	2000 K
Phase	Vapor	Vapor	Vapor
CO_2	0.9499997	0.9499997	0.9499997
C_2H_6	0.0499997	0.0499997	0.0499996
C_2H_5COOH	2.6610E-07	3.0188E-07	3.3908E-07
X C_2H_6	**5.322E-06**	**6.038E-06**	**6.782E-06**

Table A-95: Outlet moles and the equilibrium fractional conversion of methane for reaction (R A-4) obtained by using the Peng-Robinson equation of state in Aspen at varying temperatures and 50 atm.

50 atm	300 K	400 K	500 K	600 K	700 K
Phase	Vapor	Vapor	Vapor	Vapor	Vapor
CO_2	0.9500000	0.9500000	0.9500000	0.9500000	0.9500000
C_2H_6	0.0500000	0.0500000	0.0499999	0.0499999	0.0499999
C_2H_5COOH	4.4457E-10	1.6897E-09	5.4944E-09	1.3243E-08	2.6066E-08
X C_2H_6	**8.891E-09**	**3.379E-08**	**1.099E-07**	**2.649E-07**	**5.213E-07**

50 atm	800 K	900 K	1000 K	1100 K	1200 K
Phase	Vapor	Vapor	Vapor	Vapor	Vapor
CO_2	0.9500000	0.9499999	0.9499999	0.9499999	0.9499998
C_2H_6	0.0499999	0.0499999	0.0499999	0.0499998	0.0499998
C_2H_5COOH	4.4671E-08	6.9377E-08	1.0020E-07	1.3696E-07	1.7933E-07
X C_2H_6	**8.934E-07**	**1.388E-06**	**2.004E-06**	**2.739E-06**	**3.587E-06**

50 atm	1300 K	1400 K	1500 K	1600 K	1700 K
Phase	Vapor	Vapor	Vapor	Vapor	Vapor
CO_2	0.9499998	0.9499997	0.9499997	0.9499996	0.9499995
C_2H_6	0.0499997	0.0499997	0.0499996	0.0499996	0.0499995
C_2H_5COOH	2.2697E-07	2.7947E-07	3.3645E-07	3.9753E-07	4.6237E-07
X C_2H_6	**4.539E-06**	**5.589E-06**	**6.729E-06**	**7.951E-06**	**9.247E-06**

50 atm	1800 K	1900 K	2000 K
Phase	Vapor	Vapor	Vapor
CO_2	0.9499995	0.9499994	0.9499993
C_2H_6	0.0499994	0.0499994	0.0499993
C_2H_5COOH	5.3066E-07	6.0209E-07	6.7641E-07
X C_2H_6	**1.061E-05**	**1.204E-05**	**1.353E-05**

Table A-96: Outlet moles and the equilibrium fractional conversion of methane for reaction (R A-4) obtained by using the Peng-Robinson equation of state in Aspen at varying temperatures and 100 atm.

100 atm	300 K	400 K	500 K	600 K	700 K
Phase	Liquid	Vapor	Vapor	Vapor	Vapor
CO_2	0.9499999	0.9500000	0.9500000	0.9500000	0.9499999
C_2H_6	0.0499999	0.0499999	0.0499999	0.0499999	0.0499999
C_2H_5COOH	9.1171E-08	5.9346E-09	1.3872E-08	2.9793E-08	5.5538E-08
X C_2H_6	**1.823E-06**	**1.187E-07**	**2.774E-07**	**5.959E-07**	**1.111E-06**

100 atm	800 K	900 K	1000 K	1100 K	1200 K
Phase	Vapor	Vapor	Vapor	Vapor	Vapor
CO_2	0.9499999	0.9499999	0.9499998	0.9499997	0.9499996
C_2H_6	0.0499999	0.0499998	0.0499998	0.0499997	0.0499996
C_2H_5COOH	9.2462E-08	1.4124E-07	2.0199E-07	2.7444E-07	3.5806E-07
X C_2H_6	**1.849E-06**	**2.825E-06**	**4.040E-06**	**5.489E-06**	**7.161E-06**

100 atm	1300 K	1400 K	1500 K	1600 K	1700 K
Phase	Vapor	Vapor	Vapor	Vapor	Vapor
CO_2	0.9499995	0.9499994	0.9499993	0.9499992	0.9499991
C_2H_6	0.0499995	0.0499994	0.0499993	0.0499992	0.0499990
C_2H_5COOH	4.5218E-07	5.5608E-07	6.6903E-07	7.9030E-07	9.1922E-07
X C_2H_6	**9.044E-06**	**1.112E-05**	**1.338E-05**	**1.581E-05**	**1.838E-05**

100 atm	1800 K	1900 K	2000 K
Phase	Vapor	Vapor	Vapor
CO_2	0.9499989	0.9499988	0.9499987
C_2H_6	0.0499989	0.0499988	0.0499986
C_2H_5COOH	1.0552E-06	1.1976E-06	1.3459E-06
X C_2H_6	**2.110E-05**	**2.395E-05**	**2.692E-05**

Table A-97: Outlet moles and the equilibrium fractional conversion of methane for reaction (R A-4) obtained by using the Peng-Robinson equation of state in Aspen at varying temperatures and 150 atm.

150 atm	300 K	400 K	500 K	600 K	700 K
Phase	Liquid	Vapor	Vapor	Vapor	Vapor
CO_2	0.9499998	0.9500000	0.9500000	0.9500000	0.9499999
C_2H_6	0.0499998	0.0499999	0.0499999	0.0499999	0.0499999
C_2H_5COOH	1.6824E-07	1.5252E-08	2.5756E-08	4.9680E-08	8.8149E-08
X C_2H_6	**3.365E-06**	**3.050E-07**	**5.151E-07**	**9.936E-07**	**1.763E-06**

150 atm	800 K	900 K	1000 K	1100 K	1200 K
Phase	Vapor	Vapor	Vapor	Vapor	Vapor
CO_2	0.9499999	0.9499998	0.9499997	0.9499996	0.9499995
C_2H_6	0.0499998	0.0499997	0.0499996	0.0499995	0.0499994
EA	1.4297E-07	2.1515E-07	3.0498E-07	4.1213E-07	5.3594E-07
X C_2H_6	**2.859E-06**	**4.303E-06**	**6.100E-06**	**8.243E-06**	**1.072E-05**

150 atm	1300 K	1400 K	1500 K	1600 K	1700 K
Phase	Vapor	Vapor	Vapor	Vapor	Vapor
CO_2	0.9499993	0.9499992	0.9499990	0.9499988	0.9499986
C_2H_6	0.0499993	0.0499992	0.0499990	0.0499988	0.0499986
C_2H_5COOH	6.7548E-07	8.2976E-07	9.9771E-07	1.1783E-06	1.3706E-06
X C_2H_6	**1.351E-05**	**1.660E-05**	**1.995E-05**	**2.357E-05**	**2.741E-05**

150 atm	1800 K	1900 K	2000 K
Phase	Vapor	Vapor	Vapor
CO_2	0.9499984	0.9499982	0.9499980
C_2H_6	0.0499984	0.0499982	0.0499979
C_2H_5COOH	1.5736E-06	1.7864E-06	2.0084E-06
X C_2H_6	**3.147E-05**	**3.573E-05**	**4.017E-05**

Table A-98: Outlet moles and the equilibrium fractional conversion of methane for reaction (R A-4) obtained by using the Peng-Robinson equation of state in Aspen at varying temperatures and 200 atm.

200 atm	300 K	400 K	500 K	600 K	700 K
Phase	Liquid	Vapor	Vapor	Vapor	Vapor
CO_2	0.9499998	0.9500000	0.9500000	0.9499999	0.9499999
C_2H_6	0.0499997	0.0499999	0.0499999	0.0499999	0.0499998
C_2H_5COOH	2.3643E-07	3.2217E-08	4.1491E-08	7.2776E-08	1.2357E-07
X C_2H_6	**4.729E-06**	**6.443E-07**	**8.298E-07**	**1.456E-06**	**2.471E-06**

200 atm	800 K	900 K	1000 K	1100 K	1200 K
Phase	Vapor	Vapor	Vapor	Vapor	Vapor
CO_2	0.9499998	0.9499997	0.9499996	0.9499994	0.9499993
C_2H_6	0.0499998	0.0499997	0.0499995	0.0499994	0.0499992
C_2H_5COOH	1.9578E-07	2.9072E-07	4.0880E-07	5.4974E-07	7.1275E-07
X C_2H_6	**3.916E-06**	**5.814E-06**	**8.176E-06**	**1.099E-05**	**1.425E-05**

200 atm	1300 K	1400 K	1500 K	1600 K	1700 K
Phase	Vapor	Vapor	Vapor	Vapor	Vapor
CO_2	0.9499991	0.9499989	0.9499987	0.9499984	0.9499982
C_2H_6	0.0499991	0.0499989	0.0499986	0.0499984	0.0499981
C_2H_5COOH	8.9673E-07	1.1004E-06	1.3225E-06	1.5616E-06	1.8165E-06
X C_2H_6	**1.793E-05**	**2.201E-05**	**2.645E-05**	**3.123E-05**	**3.633E-05**

200 atm	1800 K	1900 K	2000 K
Phase	Vapor	Vapor	Vapor
CO_2	0.9499979	0.9499976	0.9499973
C_2H_6	0.0499979	0.0499976	0.0499973
C_2H_5COOH	2.0859E-06	2.3688E-06	2.6640E-06
X C_2H_6	**4.172E-05**	**4.738E-05**	**5.328E-05**

Table A-99: Equilibrium fractional conversion of methane for reaction (R A-4) obtained by using the Peng-Robinson equation of state in Aspen at varying temperatures and 1 - 50 atm.

T (K)	1 atm	10 atm	25 atm	50 atm
300 K	3.745E-11	4.638E-10	1.740E-09	8.891E-09
400 K	4.046E-10	4.431E-09	1.293E-08	3.379E-08
500 K	1.727E-09	1.806E-08	4.864E-08	1.099E-07
600 K	4.669E-09	4.782E-08	1.243E-07	2.649E-07
700 K	9.731E-09	9.861E-08	2.519E-07	5.213E-07
800 K	1.721E-08	1.733E-07	4.384E-07	8.934E-07
900 K	2.721E-08	2.731E-07	6.870E-07	1.388E-06
1000 K	3.971E-08	3.978E-07	9.975E-07	2.004E-06
1100 K	5.463E-08	5.466E-07	1.368E-06	2.739E-06
1200 K	7.182E-08	7.181E-07	1.795E-06	3.587E-06
1300 K	9.111E-08	9.105E-07	2.274E-06	4.539E-06
1400 K	1.123E-07	1.122E-06	2.802E-06	5.589E-06
1500 K	1.353E-07	1.352E-06	3.374E-06	6.729E-06
1600 K	1.599E-07	1.598E-06	3.987E-06	7.951E-06
1700 K	1.860E-07	1.858E-06	4.638E-06	9.247E-06
1800 K	2.135E-07	2.133E-06	5.322E-06	1.061E-05
1900 K	2.421E-07	2.419E-06	6.038E-06	1.204E-05
2000 K	2.719E-07	2.717E-06	6.782E-06	1.353E-05

NOTE: Values in bold indicate liquid phase.

Table A-100: Equilibrium fractional conversion of methane for reaction (R A-4) obtained by using the Peng-Robinson equation of state in Aspen at varying temperatures and 100 - 200 atm.

T (K)	100 atm	150 atm	200 atm
300 K	**1.823E-06**	**3.365E-06**	**4.729E-06**
400 K	1.187E-07	**3.050E-07**	**6.443E-07**
500 K	2.774E-07	5.151E-07	**8.298E-07**
600 K	5.959E-07	9.936E-07	1.456E-06
700 K	1.111E-06	1.763E-06	2.471E-06
800 K	1.849E-06	2.859E-06	3.916E-06
900 K	2.825E-06	4.303E-06	5.814E-06
1000 K	4.040E-06	6.100E-06	8.176E-06
1100 K	5.489E-06	8.243E-06	1.099E-05
1200 K	7.161E-06	1.072E-05	1.425E-05
1300 K	9.044E-06	1.351E-05	1.793E-05
1400 K	1.112E-05	1.660E-05	2.201E-05
1500 K	1.338E-05	1.995E-05	2.645E-05
1600 K	1.581E-05	2.357E-05	3.123E-05
1700 K	1.838E-05	2.741E-05	3.633E-05
1800 K	2.110E-05	3.147E-05	4.172E-05
1900 K	2.395E-05	3.573E-05	4.738E-05
2000 K	2.692E-05	4.017E-05	5.328E-05

NOTE: Values in bold indicate liquid phase.

A.6. REFERENCES

1. Chemical.Rubber.Company, *CRC Handbook of Chemistry and Physics*. 83 ed. 2002, Cleveland: Chemical Rubber Company Press.

APPENDIX B:

OVERCOMING THERMODYNAMICS

B.1. METHYL ACETATE

Equilibrium thermodynamic calculations were performed for the formation of methyl-acetate (CH_3COOCH_3) from carbon dioxide, methane, and methanol (CH_3OH):

$$CO_2 + CH_4 + CH_3OH \leftrightarrow CH_3COOCH_3 + H_2O \quad \text{(R B-1)}$$

Acetic acid was allowed in the system, thus permitting the following reactions:

$$CO_2 + CH_4 \leftrightarrow CH_3COOH \quad \text{(R B-2)}$$

$$CH_3OH + CH_3COOH \leftrightarrow CH_3COOCH_3 + H_2O \quad \text{(R B-3)}$$

The side reaction of methanol decomposition:

$$4\ CH_3OH \leftrightarrow CO_2 + 3\ CH_4 + 2\ H_2O \quad \text{(R B-4)}$$

was restricted by setting the extent of that reaction to zero.

The equilibrium thermodynamic calculations for reaction (R B-1) were performed using the AspenPlus™ engineering simulation software. The RGIBBS reactor model was used to perform a Gibbs free energy minimization on the system to give the chemical and phase equilibrium composition at various temperatures and pressures. These calculations do not take into account any surface interactions. Molecular interactions are taken into account by the equation of state. The inlet composition, inlet temperature, inlet pressure, reactor temperature and reactor pressure were specified for each reaction. The inlet conditions were set equal to the reactor conditions.

A stoichiometric inlet composition of 0.333 mole fraction of CO_2, 0.333 mole fraction of CH_4 and 0.333 mole fraction of CH_3OH was used. The AspenPlus™ calculations were performed for a wide range of temperatures and pressures, 1 - 200 atm and 300 - 2000 K. The calculations were performed using the Peng-Robinson equation of state.

Interaction parameters of 0.0919 for CO_2 and CH_4, 0.230 for CO_2 and CH_3OH, -0.0493 for CO_2 and CH_3COOCH_3, 0.1200 for CO_2 and H_2O and -0.0778 for H_2O and CH_3OH obtained from the AspenPlus™ data base were used. No other interaction parameters were available, thus a default of 0.0 was used for all other interaction parameters.

The equilibrium fractional conversion of methane (X CH_4) was calculated using:

$$X\ CH_4 = \#\ \text{Moles of } CH_4 \text{ reacted} / \#\ \text{Inlet moles of } CH_4 \qquad \text{(E B-1)}$$

When the outlet moles of methane given by AspenPlus™ did not have enough significant figures, the sum of outlet moles of acetic acid and methyl formate was used as the number of moles of methane that reacted.

The equilibrium fractional conversion of methanol (X CH_3OH) was calculated using:

$$X\ CH_3OH = \#\ \text{Moles of } CH_3OH \text{ reacted} / \#\ \text{Inlet moles of } CH_3OH \qquad \text{(E B-2)}$$

When the outlet moles of methanol given by AspenPlus™ did not have enough significant figures, the number of outlet moles of methyl formate was used as the number of moles of methanol that reacted.

The equilibrium yield of methyl acetate (Y MA) was calculated using:

$$Y\ MA = \text{Outlet } CH_3COOCH_3 \,/\, \text{Outlet } CH_3COOCH_3 + CH_3COOH \qquad \text{(E B-3)}$$

Data from these calculations can be found in tables B-1 to B-10.

Table B-1: Equilibrium outlet moles, X CH_4, X CH_3OH and Y MA for reaction (R B-1) obtained from AspenPlus™ using the Peng-Robinson equation of state and stoichiometric inlet composition from 300 – 2000 K and 1 atm.

1 atm	300 K		400 K	500 K	600 K
Phase	Liquid	Vapor	Vapor	Vapor	Vapor
CO_2	0.0006590	0.3326678	0.3333260	0.3333215	0.3333169
CH_4	0.0000631	0.3332637	0.3333260	0.3333215	0.3333169
CH_3OH	1.8948570	0.1438411	0.3333326	0.3333215	0.3333169
H_2O	5.3392E-06	1.1847E-06	7.3279E-06	1.1785E-05	1.6397E-05
CH_3COOH	8.8096E-13	7.5054E-14	1.8547E-12	1.5835E-11	6.3732E-11
CH_3COOCH_3	1.3478E-06	5.1761E-06	7.3279E-06	1.1785E-05	1.6397E-05
X CH_4	**1.9572E-05**		**2.1984E-05**	**3.5355E-05**	**4.9192E-05**
X CH_3OH	**1.9572E-05**		**2.1984E-05**	**3.5355E-05**	**4.9192E-05**
Y MA	**0.9999999**		**0.9999997**	**0.9999987**	**0.9999961**

1 atm	700 K	800 K	900 K	1000 K	1100 K
Phase	Vapor	Vapor	Vapor	Vapor	Vapor
CO_2	0.3333123	0.3333078	0.3333034	0.3332991	0.3332950
CH_4	0.3333123	0.3333078	0.3333034	0.3332991	0.3332950
CH_3OH	0.3333123	0.3333078	0.3333034	0.3332991	0.3332950
H_2O	2.1005E-05	2.5539E-05	2.9964E-05	3.4249E-05	3.8372E-05
CH_3COOH	1.7546E-10	3.8247E-10	7.1430E-10	1.1965E-09	1.8499E-09
CH_3COOCH_3	2.1005E-05	2.5539E-05	2.9964E-05	3.4249E-05	3.8372E-05
X CH_4	**6.3015E-05**	**7.6619E-05**	**8.9893E-05**	**1.0275E-04**	**1.1512E-04**
X CH_3OH	**6.3014E-05**	**7.6618E-05**	**8.9891E-05**	**1.0275E-04**	**1.1512E-04**
Y MA	**0.9999916**	**0.9999850**	**0.9999762**	**0.9999651**	**0.9999518**

Table B-1 continued

1 atm	1200 K	1300 K	1400 K	1500 K	1600 K
Phase	Vapor	Vapor	Vapor	Vapor	Vapor
CO_2	0.3332910	0.3332873	0.3328370	0.3332804	0.3332773
CH_4	0.3332910	0.3332873	0.3328370	0.3332804	0.3332773
CH_3OH	0.3332910	0.3332873	0.3328370	0.3332804	0.3332773
H_2O	4.2314E-05	4.6060E-05	4.9602E-05	5.2937E-05	5.6063E-05
CH_3COOH	2.6896E-09	3.7260E-09	4.9639E-09	6.4042E-09	8.0440E-09
CH_3COOCH_3	4.2314E-05	4.6060E-05	4.9602E-05	5.2937E-05	5.6063E-05
X CH_4	**1.2695E-04**	**1.3819E-04**	**1.4882E-04**	**1.5883E-04**	**1.6821E-04**
X CH_3OH	**1.2694E-04**	**1.3818E-04**	**1.4881E-04**	**1.5881E-04**	**1.6819E-04**
Y MA	**0.9999364**	**0.9999191**	**0.9998999**	**0.9998790**	**0.9998565**

1 atm	1700 K	1800 K	1900 K	2000 K
Phase	Vapor	Vapor	Vapor	Vapor
CO_2	0.3332743	0.3332716	0.3332691	0.3332667
CH_4	0.3332743	0.3332716	0.3332691	0.3332667
CH_3OH	0.3332743	0.3332716	0.3332691	0.3332667
H_2O	5.8985E-05	6.1708E-05	6.4239E-05	6.6587E-05
CH_3COOH	9.8772E-09	1.1896E-08	1.4089E-08	1.6447E-08
CH_3COOCH_3	5.8985E-05	6.1708E-05	6.4239E-05	6.6587E-05
X CH_4	**1.7698E-04**	**1.8516E-04**	**1.9276E-04**	**1.9981E-04**
X CH_3OH	**1.7696E-04**	**1.8512E-04**	**1.9272E-04**	**1.9976E-04**
Y MA	**0.9998326**	**0.9998073**	**0.9997807**	**0.9997531**

Table B-2: Equilibrium outlet moles, X CH_4, X CH_3OH and Y MA for reaction (R B-1) obtained from AspenPlus™ using the Peng-Robinson equation of state and stoichiometric inlet composition from 300 – 2000 K and 10 atm.

10 atm	300 K		400 K	500 K	600 K
Phase	Liquid	Vapor	Vapor	Vapor	Vapor
CO_2	0.0134645	0.3198105	0.3333092	0.3332952	0.3332808
CH_4	0.0013935	0.3318816	0.3333092	0.3332952	0.3332808
CH_3OH	0.3198794	0.0133955	0.3333092	0.3332952	0.3332808
H_2O	5.7583E-05	7.4304E-07	2.4112E-05	3.8104E-05	5.2566E-05
CH_3COOH	3.0860E-10	2.6291E-11	2.1886E-11	1.6657E-10	6.5616E-10
CH_3COOCH_3	4.8590E-05	9.7355E-06	2.4112E-05	3.8104E-05	5.2566E-05
X CH_4	**1.7498E-04**		**7.2335E-05**	**1.1431E-04**	**1.5770E-04**
X CH_3OH	**1.7498E-04**		**7.2335E-05**	**1.1431E-04**	**1.5770E-04**
Y MA	**0.9999943**		**0.9999991**	**0.9999956**	**0.9999875**

10 atm	700 K	800 K	900 K	1000 K	1100 K
Phase	Vapor	Vapor	Vapor	Vapor	Vapor
CO_2	0.3332663	0.3332521	0.3332382	0.3332247	0.3332117
CH_4	0.3332663	0.3332521	0.3332382	0.3332247	0.3332117
CH_3OH	0.3332663	0.3332521	0.3332382	0.3332247	0.3332117
H_2O	6.7016E-05	8.1249E-05	9.5146E-05	1.0862E-04	1.2158E-04
CH_3COOH	1.7857E-09	3.8669E-09	7.1928E-09	1.1990E-08	1.7178E-08
CH_3COOCH_3	6.7016E-05	8.1249E-05	9.5146E-05	1.0862E-04	1.2158E-04
X CH_4	**2.0105E-04**	**2.4376E-04**	**2.8546E-04**	**3.2589E-04**	**3.6480E-04**
X CH_3OH	**2.0105E-04**	**2.4375E-04**	**2.8544E-04**	**3.2585E-04**	**3.6475E-04**
Y MA	**0.9999734**	**0.9999524**	**0.9999244**	**0.9998896**	**0.9998587**

Table B-2 continued

10 atm	1200 K	1300 K	1400 K	1500 K	1600 K
Phase	Vapor	Vapor	Vapor	Vapor	Vapor
CO_2	0.3331993	0.3331876	0.3331764	0.3331658	0.3331559
CH_4	0.3331993	0.3331876	0.3331764	0.3331658	0.3331559
CH_3OH	0.3331993	0.3331876	0.3331764	0.3331659	0.3331560
H_2O	1.3399E-04	1.4578E-04	1.5694E-04	1.6744E-04	1.7729E-04
CH_3COOH	2.6840E-08	3.7121E-08	4.9077E-08	6.3844E-08	7.6889E-08
CH_3COOCH_3	1.3399E-04	1.4578E-04	1.5694E-04	1.6744E-04	1.7729E-04
X CH_4	**4.0204E-04**	**4.3745E-04**	**4.7095E-04**	**5.0251E-04**	**5.3210E-04**
X CH_3OH	**4.0196E-04**	**4.3734E-04**	**4.7081E-04**	**5.0231E-04**	**5.3187E-04**
Y MA	**0.9997997**	**0.9997454**	**0.9996874**	**0.9996188**	**0.9995665**

10 atm	1700 K	1800 K	1900 K	2000 K
Phase	Vapor	Vapor	Vapor	Vapor
CO_2	0.3331467	0.3331382	0.3331302	0.3331227
CH_4	0.3331467	0.3331382	0.3331302	0.3331227
CH_3OH	0.3331468	0.3331383	0.3331303	0.3331229
H_2O	1.8650E-04	1.9508E-04	2.0306E-04	2.1046E-04
CH_3COOH	9.8699E-08	1.1888E-07	1.4080E-07	1.6436E-07
CH_3COOCH_3	1.8650E-04	1.9508E-04	2.0306E-04	2.1046E-04
X CH_4	**5.5978E-04**	**5.8559E-04**	**6.0959E-04**	**6.3187E-04**
X CH_3OH	**5.5949E-04**	**5.8523E-04**	**6.0917E-04**	**6.3138E-04**
Y MA	**0.9994711**	**0.9993910**	**0.9993071**	**0.9992197**

Table B-3: Equilibrium outlet moles, X CH_4, X CH_3OH and Y MA for reaction (R B-1) obtained from AspenPlus™ using the Peng-Robinson equation of state and stoichiometric inlet composition from 300 – 2000 K and 25 atm.

25 atm	300 K		400 K	500 K	600 K
Phase	Liquid	Vapor	Vapor	Vapor	Vapor
CO_2	0.0353653	0.2978304	0.3332924	0.3332708	0.3332483
CH_4	0.0042002	0.3289955	0.3332924	0.3332708	0.3332483
CH_3OH	0.3268179	0.0063778	0.3332924	0.3332708	0.3332483
H_2O	1.3671E-04	8.9022E-07	4.0948E-05	6.2561E-05	8.5026E-05
CH_3COOH	3.0860E-10	2.6291E-11	6.4501E-11	4.5287E-10	1.7203E-09
CH_3COOCH_3	1.2674E-04	1.0861E-05	4.0948E-05	6.2561E-05	8.5026E-05
X CH_4	**4.1281E-04**		**1.2284E-04**	**1.8768E-04**	**2.5508E-04**
X CH_3OH	**4.1281E-04**		**1.2284E-04**	**1.8768E-04**	**2.5508E-04**
Y MA	**0.9999976**		**0.9999984**	**0.9999928**	**0.9999798**

25 atm	700 K	800 K	900 K	1000 K	1100 K
Phase	Vapor	Vapor	Vapor	Vapor	Vapor
CO_2	0.3332258	0.3332036	0.3331818	0.3331607	0.3331404
CH_4	0.3332258	0.3332036	0.3331818	0.3331607	0.3331404
CH_3OH	0.3332258	0.3332036	0.3331818	0.3331607	0.3331404
H_2O	1.0754E-04	1.2976E-04	1.5149E-04	1.7259E-04	1.9292E-04
CH_3COOH	4.5940E-09	9.8415E-09	1.8187E-08	3.0261E-08	4.6581E-08
CH_3COOCH_3	1.0754E-04	1.2976E-04	1.5149E-04	1.7259E-04	1.9292E-04
X CH_4	**3.2263E-04**	**3.8931E-04**	**4.5453E-04**	**5.1786E-04**	**5.7890E-04**
X CH_3OH	**3.2261E-04**	**3.8928E-04**	**4.5448E-04**	**5.1777E-04**	**5.7876E-04**
Y MA	**0.9999573**	**0.9999242**	**0.9998800**	**0.9998247**	**0.9997586**

Table B-3 continued

25 atm	1200 K	1300 K	1400 K	1500 K	1600 K
Phase	Vapor	Vapor	Vapor	Vapor	Vapor
CO_2	0.3331209	0.3331023	0.3330848	0.3330682	0.3330527
CH_4	0.3331209	0.3331023	0.3330848	0.3330682	0.3330527
CH_3OH	0.3331210	0.3331024	0.3330849	0.3330684	0.3330529
H_2O	2.1238E-04	2.3090E-04	2.4843E-04	2.6494E-04	2.8043E-04
CH_3COOH	6.7530E-08	9.3363E-08	1.2422E-07	1.6011E-07	2.0098E-07
CH_3COOCH_3	2.1238E-04	2.3090E-04	2.4843E-04	2.6494E-04	2.8043E-04
X CH_4	**6.3735E-04**	**6.9299E-04**	**7.4566E-04**	**7.9530E-04**	**8.4189E-04**
X CH_3OH	**6.3715E-04**	**6.9271E-04**	**7.4528E-04**	**7.9482E-04**	**8.4129E-04**
Y MA	**0.9996821**	**0.9995958**	**0.9995002**	**0.9993960**	**0.9992838**

25 atm	1700 K	1800 K	1900 K	2000 K
Phase	Vapor	Vapor	Vapor	Vapor
CO_2	0.3330382	0.3330246	0.3330120	0.3330003
CH_4	0.3330382	0.3330246	0.3330120	0.3330003
CH_3OH	0.3330384	0.3330249	0.3330124	0.3330007
H_2O	2.9492E-04	3.0842E-04	3.2098E-04	3.3264E-04
CH_3COOH	2.4667E-07	2.9700E-07	3.5170E-07	4.1051E-07
CH_3COOCH_3	2.9492E-04	3.0842E-04	3.2098E-04	3.3264E-04
X CH_4	**8.8549E-04**	**9.2616E-04**	**9.6400E-04**	**9.9915E-04**
X CH_3OH	**8.8475E-04**	**9.2527E-04**	**9.6295E-04**	**9.9791E-04**
Y MA	**0.9991643**	**0.9990380**	**0.9989055**	**0.9987674**

Table B-4: Equilibrium outlet moles, X CH_4, X CH_3OH and Y MA for reaction (R B-1) obtained from AspenPlus™ using the Peng-Robinson equation of state and stoichiometric inlet composition from 300 – 2000 K and 50 atm.

50 atm	300 K		400 K		500 K
Phase	Liquid	Vapor	Liquid	Vapor	Vapor
CO_2	0.0711916	0.2618875	0.0114118	0.3218196	0.3332390
CH_4	0.0107619	0.3223172	0.0042463	0.3289851	0.3332390
CH_3OH	0.3285893	0.0044899	0.1491311	0.1841004	0.3332390
H_2O	2.5288E-04	1.2732E-06	6.2558E-05	3.9357E-05	9.4345E-05
CH_3COOH	3.0557E-10	2.6033E-11	1.5802E-10	1.3462E-11	1.0396E-09
CH_3COOCH_3	2.4123E-04	1.2927E-05	3.8772E-05	6.3144E-05	9.4345E-05
X CH_4	**7.6246E-04**		**3.0575E-04**		**2.8304E-04**
X CH_3OH	**7.6246E-04**		**3.0575E-04**		**2.8303E-04**
Y MA	**0.9999987**		**0.9999983**		**0.9999890**

50 atm	700 K	600 K	800 K	900 K	1000 K
Phase	Vapor	Vapor	Vapor	Vapor	Vapor
CO_2	0.3331775	0.3332085	0.3331468	0.3331166	0.3330872
CH_4	0.3331775	0.3332085	0.3331468	0.3331166	0.3330872
CH_3OH	0.3331775	0.3332085	0.3331468	0.3331166	0.3330873
H_2O	1.5580E-04	1.2485E-04	1.8653E-04	2.1671E-04	2.4608E-04
CH_3COOH	9.6198E-09	3.7154E-09	2.0252E-08	3.7035E-08	6.1216E-08
CH_3COOCH_3	1.5580E-04	1.2485E-04	1.8653E-04	2.1671E-04	2.4608E-04
X CH_4	**4.6742E-04**	**3.7455E-04**	**5.5965E-04**	**6.5024E-04**	**7.3841E-04**
X CH_3OH	**4.6739E-04**	**3.7454E-04**	**5.5959E-04**	**6.5012E-04**	**7.3823E-04**
Y MA	**0.9999383**	**0.9999702**	**0.9998914**	**0.9998291**	**0.9997513**

Table B-4 continued

50 atm	1200 K	1100 K	1300 K	1400 K	1500 K
Phase	Vapor	Vapor	Vapor	Vapor	Vapor
CO_2	0.3330316	0.3330588	0.3330056	0.3329811	0.3329578
CH_4	0.3330316	0.3330588	0.3330056	0.3329811	0.3329578
CH_3OH	0.3330317	0.3330589	0.3330058	0.3329813	0.3329581
H_2O	3.0163E-04	2.7444E-04	3.2753E-04	3.5207E-04	3.7521E-04
CH_3COOH	1.3562E-07	9.3822E-08	1.8714E-07	2.4864E-07	3.2020E-07
CH_3COOCH_3	3.0163E-04	2.7444E-04	3.2753E-04	3.5207E-04	3.7521E-04
X CH_4	**9.0529E-04**	**8.2360E-04**	**9.8316E-04**	**1.0570E-03**	**1.1266E-03**
X CH_3OH	**9.0489E-04**	**8.2331E-04**	**9.8260E-04**	**1.0562E-03**	**1.1256E-03**
Y MA	**0.9995506**	**0.9996582**	**0.9994290**	**0.9992943**	**0.9991473**

50 atm	1700 K	1600 K	1800 K	1900 K	2000 K
Phase	Vapor	Vapor	Vapor	Vapor	Vapor
CO_2	0.3329156	0.3329360	0.3328965	0.3328788	0.3328623
CH_4	0.3329156	0.3329360	0.3328965	0.3328788	0.3328623
CH_3OH	0.3329161	0.3329364	0.3328971	0.3328795	0.3328631
H_2O	4.1726E-04	3.9694E-04	4.3622E-04	4.5387E-04	4.7025E-04
CH_3COOH	4.9279E-07	4.0167E-07	5.9316E-07	7.0229E-07	8.1964E-07
CH_3COOCH_3	4.1726E-04	3.9694E-04	4.3622E-04	4.5387E-04	4.7025E-04
X CH_4	**1.2533E-03**	**1.1920E-03**	**1.3105E-03**	**1.3637E-03**	**1.4132E-03**
X CH_3OH	**1.2518E-03**	**1.1908E-03**	**1.3087E-03**	**1.3616E-03**	**1.4107E-03**
Y MA	**0.9988204**	**0.9989891**	**0.9986421**	**0.9984550**	**0.9982600**

Table B-5: Equilibrium outlet moles, X CH_4, X CH_3OH and Y MA for reaction (R B-1) obtained from AspenPlus™ using the Peng-Robinson equation of state and stoichiometric inlet composition from 300 – 2000 K and 100 atm.

100 atm	300 K		400 K		500 K
Phase	Liquid	Vapor	Liquid	Vapor	Vapor
CO_2	0.1255278	0.2073816	0.0373975	0.2957209	0.3331812
CH_4	0.0298722	0.3030372	0.0167166	0.3164017	0.3331812
CH_3OH	0.3276956	0.0052138	0.2143848	0.1187336	0.3331812
H_2O	4.2132E-04	2.5854E-06	1.6504E-04	4.9871E-05	1.5213E-04
CH_3COOH	2.9950E-10	2.5516E-11	5.7091E-10	4.8639E-11	2.7048E-09
CH_3COOCH_3	4.0097E-04	2.2931E-05	1.2459E-04	9.0326E-05	1.5213E-04
X CH_4	**1.2717E-03**		**6.4475E-04**		**4.5640E-04**
X CH_3OH	**1.2717E-03**		**6.4474E-04**		**4.5639E-04**
Y MA	**0.9999992**		**0.9999971**		**0.9999822**

100 atm	700 K	600 K	800 K	900 K	1000 K
Phase	Vapor	Vapor	Vapor	Vapor	Vapor
CO_2	0.3331026	0.3331435	0.3330612	0.3330200	0.3329797
CH_4	0.3331026	0.3331435	0.3330612	0.3330200	0.3329797
CH_3OH	0.3331026	0.3331435	0.3330612	0.3330201	0.3329798
H_2O	2.3071E-04	1.8988E-04	2.7213E-04	3.1323E-04	3.5350E-04
CH_3COOH	2.0947E-08	8.5763E-09	4.2693E-08	7.6568E-08	1.2502E-07
CH_3COOCH_3	2.3071E-04	1.8988E-04	2.7213E-04	3.1323E-04	3.5350E-04
X CH_4	**6.9219E-04**	**5.6966E-04**	**8.1652E-04**	**9.3993E-04**	**1.0609E-03**
X CH_3OH	**6.9212E-04**	**5.6963E-04**	**8.1639E-04**	**9.3970E-04**	**1.0605E-03**
Y MA	**0.9999092**	**0.9999548**	**0.9998431**	**0.9997556**	**0.9996465**

Table B-5 continued

100 atm	1200 K	1100 K	1300 K	1400 K	1500 K
Phase	Vapor	Vapor	Vapor	Vapor	Vapor
CO_2	0.3329029	0.3329406	0.3328669	0.3328328	0.3328005
CH_4	0.3329029	0.3329406	0.3328669	0.3328328	0.3328005
CH_3OH	0.3329032	0.3329408	0.3328673	0.3328333	0.3328011
H_2O	4.3012E-04	3.9256E-04	4.6600E-04	5.0005E-04	5.3222E-04
CH_3COOH	2.7330E-07	1.9008E-07	3.7573E-07	4.9797E-07	6.4016E-07
CH_3COOCH_3	4.3012E-04	3.9256E-04	4.6600E-04	5.0005E-04	5.3222E-04
X CH_4	**1.2912E-03**	**1.1782E-03**	**1.3991E-03**	**1.5017E-03**	**1.5986E-03**
X CH_3OH	**1.2904E-03**	**1.1777E-03**	**1.3980E-03**	**1.5002E-03**	**1.5966E-03**
Y MA	**0.9993650**	**0.9995160**	**0.9991944**	**0.9990052**	**0.9987986**

100 atm	1700 K	1600 K	1800 K	1900 K	2000 K
Phase	Vapor	Vapor	Vapor	Vapor	Vapor
CO_2	0.3327416	0.3327701	0.3327149	0.3326901	0.3326670
CH_4	0.3327416	0.3327701	0.3327149	0.3326901	0.3326670
CH_3OH	0.3327426	0.3327709	0.3327161	0.3326915	0.3326686
H_2O	5.9078E-04	5.6246E-04	6.1724E-04	6.4187E-04	6.6476E-04
CH_3COOH	9.8328E-07	8.0211E-07	1.1829E-06	1.4001E-06	1.6338E-06
CH_3COOCH_3	5.9078E-04	5.6246E-04	6.1724E-04	6.4187E-04	6.6476E-04
X CH_4	**1.7753E-03**	**1.6898E-03**	**1.8553E-03**	**1.9298E-03**	**1.9992E-03**
X CH_3OH	**1.7723E-03**	**1.6874E-03**	**1.8517E-03**	**1.9256E-03**	**1.9943E-03**
Y MA	**0.9983384**	**0.9985759**	**0.9980872**	**0.9978235**	**0.9975484**

Table B-6: Equilibrium outlet moles, X CH_4, X CH_3OH and Y MA for reaction (R B-1) obtained from AspenPlus™ using the Peng-Robinson equation of state and stoichiometric inlet composition from 300 – 2000 K and 150 atm.

150 atm	300 K		400 K		500 K
Phase	Liquid	Vapor	Liquid	Vapor	Vapor
CO_2	0.1519112	0.1808929	0.0628004	0.0270225	0.3331216
CH_4	0.0507394	0.2820647	0.0339414	0.2990834	0.3331216
CH_3OH	0.3239590	0.0088452	0.2216130	0.1114119	0.3331216
H_2O	5.2405E-04	5.1463E-06	2.3776E-04	7.0668E-05	2.1172E-04
CH_3COOH	2.9343E-10	2.4999E-11	1.5008E-09	1.2786E-10	5.1481E-09
CH_3COOCH_3	4.8124E-04	4.7953E-05	1.8725E-04	1.2118E-04	2.1172E-04
X CH_4	**1.5876E-03**		**9.2528E-04**		**6.3517E-04**
X CH_3OH	**1.5876E-03**		**9.2528E-04**		**6.3516E-04**
Y MA	**0.9999994**		**0.9999947**		**0.9999757**

150 atm	700 K	600 K	800 K	900 K	1000 K
Phase	Vapor	Vapor	Vapor	Vapor	Vapor
CO_2	0.3330384	0.3330844	0.3329902	0.3329417	0.3328938
CH_4	0.3330384	0.3330844	0.3329902	0.3329417	0.3328938
CH_3OH	0.3330384	0.3330844	0.3329903	0.3329418	0.3328940
H_2O	2.9491E-04	2.4895E-04	3.4308E-04	3.9154E-04	4.3938E-04
CH_3COOH	3.3905E-08	1.4630E-08	6.7126E-08	1.1831E-07	1.9105E-07
CH_3COOCH_3	2.9491E-04	2.4895E-04	3.4308E-04	3.9154E-04	4.3938E-04
X CH_4	**8.8483E-04**	**7.4689E-04**	**1.0294E-03**	**1.1750E-03**	**1.3187E-03**
X CH_3OH	**8.8473E-04**	**7.4685E-04**	**1.0292E-03**	**1.1746E-03**	**1.3181E-03**
Y MA	**0.9998850**	**0.9999412**	**0.9998044**	**0.9996979**	**0.9995654**

Table B-6 continued

150 atm	1200 K	1100 K	1300 K	1400 K	1500 K
Phase	Vapor	Vapor	Vapor	Vapor	Vapor
CO_2	0.3328019	0.3328470	0.3327587	0.3327176	0.3326785
CH_4	0.3328019	0.3328470	0.3327587	0.3327176	0.3326785
CH_3OH	0.3328023	0.3328473	0.3327593	0.3327183	0.3326795
H_2O	5.3100E-04	4.8600E-04	5.7407E-04	6.1504E-04	6.5379E-04
CH_3COOH	4.1263E-07	2.8838E-07	5.6541E-07	7.4765E-07	9.5963E-07
CH_3COOCH_3	5.3100E-04	4.8600E-04	5.7407E-04	6.1504E-04	6.5379E-04
X CH_4	**1.5942E-03**	**1.4589E-03**	**1.7239E-03**	**1.8474E-03**	**1.9643E-03**
X CH_3OH	**1.5930E-03**	**1.4580E-03**	**1.7222E-03**	**1.8451E-03**	**1.9614E-03**
Y MA	**0.9992235**	**0.9994070**	**0.9990161**	**0.9987859**	**0.9985344**

150 atm	1700 K	1600 K	1800 K	1900 K	2000 K
Phase	Vapor	Vapor	Vapor	Vapor	Vapor
CO_2	0.3326073	0.3326419	0.3325751	0.3325450	0.3325169
CH_4	0.3326073	0.3326419	0.3325751	0.3325450	0.3325169
CH_3OH	0.3326088	0.3326431	0.3325769	0.3325471	0.3325193
H_2O	7.2449E-04	6.9027E-04	7.5647E-04	7.8628E-04	8.1400E-04
CH_3COOH	1.4713E-06	1.2011E-06	1.7692E-06	2.0934E-06	2.4423E-06
CH_3COOCH_3	7.2449E-04	6.9027E-04	7.5647E-04	7.8628E-04	8.1400E-04
X CH_4	**2.1779E-03**	**2.0744E-03**	**2.2747E-03**	**2.3651E-03**	**2.4493E-03**
X CH_3OH	**2.1735E-03**	**2.0708E-03**	**2.2694E-03**	**2.3588E-03**	**2.4420E-03**
Y MA	**0.9979733**	**0.9982630**	**0.9976667**	**0.9973447**	**0.9970086**

Table B-7: Equilibrium outlet moles, X CH_4, X CH_3OH and Y MA for reaction (R B-1) obtained from AspenPlus™ using the Peng-Robinson equation of state and stoichiometric inlet composition from 300 – 2000 K and 200 atm.

200 atm	300 K		400 K		500 K
Phase	Liquid	Vapor	Liquid	Vapor	Vapor
CO_2	0.1647918	0.1679380	0.0872571	0.2456916	0.3330590
CH_4	0.0696186	0.2631112	0.0574614	0.2754873	0.3330590
CH_3OH	0.3180600	0.0146698	0.2097022	0.1232466	0.3330590
H_2O	5.9410E-04	9.4307E-06	2.7711E-04	1.0741E-04	2.7431E-04
CH_3COOH	2.8740E-10	2.4485E-11	3.1646E-09	2.6961E-10	8.4397E-09
CH_3COOCH_3	5.1719E-04	8.6335E-05	2.2246E-04	1.6206E-04	2.7431E-04
X CH_4	**1.8106E-03**		**1.1536E-03**		**8.2294E-04**
X CH_3OH	**1.8106E-03**		**1.1536E-03**		**8.2292E-04**
Y MA	**0.9999995**		**0.9999911**		**0.9999692**

200 atm	700 K	600 K	800 K	900 K	1000 K
Phase	Vapor	Vapor	Vapor	Vapor	Vapor
CO_2	0.3329791	0.3330274	0.3329263	0.3328273	0.3328186
CH_4	0.3329791	0.3330274	0.3329263	0.3328273	0.3328186
CH_3OH	0.3329791	0.3330274	0.3329264	0.3328275	0.3328189
H_2O	3.5423E-04	3.0597E-04	4.0693E-04	4.6082E-04	5.1444E-04
CH_3COOH	4.8369E-08	2.1851E-08	9.3335E-08	1.6197E-07	2.5898E-07
CH_3COOCH_3	3.5423E-04	3.0597E-04	4.0693E-04	4.6082E-04	5.1444E-04
X CH_4	**1.0628E-03**	**9.1796E-04**	**1.2211E-03**	**1.3829E-03**	**1.5441E-03**
X CH_3OH	**1.0627E-03**	**9.1790E-04**	**1.2208E-03**	**1.3825E-03**	**1.5433E-03**
Y MA	**0.9998635**	**0.9999286**	**0.9997707**	**0.9996487**	**0.9994968**

Table B-7 continued

200 atm	1200 K	1100 K	1300 K	1400 K	1500 K
Phase	Vapor	Vapor	Vapor	Vapor	Vapor
CO_2	0.3327149	0.3327660	0.3326659	0.3326192	0.3325749
CH_4	0.3327149	0.3327660	0.3326659	0.3326192	0.3325749
CH_3OH	0.3327155	0.3327664	0.3326667	0.3326202	0.3325762
H_2O	6.1782E-04	5.6697E-04	6.6663E-04	7.1313E-04	7.5718E-04
CH_3COOH	5.5328E-07	3.8838E-07	7.5585E-07	9.9739E-07	1.2783E-06
CH_3COOCH_3	6.1782E-04	5.6697E-04	6.6663E-04	7.1313E-04	7.5718E-04
X CH_4	**1.8551E-03**	**1.7021E-03**	**2.0021E-03**	**2.1424E-03**	**2.2754E-03**
X CH_3OH	**1.8535E-03**	**1.7009E-03**	**1.9999E-03**	**2.1394E-03**	**2.2715E-03**
Y MA	**0.9991053**	**0.9993155**	**0.9988674**	**0.9986033**	**0.9983146**

200 atm	1700 K	1600 K	1800 K	1900 K	2000 K
Phase	Vapor	Vapor	Vapor	Vapor	Vapor
CO_2	0.3324937	0.3325330	0.3324568	0.3324224	0.3323903
CH_4	0.3324937	0.3325330	0.3324568	0.3324224	0.3323903
CH_3OH	0.3324957	0.3325346	0.3324592	0.3324252	0.3323935
H_2O	8.3768E-04	7.9870E-04	8.7415E-04	9.0817E-04	9.3983E-04
CH_3COOH	1.9567E-06	1.5984E-06	2.3519E-06	2.7821E-06	3.2453E-06
CH_3COOCH_3	8.3768E-04	7.9870E-04	8.7415E-04	9.0817E-04	9.3983E-04
X CH_4	**2.5189E-03**	**2.4009E-03**	**2.6295E-03**	**2.7329E-03**	**2.8292E-03**
X CH_3OH	**2.5130E-03**	**2.3961E-03**	**2.6225E-03**	**2.7245E-03**	**2.8195E-03**
Y MA	**0.9976696**	**0.9980027**	**0.9973168**	**0.9969460**	**0.9965588**

Table B-8: Equilibrium fractional conversion of methane (X CH_4) for reaction (R B-1) obtained from AspenPlus™ using the Peng-Robinson equation of state and stoichiometric inlet composition from 300 – 2000 K and 1 - 200 atm.

T (K)	1 atm	10 atm	25 atm	50 atm
300 K	**1.9572E-05**	**1.7498E-04**	**4.1281E-04**	**7.6246E-04**
400 K	2.1984E-05	7.2335E-05	1.2284E-04	**3.0575E-04**
500 K	3.5355E-05	1.1431E-04	1.8768E-04	2.8304E-04
600 K	4.9192E-05	1.5770E-04	2.5508E-04	3.7455E-04
700 K	6.3015E-05	2.0105E-04	3.2263E-04	4.6742E-04
800 K	7.6619E-05	2.4376E-04	3.8931E-04	5.5965E-04
900 K	8.9893E-05	2.8546E-04	4.5453E-04	6.5024E-04
1000 K	1.0275E-04	3.2589E-04	5.1786E-04	7.3841E-04
1100 K	1.1512E-04	3.6480E-04	5.7890E-04	8.2360E-04
1200 K	1.2695E-04	4.0204E-04	6.3735E-04	9.0529E-04
1300 K	1.3819E-04	4.3745E-04	6.9299E-04	9.8316E-04
1400 K	1.4882E-04	4.7095E-04	7.4566E-04	1.0570E-03
1500 K	1.5883E-04	5.0251E-04	7.9530E-04	1.1266E-03
1600 K	1.6821E-04	5.3210E-04	8.4189E-04	1.1920E-03
1700 K	1.7698E-04	5.5978E-04	8.8549E-04	1.2533E-03
1800 K	1.8516E-04	5.8559E-04	9.2616E-04	1.3105E-03
1900 K	1.9276E-04	6.0959E-04	9.6400E-04	1.3637E-03
2000 K	1.9981E-04	6.3187E-04	9.9915E-04	1.4132E-03

NOTE: Values in bold indicates presence of both liquid and vapor phases.

Table B-8 continued

T (K)	100 atm	150 atm	200 atm
300 K	**1.2717E-03**	**1.5876E-03**	**1.8106E-03**
400 K	**6.4475E-04**	**9.2528E-04**	**1.1536E-03**
500 K	4.5640E-04	6.3517E-04	8.2294E-04
600 K	5.6966E-04	7.4689E-04	9.1796E-04
700 K	6.9219E-04	8.8483E-04	1.0628E-03
800 K	8.1652E-04	1.0294E-03	1.2211E-03
900 K	9.3993E-04	1.1750E-03	1.3829E-03
1000 K	1.0609E-03	1.3187E-03	1.5441E-03
1100 K	1.1782E-03	1.4589E-03	1.7021E-03
1200 K	1.2912E-03	1.5942E-03	1.8551E-03
1300 K	1.3991E-03	1.7239E-03	2.0021E-03
1400 K	1.5017E-03	1.8474E-03	2.1424E-03
1500 K	1.5986E-03	1.9643E-03	2.2754E-03
1600 K	1.6898E-03	2.0744E-03	2.4009E-03
1700 K	1.7753E-03	2.1779E-03	2.5189E-03
1800 K	1.8553E-03	2.2747E-03	2.6295E-03
1900 K	1.9298E-03	2.3651E-03	2.7329E-03
2000 K	1.9992E-03	2.4493E-03	2.8292E-03

NOTE: Values in bold indicates presence of both liquid and vapor phases.

Table B-9: Equilibrium fractional conversion of methanol (X CH_3OH) for reaction (R B-1) obtained from AspenPlus™ using the Peng-Robinson equation of state and stoichiometric inlet composition from 300 – 2000 K and 1 - 200 atm.

T (K)	1 atm	10 atm	25 atm	50 atm
300 K	**1.9572E-05**	**1.7498E-04**	**4.1281E-04**	**7.6246E-04**
400 K	2.1984E-05	7.2335E-05	1.2284E-04	**3.0575E-04**
500 K	3.5355E-05	1.1431E-04	1.8768E-04	2.8303E-04
600 K	4.9192E-05	1.5770E-04	2.5508E-04	3.7454E-04
700 K	6.3014E-05	2.0105E-04	3.2261E-04	4.6739E-04
800 K	7.6618E-05	2.4375E-04	3.8928E-04	5.5959E-04
900 K	8.9891E-05	2.8544E-04	4.5448E-04	6.5012E-04
1000 K	1.0275E-04	3.2585E-04	5.1777E-04	7.3823E-04
1100 K	1.1512E-04	3.6475E-04	5.7876E-04	8.2331E-04
1200 K	1.2694E-04	4.0196E-04	6.3715E-04	9.0489E-04
1300 K	1.3818E-04	4.3734E-04	6.9271E-04	9.8260E-04
1400 K	1.4881E-04	4.7081E-04	7.4528E-04	1.0562E-03
1500 K	1.5881E-04	5.0231E-04	7.9482E-04	1.1256E-03
1600 K	1.6819E-04	5.3187E-04	8.4129E-04	1.1908E-03
1700 K	1.7696E-04	5.5949E-04	8.8475E-04	1.2518E-03
1800 K	1.8512E-04	5.8523E-04	9.2527E-04	1.3087E-03
1900 K	1.9272E-04	6.0917E-04	9.6295E-04	1.3616E-03
2000 K	1.9976E-04	6.3138E-04	9.9791E-04	1.4107E-03

NOTE: Values in bold indicates presence of both liquid and vapor phases.

Table B-9 continued

T (K)	100 atm	150 atm	200 atm
300 K	**1.2717E-03**	**1.5876E-03**	**1.8106E-03**
400 K	**6.4474E-04**	**9.2528E-04**	**1.1536E-03**
500 K	4.5639E-04	6.3516E-04	8.2292E-04
600 K	5.6963E-04	7.4685E-04	9.1790E-04
700 K	6.9212E-04	8.8473E-04	1.0627E-03
800 K	8.1639E-04	1.0292E-03	1.2208E-03
900 K	9.3970E-04	1.1746E-03	1.3825E-03
1000 K	1.0605E-03	1.3181E-03	1.5433E-03
1100 K	1.1777E-03	1.4580E-03	1.7009E-03
1200 K	1.2904E-03	1.5930E-03	1.8535E-03
1300 K	1.3980E-03	1.7222E-03	1.9999E-03
1400 K	1.5002E-03	1.8451E-03	2.1394E-03
1500 K	1.5966E-03	1.9614E-03	2.2715E-03
1600 K	1.6874E-03	2.0708E-03	2.3961E-03
1700 K	1.7723E-03	2.1735E-03	2.5130E-03
1800 K	1.8517E-03	2.2694E-03	2.6225E-03
1900 K	1.9256E-03	2.3588E-03	2.7245E-03
2000 K	1.9943E-03	2.4420E-03	2.8195E-03

NOTE: Values in bold indicates presence of both liquid and vapor phases.

Table B-10: Equilibrium fractional yield of methyl acetate (Y MA) for reaction (R B-1) obtained from AspenPlus™ using the Peng-Robinson equation of state and stoichiometric inlet composition from 300 – 2000 K and 1 - 200 atm.

T (K)	1 atm	10 atm	25 atm	50 atm
300 K	**0.9999999**	**0.9999943**	**0.9999976**	**0.9999987**
400 K	0.9999997	0.9999991	0.9999984	**0.9999983**
500 K	0.9999987	0.9999956	0.9999928	0.9999890
600 K	0.9999961	0.9999875	0.9999798	0.9999702
700 K	0.9999916	0.9999734	0.9999573	0.9999383
800 K	0.9999850	0.9999524	0.9999242	0.9998914
900 K	0.9999762	0.9999244	0.9998800	0.9998291
1000 K	0.9999651	0.9998896	0.9998247	0.9997513
1100 K	0.9999518	0.9998587	0.9997586	0.9996582
1200 K	0.9999364	0.9997997	0.9996821	0.9995506
1300 K	0.9999191	0.9997454	0.9995958	0.9994290
1400 K	0.9998999	0.9996874	0.9995002	0.9992943
1500 K	0.9998790	0.9996188	0.9993960	0.9991473
1600 K	0.9998565	0.9995665	0.9992838	0.9989891
1700 K	0.9998326	0.9994711	0.9991643	0.9988204
1800 K	0.9998073	0.9993910	0.9990380	0.9986421
1900 K	0.9997807	0.9993071	0.9989055	0.9984550
2000 K	0.9997531	0.9992197	0.9987674	0.9982600

NOTE: Values in bold indicates presence of both liquid and vapor phases.

Table B-10 continued

T (K)	100 atm	150 atm	200 atm
300 K	**0.9999992**	**0.9999994**	**0.9999995**
400 K	**0.9999971**	**0.9999947**	**0.9999911**
500 K	0.9999822	0.9999757	0.9999692
600 K	0.9999548	0.9999412	0.9999286
700 K	0.9999092	0.9998850	0.9998635
800 K	0.9998431	0.9998044	0.9997707
900 K	0.9997556	0.9996979	0.9996487
1000 K	0.9996465	0.9995654	0.9994968
1100 K	0.9995160	0.9994070	0.9993155
1200 K	0.9993650	0.9992235	0.9991053
1300 K	0.9991944	0.9990161	0.9988674
1400 K	0.9990052	0.9987859	0.9986033
1500 K	0.9987986	0.9985344	0.9983146
1600 K	0.9985759	0.9982630	0.9980027
1700 K	0.9983384	0.9979733	0.9976696
1800 K	0.9980872	0.9976667	0.9973168
1900 K	0.9978235	0.9973447	0.9969460
2000 K	0.9975484	0.9970086	0.9965588

NOTE: Values in bold indicates presence of both liquid and vapor phases.

B.2. ACETIC ANHYDRIDE

Equilibrium thermodynamic calculations were performed for the formation of acetic anhydride ($(CH_3CO)_2O$) from carbon dioxide, methane and ketene (CH_2CO):

$$CO_2 + CH_4 + CH_2CO \leftrightarrow (CH_3CO)_2O \qquad \text{(R B-5)}$$

Acetic acid was allowed in the system, thus also permitting the following reactions:

$$CO_2 + CH_4 \leftrightarrow CH_3COOH \qquad \text{(R B-2)}$$

$$CH_3COOH + CH_2CO \leftrightarrow (CH_3CO)_2O \qquad \text{(R B-6)}$$

The equilibrium thermodynamic calculations for reaction (R B-5) were performed using the AspenPlus™ engineering simulation software. The RGIBBS reactor model was used to perform a Gibbs free energy minimization on the system to give the chemical and phase equilibrium composition at various temperatures and pressures. These calculations do not take into account any surface interactions. Molecular interactions are taken into account in the Peng-Robinson equation of state. The inlet composition, inlet temperature, inlet pressure, reactor temperature and reactor pressure were specified for each reaction. The inlet conditions were set equal to the reactor conditions.

A stoichiometric inlet composition of 0.333 mole fraction of CO_2, 0.333 mole fraction of CH_4 and 0.333 mole fraction of CH_2CO was used. The AspenPlus™ calculations were performed for a wide range of temperatures and pressures, 1 - 200 atm and 300 - 2000 K. The calculations were performed using the Peng-Robinson equation of state.

An interaction parameter of 0.0919 for CO_2 and CH_4 obtained from the AspenPlus™ data base were used. No other interaction parameters were available, thus a default of 0.0 was used for all other interaction parameters.

The equilibrium fractional conversion of methane (X CH_4) was calculated using:

$$X\ CH_4 = \#\ \text{Moles of } CH_4 \text{ reacted} / \#\ \text{Inlet moles of } CH_4 \qquad \text{(E B-1)}$$

When the outlet moles of methane given by AspenPlus™ did not have enough significant figures, the number of outlet moles of acetic acid and acetic anhydride was used as the number of moles of methane that reacted.

The equilibrium fractional conversion of ketene (X CH_2CO) was calculated using:

$$X\ CH_2CO = \#\ \text{Moles of } CH_2CO \text{ reacted} / \#\ \text{Inlet moles of } CH_2CO \qquad \text{(E B-4)}$$

When the outlet moles of ketene given by AspenPlus™ did not have enough significant figures, the number of outlet moles of acetic anhydride was used as the number of moles of methane that reacted.

The equilibrium yield of acetic anhydride (Y Anhydride) was calculated using:

$$Y\ \text{Anhydride} = \text{Outlet } (CH_3CO)_2O / \text{Outlet } (CH_3CO)_2O + CH_3COOH \qquad \text{(E B-5)}$$

Data from these calculations can be found in tables B-11 to B-20.

Table B-11: Equilibrium outlet moles, X CH_4, X CH_2CO and Y Anhydride for reaction (R B - 5) obtained from AspenPlus™ using the Peng-Robinson equation of state and stoichiometric inlet composition from 300 – 2000 K and 1 atm.

1 atm	300 K	400 K	500 K	600 K	700 K
Phase	Vapor	Vapor	Vapor	Vapor	Vapor
CO_2	0.3333224	0.3333333	0.3333333	0.3333333	0.3333333
CH_4	0.3333224	0.3333333	0.3333333	0.3333333	0.3333333
CH_2CO	0.3333224	0.3333333	0.3333333	0.3333333	0.3333333
CH_3COOH	6.0018E-14	1.8547E-12	1.5835E-11	6.3732E-11	1.7546E-10
$(CH_3CO)_2O$	1.0957E-05	3.2998E-08	9.5253E-10	8.9417E-11	1.6789E-11
X CH_4	**3.2870E-05**	**9.9000E-08**	**2.9051E-09**	**4.5945E-10**	**5.7675E-10**
X CH_2CO	**3.2870E-05**	**9.8995E-08**	**2.8576E-09**	**2.6825E-10**	**5.0367E-11**
Y Anhydride	**1.0000000**	**0.9999438**	**0.9836477**	**0.5838562**	**0.0873295**

1 atm	800 K	900 K	1000 K	1100 K	1200 K
Phase	Vapor	Vapor	Vapor	Vapor	Vapor
CO_2	0.3333333	0.3333333	0.3333333	0.3333333	0.3333333
CH_4	0.3333333	0.3333333	0.3333333	0.3333333	0.3333333
CH_2CO	0.3333333	0.3333333	0.3333333	0.3333333	0.3333333
CH_3COOH	3.8247E-10	7.1430E-10	1.1965E-09	1.8499E-09	2.6896E-09
$(CH_3CO)_2O$	4.8954E-12	1.5570E-12	7.7314E-13	5.1672E-13	3.2312E-13
X CH_4	**1.1621E-09**	**2.1476E-09**	**3.5919E-09**	**5.5512E-09**	**8.0698E-09**
X CH_2CO	**1.4686E-11**	**4.6710E-12**	**2.3194E-12**	**1.5502E-12**	**9.6936E-13**
Y Anhydride	**0.0126377**	**2.1750E-03**	**6.4573E-04**	**2.7925E-04**	**1.2012E-04**

Table B-11 continued

1 atm	1300 K	1400 K	1500 K	1600 K	1700 K
Phase	Vapor	Vapor	Vapor	Vapor	Vapor
CO_2	0.3333333	0.3333333	0.3333333	0.3333333	0.3333333
CH_4	0.3333333	0.3333333	0.3333333	0.3333333	0.3333333
CH_2CO	0.3333333	0.3333333	0.3333333	0.3333333	0.3333333
CH_3COOH	3.7260E-09	4.9639E-09	6.4042E-09	8.0440E-09	9.8772E-09
$(CH_3CO)_2O$	2.1981E-13	1.5966E-13	1.2211E-13	9.7328E-14	8.0213E-14
X CH_4	**1.1179E-08**	**1.4892E-08**	**1.9213E-08**	**2.4132E-08**	**2.9632E-08**
X CH_2CO	**6.5943E-13**	**4.7898E-13**	**3.6633E-13**	**2.9198E-13**	**2.4064E-13**
Y Anhydride	**5.8991E-05**	**3.2163E-05**	**1.9067E-05**	**1.2099E-05**	**8.1210E-06**

1 atm	1800 K	1900 K	2000 K
Phase	Vapor	Vapor	Vapor
CO_2	0.3333333	0.3333333	0.3333333
CH_4	0.3333333	0.3333333	0.3333333
CH_2CO	0.3333333	0.3333333	0.3333333
CH_3COOH	1.1896E-08	1.4089E-08	1.6447E-08
$(CH_3CO)_2O$	6.7944E-14	5.8872E-14	5.1986E-14
X CH_4	**3.5687E-08**	**4.2267E-08**	**4.9340E-08**
X CH_2CO	**2.0383E-13**	**1.7662E-13**	**1.5596E-13**
Y Anhydride	**5.7117E-06**	**4.1785E-06**	**3.1609E-06**

Table B-12: Equilibrium outlet moles, X CH_4, X CH_2CO and Y Anhydride for reaction (R B - 5) obtained from AspenPlus™ using the Peng-Robinson equation of state and stoichiometric inlet composition from 300 – 2000 K and 10 atm.

10 atm	300 K	400 K	500 K	600 K	700 K
Phase	Vapor	Vapor	Vapor	Vapor	Vapor
CO_2	0.3320204	0.3333297	0.3333332	0.3333333	0.3333333
CH_4	0.3320204	0.3333297	0.3333332	0.3333333	0.3333333
CH_2CO	0.3320204	0.3333297	0.3333332	0.3333333	0.3333333
CH_3COOH	7.5142E-13	2.1886E-11	1.6657E-10	6.5616E-10	1.7857E-09
$(CH_3CO)_2O$	1.3129E-03	3.5963E-06	9.9538E-08	9.1726E-09	1.7054E-09
X CH_4	**3.9387E-03**	**1.0789E-05**	**2.9911E-07**	**2.9486E-08**	**1.0473E-08**
X CH_2CO	**3.9387E-03**	**1.0789E-05**	**2.9861E-07**	**2.7518E-08**	**5.1161E-09**
Y Anhydride	**1.0000000**	**0.9999939**	**0.9983294**	**0.9332410**	**0.4884978**

10 atm	800 K	900 K	1000 K	1100 K	1200 K
Phase	Vapor	Vapor	Vapor	Vapor	Vapor
CO_2	0.3333333	0.3333333	0.3333333	0.3333333	0.3333333
CH_4	0.3333333	0.3333333	0.3333333	0.3333333	0.3333333
CH_2CO	0.3333333	0.3333333	0.3333333	0.3333333	0.3333333
CH_3COOH	3.8669E-09	1.6822E-11	1.1990E-08	1.7178E-08	2.6840E-08
$(CH_3CO)_2O$	4.9446E-10	1.9303E-10	9.2793E-11	5.1835E-11	3.2374E-11
X CH_4	**1.3084E-08**	**6.2956E-10**	**3.6250E-08**	**5.1690E-08**	**8.0617E-08**
X CH_2CO	**1.4834E-09**	**5.7909E-10**	**2.7838E-10**	**1.5551E-10**	**9.7122E-11**
Y Anhydride	**0.1133719**	**0.9198387**	**7.6795E-03**	**3.0084E-03**	**1.2047E-03**

Table B-12 continued

10 atm	1300 K	1400 K	1500 K	1600 K	1700 K
Phase	Vapor	Vapor	Vapor	Vapor	Vapor
CO_2	0.3333333	0.3333333	0.3333333	0.3333333	0.3333332
CH_4	0.3333333	0.3333333	0.3333333	0.3333333	0.3333332
CH_2CO	0.3333333	0.3333333	0.3333333	0.3333333	0.3333333
CH_3COOH	3.7121E-08	4.9077E-08	6.3844E-08	7.6889E-08	9.8699E-08
$(CH_3CO)_2O$	2.2009E-11	1.5979E-11	1.2217E-11	9.7352E-12	8.0221E-12
X CH_4	**1.1143E-07**	**1.4728E-07**	**1.9157E-07**	**2.3070E-07**	**2.9612E-07**
X CH_2CO	**6.6027E-11**	**4.7937E-11**	**3.6651E-11**	**2.9206E-11**	**2.4066E-11**
Y Anhydride	**5.9254E-04**	**3.2549E-04**	**1.9132E-04**	**1.2660E-04**	**8.1272E-05**

10 atm	1800 K	1900 K	2000 K
Phase	Vapor	Vapor	Vapor
CO_2	0.3333332	0.3333332	0.3333332
CH_4	0.3333332	0.3333332	0.3333332
CH_2CO	0.3333333	0.3333332	0.3333332
CH_3COOH	1.1888E-07	1.4080E-07	1.6436E-07
$(CH_3CO)_2O$	6.7944E-12	5.8867E-12	5.1979E-12
X CH_4	**3.5665E-07**	**4.2241E-07**	**4.9308E-07**
X CH_2CO	**2.0383E-11**	**1.7660E-11**	**1.5594E-11**
Y Anhydride	**5.7151E-05**	**4.1807E-05**	**3.1625E-05**

Table B-13: Equilibrium outlet moles, X CH_4, X CH_2CO and Y Anhydride for reaction (R B - 5) obtained from AspenPlus™ using the Peng-Robinson equation of state and stoichiometric inlet composition from 300 – 2000 K and 25 atm.

25 atm	300 K	400 K	500 K	600 K	700 K
Phase	Liquid	Vapor	Vapor	Vapor	Vapor
CO_2	0.0177050	0.3333075	0.3333327	0.3333333	0.3333333
CH_4	0.0177050	0.3333075	0.3333327	0.3333333	0.3333333
CH_2CO	0.0177050	0.3333075	0.3333327	0.3333333	0.3333333
CH_3COOH	3.3489E-10	6.4501E-11	4.5287E-10	1.7203E-09	4.5940E-09
$(CH_3CO)_2O$	0.3156283	2.5843E-05	6.6900E-07	5.9763E-08	1.0933E-08
X CH_4	**0.9468849**	**7.7529E-05**	**2.0084E-06**	**1.8445E-07**	**4.6581E-08**
X CH_2CO	**0.9468849**	**7.7529E-05**	**2.0070E-06**	**1.7929E-07**	**3.2799E-08**
Y Anhydride	**1.0000000**	**0.9999975**	**0.9993235**	**0.9720195**	**0.7041297**

25 atm	800 K	900 K	1000 K	1100 K	1200 K
Phase	Vapor	Vapor	Vapor	Vapor	Vapor
CO_2	0.3333333	0.3333333	0.3333333	0.3333333	0.3333333
CH_4	0.3333333	0.3333333	0.3333333	0.3333333	0.3333333
CH_2CO	0.3333333	0.3333333	0.3333333	0.3333333	0.3333333
CH_3COOH	9.8415E-09	1.8187E-08	3.0261E-08	4.6581E-08	6.7530E-08
$(CH_3CO)_2O$	3.1408E-09	1.2194E-09	5.8404E-10	3.2549E-10	2.0297E-10
X CH_4	**3.8947E-08**	**5.8218E-08**	**9.2536E-08**	**1.4072E-07**	**2.0320E-07**
X CH_2CO	**9.4223E-09**	**3.6582E-09**	**1.7521E-09**	**9.7647E-10**	**6.0891E-10**
Y Anhydride	**0.2419292**	**0.0628361**	**0.0189345**	**6.9392E-03**	**2.9966E-03**

Table B-13 continued

25 atm	1300 K	1400 K	1500 K	1600 K	1700 K
Phase	Vapor	Vapor	Vapor	Vapor	Vapor
CO_2	0.3333332	0.3333332	0.3333332	0.3333331	0.3333331
CH_4	0.3333332	0.3333332	0.3333332	0.3333331	0.3333331
CH_2CO	0.3333333	0.3333333	0.3333333	0.3333333	0.3333333
CH_3COOH	9.3363E-08	1.2422E-07	1.6011E-07	2.0098E-07	2.4667E-07
$(CH_3CO)_2O$	1.3784E-10	9.9994E-11	7.6413E-11	6.0870E-11	5.0146E-11
X CH_4	**2.8050E-07**	**3.7294E-07**	**4.8056E-07**	**6.0311E-07**	**7.4017E-07**
X CH_2CO	**4.1352E-10**	**2.9998E-10**	**2.2924E-10**	**1.8261E-10**	**1.5044E-10**
Y Anhydride	**1.4742E-03**	**8.0436E-04**	**4.7703E-04**	**3.0278E-04**	**2.0325E-04**

25 atm	1800 K	1900 K	2000 K
Phase	Vapor	Vapor	Vapor
CO_2	0.3333330	0.3333330	0.3333329
CH_4	0.3333330	0.3333330	0.3333329
CH_2CO	0.3333333	0.3333333	0.3333333
CH_3COOH	2.9700E-07	3.5170E-07	4.1051E-07
$(CH_3CO)_2O$	4.2464E-11	3.6787E-11	3.2480E-11
X CH_4	**8.9112E-07**	**1.0552E-06**	**1.2316E-06**
X CH_2CO	**1.2739E-10**	**1.1036E-10**	**9.7440E-11**
Y Anhydride	**1.4296E-04**	**1.0459E-04**	**7.9116E-05**

Table B-14: Equilibrium outlet moles, X CH_4, X CH_2CO and Y Anhydride for reaction (R B - 5) obtained from AspenPlus™ using the Peng-Robinson equation of state and stoichiometric inlet composition from 300 – 2000 K and 50 atm.

50 atm	300 K	400 K	500 K	600 K	700 K
Phase	Liquid	Vapor	Vapor	Vapor	Vapor
CO_2	0.0175036	0.3332012	0.3333303	0.3333331	0.3333333
CH_4	0.0175036	0.3332012	0.3333303	0.3333331	0.3333333
CH_2CO	0.0175036	0.3332012	0.3333330	0.3333331	0.3333333
CH_3COOH	3.3160E-10	1.7148E-10	1.0396E-09	3.7154E-09	9.6198E-09
$(CH_3CO)_2O$	0.3158297	1.3218E-04	3.0127E-06	2.5552E-07	4.5537E-08
X CH_4	**0.9474891**	**3.9653E-04**	**9.0412E-06**	**7.7769E-07**	**1.6547E-07**
X CH_2CO	**0.9474891**	**3.9653E-04**	**9.0380E-06**	**7.6655E-07**	**1.3661E-07**
Y Anhydride	**1.0000000**	**0.9999987**	**0.9996551**	**0.9856675**	**0.8255921**

50 atm	800 K	900 K	1000 K	1100 K	1200 K
Phase	Vapor	Vapor	Vapor	Vapor	Vapor
CO_2	0.3333333	0.3333333	0.3333333	0.3333332	0.3333332
CH_4	0.3333333	0.3333333	0.3333333	0.3333332	0.3333332
CH_2CO	0.3333333	0.3333333	0.3333333	0.3333333	0.3333333
CH_3COOH	2.0252E-08	3.7035E-08	6.1216E-08	9.3822E-08	1.3562E-07
$(CH_3CO)_2O$	1.2890E-08	4.9023E-09	2.3624E-09	1.3117E-09	8.1589E-10
X CH_4	**9.9428E-08**	**1.2581E-07**	**1.9074E-07**	**2.8540E-07**	**4.0932E-07**
X CH_2CO	**3.8671E-08**	**1.4707E-08**	**7.0871E-09**	**3.9350E-09**	**2.4477E-09**
Y Anhydride	**0.3889352**	**0.1168973**	**0.0371566**	**1.3788E-02**	**5.9799E-03**

Table B-14 continued

50 atm	1300 K	1400 K	1500 K	1600 K	1700 K
Phase	Vapor	Vapor	Vapor	Vapor	Vapor
CO_2	0.3333331	0.3333331	0.3333330	0.3333329	0.3333328
CH_4	0.3333331	0.3333331	0.3333330	0.3333329	0.3333328
CH_2CO	0.3333333	0.3333333	0.3333333	0.3333333	0.3333333
CH_3COOH	1.8714E-07	2.4864E-07	3.2020E-07	4.0167E-07	4.9279E-07
$(CH_3CO)_2O$	5.5313E-10	4.0080E-10	3.0602E-10	2.4363E-10	2.0063E-10
X CH_4	**5.6308E-07**	**7.4713E-07**	**9.6151E-07**	**1.2057E-06**	**1.4790E-06**
X CH_2CO	**1.6594E-09**	**1.2024E-09**	**9.1806E-10**	**7.3089E-10**	**6.0189E-10**
Y Anhydride	**2.9470E-03**	**1.6093E-03**	**9.5481E-04**	**6.0617E-04**	**4.0696E-04**

50 atm	1800 K	1900 K	2000 K
Phase	Vapor	Vapor	Vapor
CO_2	0.3333327	0.3333326	0.3333325
CH_4	0.3333327	0.3333326	0.3333325
CH_2CO	0.3333333	0.3333333	0.3333333
CH_3COOH	5.9316E-07	7.0229E-07	8.1964E-07
$(CH_3CO)_2O$	1.6985E-10	1.4711E-10	1.2988E-10
X CH_4	**1.7800E-06**	**2.1073E-06**	**2.4593E-06**
X CH_2CO	**5.0955E-10**	**4.4133E-10**	**3.8964E-10**
Y Anhydride	**2.8627E-04**	**2.0943E-04**	**1.5844E-04**

Table B-15: Equilibrium outlet moles, X CH_4, X CH_2CO and Y Anhydride for reaction (R B - 5) obtained from AspenPlus™ using the Peng-Robinson equation of state and stoichiometric inlet composition from 300 – 2000 K and 100 atm.

100 atm	300 K	400 K	500 K	600 K	700 K
Phase	Liquid	Vapor	Vapor	Vapor	Vapor
CO_2	0.0171247	0.3324577	0.3333183	0.3333322	0.3333331
CH_4	0.0171247	0.3324577	0.3333183	0.3333322	0.3333331
CH_2CO	0.0171247	0.3324577	0.3333183	0.3333322	0.3333331
CH_3COOH	3.2502E-10	6.1955E-10	2.7048E-09	8.5763E-09	2.0947E-08
$(CH_3CO)_2O$	0.3162086	8.7567E-04	1.5053E-05	1.1550E-06	1.9610E-07
X CH_4	**0.9486258**	**2.6270E-03**	**4.5167E-05**	**3.4906E-06**	**6.5115E-07**
X CH_2CO	**0.9486258**	**2.6270E-03**	**4.5158E-05**	**3.4649E-06**	**5.8831E-07**
Y Anhydride	**1.0000000**	**0.9999993**	**0.9998203**	**0.9926291**	**0.9034923**

100 atm	800 K	900 K	1000 K	1100 K	1200 K
Phase	Vapor	Vapor	Vapor	Vapor	Vapor
CO_2	0.3333332	0.3333332	0.3333332	0.3333331	0.3333331
CH_4	0.3333332	0.3333332	0.3333332	0.3333331	0.3333331
CH_2CO	0.3333333	0.3333333	0.3333333	0.3333333	0.3333333
CH_3COOH	4.2693E-08	7.6568E-08	1.2502E-07	1.9008E-07	2.7330E-07
$(CH_3CO)_2O$	5.4039E-08	2.0460E-08	9.6446E-09	5.3189E-09	3.2934E-09
X CH_4	**2.9020E-07**	**2.9108E-07**	**4.0399E-07**	**5.8619E-07**	**8.2977E-07**
X CH_2CO	**1.6212E-07**	**6.1380E-08**	**2.8934E-08**	**1.5957E-08**	**9.8801E-09**
Y Anhydride	**0.5586426**	**0.2108668**	**0.0716197**	**0.0272209**	**0.0119071**

Table B-15 continued

100 atm	1300 K	1400 K	1500 K	1600 K	1700 K
Phase	Vapor	Vapor	Vapor	Vapor	Vapor
CO_2	0.3333330	0.3333328	0.3333327	0.3333325	0.3333323
CH_4	0.3333330	0.3333328	0.3333327	0.3333325	0.3333323
CH_2CO	0.3333333	0.3333333	0.3333333	0.3333333	0.3333333
CH_3COOH	3.7573E-07	4.9797E-07	6.4016E-07	8.0211E-07	9.8328E-07
$(CH_3CO)_2O$	2.2257E-09	1.6092E-09	1.2268E-07	9.7564E-10	8.0283E-10
X CH_4	**1.1339E-06**	**1.4987E-06**	**2.2885E-06**	**2.4093E-06**	**2.9523E-06**
X CH_2CO	**6.6771E-09**	**4.8276E-09**	**3.6804E-07**	**2.9269E-09**	**2.4085E-09**
Y Anhydride	**5.8888E-03**	**3.2211E-03**	**1.6082E-01**	**1.2149E-03**	**8.1581E-04**

100 atm	1800 K	1900 K	2000 K
Phase	Vapor	Vapor	Vapor
CO_2	0.3333321	0.3333319	0.3333317
CH_4	0.3333321	0.3333319	0.3333317
CH_2CO	0.3333333	0.3333333	0.3333333
CH_3COOH	1.1829E-06	1.4001E-06	1.6338E-06
$(CH_3CO)_2O$	6.7930E-10	5.8817E-10	5.1914E-10
X CH_4	**3.5508E-06**	**4.2021E-06**	**4.9028E-06**
X CH_2CO	**2.0379E-09**	**1.7645E-09**	**1.5574E-09**
Y Anhydride	**5.7392E-04**	**4.1991E-04**	**3.1766E-04**

Table B-16: Equilibrium outlet moles, X CH_4, X CH_2CO and Y Anhydride for reaction (R B - 5) obtained from AspenPlus™ using the Peng-Robinson equation of state and stoichiometric inlet composition from 300 – 2000 K and 100 atm.

150 atm	300 K	400 K	500 K	600 K	700 K
Phase	Liquid	Vapor	Vapor	Vapor	Vapor
CO_2	0.0167741	0.3302119	0.3332922	0.3333304	0.3333328
CH_4	0.0167741	0.3302119	0.3332922	0.3333304	0.3333328
CH_2CO	0.0167741	0.3302119	0.3332922	0.3333304	0.3333329
CH_3COOH	3.1843E-10	1.6287E-09	5.1481E-09	1.4630E-08	3.3905E-08
$(CH_3CO)_2O$	0.3165591	3.1214E-03	4.1174E-05	2.8921E-06	4.7076E-07
X CH_4	**0.9496773**	**9.3643E-03**	**1.2354E-04**	**8.7201E-06**	**1.5140E-06**
X CH_2CO	**0.9496773**	**9.3643E-03**	**1.2352E-04**	**8.6762E-06**	**1.4123E-06**
Y Anhydride	**1.0000000**	**0.9999995**	**0.9998750**	**0.9949668**	**0.9328167**

150 atm	800 K	900 K	1000 K	1100 K	1200 K
Phase	Vapor	Vapor	Vapor	Vapor	Vapor
CO_2	0.3333331	0.3333332	0.3333331	0.3333330	0.3333329
CH_4	0.3333331	0.3333332	0.3333331	0.3333330	0.3333329
CH_2CO	0.3333332	0.3333333	0.3333333	0.3333333	0.3333333
CH_3COOH	6.7126E-08	1.1831E-07	1.9105E-07	2.8838E-07	4.1263E-07
$(CH_3CO)_2O$	1.2672E-07	4.7305E-08	2.2099E-08	1.2114E-08	7.4706E-09
X CH_4	**5.8154E-07**	**4.9683E-07**	**6.3945E-07**	**9.0148E-07**	**1.2603E-06**
X CH_2CO	**3.8016E-07**	**1.4191E-07**	**6.6296E-08**	**3.6343E-08**	**2.2412E-08**
Y Anhydride	**0.6537162**	**0.2856384**	**0.1036761**	**0.0403149**	**0.0177829**

Table B-16 continued

150 atm	1300 K	1400 K	1500 K	1600 K	1700 K
Phase	Vapor	Vapor	Vapor	Vapor	Vapor
CO_2	0.3333328	0.3333326	0.3333324	0.3333321	0.3333319
CH_4	0.3333328	0.3333326	0.3333324	0.3333321	0.3333319
CH_2CO	0.3333333	0.3333333	0.3333333	0.3333333	0.3333333
CH_3COOH	5.6541E-07	7.4765E-07	9.5963E-07	1.2011E-06	1.4713E-06
$(CH_3CO)_2O$	5.0345E-09	3.6328E-09	2.7657E-09	2.1973E-09	1.8069E-09
X CH_4	**1.7113E-06**	**2.2538E-06**	**2.8872E-06**	**3.6099E-06**	**4.4193E-06**
X CH_2CO	**1.5103E-08**	**1.0898E-08**	**8.2971E-09**	**6.5919E-09**	**5.4206E-09**
Y Anhydride	**8.8256E-03**	**4.8355E-03**	**2.8738E-03**	**1.8261E-03**	**1.2266E-03**

150 atm	1800 K	1900 K	2000 K
Phase	Vapor	Vapor	Vapor
CO_2	0.3333316	0.3333312	0.3333309
CH_4	0.3333316	0.3333312	0.3333309
CH_2CO	0.3333333	0.3333333	0.3333333
CH_3COOH	1.7692E-06	2.0934E-06	2.4423E-06
$(CH_3CO)_2O$	1.5281E-09	1.3227E-09	1.1672E-09
X CH_4	**5.3122E-06**	**6.2841E-06**	**7.3305E-06**
X CH_2CO	**4.5844E-09**	**3.9682E-09**	**3.5016E-09**
Y Anhydride	**8.6299E-04**	**6.3146E-04**	**4.7768E-04**

Table B-17: Equilibrium outlet moles, X CH_4, X CH_2CO and Y Anhydride for reaction (R B - 5) obtained from AspenPlus™ using the Peng-Robinson equation of state and stoichiometric inlet composition from 300 – 2000 K and 200 atm.

200 atm	300 K	400 K	500 K	600 K	700 K
Phase	Liquid	Vapor	Vapor	Vapor	Vapor
CO_2	0.0164483	0.3254755	0.3332472	0.3333277	0.3333324
CH_4	0.0164483	0.3254755	0.3332472	0.3333277	0.3333324
CH_2CO	0.0164483	0.3254755	0.3324720	0.3333277	0.3333324
CH_3COOH	3.1188E-10	3.4342E-09	8.4397E-09	2.1851E-08	4.8369E-08
$(CH_3CO)_2O$	0.3168850	7.8579E-03	8.6151E-05	5.6358E-06	8.8544E-07
X CH_4	**0.9506550**	**0.0235736**	**2.5848E-04**	**1.6973E-05**	**2.8014E-06**
X CH_2CO	**0.9506550**	**0.0235736**	**2.5845E-04**	**1.6907E-05**	**2.6563E-06**
Y Anhydride	**1.0000000**	**0.9999996**	**0.9999020**	**0.9961378**	**0.9482027**

200 atm	800 K	900 K	1000 K	1100 K	1200 K
Phase	Vapor	Vapor	Vapor	Vapor	Vapor
CO_2	0.3333330	0.3333331	0.3333330	0.3333329	0.3333328
CH_4	0.3333330	0.3333331	0.3333330	0.3333329	0.3333328
CH_2CO	0.3333331	0.3333332	0.3333333	0.3333333	0.3333333
CH_3COOH	9.3335E-08	1.6197E-07	2.5898E-07	3.8838E-07	5.5328E-07
$(CH_3CO)_2O$	2.3362E-07	8.6148E-08	3.9927E-08	2.1773E-08	1.3378E-08
X CH_4	**9.8087E-07**	**7.4434E-07**	**8.9673E-07**	**1.2305E-06**	**1.7000E-06**
X CH_2CO	**7.0086E-07**	**2.5844E-07**	**1.1978E-07**	**6.5318E-08**	**4.0134E-08**
Y Anhydride	**0.7145326**	**0.3472130**	**0.1335762**	**0.0530845**	**0.0236088**

Table B-17 continued

200 atm	1300 K	1400 K	1500 K	1600 K	1700 K
Phase	Vapor	Vapor	Vapor	Vapor	Vapor
CO_2	0.3333326	0.3333323	0.3333320	0.3333317	0.3333314
CH_4	0.3333326	0.3333323	0.3333320	0.3333317	0.3333314
CH_2CO	0.3333333	0.3333333	0.3333333	0.3333333	0.3333333
CH_3COOH	7.5585E-07	9.9739E-07	1.2783E-06	1.5984E-06	1.9567E-06
$(CH_3CO)_2O$	8.9928E-09	6.4775E-09	4.9252E-09	3.9095E-09	3.2128E-09
X CH_4	**2.2945E-06**	**3.0116E-06**	**3.8498E-06**	**4.8070E-06**	**5.8798E-06**
X CH_2CO	**2.6978E-08**	**1.9433E-08**	**1.4776E-08**	**1.1728E-08**	**9.6383E-09**
Y Anhydride	**0.0117577**	**6.4526E-03**	**3.8380E-03**	**2.4399E-03**	**1.6392E-03**

200 atm	1800 K	1900 K	2000 K
Phase	Vapor	Vapor	Vapor
CO_2	0.3333310	0.3333305	0.3333301
CH_4	0.3333310	0.3333305	0.3333301
CH_2CO	0.3333333	0.3333333	0.3333333
CH_3COOH	2.3519E-06	2.7821E-06	3.2453E-06
$(CH_3CO)_2O$	2.7160E-09	2.3502E-09	2.0735E-09
X CH_4	**7.0637E-06**	**8.3533E-06**	**9.7422E-06**
X CH_2CO	**8.1479E-09**	**7.0505E-09**	**6.2205E-09**
Y Anhydride	**1.1535E-03**	**8.4404E-04**	**6.3852E-04**

Table B-18: Equilibrium fractional conversion of methane (X CH_4) for reaction (R B-5) obtained from AspenPlus™ using the Peng-Robinson equation of state and stoichiometric inlet composition from 300 – 2000 K and 1 - 200 atm.

T (K)	1 atm	10 atm	25 atm	50 atm
300 K	3.2870E-05	3.9387E-03	**0.9468849**	**0.9474891**
400 K	9.9000E-08	1.0789E-05	7.7529E-05	3.9653E-04
500 K	2.9051E-09	2.9911E-07	2.0084E-06	9.0412E-06
600 K	4.5945E-10	2.9486E-08	1.8445E-07	7.7769E-07
700 K	5.7675E-10	1.0473E-08	4.6581E-08	1.6547E-07
800 K	1.1621E-09	1.3084E-08	3.8947E-08	9.9428E-08
900 K	2.1476E-09	2.2158E-08	5.8218E-08	1.2581E-07
1000 K	3.5919E-09	3.6250E-08	9.2536E-08	1.9074E-07
1100 K	5.5512E-09	5.1690E-08	1.4072E-07	2.8540E-07
1200 K	8.0698E-09	8.0617E-08	2.0320E-07	4.0932E-07
1300 K	1.1179E-08	1.1143E-07	2.8050E-07	5.6308E-07
1400 K	1.4892E-08	1.4728E-07	3.7294E-07	7.4713E-07
1500 K	1.9213E-08	1.9157E-07	4.8056E-07	9.6151E-07
1600 K	2.4132E-08	2.3070E-07	6.0311E-07	1.2057E-06
1700 K	2.9632E-08	2.9612E-07	7.4017E-07	1.4790E-06
1800 K	3.5687E-08	3.5665E-07	8.9112E-07	1.7800E-06
1900 K	4.2267E-08	4.2241E-07	1.0552E-06	2.1073E-06
2000 K	4.9340E-08	4.9308E-07	1.2316E-06	2.4593E-06

NOTE: Values in bold indicates liquid phase.

Table B-18 continued

T (K)	100 atm	150 atm	200 atm
300 K	**0.9486258**	**0.9496773**	**0.9506550**
400 K	2.6270E-03	9.3643E-03	2.3574E-02
500 K	4.5167E-05	1.2354E-04	2.5848E-04
600 K	3.4906E-06	8.7201E-06	1.6973E-05
700 K	6.5115E-07	1.5140E-06	2.8014E-06
800 K	2.9020E-07	5.8154E-07	9.8087E-07
900 K	2.9108E-07	4.9683E-07	7.4434E-07
1000 K	4.0399E-07	6.3945E-07	8.9673E-07
1100 K	5.8619E-07	9.0148E-07	1.2305E-06
1200 K	8.2977E-07	1.2603E-06	1.7000E-06
1300 K	1.1339E-06	1.7113E-06	2.2945E-06
1400 K	1.4987E-06	2.2538E-06	3.0116E-06
1500 K	1.9242E-06	2.8872E-06	3.8498E-06
1600 K	2.4093E-06	3.6099E-06	4.8070E-06
1700 K	2.9523E-06	4.4193E-06	5.8798E-06
1800 K	3.5508E-06	5.3122E-06	7.0637E-06
1900 K	4.2021E-06	6.2841E-06	8.3533E-06
2000 K	4.9028E-06	7.3305E-06	9.7422E-06

NOTE: Values in bold indicates liquid phase.

Table B-19: Equilibrium fractional conversion of ketene (X CH_2CO) for reaction (R B-5) obtained from AspenPlus™ using the Peng-Robinson equation of state and stoichiometric inlet composition from 300 – 2000 K and 1 - 200 atm.

T (K)	1 atm	10 atm	25 atm	50 atm
300 K	3.2870E-05	3.9387E-03	**0.9468849**	**0.9474891**
400 K	9.8995E-08	1.0789E-05	7.7529E-05	3.9653E-04
500 K	2.8576E-09	2.9861E-07	2.0070E-06	9.0380E-06
600 K	2.6825E-10	2.7518E-08	1.7929E-07	7.6655E-07
700 K	5.0367E-11	5.1161E-09	3.2799E-08	1.3661E-07
800 K	1.4686E-11	1.4834E-09	9.4223E-09	3.8671E-08
900 K	4.6710E-12	5.7915E-10	3.6582E-09	1.4707E-08
1000 K	2.3194E-12	2.7838E-10	1.7521E-09	7.0871E-09
1100 K	1.5502E-12	1.5551E-10	9.7647E-10	3.9350E-09
1200 K	9.6936E-13	9.7122E-11	6.0891E-10	2.4477E-09
1300 K	6.5943E-13	6.6027E-11	4.1352E-10	1.6594E-09
1400 K	4.7898E-13	4.7937E-11	2.9998E-10	1.2024E-09
1500 K	3.6633E-13	3.6651E-11	2.2924E-10	9.1806E-10
1600 K	2.9198E-13	2.9206E-11	1.8261E-10	7.3089E-10
1700 K	2.4064E-13	2.4066E-11	1.5044E-10	6.0189E-10
1800 K	2.0383E-13	2.0383E-11	1.2739E-10	5.0955E-10
1900 K	1.7662E-13	1.7660E-11	1.1036E-10	4.4133E-10
2000 K	1.5596E-13	1.5594E-11	9.7440E-11	3.8964E-10

NOTE: Values in bold indicates liquid phase.

Table B-19 continued

T (K)	100 atm	150 atm	200 atm
300 K	**0.9486258**	**0.9496773**	**0.9506550**
400 K	2.6270E-03	9.3643E-03	0.0235736
500 K	4.5158E-05	1.2352E-04	2.5845E-04
600 K	3.4649E-06	8.6762E-06	1.6907E-05
700 K	5.8831E-07	1.4123E-06	2.6563E-06
800 K	1.6212E-07	3.8016E-07	7.0086E-07
900 K	6.1380E-08	1.4191E-07	2.5844E-07
1000 K	2.8934E-08	6.6296E-08	1.1978E-07
1100 K	1.5957E-08	3.6343E-08	6.5318E-08
1200 K	9.8801E-09	2.2412E-08	4.0134E-08
1300 K	6.6771E-09	1.5103E-08	2.6978E-08
1400 K	4.8276E-09	1.0898E-08	1.9433E-08
1500 K	3.6804E-09	8.2971E-09	1.4776E-08
1600 K	2.9269E-09	6.5919E-09	1.1728E-08
1700 K	2.4085E-09	5.4206E-09	9.6383E-09
1800 K	2.0379E-09	4.5844E-09	8.1479E-09
1900 K	1.7645E-09	3.9682E-09	7.0505E-09
2000 K	1.5574E-09	3.5016E-09	6.2205E-09

NOTE: Values in bold indicates liquid phase.

Table B-20: Equilibrium fractional yield of acetic anhydride (Y Anhydride) for reaction (R B-5) obtained from AspenPlus™ using the Peng-Robinson equation of state and stoichiometric inlet composition from 300 – 2000 K and 1 - 200 atm.

T (K)	1 atm	10 atm	25 atm	50 atm
300 K	1.0000000	1.0000000	**1.0000000**	**1.0000000**
400 K	0.9999438	0.9999939	0.9999975	0.9999987
500 K	0.9836477	0.9983294	0.9993235	0.9996551
600 K	0.5838562	0.9332410	0.9720195	0.9856675
700 K	0.0873295	0.4884978	0.7041297	0.8255921
800 K	0.0126377	0.1133719	0.2419292	0.3889352
900 K	2.1750E-03	0.0261377	0.0628361	0.1168973
1000 K	6.4573E-04	7.6795E-03	0.0189345	0.0371566
1100 K	2.7925E-04	3.0084E-03	6.9392E-03	0.0137877
1200 K	1.2012E-04	1.2047E-03	2.9966E-03	5.9799E-03
1300 K	5.8991E-05	5.9254E-04	1.4742E-03	2.9470E-03
1400 K	3.2163E-05	3.2549E-04	8.0436E-04	1.6093E-03
1500 K	1.9067E-05	1.9132E-04	4.7703E-04	9.5481E-04
1600 K	1.2099E-05	1.2660E-04	3.0278E-04	6.0617E-04
1700 K	8.1210E-06	8.1272E-05	2.0325E-04	4.0696E-04
1800 K	5.7117E-06	5.7151E-05	1.4296E-04	2.8627E-04
1900 K	4.1785E-06	4.1807E-05	1.0459E-04	2.0943E-04
2000 K	3.1609E-06	3.1625E-05	7.9116E-05	1.5844E-04

NOTE: Values in bold indicates liquid phase.

Table B-20 continued

T (K)	100 atm	150 atm	200 atm
300 K	**1.0000000**	**1.0000000**	**1.0000000**
400 K	0.9999993	0.9999995	0.9999996
500 K	0.9998203	0.9998750	0.9999020
600 K	0.9926291	0.9949668	0.9961378
700 K	0.9034923	0.9328167	0.9482027
800 K	0.5586426	0.6537162	0.7145326
900 K	0.2108668	0.2856384	0.3472130
1000 K	0.0716197	0.1036761	0.1335762
1100 K	0.0272209	0.0403149	0.0530845
1200 K	0.0119071	0.0177829	0.0236088
1300 K	5.8888E-03	8.8256E-03	0.0117577
1400 K	3.2211E-03	4.8355E-03	6.4526E-03
1500 K	1.9127E-03	2.8738E-03	3.8380E-03
1600 K	1.2149E-03	1.8261E-03	2.4399E-03
1700 K	8.1581E-04	1.2266E-03	1.6392E-03
1800 K	5.7392E-04	8.6299E-04	1.1535E-03
1900 K	4.1991E-04	6.3146E-04	8.4404E-04
2000 K	3.1766E-04	4.7768E-04	6.3852E-04

NOTE: Values in bold indicates liquid phase.

B.3. VINYL ACETATE FROM ETHYLENE AND OXYGEN

Equilibrium thermodynamic calculations were performed for the formation of vinyl acetate ($CH_3CO_2CH=CH_2$) from carbon dioxide, methane, ethylene (C_2H_4) and oxygen:

$$CO_2 + CH_4 + C_2H_4 + ½\ O_2 \leftrightarrow CH_3CO_2CH=CH_2 + H_2O \qquad \text{(R B-7)}$$

Acetic acid was allowed in the system, thus permitting the following reactions:

$$CO_2 + CH_4 \leftrightarrow CH_3COOH \qquad \text{(R B-2)}$$

$$CH_3COOH + C_2H_4 + ½\ O_2 \leftrightarrow CH_3CO_2CH=CH_2 + H_2O \qquad \text{(R B-8)}$$

Equilibrium thermodynamic calculations were performed on this system. The side reactions of methane combustion:

$$CH_4 + 2\ O_2 \leftrightarrow CO_2 + H_2O \qquad \text{(R B-9)}$$

ethylene combustion:

$$C_2H_4 + 2\ O_2 \leftrightarrow 2\ CO_2 + H_2O \qquad \text{(R B-10)}$$

and partial oxidation of ethylene:

$$C_2H_4 + O_2 \leftrightarrow CO_2 + CH_4 \qquad \text{(R B-11)}$$

were restricted by setting the extents of those reactions to zero.

The equilibrium thermodynamic calculations for reaction (R B-7) were performed using the AspenPlus™ engineering simulation software. The RGIBBS reactor model was used to perform a Gibbs free energy minimization on the system to give the chemical and phase equilibrium composition at various temperatures and pressures. These calculations do not take into account any surface interactions. Molecular interactions are taken into account

in the Peng-Robinson equation of state. The inlet composition, inlet temperature, inlet pressure, reactor temperature and reactor pressure were specified for each reaction. The inlet conditions were set equal to the reactor conditions.

A stoichiometric inlet composition of 0.286 mole fraction of CO_2, 0.286 mole fraction of CH_4, and 0.286 mole fraction of C_2H_4 and 0.142 mole fraction of O_2 was used. The AspenPlus™ calculations were performed for a wide range of temperatures and pressures, 1 - 200 K atm and 300 – 2000 K. The calculations were performed using the Peng-Robinson equation of state.

Interaction parameters of 0.0919 for CO_2 and CH_4, 0.0552 for CO_2 and C_2H_4, and 0.0215 for CH_4 and C_2H_4 obtained from the AspenPlus™ data base were used. No other interaction parameters were available, thus a default of 0.0 was used for all other interaction parameters.

The equilibrium fractional conversion of methane (X CH_4) was calculated using:

$$X\ CH_4 = \#\ \text{Moles of } CH_4 \text{ reacted} / \#\ \text{Inlet moles of } CH_4 \qquad \text{(E B-1)}$$

When the outlet moles of methane given by AspenPlus™ did not have enough significant figures, the sum of outlet moles of acetic acid and vinyl acetate was used as the number of moles of methane that reacted.

The equilibrium fractional conversion of ethylene (X C_2H_4) was calculated using:

$$X\ C_2H_4 = \#\ \text{Moles of } C_2H_4 \text{ reacted} / \#\ \text{Inlet moles of } C_2H_4 \qquad \text{(E B-6)}$$

When the outlet moles of methanol given by AspenPlus™ did not have enough significant figures, the number of outlet moles of vinyl acetate was used as the number of moles of ethylene that reacted.

The equilibrium yield of vinyl acetate (Y VA) was calculated using:

$$Y\ VA = \text{Outlet } CH_3CO_2CH{=}CH_2 / \text{Outlet } CH_3CO_2CH{=}CH_2 + CH_3COOH \qquad \text{(E B-7)}$$

Data from these calculations can be found in tables B-21 to B-30.

Table B-21: Equilibrium outlet moles, X CH_4, X C_2H_4 and Y VA for reaction (R B - 7) obtained from AspenPlus™ using the Peng-Robinson equation of state and stoichiometric inlet composition from 300 – 2000 K and 1 atm.

1 atm	300 K	400 K	500 K	600 K	700 K
Phase	Liquid	Vapor	Vapor	Vapor	Vapor
CO_2	1.1559E-07	2.6563E-03	0.0281700	0.1187654	0.2249001
CH_4	1.1559E-07	2.6563E-03	0.0281700	0.1187654	0.2249001
C_2H_4	1.1559E-07	2.6563E-03	0.0281700	0.1187654	0.2249001
O_2	4.2795E-08	1.3281E-03	0.0140849	0.0593826	0.1124500
H_2O	0.2857142	0.2830580	0.2575443	0.1669489	0.0608141
CH_3COOH	3.0824E-20	2.2956E-16	1.8589E-13	1.0817E-11	8.7888E-11
Vinyl Acetate	0.2857142	0.2830580	0.2575443	0.1669489	0.0608141
X CH_4	**0.9999997**	**0.9907030**	**0.9014051**	**0.5843212**	**0.2128494**
X C_2H_4	**0.9999997**	**0.9907030**	**0.9014051**	**0.5843212**	**0.2128494**
Y VA	**1.0000000**	**1.0000000**	**1.0000000**	**1.0000000**	**1.0000000**

1 atm	800 K	900 K	1000 K	1100 K	1200 K
Phase	Vapor	Vapor	Vapor	Vapor	Vapor
CO_2	0.2677325	0.2795559	0.2831586	0.2844714	0.2850306
CH_4	0.2677325	0.2795559	0.2831586	0.2844717	0.2850306
C_2H_4	0.2677325	0.2795559	0.2831586	0.2844714	0.2850306
O_2	0.1338662	0.1397780	0.1415793	0.1422357	0.1425153
H_2O	0.0179818	6.1584E-03	2.5556E-03	1.2429E-03	6.8365E-04
CH_3COOH	2.5352E-10	5.0697E-10	8.6662E-10	1.3496E-09	1.9685E-09
Vinyl Acetate	0.0179818	6.1584E-03	2.5557E-03	1.2429E-03	6.8365E-04
X CH_4	**0.0629363**	**0.0215542**	**8.9448E-03**	**4.3503E-03**	**2.3928E-03**
X C_2H_4	**0.0629363**	**0.0215542**	**8.9448E-03**	**4.3503E-03**	**2.3928E-03**
Y VA	**1.0000000**	**0.9999999**	**0.9999997**	**0.9999989**	**0.9999971**

Table B-21 continued

1 atm	1300 K	1400 K	1500 K	1600 K	1700 K
Phase	Vapor	Vapor	Vapor	Vapor	Vapor
CO_2	0.2853006	0.2854141	0.2855276	0.2855787	0.2856119
CH_4	0.2853006	0.2854141	0.2855276	0.2855787	0.2856119
C_2H_4	0.2853006	0.2854141	0.2855276	0.2855787	0.2856119
O_2	0.1426503	0.1427071	0.1427638	0.1427893	0.1428059
H_2O	4.1365E-04	2.8017E-04	1.8669E-04	1.3559E-04	1.0243E-04
CH_3COOH	2.7310E-09	3.7156E-09	4.7002E-09	5.9053E-09	7.2525E-09
Vinyl Acetate	4.1365E-04	2.8017E-04	1.8669E-04	1.3559E-04	1.0243E-04
X CH_4	**1.4478E-03**	**9.8061E-04**	**6.5343E-04**	**4.7457E-04**	**3.5852E-04**
X C_2H_4	**1.4478E-03**	**9.8060E-04**	**6.5342E-04**	**4.7455E-04**	**3.5850E-04**
Y VA	**0.9999934**	**0.9999867**	**0.9999748**	**0.9999564**	**0.9999292**

1 atm	1800 K	1900 K	2000 K
Phase	Vapor	Vapor	Vapor
CO_2	0.2856343	0.2856502	0.2856616
CH_4	0.2856343	0.2856502	0.2856616
C_2H_4	0.2856343	0.2856502	0.2856617
O_2	0.1428172	0.1428251	0.1428308
H_2O	7.9944E-05	6.4122E-05	4.9532E-05
CH_3COOH	8.7357E-09	1.0348E-08	1.2080E-08
Vinyl Acetate	7.9944E-05	6.4122E-05	4.9532E-05
X CH_4	**2.7983E-04**	**2.2446E-04**	**1.7340E-04**
X C_2H_4	**2.7980E-04**	**2.2443E-04**	**1.7336E-04**
Y VA	**0.9998907**	**0.9998387**	**0.9997562**

Table B-22: Equilibrium outlet moles, X CH_4, X C_2H_4 and Y VA for reaction (R B - 7) obtained from AspenPlus™ using the Peng-Robinson equation of state and stoichiometric inlet composition from 300 – 2000 K and 10 atm.

10 atm	300 K	400 K	500 K	600 K	700 K
Phase	Liquid	Liquid	Vapor	Vapor	Vapor
CO_2	1.1542E-07	2.3497E-05	0.0100907	0.0492667	0.1313426
CH_4	1.1454E-07	2.3497E-05	0.0100907	0.0492667	0.1313426
C_2H_4	1.1454E-07	2.3497E-05	1.0091E-02	0.0492667	0.1313426
O_2	4.2271E-08	1.1734E-05	5.0454E-03	0.0246333	0.0656712
H_2O	0.2857142	0.2856908	0.2756235	0.2364475	0.1543717
CH_3COOH	3.0444E-20	1.4819E-15	2.9049E-13	2.3200E-11	3.6475E-10
Vinyl Acetate	0.2857142	0.2856908	0.2756235	0.2364475	0.1543717
X CH_4	**0.9999997**	**0.9999178**	**0.9646823**	**0.8275663**	**0.5403010**
X C_2H_4	**0.9999997**	**0.9999178**	**0.9646823**	**0.8275663**	**0.5403010**
Y VA	**1.0000000**	**1.0000000**	**1.0000000**	**1.0000000**	**1.0000000**

10 atm	800 K	900 K	1000 K	1100 K	1200 K
Phase	Vapor	Vapor	Vapor	Vapor	Vapor
CO_2	0.2127866	0.2552016	0.2721010	0.2789066	0.2819248
CH_4	0.2127866	0.2552016	0.2721010	0.2789066	0.2819248
C_2H_4	0.2127866	0.2552016	0.2721010	0.2789067	0.2819248
O_2	0.1063933	0.1276008	0.1360505	0.1394533	0.1409624
H_2O	0.0729276	0.0305126	0.0136133	6.8076E-03	3.7895E-03
CH_3COOH	1.7705E-09	4.4127E-09	8.1646E-09	1.3107E-08	1.9366E-08
Vinyl Acetate	0.0729276	0.0305126	0.0136133	6.8076E-03	3.7895E-03
X CH_4	**0.2552466**	**0.1067941**	**0.0476466**	**0.0238268**	**0.0132631**
X C_2H_4	**0.2552466**	**0.1067941**	**0.0476466**	**0.0238267**	**0.0132631**
Y VA	**1.0000000**	**0.9999999**	**0.9999994**	**0.9999981**	**0.9999949**

Table B-22 continued

10 atm	1300 K	1400 K	1500 K	1600 K	1700 K
Phase	Vapor	Vapor	Vapor	Vapor	Vapor
CO_2	0.2834082	0.2842060	0.2846686	0.2849540	0.2851395
CH_4	0.2834082	0.2842060	0.2846686	0.2849540	0.2851395
C_2H_4	0.2834083	0.2842060	0.2846686	0.2849541	0.2851396
O_2	0.1417041	0.1421030	0.1423343	0.1424770	0.1425698
H_2O	2.3060E-03	1.5083E-03	1.0457E-03	7.6021E-04	5.7677E-04
CH_3COOH	2.7035E-08	3.6164E-08	4.6766E-08	5.8823E-08	7.2296E-08
Vinyl Acetate	2.3060E-03	1.5083E-03	1.0457E-03	7.6021E-04	5.7468E-04
X CH_4	**8.0712E-03**	**5.2790E-03**	**3.6600E-03**	**2.6610E-03**	**2.0116E-03**
X C_2H_4	**8.0711E-03**	**5.2789E-03**	**3.6598E-03**	**2.6607E-03**	**2.0114E-03**
Y VA	**0.9999883**	**0.9999760**	**0.9999553**	**0.9999226**	**0.9998742**

10 atm	1800 K	1900 K	2000 K
Phase	Vapor	Vapor	Vapor
CO_2	0.2852655	0.2853542	0.2854186
CH_4	0.2852655	0.2853542	0.2854186
C_2H_4	0.2852656	0.2853543	0.2854187
O_2	0.1426328	0.1426771	0.1427093
H_2O	4.4873E-04	3.6004E-04	2.9559E-04
CH_3COOH	8.7125E-08	1.0324E-07	1.2055E-07
Vinyl Acetate	4.4873E-04	3.6004E-04	2.9559E-04
X CH_4	**1.5709E-03**	**1.2605E-03**	**1.0350E-03**
X C_2H_4	**1.5706E-03**	**1.2601E-03**	**1.0346E-03**
Y VA	**0.9998059**	**0.9997133**	**0.9995923**

Table B-23: Equilibrium outlet moles, X CH_4, X C_2H_4 and Y VA for reaction (R B - 7) obtained from AspenPlus™ using the Peng-Robinson equation of state and stoichiometric inlet composition from 300 – 2000 K and 25 atm.

25 atm	300 K	400 K	500 K	600 K	700 K
Phase	Liquid	Liquid	Vapor	Vapor	Vapor
CO_2	7.0102E-08	2.3184E-05	6.0522E-03	0.0503743	0.0946963
CH_4	7.0102E-08	2.3184E-05	6.0522E-03	0.0503743	0.0946963
C_2H_4	7.0102E-08	2.3184E-05	6.0522E-03	0.0503743	0.0946963
O_2	2.0051E-08	1.1577E-05	3.0261E-03	0.0251871	0.0473481
H_2O	2.8571E-01	2.8569E-01	2.7966E-01	0.2353400	0.1910179
CH_3COOH	9.3560E-21	1.4317E-15	3.6057E-13	2.7137E-10	5.4238E-10
Vinyl Acetate	0.2857142	0.2856911	0.2796621	0.2353400	0.1910179
X CH_4	**0.9999997**	**0.9999189**	**0.9788174**	**0.8236900**	**0.6685627**
X C_2H_4	**0.9999997**	**0.9999189**	**0.9788174**	**0.8236900**	**0.6685627**
Y VA	**1.0000000**	**1.0000000**	**1.0000000**	**1.0000000**	**1.0000000**

25 atm	800 K	900 K	1000 K	1100 K	1200 K
Phase	Vapor	Vapor	Vapor	Vapor	Vapor
CO_2	0.1752590	0.2323265	0.2602048	0.2725751	0.2783025
CH_4	0.1752590	0.2323265	0.2602048	0.2725751	0.2783025
C_2H_4	0.1752591	0.2323266	0.2602048	0.2725752	0.2783026
O_2	0.0876295	0.1161633	0.1301024	0.1362876	0.1391513
H_2O	0.1104552	0.0533877	0.0255095	0.0131391	7.4117E-03
CH_3COOH	3.2874E-09	9.5940E-09	1.9125E-08	3.1698E-08	4.7511E-08
Vinyl Acetate	0.1104552	0.0533877	0.0255095	0.0131391	7.4117E-03
X CH_4	**0.3865932**	**0.1868570**	**0.0892833**	**0.0459870**	**0.0259411**
X C_2H_4	**0.3865932**	**0.1868570**	**0.0892833**	**0.0459869**	**0.0259409**
Y VA	**1.0000000**	**0.9999998**	**0.9999993**	**0.9999976**	**0.9999936**

Table B-23 continued

25 atm	1300 K	1400 K	1500 K	1600 K	1700 K
Phase	Vapor	Vapor	Vapor	Vapor	Vapor
CO_2	0.2811747	0.2827350	0.2836447	0.2842079	0.2845746
CH_4	0.2811747	0.2827350	0.2836447	0.2842079	0.2845746
C_2H_4	0.2811748	0.2827351	0.2836449	0.2842080	0.2845748
O_2	0.1405874	0.1413676	0.1418224	0.1421040	0.1422874
H_2O	4.5395E-03	2.9792E-03	2.0694E-03	1.5624E-03	1.1395E-03
CH_3COOH	6.6788E-08	8.9667E-08	1.1620E-07	1.4634E-07	1.8001E-07
Vinyl Acetate	4.5395E-03	2.9792E-03	2.0694E-03	1.5062E-03	1.1395E-03
X CH_4	**0.0158886**	**0.0104274**	**7.2434E-03**	**5.2724E-03**	**3.9888E-03**
X C_2H_4	**0.0158884**	**0.0104271**	**7.2430E-03**	**5.2718E-03**	**3.9881E-03**
Y VA	**0.9999853**	**0.9999699**	**0.9999439**	**0.9999029**	**0.9998420**

25 atm	1800 K	1900 K	2000 K
Phase	Vapor	Vapor	Vapor
CO_2	0.2848239	0.2849995	0.2851272
CH_4	0.2848239	0.2849995	0.2851272
C_2H_4	0.2848241	0.2849995	0.2851275
O_2	0.1424120	0.1424999	0.1425638
H_2O	8.9019E-04	7.1449E-04	5.8674E-04
CH_3COOH	2.1706E-07	2.5731E-07	3.0057E-07
Vinyl Acetate	8.9019E-04	7.1449E-04	5.8674E-04
X CH_4	**3.1164E-03**	**2.5016E-03**	**2.0547E-03**
X C_2H_4	**3.1157E-03**	**2.5007E-03**	**2.0536E-03**
Y VA	**0.9997562**	**0.9996400**	**0.9994880**

Table B-24: Equilibrium outlet moles, X CH_4, X C_2H_4 and Y VA for reaction (R B - 7) obtained from AspenPlus™ using the Peng-Robinson equation of state and stoichiometric inlet composition from 300 – 2000 K and 50 atm.

50 atm	300 K	400 K	500 K	600 K	700 K
Phase	Liquid	Liquid	Vapor	Vapor	Vapor
CO_2	1.0878E-07	2.2699E-05	0.0109042	0.0217858	0.0827193
CH_4	1.0878E-07	2.2699E-05	0.0109042	0.0217858	0.0827193
C_2H_4	1.0878E-07	2.2699E-05	0.0109042	0.0217858	0.0827193
O_2	3.9391E-08	1.1335E-05	5.4521E-03	0.0108929	0.0413596
H_2O	0.2857142	0.2856916	0.2748100	0.2639284	0.2029950
CH_3COOH	2.8092E-20	1.4774E-15	1.8150E-11	3.6299E-11	2.4780E-09
Vinyl Acetate	0.2857142	0.2856916	0.2748100	0.2639284	0.2029950
X CH_4	**0.9999997**	**0.9999206**	**0.9618350**	**0.9237494**	**0.7104823**
X C_2H_4	**0.9999997**	**0.9999206**	**0.9618350**	**0.9237494**	**0.7104823**
Y VA	**1.0000000**	**1.0000000**	**1.0000000**	**1.0000000**	**1.0000000**

50 atm	800 K	900 K	1000 K	1100 K	1200 K
Phase	Vapor	Vapor	Vapor	Vapor	Vapor
CO_2	0.1436528	0.2080848	0.2458360	0.2644405	0.2735121
CH_4	0.1436528	0.2080848	0.2458360	0.2644405	0.2735121
C_2H_4	0.1436528	0.2080849	0.2458361	0.2644405	0.2735122
O_2	0.0718263	0.1040424	0.1229180	0.1322203	0.1367561
H_2O	0.1420615	0.0776294	0.0398782	0.0212737	0.0122020
CH_3COOH	4.9197E-09	1.6381E-08	3.5300E-08	6.0751E-08	9.2694E-08
Vinyl Acetate	0.1420615	0.0776294	0.0398782	0.0212737	0.0122020
X CH_4	**0.4972153**	**0.2717030**	**0.1395738**	**0.0744582**	**0.0427073**
X C_2H_4	**0.4972153**	**0.2717029**	**0.1395737**	**0.0744580**	**0.0427070**
Y VA	**1.0000000**	**0.9999998**	**0.9999991**	**0.9999971**	**0.9999924**

Table B-24 continued

50 atm	1300 K	1400 K	1500 K	1600 K	1700 K
Phase	Vapor	Vapor	Vapor	Vapor	Vapor
CO_2	0.2781784	0.2807468	0.2822549	0.2831925	0.2838046
CH_4	0.2781784	0.2807468	0.2822549	0.2831925	0.2838046
C_2H_4	0.2781785	0.2807469	0.2822552	0.2831928	0.2838049
O_2	0.1390892	0.1403735	0.1411276	0.1415964	0.1419025
H_2O	7.5358E-03	4.9674E-03	3.4591E-03	2.5215E-03	1.9093E-03
CH_3COOH	1.3146E-07	1.7733E-07	2.3041E-07	2.9066E-07	3.5792E-07
Vinyl Acetate	7.5358E-03	4.9674E-03	3.4591E-03	2.5215E-03	1.9093E-03
X CH_4	**0.0263758**	**0.0173863**	**1.2108E-02**	**8.8263E-03**	**6.6839E-03**
X C_2H_4	**0.0263753**	**0.0173857**	**1.2107E-02**	**8.8253E-03**	**6.6827E-03**
Y VA	**0.9999826**	**0.9999643**	**0.9999334**	**0.9998847**	**0.9998126**

50 atm	1800 K	1900 K	2000 K
Phase	Vapor	Vapor	Vapor
CO_2	0.2842213	0.2845152	0.2847291
CH_4	0.2842213	0.2845152	0.2847281
C_2H_4	0.2842217	0.2845158	0.2847297
O_2	0.1421108	0.1422579	0.1423648
H_2O	1.4926E-03	1.1985E-03	9.8458E-04
CH_3COOH	4.3192E-07	5.1231E-07	5.9870E-07
Vinyl Acetate	1.4626E-03	1.1985E-03	9.8458E-04
X CH_4	**5.1206E-03**	**4.1967E-03**	**3.4481E-03**
X C_2H_4	**5.1191E-03**	**4.1949E-03**	**3.4460E-03**
Y VA	**0.9997048**	**0.9995727**	**0.9993923**

Table B-25: Equilibrium outlet moles, X CH_4, X C_2H_4 and Y VA for reaction (R B - 7) obtained from AspenPlus™ using the Peng-Robinson equation of state and stoichiometric inlet composition from 300 – 2000 K and 100 atm.

100 atm	300 K	400 K	500 K	600 K	700 K
Phase	Liquid	Liquid	Liquid	Vapor	Vapor
CO_2	9.4389E-08	2.1849E-05	6.6009E-04	0.0124143	0.0619558
CH_4	9.4389E-08	2.1849E-05	6.6009E-04	0.1241430	0.1178201
C_2H_4	9.4389E-08	2.1849E-05	6.6009E-04	0.1241430	0.1178201
O_2	3.2195E-08	1.0909E-05	3.3003E-04	6.2072E-03	0.0309779
H_2O	0.2857142	0.2856924	0.2850542	0.2732999	0.2237585
CH_3COOH	1.8728E-20	1.4697E-15	9.1817E-13	4.7658E-11	3.5457E-09
Vinyl Acetate	0.2857142	0.2856924	0.2850542	0.2732999	0.2237585
X CH_4	**0.9999997**	**0.9999234**	**0.9976897**	**0.9565497**	**0.7831548**
X C_2H_4	**0.9999997**	**0.9999234**	**0.9976897**	**0.9565497**	**0.7831548**
Y VA	**1.0000000**	**1.0000000**	**1.0000000**	**1.0000000**	**1.0000000**

100 atm	800 K	900 K	1000 K	1100 K	1200 K
Phase	Vapor	Vapor	Vapor	Vapor	Vapor
CO_2	0.1114972	0.1782086	0.2254423	0.2519633	0.2658701
CH_4	0.1114972	0.1782086	0.2254423	0.2519633	0.2658701
C_2H_4	0.1114972	0.1782086	0.2254424	0.2519634	0.2658703
O_2	0.0557486	0.0891042	0.1127212	0.1259817	0.1329351
H_2O	0.1742171	0.1075057	0.0602719	0.0337509	0.0198440
CH_3COOH	7.0438E-09	2.6578E-08	6.2796E-08	1.1376E-07	1.7817E-07
Vinyl Acetate	0.1742171	0.1075057	0.0602719	0.0337509	0.0198440
X CH_4	**0.6097599**	**0.3762700**	**0.2109519**	**0.1181285**	**0.0694546**
X C_2H_4	**0.6097599**	**0.3762700**	**0.2109517**	**0.1181282**	**0.0694540**
Y VA	**1.0000000**	**0.9999998**	**0.9999990**	**0.9999966**	**0.9999910**

Table B-25 continued

100 atm	1300 K	1400 K	1500 K	1600 K	1700 K
Phase	Vapor	Vapor	Vapor	Vapor	Vapor
CO_2	0.2733011	0.2774752	0.2799540	0.2815052	0.2825219
CH_4	0.2733011	0.2774752	0.2799540	0.2815052	0.2825219
C_2H_4	0.2733014	0.2774755	0.2799545	0.2815057	0.2825227
O_2	0.1366507	0.1387377	0.1399772	0.1407529	0.1412613
H_2O	0.0124129	8.2388E-03	5.7598E-03	4.2086E-03	3.1916E-03
CH_3COOH	2.5611E-07	3.4801E-07	4.5410E-07	5.7436E-07	7.0850E-07
Vinyl Acetate	0.0124129	8.2388E-03	5.7598E-03	4.2086E-03	3.1916E-03
X CH_4	**0.0434460**	**0.0288369**	**0.0201610**	**0.0147320**	**0.0111732**
X C_2H_4	**0.0434452**	**0.0288357**	**0.0201594**	**0.0147300**	**0.0111707**
Y VA	**0.9999794**	**0.9999578**	**0.9999212**	**0.9998635**	**0.9997781**

100 atm	1800 K	1900 K	2000 K
Phase	Vapor	Vapor	Vapor
CO_2	0.2832159	0.2837063	0.2840635
CH_4	0.2832159	0.2837063	0.2840635
C_2H_4	0.2832168	0.2837073	0.2840647
O_2	0.1416084	0.1418537	0.1420324
H_2O	2.4975E-03	2.0069E-03	1.6496E-03
CH_3COOH	8.5603E-07	1.0163E-06	1.1886E-06
Vinyl Acetate	2.4975E-03	2.0069E-03	1.6496E-03
X CH_4	**8.7444E-03**	**7.0278E-03**	**5.7776E-03**
X C_2H_4	**8.7414E-03**	**7.0243E-03**	**5.7735E-03**
Y VA	**0.9996574**	**0.9994939**	**0.9992800**

Table B-26: Equilibrium outlet moles, X CH_4, X C_2H_4 and Y VA for reaction (R B - 7) obtained from AspenPlus™ using the Peng-Robinson equation of state and stoichiometric inlet composition from 300 – 2000 K and 150 atm.

150 atm	300 K	400 K	500 K	600 K	700 K
Phase	Liquid	Liquid	Vapor	Vapor	Vapor
CO_2	7.9997E-08	2.1121E-05	6.0182E-04	9.1788E-03	0.0303708
CH_4	7.9997E-08	2.1121E-05	6.0182E-04	0.0650431	0.0303708
C_2H_4	7.9997E-08	2.1121E-05	6.0182E-04	0.0650431	0.0303708
O_2	2.4998E-08	1.0545E-05	3.0089E-04	4.5894E-03	0.0151854
H_2O	0.2857142	0.2856932	0.2851125	0.2765355	0.2553434
CH_3COOH	9.3640E-21	1.4902E-15	9.3393E-13	5.6117E-11	1.2042E-09
Vinyl Acetate	0.2857142	0.2856932	0.2851125	0.2765355	0.2553434
X CH_4	**0.9999997**	**0.9999262**	**0.9978936**	**0.9678743**	**0.8937019**
X C_2H_4	**0.9999997**	**0.9999262**	**0.9978936**	**0.9678743**	**0.8937019**
Y VA	**1.0000000**	**1.0000000**	**1.0000000**	**1.0000000**	**1.0000000**

150 atm	800 K	900 K	1000 K	1100 K	1200 K
Phase	Vapor	Vapor	Vapor	Vapor	Vapor
CO_2	0.0930922	0.1586412	0.2104027	0.2420530	0.2595496
CH_4	0.0930922	0.1586412	0.2104027	0.2420530	0.2595496
C_2H_4	0.0930922	0.1586412	0.2104027	0.2420532	0.2595498
O_2	0.0465461	0.0793206	0.1052014	0.1210266	0.1297749
H_2O	0.1926220	0.1270730	0.0753115	0.0436611	0.0261644
CH_3COOH	8.5633E-09	3.4454E-08	8.6157E-08	1.6180E-07	2.5851E-07
Vinyl Acetate	0.1926220	0.1270730	0.0753115	0.0436611	0.0261644
X CH_4	**0.6741770**	**0.4447556**	**0.2635906**	**0.1528144**	**0.0915763**
X C_2H_4	**0.6741770**	**0.4447555**	**0.2635903**	**0.1528139**	**0.0915754**
Y VA	**1.0000000**	**0.9999997**	**0.9999989**	**0.9999963**	**0.9999901**

Table B-26 continued

150 atm	1300 K	1400 K	1500 K	1600 K	1700 K
Phase	Vapor	Vapor	Vapor	Vapor	Vapor
CO_2	0.2691792	0.2746773	0.2779728	0.2800463	0.2814101
CH_4	0.2691792	0.2746773	0.2779728	0.2800463	0.2841010
C_2H_4	0.2691796	0.2746778	0.2779735	0.2800472	0.2814111
O_2	0.1345898	0.1373389	0.1389867	0.1400236	0.1407056
H_2O	0.0165346	0.0110364	7.7408E-03	5.6671E-03	4.3032E-03
CH_3COOH	3.7561E-07	5.1343E-07	6.7229E-07	8.5220E-07	1.0528E-06
Vinyl Acetate	0.0165346	0.0110364	7.7408E-03	5.6671E-03	4.3032E-03
X CH_4	**0.0578724**	**0.0386292**	**0.0270951**	**0.0198379**	**0.0150647**
X C_2H_4	**0.0578711**	**0.0386274**	**0.0270928**	**0.0198349**	**0.0150611**
Y VA	**0.9999773**	**0.9999535**	**0.9999132**	**0.9998496**	**0.9997554**

150 atm	1800 K	1900 K	2000 K
Phase	Vapor	Vapor	Vapor
CO_2	0.2823428	0.2830030	0.2834843
CH_4	0.2823428	0.2830030	0.2834843
C_2H_4	0.2823441	0.2830045	0.2834860
O_2	0.1411720	0.1415022	0.1417430
H_2O	3.3702E-03	2.7098E-03	2.2283E-03
CH_3COOH	1.2733E-06	1.5130E-06	1.7706E-06
Vinyl Acetate	3.3702E-03	2.7098E-03	2.2283E-03
X CH_4	**1.1800E-02**	**9.4896E-03**	**7.8051E-03**
X C_2H_4	**1.1796E-02**	**9.4843E-03**	**7.7989E-03**
Y VA	**0.9996223**	**0.9994420**	**0.9992060**

Table B-27: Equilibrium outlet moles, X CH_4, X C_2H_4 and Y VA for reaction (R B - 7) obtained from AspenPlus™ using the Peng-Robinson equation of state and stoichiometric inlet composition from 300 – 2000 K and 200 atm.

200 atm	300 K	400 K	500 K	600 K	700 K
Phase	Liquid	Liquid	Liquid	Vapor	Vapor
CO_2	6.5605E-08	2.7180E-05	5.4354E-04	5.9432E-03	0.0432228
CH_4	6.5605E-08	2.7180E-05	5.4354E-04	5.9432E-03	0.0432228
C_2H_4	6.5605E-08	2.7180E-05	5.4354E-04	5.9432E-03	0.0432228
O_2	1.7802E-08	1.3589E-05	2.7176E-04	2.9716E-03	0.0216113
H_2O	0.2857142	0.2854425	0.2851707	0.2797711	0.2424915
CH_3COOH	0.0000000	1.5302E-15	9.4968E-13	6.4576E-11	4.9216E-09
Vinyl Acetate	0.2857142	0.2854425	0.2851707	0.2797711	0.2424915
X CH_4	**0.9999997**	**0.9990486**	**0.9980975**	**0.9791989**	**0.8487203**
X C_2H_4	**0.9999997**	**0.9990486**	**0.9980975**	**0.9791989**	**0.8487203**
Y VA	**1.0000000**	**1.0000000**	**1.0000000**	**1.0000000**	**1.0000000**

200 atm	800 K	900 K	1000 K	1100 K	1200 K
Phase	Vapor	Vapor	Vapor	Vapor	Vapor
CO_2	0.0805023	0.1441137	0.1983349	0.2336596	0.2540240
CH_4	0.0805023	0.1441137	0.1983349	0.2336596	0.2540240
C_2H_4	0.0805023	0.1441137	0.1983350	0.2336598	0.2540243
O_2	0.0402511	0.0720568	0.0991674	0.1168299	0.1270122
H_2O	0.2052119	0.1416006	0.0873793	0.0520544	0.0316899
CH_3COOH	9.7787E-09	4.0986E-08	1.0670E-07	2.0605E-07	3.3463E-07
Vinyl Acetate	0.2052119	0.1416006	0.0873793	0.0520544	0.0316899
X CH_4	**0.7182417**	**0.4956022**	**0.3058279**	**0.1821911**	**0.1109158**
X C_2H_4	**0.7182417**	**0.4956021**	**0.3058276**	**0.1821904**	**0.1109147**
Y VA	**1.0000000**	**0.9999997**	**0.9999988**	**0.9999960**	**0.9999894**

Table B-27 continued

200 atm	1300 K	1400 K	1500 K	1600 K	1700 K
Phase	Vapor	Vapor	Vapor	Vapor	Vapor
CO_2	0.2655115	0.2721629	0.2761820	0.2787230	0.2803992
CH_4	0.2655115	0.2721629	0.2761820	0.2787230	0.2803992
C_2H_4	0.2655120	0.2721635	0.2761829	0.2787241	0.2804006
O_2	0.1327560	0.1360818	0.1380914	0.1393621	0.1402003
H_2O	0.0202023	0.0135507	9.5314E-03	6.9905E-03	5.3137E-03
CH_3COOH	4.9067E-07	6.7419E-07	8.8552E-07	1.1247E-06	1.3912E-06
Vinyl Acetate	0.0202023	0.0135507	9.5314E-03	6.9902E-03	5.3137E-03
X CH_4	**0.0707098**	**0.0474298**	**0.0333630**	**0.0244695**	**0.0186027**
X C_2H_4	**0.0707081**	**0.0474275**	**0.0333599**	**0.0244655**	**0.0185978**
Y VA	**0.9999757**	**0.9999502**	**0.9999071**	**0.9998391**	**0.9997383**

200 atm	1800 K	1900 K	2000 K
Phase	Vapor	Vapor	Vapor
CO_2	0.2815479	0.2823619	0.2829558
CH_4	0.2815479	0.2823619	0.2829558
C_2H_4	0.2815496	0.2823639	0.2829581
O_2	0.1407748	0.1411819	0.1414791
H_2O	4.1648E-03	3.3504E-03	2.7561E-03
CH_3COOH	1.6843E-06	2.0027E-06	2.3451E-06
Vinyl Acetate	4.1647E-03	3.3504E-03	2.7561E-03
X CH_4	**0.0145824**	**0.0117335**	**9.6547E-03**
X C_2H_4	**0.0145765**	**0.0117265**	**9.6465E-03**
Y VA	**0.9995957**	**0.9994026**	**0.9991499**

Table B-28: Equilibrium fractional conversion of methane (X CH_4) for reaction (R B-7) obtained from AspenPlus™ using the Peng-Robinson equation of state and stoichiometric inlet composition from 300 – 2000 K and 1 - 200 atm.

T (K)	1 atm	10 atm	25 atm	50 atm
300 K	**0.9999997**	**0.9999997**	**0.9999997**	**0.9999997**
400 K	0.9907030	**0.9999178**	**0.9999189**	**0.9999206**
500 K	0.9014051	0.9646823	0.9788174	0.9618350
600 K	0.5843212	0.8275663	0.8236900	0.9237494
700 K	0.2128494	0.5403010	0.6685627	0.7104823
800 K	0.0629363	0.2552466	0.3865932	0.4972153
900 K	0.0215542	0.1067941	0.1868570	0.2717030
1000 K	8.9448E-03	0.0476466	0.0892833	0.1395738
1100 K	4.3503E-03	0.0238268	0.0459870	0.0744582
1200 K	2.3928E-03	0.0132631	0.0259411	0.0427073
1300 K	1.4478E-03	8.0712E-03	0.0158886	0.0263758
1400 K	9.8061E-04	5.2790E-03	0.0104274	0.0173863
1500 K	6.5343E-04	3.6600E-03	7.2434E-03	0.0121077
1600 K	4.7457E-04	2.6610E-03	5.2724E-03	8.8263E-03
1700 K	3.5852E-04	2.0116E-03	3.9888E-03	6.6839E-03
1800 K	2.7983E-04	1.5709E-03	3.1164E-03	5.1206E-03
1900 K	2.2446E-04	1.2605E-03	2.5016E-03	4.1967E-03
2000 K	1.7340E-04	1.0350E-03	2.0547E-03	3.4481E-03

NOTE: Values in bold indicates liquid phase.

Table B-28 continued

T (K)	100 atm	150 atm	200 atm
300 K	**0.9999997**	**0.9999997**	**0.9999997**
400 K	**0.9999234**	**0.9999262**	**0.9990486**
500 K	0.9976897	0.9978936	**0.9980975**
600 K	0.9565497	0.9678743	0.9791989
700 K	0.7831548	0.8937019	0.8487203
800 K	0.6097599	0.6741770	0.7182417
900 K	0.3762700	0.4447556	0.4956022
1000 K	0.2109519	0.2635906	0.3058279
1100 K	0.1181285	0.1528144	0.1821911
1200 K	0.0694546	0.0915763	0.1109158
1300 K	0.0434460	0.0578724	0.0707098
1400 K	0.0288369	0.0386292	0.0474298
1500 K	0.0201610	0.0270951	0.0333630
1600 K	0.0147320	0.0198379	0.0244695
1700 K	0.0111732	0.0150647	0.0186027
1800 K	8.7444E-03	0.0118001	0.0145824
1900 K	7.0278E-03	9.4896E-03	0.0117335
2000 K	5.7776E-03	7.8051E-03	9.6547E-03

NOTE: Values in bold indicates liquid phase.

Table B-29: Equilibrium fractional conversion of ethylene (X C_2H_4) for reaction (R B-7) obtained from AspenPlus™ using the Peng-Robinson equation of state and stoichiometric inlet composition from 300 – 2000 K and 1 - 200 atm.

T (K)	1 atm	10 atm	25 atm	50 atm
300 K	**0.9999997**	**0.9999997**	**0.9999997**	**0.9999997**
400 K	0.9907030	**0.9999178**	**0.9999189**	**0.9999206**
500 K	0.9014051	0.9646823	0.9788174	0.9618350
600 K	0.5843212	0.8275663	0.8236900	0.9237494
700 K	0.2128494	0.5403010	0.6685627	0.7104823
800 K	0.0629363	0.2552466	0.3865932	0.4972153
900 K	0.0215542	0.1067941	0.1868570	0.2717029
1000 K	8.9448E-03	0.0476466	0.0892833	0.1395737
1100 K	4.3503E-03	0.0238267	0.0459869	0.0744580
1200 K	2.3928E-03	0.0132631	0.0259409	0.0427070
1300 K	1.4478E-03	8.0711E-03	0.0158884	0.0263753
1400 K	9.8060E-04	5.2789E-03	0.0104271	0.0173857
1500 K	6.5342E-04	3.6598E-03	7.2430E-03	0.0121069
1600 K	4.7455E-04	2.6607E-03	5.2718E-03	8.8253E-03
1700 K	3.5850E-04	2.0114E-03	3.9881E-03	6.6827E-03
1800 K	2.7980E-04	1.5706E-03	3.1157E-03	5.1191E-03
1900 K	2.2443E-04	1.2601E-03	2.5007E-03	4.1949E-03
2000 K	1.7336E-04	1.0346E-03	2.0536E-03	3.4460E-03

NOTE: Values in bold indicates liquid phase.

Table B-29 continued

T (K)	100 atm	150 atm	200 atm
300 K	**0.9999997**	**0.9999997**	**0.9999997**
400 K	**0.9999234**	**0.9999262**	**0.9990486**
500 K	0.9976897	0.9978936	**0.9980975**
600 K	0.9565497	0.9678743	0.9791989
700 K	0.7831548	0.8937019	0.8487203
800 K	0.6097599	0.6741770	0.7182417
900 K	0.3762700	0.4447555	0.4956021
1000 K	0.2109517	0.2635903	0.3058276
1100 K	0.1181282	0.1528139	0.1821904
1200 K	0.0694540	0.0915754	0.1109147
1300 K	0.0434452	0.0578711	0.0707081
1400 K	0.0288357	0.0386274	0.0474275
1500 K	0.0201594	0.0270928	0.0333599
1600 K	0.0147300	0.0198349	0.0244655
1700 K	0.0111707	0.0150611	0.0185978
1800 K	8.7414E-03	0.0117956	0.0145765
1900 K	7.0243E-03	9.4843E-03	0.0117265
2000 K	5.7735E-03	7.7989E-03	9.6465E-03

NOTE: Values in bold indicates liquid phase.

Table B-30: Equilibrium fractional yield of vinyl acetate (Y VA) for reaction (R B-7) obtained from AspenPlus™ using the Peng-Robinson equation of state and stoichiometric inlet composition from 300 – 2000 K and 1 - 200 atm.

T (K)	1 atm	10 atm	25 atm	50 atm
300 K	**1.0000000**	**1.0000000**	**1.0000000**	**1.0000000**
400 K	1.0000000	**1.0000000**	**1.0000000**	**1.0000000**
500 K	1.0000000	1.0000000	1.0000000	1.0000000
600 K	1.0000000	1.0000000	1.0000000	1.0000000
700 K	1.0000000	1.0000000	1.0000000	1.0000000
800 K	1.0000000	1.0000000	1.0000000	1.0000000
900 K	0.9999999	0.9999999	0.9999998	0.9999998
1000 K	0.9999997	0.9999994	0.9999993	0.9999991
1100 K	0.9999989	0.9999981	0.9999976	0.9999971
1200 K	0.9999971	0.9999949	0.9999936	0.9999924
1300 K	0.9999934	0.9999883	0.9999853	0.9999826
1400 K	0.9999867	0.9999760	0.9999699	0.9999643
1500 K	0.9999748	0.9999553	0.9999439	0.9999334
1600 K	0.9999564	0.9999226	0.9999029	0.9998847
1700 K	0.9999292	0.9998742	0.9998420	0.9998126
1800 K	0.9998907	0.9998059	0.9997562	0.9997048
1900 K	0.9998387	0.9997133	0.9996400	0.9995727
2000 K	0.9997562	0.9995923	0.9994880	0.9993923

NOTE: Values in bold indicates liquid phase.

Table B-30 continued

T (K)	100 atm	150 atm	200 atm
300 K	**1.0000000**	**1.0000000**	**1.0000000**
400 K	**1.0000000**	**1.0000000**	**1.0000000**
500 K	1.0000000	1.0000000	**1.0000000**
600 K	1.0000000	1.0000000	1.0000000
700 K	1.0000000	1.0000000	1.0000000
800 K	1.0000000	1.0000000	1.0000000
900 K	0.9999998	0.9999997	0.9999997
1000 K	0.9999990	0.9999989	0.9999988
1100 K	0.9999966	0.9999963	0.9999960
1200 K	0.9999910	0.9999901	0.9999894
1300 K	0.9999794	0.9999773	0.9999757
1400 K	0.9999578	0.9999535	0.9999502
1500 K	0.9999212	0.9999132	0.9999071
1600 K	0.9998635	0.9998496	0.9998391
1700 K	0.9997781	0.9997554	0.9997383
1800 K	0.9996574	0.9996223	0.9995957
1900 K	0.9994939	0.9994420	0.9994026
2000 K	0.9992800	0.9992060	0.9991499

NOTE: Values in bold indicates liquid phase.

B.4. VINYL ACETATE FROM ACETYLENE

Equilibrium thermodynamic calculations were performed for the formation of vinyl acetate ($CH_3CO_2CH=CH_2$) from carbon dioxide, methane, acetylene (C_2H_2):

$$CO_2 + CH_4 + C_2H_2 \leftrightarrow CH_3CO_2CH=CH_2 \qquad \text{(R B-12)}$$

Acetic acid was allowed in the system, thus permitting the following reactions:

$$CO_2 + CH_4 \leftrightarrow CH_3COOH \qquad \text{(R B-2)}$$

$$CH_3COOH + C_2H_2 \leftrightarrow CH_3CO_2CH=CH_2 \qquad \text{(R B-13)}$$

The equilibrium thermodynamic calculations for reaction (R B-12) were performed using the AspenPlus™ engineering simulation software. The RGIBBS reactor model was used to perform a Gibbs free energy minimization on the system to give the chemical and phase equilibrium composition at various temperatures and pressures. These calculations do not take into account any surface interactions. Molecular interactions are taken into account in the Peng-Robinson equation of state. The inlet composition, inlet temperature, inlet pressure, reactor temperature and reactor pressure were specified for each reaction. The inlet conditions were set equal to the reactor conditions.

A stoichiometric inlet composition of 0.333 mole fraction of CO_2, 0.333 mole fraction of CH_4 and 0.333 mole fraction of C_2H_2 was used. The AspenPlus™ calculations were performed for a wide range of temperatures and pressures, 1 - 200 atm and 300 - 2000 K. The calculations were performed using the Peng-Robinson equation of state.

An interaction parameter of 0.0919 for CO_2 and CH_4 obtained from the AspenPlus™ data base were used. No other interaction parameters were available, thus a default of 0.0 was used for all other interaction parameters.

The equilibrium fractional conversion of methane (X CH_4) was calculated using:

$$X\ CH_4 = \#\ Moles\ of\ CH_4\ reacted\ /\ \#\ Inlet\ moles\ of\ CH_4 \qquad (E\ B\text{-}1)$$

When the outlet moles of methane given by AspenPlus™ did not have enough significant figures, the sum of outlet moles of acetic acid and vinyl acetate was used as the number of moles of methane that reacted.

The equilibrium fractional conversion of acetylene (X C_2H_2) was calculated using:

$$X\ C_2H_2 = \#\ Moles\ of\ C_2H_2\ reacted\ /\ \#\ Inlet\ moles\ of\ C_2H_2 \qquad (E\ B\text{-}8)$$

When the outlet moles of methanol given by AspenPlus™ did not have enough significant figures, the number of outlet moles of vinyl acetate was used as the number of moles of ethylene that reacted.

The equilibrium yield of vinyl acetate (Y VA) was calculated using:

$$Y\ VA = Outlet\ CH_3CO_2CH{=}CH_2\ /\ Outlet\ CH_3CO_2CH{=}CH_2 + CH_3COOH \qquad (E\ B\text{-}7)$$

Data from these calculations can be found in tables B-31 to B-40.

Table B-31: Equilibrium outlet moles, X CH_4, X C_2H_2 and Y VA for reaction (R B - 12) obtained from AspenPlus™ using the Peng-Robinson equation of state and stoichiometric inlet composition from 300 – 2000 K and 1 atm.

1 atm	300 K	400 K	500 K	600 K	700 K
Phase	Vapor	Vapor	Vapor	Vapor	Vapor
CO_2	0.3308946	0.3333321	0.3333333	0.3333333	0.3333333
CH_4	0.3308946	0.3333321	0.3333333	0.3333333	0.3333333
C_2H_2	0.3308946	0.3333321	0.3333333	0.3333333	0.3333333
CH_3COOH	0.0000000	1.9847E-12	1.5820E-11	6.3699E-11	1.7538E-10
Vinyl Acetate	2.4387E-03	1.2330E-06	1.2113E-08	5.4910E-10	6.0908E-11
X CH_4	**7.3161E-03**	**3.6991E-06**	**3.6387E-08**	**1.8384E-09**	**7.0886E-10**
X C_2H_2	**7.3161E-03**	**3.6991E-06**	**3.6340E-08**	**1.6473E-09**	**1.8272E-10**
Y VA	**1.0000000**	**0.9999984**	**0.9986957**	**0.8960524**	**0.2577702**

1 atm	800 K	900 K	1000 K	1100 K	1200 K
Phase	Vapor	Vapor	Vapor	Vapor	Vapor
CO_2	0.3333333	0.3333333	0.3333333	0.3333333	0.3333333
CH_4	0.3333333	0.3333333	0.3333333	0.3333333	0.3333333
C_2H_2	0.3333333	0.3333333	0.3333333	0.3333333	0.3333333
CH_3COOH	3.8236E-10	7.1415E-10	1.1964E-09	1.9505E-09	2.6894E-09
Vinyl Acetate	1.1939E-11	2.4340E-12	7.4800E-13	3.9507E-13	2.1291E-13
X CH_4	**1.1829E-09**	**2.1498E-09**	**3.5913E-09**	**5.8527E-09**	**8.0688E-09**
X C_2H_2	**3.5817E-11**	**7.3020E-12**	**2.2440E-12**	**1.1852E-12**	**6.3873E-13**
Y VA	**0.0302791**	**3.3967E-03**	**6.2484E-04**	**2.0250E-04**	**7.9160E-05**

Table B-31 continued

1 atm	1300 K	1400 K	1500 K	1600 K	1700 K
Phase	Vapor	Vapor	Vapor	Vapor	Vapor
CO_2	0.3333333	0.3333333	0.3333333	0.3333333	0.3333333
CH_4	0.3333333	0.3333333	0.3333333	0.3333333	0.3333333
C_2H_2	0.3333333	0.3333333	0.3333333	0.3333333	0.3333333
CH_3COOH	3.7257E-09	4.9636E-09	6.4040E-09	8.0437E-09	9.8770E-09
Vinyl Acetate	1.3484E-13	9.8930E-14	8.1838E-14	5.9418E-14	4.5081E-14
X CH_4	**1.1177E-08**	**1.4891E-08**	**1.9212E-08**	**2.4131E-08**	**2.9631E-08**
X C_2H_2	**4.0452E-13**	**2.9679E-13**	**2.4551E-13**	**1.7825E-13**	**1.3524E-13**
Y VA	**3.6191E-05**	**1.9931E-05**	**1.2779E-05**	**7.3868E-06**	**4.5642E-06**

1 atm	1800 K	1900 K	2000 K
Phase	Vapor	Vapor	Vapor
CO_2	0.3333333	0.3333333	0.3333333
CH_4	0.3333333	0.3333333	0.3333333
C_2H_2	0.3333333	0.3333333	0.3333333
CH_3COOH	1.1895E-08	1.4089E-08	1.6446E-08
Vinyl Acetate	3.5385E-14	2.8730E-14	2.3850E-14
X CH_4	**3.5686E-08**	**4.2267E-08**	**4.9339E-08**
X C_2H_2	**1.0616E-13**	**8.6190E-14**	**7.1550E-14**
Y VA	**2.9747E-06**	**2.0392E-06**	**1.4502E-06**

Table B-32: Equilibrium outlet moles, X CH_4, X C_2H_2 and Y VA for reaction (R B - 12) obtained from AspenPlus™ using the Peng-Robinson equation of state and stoichiometric inlet composition from 300 – 2000 K and 10 atm.

10 atm	300 K	400 K	500 K	600 K	700 K
Phase	Liquid	Vapor	Vapor	Vapor	Vapor
CO_2	6.3062E-03	0.3332037	0.3333321	0.3333333	0.3333333
CH_4	6.3062E-03	0.3332037	0.3333321	0.3333333	0.3333333
C_2H_2	6.3062E-03	0.3332037	0.3333321	0.3333333	0.3333333
CH_3COOH	2.1837E-11	2.1519E-11	1.6501E-10	6.5225E-10	1.7785E-09
Vinyl Acetate	0.3270271	1.2965E-04	1.2450E-06	5.5808E-08	6.1532E-09
X CH_4	**9.8108E-01**	**3.8895E-04**	**3.7354E-06**	**1.6938E-07**	**2.3795E-08**
X C_2H_2	**9.8108E-01**	**3.8895E-04**	**3.7349E-06**	**1.6742E-07**	**1.8460E-08**
Y VA	**1.0000000**	**0.9999998**	**0.9998675**	**0.9884476**	**0.7757751**

10 atm	800 K	900 K	1000 K	1100 K	1200 K
Phase	Vapor	Vapor	Vapor	Vapor	Vapor
CO_2	0.3333333	0.3333333	0.3333333	0.3333333	0.3333333
CH_4	0.3333333	0.3333333	0.3333333	0.3333333	0.3333333
C_2H_2	0.3333333	0.3333333	0.3333333	0.3333333	0.3333333
CH_3COOH	3.8559E-09	7.1779E-09	1.2000E-08	1.8528E-08	2.6916E-08
Vinyl Acetate	1.2019E-09	3.4495E-10	1.2968E-10	5.9277E-11	3.1338E-11
X CH_4	**1.5174E-08**	**2.2569E-08**	**3.6388E-08**	**5.5761E-08**	**8.0843E-08**
X C_2H_2	**3.6057E-09**	**1.0349E-09**	**3.8904E-10**	**1.7783E-10**	**9.4014E-11**
Y VA	**0.2376331**	**4.5854E-02**	**0.0106915**	**3.1892E-03**	**1.1629E-03**

Table B-32 continued

10 atm	1300 K	1400 K	1500 K	1600 K	1700 K
Phase	Vapor	Vapor	Vapor	Vapor	Vapor
CO_2	0.3333333	0.3333333	0.3333333	0.3333333	0.3333332
CH_4	0.3333333	0.3333333	0.3333333	0.3333333	0.3333332
C_2H_2	0.3333333	0.3333333	0.3333333	0.3333333	0.3333333
CH_3COOH	3.7266E-08	4.9630E-08	6.4016E-08	8.0395E-08	9.8708E-08
Vinyl Acetate	1.8540E-11	1.1902E-11	8.1904E-12	5.9482E-12	4.5124E-12
X CH_4	**1.1185E-07**	**1.4893E-07**	**1.9207E-07**	**2.4120E-07**	**2.9614E-07**
X C_2H_2	**5.5620E-11**	**3.5706E-11**	**2.4571E-11**	**1.7845E-11**	**1.3537E-11**
Y VA	**4.9725E-04**	**2.3976E-04**	**1.2793E-04**	**7.3982E-05**	**4.5713E-05**

10 atm	1800 K	1900 K	2000 K
Phase	Vapor	Vapor	Vapor
CO_2	0.3333332	0.3333332	0.3333332
CH_4	0.3333332	0.3333332	0.3333332
C_2H_2	0.3333333	0.3333333	0.3333333
CH_3COOH	1.1887E-07	1.4079E-07	1.6435E-07
Vinyl Acetate	3.5475E-12	2.8730E-12	2.3796E-12
X CH_4	**3.5663E-07**	**4.2238E-07**	**4.9305E-07**
X C_2H_2	**1.0643E-11**	**8.6190E-12**	**7.1388E-12**
Y VA	**2.9842E-05**	**2.0406E-05**	**1.4479E-05**

Table B-33: Equilibrium outlet moles, X CH_4, X C_2H_2 and Y VA for reaction (R B - 12) obtained from AspenPlus™ using the Peng-Robinson equation of state and stoichiometric inlet composition from 300 – 2000 K and 25 atm.

25 atm	300 K	400 K	500 K	600 K	700 K
Phase	Liquid	Vapor	Vapor	Vapor	Vapor
CO_2	6.2464E-03	0.3324536	0.3333252	0.3333330	0.3333333
CH_4	6.2464E-03	0.3324536	0.3333252	0.3333330	0.3333333
C_2H_2	6.2464E-03	0.3324536	0.3333252	0.3333330	0.3333333
CH_3COOH	2.1734E-11	6.1553E-11	4.4215E-10	1.6747E-09	4.5484E-09
Vinyl Acetate	0.3270869	8.7969E-04	8.1382E-06	3.5811E-07	3.9098E-08
X CH_4	**0.9812607**	**2.6391E-03**	**2.4416E-05**	**1.0794E-06**	**1.3094E-07**
X C_2H_2	**0.9812607**	**2.6391E-03**	**2.4415E-05**	**1.0743E-06**	**1.1729E-07**
Y VA	**1.0000000**	**0.9999999**	**0.9999457**	**0.9953452**	**0.8957911**

25 atm	800 K	900 K	1000 K	1100 K	1200 K
Phase	Vapor	Vapor	Vapor	Vapor	Vapor
CO_2	0.3333333	0.3333333	0.3333333	0.3333333	0.3333333
CH_4	0.3333333	0.3333333	0.3333333	0.3333333	0.3333333
C_2H_2	0.3333333	0.3333333	0.3333333	0.3333333	0.3333333
CH_3COOH	9.7726E-09	1.8094E-08	3.0146E-08	4.6446E-08	6.7379E-08
Vinyl Acetate	7.5936E-09	2.1717E-09	8.1454E-10	3.7178E-10	1.9634E-10
X CH_4	**5.2098E-08**	**6.0796E-08**	**9.2881E-08**	**1.4045E-07**	**2.0273E-07**
X C_2H_2	**2.2781E-08**	**6.5151E-09**	**2.4436E-09**	**1.1153E-09**	**5.8902E-10**
Y VA	**0.4372641**	**0.1071625**	**0.0263091**	**7.9411E-03**	**2.9055E-03**

Table B-33 continued

25 atm	1300 K	1400 K	1500 K	1600 K	1700 K
Phase	Vapor	Vapor	Vapor	Vapor	Vapor
CO_2	0.3333332	0.3333332	0.3333332	0.3333331	0.3333331
CH_4	0.3333332	0.3333332	0.3333332	0.3333331	0.3333331
C_2H_2	0.3333333	0.3333333	0.3333333	0.3333333	0.3333333
CH_3COOH	9.3201E-08	1.2405E-07	1.5994E-07	2.0081E-07	2.4651E-07
Vinyl Acetate	1.1585E-10	7.4480E-11	5.1233E-11	3.7197E-11	2.8213E-11
X CH_4	**2.7995E-07**	**3.7236E-07**	**4.7997E-07**	**6.0254E-07**	**7.3962E-07**
X C_2H_2	**3.4755E-10**	**2.2344E-10**	**1.5370E-10**	**1.1159E-10**	**8.4639E-11**
Y VA	**1.2415E-03**	**6.0006E-04**	**3.2023E-04**	**1.8520E-04**	**1.1444E-04**

25 atm	1800 K	1900 K	2000 K
Phase	Vapor	Vapor	Vapor
CO_2	0.3333330	0.3333330	0.3333329
CH_4	0.3333330	0.3333330	0.3333329
C_2H_2	0.3333333	0.3333333	0.3333333
CH_3COOH	2.9685E-07	3.5156E-07	4.1039E-07
Vinyl Acetate	2.2179E-11	1.7959E-11	1.4907E-11
X CH_4	**8.9060E-07**	**1.0547E-06**	**1.2312E-06**
X C_2H_2	**6.6537E-11**	**5.3877E-11**	**4.4721E-11**
Y VA	**7.4710E-05**	**5.1081E-05**	**3.6323E-05**

Table B-34: Equilibrium outlet moles, X CH_4, X C_2H_2 and Y VA for reaction (R B - 12) obtained from AspenPlus™ using the Peng-Robinson equation of state and stoichiometric inlet composition from 300 – 2000 K and 50 atm.

50 atm	300 K	400 K	500 K	600 K	700 K
Phase	Liquid	Vapor	Vapor	Vapor	Vapor
CO_2	6.1509E-03	0.3293186	0.3332983	0.3333318	0.3333332
CH_4	6.1509E-03	0.3293186	0.3332983	0.3333318	0.3333332
C_2H_2	6.1509E-03	0.3293186	0.3332983	0.3333318	0.3333332
CH_3COOH	2.1556E-11	1.5399E-10	9.8999E-10	3.6076E-09	9.4337E-09
Vinyl Acetate	0.3271825	4.0147E-03	3.4990E-05	1.4939E-06	1.6056E-07
X CH_4	**0.9815475**	**0.0120440**	**1.0497E-04**	**4.4925E-06**	**5.0997E-07**
X C_2H_2	**0.9815475**	**0.0120440**	**1.0497E-04**	**4.4816E-06**	**4.8167E-07**
Y VA	**1.0000000**	**1.0000000**	**0.9999717**	**0.9975909**	**0.9445049**

50 atm	800 K	900 K	1000 K	1100 K	1200 K
Phase	Vapor	Vapor	Vapor	Vapor	Vapor
CO_2	0.3333333	0.3333333	0.3333333	0.3333332	0.3333332
CH_4	0.3333333	0.3333333	0.3333333	0.3333332	0.3333332
C_2H_2	0.3333333	0.3333333	0.3333333	0.3333333	0.3333333
CH_3COOH	1.9977E-08	3.6668E-08	6.0763E-08	9.3293E-08	1.3503E-07
Vinyl Acetate	3.0902E-08	8.7885E-09	3.2845E-09	1.4955E-09	7.8847E-10
X CH_4	**1.5264E-07**	**1.3637E-07**	**1.9214E-07**	**2.8436E-07**	**4.0747E-07**
X C_2H_2	**9.2707E-08**	**2.6366E-08**	**9.8534E-09**	**4.4864E-09**	**2.3654E-09**
Y VA	**0.6073653**	**0.1933408**	**0.0512818**	**0.0157771**	**5.8052E-03**

Table B-34 continued

50 atm	1300 K	1400 K	1500 K	1600 K	1700 K
Phase	Vapor	Vapor	Vapor	Vapor	Vapor
CO_2	0.3333331	0.3333331	0.3333330	0.3333329	0.3333328
CH_4	0.3333331	0.3333331	0.3333330	0.3333329	0.3333328
C_2H_2	0.3333333	0.3333333	0.3333333	0.3333333	0.3333333
CH_3COOH	1.8651E-07	2.4798E-07	3.1953E-07	4.0101E-07	4.9216E-07
Vinyl Acetate	4.6468E-10	2.9850E-10	2.0521E-10	1.4892E-10	1.1292E-10
X CH_4	**5.6091E-07**	**7.4485E-07**	**9.5920E-07**	**1.2035E-06**	**1.4768E-06**
X C_2H_2	**1.3940E-09**	**8.9550E-10**	**6.1563E-10**	**4.4676E-10**	**3.3876E-10**
Y VA	**2.4853E-03**	**1.2023E-03**	**6.4181E-04**	**3.7122E-04**	**2.2939E-04**

50 atm	1800 K	1900 K	2000 K
Phase	Vapor	Vapor	Vapor
CO_2	0.3333327	0.3333326	0.3333325
CH_4	0.3333327	0.3333326	0.3333325
C_2H_2	0.3333333	0.3333333	0.3333333
CH_3COOH	5.9257E-07	7.0175E-07	8.1916E-07
Vinyl Acetate	8.8746E-11	7.1852E-11	5.9633E-11
X CH_4	**1.7780E-06**	**2.1055E-06**	**2.4577E-06**
X C_2H_2	**2.6624E-10**	**2.1556E-10**	**1.7890E-10**
Y VA	**1.4974E-04**	**1.0238E-04**	**7.2792E-05**

Table B-35: Equilibrium outlet moles, X CH_4, X C_2H_2 and Y VA for reaction (R B - 12) obtained from AspenPlus™ using the Peng-Robinson equation of state and stoichiometric inlet composition from 300 – 2000 K and 100 atm.

100 atm	300 K	400 K	500 K	600 K	700 K
Phase	Liquid	Vapor	Vapor	Vapor	Vapor
CO_2	5.9735E-03	0.3128089	0.3331735	0.3333269	0.3333326
CH_4	5.9735E-03	0.3128089	0.3331735	0.3333269	0.3333326
C_2H_2	5.9735E-03	0.3128089	0.3331735	0.3333269	0.3333327
CH_3COOH	2.1178E-11	4.8472E-10	2.4502E-09	8.1005E-09	2.0181E-08
Vinyl Acetate	0.3273598	0.0205244	1.5986E-04	6.4516E-06	6.7384E-07
X CH_4	**0.9820794**	**0.0615732**	**4.7958E-04**	**1.9379E-05**	**2.0821E-06**
X C_2H_2	**0.9820794**	**0.0615732**	**4.7957E-04**	**1.9355E-05**	**2.0215E-06**
Y VA	**1.0000000**	**1.0000000**	**0.9999847**	**0.9987460**	**0.9709215**

100 atm	800 K	900 K	1000 K	1100 K	1200 K
Phase	Vapor	Vapor	Vapor	Vapor	Vapor
CO_2	0.3333332	0.3333332	0.3333332	0.3333331	0.3333331
CH_4	0.3333332	0.3333332	0.3333332	0.3333331	0.3333331
C_2H_2	0.3333332	0.3333333	0.3333333	0.3333333	0.3333333
CH_3COOH	4.1599E-08	7.5136E-08	1.2327E-07	1.8804E-07	2.7103E-07
Vinyl Acetate	1.2759E-07	3.5919E-08	1.3336E-08	6.0452E-09	3.1774E-09
X CH_4	**5.0755E-07**	**3.3317E-07**	**4.0981E-07**	**5.8227E-07**	**8.2263E-07**
X C_2H_2	**3.8276E-07**	**1.0776E-07**	**4.0007E-08**	**1.8135E-08**	**9.5323E-09**
Y VA	**0.7541211**	**0.3234353**	**0.0976233**	**0.0311463**	**0.0115876**

Table B-35 continued

100 atm	1300 K	1400 K	1500 K	1600 K	1700 K
Phase	Vapor	Vapor	Vapor	Vapor	Vapor
CO_2	0.3333330	0.3333328	0.3333327	0.3333325	0.3333324
CH_4	0.3333330	0.3333328	0.3333327	0.3333325	0.3333324
C_2H_2	0.3333333	0.3333333	0.3333333	0.3333333	0.3333333
CH_3COOH	3.7330E-07	4.9543E-07	6.3759E-07	7.9957E-07	9.8083E-07
Vinyl Acetate	1.8685E-09	1.1984E-09	8.2295E-10	5.9674E-10	4.5220E-10
X CH_4	**1.1255E-06**	**1.4899E-06**	**1.9152E-06**	**2.4005E-06**	**2.9439E-06**
X C_2H_2	**5.6056E-09**	**3.5953E-09**	**2.4689E-09**	**1.7902E-09**	**1.3566E-09**
Y VA	**4.9805E-03**	**2.4131E-03**	**1.2890E-03**	**7.4577E-04**	**4.6082E-04**

100 atm	1800 K	1900 K	2000 K
Phase	Vapor	Vapor	Vapor
CO_2	0.3333322	0.3333319	0.3333317
CH_4	0.3333322	0.3333319	0.3333317
C_2H_2	0.3333333	0.3333333	0.3333333
CH_3COOH	1.1806E-06	1.3980E-06	1.6319E-06
Vinyl Acetate	3.5524E-10	2.8752E-10	2.3857E-10
X CH_4	**3.5430E-06**	**4.1949E-06**	**4.8964E-06**
X C_2H_2	**1.0657E-09**	**8.6256E-10**	**7.1571E-10**
Y VA	**3.0080E-04**	**2.0562E-04**	**1.4617E-04**

Table B-36: Equilibrium outlet moles, X CH_4, X C_2H_2 and Y VA for reaction (R B - 12) obtained fom AspenPlus™ using the Peng-Robinson equation of state and stoichiometric inlet composition from 300 – 2000 K and 150 atm.

150 atm	300 K	400 K	500 K	600 K	700 K
Phase	Liquid	Vapor	Vapor	Vapor	Vapor
CO_2	5.8119E-03	0.2740367	0.3329297	0.3333178	0.3333317
CH_4	5.8119E-03	0.2740367	0.3329297	0.3333178	0.3333317
C_2H_2	5.8119E-03	0.2740367	0.3329297	0.3333178	0.3333318
CH_3COOH	2.0783E-11	1.2285E-09	4.4556E-09	1.3483E-08	3.2157E-08
Vinyl Acetate	0.3275215	0.0592966	4.0365E-04	1.5523E-05	1.5819E-06
X CH_4	**0.9825645**	**0.1778898**	**1.2110E-03**	**4.6608E-05**	**4.8420E-06**
X C_2H_2	**0.9825645**	**0.1778898**	**1.2109E-03**	**4.6568E-05**	**4.7456E-06**
Y VA	**1.0000000**	**1.0000000**	**0.9999890**	**0.9991321**	**0.9800762**

150 atm	800 K	900 K	1000 K	1100 K	1200 K
Phase	Vapor	Vapor	Vapor	Vapor	Vapor
CO_2	0.3333330	0.3333331	0.3333331	0.3333330	3.3333E-01
CH_4	0.3333330	0.3333331	0.3333331	0.3333330	3.3333E-01
C_2H_2	0.3333330	0.3333333	0.3333333	0.3333333	3.3333E-01
CH_3COOH	6.4697E-08	1.1518E-07	1.8725E-07	2.8398E-07	4.0774E-07
Vinyl Acetate	2.9529E-07	8.2403E-08	3.0417E-08	1.3734E-08	7.1987E-09
X CH_4	**1.0800E-06**	**5.9274E-07**	**6.5300E-07**	**8.9315E-07**	**1.2448E-06**
X C_2H_2	**8.8588E-07**	**2.4721E-07**	**9.1250E-08**	**4.1201E-08**	**2.1596E-08**
Y VA	**0.8202804**	**0.4170636**	**0.1397392**	**0.0461296**	**0.0173489**

Table B-36 continued

150 atm	1300 K	1400 K	1500 K	1600 K	1700 K
Phase	Vapor	Vapor	Vapor	Vapor	Vapor
CO_2	0.3333328	0.3333326	0.3333324	0.3333321	0.3333319
CH_4	0.3333328	0.3333326	0.3333324	0.3333321	0.3333319
C_2H_2	0.3333333	0.3333333	0.3333333	0.3333333	0.3333333
CH_3COOH	5.6015E-07	7.4216E-07	9.5406E-07	1.1956E-06	1.4660E-06
Vinyl Acetate	4.2249E-09	2.7059E-09	1.8562E-09	1.3449E-09	1.0186E-09
X CH_4	**1.6931E-06**	**2.2346E-06**	**2.8677E-06**	**3.5907E-06**	**4.4010E-06**
X C_2H_2	**1.2675E-08**	**8.1178E-09**	**5.5686E-09**	**4.0348E-09**	**3.0558E-09**
Y VA	**7.4860E-03**	**3.6328E-03**	**1.9418E-03**	**1.1237E-03**	**6.9434E-04**

150 atm	1800 K	1900 K	2000 K
Phase	Vapor	Vapor	Vapor
CO_2	0.3333316	0.3333312	0.3333309
CH_4	0.3333316	0.3333312	0.3333309
C_2H_2	0.3333333	0.3333333	0.3333333
CH_3COOH	1.7642E-06	2.0888E-06	2.4383E-06
Vinyl Acetate	7.9985E-10	6.4717E-10	5.3687E-10
X CH_4	**5.2949E-06**	**6.2683E-06**	**7.3164E-06**
X C_2H_2	**2.3996E-09**	**1.9415E-09**	**1.6106E-09**
Y VA	**4.5318E-04**	**3.0973E-04**	**2.2014E-04**

Table B-37: Equilibrium outlet moles, X CH_4, X C_2H_2 and Y VA for reaction (R B - 12) obtained from AspenPlus™ using the Peng-Robinson equation of state and stoichiometric inlet composition from 300 – 2000 K and 200 atm.

200 atm	300 K	400 K	500 K	600 K	700 K
Phase	Liquid	Liquid	Vapor	Vapor	Vapor
CO_2	5.6635E-03	0.1888888	0.3325429	0.3333041	0.3333304
CH_4	5.6635E-03	0.1888888	0.3325429	0.3333041	0.3333304
C_2H_2	5.6635E-03	0.1888888	0.3325429	0.3333041	0.3333304
CH_3COOH	2.0371E-11	3.6750E-09	7.0390E-09	1.9722E-08	4.5257E-08
Vinyl Acetate	0.3276698	0.1444445	7.9043E-04	2.9243E-05	2.9192E-06
X CH_4	**0.9830094**	**0.4333335**	**2.3713E-03**	**8.7788E-05**	**8.8935E-06**
X C_2H_2	**0.9830094**	**0.4333335**	**2.3713E-03**	**8.7729E-05**	**8.7577E-06**
Y VA	**1.0000000**	**1.0000000**	**0.9999911**	**0.9993260**	**0.9847337**

200 atm	800 K	900 K	1000 K	1100 K	1200 K
Phase	Vapor	Vapor	Vapor	Vapor	Vapor
CO_2	0.3333327	0.3333330	0.3333330	0.3333329	0.3333328
CH_4	0.3333327	0.3333330	0.3333330	0.3333329	0.3333328
C_2H_2	0.3333338	0.3333332	0.3333333	0.3333333	0.3333333
CH_3COOH	8.9103E-08	1.5657E-07	2.5247E-07	3.8087E-07	5.4493E-07
Vinyl Acetate	5.3838E-07	1.4909E-07	5.4750E-08	2.4634E-08	1.2880E-08
X CH_4	**1.8824E-06**	**9.1698E-07**	**9.2167E-07**	**1.2165E-06**	**1.6734E-06**
X C_2H_2	**1.6151E-06**	**4.4726E-07**	**1.6425E-07**	**7.3901E-08**	**3.8640E-08**
Y VA	**0.8579984**	**0.4877560**	**0.1782098**	**0.0607482**	**0.0230904**

Table B-37 continued

200 atm	1300 K	1400 K	1500 K	1600 K	1700 K
Phase	Vapor	Vapor	Vapor	Vapor	Vapor
CO_2	0.3333326	0.3333323	0.3333321	0.3333317	3.3333E-01
CH_4	0.3333326	0.3333323	0.3333321	0.3333317	3.3333E-01
C_2H_2	0.3333333	0.3333333	0.3333333	0.3333333	3.3333E-01
CH_3COOH	7.4688E-07	9.8801E-07	1.2688E-06	1.5889E-06	1.9475E-06
Vinyl Acetate	7.5457E-09	4.8264E-09	3.3076E-09	2.3948E-09	1.8128E-09
X CH_4	**2.2633E-06**	**2.9785E-06**	**3.8163E-06**	**4.7740E-06**	**5.8481E-06**
X C_2H_2	**2.2637E-08**	**1.4479E-08**	**9.9227E-09**	**7.1845E-09**	**5.4383E-09**
Y VA	**0.0100020**	**4.8613E-03**	**2.6001E-03**	**1.5049E-03**	**9.2993E-04**

200 atm	1800 K	1900 K	2000 K
Phase	Vapor	Vapor	Vapor
CO_2	0.3333310	0.3333306	0.3333301
CH_4	0.3333310	0.3333306	0.3333301
C_2H_2	0.3333333	0.3333333	0.3333333
CH_3COOH	2.3432E-06	2.7741E-06	3.2383E-06
Vinyl Acetate	1.4229E-09	1.1510E-09	9.5458E-10
X CH_4	**7.0339E-06**	**8.3258E-06**	**9.7176E-06**
X C_2H_2	**4.2688E-09**	**3.4529E-09**	**2.8637E-09**
Y VA	**6.0689E-04**	**4.1472E-04**	**2.9469E-04**

Table B-38: Equilibrium fractional conversion of methane (X CH_4) for reaction (R B-12) obtained from AspenPlus™ using the Peng-Robinson equation of state and stoichiometric inlet composition from 300 – 2000 K and 1 - 200 atm.

T (K)	1 atm	10 atm	25 atm	50 atm
300 K	7.3161E-03	**0.9810813**	**0.9812607**	**0.9815475**
400 K	3.6991E-06	3.8895E-04	2.6391E-03	0.0120440
500 K	3.6387E-08	3.7354E-06	2.4416E-05	1.0497E-04
600 K	1.8384E-09	1.6938E-07	1.0794E-06	4.4925E-06
700 K	7.0886E-10	2.3795E-08	1.3094E-07	5.0997E-07
800 K	1.1829E-09	1.5174E-08	5.2098E-08	1.5264E-07
900 K	2.1498E-09	2.2569E-08	6.0796E-08	1.3637E-07
1000 K	3.5913E-09	3.6388E-08	9.2881E-08	1.9214E-07
1100 K	5.8527E-09	5.5761E-08	1.4045E-07	2.8436E-07
1200 K	8.0688E-09	8.0843E-08	2.0273E-07	4.0747E-07
1300 K	1.1177E-08	1.1185E-07	2.7995E-07	5.6091E-07
1400 K	1.4891E-08	1.4893E-07	3.7236E-07	7.4485E-07
1500 K	1.9212E-08	1.9207E-07	4.7997E-07	9.5920E-07
1600 K	2.4131E-08	2.4120E-07	6.0254E-07	1.2035E-06
1700 K	2.9631E-08	2.9614E-07	7.3962E-07	1.4768E-06
1800 K	3.5686E-08	3.5663E-07	8.9060E-07	1.7780E-06
1900 K	4.2267E-08	4.2238E-07	1.0547E-06	2.1055E-06
2000 K	4.9339E-08	4.9305E-07	1.2312E-06	2.4577E-06

NOTE: Values in bold indicates liquid phase.

Table B-38 continued

T (K)	100 atm	150 atm	200 atm
300 K	**0.9820794**	**0.9825645**	**0.9830094**
400 K	0.0615732	0.1778898	**0.4333335**
500 K	4.7958E-04	1.2110E-03	2.3713E-03
600 K	1.9379E-05	4.6608E-05	8.7788E-05
700 K	2.0821E-06	4.8420E-06	8.8935E-06
800 K	5.0755E-07	1.0800E-06	1.8824E-06
900 K	3.3317E-07	5.9274E-07	9.1698E-07
1000 K	4.0981E-07	6.5300E-07	9.2167E-07
1100 K	5.8227E-07	8.9315E-07	1.2165E-06
1200 K	8.2263E-07	1.2448E-06	1.6734E-06
1300 K	1.1255E-06	1.6931E-06	2.2633E-06
1400 K	1.4899E-06	2.2346E-06	2.9785E-06
1500 K	1.9152E-06	2.8677E-06	3.8163E-06
1600 K	2.4005E-06	3.5907E-06	4.7740E-06
1700 K	2.9439E-06	4.4010E-06	5.8481E-06
1800 K	3.5430E-06	5.2949E-06	7.0339E-06
1900 K	4.1949E-06	6.2683E-06	8.3258E-06
2000 K	4.8964E-06	7.3164E-06	9.7176E-06

NOTE: Values in bold indicates liquid phase.

Table B-39: Equilibrium fractional conversion of ethylene (X C_2H_2) for reaction (R B-12) obtained from AspenPlus™ using the Peng-Robinson equation of state and stoichiometric inlet composition from 300 – 2000 K and 1 - 200 atm.

T (K)	1 atm	10 atm	25 atm	50 atm
300 K	7.3161E-03	**0.9810813**	**0.9812607**	**0.9815475**
400 K	3.6991E-06	3.8895E-04	2.6391E-03	0.0120440
500 K	3.6340E-08	3.7349E-06	2.4415E-05	1.0497E-04
600 K	1.6473E-09	1.6742E-07	1.0743E-06	4.4816E-06
700 K	1.8272E-10	1.8460E-08	1.1729E-07	4.8167E-07
800 K	3.5817E-11	3.6057E-09	2.2781E-08	9.2707E-08
900 K	7.3020E-12	1.0349E-09	6.5151E-09	2.6366E-08
1000 K	2.2440E-12	3.8904E-10	2.4436E-09	9.8534E-09
1100 K	1.1852E-12	1.7783E-10	1.1153E-09	4.4864E-09
1200 K	6.3873E-13	9.4014E-11	5.8902E-10	2.3654E-09
1300 K	4.0452E-13	5.5620E-11	3.4755E-10	1.3940E-09
1400 K	2.9679E-13	3.5706E-11	2.2344E-10	8.9550E-10
1500 K	2.4551E-13	2.4571E-11	1.5370E-10	6.1563E-10
1600 K	1.7825E-13	1.7845E-11	1.1159E-10	4.4676E-10
1700 K	1.3524E-13	1.3537E-11	8.4639E-11	3.3876E-10
1800 K	1.0616E-13	1.0643E-11	6.6537E-11	2.6624E-10
1900 K	8.6190E-14	8.6190E-12	5.3877E-11	2.1556E-10
2000 K	7.1550E-14	7.1388E-12	4.4721E-11	1.7890E-10

NOTE: Values in bold indicates liquid phase.

Table B-39 continued

T (K)	100 atm	150 atm	200 atm
300 K	**0.9820794**	**0.9825645**	**0.9830094**
400 K	0.0615732	0.1778898	**0.4333335**
500 K	4.7957E-04	1.2109E-03	2.3713E-03
600 K	1.9355E-05	4.6568E-05	8.7729E-05
700 K	2.0215E-06	4.7456E-06	8.7577E-06
800 K	3.8276E-07	8.8588E-07	1.6151E-06
900 K	1.0776E-07	2.4721E-07	4.4726E-07
1000 K	4.0007E-08	9.1250E-08	1.6425E-07
1100 K	1.8135E-08	4.1201E-08	7.3901E-08
1200 K	9.5323E-09	2.1596E-08	3.8640E-08
1300 K	5.6056E-09	1.2675E-08	2.2637E-08
1400 K	3.5953E-09	8.1178E-09	1.4479E-08
1500 K	2.4689E-09	5.5686E-09	9.9227E-09
1600 K	1.7902E-09	4.0348E-09	7.1845E-09
1700 K	1.3566E-09	3.0558E-09	5.4383E-09
1800 K	1.0657E-09	2.3996E-09	4.2688E-09
1900 K	8.6256E-10	1.9415E-09	3.4529E-09
2000 K	7.1571E-10	1.6106E-09	2.8637E-09

NOTE: Values in bold indicates liquid phase.

Table B-40: Equilibrium fractional yield of vinyl acetate (Y VA) for reaction (R B-12) obtained from AspenPlus™ using the Peng-Robinson equation of state and stoichiometric inlet composition from 300 – 2000 K and 1 - 200 atm.

T (K)	1 atm	10 atm	25 atm	50 atm
300 K	1.0000000	**1.0000000**	**1.0000000**	**1.0000000**
400 K	0.9999984	0.9999998	0.9999999	1.0000000
500 K	0.9986957	0.9998675	0.9999457	0.9999717
600 K	0.8960524	0.9884476	0.9953452	0.9975909
700 K	0.2577702	0.7757751	0.8957911	0.9445049
800 K	0.0302791	0.2376331	0.4372641	0.6073653
900 K	3.3967E-03	0.0458535	0.1071625	0.1933408
1000 K	6.2484E-04	0.0106915	0.0263091	0.0512818
1100 K	2.0250E-04	3.1892E-03	7.9411E-03	0.0157771
1200 K	7.9160E-05	1.1629E-03	2.9055E-03	5.8052E-03
1300 K	3.6191E-05	4.9725E-04	1.2415E-03	2.4853E-03
1400 K	1.9931E-05	2.3976E-04	6.0006E-04	1.2023E-03
1500 K	1.2779E-05	1.2793E-04	3.2023E-04	6.4181E-04
1600 K	7.3868E-06	7.3982E-05	1.8520E-04	3.7122E-04
1700 K	4.5642E-06	4.5713E-05	1.1444E-04	2.2939E-04
1800 K	2.9747E-06	2.9842E-05	7.4710E-05	1.4974E-04
1900 K	2.0392E-06	2.0406E-05	5.1081E-05	1.0238E-04
2000 K	1.4502E-06	1.4479E-05	3.6323E-05	7.2792E-05

NOTE: Values in bold indicates liquid phase.

Table B-40 continued

T (K)	100 atm	150 atm	200 atm
300 K	**1.0000000**	**1.0000000**	**1.0000000**
400 K	1.0000000	1.0000000	**1.0000000**
500 K	0.9999847	0.9999890	0.9999911
600 K	0.9987460	0.9991321	0.9993260
700 K	0.9709215	0.9800762	0.9847337
800 K	0.7541211	0.8202804	0.8579984
900 K	0.3234353	0.4170636	0.4877560
1000 K	0.0976233	0.1397392	0.1782098
1100 K	0.0311463	0.0461296	0.0607482
1200 K	0.0115876	0.0173489	0.0230904
1300 K	4.9805E-03	7.4860E-03	1.0002E-02
1400 K	2.4131E-03	3.6328E-03	4.8613E-03
1500 K	1.2890E-03	1.9418E-03	2.6001E-03
1600 K	7.4577E-04	1.1237E-03	1.5049E-03
1700 K	4.6082E-04	6.9434E-04	9.2993E-04
1800 K	3.0080E-04	4.5318E-04	6.0689E-04
1900 K	2.0562E-04	3.0973E-04	4.1472E-04
2000 K	1.4617E-04	2.2014E-04	2.9469E-04

NOTE: Values in bold indicates liquid phase.

APPENDIX C:

MASS SPECTRA OF PURE COMPOUNDS

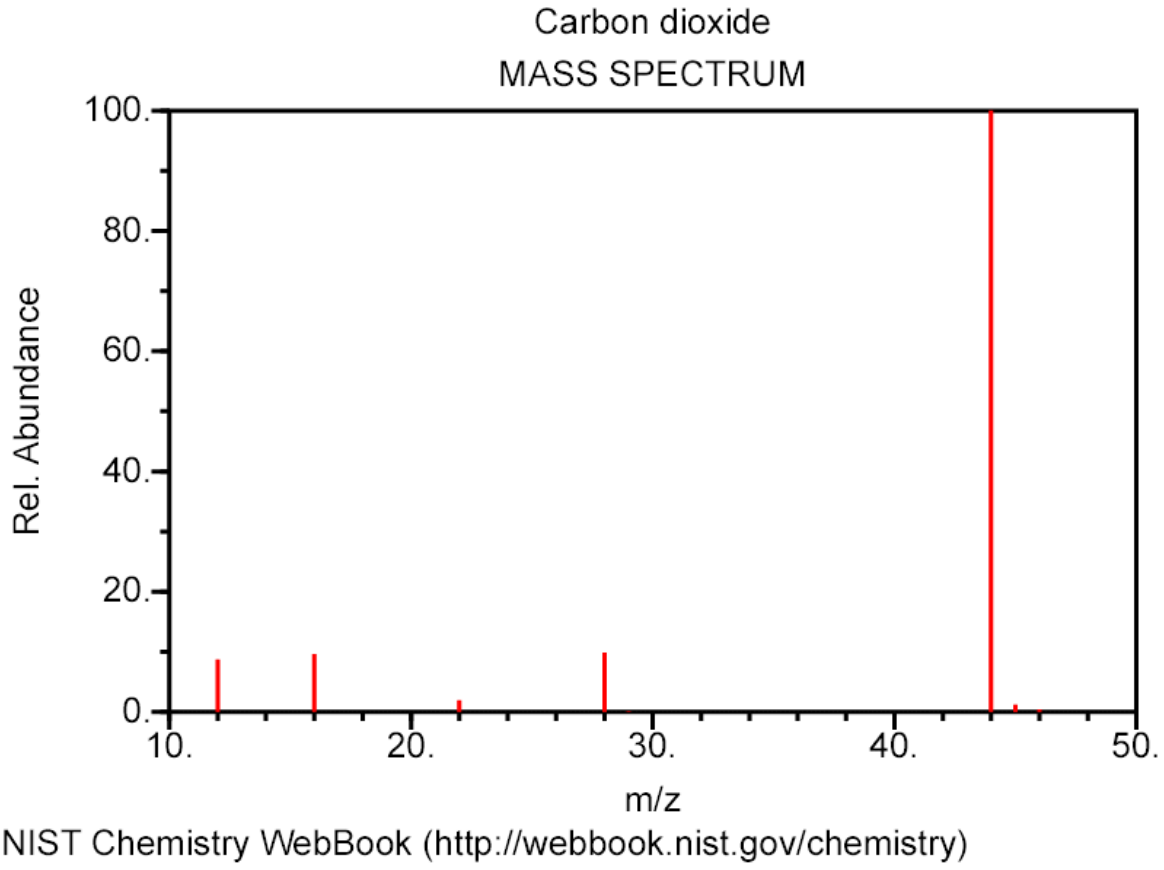

Figure C-1: Mass Spectrum of Carbon Dioxide

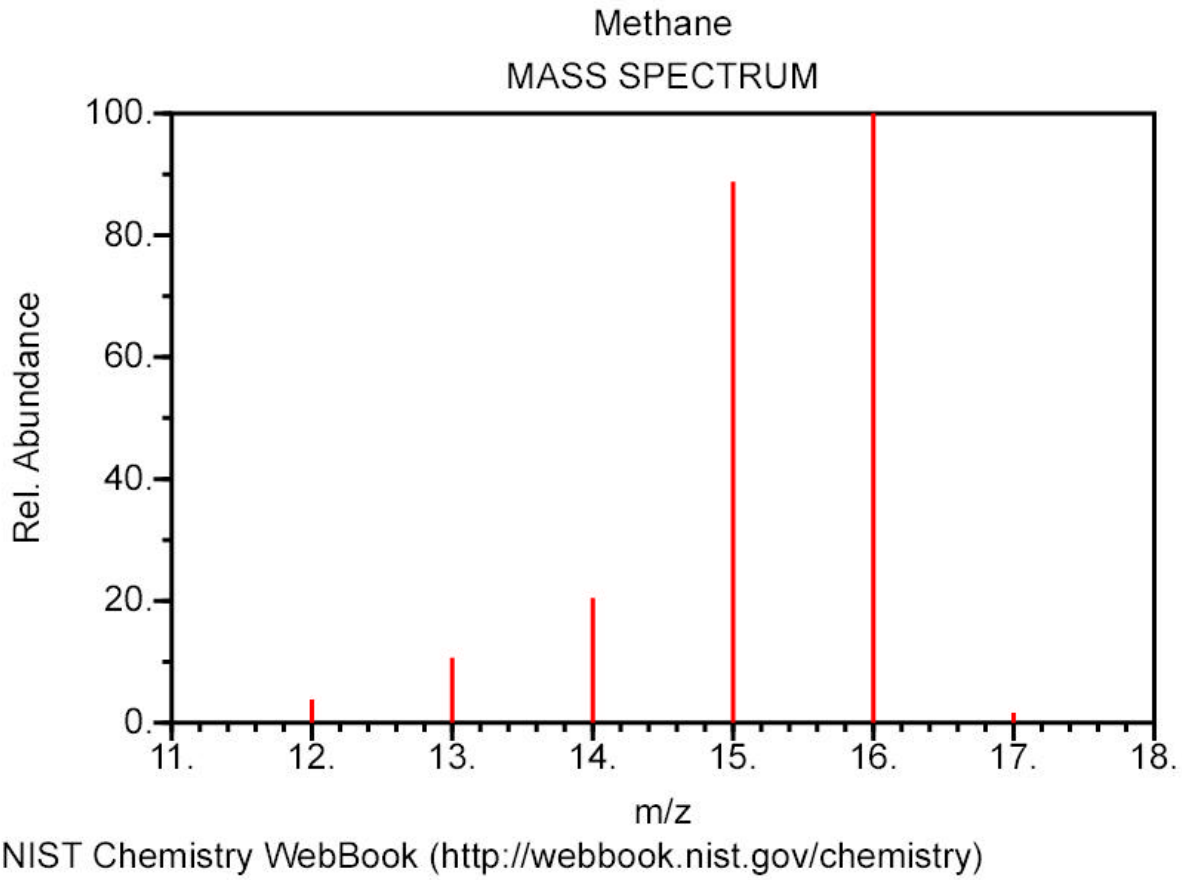

Figure C-2: Mass Spectrum of Methane

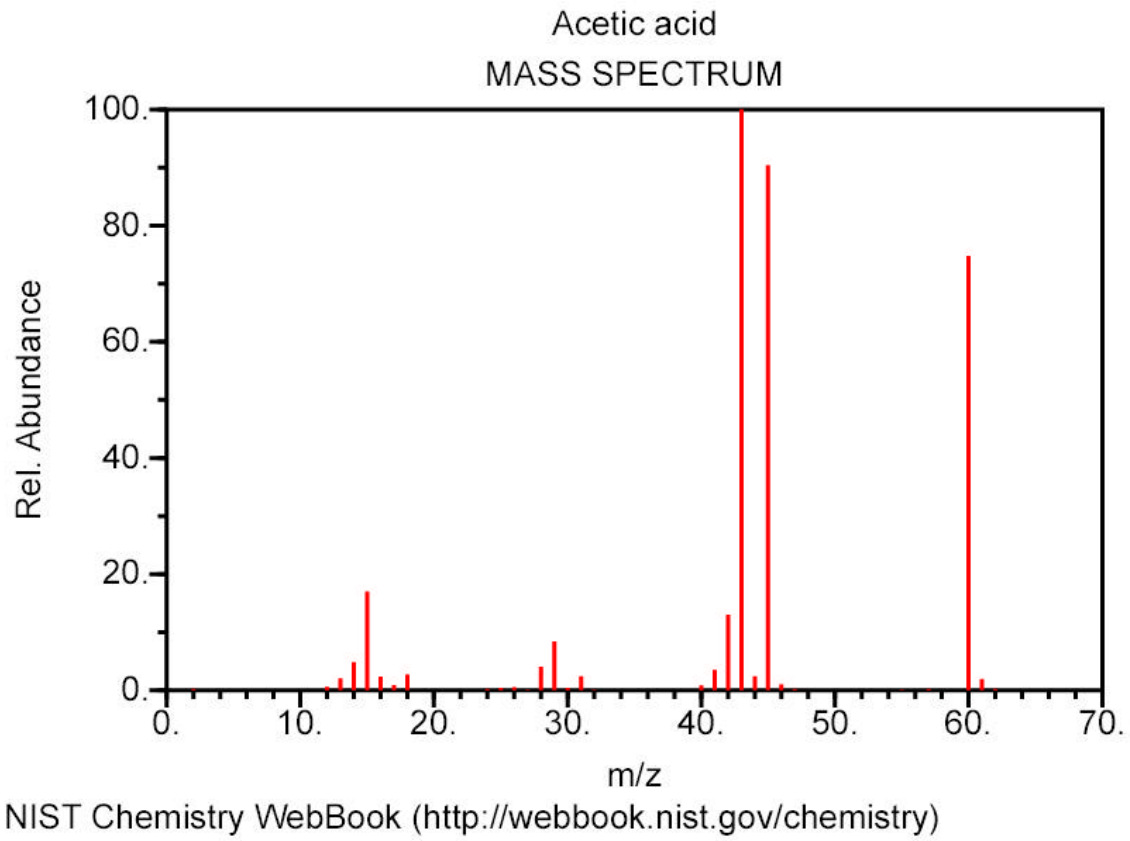

Figure C-3: Mass Spectrum of Acetic Acid

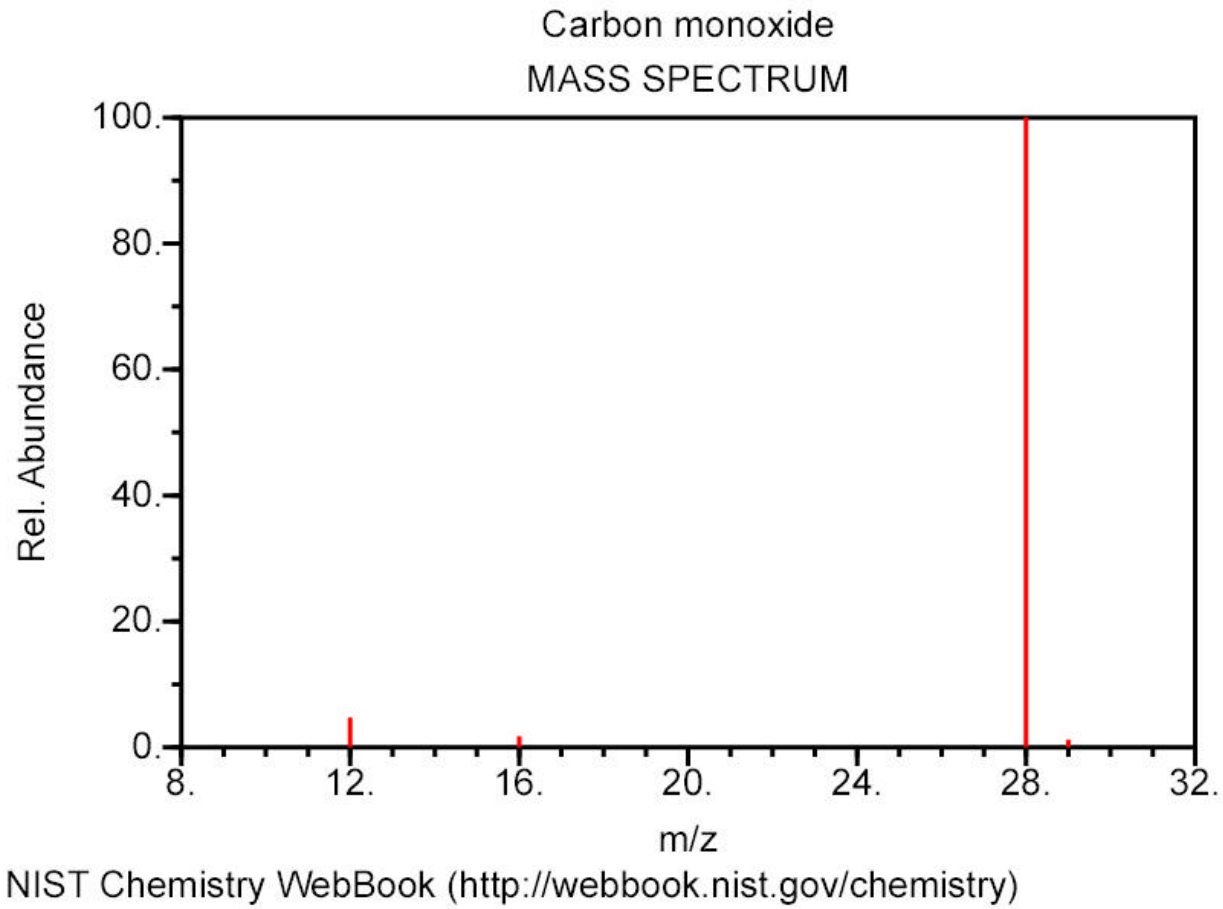

Figure C-4: Mass Spectrum of Carbon Monoxide

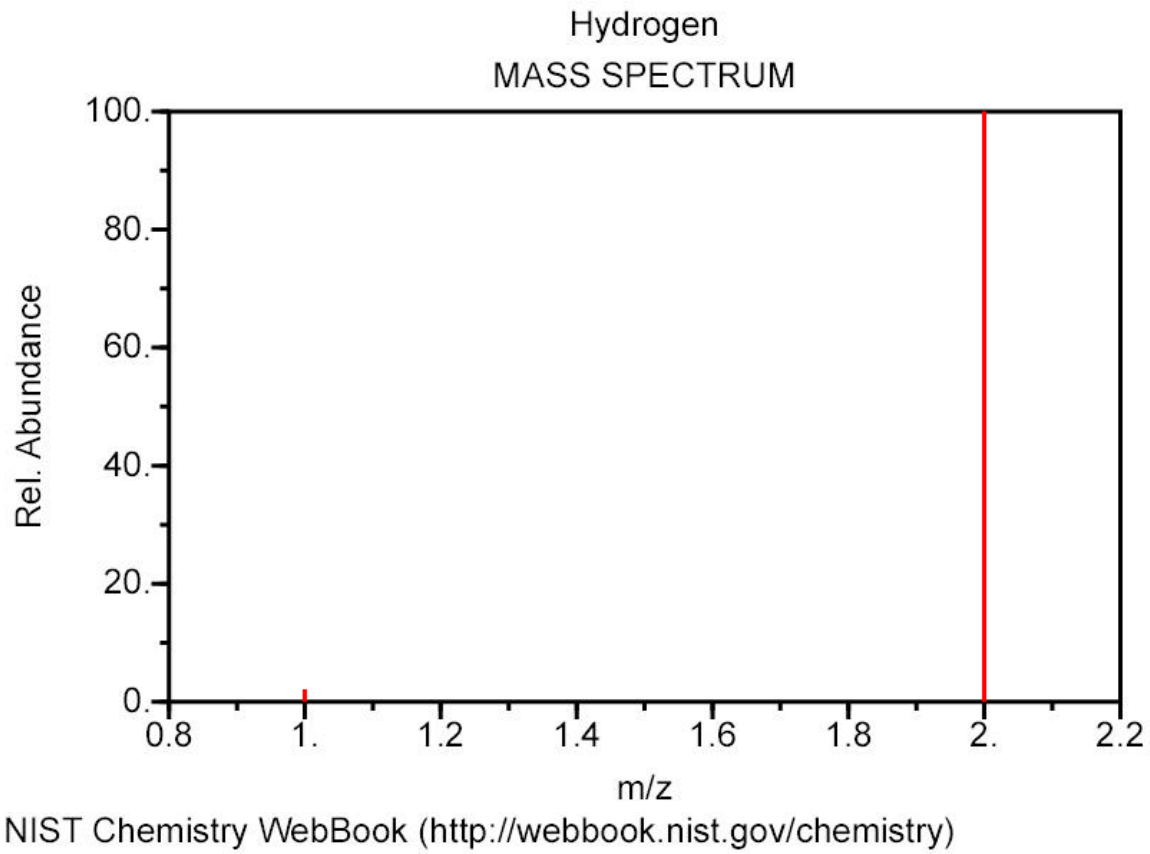

Figure C-5: Mass Spectrum of Hydrogen

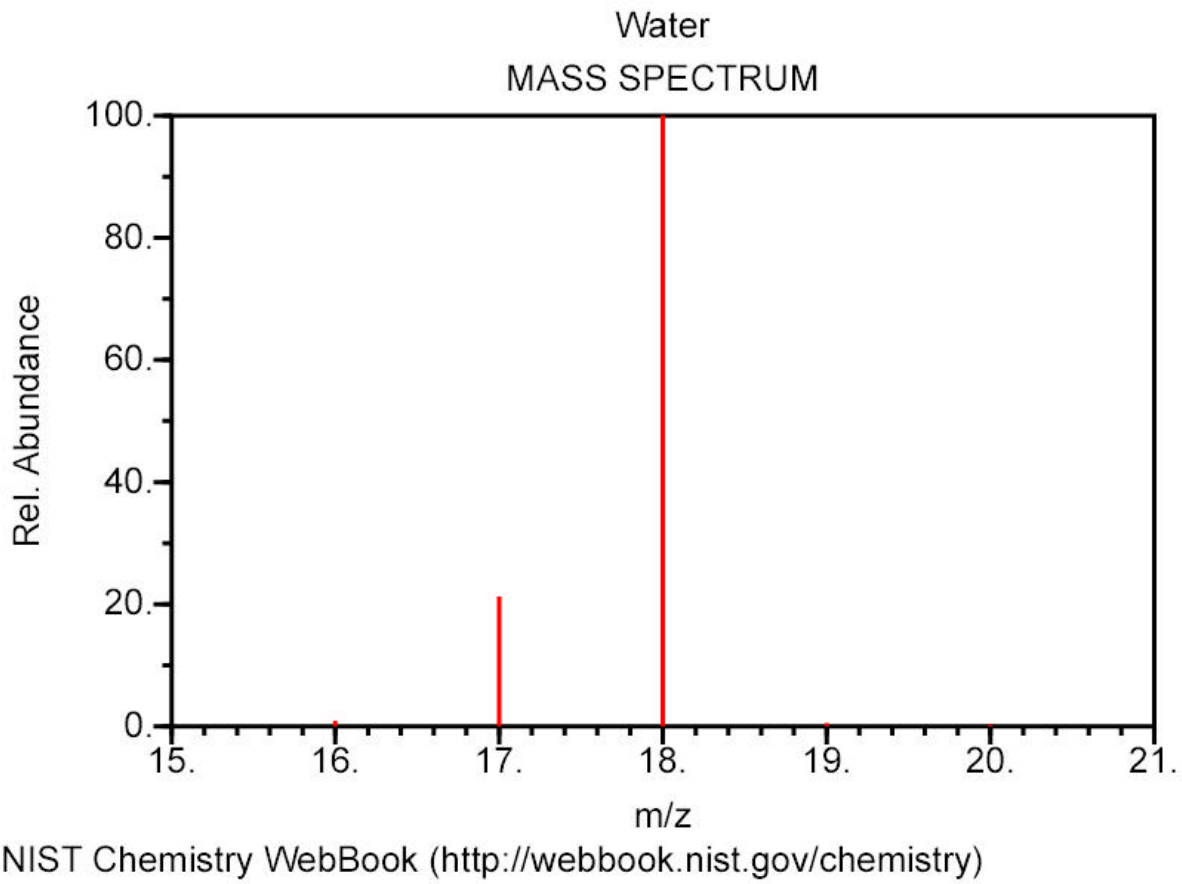

Figure C-6: Mass Spectrum of Water

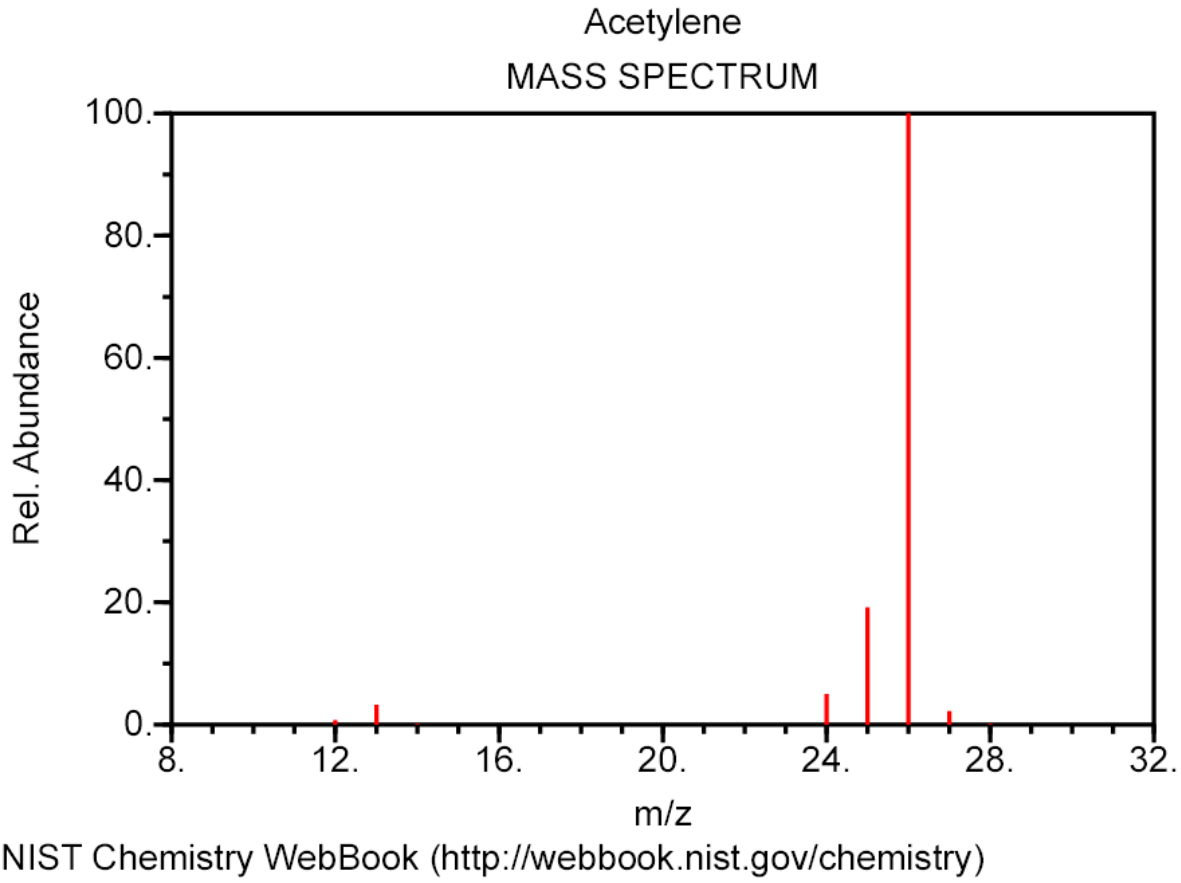

Figure C-7: Mass Spectrum of Acetylene

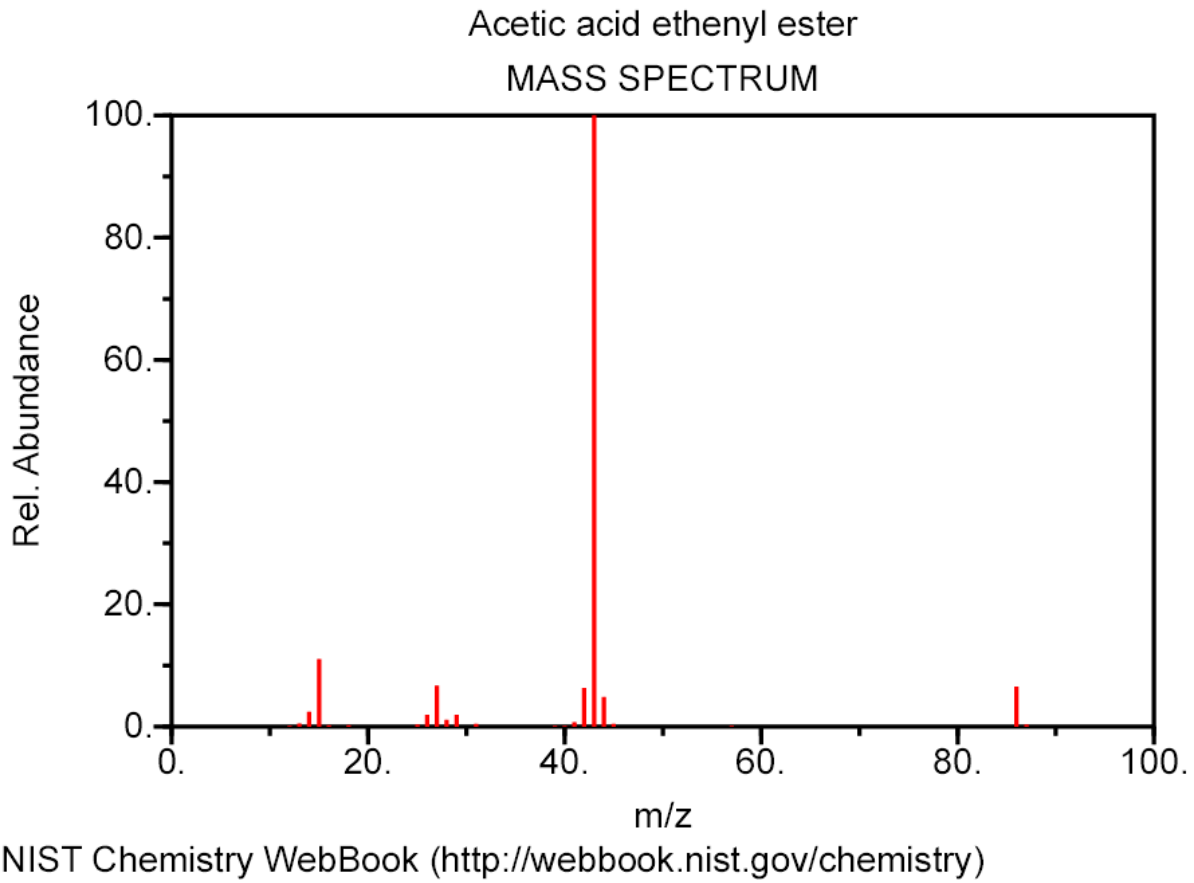

Figure C-8: Mass Spectrum of Acetylene

APPENDIX D:

REACTION DATA

D.1. 5% PD/ALUMINA

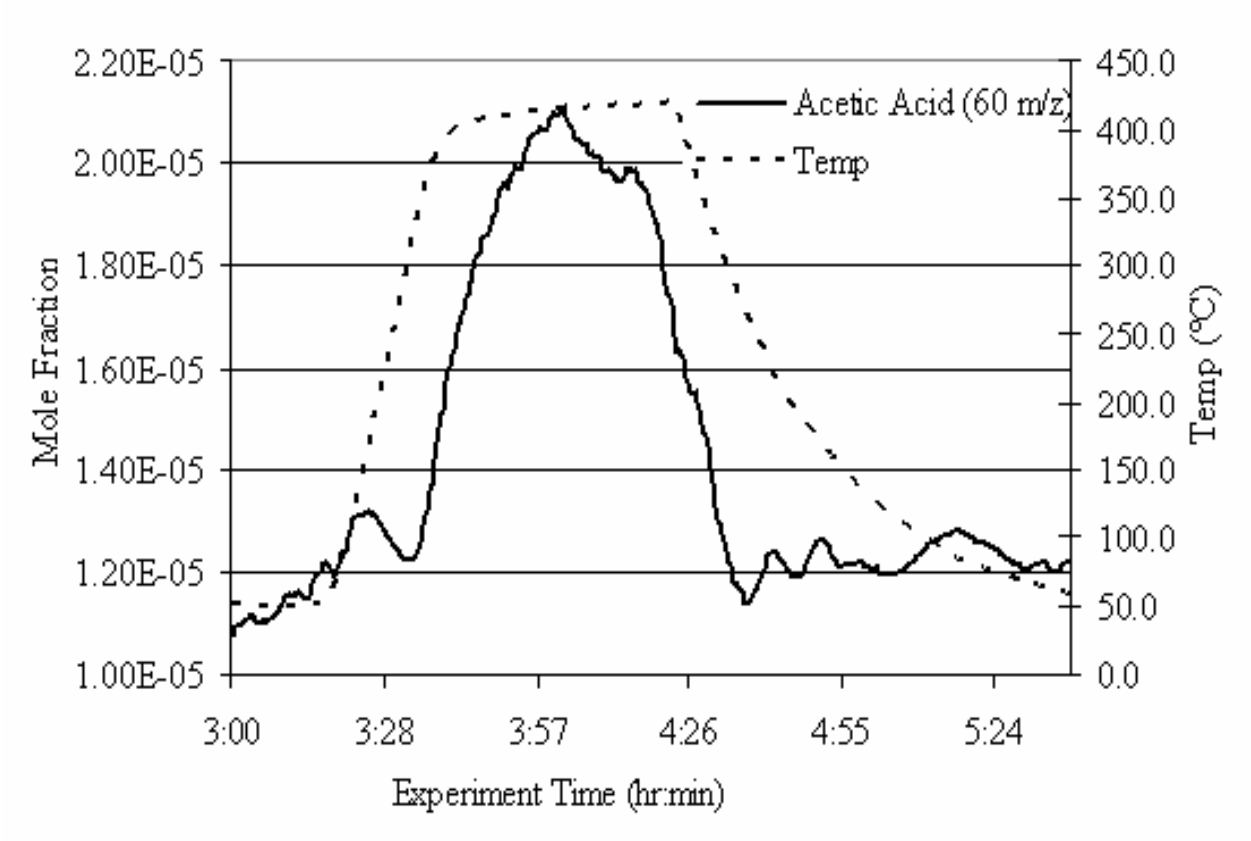

Figure D-1: Acetic acid mole fraction and temperature for helium pretreated 5% Pd/alumina exposed to 35% carbon dioxide 65% methane

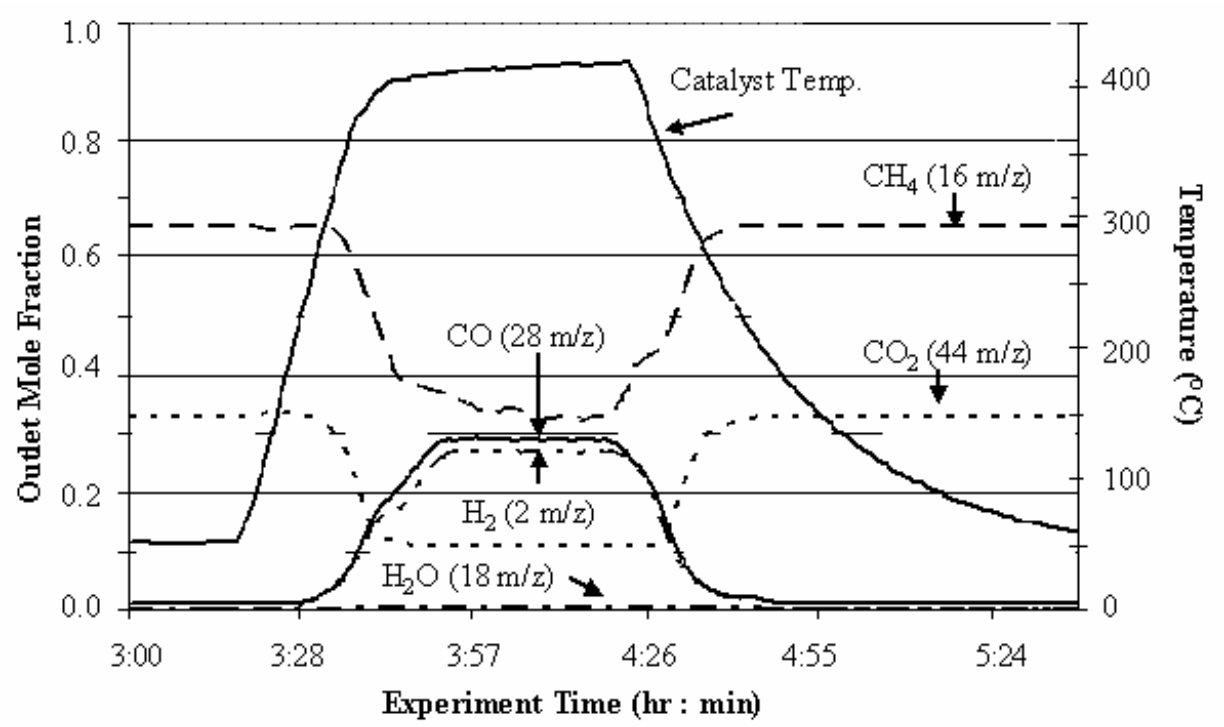

Figure D-2: CO_2, CH_4, CO, H_2 and H_2O mole fractions and temperature for helium pretreated 5% Pd/alumina exposed to 35% carbon dioxide 65% methane

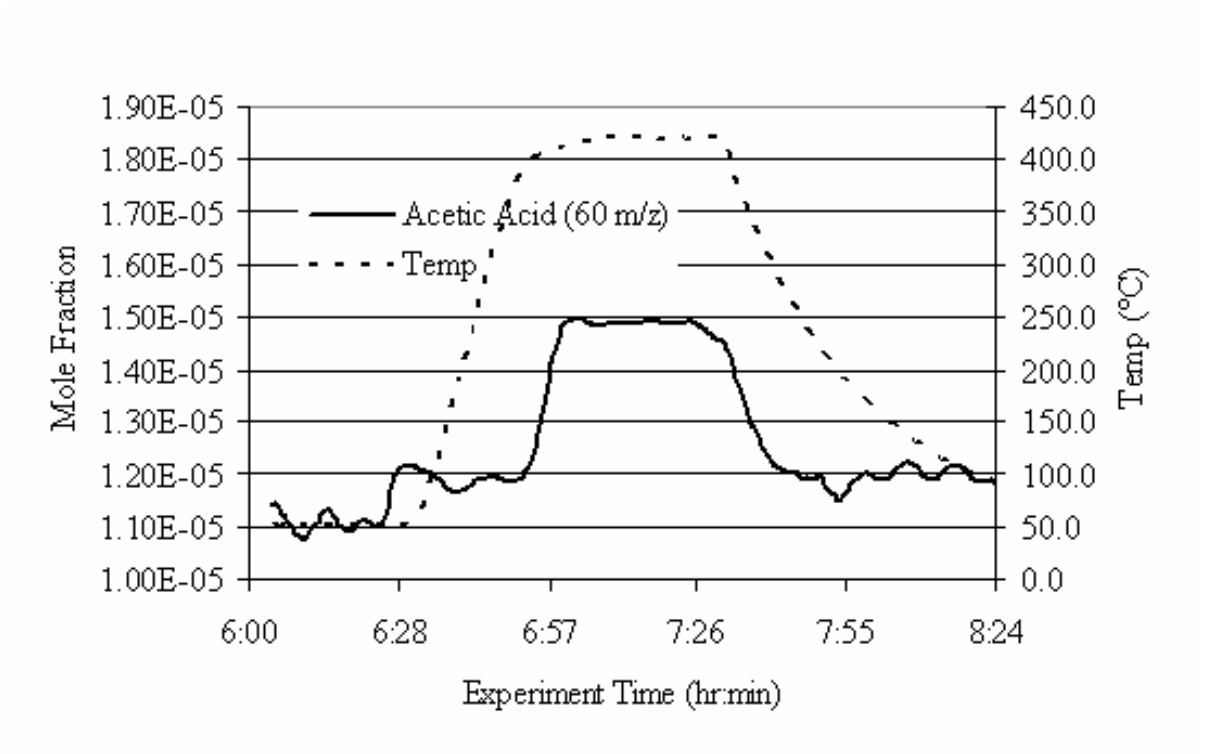

Figure D-3: Acetic acid mole fraction and temperature for helium pretreated 5% Pd/alumina exposed to 47% carbon dioxide 53% methane

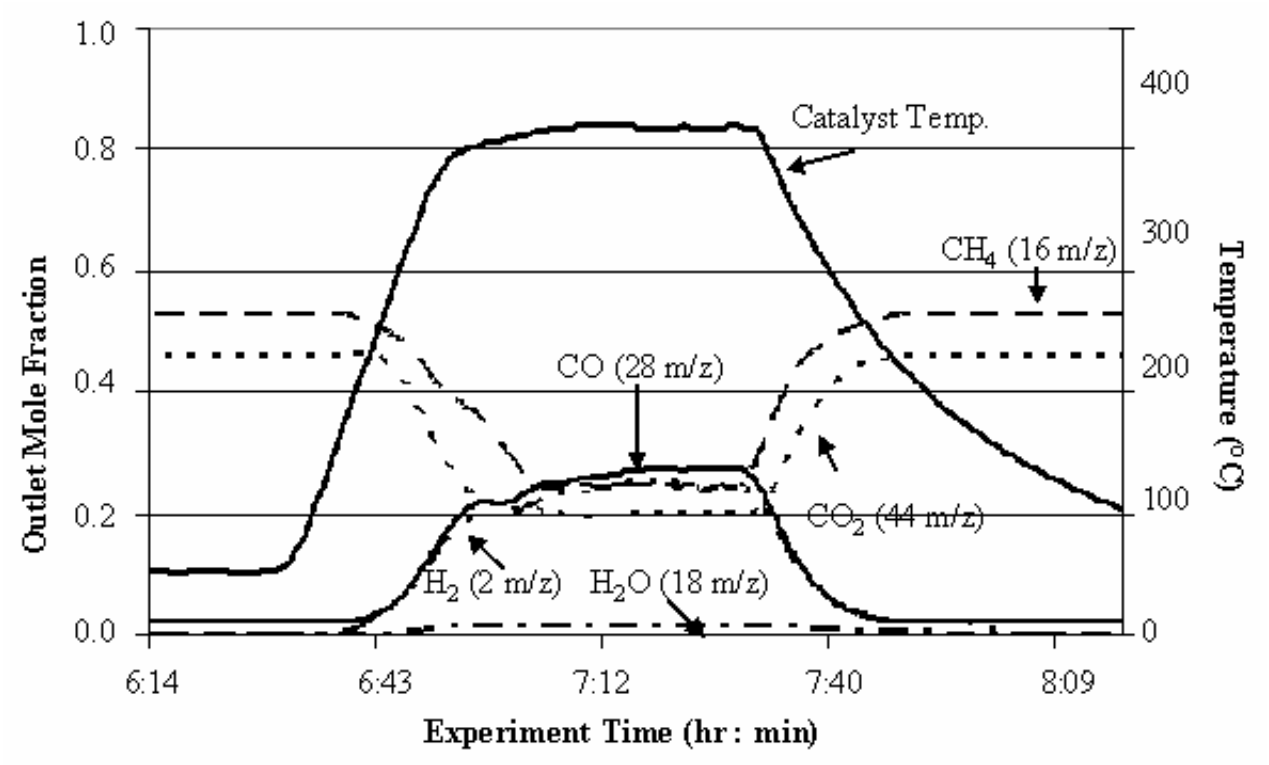

Figure D-4: CO_2, CH_4, CO, H_2 and H_2O mole fractions and temperature for helium pretreated 5% Pd/alumina exposed to 47% carbon dioxide 53% methane

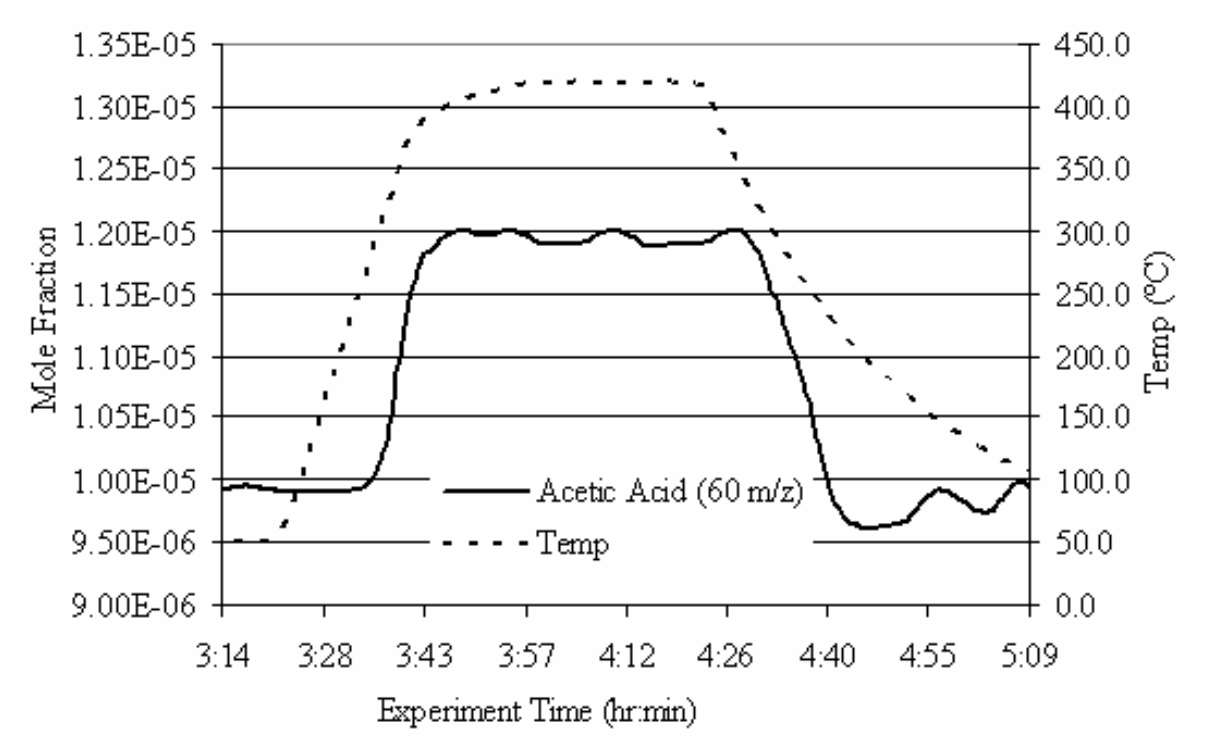

Figure D-5: Acetic acid mole fraction and temperature for helium pretreated 5% Pd/alumina exposed to 80% carbon dioxide 20% methane

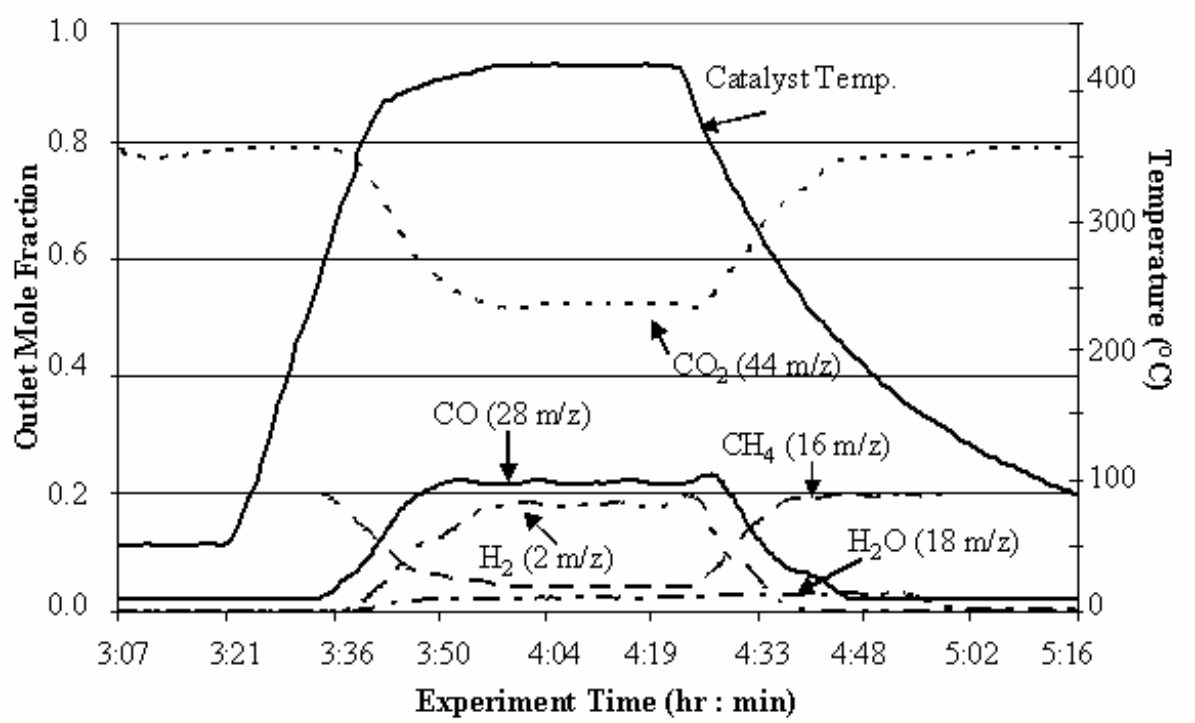

Figure D-6: CO_2, CH_4, CO, H_2 and H_2O mole fractions and temperature for helium pretreated 5% Pd/alumina exposed to 80% carbon dioxide 20% methane

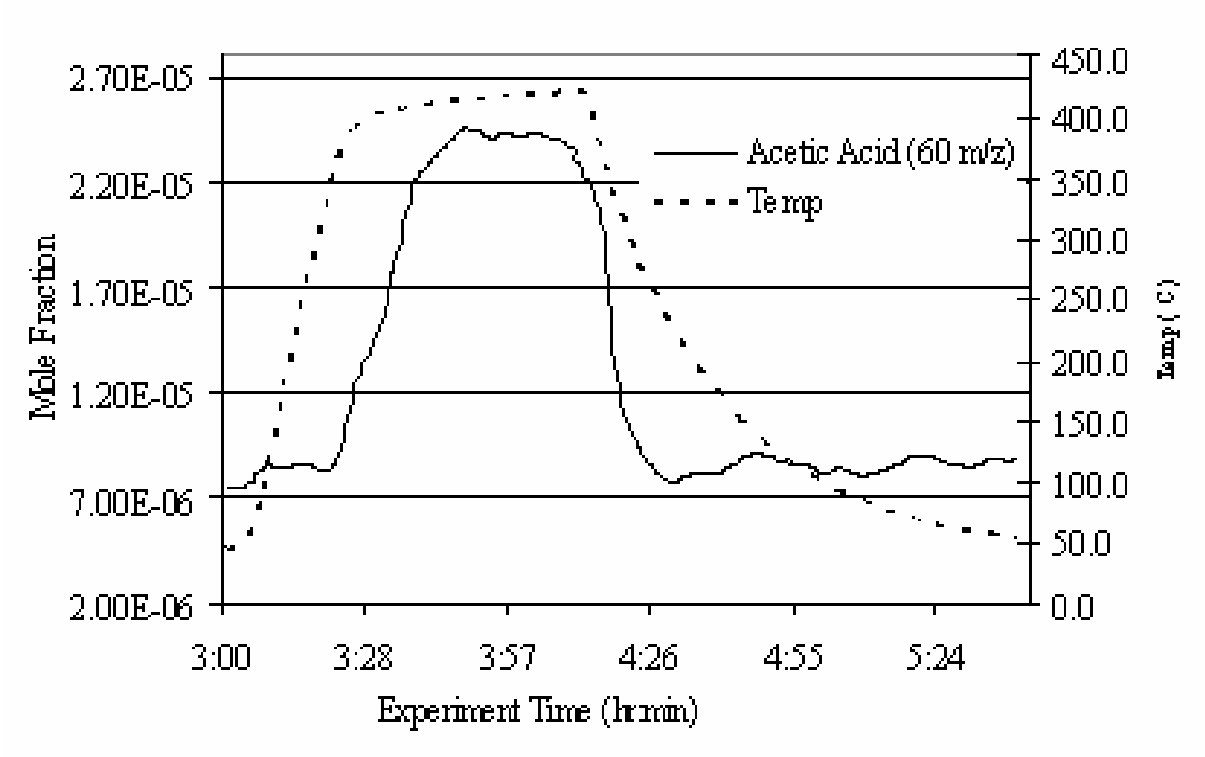

Figure D-7: Acetic acid mole fraction and temperature for carbon dioxide pretreated 5% Pd/alumina exposed to 35% carbon dioxide 65% methane

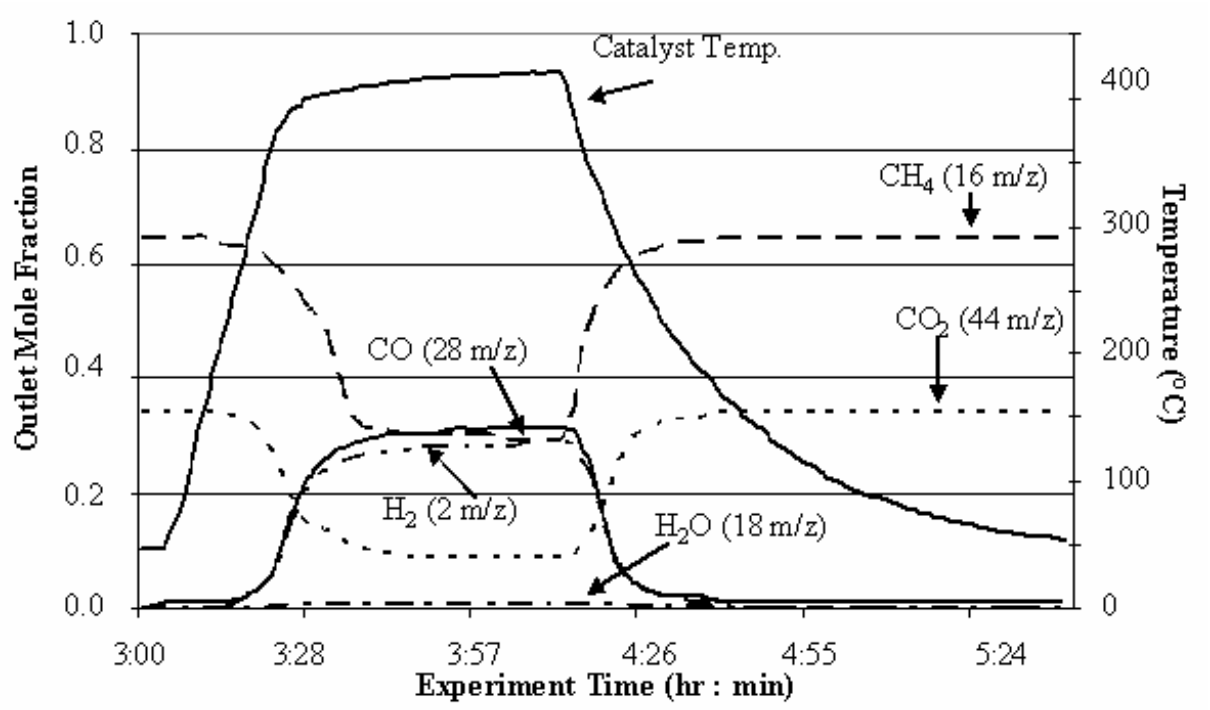

Figure D-8: CO_2, CH_4, CO, H_2 and H_2O mole fractions and temperature for carbon dioxide pretreated 5% Pd/alumina exposed to 35% carbon dioxide 65% methane

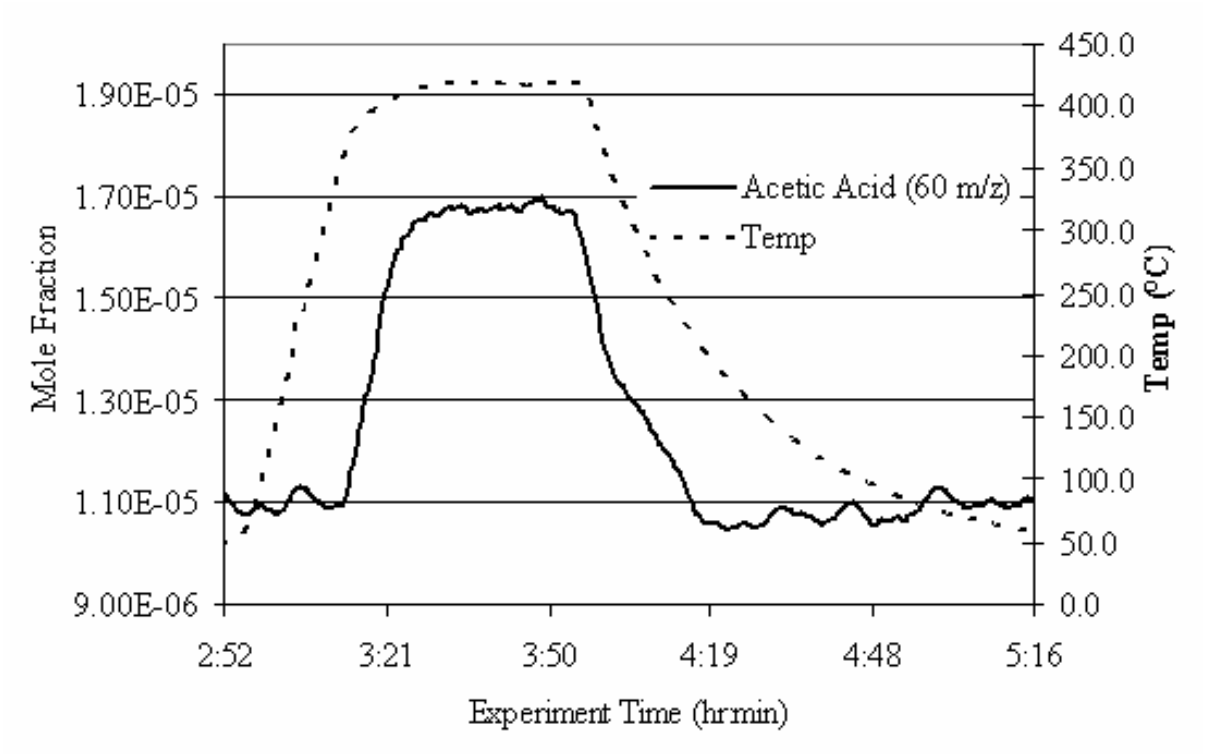

Figure D-9: Acetic acid mole fraction and temperature for carbon dioxide pretreated 5% Pd/alumina exposed to 53% carbon dioxide 47% methane

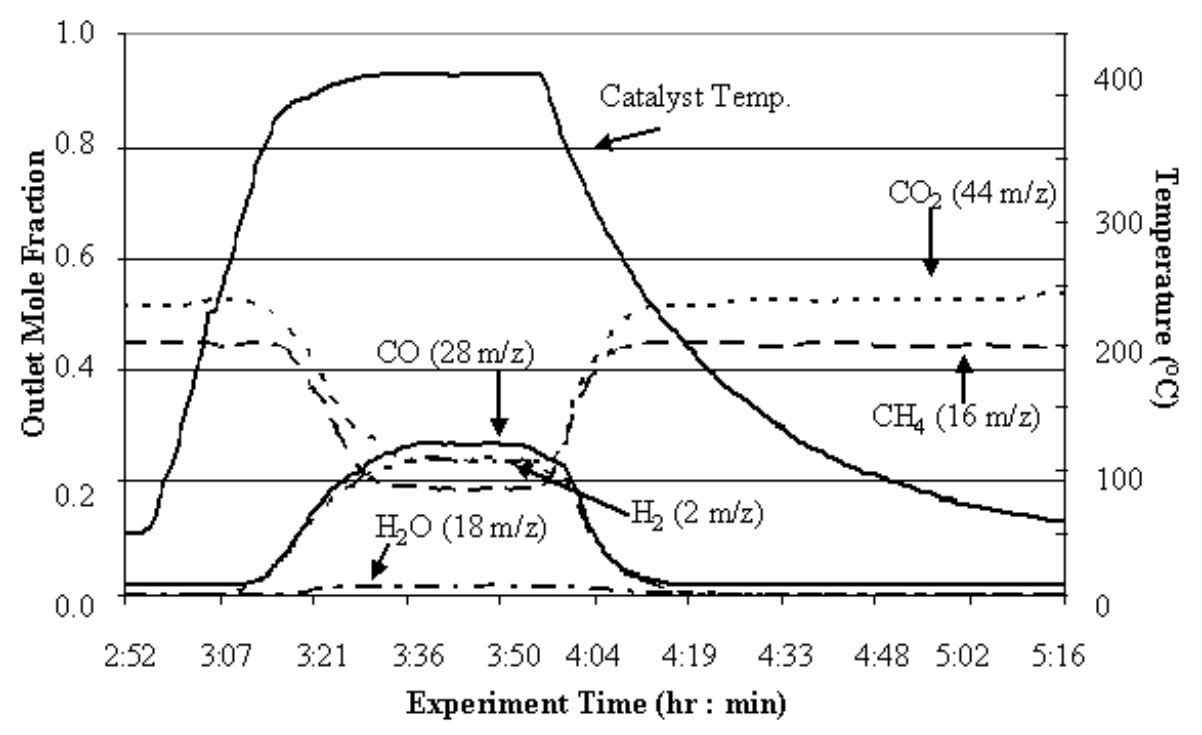

Figure D-10: CO_2, CH_4, CO, H_2 and H_2O mole fractions and temperature for carbon dioxide pretreated 5% Pd/alumina exposed to 53% carbon dioxide 47% methane

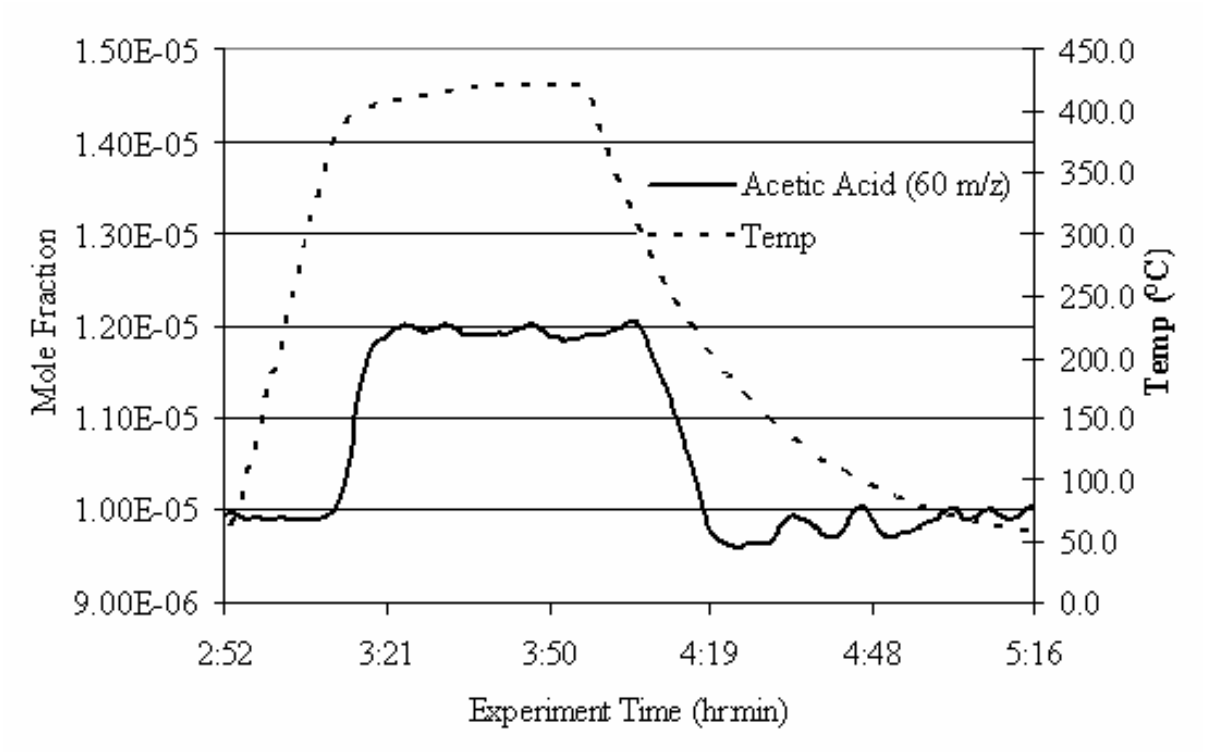

Figure D-11: Acetic acid mole fraction and temperature for carbon dioxide pretreated 5% Pd/alumina exposed to 23% carbon dioxide 77% methane

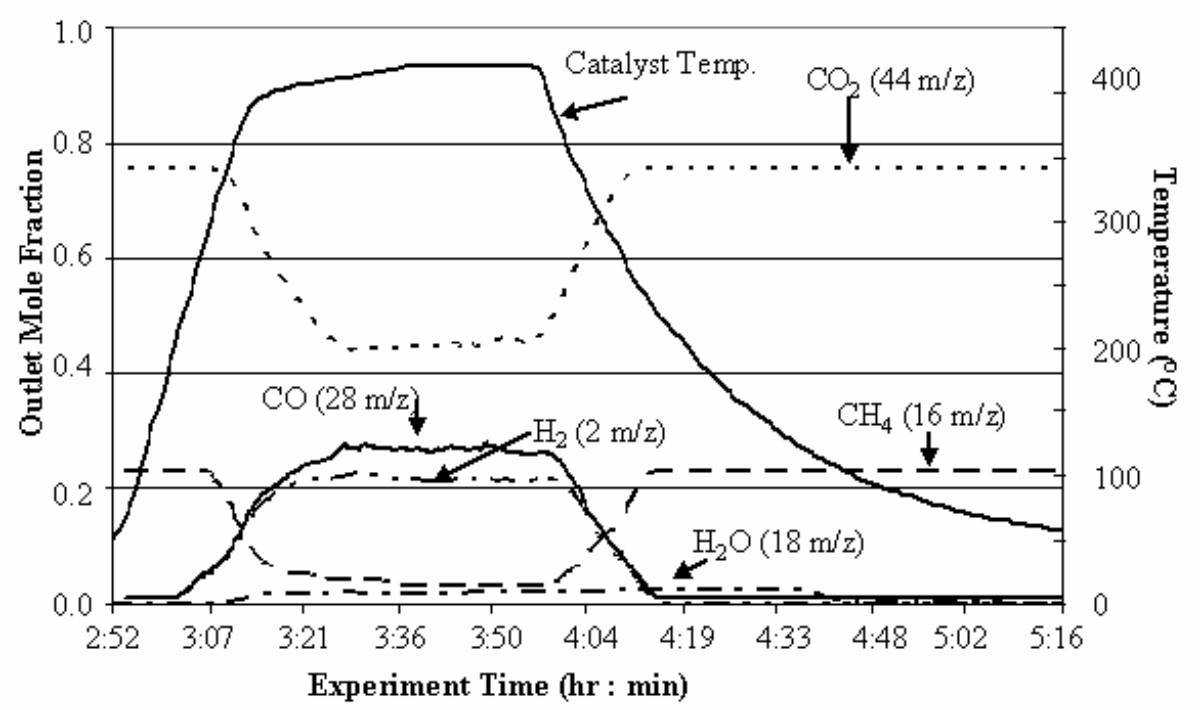

Figure D-12: CO_2, CH_4, CO, H_2 and H_2O mole fractions and temperature for carbon dioxide pretreated 5% Pd/alumina exposed to 23% carbon dioxide 77% methane

D.2. 5% PT/ALUMINA

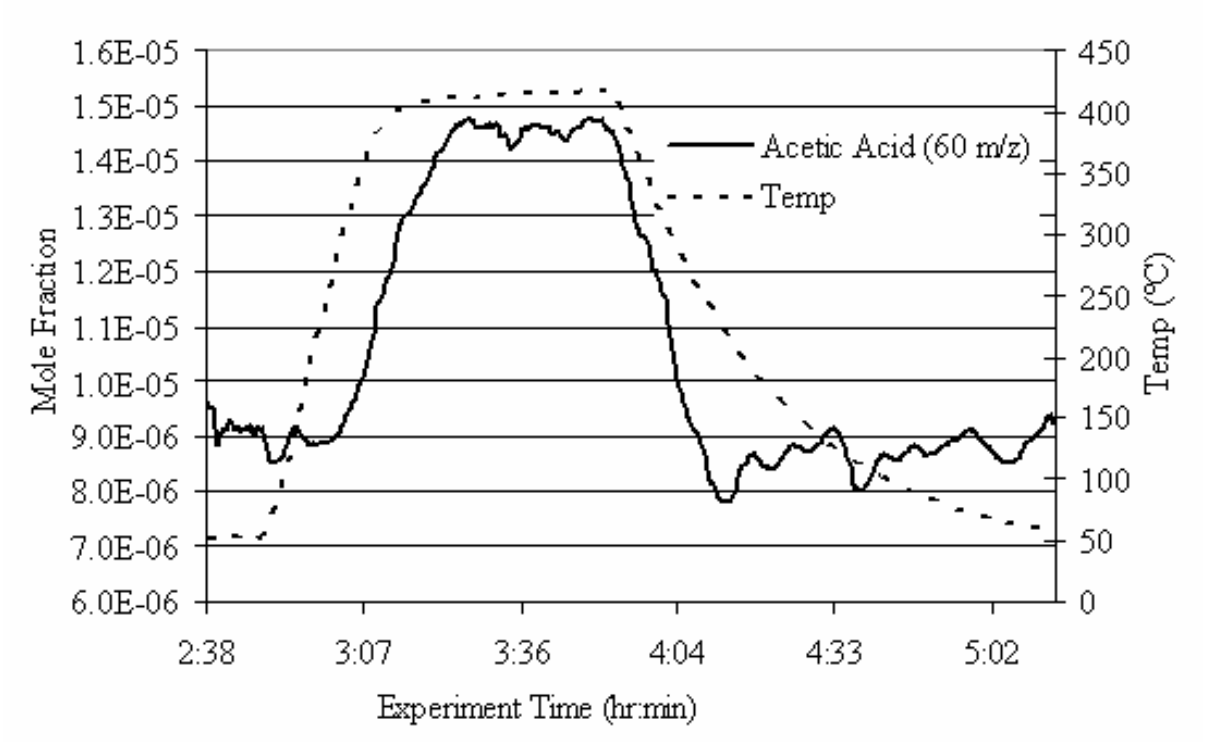

Figure D-13: Acetic acid mole fraction and temperature for helium pretreated 5% Pt/alumina exposed to 35% carbon dioxide 65% methane

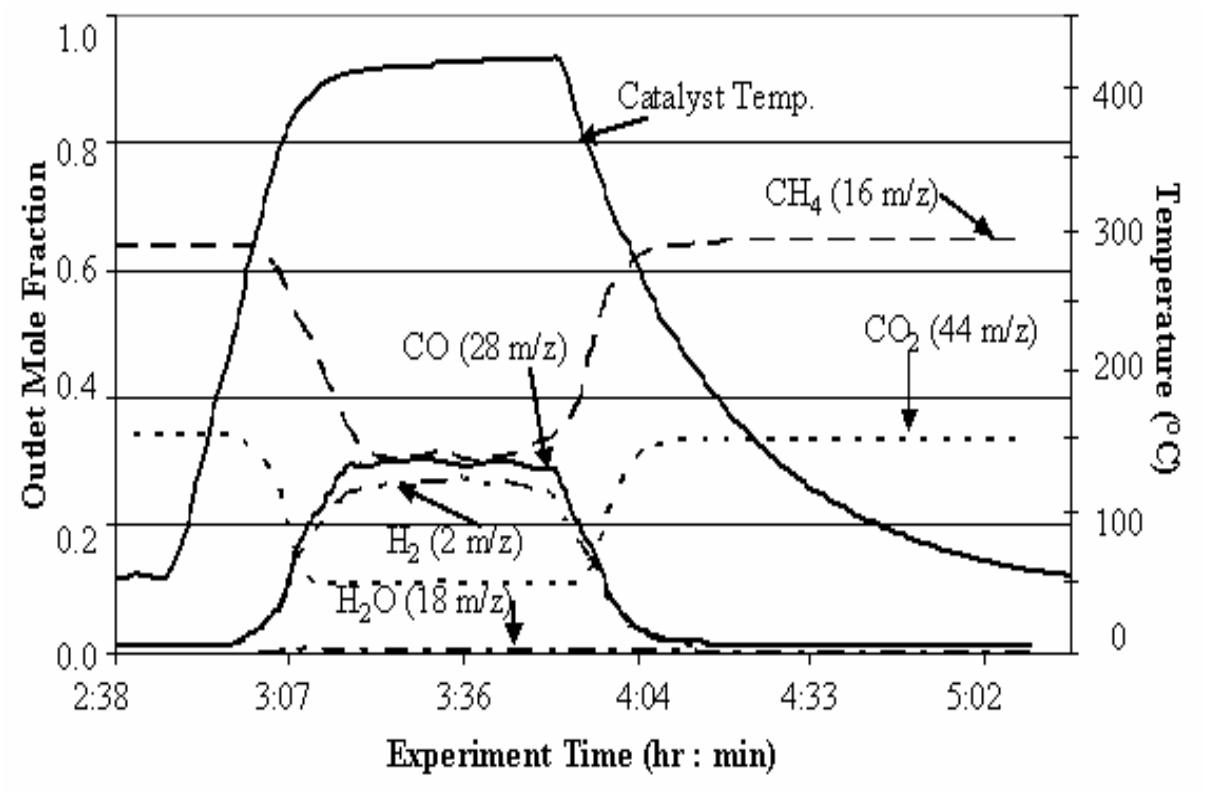

Figure D-14: CO_2, CH_4, CO, H_2 and H_2O mole fractions and temperature for helium pretreated 5% Pt/alumina exposed to 35% carbon dioxide 65% methane

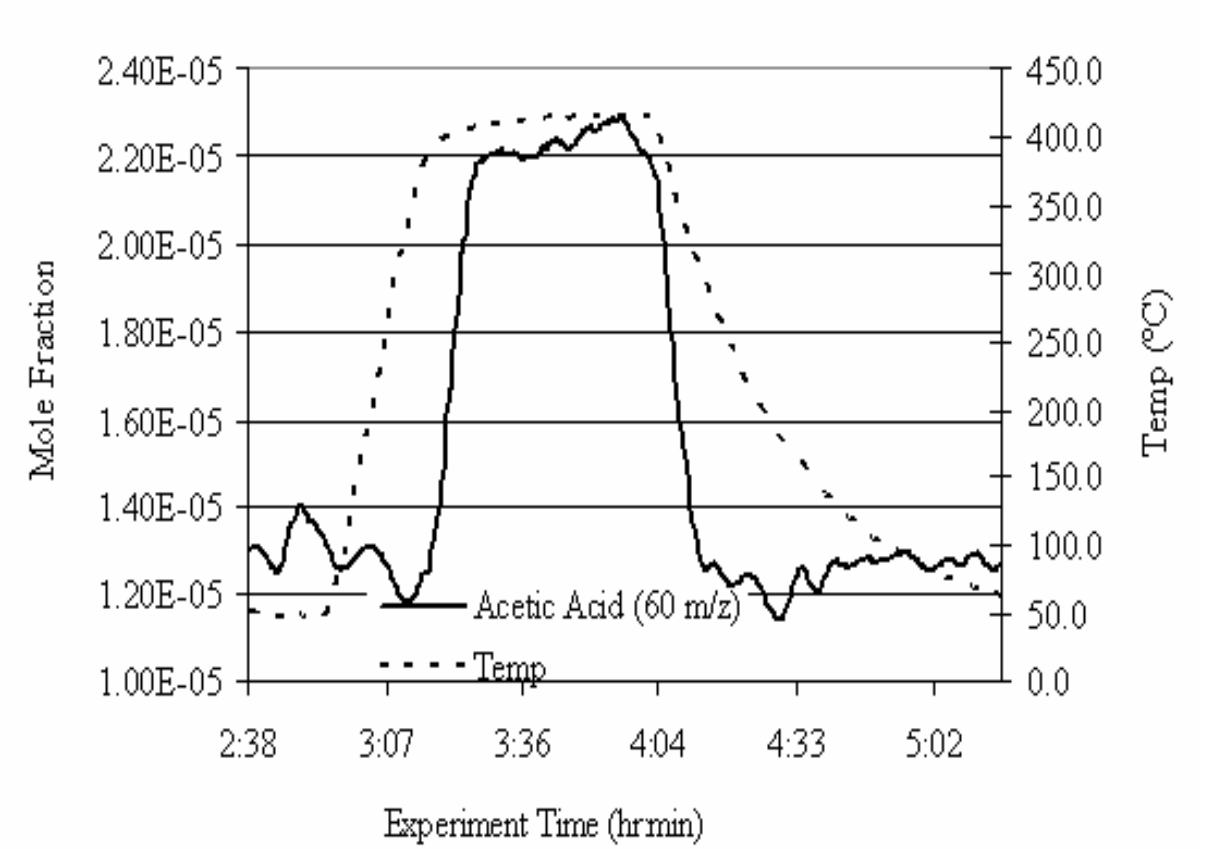

Figure D-15: Acetic acid mole fraction and temperature for helium pretreated 5% Pt/alumina exposed to 48% carbon dioxide 52% methane

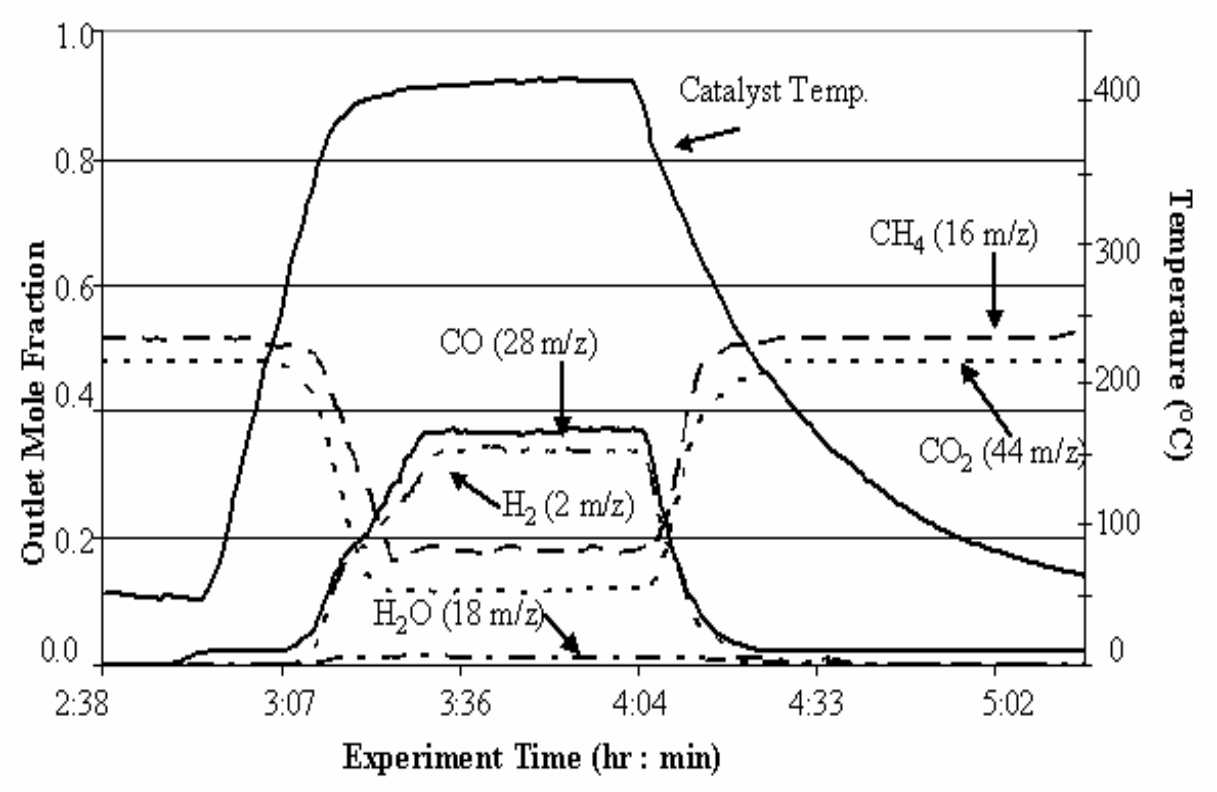

Figure D-16: CO_2, CH_4, CO, H_2 and H_2O mole fractions and temperature for helium pretreated 5% Pt/alumina exposed to 48% carbon dioxide 52% methane

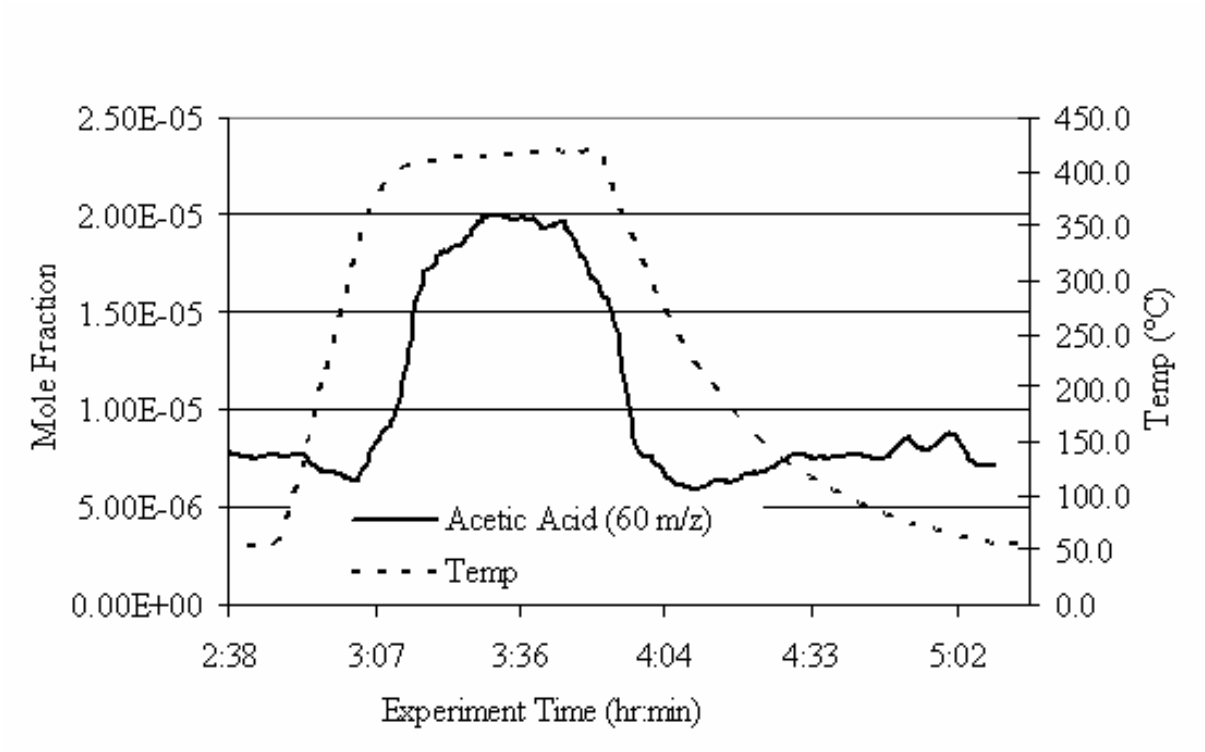

Figure D-17: Acetic acid mole fraction and temperature for helium pretreated 5% Pt/alumina exposed to 80% carbon dioxide 20% methane

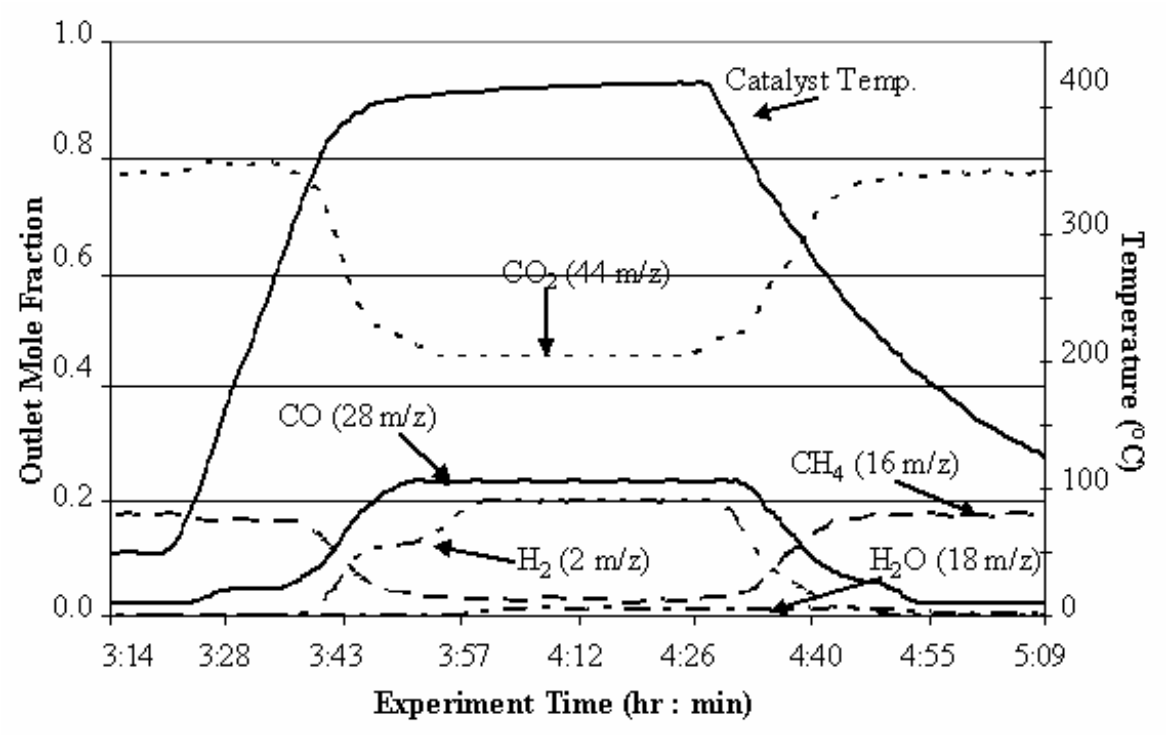

Figure D-18: CO_2, CH_4, CO, H_2 and H_2O mole fractions and temperature for helium pretreated 5% Pt/alumina exposed to 80% carbon dioxide 20% methane

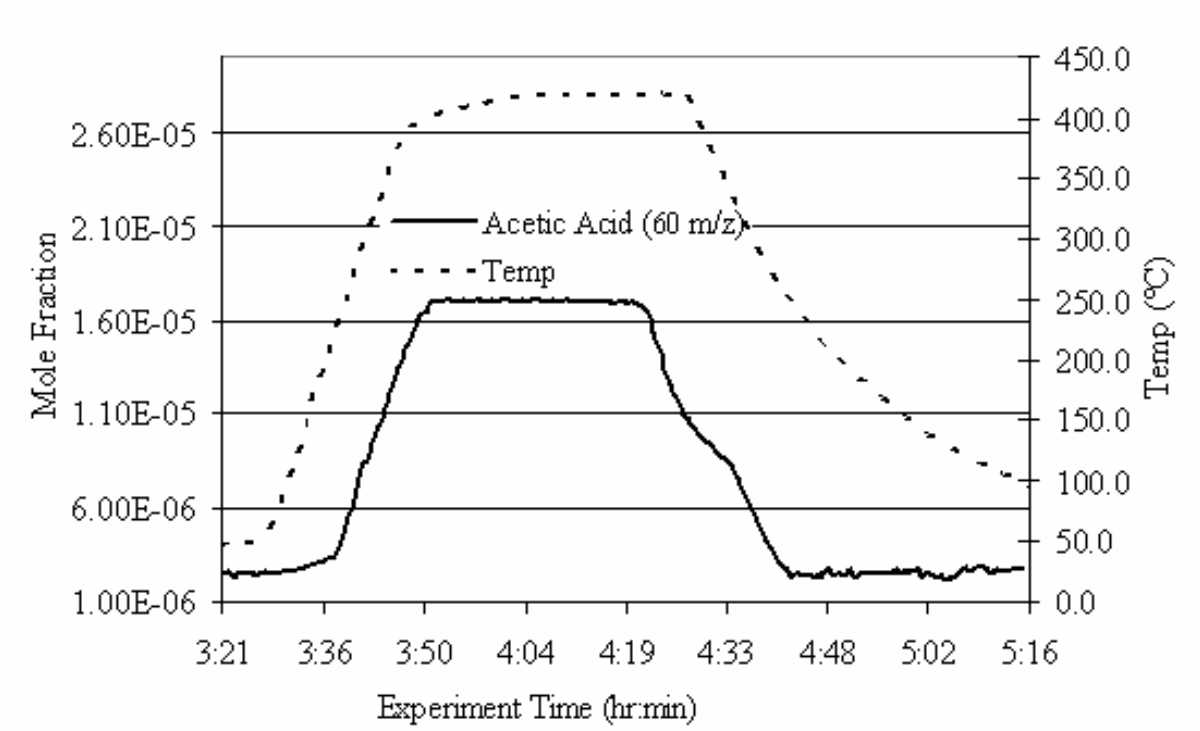

Figure D-19: Acetic acid mole fraction and temperature for helium pretreated 5% Pt/alumina exposed to 36% carbon dioxide 64% methane

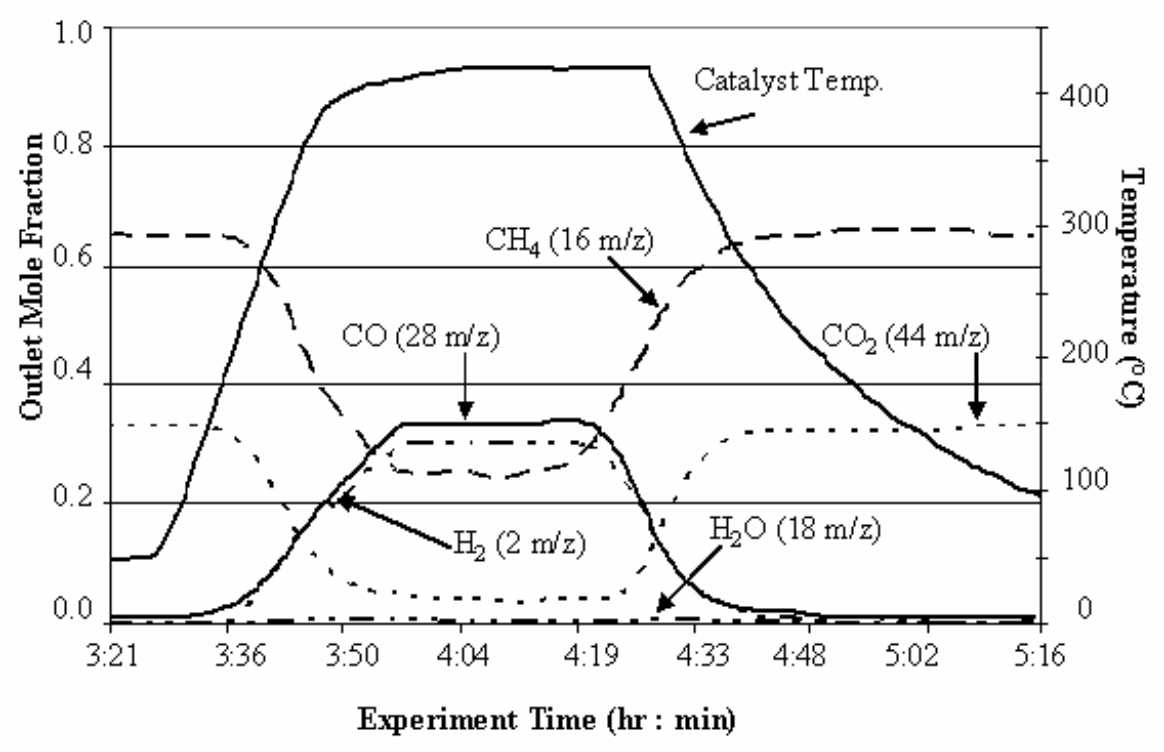

Figure D-20: CO_2, CH_4, CO, H_2 and H_2O mole fractions and temperature for helium pretreated 5% Pt/alumina exposed to 36% carbon dioxide 64% methane

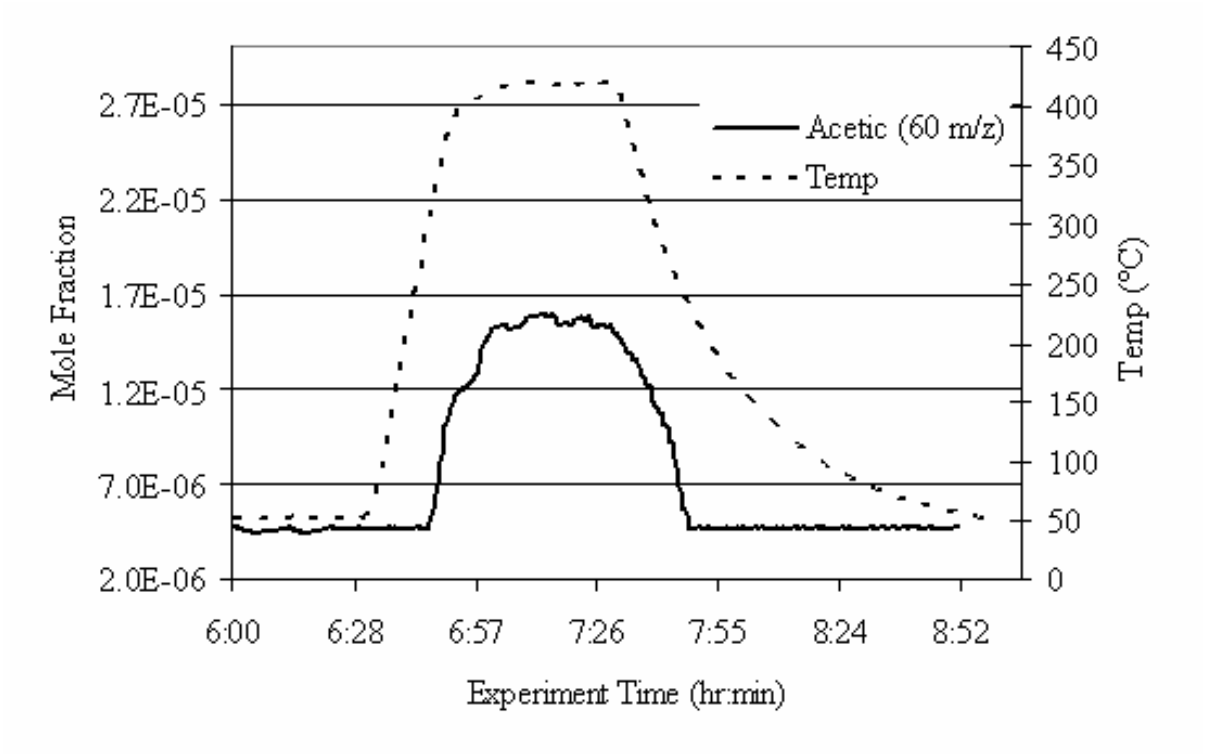

Figure D-21: Acetic acid mole fraction and temperature for helium pretreated 5% Pt/alumina exposed to 48% carbon dioxide 52% methane

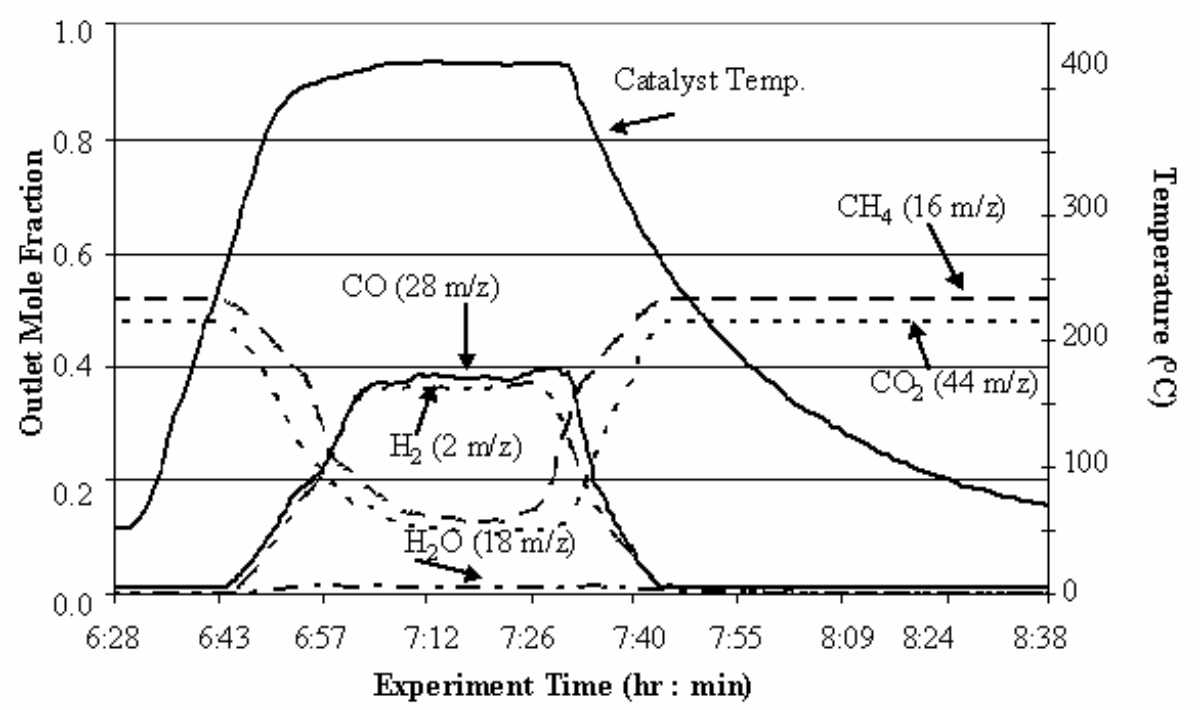

Figure D-22: CO_2, CH_4, CO, H_2 and H_2O mole fractions and temperature for helium pretreated 5% Pt/alumina exposed to 48% carbon dioxide 52% methane

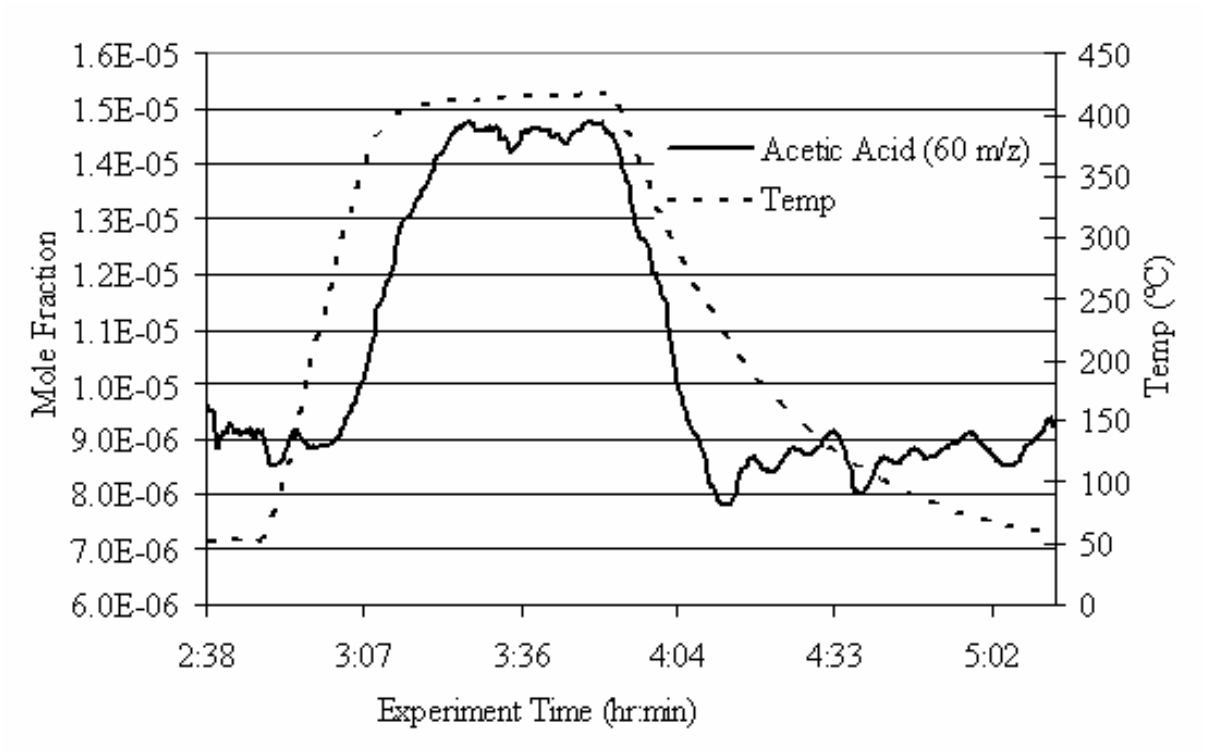

Figure D-23: Acetic acid mole fraction and temperature for helium pretreated 5% Pt/alumina exposed to 83% carbon dioxide 17% methane

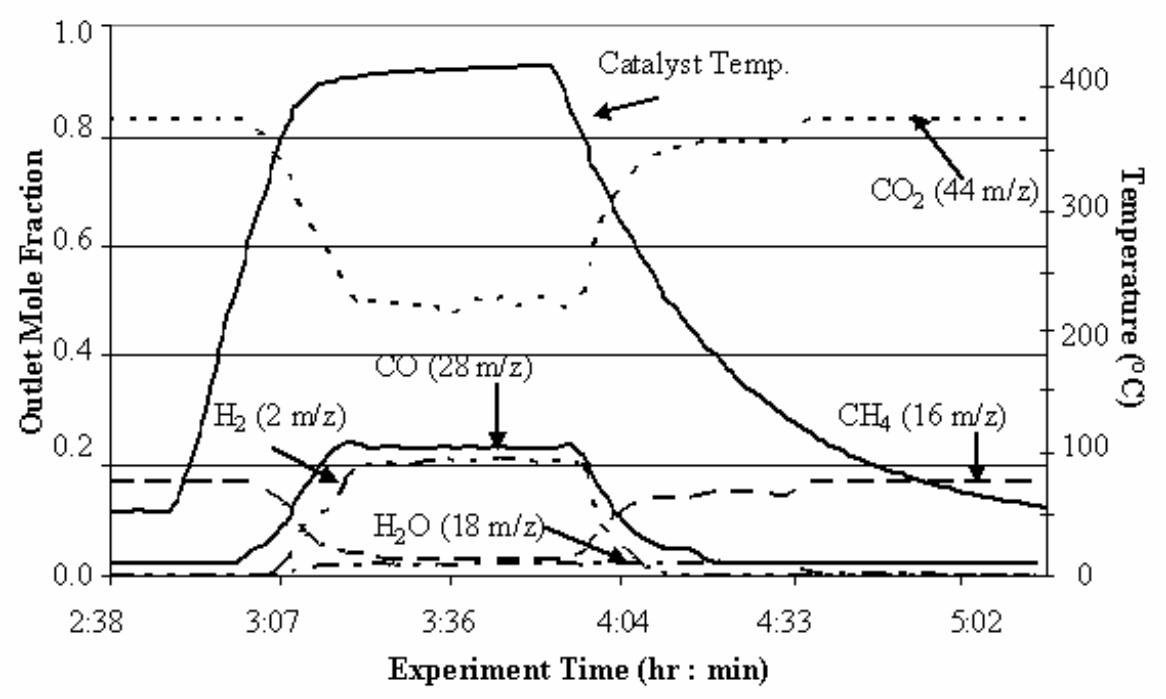

Figure D-24: CO_2, CH_4, CO, H_2 and H_2O mole fractions and temperature for helium pretreated 5% Pt/alumina exposed to 83% carbon dioxide 17% methane